CENTRAL REGULATION OF METABOLISM

EDITED BY: Hu Huang, Alexander K. Murashov, Tiemin Liu,
Srinivas Sriramula and Jessica M. Ellis
PUBLISHED IN: Frontiers in Endocrinology and Frontiers in Neuroscience

frontiers Research Topics

ISSN 1664-8714
ISBN 978-2-88974-836-5
DOI 10.3389/978-2-88974-836-5

About Frontiers

Frontiers is more than just an open-access publisher of scholarly articles: it is a pioneering approach to the world of academia, radically improving the way scholarly research is managed. The grand vision of Frontiers is a world where all people have an equal opportunity to seek, share and generate knowledge. Frontiers provides immediate and permanent online open access to all its publications, but this alone is not enough to realize our grand goals.

Frontiers Journal Series

The Frontiers Journal Series is a multi-tier and interdisciplinary set of open-access, online journals, promising a paradigm shift from the current review, selection and dissemination processes in academic publishing. All Frontiers journals are driven by researchers for researchers; therefore, they constitute a service to the scholarly community. At the same time, the Frontiers Journal Series operates on a revolutionary invention, the tiered publishing system, initially addressing specific communities of scholars, and gradually climbing up to broader public understanding, thus serving the interests of the lay society, too.

Dedication to Quality

Each Frontiers article is a landmark of the highest quality, thanks to genuinely collaborative interactions between authors and review editors, who include some of the world's best academicians. Research must be certified by peers before entering a stream of knowledge that may eventually reach the public - and shape society; therefore, Frontiers only applies the most rigorous and unbiased reviews.
Frontiers revolutionizes research publishing by freely delivering the most outstanding research, evaluated with no bias from both the academic and social point of view. By applying the most advanced information technologies, Frontiers is catapulting scholarly publishing into a new generation.

What are Frontiers Research Topics?

Frontiers Research Topics are very popular trademarks of the Frontiers Journals Series: they are collections of at least ten articles, all centered on a particular subject. With their unique mix of varied contributions from Original Research to Review Articles, Frontiers Research Topics unify the most influential researchers, the latest key findings and historical advances in a hot research area! Find out more on how to host your own Frontiers Research Topic or contribute to one as an author by contacting the Frontiers Editorial Office: frontiersin.org/about/contact

CENTRAL REGULATION OF METABOLISM

Topic Editors:
Hu Huang, East Carolina University, United States
Alexander K. Murashov, East Carolina University, United States
Tiemin Liu, Fudan University, China
Srinivas Sriramula, East Carolina University, United States
Jessica M. Ellis, East Carolina University, United States

Citation: Huang, H., Murashov, A. K., Liu, T., Sriramula, S., Ellis, J. M., eds. (2022). Central Regulation of Metabolism. Lausanne: Frontiers Media SA.
doi: 10.3389/978-2-88974-836-5

Table of Contents

frontiers in Endocrinology

MINI REVIEW
published: 09 February 2021
doi: 10.3389/fendo.2020.622581

Tissue-Specific Approaches Reveal Diverse Metabolic Functions of Rho-Kinase 1

Taylor Landry[1,2,3], *Daniel Shookster*[1,2,3] *and Hu Huang*[1,2,3,4]*

[1] East Carolina Diabetes and Obesity Institute, East Carolina University, Greenville, NC, United States, [2] Department of Kinesiology, East Carolina University, Greenville, NC, United States, [3] Human Performance Laboratory, College of Human Performance and Health, East Carolina University, Greenville, NC, United States, [4] Department of Physiology, East Carolina University, Greenville, NC, United States

Rho-kinase 1 (ROCK1) has been implicated in diverse metabolic functions throughout the body, with promising evidence identifying ROCK1 as a therapeutic target in diabetes and obesity. Considering these metabolic roles, several pharmacological inhibitors have been developed to elucidate the mechanisms underlying ROCK1 function. Y27632 and fasudil are two common ROCK1 inhibitors; however, they have varying non-specific selectivity to inhibit other AGC kinase subfamily members and whole-body pharmacological approaches lack tissue-specific insight. As a result, interpretation of studies with these inhibitors is difficult, and alternative approaches are needed to elucidate ROCK1's tissue specific metabolic functions. Fortunately, recent technological advances utilizing molecular carriers or genetic manipulation have facilitated discovery of ROCK1's tissue-specific mechanisms of action. In this article, we review the tissue-specific roles of ROCK1 in the regulation of energy balance and substrate utilization. We highlight prominent metabolic roles in liver, adipose, and skeletal muscle, in which ROCK1 regulates energy expenditure, glucose uptake, and lipid metabolism *via* inhibition of AMPK2α and paradoxical modulation of insulin signaling. Compared to ROCK1's roles in peripheral tissues, we also describe contradictory functions of ROCK1 in the hypothalamus to increase energy expenditure and decrease food intake *via* leptin signaling. Furthermore, dysregulated ROCK1 activity in either of these tissues results in metabolic disease phenotypes. Overall, tissue-specific approaches have made great strides in deciphering the many critical metabolic functions of ROCK1 and, ultimately, may facilitate the development of novel treatments for metabolic disorders.

Keywords: Rho-kinase, metabolism, energy balance, glucose metabolism, lipid metabolism

OPEN ACCESS

Edited by:
Lee E. Eiden,
National Institutes of Health (NIH), United States

Reviewed by:
Klaas Poelstra,
University of Groningen, Netherlands
Jin Kwon Jeong,
George Washington University, United States

***Correspondence:**
Hu Huang
huangh@ecu.edu

Specialty section:
This article was submitted to Neuroendocrine Science, a section of the journal Frontiers in Endocrinology

Received: *28 October 2020*
Accepted: *22 December 2020*
Published: *09 February 2021*

Citation:
Landry T, Shookster D and Huang H (2021) Tissue-Specific Approaches Reveal Diverse Metabolic Functions of Rho-Kinase 1. Front. Endocrinol. 11:622581. doi: 10.3389/fendo.2020.622581

INTRODUCTION

Rho-kinase (ROCK) belongs to the protein kinase A/G/C (AGC) subfamily of serine/threonine protein kinases and is a major downstream effector of small GTPase RhoA (1). The two ROCK isoforms, ROCK1 and ROCK2, each contain a kinase domain at its N-terminus, a central coiled-coil domain, and a pleckstrin-homology domain split by a cysteine-rich region at its

C-terminus (2–4). ROCK1 and ROCK2 share 65% amino acid homology and have been implicated in a variety of cellular functions, including smooth-muscle contraction and actin cytoskeleton arrangement; however, these isoforms also perform independent functions due to differences in their structure, subcellular localization, and gene distribution (5, 6). For example, ROCK1 has uniquely been identified as an important regulator of energy balance and substrate metabolism. Pharmacological ROCK1 inhibitors, like Y-27632 and fasudil (HA1077), have been valuable to elucidating ROCK1's diverse metabolic roles (7–12); however, both these compounds have varying selectivity to also inhibit ROCK2 and other AGC kinase subfamily members. The nonspecific and systemic effects of these inhibitors make interpretation of studies in which they are used challenging (13); therefore, alternative approaches to investigating ROCK1 function are required to understand its tissue-specific metabolic functions.

In this article, we review the physiological roles of ROCK1 in the regulation of energy balance and substrate utilization. We describe novel insights into ROCK1's tissue-specific functions facilitated by recent technological advances and highlight prominent roles in liver, adipose, skeletal muscle, and hypothalamus. Furthermore, emerging evidence suggests ROCK1 is a molecular mediator underlying the pathogenesis of diabetes and obesity.

ROCK1 IN LIVER

Hepatic ROCK1 Overactivity Is Associated With Metabolic Disease States-

To date, the most well-documented metabolic roles of ROCK1 are observed in liver, with clear connections demonstrated between hepatic ROCK1 overactivity and humans or rodents with metabolic disorders (14–21). For example, in humans, liver ROCK1 protein content positively correlates with BMI, liver triglycerides (TG's), and markers of liver damage including alanine transaminase and aspartate transaminase (14). Moreover, elevated hepatic ROCK1 activity has consistently been observed in a plethora of models of disordered metabolism including: humans with fatty liver disease (14), DIO mice (14), db/db mice (14), ob/ob mice (14), TNFα-treated hepatocytes (15), endothelial nitric oxide synthase (eNOS) deficient mice (16), palmitate-treated hepG2 cells (21), palmitate metabolite lysophosphatidylcholine (LPS) -treated Huh7 cells (20), LPS-treated mice (15), and DIO streptozotocin-treated rats (18). Consequently, ROCK1's role in homeostatic and disordered liver metabolism has been an important subject of investigation.

The causal relationship between hepatic ROCK1 and metabolic disease has been investigated using a constitutively active ROCK1-specific mutant in the liver (L-CA-ROCK1), which increases ROCK1 activity 2-fold (14). In chow-fed L-CA-ROCK1 mice, body weight is normal, however fasting glucose levels and lipogenic gene expression including fatty acid synthase (FAS) and stearoyl-CoA desaturase (SCD1) is elevated. DIO L-CA-ROCK1 mice experience a more striking phenotype, characterized by accelerated obesity, insulin resistance, hepatic steatosis, hyperglycemia, and dyslipidemia. These mice also have decreased thermogenic gene expression indicated by decreased peroxisome proliferator-activated receptor gamma coactivator 1-alpha (PGC1α) and uncoupling protein 1 (UCP1) mRNA in brown adipose tissue (BAT) and/or white adipose tissue (WAT). Overall, the L-CA-ROCK1 phenotype demonstrates a possible causal role of hepatic ROCK1 overactivity in metabolic disease pathologies, identifying a potential therapeutic target in liver ROCK1 to treat obesity and diabetes.

Inhibition of Liver ROCK1 Protects Against Metabolic Disease Pathologies-

Several studies have investigated the therapeutic potential of genetically or chemically inhibiting ROCK1 in various models of disordered liver metabolism (14–17, 20). One mouse model of liver ROCK1-deficiency (L-ROCK1$^{-/-}$), in which hepatic ROCK1 activity was specifically knocked down 80%, resulted in significant protection from DIO and related comorbidities (14). In chow-fed L-ROCK1$^{-/-}$ mice, there are no differences in body weight, body composition, or food intake; however, in DIO L-ROCK1$^{-/-}$ mice, body weight and adiposity are reduced, at least in part, due to elevated energy expenditure and locomotor activity. Increases in energy expenditure may be due to augmented thermogenic gene expression in BAT (PGC1α, UCP1, COX7a1, COX8b, and ELOVL3) and WAT (COX8b) (14).

ROCK1 inhibition also improves insulin sensitivity, glucose clearance, fatty liver, and circulating lipid levels (14–17, 22). Chow-fed, DIO, and db/db L-ROCK1$^{-/-}$ mice experience improved glucose clearance and insulin sensitivity, as well as decreased liver weight, TG's, and cholesterol content (14). Supporting these findings, Y-27632 treatment in primary mouse hepatocytes abolishes TNFα-induced insulin resistance (15). L-ROCK1$^{-/-}$ mice also have decreased lipogenic gene expression (FAS, SCD1, SREBP1c, and ELOVL2), despite no observed differences in gene expression involved glucose metabolism (14). Overall, studies have observed encouraging therapeutic potential of liver-specific ROCK1 inhibition in metabolic disease models, demonstrated by increased energy expenditure, improved insulin sensitivity, and attenuated lipid accumulation. These results underscore the value of determining the molecular mechanisms underlying ROCK1 function to further understand the pathology of diabetes and obesity.

Hepatic ROCK1 Negatively Regulates AMPK Activity-

The effects of ROCK1 inhibition on energy balance and lipid metabolism are abolished in AMPKα2$^{-/-}$ mice, suggesting a mechanistic relationship between liver ROCK1 and AMPK in metabolic regulation (16, 17). Hepatic ROCK1 decreases phosphorylation (thr172) and activity of AMPK, which is the proposed mechanism through which ROCK1 increases gene expression and decreases phosphorylation of ACC^{ser79} and

SREBP1^{ser372} to increase lipogenesis (14, 16, 17). Interestingly, therapeutic agents metformin and paeoniflorin target hepatic ROCK1/AMPK signaling to improve steatosis and dyslipidemia in DIO mice (14) and palmitate treated HepG2 cells, respectively (21). In summary, hepatic ROCK1 appears to have a prominent role in promoting lipogenesis *via* suppression of AMPK activity and subsequent elevations in AMPK's downstream targets SREBP1c and ACC. At this time, the upstream molecular mediators of ROCK1 pathologies are less clear, but a recent study determining TNFα stimulates NF-κB to activate hepatic ROCK1 in primary hepatocytes and LPS-treated mice may suggest the involvement of inflammatory pathways.

Interestingly, the ability of hepatic ROCK1 inhibition to improve glucose metabolism was found to be AMPKα2 independent, suggesting an alternative, not yet discovered mechanism (14, 16, 17). The role of ROCK1 in the regulation of insulin signaling is complex and tissue specific, with some studies reporting ROCK1 directly reduces phosphorylation of the tyrosine^{612} residue (23, 24) and induces phosphorylation of the serine$^{632/635}$ residues (25, 26) on insulin receptor substrate 1 (IRS1). Consequently, ROCK1 activity has been associated with impaired insulin signaling in smooth muscle (23, 27), fibroblasts (28), adipose tissue (24), heart (29, 30), and leukocytes (31). Conversely, some studies observe ROCK1 to facilitate glucose uptake in adipocytes (25, 32, 33) and skeletal muscle (25, 33–35). These convoluted results are most likely due to differences in experimental models and the tissue-specific differences in ROCK1-mediated regulation of insulin signaling should be considered when developing therapeutic agents.

ROCK1 AND ADIPOSE TISSUE

Adipocyte-Specific ROCK1 Inhibition Is Therapeutic in Models of Metabolic Disease-

ROCK1 activity is elevated in the adipose tissue of DIO and db/db mice, and adipocyte-specific inhibition of ROCK1 rescues many metabolic disease pathologies (24, 36). While adipose-specific ROCK1 disruption by 50% has no obvious phenotype in healthy mice (24), DIO mice experience improved insulin sensitivity and glucose clearance, despite no changes in adipogenesis, energy balance, or inflammation (24). The benefits are even greater when adipocyte-specific ROCK1 activity is reduced by ~83% (36), resulting in attenuated HFD-induced weight gain and improved insulin sensitivity independent of body weight changes. Furthermore, fasting insulin, fasting glucose, FFA's, adipocyte growth, and macrophage infiltration are all reduced. Despite this encouraging therapeutic potential, the mechanisms underlying ROCK1-mediated adipose pathologies remain relatively unexplored.

ROCK1 Is Critical to Adipose Insulin Signaling-

Despite the glucose-lowering effects of ROCK1 inhibition in mouse models of metabolic disease (24, 36), ROCK1 inhibition in cultured adipocytes impairs insulin-stimulated glucose uptake (25, 32, 33). ROCK1 activity is critical to insulin-stimulated phosphorylation of IRS1$^{ser632/635}$ and PI3kinase activity (25, 32). Interestingly, insulin directly stimulates rho membrane translocation *via* PI3kinase in adipocytes (37), and PI3kinase inhibition abolishes ROCK1-mediated glucose transport (33). This suggests a circuitous, poorly understood, regulatory mechanism of insulin signaling, in which ROCK1 is both downstream and upstream of PI3kinase. Overall, ROCK1's role in insulin signaling is complex, and the opposing effects of adipocyte-specific ROCK1 inhibition in healthy vs. pathological models, indicates an importance of basal ROCK1 activity to glucose homeostasis but also implicates its overactivity in metabolic disease pathologies.

Adipose ROCK1 Is Involved in Adipocyte Differentiation and Lipid Metabolism-

Studies utilizing primary human and rodent adipocytes have revealed ROCK1 also regulates adipocyte differentiation and storage. For example, silencing of the ROCK1 antagonist "deleted in liver cancer 1" in both white and brown cultured adipocytes, and subsequent overactivation of ROCK1, results in decreased adipocyte differentiation, lipid accumulation, and adipogenic gene expression (fatty acid binding protein 4; FABP4 and adiponectin) (38, 39). Additional impairments in thermogenic (UCP1 and ELOVL3) and mitochondrial (cox7a1 and cox5b) gene expression are observed in BAT, as well as reduced mitochondrial respiration (38). Increased ROCK1 activity in cultured human adipocytes has also been shown to impair lipolysis and reduce protein levels of phosphorylated hormone sensitive lipase^{ser660} and adipose TG lipase (40). Overall, while these studies lack in-depth mechanistic insight, their findings suggest adipose ROCK1 is a physiological negative regulator of adipogenesis, lipolysis, and thermogenesis.

ROCK1 AND SKELETAL MUSCLE METABOLISM

Skeletal Muscle ROCK1 Overactivity Is Associated With Metabolic Disease States-

Similar to adipose and liver, skeletal muscle ROCK1 expression and activity are elevated in rodent models of metabolic disease (26, 41–43). Conversely, one study observed no differences in basal vastus lateralis (VL) ROCK1 protein expression or activity between obese and lean humans (35), highlighting the importance of considering potential differences between rodent and human ROCK1 function. Further supporting the hypothesis that overactive ROCK1 is involved in metabolic disease pathologies, at least in mice, constitutively active skeletal muscle-specific ROCK1 (SM-CA-ROCK1) results in early-onset obesity, even when eating a normal diet (44). These mice exhibit reduced physical activity, decreased energy expenditure, impaired glucose clearance and insulin sensitivity, elevated fasting TG's and cholesterol, and increased respiratory

exchange ratio suggesting decreased fat utilization. They also experience decreased thermogenic gene expression in BAT and WAT, as well as reduced mitochondrial size and content specifically in Type I muscle fibers. Lastly, myogenic gene expression is altered in these mice including reduced irisin and IL13 mRNA by 60% and 25%, respectively.

Skeletal Muscle ROCK1 Paradoxically Regulates Insulin Signaling-

The metabolic dysfunctions of SM-CA-ROCK1 mice may be due to impaired insulin signaling (41, 42). Lipid-induced geranylgeranyl diphosphate synthase 1 (GGPPS), a branchpoint enzyme in the mevalonate pathway involved in cholesterol synthesis, activates RhoA/ROCK1 signaling in muscle, which then increases inhibitory phosphorylation of $IRS1^{ser307}$ to inhibit downstream signaling (41). This phenomenon is rescued in muscle-specific GGPPS knockout mice, as is insulin sensitivity and glucose homeostasis (41). ROCK1 also activates phosphatase and tensin homolog to inhibit phosphorylation of AKT in cultured myotubes, providing another mechanism for ROCK1-mediated negative regulation of insulin signaling (43). Interestingly, in L6 myotubes, insulin inhibits ROCK1 to promote AMPK2α activity and subsequently inhibit the lipogenic transcription factor SREBP-1c (42). This suggests a mechanism in which insulin may inhibit ROCK1 activity to prevent inhibitory IRS1 phosphorylation and ultimately facilitate downstream insulin signaling.

The association between skeletal muscle ROCK1 and metabolic dysfunction has been well-documented in animal models; however, much like ROCK1 in adipose tissue, basal ROCK1 activity may be essential to skeletal muscle glucose uptake. In humans, VL ROCK1 activity positively correlates with glucose disposal in lean subjects, while insulin-stimulated ROCK1 activity is impaired in those with diabetes or obesity, possibly due to elevated levels of the ROCK1 antagonist RhoE (35). Furthermore, systemic ROCK1 knockout impairs skeletal muscle insulin signaling, and ROCK1 suppression in myoblasts blunts glucose uptake in a PI3kinase-dependent manner (25, 33, 34). Overall, ROCK1-modulated glucose uptake in skeletal muscle is similarly paradoxical to its role in adipose tissue, both regarding mechanisms and complexity (Section 3.2) (25, 33).

SUMMARY OF ROCK1 IN PERIPHERAL TISSUES

To date, similar metabolic roles of ROCK1 have been identified in liver, skeletal muscle, and adipose tissue. ROCK1 in peripheral tissues inhibits AMPK2α, which results in changes in gene expression and downstream phosphorylation events to ultimately decrease energy expenditure and increase lipogenesis. ROCK1 also interferes with insulin signaling to increase blood glucose levels and ROCK1 overactivity is associated with metabolic disease states and related comorbidities including obesity, insulin resistance, and dyslipidemia. Despite this, increasing evidence suggests basal ROCK1 activity is also paradoxically essential to glucose disposal and insulin/PI3kinase signaling (**Figure 1**). Overall homeostatic ROCK1 function in peripheral tissues appears to be critical to metabolic health and future studies should focus on the differences between healthy and pathological ROCK1 activity.

ROCK1 IN THE CENTRAL NERVOUS SYSTEM (CNS)

Hypothalamic ROCK1 Regulates Metabolism-

Unlike liver, adipose, and skeletal muscle, ROCK1 activity in the hypothalamus is reduced in db/db and DIO mice (45). Furthermore, hypothalamic ROCK1 knockout in healthy mice results in excessive food intake, dyslipidemia, and obesity, while ROCK1 overexpression has opposite effects (45, 46). One study observed fasudil treatment to increase food intake and gene expression of the orexigenic neuropeptide, neuropeptide Y, which is predominantly expressed in the arcuate nucleus of the hypothalamus (ARC) (47). Considering this, studies have identified novel roles for hypothalamic ROCK1 to regulate energy balance *via* ARC neuron populations.

ROCK1 Regulates ARC Neurons-

The ARC, located in the medio-basal hypothalamus, contains both the orexigenic neuropeptide Y/agouti-related peptide (NPY/AgRP) -expressing and the anorexic proopiomelanocortin-expressing neuron populations (48–50). Disruption of ROCK1 in either of these neuron populations results in disordered neuronal activity and metabolism (45, 46). For example, deletion of ROCK1 in NPY/AgRP neurons results in increased NPY/AgRP activity and accelerated weight gain in chow-fed and DIO mice. These mice exhibit decreased resting energy expenditure and locomotor activity with increased serum TG's (45, 46). Similarly, ROCK1 deletion in POMC neurons leads to POMC hypoactivity and obesity due to reduced locomotor activity, while whole-ARC ROCK1 deletion has even greater effects (46).

Tyrosine hydroxylase is the rate-limiting enzyme in dopamine synthesis (51), and activation of tyrosine hydroxylase-expressing (TH) neurons in the ARC has recently been shown to increase food intake and body weight (52). While RhoA deletion in TH neurons (RhoA-$TH^{-/-}$) has no effects on energy balance in chow-fed mice, DIO RhoA-$TH^{-/-}$ mice experience accelerated weight gain and adiposity due to increased food intake, despite no differences in energy expenditure or glucose regulation (53). Additionally, hypothalamic NPY and AgRP mRNA is elevated in RhoA-$TH^{-/-}$ mice, suggesting RhoA/ROCK1 in TH neurons likely regulates other post-synaptic neuron populations as well (53). Overall, studies in the hypothalamus highlight a prominent role for ROCK1 to regulate ARC neurons involved in metabolic regulation; however, nonspecific ROCK1 knockdown in the

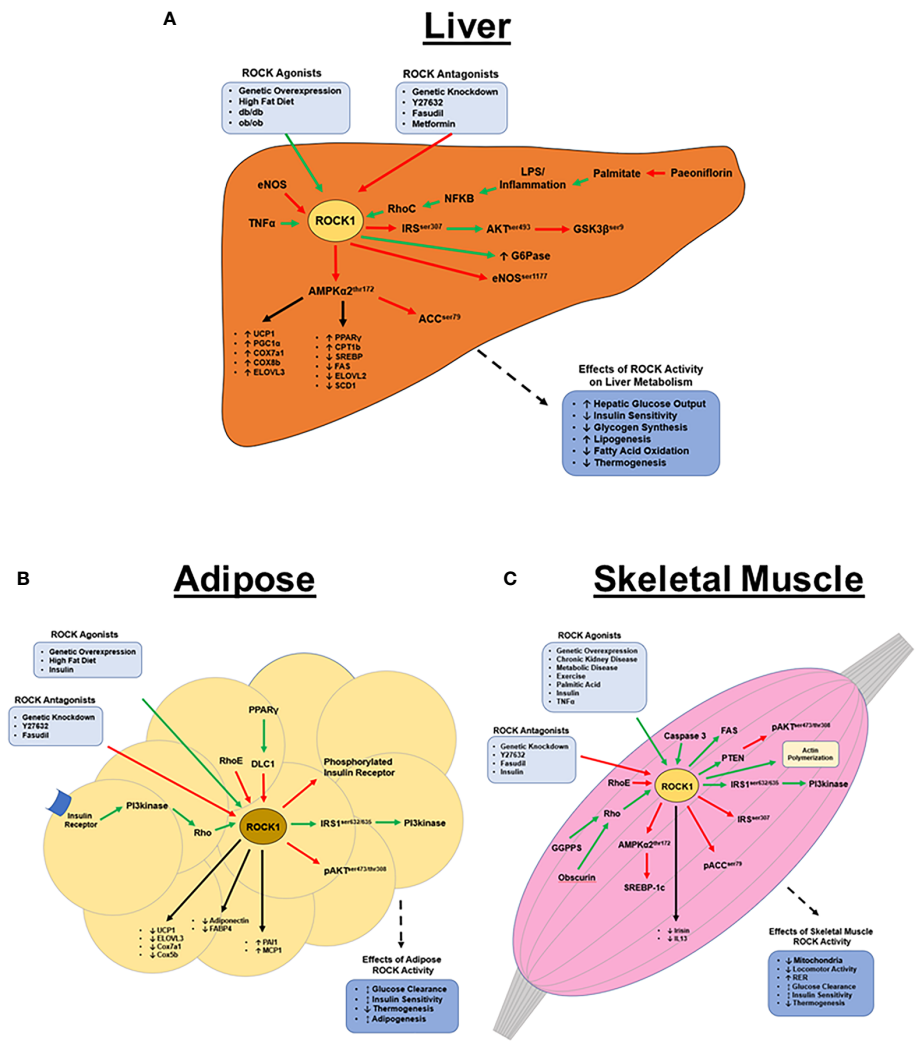

FIGURE 1 | ROCK1's metabolic functions in peripheral tissues. **(A)** Hepatic ROCK1 overactivity is associated with disordered metabolic regulation; conversely, downregulation of ROCK1 is therapeutic in metabolic disease models. ROCK1 primarily regulates lipid metabolism and thermogenesis *via* AMPK signaling, however the mechanisms underlying ROCK1's role in insulin signaling remain unclear. The pathophysiology of ROCK1 overactivity in metabolic disease is poorly understood, however sustained inflammation and subsequent NF-κB signaling may be an upstream ROCK1 agonist. **(B)** Basal adipose ROCK1 activity is critical to homeostatic glucose metabolism; however, overactivity of ROCK1 is associated with metabolic disease phenotypes. ROCK1 is a negative regulator of thermogenic, adipogenic, and mitochondrial gene expression. Mechanistically, insulin and PI3kinase signaling are upstream activators of ROCK, while RhoE and DLC1 are antagonists. Downstream of ROCK1 includes a paradoxical insulin signaling mechanism, where ROCK1 activates IRS1 and PI3kinase, but also attenuates activation of insulin receptor and AKT. **(C)** Similar to in adipose, ROCK1 paradoxically regulates glucose metabolism in skeletal muscle. Basal ROCK1 function is critical to glucose regulation, but overactivity is associated with metabolic disease. ROCK1 regulates metabolism in skeletal muscle by downregulating AMPK, ACC, and AKT signaling, but also activates PI3kinase, FAS, and SREBP-1c. (Green arrows indicate activation; red arrows indicate inhibition; black arrows indicate regulation of gene expression).

hypothalamus results in a much more robust metabolic phenotype (45, 46, 53). Thus, ROCK1 likely regulates other, currently unidentified, neuron populations, in addition to NPY/AgRP, POMC, and TH neurons.

ROCK1 Facilitates Hypothalamic Leptin Signaling-

Leptin is a potent adipokine that regulates ARC neurons to increase energy expenditure and suppress food intake (48, 53, 54). Deficiency in leptin, its receptor (LepR), or its downstream signaling results in hyperphagia, hyperglycemia, and obesity (48, 55). Interestingly, RhoA or ROCK1 deletion in NPY/AgRP, POMC, or TH neurons impairs leptin-mediated signaling and regulation of these respective neurons (45, 46, 53). Furthermore, hyper-leptinemia is observed in hypothalamic ROCK1 knockout mice, suggesting the involvement of ROCK1 in the development of leptin resistance seen in metabolic disease states (45, 46, 56).

Considering the strong association between ROCK1 and leptin activity, ROCK1 has been identified as a cell signaling molecule directly involved in LepR action. Following leptin binding to LepR, ROCK1 phosphorylates JAK2, which stimulates dimerization and phosphorylation of STAT3 (46). Phosphorylated STAT3 stimulates nuclear translocation and transcription of target genes, including POMC and signal of cytokine signaling 3 (SOCS3), each of which act to maintain energy homeostasis (57, 58). In addition to this leptin➔ROCK1➔JAK2➔STAT3 signaling mechanism, ROCK1 likely functions *via* other signaling pathways as well. For example, RhoA deletion in TH neurons also increases sensitivity to the hunger-inducing hormone ghrelin through unknown mechanisms (53). Insulin also modulates NPY/AgRP and POMC neurons and, like in peripheral tissues, may also facilitate hypothalamic ROCK1 function (54, 59–61).

Summary of ROCK1 in the CNS-

In summary, hypothalamic ROCK1 regulates various neuron populations, including NPY/AgRP, POMC, and TH neurons, to decrease food intake and increase energy expenditure, with no obvious effects on glucose metabolism. Mechanistically, ROCK1 directly mediates leptin signaling and impairs ghrelin signaling through unknown mechanisms and the importance of these functions is underscored by obesity manifesting when hypothalamic ROCK1 function is impaired (**Figure 2**). The seemingly conflicting functions of central and peripheral ROCK1 are teleologically perplexing, and the reasons for these

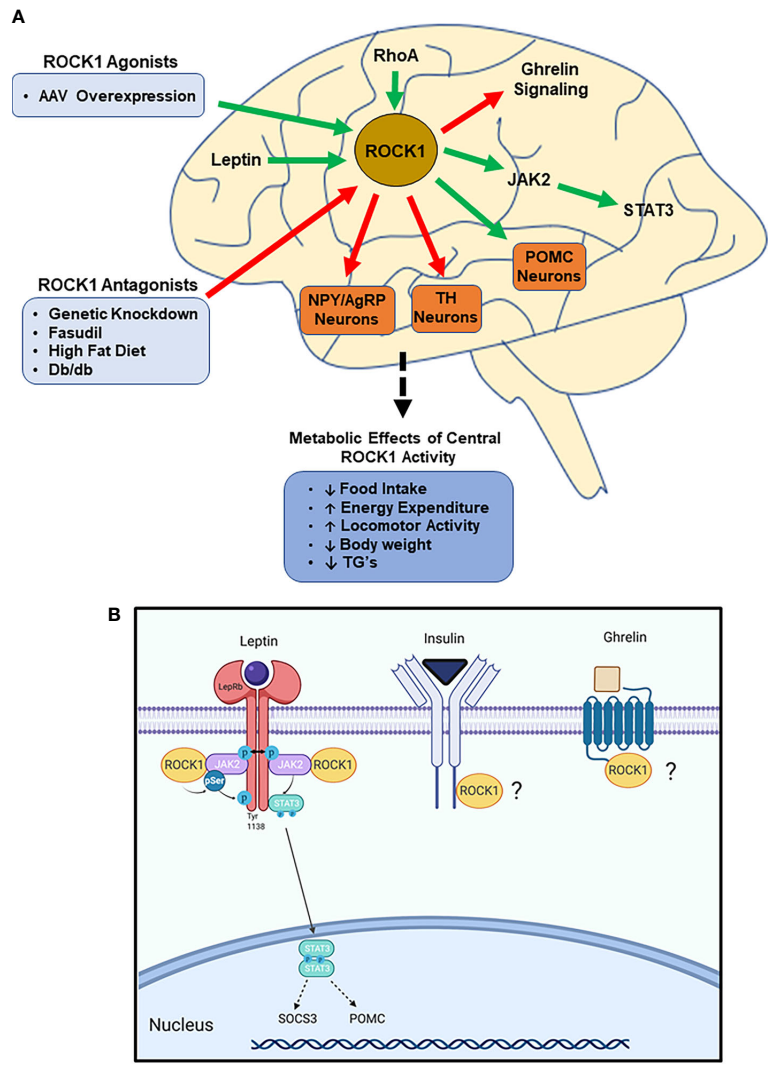

FIGURE 2 | ROCK1 is critical to central nervous system (CNS)-mediated regulation of energy homeostasis. **(A)** Impaired ROCK1 activity in the hypothalamus is associated with disordered energy homeostasis. ROCK1 inhibits NPY/AgRP and TH neurons, while stimulating POMC neurons. Mechanistically, ROCK1 facilitates leptin signaling and attenuates ghrelin signaling. (Green arrows indicate activation; red arrows indicate inhibition). **(B)** Following leptin binding to LepR, ROCK1 phosphorylates JAK2, which stimulates dimerization and phosphorylation of STAT3. Subsequent STAT3 nuclear translocation elicits transcriptional changes including increased POMC and SOCS3 mRNA. Other potential mediators of hypothalamic ROCK1 action may be ghrelin and insulin receptor signaling.

differences are unclear. Despite this. the various tissue-specific models described in this review cumulatively indicate both hypo- and hyper-ROCK1 activity have drastic metabolic effects, clearly demonstrating the critical nature of maintaining homeostatic ROCK1 function.

CONCLUDING REMARKS

Many studies have used chemical inhibitors and whole-body genetic manipulation to identify ROCK1 as a prominent homeostatic regulator of diverse metabolic functions; however, these studies are limited in their isoform and tissue-specific insight. Recently, technological advances have facilitated development of novel models utilizing tissue-specific approaches, which have greatly enhanced our understanding of ROCK1's functions. These studies have observed critical functions for ROCK1 in various metabolic tissues, including tissue-specific action in liver, adipose tissue, skeletal muscle, and hypothalamus to regulate food intake, thermogenesis, locomotor activity, glucose metabolism, and/or lipid metabolism. The molecular mechanisms underlying these functions are complex, underscored by disease states manifesting in response to ROCK1 overactivity, despite basal ROCK1 activity being critical to homeostatic maintenance of many physiological functions. Additionally, elevated ROCK1 activity consistently is associated with various metabolic disease states, suggesting ROCK1 may be useful as a preclinical marker of diabetes and obesity. Nonspecific ROCK1 inhibitors fasudil and Y-27632 demonstrate inhibitor pharmacotherapy is beneficial for these diseases; however, adverse effects such as hypotension, insulin resistance, and obesity are observed when ROCK expression/activity is non-specifically altered or systemically downregulated (25, 32–35, 62, 63). This once again highlights the importance of tissue-specific targeting of ROCK1, for example, *via* mannose-6-phosphate carriers (62, 64, 65), vitamin-A-coupled lysosomes (66), or genetic engineering. Overall, these tissue-specific approaches will greatly facilitate deciphering the many critical metabolic functions of ROCK1 and, ultimately, may result in the development of novel treatments for metabolic 2974disorders.

AUTHOR CONTRIBUTIONS

TL and DS wrote this manuscript. HH supervised and edited the manuscript. All authors contributed to the article and approved the submitted version.

REFERENCES

1. Matsui T, Amano M, Yamamoto T, Chihara K, Nakafuku M, Ito M, et al. Rho-associated kinase, a novel serine/threonine kinase, as a putative target for small GTP binding protein Rho. *EMBO J* (1996) 15:2208–16. doi: 10.1002/j.1460-2075.1996.tb00574.x
2. Nakagawa O, Fujisawa K, Ishizaki T, Saito Y, Nakao K, Narumiya S. ROCK-I and ROCK-II, two isoforms of Rho-associated coiled-coil forming protein serine/threonine kinase in mice. *FEBS Lett* (1996) 392:189–93. doi: 10.1016/0014-5793(96)00811-3
3. Ishizaki T, Maekawa M, Fujisawa K, Okawa K, Iwamatsu A, Fujita A, et al. The small GTP-binding protein Rho binds to and activates a 160 kDa Ser/Thr protein kinase homologous to myotonic dystrophy kinase. *EMBO J* (1996) 15:1885–93. doi: 10.1002/j.1460-2075.1996.tb00539.x
4. Leung T, Manser E, Tan L, Lim L. A novel serine/threonine kinase binding the Ras-related RhoA GTPase which translocates the kinase to peripheral membranes. *J Biol Chem* (1995) 270:29051–4. doi: 10.1074/JBC.270.49.29051
5. Amano M, Fukata Y, Kaibuchi K. Regulation and Functions of Rho-Associated Kinase. *Exp Cell Res* (2000) 261:44–51. doi: 10.1006/excr.2000.5046
6. Riento K, Ridley AJ. ROCKs: multifunctional kinases in cell behaviour. *Nat Rev Mol Cell Biol* (2003) 4:446–56. doi: 10.1038/nrm1128
7. Vicari RM, Chaitman B, Keefe D, Smith WB, Chrysant SG, Tonkon MJ, et al. Efficacy and Safety of Fasudil in Patients With Stable Angina. *J Am Coll Cardiol* (2005) 46:1803–11. doi: 10.1016/j.jacc.2005.07.047
8. Liao JK, Seto M, Noma K. Rho Kinase (ROCK) Inhibitors. *J Cardiovasc Pharmacol* (2007) 50:17–24. doi: 10.1097/FJC.0b013e318070d1bd
9. Narumiya S, Ishizaki T, Uehata M. Use and properties of ROCK-specific inhibitor Y-27632. *Methods Enzymol* (2000) 325:273–84. doi: 10.1016/s0076-6879(00)25449-9
10. Ono-Saito N, Niki I, Hidaka H. H-Series Protein Kinase Inhibitors and Potential Clinical Applications. *Pharmacol Ther* (1999) 82:123–31. doi: 10.1016/S0163-7258(98)00070-9
11. Hirooka Y, Shimokawa H. Therapeutic Potential of Rho-Kinase Inhibitors in Cardiovascular Diseases. *Am J Cardiovasc Drugs* (2005) 5:31–9. doi: 10.2165/00129784-200505010-00005
12. Hu E, Lee D. Rho kinase as potential therapeutic target for cardiovascular diseases: opportunities and challenges. *Expert Opin Ther Targ* (2005) 9:715–36. doi: 10.1517/14728222.9.4.715
13. Tamura M, Nakao H, Yoshizaki H, Shiratsuchi M, Shigyo H, Yamada H, et al. Development of specific Rho-kinase inhibitors and their clinical application. *Biochim Biophys Acta Proteins Proteom* (2005) 1754:245–52. doi: 10.1016/J.BBAPAP.2005.06.015
14. Huang H, Lee S-H, Sousa-Lima I, Kim SS, Hwang WM, Dagon Y, et al. Rho-kinase/AMPK axis regulates hepatic lipogenesis during overnutrition. *J Clin Invest* (2018) 128:5335–50. doi: 10.1172/JCI63562
15. Okin D, Medzhitov R. The Effect of Sustained Inflammation on Hepatic Mevalonate Pathway Results in Hyperglycemia. *Cell* (2016) 165:343–56. doi: 10.1016/J.CELL.2016.02.023
16. Noda K, Godo S, Saito H, Tsutsui M, Shimokawa H. Opposing Roles of Nitric Oxide and Rho-Kinase in Lipid Metabolism in Mice. *Tohoku J Exp Med* (2015) 235:171–83. doi: 10.1620/tjem.235.171
17. Noda K, Nakajima S, Godo S, Saito H, Ikeda S, Shimizu T, et al. Rho-Kinase Inhibition Ameliorates Metabolic Disorders through Activation of AMPK Pathway in Mice. *PloS One* (2014) 9:e110446. doi: 10.1371/journal.pone.0110446
18. Gupta J, Gaikwad AB, Tikoo K. Hepatic expression profiling shows involvement of PKC epsilon, DGK eta, Tnfaip, and Rho kinase in type 2 diabetic nephropathy rats. *J Cell Biochem* (2010) 111:944–54. doi: 10.1002/jcb.22783
19. Zhou H, Fang C, Zhang L, Deng Y, Wang M, Meng F. Fasudil hydrochloride hydrate, a Rho-kinase inhibitor, ameliorates hepatic fibrosis in rats with type 2 diabetes. *Chin Med J (Engl)* (2014) 127:225–31. doi: 10.3760/cma.j.issn.0366-6999.20131917
20. Hirsova P, Ibrahim SH, Krishnan A, Verma VK, Bronk SF, Werneburg NW, et al. Lipid-Induced Signaling Causes Release of Inflammatory Extracellular Vesicles From Hepatocytes. *Gastroenterology* (2016) 150:956–67. doi: 10.1053/j.gastro.2015.12.037
21. Ma Z, Liu H, Wang W, Guan S, Yi J, Chu L. Paeoniflorin suppresses lipid accumulation and alleviates insulin resistance by regulating the Rho kinase/IRS-1 pathway in palmitate-induced HepG2Cells. *Biomed Pharmacother* (2017) 90:361–7. doi: 10.1016/J.BIOPHA.2017.03.087

22. Ma Z, Zhang J, Ji E, Cao G, Li G, Chu L. Rho kinase inhibition by fasudil exerts antioxidant effects in hypercholesterolemic rats. *Clin Exp Pharmacol Physiol* (2011) 38:688–94. doi: 10.1111/j.1440-1681.2011.05561.x
23. Begum N, Sandu OA, Ito M, Lohmann SM, Smolenski A. Active Rho kinase (ROK-alpha) associates with insulin receptor substrate-1 and inhibits insulin signaling in vascular smooth muscle cells. *J Biol Chem* (2002) 277:6214–22. doi: 10.1074/jbc.M110508200
24. Lee S-H, Huang H, Choi K, Lee DH, Shi J, Liu T, et al. ROCK1 isoform-specific deletion reveals a role for diet-induced insulin resistance. *Am J Physiol Metab* (2014) 306:E332–43. doi: 10.1152/ajpendo.00619.2013
25. Furukawa N, Ongusaha P, Jahng WJ, Araki K, Choi CS, Kim H-J, et al. Role of Rho-kinase in regulation of insulin action and glucose homeostasis. *Cell Metab* (2005) 2:119–29. doi: 10.1016/J.CMET.2005.06.011
26. Kanda T, Wakino S, Homma K, Yoshioka K, Tatematsu S, Hasegawa K, et al. Rho-kinase as a molecular target for insulin resistance and hypertension. *FASEB J* (2006) 20:169–71. doi: 10.1096/fj.05-4197fje
27. Song P, Zhang M, Wang S, Xu J, Choi HC, Zou M-H. Thromboxane A_2 Receptor Activates a Rho-associated Kinase/LKB1/PTEN Pathway to Attenuate Endothelium Insulin Signaling. *J Biol Chem* (2009) 284:17120–8. doi: 10.1074/jbc.M109.012583
28. Sordella R, Classon M, Hu K-Q, Matheson SF, Brouns MR, Fine B, et al. Modulation of CREB Activity by the Rho GTPase Regulates Cell and Organism Size during Mouse Embryonic Development. *Dev Cell* (2002) 2:553–65. doi: 10.1016/S1534-5807(02)00162-4
29. Lin G, Craig G, Zhang L, Yuen V, Allard M, Mcneill J, et al. Acute inhibition of Rho-kinase improves cardiac contractile function in streptozotocin-diabetic rats. *Cardiovasc Res* (2007) 75:51–8. doi: 10.1016/j.cardiores.2007.03.009
30. Wingard C, Fulton D, Husain S. Altered Penile Vascular Reactivity and Erection in the Zucker Obese-Diabetic Rat. *J Sex Med* (2007) 4:348–63. doi: 10.1111/j.1743-6109.2007.00439.x
31. Liu P-Y, Chen J-H, Lin L-J, Liao JK. Increased Rho kinase activity in a Taiwanese population with metabolic syndrome. *J Am Coll Cardiol* (2007) 49:1619–24. doi: 10.1016/j.jacc.2006.12.043
32. Standaert M, Bandyopadhyay G, Galloway L, Ono Y, Mukai H, Farese R. Comparative effects of GTPgammaS and insulin on the activation of Rho, phosphatidylinositol 3-kinase, and protein kinase N in rat adipocytes. Relationship to glucose transport. *J Biol Chem* (1998) 273:7470–7. doi: 10.1074/jbc.273.13.7470
33. Chun K-H, Araki K, Jee Y, Lee D-H, Oh B-C, Huang H, et al. Regulation of Glucose Transport by ROCK1 Differs from That of ROCK2 and Is Controlled by Actin Polymerization. *Endocrinology* (2012) 153:1649–62. doi: 10.1210/en.2011-1036
34. Lee DH, Shi J, Jeoung NH, Kim MS, Zabolotny JM, Lee SW, et al. Targeted disruption of ROCK1 causes insulin resistance in vivo. *J Biol Chem* (2009) 284:11776–80. doi: 10.1074/jbc.C900014200
35. Chun K-H, Choi K-D, Lee D-H, Jung Y, Henry RR, Ciaraldi TP, et al. In vivo activation of ROCK1 by insulin is impaired in skeletal muscle of humans with type 2 diabetes. *Am J Physiol Metab* (2011) 300:E536–42. doi: 10.1152/ajpendo.00538.2010
36. Hara Y, Wakino S, Tanabe Y, Saito M, Tokuyama H, Washida N, et al. Rho and Rho-kinase activity in adipocytes contributes to a vicious cycle in obesity that may involve mechanical stretch. *Sci Signal* (2011) 4:ra3–3. doi: 10.1126/scisignal.2001227
37. Karnam P, Standaert ML, Galloway L, Farese RV. Activation and translocation of Rho (and ADP ribosylation factor) by insulin in rat adipocytes. Apparent involvement of phosphatidylinositol 3-kinase. *J Biol Chem* (1997) 272:6136–40. doi: 10.1074/JBC.272.10.6136
38. Sim CK, Kim S-Y, Brunmeir R, Zhang Q, Li H, Dharmasegaran D, et al. Regulation of white and brown adipocyte differentiation by RhoGAP DLC1. *PloS One* (2017) 12:e0174761. doi: 10.1371/journal.pone.0174761
39. Takahashi N, Nobusue H, Shimizu T, Sugihara E, Yamaguchi-Iwai S, Onishi N, et al. ROCK inhibition induces terminal adipocyte differentiation and suppresses tumorigenesis in chemoresistant osteosarcoma cells. *Cancer Res* (2019) 79:3088–99. doi: 10.1158/0008-5472.CAN-18-2693
40. Dankel SN, Røst TH, Kulyté A, Fandalyuk Z, Skurk T, Hauner H, et al. The Rho GTPase RND3 regulates adipocyte lipolysis. *Metabolism* (2019) 101:153999. doi: 10.1016/j.metabol.2019.153999
41. Tao W, Wu J, Xie BX, Zhao YY, Shen N, Jiang S, et al. Lipid-induced muscle insulin resistance is mediated by GGPPS via modulation of the RhoA/Rho kinase signaling pathway. *J Biol Chem* (2015) 290:20086–97. doi: 10.1074/jbc.M115.657742
42. Tang S, Wu W, Tang W, Ge Z, Wang H, Hong T, et al. Suppression of Rho-kinase 1 is responsible for insulin regulation of the AMPK/SREBP-1c pathway in skeletal muscle cells exposed to palmitate. *Acta Diabetol* (2017) 54:635–44. doi: 10.1007/s00592-017-0976-z
43. Peng H, Cao J, Yu R, Danesh F, Wang Y, Mitch WE, et al. CKD stimulates muscle protein loss via rho-associated protein kinase 1 activation. *J Am Soc Nephrol* (2016) 27:509–19. doi: 10.1681/ASN.2014121208
44. Zhou X, Li R, Liu X, Wang L, Hui P, Chan L, et al. ROCK1 reduces mitochondrial content and irisin production in muscle suppressing adipocyte browning and impairing insulin sensitivity. *Sci Rep* (2016) 6:1–14. doi: 10.1038/srep29669
45. Huang H, Lee SH, Ye C, Lima IS, Oh B-C, Lowell BB, et al. ROCK1 in AgRP Neurons Regulates Energy Expenditure and Locomotor Activity in Male Mice. *Endocrinology* (2013) 154:3660–70. doi: 10.1210/en.2013-1343
46. Huang H, Kong D, Byun KH, Ye C, Koda S, Lee DH, et al. Rho-kinase regulates energy balance by targeting hypothalamic leptin receptor signaling. *Nat Neurosci* (2012) 15:1391–8. doi: 10.1038/nn.3207
47. Butruille L, Mayeur S, Duparc T, Knauf C, Moitrot E, Fajardy I, et al. Prenatal fasudil exposure alleviates fetal growth but programs hyperphagia and overweight in the adult male rat. *Eur J Pharmacol* (2012) 689:278–84. doi: 10.1016/j.ejphar.2012.05.040
48. Huo L, Gamber K, Greeley S, Silva J, Huntoon N, Leng XH, et al. Leptin-Dependent Control of Glucose Balance and Locomotor Activity by POMC Neurons. *Cell Metab* (2009) 9:537–47. doi: 10.1016/j.cmet.2009.05.003
49. Krashes MJ, Koda S, Ye C, Rogan SC, Adams AC, Cusher DS, et al. Rapid, reversible activation of AgRP neurons drives feeding behavior in mice. *J Clin Invest* (2011) 121:1424–8. doi: 10.1172/JCI46229
50. Morton GJ, Cummings DE, Baskin DG, Barsh GS, Schwartz MW. Central nervous system control of food intake and body weight. *Nature* (2006) 443:289–95. doi: 10.1038/nature05026
51. Daubner SC, Le T, Wang S. Tyrosine hydroxylase and regulation of dopamine synthesis. *Arch Biochem Biophys* (2011) 508:1–12. doi: 10.1016/j.abb.2010.12.017
52. Zhang X, Van Den Pol AN. Hypothalamic arcuate nucleus tyrosine hydroxylase neurons play orexigenic role in energy homeostasis. *Nat Neurosci* (2016) 19:1341–7. doi: 10.1038/nn.4372
53. Skov LJ, Ratner C, Hansen NW, Thompson JJ, Egerod KL, Burm H, et al. RhoA in tyrosine hydroxylase neurones regulates food intake and body weight via altered sensitivity to peripheral hormones. *J Neuroendocrinol* (2019) 31:e12761. doi: 10.1111/jne.12761
54. Varela L, Horvath TL. Leptin and insulin pathways in POMC and AgRP neurons that modulate energy balance and glucose homeostasis. *EMBO Rep* (2012) 13:1079–86. doi: 10.1038/embor.2012.174
55. Cohen P, Zhao C, Cai X, Montez JM, Rohani SC, Feinstein P, et al. Selective deletion of leptin receptor in neurons leads to obesity. *J Clin Invest* (2001) 108:1113–21. doi: 10.1172/JCI13914
56. Frederich RC, Hamann A, Anderson S, Löllmann B, Lowell BB, Flier JS. Leptin levels reflect body lipid content in mice: Evidence for diet-induced resistance to leptin action. *Nat Med* (1995) 1:1311–4. doi: 10.1038/nm1295-1311
57. Gong L, Yao F, Hockman K, Heng HH, Morton GJ, Takeda K, et al. Signal transducer and activator of transcription-3 is required in hypothalamic agouti-related protein/neuropeptide Y neurons for normal energy homeostasis. *Endocrinology* (2008) 149:3346–54. doi: 10.1210/en.2007-0945
58. Xu AW, Ste-Marie L, Kaelin CB, Barsh GS. Inactivation of signal transducer and activator of transcription 3 in proopiomelanocortin (Pomc) neurons causes decreased Pomc expression, mild obesity, and defects in compensatory refeeding. *Endocrinology* (2007) 148:72–80. doi: 10.1210/en.2006-1119
59. Al-Qassab H, Smith MA, Irvine EE, Guillermet-Guibert J, Claret M, Choudhury AI, et al. Dominant Role of the p110β Isoform of PI3K over p110α in Energy Homeostasis Regulation by POMC and AgRP Neurons. *Cell Metab* (2009) 10:343–54. doi: 10.1016/J.CMET.2009.09.008
60. Könner AC, Janoschek R, Plum L, Jordan SD, Rother E, Ma X, et al. Insulin Action in AgRP-Expressing Neurons Is Required for Suppression of Hepatic Glucose Production. *Cell Metab* (2007) 5:438–49. doi: 10.1016/j.cmet.2007.05.004

61. Mayer CM, Belsham DD. Insulin directly regulates NPY and AgRP gene expression via the MAPK MEK/ERK signal transduction pathway in mHypoE-46 hypothalamic neurons. *Mol Cell Endocrinol* (2009) 307:99–108. doi: 10.1016/j.mce.2009.02.031
62. Klein S, Van Beuge MM, Granzow M, Beljaars L, Schierwagen R, Kilic S, et al. HSC-specific inhibition of Rho-kinase reduces portal pressure in cirrhotic rats without major systemic effects. *J Hepatol* (2012) 57:1220–7. doi: 10.1016/J.JHEP.2012.07.033
63. Anegawa G, Kawanaka H, Yoshida D, Konishi K, Yamaguchi S, Kinjo N, et al. Defective endothelial nitric oxide synthase signaling is mediated by rho-kinase activation in rats with secondary biliary cirrhosis. *Hepatology* (2008) 47:966–77. doi: 10.1002/hep.22089
64. Klein S, Frohn F, Magdaleno F, Reker-Smit C, Schierwagen R, Schierwagen I, et al. Rho-kinase inhibitor coupled to peptide-modified albumin carrier reduces portal pressure and increases renal perfusion in cirrhotic rats. *Sci Rep* (2019) 9:2256. doi: 10.1038/s41598-019-38678-5
65. van Beuge MM, Prakash J, Lacombe M, Gosens R, Post E, Reker-Smit C, et al. Reduction of fibrogenesis by selective delivery of a Rho kinase inhibitor to hepatic stellate cells in mice. *J Pharmacol Exp Ther* (2011) 337:628–35. doi: 10.1124/jpet.111.179143
66. Okimoto S, Kuroda S, Tashiro H, Kobayashi T, Taogoshi T, Matsuo H, et al. Vitamin A-coupled liposomal Rho-kinase inhibitor ameliorates liver fibrosis without systemic adverse effects. *Hepatol Res* (2019) 49(6):663–75. doi: 10.1111/hepr.13317

Conflict of Interest: The authors declare that the research was conducted in the absence of any commercial or financial relationships that could be construed as a potential conflict of interest.

frontiers in Neuroscience

ORIGINAL RESEARCH
published: 10 February 2021
doi: 10.3389/fnins.2021.631311

Negative Modulation of the Metabotropic Glutamate Receptor Type 5 as a Potential Therapeutic Strategy in Obesity and Binge-Like Eating Behavior

Tadeu P. D. Oliveira[1†], Bruno D. C. Gonçalves[1†], Bruna S. Oliveira[2], Antonio Carlos P. de Oliveira[1], Helton J. Reis[1], Claudia N. Ferreira[3], Daniele C. Aguiar[1], Aline S. de Miranda[2], Fabiola M. Ribeiro[4], Erica M. L. Vieira[1], András Palotás[5,6] and Luciene B. Vieira[1]**

[1] Departamento de Farmacologia, Instituto de Ciências Biológicas, Universidade Federal de Minas Gerais, Belo Horizonte, Brazil, [2] Departamento de Morfologia, Instituto de Ciências Biológicas, Universidade Federal de Minas Gerais, Belo Horizonte, Brazil, [3] Colégio Técnico, Universidade Federal de Minas Gerais, Belo Horizonte, Brazil, [4] Departamento de Bioquimica e Imunologia, Instituto de Ciências Biológicas, Universidade Federal de Minas Gerais, Belo Horizonte, Brazil, [5] Asklepios-Med (Private Medical Practice and Research Center), Szeged, Hungary, [6] Institute of Fundamental Medicine and Biology, Kazan Federal University, Kazan, Russia

Obesity is a multifactorial disease, which in turn contributes to the onset of comorbidities, such as diabetes and atherosclerosis. Moreover, there are only few options available for treating obesity, and most current pharmacotherapy causes severe adverse effects, while offering minimal weight loss. Literature shows that metabotropic glutamate receptor 5 (mGluR5) modulates central reward pathways. Herein, we evaluated the effect of VU0409106, a negative allosteric modulator (NAM) of mGluR5 in regulating feeding and obesity parameters. Diet-induced obese C57BL/6 mice were treated for 14 days with VU0409106, and food intake, body weight, inflammatory/hormonal levels, and behavioral tests were performed. Our data suggest reduction of feeding, body weight, and adipose tissue inflammation in mice treated with high-fat diet (HFD) after chronic treatment with VU0409106. Furthermore, a negative modulation of mGluR5 also reduces binge-like eating, the most common type of eating disorder. Altogether, our results pointed out mGluR5 as a potential target for treating obesity, as well as related disorders.

Keywords: obesity, mGluR5, high-fat, inflammation, glutamate

OPEN ACCESS

Edited by:
Srinivas Sriramula, East Carolina University, United States

Reviewed by:
Kavaljit Chhabra, University of Rochester, United States
Abdel Abdel-Rahman, The Brody School of Medicine at East Carolina University, United States

***Correspondence:**
András Palotás
palotas@asklepios-med.eu
Luciene B. Vieira
lubvieira@icb.ufmg.br

† These authors have contributed equally to this work

Specialty section:
This article was submitted to Neuroendocrine Science, a section of the journal Frontiers in Neuroscience

Received: *19 November 2020*
Accepted: *06 January 2021*
Published: *10 February 2021*

Citation:
Oliveira TPD, Gonçalves BDC, Oliveira BS, de Oliveira ACP, Reis HJ, Ferreira CN, Aguiar DC, de Miranda AS, Ribeiro FM, Vieira EML, Palotás A and Vieira LB (2021) Negative Modulation of the Metabotropic Glutamate Receptor Type 5 as a Potential Therapeutic Strategy in Obesity and Binge-Like Eating Behavior. Front. Neurosci. 15:631311. doi: 10.3389/fnins.2021.631311

HIGHLIGHTS

- VU0409106 is a negative allosteric modulator of mGluR5.
- VU0409106 reduces food consumption, body weight, and anxiety behavior of mice treated with high-fat diet.
- VU0409106 decreases inflammatory cytokines in the adipose tissue.
- VU0409106 treatment was able to reduce binge-like eating in mice.

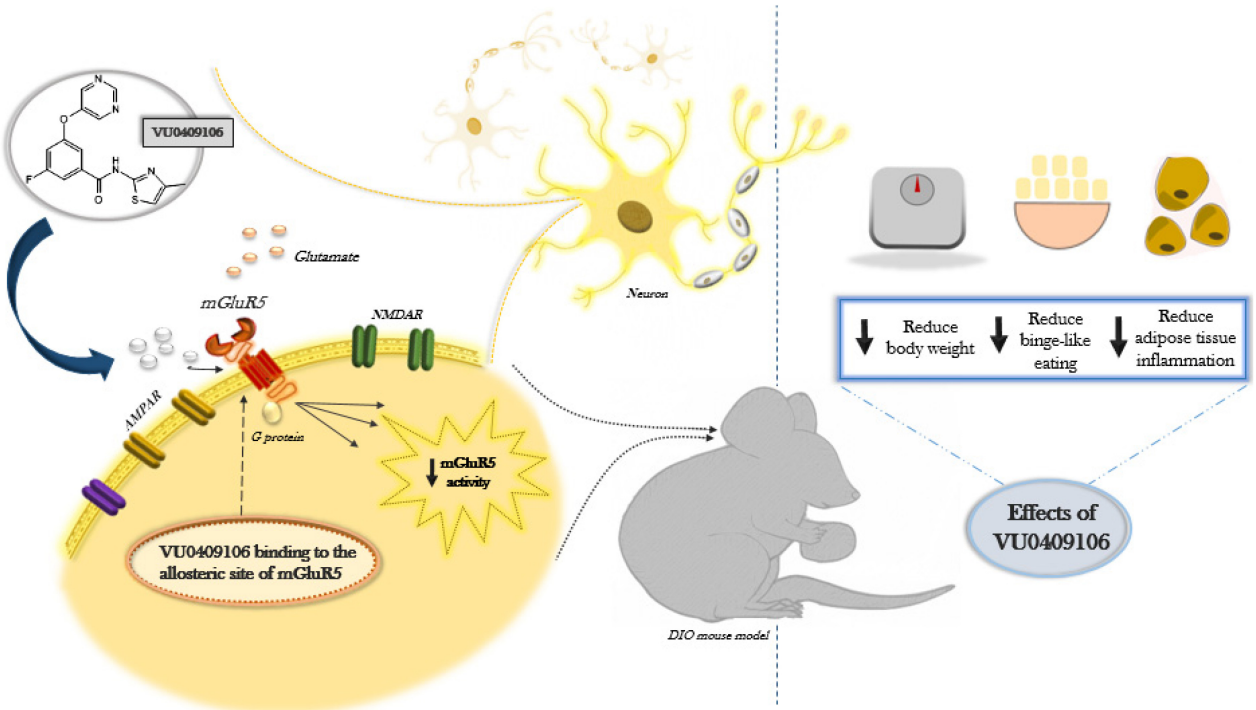

GRAPHICAL ABSTRACT | Diet-induced obese (DIO) C57BL/6 mice were treated for 14 days with VU0409106, a negative allosteric modulator of mGluR5. Food intake, body weight, inflammatory/hormonal levels, and behavioral tests were performed. Our data suggest reduction of feeding, body weight, and adipose tissue inflammation in DIO mice after chronic treatment with VU0409106.

INTRODUCTION

Obesity prevalence is expanding in most countries according to the World Health Organization (Blüher, 2019). In fact, worldwide obesity numbers nearly tripled since 1975 (Blüher, 2019). Obesity is defined as an abnormal accumulation of body fat, associated with genetics, hormones, and environmental factors (González-Muniesa et al., 2017). The growing accessibility to highly palatable food, rich in fats and sugars, and reduced energy expenditure and sedentary lifestyle are considered the main environmental factors contributing to weight gain (Ravussin et al., 1988; Hill and Peters, 1998).

Obesity also increases the risk of several chronic conditions, including cardiovascular diseases, diabetes, cancer, psychiatric disorders, and many others (Kopelman, 2007). Changes leading to a series of physiological imbalances can be established in obese individuals, such as dyslipidemia and chronic inflammatory response (Dandona et al., 2004; Van Gaal et al., 2006). Besides, the progressive adipose tissue expansion in obesity is associated with insufficient angiogenesis, leading to hypoxia, cellular stress, oxidative damage, and necrosis, triggering an inflammatory response from adipocytes and local immune cells that becomes chronic in the context of long term obesity (Wood et al., 2009). Furthermore, a low-grade chronic inflammatory response can result in increased circulating levels of proinflammatory cytokines, leading to the onset of insulin resistance, diabetes, atherosclerosis, osteoarthritis, and so on (Dandona et al., 2004; Van Gaal et al., 2006; Kopelman, 2007; Wood et al., 2009).

Psychiatric disorders, including anxiety, depression, and binge eating, are also linked to obesity, yet there is still debate about whether they constitute cause or consequence of this disease (de Zwaan, 2001; Wurtman and Wurtman, 2018). Either way, efforts to reduce body weight and adiposity can be hampered by depression, anxiety, and other mood disorders, as these conditions can also promote weight gain (Collins et al., 2016). In agreement, some evidence shows a link between high-fat diet (HFD) consumption and the development of depression and anxiety, in animal models (Sharma and Fulton, 2013; Gancheva et al., 2017). Moreover, consumption of HFD might lead to neural adaptations in brain reward circuitry, a key area involved in binge eating and other addictive-like aspects of feeding behavior (Sharma and Fulton, 2013; Murray et al., 2014).

The metabotropic glutamate receptor 5 (mGluR5) is a G-protein–coupled receptor, associated with an intracellular rise in $[Ca^{2+}]_i$ through G_q/G_{11} protein signaling, increasing the activity of PLC and the levels of IP_3 and DAG (Niswender and Conn, 2010). There is evidence that mGluR5 may underlie obesity pathophysiology. For instance, the knockout of mGluR5 gene, as well as treatment with MTEP, a NAM of mGluR5,

Abbreviations: HFD, High-fat diet; CHPG, 2-Chloro-5-hydroxyphenylglycine; CD, Control diet; CNS, Central nervous system; mGluR5, Metabotropic glutamate receptor 5; PLC, Phospholipase C; IP3, Inositol 3-phosphate; DAG, Diacylglycerol; NAM, Negative allosteric modulator; DIO, Diet-induced obesity/diet-induced obese; TNF, Tumor necrosis factor; IFN-γ, Interferon gamma; IL, Interleukin; MCP-1, Monocyte chemoattractant protein; VEH, Vehicle; IP, Intraperitoneal route; MTEP, [3-[(2-Methyl-1,3-thiazol-4-yl)-ethynyl]-pyridine.

decreased body weight, plasma leptin and insulin levels, food intake, and feeding after food deprivation (Bradbury et al., 2005). Accordingly, CHPG, an mGluR5 agonist, stimulates food intake in mice, supporting a role of this receptor in mediating appetite and feeding (Ploj et al., 2010). Herein, we used a NAM of mGluR5, VU0409106, to investigate the effects of reducing mGluR5 activity over different aspects related to obesity, including binge-like eating. Compared to MTEP and related compounds, VU0409106 was recently synthesized, exhibiting improved pharmacokinetics and *in vivo* activity on reducing compulsion behavior without affecting motor behavior in mice (Varty et al., 2005; Koros et al., 2007; Felts et al., 2013).

Our results indicated that obese mice chronically injected with VU0409106 showed reduced body weight and adipose tissue inflammation. Locomotor activity and compulsive behavior were assessed, and the compound seems to reduce compulsive behavior in treated mice. Furthermore, our data confirm that the treatment with this drug was able to reduce binge-like eating in mice.

MATERIALS AND METHODS

Animals

All procedures used in this study were approved and strictly followed the ethical principles of animal experimentation adopted by the Ethics Committee on Animal Use of Federal University of Minas Gerais and institutionally approved under protocol number 350/2015. Male C57BL/6 mice aging from 3 to 15 weeks were used. After weaning, mice were provided with *ad libitum* water and either HFD with 45% of total calories from fat, or control diet (CD) with 10% of total calories from fat (**Supplementary Material**). Diet was obtained from Rhoster® Industry and Commerce (São Paulo, Brazil). All animals were housed in groups (two per box) and in conditions of 25°C, a 12 h light–dark cycle, with lights on 7 AM and off on 7 PM, and food and water *ad libitum*.

Drugs

The compound VU0409106 was purchased from Tocris Bioscience© (Bristol, United Kingdom). Fluoxetine hydrochloride was donated by Infinity Pharma© (RJ, Brazil). The drugs were dissolved by sonication into vehicle (VEH) consisting of 10% Tween 80 (Sigma–Aldrich) and 90% physiological saline solution and administered via intraperitoneal route (IP). The doses of VU0409106 (50 mg) prepared were as follows: 3, 7.5, and 15 mg/kg. Fluoxetine, a selective serotonin reuptake inhibitor, was used at doses of 10 mg/kg as a positive control on reducing food consumption and body weight. After preparation, solutions were stored in the freezer at a temperature of −20°C until use.

Diet-Induced Obesity

Mice were placed on HFD from weaning (third week), and body weight was measured weekly. At midweeks 12th and 14th, daily body weight and food intake were assessed in the morning (14 days). During this period, food intake was calculated by placing preweighed food in the cage daily. Consumption was normalized by mice body weight. At the beginning of the 15th week, mice were made to fast (7 AM–1 PM) and euthanized (**Figure 1**).

Chronic Treatment in Obese Mice

The same protocol of diet-induced obesity (DIO) was used to assess the effects of 14 days treatment of obese mice with VU0409106 (**Figure 1**). Through the 12th to 14th week, mice were injected in the morning daily, via the IP route, with VEH, VU0409106 3 mg/kg, VU0409106 7.5 mg/kg, or fluoxetine 10 mg/kg. Those doses were based on previously reported data (Yen et al., 1987; Niswender and Conn, 2010; Felts et al., 2013). Daily food intake and body weight were measured, and after the period of treatment, the hypothalamus, serum, and epididymal adipose tissue were collected and properly stored for subsequent analysis.

Fasting-Induced Food Intake Protocol

In order to assess the effects of VU0409106 on binge-like eating behavior, mice were fed with CD from weaning, and they were isolated in their cages at the beginning of the 11th week for 7 days for habituation. At the beginning of the 12th week, animals were deprived of food for 14 h (1 h prior to lights out, until 1 h after lights on). Thirty minutes before lights on, animals were treated with vehicle (VEH) or VU0409106 at doses of 3, 7.5, or 15 mg/kg or fluoxetine 10 mg/kg. After 14 h fasting, preweighed CD was reintroduced in cages, and food intake was measured at 15, 30, 60, and 210 min after refeeding. Food intake (milligrams) was normalized to body weight (grams).

Intermittent HFD-Induced Food Intake Protocol

A second protocol to assess the effects of VU0409106 on binge-like eating behavior was conducted. Mice at 10 weeks of age were subjected to intermittent or continuous HFD, as described in the **Supplementary Material**. Previous work demonstrated that successive cycle of 24-h intermittent exposure to HFD induces binge-like eating in mice (Czyzyk et al., 2010). At the 12th week of age, these mice were injected with either VEH; VU0409106 at doses of 3, 7.5, or 15 mg/kg; or fluoxetine 10 mg/kg, 30 min prior to another presentation of preweighed HFD to the mice of the intermittent group. Food intake was measured 2.5 and 24 h after HFD presentation.

Sample Processing

The hypothalamus and epididymal adipose tissue were rapidly collected and homogenized in an extraction solution (100 mg of tissue per milliliter), containing 0.4 M NaCl, 0.05% Tween 20, 0.5% bovine serum albumin, 0.1 mM phenyl methyl sulfonyl fluoride, 0.1 mM benzethonium chloride, 10 mM EDTA, and 20 KIU aprotinin, using Ultra-Turrax. Lysates were centrifuged at 13,000*g* for 10 min at 4°C; supernatants were collected and stocked at −70°C until use. Blood samples were also obtained, centrifuged at 1,500*g* for 10 min at 4°C, and the serum was collected and stocked at −70°C until use.

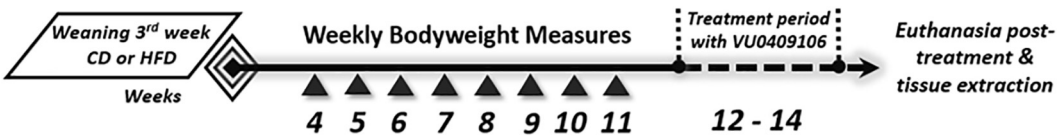

FIGURE 1 | Scheme of diet-induced obesity (DIO) and chronic drug treatment. Three-week-old C57BL/6 mice were divided into control diet group (CD) and high-fat diet group (HFD). Animals were fed *ad libitum* throughout the experiment. At the 12th and 14th day, daily body weight and food intake were assessed for 14 days. In the last day of treatment, mice were submitted to behavioral experiments and afterward to biochemical analysis.

Cytokines and Endocrine Markers Analysis

The concentration of the cytokines interleukin 6 (IL-6), IL-10, IL-12p70, interferon γ (IFN-γ), and tumor necrosis factor α (TNF-α), and chemokine monocyte chemoattractant protein 1 (MCP-1) was determined using a mouse CBA kit (BD Biosciences, San Diego, CA) and acquired on a FACS CANTO II flow cytometer (Becton Dickinson, San Jose, CA). The samples were incubated with capture microspheres (beads) covered by specifics antibodies to the respective cytokines and chemokines, as well as the proteins of the standard curve. Then, the color reagent was added, and the samples were incubated for 3 h, at room temperature, and protected from light. Then, the plate wells were washed with the Wash Buffer® washing solution, provided in the kit, and subjected to centrifugation for 5 min at 200 rpm at room temperature. The supernatant was then aspirated and discarded. The precipitate containing the microspheres was then suspended with 300 μL of Wash Buffer®. The CBA results were analyzed by employing the software FCAP Array version 3.0 (Soft Flow Inc., Pécs, Hungary). Leptin, adiponectin, and insulin levels were detected by enzyme-linked immunosorbent assay (R&D Systems, Minneapolis, MN) in accordance to the manufacturer's instructions. Total cholesterol and triglyceride assays were measured by specific kits from Bioclin® (MG, Brazil). The monoreagent cholesterol and triglycerides kit are based on a colorimetric enzymatic test, in which a substrate is formed in which the color produced is directly proportional to the concentration of analyze, and its intensity is determined in a spectrophotometer at 500 nm.

Glucose Measurement

All tests were performed in the morning with 6 h–fasted mice, and tail vein blood sample was collected. Blood glucose test was performed on mice at three different times: after weaning, before 14 days drug treatment, and after drug treatment. For measurements, *-chek active* device was used.

Open-Field Test

To evaluate the locomotor activity, an open-field test was performed. In the afternoon, the animals were removed from the bioterium and taken to the test room, where the apparatus used in the experiment was located (the animals were not deprived from food or water). The habituation period was 30 min. After habituation, animals were placed in the apparatus (PhenoTyper®System; Noldus, Information Technology, Leesburg, VA, United States) and remained in the test for 30 min. The apparatus has an opaque plastic arena (30 × 30 cm), and animals could explore freely the entire area. The total distance traveled (cm) was analyzed using Ethovision XT software (Noldus, Information Technology, Leesburg, VA, United States).

Marble-Burying Test

The basic protocol for this experiment was performed according to Nature Protocols (Deacon, 2006). For that, acrylic boxes measuring 29 × 17.5 cm in length, 20 spheres (marbles), and wood shavings were used. A quantity of wood shavings was placed, filling the boxes approximately 7 cm and forming a flat and compact surface. Twenty spheres were placed in rows (4 × 5) in the box on the shavings evenly spaced, with each space about 4 cm apart between the spheres. The animals faced the test in the morning. Before being taken to the experimental room, animals were kept for 30 min in packaging (there was no water or food deprivation). The drugs were administered 15 min before starting the behavioral test. The duration of the test was 30 min. The analyses were performed after the tests. The number of spheres buried and not buried was quantified. For the sphere to be considered buried, two-thirds of its dimension should be below the level of shavings. The same experimenter blindly analyzed all the tests performed.

Statistics

Data are presented as mean ± SEM. All graphs and analyses were performed using GraphPad Prism 5.0 (GraphPad Software, San Diego). Before statistical tests, all data were analyzed by Grubbs ESD method for outlier detection, and extreme values were excluded from the analysis. Gaussian distribution of data was confirmed by Kolmogorov–Smirnov normality test. A comparison between two groups was performed by Student *t*-test. Three or more groups were analyzed by one-way analysis of variance (ANOVA) followed by Bonferroni *post hoc* test. The two-way ANOVA, followed by the Bonferroni *post hoc* was used in cases of two independent variables. In all cases, significance was defined by $p < 0.05$.

RESULTS

DIO and Chronic Treatment With VU0409106 in Mice

Mice fed with HFD exhibited significantly higher body weight since the second week (two-way ANOVA, $F_{(2,23)} = 10.52$,

TABLE 1 | Wild-type C57BL/6 mice after 11 weeks on HFD or CD.

	HFD	CD
Serum insulin (pg/mL)	1.725 ± 0.208	2.088 ± 0.239
Serum triglycerides (mg/dL)	61.38 ± 5.382	59.50 ± 8.379
Serum adiponectin (pg/mL)	188.9 ± 18.24	178.5 ± 27.57
Hypothalamic adiponectin (pg/mg)	25.68 ± 4.849*	12.42 ± 2.412
Adipose tissue adiponectin (pg/mg)	29.17 ± 7.737	36.91 ± 5.978
Hypothalamic IL-12p70 (pg/mg)	2.824 ± 0.686	2.822 ± 0.388
Hypothalamic TNF-α (pg/mg)	1.465 ± 0.170	1.551 ± 0.151
Hypothalamic IFN-γ (pg/mg)	0.481 ± 0.059	0.5415 ± 0.089
Hypothalamic MCP-1 (pg/mg)	8.536 ± 1.897	9.497 ± 1.517
Hypothalamic IL-10 (pg/mg)	1.510 ± 0.137	1.588 ± 0.154
Hypothalamic IL-6 (pg/mg)	1.364 ± 0.198	1.221 ± 0.116
Serum IL-12p70 (pg/mL)	17.27 ± 4.598	24.36 ± 6.843
Serum TNF-α (pg/mL)	15.33 ± 3.330	15.03 ± 3.186
Serum IFN-γ (pg/mL)	2.590 ± 0.332	3.106 ± 0.486
Serum MCP-1 (pg/mL)	94.64 ± 15.06	89.18 ± 15.02
Serum IL-10 (pg/mL)	15.35 ± 4.324	18.95 ± 4.613
Serum IL-6 (pg/mL)	7.391 ± 1.480	8.053 ± 1.475

**Statistically different from control diet–treated mice, $p < 0.05$, Student's t-test, $n = 6–8$.*

p = 0.0004) (**Supplementary Figure 1A**). In addition, HFD group showed higher levels of total cholesterol (unpaired t-test, t_{16} = 2.335, p = 0.0329) (**Supplementary Figure 1B**), serum leptin (unpaired t-test, t_{13} = 2.184, p = 0.0479) (**Supplementary Figure 1C**), and also epididymal adipose tissue leptin levels (unpaired t-test, t_{12} = 5.584, p = 0.027) (**Supplementary Figure 1D**). Inflammatory markers in epididymal adipose tissue at the end of the DIO protocol were also measured, and higher levels of cytokines IL-12p70, TNF-α, IFN-γ, and the chemokine MCP-1 were detected (unpaired t-test, IL-12.70 t_{10} = 2.506, p = 0.0311; TNF-α t_{10} = 2.567, p = 0.028; IFN-γ t_{10} = 2.835, p = 0.0177; and MCP-1 t_{11} = 2.869, p = 0.0153) (**Supplementary Figures 1E–J**). Besides, results showed an increase in hypothalamic adiponectin levels in mice fed with HFD, although no other difference regarding serum insulin, adiponectin, triglycerides, and inflammatory markers outside epididymal adipose tissue was observed between HFD and control group (**Table 1**).

Interestingly, treatment with VU0409106 7.5 mg/kg or fluoxetine 10 mg/kg promoted weight loss (one-way ANOVA, $F_{(3,29)}$ = 21.93, $p < 0.001$) and reduced food intake in HFD mice (one-way ANOVA, $F_{(3,35)}$ = 9.654, $p <$ 0.001) (**Figures 2A–C**). Besides, mice fed with CD were also treated with VU0409106, under the same protocol described for HFD mice. CD mice did not show significantly reduced body weight or food intake (**Figures 2D–F**). In order to investigate if drug treatment interferes with locomotor parameters of HFD and CD mice, the open-field test was performed. Importantly, HFD- or CD-treated mice with VU0409106 did not present reduction on total distance traveled compared to control group (**Figures 2G,H**). In addition to locomotor parameter, the effect of VU0409106 was evaluated on a model of compulsion (marble burying) in both groups. It was observed that HFD mice treated with VU0409106 7.5 mg/kg or fluoxetine 10 mg/kg buried fewer marbles compared to the control group (**Figure 2I**). Otherwise, CD mice treated with VU0409106 in all different concentrations or fluoxetine 10 mg/kg buried fewer marbles as compared to control group (**Figure 2J**).

Nonetheless, we also observed a reduction of inflammatory cytokine levels IL-12p70, TNF-α, and IFN-γ in HFD mice treated with VU0409106 7.5 mg/kg in the adipose tissue of C57BL/6 obese mice (one-way ANOVA, IL-12p70 $F_{(3,23)}$ = 3.116, p = 0.0459; TNF-α $F_{(3,24)}$ = 3.904, p = 0.021; and IFN-γ $F_{(3,27)}$ = 3.962, p = 0.0184) (**Figures 3A–C**). However, no difference was observed comparing vehicle-, VU0409106-, and fluoxetine-treated HFD mice in terms of leptin, adiponectin, total cholesterol, triglycerides, and inflammatory cytokine levels in hypothalamus or in serum (**Supplementary Materials 2–6**).

In addition, treatment with VU0409106 at both doses also reduced serum insulin levels in HFD mice (one-way ANOVA, $F_{(3,23)}$ = 5.749, p = 0.0044) (**Figure 4A**), and VU0409106 7.5 mg/kg decreased glucose levels (unpaired t-test, t_{17} = 2.936, p = 0.0092) (**Figure 4B**).

Effect of VU0409106 Treatment on Binge-Like Eating Behavior

To assess the effects of negative mGluR5 modulation on fasting-induced food intake (Bradbury et al., 2005), 12 weeks-old non-obese mice were made to fast for 14 h (1 h prior to lights off until 1 h after lights on). Thirty minutes before returning food to the cages, mice were injected with vehicle, fluoxetine 10 mg/kg, or VU0409106 at doses of 3, 7.5, or 15 mg/kg. Food intake was measured 15, 30, 60, and 210 min after food was reintroduced and normalized by body weight. Mice injected with VU0409106 7.5 and 15 mg/kg showed reduced food intake after 30 min of returning food to the cage, as compared to vehicle-treated animals (**Figure 5A**) (two-way ANOVA; interaction $F_{(12,96)}$ = 1.782, ns; group factor $F_{(3,96)}$ = 16.74, $p < 0.0001$; time factor $F_{(4,96)}$ = 105.8, $p < 0.0001$), and this reduction was even more pronounced at the end of the experiment (210 min after food presentation) (one-way ANOVA, $F_{(4,24)}$ = 8.611, p = 0.0002) (**Figure 5B**). We also assessed binge-like eating behavior in a different protocol based on intermittent HFD exposure (Czyzyk et al., 2010). Ten-week-old non-obese mice were subjected to successive cycles of HFD and developed binge-like eating behavior (**Supplementary Material**). Thirty minutes before the third cycle of HFD exposure, mice were injected with vehicle, fluoxetine 10 mg/kg, or VU0409106 at 7.5 or 15 mg/kg. Food intake was measured 2.5 and 24 h later. As shown in **Figure 5**, mice with intermittent access to HFD had considerably higher food intake (one-way ANOVA, $F_{(4,30)}$ = 17.99, $p < 0.0001$) (**Figures 5C–E**), including food intake per minute, which characterizes the binge-like eating behavior. At both tested doses of VU0409106, and also fluoxetine, results showed a reduction in binge-like eating 2.5 h after HFD presentation (**Figures 5C,D**). However, at 24 h, no difference was observed among drug-treated groups (**Figure 5E**).

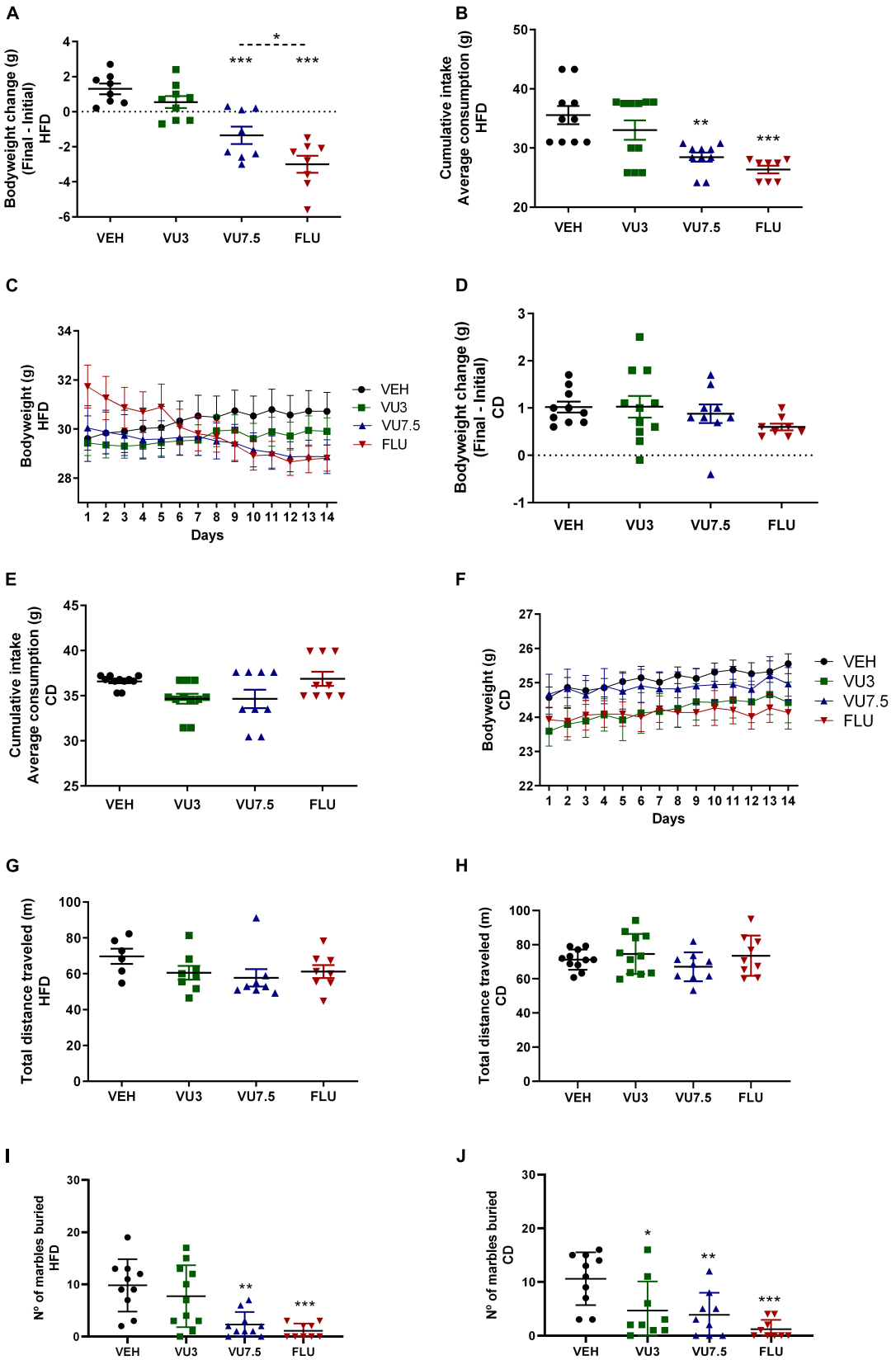

FIGURE 2 | Continued

FIGURE 2 | Effects of 14 days' treatment on body weight, cumulative intake, and behavioral tests in HFD mice and CD mice. Scatter plot representation. **(A)** Treatment with VU0409106 7.5 mg/kg or fluoxetine 10 mg/kg reduced body weight of HFD mice (n = 8–9). **(B)** Food intake of HFD mice is decreased after treatment with VU0409106 7.5 mg/kg or fluoxetine 10 mg/kg (n = 8–11). **(C)** Graphical representation showing 14 days' treatment on body weight of HFD mice. Treatment with VU0409106 (3 or 7.5 mg/kg) or fluoxetine (10 mg/kg) did not reduce body weight **(D)** or food intake **(E)** of CD mice (n = 8–11). **(F)** Graphical representation showing 14 days' treatment on body weight of CD mice. **(G)** Treatment with VU0409106 7.5 mg/kg did not alter the distance traveled of HFD mice (n = 6–8). $^{*}p < 0.05$, $^{**}p < 0.01$, and $^{***}p < 0.001$ compared to vehicle after Bonferroni multiple-comparison *post hoc* test. **(H)** Treatment with VU0409106 (3 or 7.5 mg/kg) or fluoxetine (10 mg/kg) on CD mice did not change the distance traveled comparing to the control group. **(I)** VU0409106 7.5 mg/kg or fluoxetine 10 mg/kg reduced the number of marbles buried in HFD mice (n = 9–11). $^{**}p < 0.01$ and $^{***}p < 0.001$ compared to vehicle after Bonferroni multiple-comparison *post hoc* test. **(J)** VU0409106 3 and 7.5 mg/kg or fluoxetine 10 mg/kg reduce the number of marbles buried in CD mice (n = 9–10). $^{*}p < 0.05$, $^{**}p < 0.01$, and $^{***}p < 0.001$ compared to vehicle after Bonferroni multiple-comparison *post hoc* test.

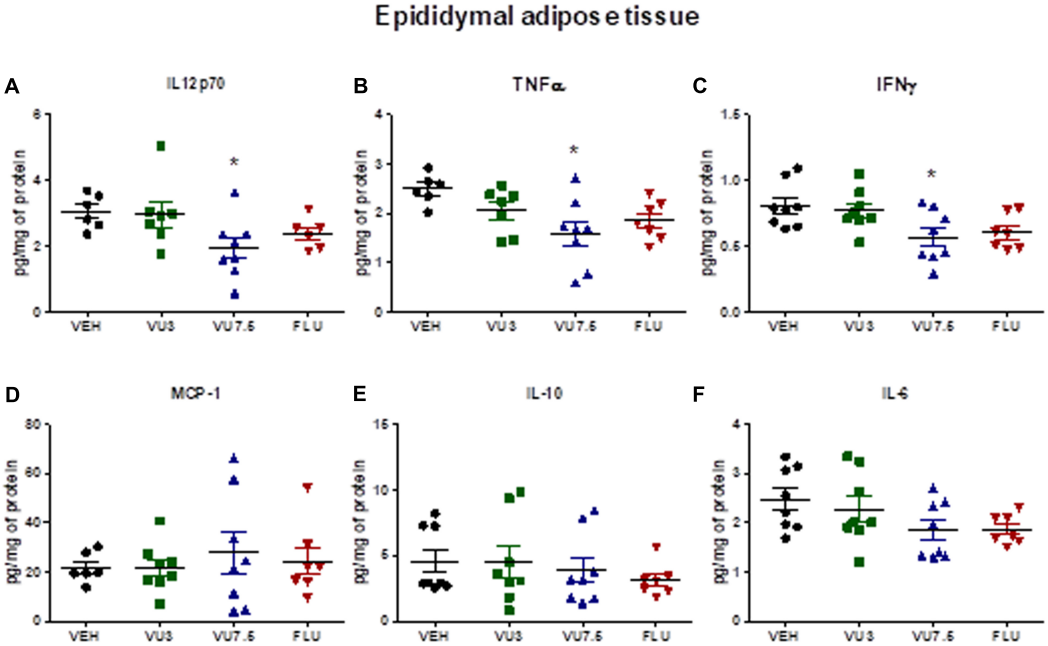

FIGURE 3 | Decreased levels of inflammatory cytokines IL-12p70, TNF-α, and IFN-γ in the epididymal adipose tissue of HFD mice after treatment with VU0409106. Fourteen days' treatment with VU0409106 7.5 mg/kg of HFD mice reduced **(A)** IL-12p70, **(B)** TNF-α, and **(C)** IFN-γ levels in the epididymal adipose tissue of HFD mice. **(D–F)** No effect of VU0409106 or fluoxetine on **(D)** MCP-1, **(E)** IL-10, or **(F)** IL-6 levels. The results are shown as mean ± *SD* from (n = 6–8). $^{*}p < 0.05$ compared to vehicle after Bonferroni multiple-comparison *post hoc* test.

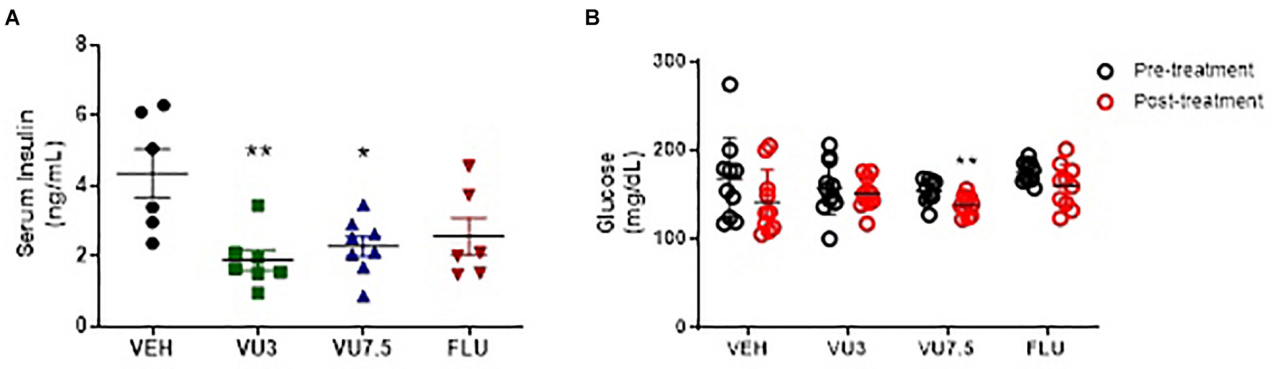

FIGURE 4 | Fourteen days' treatment with VU0409106 reduced serum insulin and glucose levels of HFD mice. **(A)** Scatter plot representation of treatment with VEH (vehicle), VU0409106 (3 or 7.5 mg/kg), and fluoxetine (10 mg/kg) (n = 7–8). $^{*}p < 0.05$ and $^{**}p < 0.01$ compared to vehicle after Bonferroni multiple-comparison *post hoc* test. **(B)** Glycaemia levels of HFD mice were measured prior (pretreatment) and after 14 days drug treatment (posttreatment). Blood samples were collected after 6-h fasting. VEH (vehicle), VU0409106 (3 or 7.5 mg/kg), and fluoxetine (10 mg/kg) (n = 10–11), $^{**}p < 0.01$ compared to vehicle after Student's t-test.

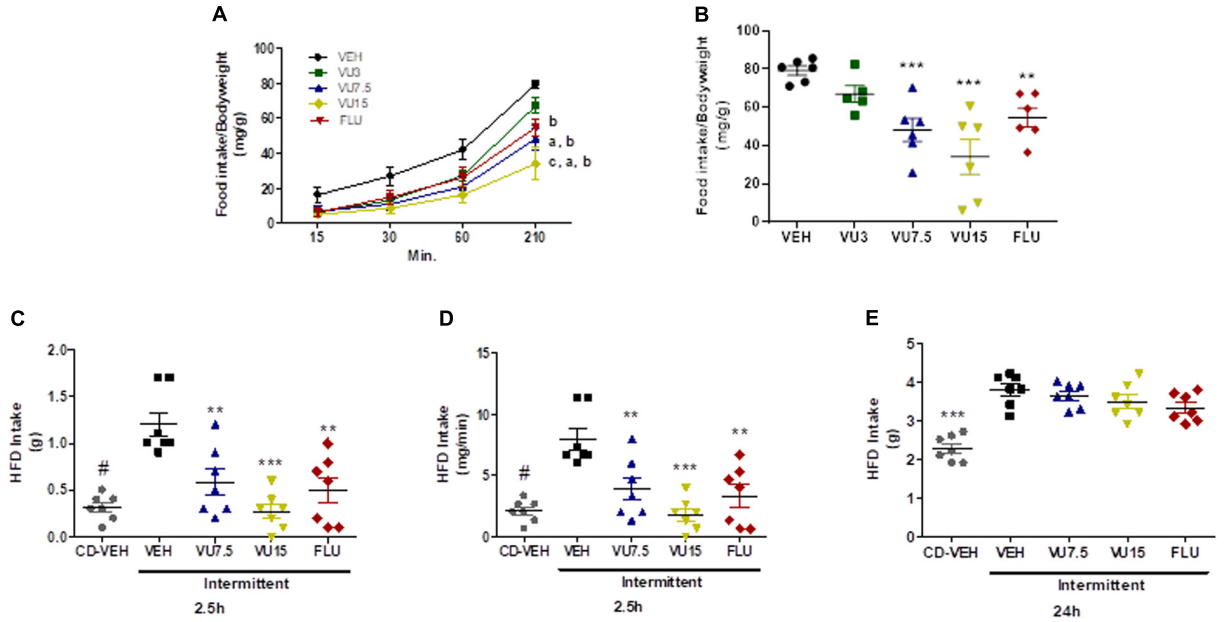

FIGURE 5 | NAM VU0409106 reduced binge-like eating behavior in C57BL/6 mice. Fasting-induced food intake results are shown in A and B. **(A)** Food intake after 15, 30, 60, and 210 min of food return to the cage (a: different from vehicle at time 60; b: different from vehicle at time 210; and c: different from vehicle at time 30 after Bonferroni multiple-comparison *post hoc* test). **(B)** Food intake at 210 min ($n = 6$), $^{**}p < 0.01$ and $^{***}p < 0.001$ compared to vehicle after Bonferroni multiple-comparison *post hoc* test. Intermittent-HFD-induced binge-like eating results are shown in **(C–E)**. HFD intakes were monitored **(C,D)** 2.5 h and **(E)** 24 h after presentation of HFD ($n = 7$), $^{\#}p < 0.05$, $^{**}p < 0.01$, and $^{***}p < 0.001$ after Bonferroni multiple-comparison *post hoc* test.

DISCUSSION

In order to assess potential therapeutic applications of mGluR5-targeting drugs in obesity, herein we focused on the role of negative modulation of mGluR5 by VU0409106 in feeding regulation, body weight, binge eating, and adipose tissue inflammation on diet-induced obese mice. Importantly, VU0409106 is a drug structurally distinct from MTEP acting as a potent and selective NAM of mGluR5 binding at recognized allosteric binding site (Felts et al., 2013). This drug crosses the blood–brain barrier, displays good central nervous system (CNS) rates following intraperitoneal injection, and also reduces compulsive behavior in mice (Felts et al., 2013), which might be an interesting tool for treating CNS-related disorders, as binge eating in the context of obesity. Besides, rodents treated with VU0409106 differently from MTEP did not show altered locomotor activity, which may be related to alterations in learning and memory, social behavior deficits, and disruption on prepulse inhibition (Varty et al., 2005; Koros et al., 2007).

In the current study, we induced obesity in mice by using a protocol with 45% HFD. Our results showed that after HFD treatment, mice showed obesity features, such as increased body weight, cholesterol, leptin levels, and inflammatory markers. It is well known that adipose tissue inflammation is a hallmark of obesity and underlies several metabolic alterations associated with this condition (Dandona et al., 2004; Buettner et al., 2007; Wood et al., 2009). Accordingly, HFD mice showed elevated levels of the chemokine MCP-1 and inflammatory cytokines IL-12p70, TNF-α, and IFN-γ in the epididymal adipose tissue, 10 weeks after introduction of HFD. These findings reinforce the presence of an inflammatory milieu as described in obesity (Dandona et al., 2004; Huh et al., 2014). Moreover, the lack of higher levels of IL-10, a pivotal anti-inflammatory cytokine, points out the absence of a counter-regulatory process, which in turn may contribute to the chronic, low-grade inflammation typical of obesity (Juge-Aubry et al., 2005).

We also investigated the levels of adiponectin, a hormone produced by adipocytes, generally found at lower levels in obese subjects (Kern et al., 2003; Nigro et al., 2014). Although no difference was observed between HFD and CD mice regarding serum or adipose tissue levels of adiponectin, higher levels of this adipokine were found in the hypothalamus of obese mice. Based on the anti-inflammatory effects of adiponectin, its increased levels in the hypothalamus may explain, at least in part, the lack of a central inflammatory response in the HFD group (Huang et al., 2008; Nigro et al., 2014). In line with this finding, an intracerebroventricular injection of adiponectin was able to reverse the elevated proinflammatory signals in the hypothalamus of HFD mice, reinforcing adiponectin anti-inflammatory role in the brain in the obesity context (Koch et al., 2014).

It has been reported that the modulation of the glutamatergic system might be a promising strategy to treat obesity (Barja-Fernandez et al., 2014; Bojanowska and Ciosek, 2016). Accordingly, we investigated whether 14 days' treatment with VU0409106 would oppose obesity in mice under HFD. The systemic administration of VU0409106 reversed weight gain and decreased food intake in HFD mice. Our data are

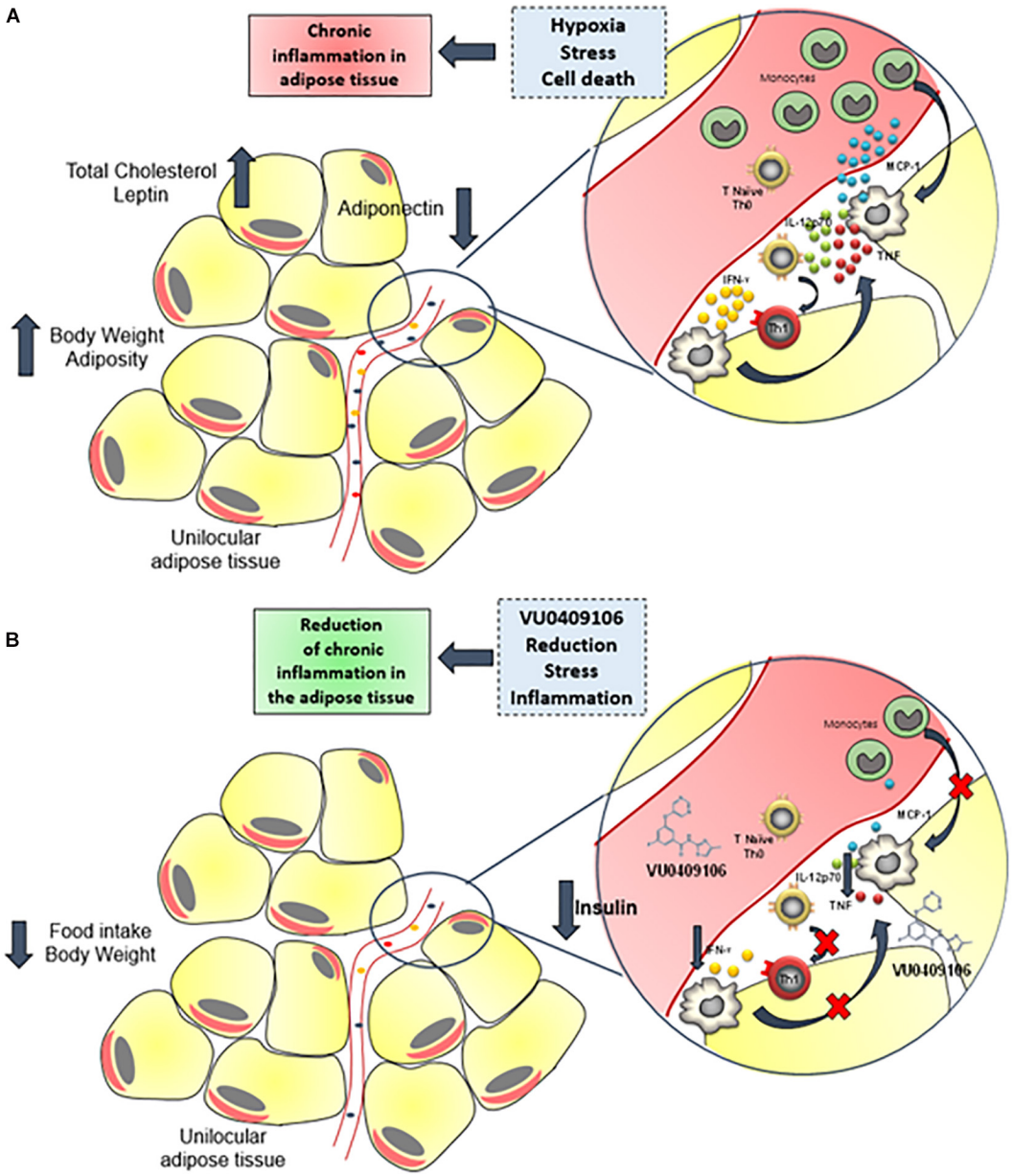

FIGURE 6 | Anti-inflammatory role of VU0409106 in the adipose tissue of obese mice. **(A)** Increased adiposity may contribute to hypoxia, stress, and cell death, which triggers an inflammatory response with enhanced local levels of inflammatory mediators, especially cytokines such as IL-12p70, TNF-α, and IFN-γ and the chemokine MCP-1 and consequent immune cell recruitment. As a result, a chronic, low-grade inflammation of adipose tissue is sustained. **(B)** Chronic administration of VU04090106 reduces food consumption and body weight and promotes an anti-inflammatory milieu.

in accordance with previous results showing that mGluR5 mediates appetite and energy balance in rodents (Bradbury et al., 2005). Also, previous data showed that MTEP, a NAM of mGluR5, decreased consumption of highly palatable food without altering consumption of the standard diet, which may explain, at least in part, the lack of treatment effect in CD mice (Bisaga et al., 2008). These results needed to be further investigated in order to clarify if the effect of VU0409016 is directly related to brain reward circuits. It is well known that eating behavior is directly affected by food taste and also that high-fat food is highly palatable (Rockwood and Bhathena, 1990; Melhorn et al., 2010; Small, 2012; Bake et al., 2014). Because of the difference in nutrient composition between diets, it is possible that VU0409106 acts by suppressing the intake of HFD more than CD as meal patterns are altered when mice are subjected to an HFD (Melhorn et al., 2010). Besides, mGluR5 is a diffuse receptor found in the brain, distributed in the following structures: olfactory bulb, anterior olfactory nucleus, olfactory tubercle, cerebral cortex, hippocampus, lateral septum, striatum, nucleus accumbens, inferior colliculus, and spinal trigeminal

nucleus (Shigemoto et al., 1993). In addition, studies show that mGluR5 is expressed in several regions of the hypothalamus as in the preoptic, suprachiasmatic nucleus, and ventrolateral region (van den Pol et al., 1995). However, among these regions, mGluR5 is strongly expressed in the ventrolateral pole of the ventromedial nucleus (an area related to metabolic balance and food intake) (van den Pol et al., 1995). As mGluR5 are expressed in key brain areas controlling feeding behavior and rewarding brain circuits, as hypothalamus, nucleus accumbens, and dorsolateral striatum, it is possible that the negative modulation of these receptors reduced the rewarding aspects induced by the palatable food in the HFD group (van den Pol et al., 1995; Boer et al., 2010; Terbeck et al., 2015). In fact, there is evidence that glutamatergic antagonists seem to be more selective in decreasing the reinforcing effect of food, which is more related to hedonic than homeostatic processes (Saper et al., 2002). Moreover, it is quite tempting to postulate that the mechanisms underlying the effects of negative modulation of mGluR5 on reducing food intake may resemble the antagonist of those receptors on decreasing self-administration and drug-seeking behavior of agents, such as alcohol, cocaine, nicotine, and opiates (Paterson and Markou, 2005; Bäckström and Hyytiä, 2006; Osborne and Olive, 2008; Rutten et al., 2011; Wang et al., 2013).

In the behavioral tests performed, no uncommon results were found. As previously described, MPEP and fluoxetine decrease the compulsive behavior of burying marbles on mice (Spooren et al., 2000; Nicolas et al., 2006; Arora et al., 2013), and the compound VU0409106 itself has a similar ability (Felts et al., 2013). In the open-field test, according to our results VU0409106 administration did not cause hyperlocomotion or sedation in treated mice. However, more side effects of the compound need to be explored.

The negative modulation of mGluR5 by VU04090106 also decreased the adipose tissue inflammation induced by HFD. It is unclear how VU0409106 decreased inflammatory markers selectively in the adipose tissue without affecting their levels in the serum or hypothalamus. Nonetheless, VU0490106-associated decrease in inflammatory signaling in the epididymal adipose tissue of HFD mice may also be dependent on the body weight loss alongside with reduced adiposity due to decreased food intake, which in turn leads to diminished stress upon adipocytes and to a decrease in local inflammation (**Figure 6**). Corroborating our findings, anti-inflammatory effects, including decrease in the expression of inflammatory cytokines, as well as in the recruitment of immune cells to the lesion site, have been also reported following negative regulation of mGluR5 in other pathological conditions, such as traumatic brain injury (Byrnes et al., 2009; Yang et al., 2017). Considering the widespread distribution of mGluR5 (e.g., CNS, liver, hepatocytes, thymus, immune cells), further studies are necessary to address the mechanisms behind VU0490106 anti-inflammatory properties in obesity (Boldyrev et al., 2005; Ferrigno et al., 2017).

An intriguing effect was observed in the serum insulin and glucose levels of HFD mice in response to the treatment with VU0409106 (**Figure 6B**). Although no difference in serum insulin level was observed between HFD and CD mice, only HFD mice had lower insulin and glucose levels after VU0409106 treatment. Likewise, lower serum insulin level after mGluR5 negative modulation was observed only in HFD mice as reported by Bradbury et al. (2005). Evidence suggests that mGluR is involved in the regulation of hormone secretion in the endocrine pancreas (Brice et al., 2002; Storto et al., 2006). The mGluR5 appears also to be required for an optimal insulin response to glucose both in clonal beta cells and mice (Storto et al., 2006). In clonal pancreatic beta cells, mGluR5 is expressed at the cell surface and also found in purified insulin-containing granules (Storto et al., 2006). Moreover, the NAM of mGluR5, MPEP, was able to inhibit glucose-stimulated $[Ca^{2+}]_i$ increase and insulin secretion in those cells (Storto et al., 2006) supporting our findings.

Binge-eating disorder is strongly linked with obesity, and binge eating *per se* is associated with a high burden of metabolic risk factors in the general population (Succurro et al., 2015; Davis, 2017). Binge-eating disorder has genetic and environmental components, being also associated with abnormalities in main cognitive areas as prefrontal cortex and the striatum (Kessler et al., 2016). In addition, glutamatergic neurotransmission is an interesting target for binge-eating disorder treatment, as it plays a role in reinforcing action of natural stimuli, such as food and drug abuse (Bisaga et al., 2008; Gass and Olive, 2008; Kalivas, 2009; Guardia et al., 2011). Thus, in order to assess the effects of negative modulation of mGluR5 in a model of binge-eating disorder, we selected two different protocols: a fasting protocol and an intermittent HFD access model, which does not involve the stress of forced fasting (Smith and Robbins, 2013). There is evidence that different neural substrates may control hunger- and non–hunger-driven food intake (Cao et al., 2014; Xu et al., 2017). Our results showed that in both protocols, the NAM VU0409106 was able to reduce the binge-like eating behavior. Fluoxetine, a selective inhibitor of reuptake of serotonin, which is largely used in the treatment of binge-eating disorders, was also effective in reducing binge-like eating in our models (Arnold et al., 2002; Guardia et al., 2011; Li et al., 2015). In addition, the role of mGluR5 on eating disorders was assessed by several authors (Bradbury et al., 2005; Bisaga et al., 2008; Guardia et al., 2011). More recently, interesting work described the part of mGluR5, *in vivo*, in bulimia nervosa (Mihov et al., 2020). In this study, the authors found higher distribution volume of mGluR5 in areas linked to processing emotional and cognitive information related to self-control, as anterior cingulate cortex and medial orbitofrontal cortex in individuals with bulimia (Mihov et al., 2020). Overall, our data confirm the role of mGluR5 on eating disorders and paved the way for the development of therapeutic strategies focused in the glutamatergic transmission for the treatment of this condition.

It is also important to highlight that our DIO model used small laboratory animals, which have different feeding patterns and compensatory mechanisms than humans, which may limit the extrapolation of the findings. And besides the limitations of this study on lacking on a deeper investigation of the mechanisms behind VU0409106 weight loss and decreased inflammatory markers on the adipose tissue, our findings may have important clinical implications. The current study confirms the role of mGluR5 on feeding and body weight regulation, pointing out this glutamatergic receptor as an important clinical target to treat

obesity and related disorders. Further research and prospective studies, however, are needed to assess and evaluate the potential of VU0409106 on long-term treatment.

CONCLUSION

This work provides first evidence of positive results on the mGluR5 NAM, VU0409106, in DIO and binge-like eating models. The weight loss achieved by VU0409106 administration was restricted to obese mice; likewise, the reduced food intake. The compound also reduced epididymal adipose tissue inflammation, suggesting that it could hold other therapeutic effects in the context of obesity and metabolic syndromes. We also showed that both hunger- and non–hunger-driven food intake, resembling binge-like eating, are suppressed by VU0409106-negative mGluR5 modulation. In summary, this work adds to previous evidence linking potential therapeutic application of mGluR5 antagonists to obesity and obesity-related disorders, paving the way for the development of translational approaches and promised treatments.

DATA AVAILABILITY STATEMENT

The original data presented in the study are included in the article/**Supplementary Material**, further inquiries can be directed to the corresponding author.

ETHICS STATEMENT

The studies involving animals were reviewed and approved by Ethics Committee on Animal Use of Federal University of Minas Gerais and institutionally approved under protocol number 350/2015.

AUTHOR CONTRIBUTIONS

LV designed the study. BG and TO performed most diet and behavioral experiments. BO, AM, and EV performed Elisa and CBA assays. CF performed analysis of triglycerides and cholesterol. DA contributed to the conception and design of diet protocols of the study. FR, HR, AO, and AP made substantial contributions to conception and design of the study and critically revised the manuscript for important intellectual content. BG, TO, and LV analyzed the results and wrote the article. All other authors revised the data and discussed the manuscript.

FUNDING

We disclosed receipt of the following financial support for the research, authorship, and/or publication of this article. This study was supported by CNPq (449578/2014-3 grants to LV and 442077/2014-9 and 400133/2014-8 grants to FR) and FAPEMIG (APQ 01995-14 to LV and CBB-RED 00012-14 to FR). This work was supported by Pró-Reitoria de Pesquisa da UFMG (PRPq/UFMG). This project was supported in part by the program of competitive growth of Kazan Federal University.

ACKNOWLEDGMENTS

We acknowledge Jeffrey P. Conn for suggesting VU0409106 to be tested. We also thank Mona Hassane for English editing.

SUPPLEMENTARY MATERIAL

The Supplementary Material for this article can be found online at: https://www.frontiersin.org/articles/10.3389/fnins.2021.631311/full#supplementary-material

REFERENCES

Arnold, L. M., McElroy, S. L., Hudson, J. I., Welge, J. A., Bennett, A. J., and Keck, P. E. (2002). A placebo-controlled, randomized trial of fluoxetine in the treatment of binge-eating disorder. *J. Clin. Psychiatry* 63, 1028–1033. doi: 10.4088/jcp.v63n1113

Arora, T., Bhowmik, M., Khanam, R., and Vohora, D. (2013). Oxcarbazepine and fluoxetine protect against mouse models of obsessive compulsive disorder through modulation of cortical serotonin and CREB pathway. *Behav. Brain Res.* 247, 146–152. doi: 10.1016/j.bbr.2013.02.038

Bäckström, P., and Hyytiä, P. (2006). Ionotropic and metabotropic glutamate receptor antagonism attenuates cue-induced cocaine seeking. *Neuropsychopharmacology* 31, 778–786. doi: 10.1038/sj.npp.1300845

Bake, T., Murphy, M., Morgan, D. G., and Mercer, J. G. (2014). Large, binge-type meals of high fat diet change feeding behaviour and entrain food anticipatory activity in mice. *Appetite* 77, 60–71.

Barja-Fernandez, S., Leis, R., Casanueva, F. F., and Seoane, L. M. (2014). Drug development strategies for the treatment of obesity: how to ensure efficacy, safety, and sustainable weight loss. *Drug Des. Devel. Ther.* 8, 2391–2400. doi: 10.2147/dddt.s53129

Bisaga, A., Danysz, W., and Foltin, R. W. (2008). Antagonism of glutamatergic NMDA and mGluR5 receptors decreases consumption of food in baboon model of binge-eating disorder. *Eur. Neuropsychopharmacol.* 18, 794–802. doi: 10.1016/j.euroneuro.2008.05.004

Blüher, M. (2019). Obesity: global epidemiology and pathogenesis. *Nat. Rev. Endocrinol.* 15, 288–298. doi: 10.1038/s41574-019-0176-8

Boer, K., Encha-Razavi, F., Sinico, M., and Aronica, E. (2010). Differential distribution of group I metabotropic glutamate receptors in developing human cortex. *Brain Res.* 1324, 24–33. doi: 10.1016/j.brainres.2010.02.005

Bojanowska, E., and Ciosek, J. (2016). Can we selectively reduce appetite for energy-dense foods? an overview of pharmacological strategies for modification of food preference behavior. *Curr. Neuropharmacol.* 14, 118–142. doi: 10.2174/1570159x14666151109103147

Boldyrev, A. A., Carpenter, D. O., and Johnson, P. (2005). Emerging evidence for a similar role of glutamate receptors in the nervous and immune systems. *J. Neurochem.* 95, 913–918. doi: 10.1111/j.1471-4159.2005.03456.x

Bradbury, M. J., Campbell, U., Giracello, D., Chapman, D., King, C., Tehrani, L., et al. (2005). Metabotropic glutamate receptor mGlu5 is a mediator of appetite and energy balance in rats and mice. *J. Pharmacol. Exp. Ther.* 313, 395–402. doi: 10.1124/jpet.104.076406

Brice, N. L., Varadi, A., Ashcroft, S. J., and Molnar, E. (2002). Metabotropic glutamate and GABA(B) receptors contribute to the modulation of glucose-stimulated insulin secretion in pancreatic beta cells. *Diabetologia* 45, 242–252. doi: 10.1007/s00125-001-0750-0

Buettner, R., Scholmerich, J., and Bollheimer, L. C. (2007). High-fat diets: modeling the metabolic disorders of human obesity in rodents. *Obesity (Silver Spring)* 15, 798–808. doi: 10.1038/oby.2007.608

Byrnes, K. R., Stoica, B., Loane, D. J., Riccio, A., Davis, M. I., and Faden, A. I. (2009). Metabotropic glutamate receptor 5 activation inhibits microglial associated inflammation and neurotoxicity. *Glia* 57, 550–560. doi: 10.1002/glia.20783

Cao, X., Xu, P., Oyola, M. G., Xia, Y., Yan, X., Saito, K., et al. (2014). Estrogens stimulate serotonin neurons to inhibit binge-like eating in mice. *J. Clin. Invest.* 124, 4351–4362. doi: 10.1172/jci74726

Collins, J., Meng, C., and Eng, A. (2016). Psychological impact of severe obesity. *Curr. Obes. Rep.* 5, 435–440. doi: 10.1007/s13679-016-0229-4

Czyzyk, T. A., Sahr, A. E., and Statnick, M. A. (2010). A model of binge-like eating behavior in mice that does not require food deprivation or stress. *Obesity (Silver Spring)* 18, 1710–1717. doi: 10.1038/oby.2010.46

Dandona, P., Aljada, A., and Bandyopadhyay, A. (2004). Inflammation: the link between insulin resistance, obesity and diabetes. *Trends Immunol.* 25, 4–7. doi: 10.1016/j.it.2003.10.013

Davis, C. (2017). A commentary on the associations among 'food addiction', binge eating disorder, and obesity: overlapping conditions with idiosyncratic clinical features. *Appetite* 115, 3–8. doi: 10.1016/j.appet.2016.11.001

de Zwaan, M. (2001). Binge eating disorder and obesity. *Int. J. Obes. Relat. Metab. Disord.* 25(Suppl. 1), S51–S55.

Deacon, R. M. (2006). Digging and marble burying in mice: simple methods for in vivo identification of biological impacts. *Nat. Protoc.* 1, 122–124. doi: 10.1038/nprot.2006.20

Felts, A. S., Rodriguez, A. L., Morrison, R. D., Venable, D. F., Manka, J. T., Bates, B. S., et al. (2013). Discovery of VU0409106: a negative allosteric modulator of mGlu5 with activity in a mouse model of anxiety. *Bioorg. Med. Chem. Lett.* 23, 5779–5785. doi: 10.1016/j.bmcl.2013.09.001

Ferrigno, A., Berardo, C., Di Pasqua, L. G., Siciliano, V., Richelmi, P., and Vairetti, M. (2017). Localization and role of metabotropic glutamate receptors subtype 5 in the gastrointestinal tract. *World J. Gastroenterol.* 23, 4500–4507. doi: 10.3748/wjg.v23.i25.4500

Gancheva, S., Galunska, B., and Zhelyazkova-Savova, M. (2017). Diets rich in saturated fat and fructose induce anxiety and depression-like behaviours in the rat: is there a role for lipid peroxidation? *Int. J. Exp. Pathol.* 98, 296–306. doi: 10.1111/iep.12254

Gass, J. T., and Olive, M. F. (2008). Glutamatergic substrates of drug addiction and alcoholism. *Biochem. Pharmacol.* 75, 218–265. doi: 10.1016/j.bcp.2007.06.039

González-Muniesa, P., Mártinez-González, M., Hu, F., Després, J. P., Matsuzawa, Y., Loos, R. J. F., et al. (2017). Obesity. *Nat. Rev. Dis. Prim.* 3, 1–18.

Guardia, D., Rolland, B., Karila, L., and Cottencin, O. (2011). GABAergic and glutamatergic modulation in binge eating: therapeutic approach. *Curr. Pharm. Des.* 17, 1396–1409. doi: 10.2174/138161211796150828

Hill, J. O., and Peters, J. C. (1998). Environmental contributions to the obesity epidemic. *Science* 280, 1371–1374. doi: 10.1126/science.280.5368.1371

Huang, H., Park, P. H., McMullen, M. R., and Nagy, L. E. (2008). Mechanisms for the anti-inflammatory effects of adiponectin in macrophages. *J Gastroenterol. Hepatol.* 23(Suppl. 1), S50–S53.

Huh, J. Y., Park, Y. J., Ham, M., and Kim, J. B. (2014). Crosstalk between adipocytes and immune cells in adipose tissue inflammation and metabolic dysregulation in obesity. *Mol. Cells* 37, 365–371. doi: 10.14348/molcells.2014.0074

Juge-Aubry, C. E., Somm, E., Pernin, A., Alizadeh, N., Giusti, V., Dayer, J. M., et al. (2005). Adipose tissue is a regulated source of interleukin-10. *Cytokine* 29, 270–274.

Kalivas, P. W. (2009). The glutamate homeostasis hypothesis of addiction. *Nat. Rev. Neurosci.* 10, 561–572. doi: 10.1038/nrn2515

Kern, P. A., di Gregorio, G. B., Lu, T., Rassouli, N., and Ranganathan, G. (2003). Adiponectin expression from human adipose tissue: relation to obesity, insulin resistance, and tumor necrosis factor-α expression. *Diabetes* 52, 1779–1785. doi: 10.2337/diabetes.52.7.1779

Kessler, R. M., Hutson, P. H., Herman, B. K., and Potenza, M. N. (2016). The neurobiological basis of binge-eating disorder. *Neurosci. Biobehav. Rev.* 63, 223–238. doi: 10.1016/j.neubiorev.2016.01.013

Koch, C. E., Lowe, C., Legler, K., Benzler, J., Boucsein, A., Böttiger, G., et al. (2014). Central adiponectin acutely improves glucose tolerance in male mice. *Endocrinology* 155, 1806–1816. doi: 10.1210/en.2013-1734

Kopelman, P. (2007). Health risks associated with overweight and obesity. *Obes. Rev.* 8(Suppl. 1), 13–17. doi: 10.1111/j.1467-789x.2007.00311.x

Koros, E., Rosenbrock, H., Birk, G., Weiss, C., and Sams-Dodd, F. (2007). The selective mGlu5 receptor antagonist MTEP, similar to NMDA receptor antagonists, induces social isolation in rats. *Neuropsychopharmacology* 32, 562–576. doi: 10.1038/sj.npp.1301133

Li, B., Shao, D., Luo, Y., Wang, P., Liu, C., Zhang, X., et al. (2015). Role of 5-HT3 receptor on food intake in fed and fasted mice. *PLoS One* 10:e0121473. doi: 10.1371/journal.pone.0121473

Melhorn, S. J., Krause, E. G., Scott, K. A., Mooney, M. R., Johnson, J. D., Woods, S. C., et al. (2010). Acute exposure to a high-fat diet alters meal patterns and body composition. *Physiol. Behav.* 99, 33–39. doi: 10.1016/j.physbeh.2009.10.004

Mihov, Y., Treyer, V., Akkus, F., Toman, E., Milos, G., Ametamey, S. M., et al. (2020). Metabotropic glutamate receptor 5 in bulimia nervosa. *Sci. Rep.* 10:6374.

Murray, S., Tulloch, A., Gold, M. S., and Avena, N. M. (2014). Hormonal and neural mechanisms of food reward, eating behaviour and obesity. *Nat. Rev. Endocrinol.* 10, 540–552. doi: 10.1038/nrendo.2014.91

Nicolas, L. B., Kolb, Y., and Prinssen, E. P. (2006). A combined marble burying-locomotor activity test in mice: a practical screening test with sensitivity to different classes of anxiolytics and antidepressants. *Eur. J. Pharmacol.* 547, 106–115. doi: 10.1016/j.ejphar.2006.07.015

Nigro, E., Scudiero, O., Monaco, M. L., Palmieri, A., Mazzarella, G., Costagliola, C., et al. (2014). New insight into adiponectin role in obesity and obesity-related diseases. *Biomed. Res. Int.* 2014:658913.

Niswender, C. M., and Conn, P. J. (2010). Metabotropic glutamate receptors: physiology, pharmacology, and disease. *Annu. Rev. Pharmacol. Toxicol.* 50, 295–322. doi: 10.1146/annurev.pharmtox.011008.145533

Osborne, M. P., and Olive, M. F. (2008). A role for mGluR5 receptors in intravenous methamphetamine self-administration. *Ann. N. Y. Acad. Sci.* 1139, 206–211. doi: 10.1196/annals.1432.034

Paterson, N. E., and Markou, A. (2005). The metabotropic glutamate receptor 5 antagonist MPEP decreased break points for nicotine, cocaine and food in rats. *Psychopharmacology (Berl)* 179, 255–261. doi: 10.1007/s00213-004-2070-9

Ploj, K., Albery-Larsdotter, S., Arlbrandt, S., Kjaer, M. B., Skantze, P. M., and Storlien, L. H. (2010). The metabotropic glutamate mGluR5 receptor agonist CHPG stimulates food intake. *Neuroreport* 21, 704–708.

Ravussin, E., Lillioja, S., Knowler, W. C., Christin, L., Freymond, D., Abbott, W. G., et al. (1988). Reduced rate of energy expenditure as a risk factor for body-weight gain. *N. Engl. J. Med.* 318, 467–472. doi: 10.1056/nejm198802253180802

Rockwood, G. A., and Bhathena, S. J. (1990). High-fat diet preference in developing and adult rats. *Physiol. Behav.* 48, 79–82. doi: 10.1016/0031-9384(90)90264-5

Rutten, K., Van Der Kam, E. L., De Vry, J., Bruckmann, W., and Tzschentke, T. M. (2011). The mGluR5 antagonist 2-methyl-6-(phenylethynyl)-pyridine (MPEP) potentiates conditioned place preference induced by various addictive and non-addictive drugs in rats. *Addict. Biol.* 16, 108–115. doi: 10.1111/j.1369-1600.2010.00235.x

Saper, C. B., Chou, T. C., and Elmquist, J. K. (2002). The need to feed: homeostatic and hedonic control of eating. *Neuron* 36, 199–211.

Sharma, S., and Fulton, S. (2013). Diet-induced obesity promotes depressive-like behaviour that is associated with neural adaptations in brain reward circuitry. *Int. J. Obes. (Lond)* 37, 382–389. doi: 10.1038/ijo.2012.48

Shigemoto, R., Nomura, S., Ohishi, H., Sugihara, H., Nakanishi, S., and Mizuno, N. (1993). Immunohistochemical localization of a metabotropic glutamate receptor, mGluR5, in the rat brain. *Neurosci. Lett.* 163, 53–57. doi: 10.1016/0304-3940(93)90227-c

Small, D. M. (2012). Flavor is in the brain. *Physiol Behav.* 107, 540–552.

Smith, D. G., and Robbins, T. W. (2013). The neurobiological underpinnings of obesity and binge eating: a rationale for adopting the food addiction model. *Biol. Psychiatry* 73, 804–810. doi: 10.1016/j.biopsych.2012.08.026

Spooren, W. P., Vassout, A., Neijt, H. C., Kuhn, R., Gasparini, F., Roux, S., et al. (2000). Anxiolytic-like effects of the prototypical metabotropic glutamate receptor 5 antagonist 2-methyl-6-(phenylethynyl)pyridine in rodents. *J. Pharmacol. Exp. Ther.* 295, 1267–1275.

Storto, M., Capobianco, L., Battaglia, G., Molinaro, G., Gradini, R., Riozzi, B., et al. (2006). Insulin secretion is controlled by mGlu5 metabotropic glutamate receptors. *Mol. Pharmacol.* 69, 1234–1241. doi: 10.1124/mol.105.018390

Succurro, E., Segura-Garcia, C., Ruffo, M., Caroleo, M., Rania, M., Aloi, M., et al. (2015). Obese patients with a binge eating disorder have an unfavorable metabolic and inflammatory profile. *Medicine (Baltimore)* 94:e2098. doi: 10.1097/md.0000000000002098

Terbeck, S., Akkus, F., Chesterman, L. P., and Hasler, G. (2015). The role of metabotropic glutamate receptor 5 in the pathogenesis of mood disorders and addiction: combining preclinical evidence with human positron emission tomography (PET) studies. *Front. Neurosci.* 9:86. doi: 10.3389/fnins.2015.00086

van den Pol, A. N., Romano, C., and Ghosh, P. (1995). Metabotropic glutamate receptor mGluR5 subcellular distribution and developmental expression in hypothalamus. *J. Comp. Neurol.* 362, 134–150. doi: 10.1002/cne.903620108

Van Gaal, L. F., Mertens, I. L., and De Block, C. E. (2006). Mechanisms linking obesity with cardiovascular disease. *Nature* 444, 875–880. doi: 10.1038/nature05487

Varty, G. B., Grilli, M., Forlani, A., Fredduzzi, S., Grzelak, M. E., Guthrie, D. H., et al. (2005). The antinociceptive and anxiolytic-like effects of the metabotropic glutamate receptor 5 (mGluR5) antagonists, MPEP and MTEP, and the mGluR1 antagonist, LY456236, in rodents: a comparison of efficacy and side-effect profiles. *Psychopharmacology (Berl)* 179, 207–217. doi: 10.1007/s00213-005-2143-4

Wang, X., Moussawi, K., Knackstedt, L., Shen, H., and Kalivas, P. W. (2013). Role of mGluR5 neurotransmission in reinstated cocaine-seeking. *Addict. Biol.* 18, 40–49. doi: 10.1111/j.1369-1600.2011.00432.x

Wood, I. S., de Heredia, F. P., Wang, B., and Trayhurn, P. (2009). Cellular hypoxia and adipose tissue dysfunction in obesity. *Proc. Nutr. Soc.* 68, 370–377. doi: 10.1017/s0029665109990206

Wurtman, J., and Wurtman, R. (2018). The trajectory from mood to obesity. *Curr. Obes. Rep.* 7, 1–5. doi: 10.1007/s13679-017-0291-6

Xu, P., He, Y., Cao, X., Valencia-Torres, L., Yan, X., Saito, K., et al. (2017). Activation of serotonin 2C receptors in dopamine neurons inhibits binge-like eating in mice. *Biol. Psychiatry.* 81, 737–747. doi: 10.1016/j.biopsych.2016.06.005

Yang, T., Liu, Y., Zhao, L., Wang, H., Yang, N., Dai, S.-S., et al. (2017). Metabotropic glutamate receptor 5 deficiency inhibits neutrophil infiltration after traumatic brain injury in mice. *Sci Rep.* 7:9998.

Yen, T. T., Wong, D. T., and Bemis, K. G. (1987). Reduction of food consumption and body weight of normal and obese mice by chronic treatment with fluoxetine: a serotoninre uptake inhibitor. *Drug Dev. Res.* 10, 37–45. doi: 10.1002/ddr.430100106

Conflict of Interest: The authors declare that the research was conducted in the absence of any commercial or financial relationships that could be construed as a potential conflict of interest.

frontiers in Endocrinology

REVIEW
published: 08 March 2021
doi: 10.3389/fendo.2021.650284

Metabolic Regulation of Hypoxia-Inducible Factors in Hypothalamus

Dan Du[1†], *Yugang Zhang*[1†], *Canjun Zhu*[2*], *Hong Chen*[1*] *and Jia Sun*[1*]

[1] Department of Endocrinology, Zhujiang Hospital, Southern Medical University, Guangzhou, China, [2] Guangdong Province Key Laboratory of Animal Nutritional Regulation, College of Animal Science, South China Agricultural University, Guangzhou, China

The earliest hypoxia-inducible factor (HIF) function was to respond to hypoxia or hypoxic conditions as a transcription factor. Recent studies have expanded our understanding of HIF, and a large amount of evidence indicates that HIF has an essential effect on central regulation of metabolism. The central nervous system's response to glucose, inflammation, and hormones' main influence on systemic metabolism are all regulated by HIF to varying degrees. In the hypothalamus, HIF mostly plays a role in inhibiting energy uptake and promoting energy expenditure, which depends not only on the single effect of HIF or a single part of the hypothalamus. In this paper, we summarize the recent progress in the central regulation of metabolism, describe in detail the role of HIF in various functions of the hypothalamus and related molecular mechanisms, and reveal that HIF is deeply involved in hypothalamic-mediated metabolic regulation.

Keywords: energy homeostasis, obesity, hypoxia-inducible factor (HIF), hypothalamus, proopiomelanocortin (POMC)

OPEN ACCESS

Edited by:
Hu Huang,
East Carolina University, United States

Reviewed by:
Yanlin He,
Pennington Biomedical Research Center, United States
Xiaodan Lu,
The People's Hospital of Jilin Province, China

***Correspondence:**
Jia Sun
sunjia@smu.edu.cn
Hong Chen
chenhong123@smu.edu.cn
Canjun Zhu
canjunzhu@scau.edu.cn

[†]These authors have contributed equally to this work and share first authorship

Specialty section:
This article was submitted to Neuroendocrine Science, a section of the journal Frontiers in Endocrinology

Received: *06 January 2021*
Accepted: *29 January 2021*
Published: *08 March 2021*

Citation:
Du D, Zhang Y, Zhu C, Chen H and Sun J (2021) Metabolic Regulation of Hypoxia-Inducible Factors in Hypothalamus. Front. Endocrinol. 12:650284. doi: 10.3389/fendo.2021.650284

INTRODUCTION

The central nervous system (CNS) receives many peripheral signals, including nutrient signals, hormone and gastric vagal afferent signals transmit and integrate peripheral energy information through a complex neural network, regulating peripheral target organs such as adipose tissue, through the nerve-body fluid pathway. The hypothalamus, a part of CNS, contains essential nuclei that function as neuroendocrine cells. It is a key regulator of systemic metabolic homeostasis because it can combine nutritional information with hormonal signals and regulate food intake as well as peripheral metabolism according to energy utilization. Glucose, leptin, insulin, and orexin play a special role in the brain, especially in the hypothalamus. These signals ultimately affect the metabolic capacity or electrical excitability of hypothalamic neurons, thereby regulating the whole body through the hypothalamus.

The metabolism of neurons is closely related to oxygen sensing. Different oxygen concentration will lead to different metabolic states. HIF is a major transcription factor that responds to hypoxia and induces or suppresses genes. HIF is a diploid, which consists of a stable α—subunit and a constitutively expressed beta subunit. There are three subtypes of HIF-α, called HIF-1α, HIF-2α, and HIF-3α (1). There is little research on HIF-3α, but HIF-1α and HIF-2α are described in detail. HIF-1α and HIF-2α are similar in structure, but the former is generally expressed *in vivo*, while the latter is more cell-specific, they both express in the brain. When oxygen is sufficient, the E3 ubiquitin ligase, known as von Hippel Lindau disease tumor suppressor (pVHL), mediates the binding of α—subunit to ubiquitin and causes α—subunit to be degraded by the proteasome (1). Besides, the prolyl hydroxylase domain (PhD) can inhibit HIF-1α through the combination of targeting

degradation and transcriptional inhibition under normoxic conditions (2). These two factors are regarded as the most common regulatory factors of HIF. But many metabolic factors such as glucose (3) and lipid (4–6), also affect the stability and expression of HIF. Functions of HIF are diverse in different organs. For example, overexpression of HIF-1α and HIF-2α is demonstrated to increase hepatic steatosis (7).

Meanwhile, ablation of intestine-specific Hif-2α can reverse high-fat diet (HFD)-induced obesity (2). As for cancer, HIF can promote the growth, invasion and metastasis of cancer cells such as breast cancer (8) and can help the pancreatic cancers metabolize glucose at higher rates that benefit their survival (9). However, HIF is not always a harmful factor in the human body, as it's a crucial protein in CNS and participates in controlling homeostasis of metabolism. The importance of HIF-1α in regulating body weight, liver metabolism and glucose homeostasis is evident (4). It is also pointed out that HIF-2α can affect the energy balance to a certain extent (10). Based on all the available evidences that we will mention below, we can conclude that HIF plays a vital role in hypothalamus-mediated systemic metabolic regulation. In this case, it is of great significance to understand the characteristics of HIF to provide a new and more robust method for the treatment of metabolic diseases. This article reviews the roles of HIF in the hypothalamus-mediated regulation of metabolism.

HYPOXIA-INDUCIBLE FACTORS INDUCED INCREASE OF GLUCOSENSING AND GLUCOSE METABOLISM IN THE HYPOTHALAMUS

Previous studies have shown that HIF deeply takes part in response to hypoxia and inflammation. However, more and more recent studies have shown that HIF can not only regulate its targeted cells but also regulate the metabolic activities of cells in other parts of the body in an indirect but profound way. For example, HIF has been shown to regulate glucose sensing in CNS. As one of the crucial nutritional sensing functions of the central nervous system, glucose sensing should not be ignored when considering metabolic disorders. Both the glucose from food and the glucose produced by the body should be adjusted correctly to maintain balance. It is necessary to study the regulation of glucose sensing and metabolism by HIF *via* CNS.

Unlike the peripheral response of pancreatic cells as the leading way to regulate blood glucose, the hypothalamus is an important part of glucose sensing (11). The process of hypothalamic neurons sensing glucose is called hypothalamic glucose sensing (HGS). Compared with the long-term regulation of hypothalamic hormone on body weight, HGS can quickly and timely regulate metabolic homeostasis.

The particular structure of the hypothalamus determines the high sensitivity and accuracy of HGS, because the arcuate nucleus (ARC) located in the medial basal hypothalamus, which contains the most important glucose-sensing cells we have found so far, mainly POMC neurons and AGRP neurons (12), is very close to the median eminence without the blood-brain barrier (13). This structural basis makes it easier for passive diffusion of body fluid to transmit nutrient and energy signals to neural networks close to the ARC without being limited like other parts of the brain. Thus, ARC can sense changes in peripheral energy metabolism earlier and then transmit information to other regions of the hypothalamus and brain. The HIF complex plays an essential role in the glucose-dependent hypothalamic control of feeding and, energy balance and hypothalamic glucose sensing based on the above structures. We can note that the functional relationship between them is not unidirectional.

Glucose levels can affect HIF in the central nervous system. In the hypothalamus, HIF can be upregulated by glucose to achieve feeding regulation through glucose sensing. There are two pathways, including recruitment of AMPK and mTOR/S6K to regulate HIF-2α protein synthesis and inhibition of PHD to prevent HIF-2α degradation (3). Furthermore, we should know that not only glucose but also its metabolites can regulate HIF in the central nervous system. Pyruvate has been reported to inhibit PHD to stabilize HIF (14). In addition, succinate and fumarate were found to upregulate the protein level of HIF-2α through inhibition of PhD (10). Through these TCA cycle intermediates, increased HIF-2α is involved in hypothalamic glucose sensing.

On the other hand, many studies have shown that HIF can mediate the activity of GLUT, which is an essential glucose channel for mediating life activities. GLUT-1, GLUT-2, and GLUT-4 are all expressed in the brain (15). GLUT-1 mainly exists in microvascular endothelial cells and astrocytes (16), while GLUT-3 and GLUT-4 mainly exist in neurons (17) GLUT-1 is the main glucose transporter in the brain, responsible for promoting glucose transport through BBB (18). Mice that did not express GLUT-2 in the brain had glucagon imbalance, and the re-expression of GLUT-2 in their astrocytes restored the correct control of glucagon levels (19). GLUT is involved in the process of HGS: Based on the description of "neuron sensor" model, neurons absorb glucose through GLUT, and then glucose is metabolized into ATP, which is considered as a factor providing glucose concentration information. It binds and closes the ATP dependent potassium channel (KATP) widely expressed in POMC and AgRP neurons (20), leading to reduced potassium outflow and neuronal depolarization. HIF-1α is a transcription factor of GLUT-1, GLUT-3 (21), and an activator of GLUT-4 (22). Under hypobaric hypoxia, the expression of GLUT-1 was similar to that of HIF-1α (23–25), both of them were upregulated (26). No one has directly studied whether HIF can increase GLUT-2 in the brain, but in the liver, the increase of GLUT-2 is due to the up-regulation of HIF-1α (27), so the similar mechanism in the brain is also worth looking forward to. There is a persuasive evidence that HIF-1α regulates GLUT-4 in the brain: 2 month administration of α-lipoic acid (LA) can inhibit the development of Alzheimer's disease, it can also significantly increase the protein and mRNA levels of GLUT-3, GLUT-4, vascular endothelial growth factor (VEGF) and heme oxygenase-1 (HO-1) in the brain of P301S mice

(a tauopathy and AD mouse model) (28); LA induced activation of brain-derived neurotrophic factor (BDNF)/tyrosine kinase receptor B (TrkB)/HIF-1α signaling pathway may be one of the most important mechanisms during the above process (28).

In general, high glucose levels increase the expression of HIF in glucose sensing cells, which are also appetite control neurons. Increased HIF affects these neurons and reduces glucose intake. The glucose sensitivity of these neurons is at least partly based on the amount of GLUT that can be regulated by HIF. In astrocytes, HIF also increases GLUT and leads to more glucose absorption and sensing, which contributes to correct glucose regulation and reduces systemic glucose levels. In the whole-body glucose regulation process, it is not only the appetite control pathway that plays a role. In addition to adjusting food intake, HGS also participates in energy homeostasis by activating insulin secretion (IS) through vagal nerve. For example, high glucose levels in the hypothalamus stimulate IS and glycogen storage, while preventing hepatic glucose production (29).

HYPOXIA-INDUCIBLE FACTORS INDUCED DECREASE OF HYPOTHALAMUS NF-KB RELATIVE INFLAMMATION

Metabolic disorders are often accompanied by inflammation in CNS (30), which can be caused by infection, high-fat diet (HFD) and hypoxia, among which HFD is the most common cause. Therefore, diet-induced obesity (DIO) in rodent model induced by HFD is one of the most widely used models to study human obesity. In the pursuit of a better treating method for obesity, it is necessary to investigate the hypothalamic inflammatory process caused by HFD. In terms of inflammation, we must mention NF-κB because it is a key protein in inflammation and is always induced by HFD.

The reason why HFD induces inflammation remains controversial. A well-known and compelling explanation is about long-chain saturated fatty acids (SFA), which have the same functional structure as lipopolysaccharide (LPS), which is responsible for binding to TLR4 (a pattern recognition receptor that recognizes molecular patterns associated with pathogens). For NF-κB, some studies have shown that SFAs activates glial proliferation of microglia and astrocytes to regulate inflammatory response (5), in this process, the LPS functional part that is composed of acylated SFA acts on TLR4 to activate NF-κB (**Figure 1**).

The activation of NF-κB induced by HFD can occur in microglia and neurons (5). For microglia, the activation of the NF-κB pathway leads to the recruitment of pro-inflammatory microglia in the hypothalamus and leads to obesity (5, 31, 32). For neurons, HFD causes neuronal stress, insulin sensitivity and leptin sensitivity reduction through the increase of NF-κB signal (33), which in turn weakens appetite inhibition and promotes overeating and intake of more HFD. For the precursor of neurons, the activation of IKKβ/NF-κB in hypothalamic neural stem cells (htNSCs) can prevent neuronal differentiation and induce consumptively damage of htNSCs, and eventually lead to the development of obesity and prediabetes (34). In addition, chronic HFD feeding impairs the function of htNSCs, HFD also activates apoptosis pathways in these cells triggered by IKKβ/NF-κB, which reduces the survival and proliferation of htNSCs (34). The injury of adult htNSCs mediated by IKKβ/NF-κB is an important neurodegenerative process in obesity and related diabetes mellitus (34).

There are at least two pathways *via* which NF-κB can activate HIF. One is an indirect way: in microglia whose main function is to communicate continuously with neurosecretory cells in the hypothalamus through IL-1β and TNF-α (pro-inflammatory cytokines), the activated IKKβ/NF-κB system can upregulate IL-1β and TNF-α, which can stabilize HIF activity by inhibiting PHD enzyme (4). Another is by NF-κB directly activating HIF: this method is not based on the effect on protein structure but is based on the mRNA expression of HIF, which can be promoted by the transport of NF-κB into the nucleus. On the opposite, HIF-1α cannot be effectively transcribed in infection or inflammation when NF-κB gene is deleted. Therefore, in the absence of NF-κB gene, HIF-1α will not have stability or activity even if exposed to adverse factors for a long time (6).

In model organisms Drosophila melanogaster and mammalian cells, the expression of NF-κB-dependent genes is inhibited by HIF-1α, such an inhibitory function is evolutionarily conserved (6). Direct deletion of HIF-1α can lead to increased NF-κB transcriptional activity by mechanisms depend on TAK and IKK as well as CDK6 (6). Inhibition of HIF-1α makes Drosophila more susceptible to death by inflammation after infection, suggesting that HIF-1α is involved in an important process of negative feedback inhibition on the NF-κB dependent defensive mechanism to achieve moderate immunity.

In the central nervous system, microglia are the main responders to LPS (35). For HIF, conditionally knocking out of isoform-specific pyruvate kinase M2 (PKM2) in cells demonstrates that the stabilization of HIF-1α can be achieved by PKM2, a key factor induced by LPS (36, 37). Therefore, LPS is a common upstream regulatory factor of HIF and NF-κB. During the induction by LPS, HIF is more likely to increase at the same time as NF-κB, rather than only after the increase of NF-κB as negative feedback. However, HIF is not the only factor that prevents NF-κB, because, in the absence of HIF, the termination of the NF-κB response still exists, which indicates that all these negative feedback points still exist (6).

Overall, in the hypothalamus, the key site of energy homeostasis regulation, central nervous system response to HFD and a high-sugar diet is primarily a quick upregulation of the NF-κB pathway. Deletion or inhibition of neuronal NF-κB pathway intermediates restores hypothalamic control of energy balance, thereby reducing the incidence of glucose intolerance and DIO (38). There are also many specific mechanisms, with which HIF prevents HFD from damaging the body, remain to be studied, some of which may be different from the crosstalk process we mentioned earlier. For example, in HFD fed mice, inhibition of HIF-1β in ARC resulted in significant weight gain and enhanced energy storage capacity (39).

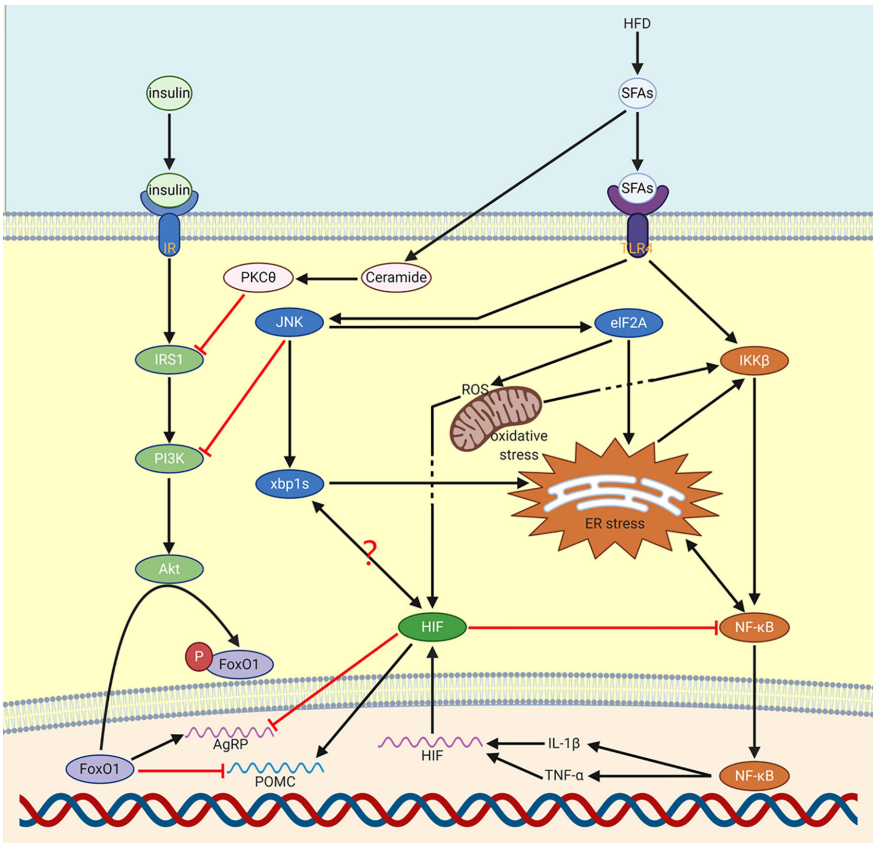

FIGURE 1 | Production of NF-κB *via* HFD. HFD increases NF-κB through SFAs. Through JNK, ER stress can be activated. Meanwhile, NF-κB and ER stress will mediate each other. NF-κB induced IL-1β and TNF-α mediate the expression of HIF. Besides, SFAs induced PKCθ and JNK reduce the function of insulin in CNS. HIF activated POMC reduces food consumption in order to decrease the influence of HFD. On the contrary, AgRP will be inhibited by HIF. It's possible that there is a relation between XBP1s and HIF.

HYPOXIA-INDUCIBLE FACTORS INDUCED REACTIVE OXYGEN SPECIES PRODUCTION DECREASE

Reactive oxygen species (ROS) are quite common substances in cells. The identified source of ROS is the mitochondrial respiratory chain complex. During aerobic respiration, oxygen is relocated to ROS after reacting with electrons. As a matter of fact, ROS can destroy human cells as well as bacteria. But the new role of ROS in diseases and health, especially metabolism, is attracting attention. In various peripheral organs, ROS are known to play a role in many signaling pathways. However, they also have a function in food intake regulation, metabolism and hormone secretion in the hypothalamus by affecting different types of neurons such as POMC and AgRP/NPY neurons (40). Different factors such as adipokines (leptin, apelin, etc.), pancreatic, intestinal hormones, nutrients (glucose, lipids, etc.) and neurotransmitters can affect the release of ROS in the hypothalamus. ROS released in CNS is involved in the development of many diseases, such as type 2 diabetes (T2D) (40).

In the brain, glucose, lipids and other common nutrients have a similar mechanism to induce mitochondrial ROS production in the hypothalamus alongside with an activity raise in mitochondrial respiration, so the central nervous system, after receiving lipid and glucose signals, can cause certain systemic metabolic regulation measures by upregulated ROS.

Also, lipid- Hypothalamic ROS can reduce food intake and increase insulin production. Through parasympathetic outflow, the release of ROS in the hypothalamus can induce an insulin peak after 1–3 min, without change in peripheral blood glucose (40). By using antioxidant molecules to clear ROS production in the brain, insulin secretion induced by brain glucose is significantly disturbed, which demonstrates the regulatory role of hypothalamic ROS in energy metabolism. ROS plays a specific role in different nerve cells. After glucose infused into ventromedial hypothalamus (VMH), through mROS production, the food intake is attenuated when re-feed after overnight fasting for a period (41). In ARC, ROS reduction mediates the activation of NPY/AgRP neurons, while ROS mediates the activation of POMC neurons (42). The ROS with

the strongest effect on POMC neurons seems to be H_2O_2, increasing H_2O_2 can cause depolarization of POMC neurons, and ICV injection of H_2O_2 can cause significant anorexia. Furthermore, only ROS itself can mediate leptin action and restore POMC function (40).

REACTIVE OXYGEN SPECIES INDUCED INCREASE OF HYPOXIA-INDUCIBLE FACTOR STABILITY

As one of the oxygen free radicals, ROS, can also regulate HIF. Low and moderate concentrations of ROS exert their functions, including regulation of HIF, by regulating cellular signaling cascades. It is worth noting that long-term inflammatory process can increase the production of ROS (43), so ROS may also play a role in DIO.

The HIF-α hydroxylation rate partly depends on the level of PhD (44). In the presence of oxygen, Fe2+, 2-oxoglutarate (2-OG) and ascorbic acid (45, 46), PhD enzymes are active and can hydroxylate conserved proline residues of the HIF-α subunit using alpha-ketoglutarate and molecular oxygen as co-substrates, which then lead to HIF-α's proteasomal degradation under non-hypoxic conditions (47, 48). A quick increase in ROS (49)can be observed within the first minute of hypoxia, which helps stabilize HIF-α protein, mainly by oxidizing central Fe(II) to Fe(III) to promote PHD enzyme inactivation (50).

The stabilizing effect of ROS on HIFs is common, H_2O_2 is the most effective ROS to inhibit PHD activity and thus interfere with HIFs degradation (51), while other types of ROS from diverse complexes of mitochondria can stabilize HIF: knockdown of GRIM-19 (NDUFA13), a subunit of complex I, can induce ROS and then stabilize HIF-1α (50). Loss of SDHB, a subunit of the iron-sulfur cluster of complex II, causes HIF stabilization through a ROS-dependent pathway. Furthermore, only SDHB loss can trigger ROS formation and can stabilize HIF in mitochondrial complex II (52). In addition, the ROS of mitochondrial complex III can also stabilize HIF, but it is not clear whether complex III ROS is necessary to induce HIF (53–55). In complex III, RISP knockdown reduced HIF-1α expression and demonstrated a link between HIF and ROS of mitochondrial complex III (56).

There is evidence that HIF can increase the glycolytic rate by upregulating the transcription of glycolytic genes (1), which reduces oxygen consumption and reduces hypoxia-induced stress, then reduces inflammation that can increase ROS. In addition, other studies have shown that mammalian HIF-1α is necessary to control the production of toxic ROS in hypoxia, as HIF-1α can activate pyruvate dehydrogenase kinase 1 (6, 57), a key factor that decreases ROS. But there is another more specific regulatory process: REDD1 protein is an essential HIF-1α effector for regulating activity of mTOR complex 1 (mTORC1) in Drosophila and mammalian cells (58); REDD1 is also a key factor in controlling ROS production under hypoxia (6)—when localizes to the mitochondria, ROS production will be reduced by REDD1 (58). Intuitively, HIF reduces ROS production, but it cannot be considered that HIF and ROS are simply antagonistic to each other. Considering that some functions of HIF and ROS overlap, such as H_2O_2, which has the strongest effect on POMC neurons, is also the most effective ROS to interfere with the degradation of HIF, this strongly indicates that HIF is more suitable to be identified as a downstream factor regulated by ROS, plays a part of the regulatory role caused by ROS, and exerts negative feedback regulation on ROS.

HYPOXIA-INDUCIBLE FACTORS INDUCED INCREASE OF LEPTIN SENSITIVITY

Leptin is produced by peripheral adipose tissue and plays a role in the CNS, which cannot be ignored when investigating the development of metabolic diseases. Leptin signals activate Janus-activated kinase (JAK)-2 through LEPR and promote later signaling through effector cascades, including signal transduction and activators in the phosphatidylinositol 3-kinase (PI3K)/AKT and transcription activator (STAT)-3 pathways, to increase POMC expression and inhibit AGRP expression, thereby promoting satiety to suppress food intake and promote energy expenditure (59). In addition, POMC promotes white fat browning, which can be caused by simultaneous activation of leptin and insulin signaling pathways in POMC neurons (60). Through the activation of POMC, leptin can also increase the secretion of α-MSH, thereby directly activating MC4R in the paraventricular hypothalamic nucleus (PVH), dorsal medial thalamus(DMH) and intermediolateral nucleus (IML), which can mediate the peripheral sympathetic outflow of SNA through direct and indirect signaling processes, ultimately increasing mitochondrial UCP-1 expression and BAT activity, resulting in increased heat production in BAT, which is one of the mechanisms that leptin increases energy expenditure.

Overall, HIF can regulate leptin and insulin simultaneously through several pathways. There are also some independent regulatory pathways for common pathways that regulate both insulin and leptin.

The relationship between HIF and leptin in the central nervous system is less clear than the one between HIF and insulin. According to existing research conclusions, HIF regulates leptin through suppressor of leptin signaling (SOCS), one of the hypothalamic signaling molecules/pathways that have been extensively studied to inhibit obesity-induced leptin resistance (61). This process involves several elements. Activated NF-κB can cause an increase in the expression of SOCS3, which prevents insulin (33) and leptin (62) signaling in the brain. This process is obvious and rapid, once exposed to HFD, overexpression of SOCS3 can be detected in AgRP neurons, inducing energy imbalance, leptin, and insulin resistance, and hyper-appetite (63). According to our conclusion, if HIF reduces NF-κB, then SOCS3 will also be reduced by HIF, then leptin and insulin sensitivity will increase. In addition, HIF can increase leptin and insulin sensitivity by reducing ER stress, which conversely regulates HIF through the PI3K/AKT pathway, as we will describe in the insulin section later.

HYPOXIA-INDUCIBLE FACTORS INDUCED INCREASE OF INSULIN SENSITIVITY

Insulin is one of the most critical hormones in the development of metabolic diseases. Insulin affects systemic metabolism and has special effects on the hypothalamus. In the peripheral body part, when blood glucose rises, insulin is released from pancreatic β cells and enters the central nervous system through the blood-brain barrier. In the central nervous system, insulin receptors can be found throughout the brain, especially in neurons of the hypothalamus, where insulin mainly acts on POMC and AgRP/NPY neurons of ARC. Through ligand-induced stimulation, insulin upregulates POMC expression and reduces food intake (4). Knockdown of insulin receptors in the central nervous system leads to gender-specific mild obesity, and obese males are resistant to insulin-mediated anorexia function imply both peripheral and central insulin resistance are included in the development of obesity (20).

HIF is one of the downstream pathways of insulin function. Indeed, both insulin and leptin can regulate HIF through the common PI3K/AKT pathway. Here, we will discuss the detailed process.

PI3K/AKT/mTOR signaling pathway is one of the main upstream regulatory pathways of HIF-1α. Through this pathway, not only the synthesis of new HIF-1α protein is increased due to the increase of translation, but also Hsp90, which maintains the stability of HIF-1α protein to prevent its degradation, is also activated and enhanced (64). The pathway itself has negative feedback, activated AKT can increase the expression of mTOR, and chronic activation of mTOR complex 1 (mTORC1) signal transduction can inhibit IRS-1, then Akt signal transduction will be reduced (65) (**Figure 2**).

MTOR can be considered as an important part of energy homeostasis regulated by CNS because it is a downstream target of PI3K pathway stimulated by insulin and has the function of regulating glucose/lipid homeostasis, body weight and energy consumption through hypothalamus (66). These functions are embodied in the hypothalamus mTORC1 through reducing the expression of AgRP and NPY, thereby reducing food intake and body weight. On the contrary, over nutrition down-regulates the activity of mTORC1 in the hypothalamus, and then causes leptin

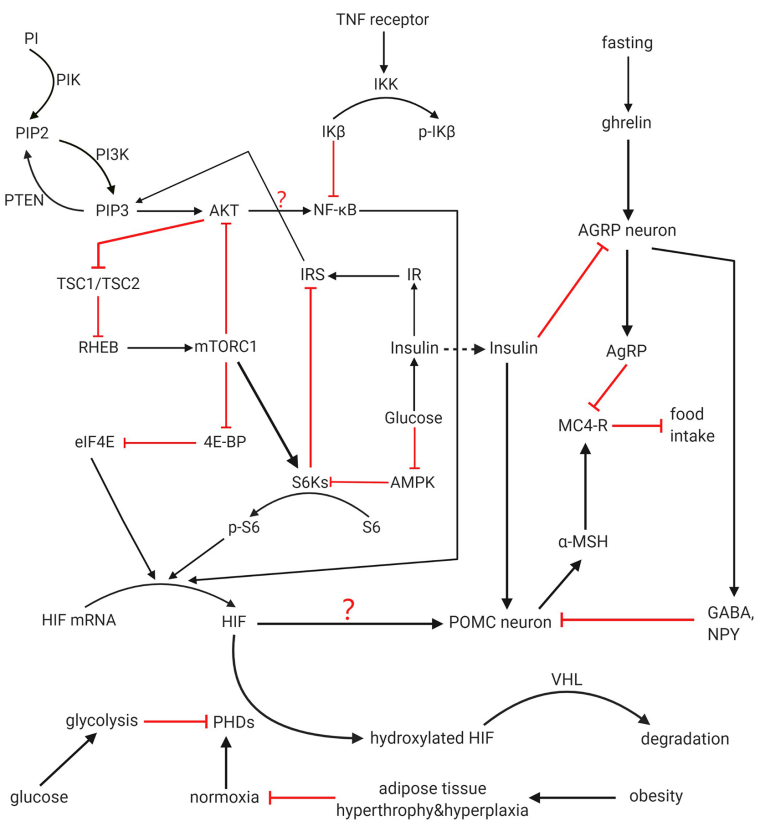

FIGURE 2 | HIF regulation and function on POMC. PI3K pathway, HIF-PHD-VHL pathway and mTOR/NF-kB/HIF pathway all participates in regulation of HIF. Crosstalk among these pathways is not completely clear. PI3K, mTOR, and NF-kB can increase expression of HIF, while PHD negatively regulate HIF and promote its degradation with VHL as a cofactor. Hypoxia among adipocytes caused by obesity downregulated the activity of PHDs. HIF works as one of the activators of POMC gene that prevent food intake. Whether the feedback from IRS to PIP3 and the function from AKT to NF-kB can finally influence the activity of HIF is not clear and demand further study. Whether these upstream activated HIF can activate all the functional effects of POMC has not been directly stated in previous articles, and it is for further study.

resistance, weight gain and excessive appetite. According to the existing studies, there is a significant relationship between mTOR and HIF. mTOR can directly improve the translation rate of HIF-1α mRNA through 5'oligopyrimidine nucleotide sequence, thus promoting the expression of HIF-1α. MTOR/S6K can promote HIF-2α protein synthesis, as the increased S6K activity will lead to the up-regulation of HIF-2α in hypothalamus when glucose is provided (3). In addition, mTORC1 can phosphorylate the binding protein 1 (4E-BP1) of eukaryotic initiation factor 4E (eIF4E) to terminate the inhibition of the latter by the former (67), then the expression of HIF will be promoted by the release of eIF4E (**Figure 3**).

HIF does assist in insulin's activity in multiple ways. In addition to inhibiting SOCS3, there are at least two methods. After stimulating the CNS with insulin, the level of HIF-2α protein in the hypothalamus of young mice increased rapidly compared with aged mice, while the activation of IR/IRS-2/Akt/FoxO1 pathway in aged mice and young mice was similar (10). This indicates the mechanism that age decreases the level of upregulating HIF-2α mediated by insulin may adopt another pathway different from IR/IRS-2/Akt/FoxO1. Like the ageing mice, HIF-2α is not increasing that much in short-term DIO mice (10). According to the analysis of physiology and molecular structure, HIF-2α can maintain the function of central insulin and promote the expression of the POMC gene. These results suggest that HIF-2α knockout in POMC neurons can cause insulin resistance and glucose intolerance, and lead to age-dependent weight gain and fat gain.

Secondly, HIF can increase insulin and leptin sensitivity by reducing endoplasmic reticulum (ER) stress. Unfolded protein response (UPR) caused by ER dysfunction is known as ER stress, which is related to metabolic diseases including insulin resistance and obesity (5) because induced ER stress prevents weight loss and anorexic functions of insulin and leptin (68). Considering that UPR may promote HIF through inositol-requiring enzyme 1α (IRE1α)-X box-binding protein 1 (XBP1) (69, 70), while IKK/NF-κB and ER stress promote each other and induce energy imbalance leading to obesity during HFD feeding (68), it can be inferred that HIF can act as downstream negative feedback to inhibit NF-κB in the process of ER stress, so as to reduce the adverse effects of this stress.

INCREASING OF SPONTANEOUS PHYSICAL ACTIVITY BY OREXIN *VIA* INDUCED INCREASE OF INSULIN SENSITIVITY

The hypothalamic neuropeptides orexin-A and orexin-B are the cleavage products of prepro-orexin (PPO). The immunoreactive neurons to OXA and OXB antibodies were mainly located in the

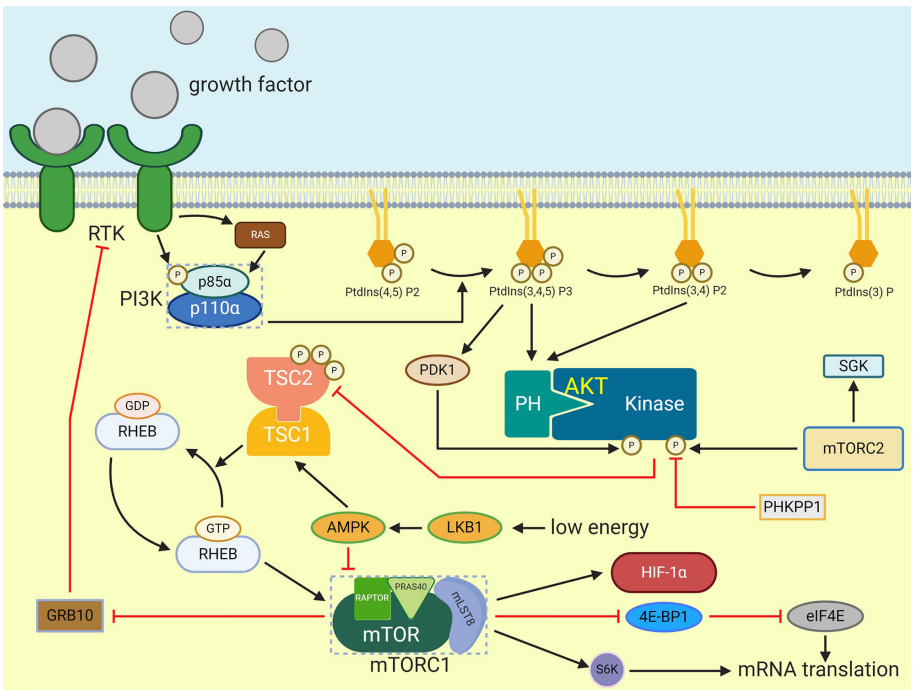

FIGURE 3 | Activation of mTORC1. Extracellular signals such as growth factor can stimulate receptor that activate PI3K which will cause PIP3 generation. PIP3 then activate AKT by phosphorylation. TSC2 is phosphorylated by AKT and then inactivate TSC1/TSC2 complex which prevent RHEB activation. After that, GTP-bounded RHEB will activate mTORC1. eIF4E-binding protein 1 and S6K can be phosphorylated by activated mTORC1, and they can enhance mRNA translation. HIF-1α is one of the mTORC1 effectors.

dorsomedial (DMH), lateral (LH) and perifornical hypothalamus (PeF) of rat, human and pig (71–73). In situ hybridization data showed that OXRs (orexin receptor-1 and -2) were widely located in the brainstem, cerebral cortex, hypothalamus and thalamus (74, 75).

There is an obvious relationship between orexin-A, orexin B and hypothalamic neuropeptides, as orexin responds to metabolic, limbic, and circadian stimuli by activating cholinergic and monoaminergic neurons in the brainstem and hypothalamus to maintain wakefulness or sleep or alertness (76), sense nutrients and regulate appetite (77). Via these processes, orexin enables the living body to achieve various changes that should be made to adapt to the environment and regulate the organism itself.

Among this series of adaptive and regulatory roles, another review highlights the ability of orexin-A to take part in counteracting the brain mechanisms responsible for obesity (78). Spontaneous physical activity (SPA) is positively correlated with obesity resistance, during SPA, the increase of non-exercise activity thermogenesis (NEAT) is the main mechanism (79). Second, there is evidence of orexin ability to increase NEAT (78). By combining these two facts, the potential of orexin in combating obesity cannot be denied. According to the above viewpoints, orexin is of great concern to researchers who want to study the mechanisms involved in combating obesity.

For a long time, many experiments have found that HIF is related to cancer and hypoxia. However, OXA has recently been proved to increase HIF-1α activity by downregulating VHL and increasing the transcription of HIF-1α gene to induce the expression of HIF-1α (77, 78). The increase of HIF-1α can also be achieved by OXA in a more indirect but specific way: OXA has been proved to activate mitogen-activated protein kinase (MAPK) pathway. Higher MAPK activity can make mice express higher levels of peroxisome proliferator-activated receptor-gamma coactivator 1 alpha (PGC-1α) in skeletal muscle. The latter is expressed throughout the brain, and its changes are associated with obesity, diabetes mellitus, pathological changes such as chronic neurodegenerative diseases (78). PGC-1α is involved in regulating HIF-1α in peripheral tissues (80), and it is speculated that the same process can be done in the hypothalamus (78). Orexin mediated HIF-1α activation leads to higher glycolysis activity and increased glucose uptake; it is an important transcription factor in mediating hormone-induced arousal and starvation (77). Data from several independent *in vitro* and rodent models support the hypothesis that OXA mediated increase of energy consumption suggests orexin's obesity resistance may be partially dependent on signaling cascades involving MAPK, PGC-1α, and HIF-1α, regulation of these pathways ultimately induces increased SPA and obesity resistance (78). In addition, anoxia induced orexin function decreasing was identified as one of the functions of HIF. Orexin reduces the expression of lactate dehydrogenase A (LDHA) and pyruvate dehydrogenase kinase 1 (PDK1) genes (LDHA converted pyruvate to lactic acid, while PDK1 phosphorylated PDH, both of which promoted pyruvate flow through anaerobic glycolysis), and when HIF-1α was knocked down, ldhA and PDK1 gene expression were even lower (77).

CONCLUSION

HIF plays an important role in hypothalamus regulation and affects systemic metabolism. Nutrition sensing, hormone induction, metabolic regulation and appetite regulation are important functions of HIF that have been discovered.

Neural cells based mainly in ARC control appetite and energy expenditure, loss of HIF will at least partially disturb these controls. However, it is not sure if appetite and energy expenditure are modulated by neurons *via* the same mechanism; after all, the target organs are different. The importance of HIF in AGRP neurons has not been studied. In addition, glucose is demonstrated to influence the stability of HIF protein, but the relation between central HIF and other nutrients like lipids and amino acids is unclear. Hence, future studies are still necessary to answer these questions.

Although most of our understanding of the physiological principles and therapeutic potential of the HIF pathways comes from laboratory studies, information obtained from these non-clinical trials will provide *in vivo* pharmacological information on agents that mimic or regulate the function of HIF. From these known contents, we can also infer that HIF has the potential to become a focus in metabolic research. This is an exciting period based on our rapidly evolving understanding of the central nervous system's role in regulating metabolism and energy balance throughout the body. Given the evidence that HIF plays an essential role in the central regulation of metabolism, the multiple effects of related drugs on metabolic diseases are likely to become an important clinical research field soon. More pharmacological, biological, and clinical experiments should be carried out to study the details of molecular signal transduction and the mechanisms involved in changing cellular responses caused by HIF in the hypothalamus and any other relevant parts of the CNS. The relation between these factors is not fully clear. A better understanding of the upstream factors that regulate hypothalamic activity can provide more options for preventing obesity and many other related metabolic diseases in the future.

AUTHOR CONTRIBUTIONS

All authors have debated the proposed scope and content of the article before drafting. All authors contributed to the article and approved the submitted version.

FUNDING

This study was supported by the National Natural Science Foundation of China (81974117) and (81774035); Guangdong Basic and Applied Basic Research Foundation (Grant No. 2019A1515010665).

ACKNOWLEDGMENTS

We would like to thank Professor Gang Shu for his valuable work of correction on review. Figures were created with BioRender.com.

REFERENCES

1. Taylor CT, Colgan SP. Regulation of immunity and inflammation by hypoxia in immunological niches. *Nat Rev Immunol* (2017) 17(12):774–85. doi: 10.1038/nri.2017.103
2. Xie C, Yagai T, Luo Y, Liang X, Chen T, Wang Q, et al. Activation of intestinal hypoxia-inducible factor 2α during obesity contributes to hepatic steatosis. *Nat Med* (2017) 23(11):1298–308. doi: 10.1038/nm.4412
3. Zhang H, Zhang G, Gonzalez FJ, Park SM, Cai D. Hypoxia-Inducible Factor Directs POMC Gene to Mediate Hypothalamic Glucose Sensing and Energy Balance Regulation. *PLoS Biol* (2011) 9(7):e1001112. doi: 10.1371/journal.pbio.1001112
4. Gaspar JM, Velloso LA. Hypoxia Inducible Factor as a Central Regulator of Metabolism – Implications for the Development of Obesity. *Front Neurosci Switz* (2018) 12:813. doi: 10.3389/fnins.2018.00813
5. Seong J, Kang JY, Sun JS, Kim KW. Hypothalamic inflammation and obesity: a mechanistic review. *Arch Pharm Res* (2019) 42(5):383–92. doi: 10.1007/s12272-019-01138-9
6. Bandarra D, Biddlestone J, Mudie S, Müller HAJ, Rocha S. HIF-1α restricts NF-κB-dependent gene expression to control innate immunity signals. *Dis Model Mech* (2015) 8(2):169–81. doi: 10.1242/dmm.017285
7. Minamishima YA, Moslehi J, Padera RF, Bronson RT, Liao R, Kaelin WJ. A feedback loop involving the Phd3 prolyl hydroxylase tunes the mammalian hypoxic response in vivo. *Mol Cell Biol* (2009) 29(21):5729–41. doi: 10.1128/MCB.00331-09
8. Briggs KJ, Koivunen P, Cao S, Backus KM, Olenchock BA, Patel H, et al. Paracrine Induction of HIF by Glutamate in Breast Cancer: EglN1 Senses Cysteine. *Cell* (2016) 166(1):126–39. doi: 10.1016/j.cell.2016.05.042
9. Shukla SK, Purohit V, Mehla K, Gunda V, Chaika NV, Vernucci E, et al. MUC1 and HIF-1alpha Signaling Crosstalk Induces Anabolic Glucose Metabolism to Impart Gemcitabine Resistance to Pancreatic Cancer. *Cancer Cell* (2017) 32(1):71–87. doi: 10.1016/j.ccell.2017.06.004
10. Wang Z, Khor S, Cai D. Age-dependent decline of hypothalamic HIF2α in response to insulin and its contribution to advanced age-associated metabolic disorders in mice. *J Biol Chem* (2019) 294(13):4946–55. doi: 10.1074/jbc.RA118.005429
11. López-Gambero AJ, Martínez F, Salazar K, Cifuentes M, Nualart F. Brain Glucose-Sensing Mechanism and Energy Homeostasis. *Mol Neurobiol* (2019) 56(2):769–96. doi: 10.1007/s12035-018-1099-4
12. Abizaid A, Horvath TL. Brain circuits regulating energy homeostasis. *Regul Pept* (2008) 149(1–3):3–10. doi: 10.1016/j.regpep.2007.10.006
13. Kalra SP, Dube MG, Pu S, Xu B, Horvath TL, Kalra PS. Interacting appetite-regulating pathways in the hypothalamic regulation of body weight. *Endocr Rev* (1999) 20(1):68–100. doi: 10.1210/edrv.20.1.0357
14. Virtue S, Vidal-Puig A. Nothing Iffy about HIF in the Hypothalamus. *PloS Biol* (2011) 9(7):e1001116. doi: 10.1371/journal.pbio.1001116
15. Mueckler M, Thorens B. The SLC2 (GLUT) family of membrane transporters. *Mol Aspects Med* (2013) 34(2-3):121–38. doi: 10.1016/j.mam.2012.07.001
16. Simpson IA, Appel NM, Hokari M, Oki J, Holman GD, Maher F, et al. Blood-brain barrier glucose transporter: effects of hypo- and hyperglycemia revisited. *J Neurochem* (1999) 72(1):238–47. doi: 10.1046/j.1471-4159.1999.0720238.x
17. Simpson FMSJ. Glucose transporter proteins in brain. *FASEB J* (1994) 8 (13):1003–11. doi: 10.1096/fasebj.8.13.7926364
18. García-Cáceres C, Quarta C, Varela L, Gao Y, Gruber T, Legutko B, et al. Astrocytic Insulin Signaling Couples Brain Glucose Uptake with Nutrient Availability. *Cell* (2016) 166(4):867–80. doi: 10.1016/j.cell.2016.07.028
19. Marty N. Regulation of glucagon secretion by glucose transporter type 2 (glut2) and astrocyte-dependent glucose sensors. *J Clin Invest* (2005) 115 (12):3545–53. doi: 10.1172/JCI26309
20. Belgardt BF, Okamura T, Brüning JC. Hormone and glucose signalling in POMC and AgRP neurons. *J Physiol* (2009) 587(22):5305–14. doi: 10.1113/jphysiol.2009.179192
21. Denko NC. Hypoxia, HIF1 and glucose metabolism in the solid tumour. *Nat Rev Cancer* (2008) 8(9):705–13. doi: 10.1038/nrc2468
22. Sakagami H, Makino Y, Mizumoto K, Isoe T, Takeda Y, Watanabe J, et al. Loss of HIF-1α impairs GLUT4 translocation and glucose uptake by the skeletal muscle cells. *Am J Physiol: Endocrinol Metab* (2014) 306(9):E1065–76. doi: 10.1152/ajpendo.00597.2012
23. Harik N, Harik SI, Kuo NT, Sakai K, Przybylski RJ, LaManna JC. Time-course and reversibility of the hypoxia-induced alterations in cerebral vascularity and cerebral capillary glucose transporter density. *Brain Res* (1996) 737(1-2):335–8. doi: 10.1016/0006-8993(96)00965-1
24. Kuo NT, Benhayon D, Przybylski RJ, Martin RJ, LaManna JC. Prolonged hypoxia increases vascular endothelial growth factor mRNA and protein in adult mouse brain. *J Appl Physiol (1985)* (1999) 86(1):260–4. doi: 10.1152/jappl.1999.86.1.260
25. Xu F, Severinghaus JW. Rat brain VEGF expression in alveolar hypoxia: possible role in high-altitude cerebral edema. *J Appl Physiol (1985)* (1998) 85 (1):53–7. doi: 10.1152/jappl.1998.85.1.53
26. Chavez JC, Agani F, Pichiule P, LaManna JC. Expression of hypoxia-inducible factor-1alpha in the brain of rats during chronic hypoxia. *J Appl Physiol (1985)* (2000) 89(5):1937–42. doi: 10.1152/jappl.2000.89.5.1937
27. Sacramento JF, Ribeiro MJ, Rodrigues T, Guarino MP, Diogo LN, Seiça R, et al. Insulin resistance is associated with tissue-specific regulation of HIF-1α and HIF-2α during mild chronic intermittent hypoxia. *Respir Physiol Neurobiol* (2016) 228:30–8. doi: 10.1016/j.resp.2016.03.007
28. Zhang Y, Yan X, Xu S, Pang Z, Li L, Yang Y, et al. α-Lipoic Acid Maintains Brain Glucose Metabolism via BDNF/TrkB/HIF-1α Signaling Pathway in P301S Mice. *Front Aging Neurosci* (2020) 12:262. doi: 10.3389/fnagi.2020.00262
29. Desmoulins L, Chrétien C, Paccoud R, Collins S, Cruciani-Guglielmacci C, Galinier A, et al. Mitochondrial Dynamin-Related Protein 1 (DRP1) translocation in response to cerebral glucose is impaired in a rat model of early alteration in hypothalamic glucose sensing. *Mol Metab* (2019) 20:166–77. doi: 10.1016/j.molmet.2018.11.007
30. Chen Y, Yu X, Liu K, Gao H, Li Y, Sun T, et al. Inhibition of Hypothalamic Inhibitor κB Kinase β/Nuclear Transcription Factor κB Pathway Attenuates Metabolism and Cardiac Dysfunction in Type 2 Diabetic Rats. *Neuroendocrinology* (2020) 110(11-12):899–913. doi: 10.1159/000504444
31. Andre C, Guzman-Quevedo O, Rey C, Remus-Borel J, Clark S, Castellanos-Jankiewicz A, et al. Inhibiting Microglia Expansion Prevents Diet-Induced Hypothalamic and Peripheral Inflammation. *Diabetes* (2017) 66(4):908–19. doi: 10.2337/db16-0586
32. Valdearcos M, Douglass JD, Robblee MM, Dorfman MD, Stifler DR, Bennett ML, et al. Microglial Inflammatory Signaling Orchestrates the Hypothalamic Immune Response to Dietary Excess and Mediates Obesity Susceptibility. *Cell Metab* (2017) 26(1):185–97. doi: 10.1016/j.cmet.2017.05.015
33. Zhang X, Zhang G, Zhang H, Karin M, Bai H, Cai D. Hypothalamic IKKβ/NF-κB and ER Stress Link Overnutrition to Energy Imbalance and Obesity. *Cell* (2008) 135(1):61–73. doi: 10.1016/j.cell.2008.07.043
34. Li J, Tang Y, Cai D. IKKβ/NF-κB disrupts adult hypothalamic neural stem cells to mediate a neurodegenerative mechanism of dietary obesity and pre-diabetes. *Nat Cell Biol* (2012) 14(10):999–1012. doi: 10.1038/ncb2562
35. Kumar H, Lim J, Kim I, Choi D. Differential regulation of HIF-3α in LPS-induced BV-2 microglial cells: Comparison and characterization with HIF-1α. *Brain Res* (2015) 1610:33–41. doi: 10.1016/j.brainres.2015.03.046
36. Palsson-McDermott EM, Curtis AM, Goel G, Lauterbach MAR, Sheedy FJ, Gleeson LE, et al. Pyruvate Kinase M2 Regulates Hif-1α Activity and IL-1β Induction and Is a Critical Determinant of the Warburg Effect in LPS-Activated Macrophages. *Cell Metab* (2015) 21(1):65–80. doi: 10.1016/j.cmet.2014.12.005
37. Luo W, Hu H, Chang R, Zhong J, Knabel M, O'Meally R, et al. Pyruvate kinase M2 is a PHD3-stimulated coactivator for hypoxia-inducible factor 1. *Cell* (2011) 145(5):732–44. doi: 10.1016/j.cell.2011.03.054
38. Douglass JD, Dorfman MD, Fasnacht R, Shaffer LD, Thaler JP. Astrocyte IKKβ/NF-κB signaling is required for diet-induced obesity and hypothalamic inflammation. *Mol Metab* (2017) 6(4):366–73. doi: 10.1016/j.molmet.2017.01.010
39. Gaspar JM, Mendes NF, Corrêa-da-Silva F, Lima-Junior JCD, Gaspar RC, Ropelle ER, et al. Downregulation of HIF complex in the hypothalamus exacerbates diet-induced obesity. *Brain Behav Immun* (2018) 73:550–61. doi: 10.1016/j.bbi.2018.06.020
40. Drougard A, Fournel A, Valet P, Knauf C. Impact of hypothalamic reactive oxygen species in the regulation of energy metabolism and food intake. *Front Neurosci* (2015) 9:56. doi: 10.3389/fnins.2015.00056
41. Carneiro L, Allard C, Guissard C, Fioramonti X, Tourrel-Cuzin C, Bailbé D, et al. Importance of mitochondrial dynamin-related protein 1 in

hypothalamic glucose sensitivity in rats. *Antioxid Redox Signal* (2012) 17 (3):433–44. doi: 10.1089/ars.2011.4254
42. Andrews ZB, Liu Z, Walllingford N, Erion DM, Borok E, Friedman JM, et al. UCP2 mediates ghrelin's action on NPY/AgRP neurons by lowering free radicals. *Nat 2008* (7206) 454:846–51. doi: 10.1038/nature07181
43. Harrison DG, Bernstein KE. 7 - Inflammation and Immunity in Hypertension. In: GL Bakris, MJ Sorrentino, editors. *Hypertension: A Companion to Braunwald"s Heart Disease*, *3rd ed.* Elsevier (2018). p. 60–69.
44. Di Conza G, Trusso CS, Loroch S, Mennerich D, Deschoemaeker S, Di Matteo M, et al. The mTOR and PP2A Pathways Regulate PHD2 Phosphorylation to Fine-Tune HIF1α Levels and Colorectal Cancer Cell Survival under Hypoxia. *Cell Rep* (2017) 18(7):1699–712. doi: 10.1016/j.celrep.2017.01.051
45. Zhao L, Liu Z, Yang F, Zhang Y, Xue Y, Miao H, et al. Intrabody against prolyl hydroxylase 2 promotes angiogenesis by stabilizing hypoxia-inducible factor-1α. *Sci Rep UK* (2019) 9(1):11861. doi: 10.1038/s41598-019-47891-1
46. Koivunen P, Serpi R, Dimova EY. Hypoxia-inducible factor prolyl 4-hydroxylase inhibition in cardiometabolic diseases. *Pharmacol Res* (2016) 114:265–73. doi: 10.1016/j.phrs.2016.11.003
47. Rey S, Semenza GL. Hypoxia-inducible factor-1-dependent mechanisms of vascularization and vascular remodelling. *Cardiovasc Res* (2010) 86(2):236–42. doi: 10.1093/cvr/cvq045
48. Kaelin WJ, Ratcliffe PJ. Oxygen sensing by metazoans: the central role of the HIF hydroxylase pathway. *Mol Cell* (2008) 30(4):393–402. doi: 10.1016/j.molcel.2008.04.009
49. Hernansanz-Agustín P, Izquierdo-Álvarez A, Sánchez-Gómez FJ, Ramos E, Villa-Piña T, Lamas S, et al. Acute hypoxia produces a superoxide burst in cells. *Free Radical Bio Med* (2014) 71:146–56. doi: 10.1016/j.freeradbiomed.2014.03.011
50. Fuhrmann DC, Brüne B. Mitochondrial composition and function under the control of hypoxia. *Redox Biol* (2017) 12:208–15. doi: 10.1016/j.redox.2017.02.012
51. Dehne N, Brüne B. Sensors, transmitters, and targets in mitochondrial oxygen shortage-a hypoxia-inducible factor relay story. *Antioxid Redox Signal* (2014) 20(2):339–52. doi: 10.1089/ars.2012.4776
52. Guzy RD, Sharma B, Bell E, Chandel NS, Schumacker PT. Loss of the SdhB, but Not the SdhA, Subunit of Complex II Triggers Reactive Oxygen Species-Dependent Hypoxia-Inducible Factor Activation and Tumorigenesis. *Mol Cell Biol* (2008) 28(2):718–31. doi: 10.1128/MCB.01338-07
53. Comito G, Calvani M, Giannoni E, Bianchini F, Calorini L, Torre E, et al. HIF-1α stabilization by mitochondrial ROS promotes Met-dependent invasive growth and vasculogenic mimicry in melanoma cells. *Free Radic Biol Med* (2011) 51(4):893–904. doi: 10.1016/j.freeradbiomed.2011.05.042
54. Klimova T, Chandel NS. Mitochondrial complex III regulates hypoxic activation of HIF. *Cell Death Differ* (2008) 15(4):660–6. doi: 10.1038/sj.cdd.4402307
55. Chua YL, Dufour E, Dassa EP, Rustin P, Jacobs HT, Taylor CT, et al. Stabilization of Hypoxia-inducible Factor-1α Protein in Hypoxia Occurs Independently of Mitochondrial Reactive Oxygen Species Production. *J Biol Chem* (2010) 285(41):31277–84. doi: 10.1074/jbc.M110.158485
56. Brunelle JK, Bell EL, Quesada NM, Vercauteren K, Tiranti V, Zeviani M, et al. Oxygen sensing requires mitochondrial ROS but not oxidative phosphorylation. *Cell Metab* (2005) 1(6):409–14. doi: 10.1016/j.cmet.2005.05.002
57. Kim J, Tchernyshyov I, Semenza GL, Dang CV. HIF-1-mediated expression of pyruvate dehydrogenase kinase: A metabolic switch required for cellular adaptation to hypoxia. *Cell Metab* (2006) 3(3):177–85. doi: 10.1016/j.cmet.2006.02.002
58. Horak P, Crawford AR, Vadysirisack DD, Nash ZM, DeYoung MP, Sgroi D, et al. Negative feedback control of HIF-1 through REDD1-regulated ROS suppresses tumorigenesis. *Proc Natl Acad Sci USA* (2010) 107(10):4675–80. doi: 10.1073/pnas.0907705107
59. Myers MG, Cowley MA, Münzberg H. Mechanisms of leptin action and leptin resistance. *Annu Rev Physiol* (2008) 70:537–56. doi: 10.1146/annurev.physiol.70.113006.100707
60. Dodd GT, Decherf S, Loh K, Simonds SE, Wiede F, Balland E, et al. Leptin and Insulin Act on POMC Neurons to Promote the Browning of White Fat. *Cell* (2015) 160(1-2):88–104. doi: 10.1016/j.cell.2014.12.022
61. Kwon O, Kim KW, Kim MS. Leptin signalling pathways in hypothalamic neurons. *Cell Mol Life Sci* (2016) 73(7):1457–77. doi: 10.1007/s00018-016-2133-1
62. Pedroso J, Ramos-Lobo AM, Donato JJ. SOCS3 as a future target to treat metabolic disorders. *Hormones (Athens)* (2019) 18(2):127–36. doi: 10.1007/s42000-018-0078-5
63. Olofsson LE, Unger EK, Cheung CC, Xu AW. Modulation of AgRP-neuronal function by SOCS3 as an initiating event in diet-induced hypothalamic leptin resistance. *Proc Natl Acad Sci* (2013) 110(8):E697–706. doi: 10.1073/pnas.1218284110
64. Choi YK, Kim C, Lee H, Jeoung D, Ha K, Kwon Y, et al. Carbon Monoxide Promotes VEGF Expression by Increasing HIF-1α Protein Level via Two Distinct Mechanisms, Translational Activation and Stabilization of HIF-1α Protein. *J Biol Chem* (2010) 285(42):32116–25. doi: 10.1074/jbc.M110.131284
65. Albert V, Hall MN. mTOR signaling in cellular and organismal energetics. *Curr Opin Cell Biol* (2015) 33:55–66. doi: 10.1016/j.ceb.2014.12.001
66. Hu F, Xu Y, Liu F. Hypothalamic roles of mTOR complex I: integration of nutrient and hormone signals to regulate energy homeostasis. *Am J Physiol Endocrinol Metab* (2016) 310(11):E994–1002. doi: 10.1152/ajpendo.00121.2016
67. Aoki M, Fujishita T. Oncogenic Roles of the PI3K/AKT/mTOR Axis. *Curr Top Microbiol Immunol* (2017) 407:153–89. doi: 10.1007/82_2017_6
68. Jais A, Brüning JC. Hypothalamic inflammation in obesity and metabolic disease. *J Clin Invest* (2017) 127(1):24–32. doi: 10.1172/JCI88878
69. Bartoszewska S, Collawn JF. Unfolded protein response (UPR) integrated signaling networks determine cell fate during hypoxia. *Cell Mol Biol Lett* (2020) 25:18. doi: 10.1186/s11658-020-00212-1
70. Xia Z, Wu S, Wei X, Liao Y, Yi P, Liu Y, et al. Hypoxic ER stress suppresses β-catenin expression and promotes cooperation between the transcription factors XBP1 and HIF1α for cell survival. *J Biol Chem* (2019) 294 (37):13811–21. doi: 10.1074/jbc.RA119.008353
71. Sakurai T, Amemiya A, Ishii M, Matsuzaki I, Chemelli RM, Tanaka H, et al. Orexins and Orexin Receptors: A Family of Hypothalamic Neuropeptides and G Protein-Coupled Receptors that Regulate Feeding Behavior. *Cell* (1998) 92 (4):573–85. doi: 10.1016/S0092-8674(00)80949-6
72. Thannickal TC, Moore RY, Nienhuis R, Ramanathan L, Gulyani S, Aldrich M, et al. Reduced number of hypocretin neurons in human narcolepsy. *Neuron* (2000) 27(3):469–74. doi: 10.1016/S0896-6273(00)00058-1
73. Ettrup KS, Sørensen JC, Bjarkam CR. The anatomy of the Göttingen minipig hypothalamus. *J Chem Neuroanat* (2010) 39(3):151–65. doi: 10.1016/j.jchemneu.2009.12.004
74. Gotter AL, Webber AL, Coleman PJ, Renger JJ, Winrow CJInternational Union of Basic and Clinical Pharmacology. LXXXVI. Orexin Receptor Function, Nomenclature and Pharmacology. *Pharmacol Rev* (2012) 64 (3):389–420. doi: 10.1124/pr.111.005546
75. Alexandre C, Andermann ML, Scammell TE. Control of arousal by the orexin neurons. *Curr Opin Neurobiol* (2013) 23(5):752–9. doi: 10.1016/j.conb.2013.04.008
76. Sakurai T. The neural circuit of orexin (hypocretin): maintaining sleep and wakefulness. *Nat Rev Neurosci* (2007) 8(3):171–81. doi: 10.1038/nrn2092
77. Sikder D, Kodadek T. The neurohormone orexin stimulates hypoxia-inducible factor-1 activity. *Gene Dev* (2007) 21(22):2995–3005. doi: 10.1101/gad.1584307
78. Butterick TA, Billington CJ, Kotz CM, Nixon JP. Orexin: Pathways to obesity resistance? *Rev Endocr Metab Disord* (2013) 14(4):357–64. doi: 10.1007/s11154-013-9259-3
79. Garland TJ, Schutz H, Chappell MA, Keeney BK, Meek TH, Copes LE, et al. The biological control of voluntary exercise, spontaneous physical activity and daily energy expenditure in relation to obesity: human and rodent perspectives. *J Exp Biol* (2011) 214(Pt 2):206–29. doi: 10.1242/jeb.048397
80. O'Hagan KA, Cocchiglia S, Zhdanov AV, Tambuwala MM, Cummins EP, Monfared M, et al. PGC-1alpha is coupled to HIF-1alpha-dependent gene expression by increasing mitochondrial oxygen consumption in skeletal muscle cells. *Proc Natl Acad Sci USA* (2009) 106(7):2188–93. doi: 10.1073/pnas.0808801106

Conflict of Interest: The authors declare that the research was conducted in the absence of any commercial or financial relationships that could be construed as a potential conflict of interest.

frontiers in Endocrinology

ORIGINAL RESEARCH
published: 16 March 2021
doi: 10.3389/fendo.2021.627343

Transcription Factor TonEBP Stimulates Hyperosmolality-Dependent Arginine Vasopressin Gene Expression in the Mouse Hypothalamus

Dong Hee Kim[1†], Kwang Kon Kim[1†], Tae Hwan Lee[1], Hyejin Eom[1], Jin Woo Kim[1], Jeong Woo Park[1], Jin Kwon Jeong[2] and Byung Ju Lee[1*]*

[1] Department of Biological Sciences, College of Natural Sciences, University of Ulsan, Ulsan, South Korea, [2] Department of Pharmacology and Physiology, School of Medicine & Health Sciences, The George Washington University, Washington, DC, United States

OPEN ACCESS

Edited by:
Hu Huang, East Carolina University, United States

Reviewed by:
Flavio S. J. De Souza, CONICET Institute of Physiology, Molecular Biology and Neurosciences (IFIBYNE), Argentina
Charles Colin Thomas Hindmarch, Queen's University, Canada

***Correspondence:**
Byung Ju Lee
bjlee@ulsan.ac.kr
Jin Kwon Jeong
jinkwon0911@gwu.edu

†These authors have contributed equally to this work and share first authorship

Specialty section:
This article was submitted to Neuroendocrine Science, a section of the journal Frontiers in Endocrinology

Received: *09 November 2020*
Accepted: *17 February 2021*
Published: *16 March 2021*

Citation:
Kim DH, Kim KK, Lee TH, Eom H, Kim JW, Park JW, Jeong JK and Lee BJ (2021) Transcription Factor TonEBP Stimulates Hyperosmolality-Dependent Arginine Vasopressin Gene Expression in the Mouse Hypothalamus. Front. Endocrinol. 12:627343. doi: 10.3389/fendo.2021.627343

The hypothalamic neuroendocrine system is strongly implicated in body energy homeostasis. In particular, the degree of production and release of arginine vasopressin (AVP) in the hypothalamus is affected by plasma osmolality, and that hypothalamic AVP is responsible for thirst and osmolality-dependent water and metabolic balance. However, the osmolality-responsive intracellular mechanism within AVP cells that regulates AVP synthesis is not clearly understood. Here, we report a role for tonicity-responsive enhancer binding protein (TonEBP), a transcription factor sensitive to cellular tonicity, in regulating osmosensitive hypothalamic AVP gene transcription. Our immunohistochemical work shows that hypothalamic AVP cellular activity, as recognized by c-fos, was enhanced in parallel with an elevation in TonEBP expression within AVP cells following water deprivation. Interestingly, our *in vitro* investigations found a synchronized pattern of TonEBP and AVP gene expression in response to osmotic stress. Those results indicate a positive correlation between hypothalamic TonEBP and AVP production during dehydration. Promoter and chromatin immunoprecipitation assays confirmed that TonEBP can bind directly to conserved binding motifs in the 5'-flanking promoter regions of the AVP gene. Furthermore, dehydration- and TonEBP-mediated hypothalamic AVP gene activation was reduced in TonEBP haploinsufficiency mice, compared with wild TonEBP homozygote animals. Therefore, our result support the idea that TonEBP is directly necessary, at least in part, for the elevation of AVP transcription in dehydration conditions. Additionally, dehydration-induced reductions in body weight were rescued in TonEBP haploinsufficiency mice. Altogether, our results demonstrate an intracellular machinery within hypothalamic AVP cells that is responsible for dehydration-induced AVP synthesis.

Keywords: TonEBP, hyperosmolality, arginine vasopressin, hypothalamus, appetite behavior

INTRODUCTION

The fluid and metabolic systems are reciprocally interconnected, and body fluid status, i.e., hydration or dehydration, strongly influences a broad spectrum of metabolic parameters, including food intake, weight gain, and energy expenditure, in both human and non-human species (1–5). Accumulated information points to the central nervous system (CNS) as a key site for crosstalk between the fluid and metabolic systems (6, 7). Within the CNS, the forebrain sensory circumventricular organs (CVOs), including the subfornical organ (SFO) and the organum vasculosum of the lamina terminalis (OVLT), form a complex molecular and cellular machinery that senses fluid information and plasma osmolality (8–12). Synaptic fibers from the SFO and OVLT project into the hypothalamic nuclei, such as the paraventricular (PVN) and supraoptic nuclei (SON) (8, 10, 13–16). Those hypothalamic nuclei have been recognized as the forebrain metabolic center; they integrate central and peripheral water and metabolic information and regulate neuroendocrine outputs, including the production and release of arginine vasopressin (AVP), in response to the body's needs.

In the brain, AVP is synthesized predominantly in magnocellular and parvocellular neurons of the PVN and SON, and then it is translocated and stored in the neurohypophysis (17, 18). Traditionally, the hypothalamic AVP system has been highlighted in the regulation of water homeostasis (3, 10, 19–21). Dehydration causes an increase in blood osmolality as fluid volume is reduced, and that water-restricted condition activates the release of hypothalamic AVP to stimulate the kidneys for water reabsorption (19–21). On the other hand, SFO excitatory neurons predict the body's need for fluid homeostasis following eating and drinking and activate the release of hypothalamic AVP to induce thirst-dependent drinking behavior in awake animals before any change in blood osmolality can occur (8, 10). Therefore, the hypothalamic AVP system plays a central role in both intero-sensory regulation and the rapid anticipatory drinking response that promotes fluid homeostasis (3).

In addition to water homeostasis, hypothalamic AVP is directly implicated in metabolism regulation. Alterations in the plasma AVP concentration are associated with the development of metabolic disorders (4, 5, 22–28). For example, AVP resistance, a chronic elevation in plasma AVP levels and decreased responsiveness of AVP receptors, is a leading factor in the development of obesity caused by increased food intake and impaired glucose metabolism (24). Overactivation of the AVP system is also common in insulin-dependent and -independent diabetic conditions (22, 23, 25) and has been linked with impaired lipid metabolism, insulin and glucose signaling, and energy expenditure (5, 26–28). On the other hand, acute activation of the hypothalamic AVP system in normal conditions increases the plasma AVP level and attenuates food intake (7).

As aforementioned, crosstalk between the water and metabolic systems occurs through the hypothalamic AVP; therefore, hypothalamic AVP is critical in the tight regulation of plasma AVP levels. To date, the mechanisms leading to the release of AVP have been well characterized (19, 21, 27, 29, 30). However, keeping in mind that plasma hyperosmolality is a powerful single stimulator for AVP production, the intracellular molecular mechanisms that activate AVP gene transcription within hypothalamic AVP cells in response to dehydration or increased plasma osmolality remain unclear.

Interestingly, a previous investigation in chickens suggested the possible involvement of tonicity-responsive enhancer binding protein (TonEBP) in hyperosmolality-dependent hypothalamic AVP gene expression (31). TonEBP is a ubiquitously distributed transcription factor that can bind to tonicity-responsive enhancer sites through a Rel-like DNA motif (32). TonEBP activity is stimulated by extracellular hypertonicity and activates the expression of downstream osmoprotective molecules in response to osmotic stress to support the survival and osmoadaptation of cells (32–36). Especially in rat brains, cells producing TonEBP have been detected in the PVN and SON, where AVP cell bodies are also densely distributed. The expression of TonEBP within those nuclei is upregulated by hypertonicity (37). However, no previous investigations have determined whether TonEBP and the AVP gene interact directly or indirectly upstream of dehydration-induced hypothalamic AVP gene transcription.

Therefore, we here investigated whether TonEBP is expressed in AVP neurons in the PVN and SON and whether it regulates AVP gene transcription in response to dehydration-induced hyperosmolality in rodents. Our results demonstrate that 1) expression of TonEBP in the PVN and SON is activated by hyperosmolality, 2) TonEBP can directly bind to the 5' flanking promoter region of the AVP gene, 3) TonEBP stimulates hyperosmolality-dependent hypothalamic AVP gene transcription, and 4) the hypothalamic TonEBP-AVP system is associated with dehydration-induced reductions in body weight. Altogether, our results provide a molecular mechanism for the regulation of osmosensitive AVP gene transcription in hypothalamic AVP cells.

MATERIALS AND METHODS

Animals

Eight-week-old C57BL/6 mice were used for animal experiments, which were conducted in accordance with the regulations of the University of Ulsan for the Care and Use of Laboratory Animals (permission number, BJL-20-050). Mice were housed in a room with a conditioned photoperiod (12-h light/dark cycle; lights on from 6:00 a.m. to 6:00 p.m.) and temperature (22–25°C) and allowed *ad libitum* access to tap water and standard pelleted mouse chow. To identify the *in vivo* effects of TonEBP on AVP mRNA expression in the hypothalamus, heterozygous TonEBP haploinsufficiency [TonEBP (+/-)] mice were used (a kind gift from Dr. H.M. Kwon, UNIST, Ulsan, South Korea). TonEBP knockout animals die during development, so TonEBP haploinsufficiency mice have been used extensively from us and other groups to study the physiological functions of TonEBP *in vivo* (38–44). To determine whether TonEBP

affects dehydration-induced energy homeostasis, drinking water was withdrawn for 48 h, starting at 10:00 a.m., with food available *ad libitum*, and the food intake and body weight of wild and TonEBP haploinsufficiency mice were measured every day for 2 days.

Immunohistochemistry (IHC)

Mice were anesthetized with tribromoethanol and transcardially perfused with phosphate buffer (PB, 0.1 M, pH 7.4), followed by a fresh fixative of 4% paraformaldehyde in PB. Brains were post-fixed overnight at 4°C, sliced to a thickness of 50 μm using a vibratome (VT1000P; Leica Microsystems, Wetzlar, Germany) and reference to the *Mouse Brain Atlas* (Paxinos G and Franklin KBJ, 2001, Academic Press, San Diego, CA, USA) to extract the PVN and SON, which were washed several times in PB. Coronal brain sections were pre-incubated with 0.2% Triton X-100 (T8787, Sigma-Aldrich, St. Louis, MO, USA) in PB for 30 min to permeabilize the tissues and cells. After further washing with PB, the sections were incubated overnight at room temperature (RT) with goat anti-TonEBP antibody (1:1000, Santa Cruz, Dallas, TX, USA, Catalogue No. sc-5501), mouse monoclonal anti-AVP antibody (1:1000, Santa Cruz, Catalogue No. sc-390723), and rabbit anti-c-Fos antibody (1:1000, Millipore, Billerica, MA, USA, Catalogue No. ABE457). The next day, the sections were washed in PB and incubated with the following secondary antibodies for 2 h at RT: Alexa Fluor 594-labeled anti-goat antibody, Alexa Fluor 594-labeled anti-rabbit antibody, or Alexa Fluor 488-labeled anti-mouse antibody (1:2000 each, Life Technologies, Carlsbad, CA, USA). Sections were mounted onto glass slides, and coverslips were placed and sealed with nail polish. Immunofluorescence images were captured using an FV1200 confocal laser-scanning microscope (Olympus America, Inc., Center Valley, PA, USA). The number of immunostained cells from both sides of the PVN and SON was measured manually by an unbiased observer using ImageJ software (National Institutes of Health, Bethesda, MD; http://rsbweb.nih.gov/ij/).

Cell Culture and Transfection

We have utilized mHypoA 2/28 cell line in this study, as this cell line was originally generated from the hypothalamus, and therefore, includes a broad library of hypothalamic neuronal phenotypes (44, 45). mHypoA 2/28 cells (CELLutions Biosystems Inc. Ontario, Canada) were maintained in high-glucose Dulbecco's Modified Eagle Medium (Hyclone, South Logan, UT, USA) supplemented with 10% fetal bovine serum and 100 U/ml penicillin-streptomycin (Hyclone) in a humidified atmosphere with 5% CO_2 at 37°C. When the cells had grown to 70% confluence, they were transiently transfected with expression vectors or small interfering RNA (siRNA) using jetPRIME® reagent (Polyplus, New York, NY, USA): expression vector pCMV-myc containing the TonEBP coding region (a gift from Dr. H.M. Kwon, 500 ng) or control pCMV-myc; TonEBP siRNA (50 nM, sense sequence, 5'-GAC CAU GGU CCA AAU GCA A-3'; antisense sequence, 5'-UUG CAU UUG GAC CAU GGU C-3') or control RNA (50 nM) with a scrambled sequence. pCMV-myc mammalian expression vector was originally developed from Clontech, and general information for this vector is available at http://www.takara.co.kr/file/manual/pdf/PT3282-5.pdf. To determine the effect of osmotic stress on TonEBP and AVP expression, the cells were treated with NaCl (50 or 100 mM) for 24 h, which did not induce cell death.

Real-Time PCR

To determine the effect of TonEBP on AVP expression during dehydration, bilateral punches of the PVN and SON were taken using 1.00 mm needles and referencing the *Stereotaxic Mouse Brain Atlas*. Samples were collected from mice that had been water-deprived for 2 days. Total RNA samples were extracted using the Sensi-TriJol™ reagent (Lugen Sci co., Ltd, Korea, Catalogue No. LGR-1117) according to the manufacturer's instructions. cDNA was synthesized using MMLV reverse transcriptase (Beams Bio., Korea, Catalogue No. #3201). After reverse transcription, real-time PCR analyses were performed with Bright-Green 2X qPCR MasterMix-ROX (abm, Vancouver, Canada) using a StepOnePlus Real-Time PCR System (Applied Biosystems, Thermo Fisher Scientific, Waltham, MA, USA) for ~40 cycles. The target DNA species were amplified by real-time PCR using the following primer sets: TonEBP sense primer, 5'-TGA CCC TTG AAC CAA CTG GA-3'; TonEBP antisense primer, 5'-GGA GCA GAA CCA GTC AA-3'; AVP sense primer, 5'-GCT TGT TTC CTG AGC CTG CT-3'; AVP antisense primer, 5'-GCT CCA TGT CAG AGA TGG CC-3'; β-actin sense primer, 5'-TGG AAT CCT GTG GCA TCC ATG AAA C -3'; β-actin antisense primer, 5'-TAA AAC GCA GCT CAG TAA CAG TCC G -3'. Data were normalized for gene expression using β-actin as an internal control, as an expression pattern of β-actin in our experimental sets did not differ between groups (data not shown). The $2^{-\Delta\Delta CT}$ method (46) was used to analyze the relative quantification of gene expression.

Promoter Assay

To determine whether TonEBP regulates AVP transcription, mHypoA cells were co-transfected with an AVP promoter-luciferase reporter vector and a TonEBP expression vector (300 ng) using jetPRIME® (Polyplus). The 5' flanking region of the rat AVP gene (-2059 to +6 bp) that we used for this promoter analysis was cloned by PCR from rat genomic DNA based on sequence information deposited in the GenBank™ database (accession number: AF112362.1). The 2,065-nucleotide-long PCR product was inserted into a luciferase reporter plasmid (pGL2-promoter vector, Promega, Madison, WI, USA), and its sequence was confirmed by DNA sequencing. This 5' flanking sequence of the rat AVP gene includes 4 conserved core domains (TGGAAANNYNY, N = any nucleotide, Y = pyrimidine nucleotide) for the binding of TonEBP (44). Transfection efficiency was normalized by co-transfecting a β-galactosidase reporter plasmid (pCMV-β-gal; Clontech, Palo Alto, CA) at 100 ng/well. Transfected cells were harvested 24 h after transfection, and luciferase activity was measured using a luciferase reporter assay system (Promega) according to the manufacturer's protocols.

Chromatin Immunoprecipitation (ChIP) Assays

mHypoA 2/28 cells were transiently transfected using jetPRIME® reagent with expression vector pCMV-myc containing the TonEBP coding region or control pCMV-myc. Independently, hypothalamic fragments were also collected from mice subjected to dehydration for 2 days. The detailed procedures and materials for the ChIP assays in this study followed a previous report (47). Briefly, both samples were lysed in 0.3 ml of cell lysis buffer (5 mM PIPES (pH 8.0), 85 mM KCl, 0.5% NP40 and protease inhibitors) for 10 min on ice, and nuclei were extracted and resuspended with nuclear lysis buffer. Chromatin was sheared by sonication and diluted 5-fold in ChIP dilution buffer. The reactions were incubated with 5 µg of rabbit anti-TonEBP antibody (Thermo Scientific, Waltham, MA, USA, Catalogue No. PA1-023) or normal rabbit IgG (Santa Cruz, Catalogue No. sc-2004) at 4°C overnight. Immune complexes were collected by reaction with 60 µl of salmon sperm DNA/protein A agarose and then washed with washing buffer that contained different concentrations of salts (150 mM–500 mM) and 0.25 M LiCl. DNA from the protein–DNA cross-links was extracted by incubating the reactions with extraction solution, and it was further purified with phenol/chloroform. PCR amplification was performed using 30 cycles of 94°C for 30 sec, 53°C for 30 sec, and 72°C for 30 sec, preceded by 94°C for 30 sec and followed by 72°C for 10 min using the following primer sets: TonEBP at -1930, forward, 5'-CCA TTC ATG AAG CAG CAC AG-3'; TonEBP at -1930, reverse, 5'-GGA AAC AGC TTC CTT GGT CA-3'; TonEBP at -1890, forward, 5'-GTT TCT GAC CAA GGA AGC-3'; TonEBP at -1890, reverse, 5'-CAG CAT AAA GTA GTG AAG GGC-3'; TonEBP at -330/-343, forward, 5'-CTG CTC CAA ACG TGC CAG-3'; TonEBP at -330/-343, reverse, 5'- GCC AGC CAT CAG GCT GT-3'.

Western Blotting Analysis

Cytoplasmic as well as nucleus-specific proteins in the PVN and SON were isolated by using the Nucleus and Cytoplasmic extraction kit (Thermo Scientific, Catalogue No. 78833), according to the manufacturer's instruction. Briefly, protein concentration was measured by the Bradford dye-binding assay (Bio-Rad, Hercules, CA, USA, Catalog No. 5000006), and then, equal amount of proteins from each sample were separated by SDS-PAGE, transferred onto the PVDF membranes by electrophoretic transfer. The membrane was blocked with 5% non-fat skim milk in TBS-tween, and then incubated with anti-TonEBP (Santa Cruz, Catalog No. sc-398171; 1:1000 dilution). The membrane was incubated with HRP-conjugated mouse secondary antibody (Cell signaling, Danver, MA, USA, Catalog No. 7076; 1:3000 dilution), and the immunoreactive signals were detected by Chemiluminescent detection reagent (Thermo Scientific, Catalog No. 34095). Protein density was normalized using an anti-Hsc70 antibody (Rockland, Limerick, PA, USA, Catalog No. 200-301-A28; 1:1000 dilution), and ImageJ software was utilized to analyze data.

Statistical Analyses

Statistical analyses were performed in GraphPad Prism 9 software (GraphPad Software, San Diego, CA, USA). All data are expressed as the mean ± SEM. Data were analyzed with a one-way or two-way analysis of variance followed by the Tukey's multiple comparison test for unequal replications. A Student's t test was used to compare the two groups.

RESULTS

Enhanced TonEBP Expression Within Hypothalamic AVP Neurons During Hyperosmolality

The activity of hypothalamic AVP cells, measured using c-Fos immunoreactivity as a molecular marker for cellular activity, is elevated under hyperosmolality conditions in multiple animal models, along with increased levels of AVP gene and protein expression (31, 48, 49). To confirm that observation in our *in vivo* animal model, we induced hyperosmolality with 2 days of water deprivation and measured c-Fos immunoreactivity in AVP cells in the PVN and SON (**Figure 1**). As expected, the activity of AVP cells in both regions was enhanced by water-deprived hyperosmolality compared with euhydrated control mice (average percentage of c-Fos positive AVP cells in the PVN: 88.9% vs. 8.6%, and in the SON: 78.8% vs. 8.6%, in hyperosmolality vs. control, respectively). Furthermore, double IHC was performed to determine whether hyperosmolality-dependent production of TonEBP occurs in hypothalamic AVP cells (**Figure 2**). In line with the findings from studies in chickens, TonEBP immunoreactivity in AVP cells in the PVN and SON was elevated in mice in the hyperosmolality condition compared with the euosmotic control animals (average percentage of TonEBP positive AVP cells in the PVN: 54.0% vs. 13.8%, and in the SON: 68.9% vs. 33.1%, in hyperosmolality vs. control, respectively). Interestingly, the intracellular distribution of TonEBP seemed to differ between the PVN and the SON. It seemed like that TonEBP immunoreactivity was abundantly accumulated in the cytoplasm of PVN AVP cells, while majority of AVP cells in the SON showed a translocation of TonEBP immunoreactivity to the nucleus. However, it was unable for us to quantify cytoplasmic- versus nucleus-specific TonEBP in AVP cells by our immunofluorescence. Therefore, we extracted cytoplasmic- or nucleus-specific proteins from the PVN and SON, and performed western blotting analysis to quantify intracellular subregion-dependent TonEBP proteins following 2 days of dehydration (**Figure 3**). Our results indicated a hyperosmolality-induced increased TonEBP translocation from the cytoplasm to the nucleus, both in the PVN and SON. Although indirect, these results support a possibility of increased intracellular TonEBP translocation to the nucleus of AVP cells in both hypothalamic regions following dehydration.

TonEBP as a Transcriptional Activator of AVP Gene Expression

Next, we used *in vitro* experiments with mHypoA cells to examine the role of TonEBP in AVP gene transcription. The mHypoA cells were transfected with either a TonEBP expression

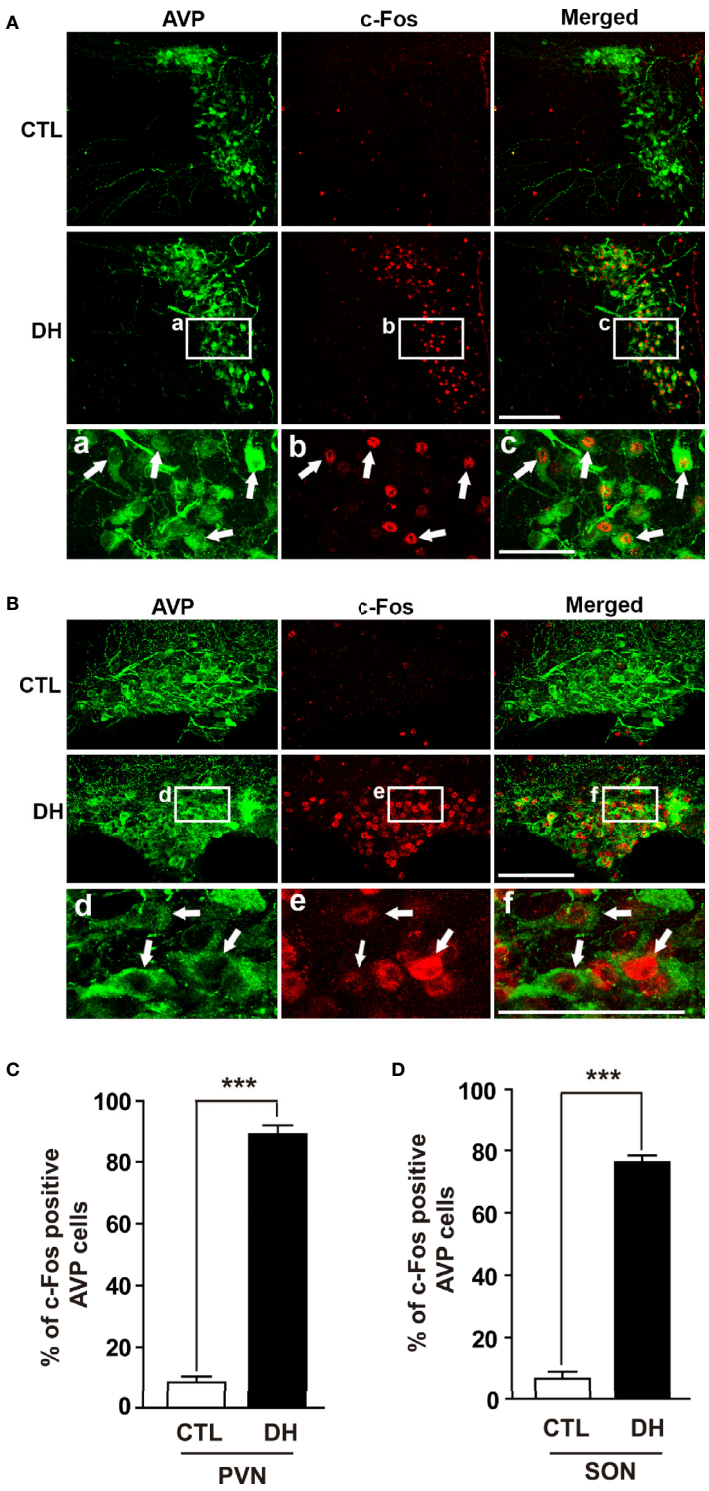

FIGURE 1 | Dehydration-induced elevation of AVP cellular activity in the PVN and SON. Double immunohistochemistry was used to quantify the activity of AVP cells in the PVN and SON in mice deprived of water for 2 days and euhydrated control mice. **(A, B)** Representative images show overall AVP-immunoreactive cells (green) and c-Fos-immunopositive (red) AVP cells in the PVN **(A)** and SON **(B)**. High magnified images from water deprived condition clearly indicate nuclear localization of c-Fos immunoreactivity in the AVP cells with arrows in both regions. **(C, D)** Quantificational analyses clearly demonstrate that dehydration resulted in an increase in c-Fos immunoreactivity within the AVP cells in both regions. CTL, euhydrated control; DH, 2 days of dehydration. N= 3 sections, each with 4 mice. Data are presented as mean ± SEM. ***$p < 0.001$. Scale bar = 100 μm.

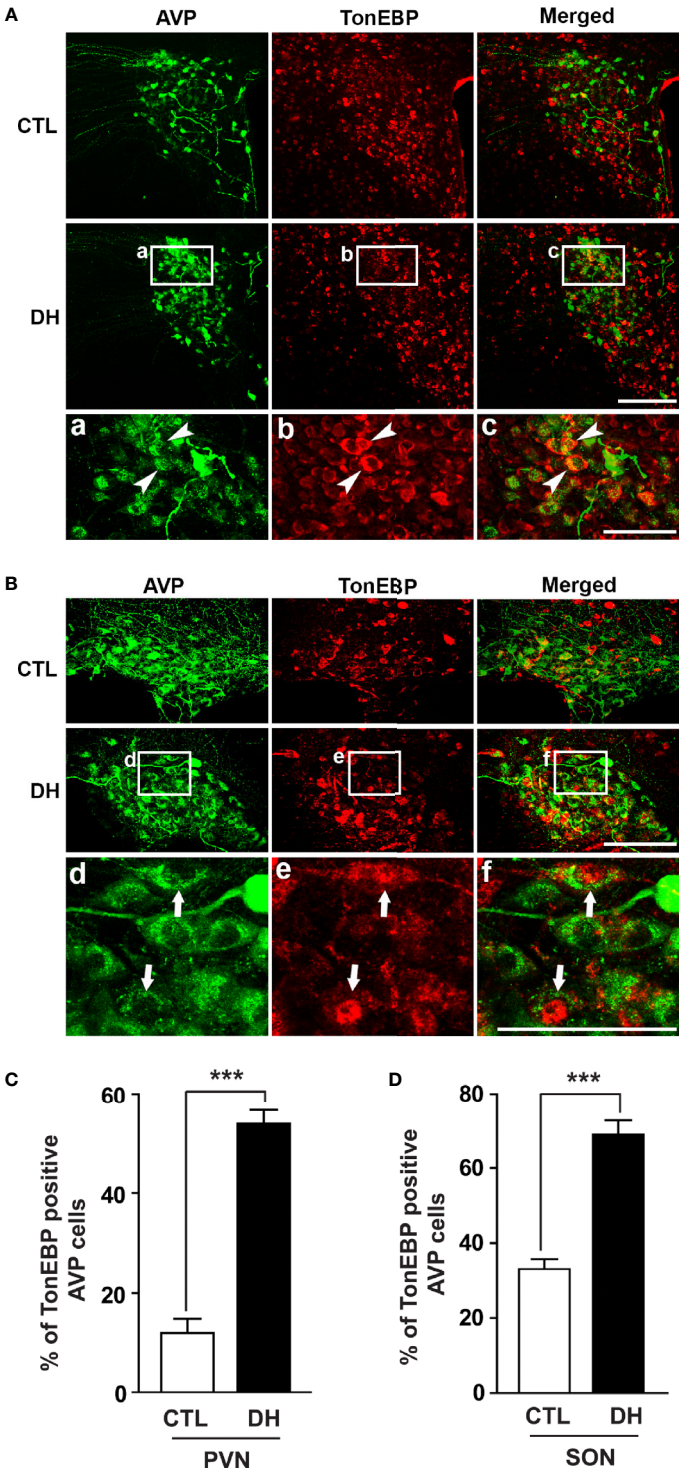

FIGURE 2 | Dehydration-induced elevation in TonEBP expression in AVP cells in the PVN and SON. Double immunohistochemistry was used to quantify the expression of TonEBP in AVP cells in the PVN and SON in mice deprived of water for 2 days and euhydrated control mice. **(A, B)** Representative images show TonEBP-immunoreactive (red) and AVP-immunoreactive cells (green) in the PVN **(A)** and SON **(B)**. Interestingly, high magnified images from dehydration condition indicate TonEBP nuclear translocation in the SON (arrows), but not in the PVN (arrow heads). **(C, D)** Quantificational analyses clearly demonstrate that dehydration resulted in an increase in TonEBP immunoreactivity in the AVP cells in both regions. CTL, euhydrated control; DH, 2 days of dehydration. N= 3 sections, each with 4 mice. Data are presented as mean ± SEM. ***$p < 0.001$. Scale bar = 100 μm.

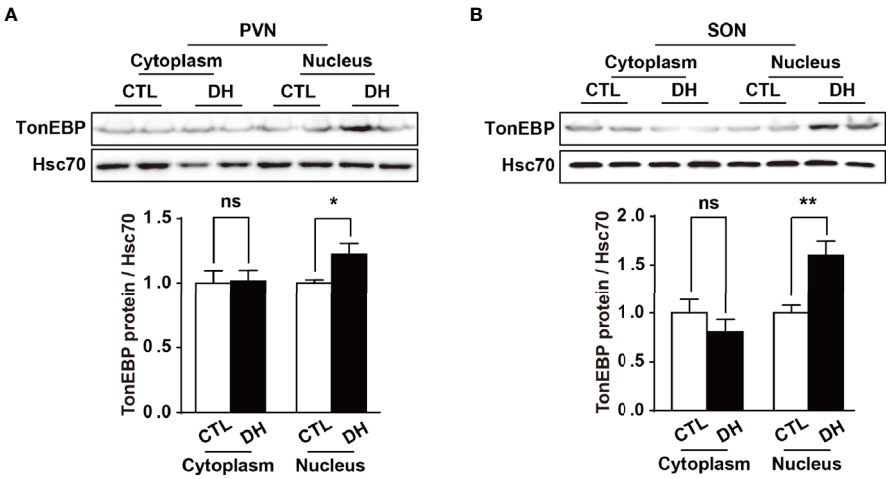

FIGURE 3 | Dehydration-induced nuclear translocation of TonEBP in the PVN and SON. Western blotting analysis was used to quantify cytoplasmic or nucleus TonEBP in the PVN and SON in mice deprived of water for 2 days and euhydrated control mice. Representative images show intracellular region-specific TonEBP proteins in the PVN **(A)** and SON **(B)**, and quantificational analyses demonstrate that dehydration resulted in an increased TonEBP nuclear translocation in both regions. CTL, euhydrated control; DH, 2 days of dehydration; N= 5 mice per group. Data are presented as mean ± SEM. *p < 0.05; **p < 0.01; ns, not significant.

vector or TonEBP siRNA to produce gain-of-function and loss-of-function of TonEBP, respectively, under normal osmotic conditions. A real-time PCR analysis measured the level of gene transcription of both TonEBP and AVP (**Figures 4A, B**). Importantly, the patterns of gene expression for TonEBP and AVP were synchronized with each other, with AVP gene transcription up- or down-regulated as the level of TonEBP moved up or down, respectively (419% in TonEBP mRNA and 280% in AVP mRNA with TonEBP overexpression; 47% in TonEBP mRNA and 43% in AVP mRNA with TonEBP siRNA). Using the same cell line, the gene expression profiles of both TonEBP and AVP were determined in different extracellular hyperosmolality conditions. To induce different degrees of extracellular hyperosmolality, different doses of NaCl were applied to the cell culture medium. As shown in **Figure 4C**, the gene expression of both molecules increased gradually following an increase in osmolality (TonEBP mRNA, 229% and 641% of control with 50 mM and 100 mM NaCl treatment, respectively; AVP mRNA, 344% and 1554% of control with 50 mM and 100 mM NaCl treatment, respectively). These results indicate that TonEBP could act as a transcriptional activator of the AVP gene in a high osmolality environment.

TonEBP Directly Regulates Hyperosmolality-Dependent AVP Gene Expression

Our results clearly demonstrate a positive correlation between TonEBP and AVP expression in response to osmotic stress. The 5'-flanking promoter region of the AVP gene is highly conserved between species, and includes multiple potential TonEBP binding sites as characterized previously (35, 50) (**Supplementary Figures 1** and **2**), so we investigated whether TonEBP can bind directly to the promoter regions of the AVP gene to activate AVP gene transcription. First, we measured AVP promoter activity in response to different levels of TonEBP by analyzing the luciferase activity of the AVP promoter *in vitro*. The activity of the AVP promoter increased in parallel with an increasing amount of transfected promoter-luciferase plasmid, indicating that the AVP promoter was functional in our cell culture conditions (**Figure 5A**). TonEBP expression vectors induced an increase in AVP promoter activity (157% increase over the control) (**Figure 5B**). On the other hand, a TonEBP siRNA–mediated blockade of endogenous TonEBP synthesis lowered the AVP promoter activity (52% of control) (**Figure 5C**). Next, we investigated direct interaction between TonEBP and the AVP promoter region from *in vitro* and *ex vivo* systems using ChIP assay technology (**Figure 5D** and **Supplementary Figure 3**). For ex vivo studies, whereas the control mice had *ad libitum* access to water, the experimental mice underwent 2 days of water deprivation to induce dehydration. Hypothalamic nuclear protein was extracted and precipitated by the TonEBP antibody, and then a set of PCR primers was used to amplify the endogenous binding motifs of the AVP promoter to TonEBP for PCR analysis. Our results demonstrate that TonEBP binds directly to the AVP promoter regions at -1930 and -1890 and between -330 and -343 and that the binding activity was elevated during dehydration (**Supplementary Figure 3**). These findings were further confirmed in *in vitro* system using the mHypoA 2/28 cell line with the expression vector containing the TonEBP coding region, and the results were similar as described above in *ex vivo* experiments (**Figure 5D**). These results indicate that enhanced binding between TonEBP and the AVP gene promoter directly activates dehydration-dependent AVP gene transcription.

To confirm our findings *in vivo*, we adapted a mouse model with TonEBP haploinsufficiency and measured the mRNA levels of TonEBP and AVP in the PVN and SON under dehydration (**Figures 6A, B**). The use of TonEBP haploinsufficiency (+/-) mice is necessary because homozygous TonEBP knockout (-/-) is

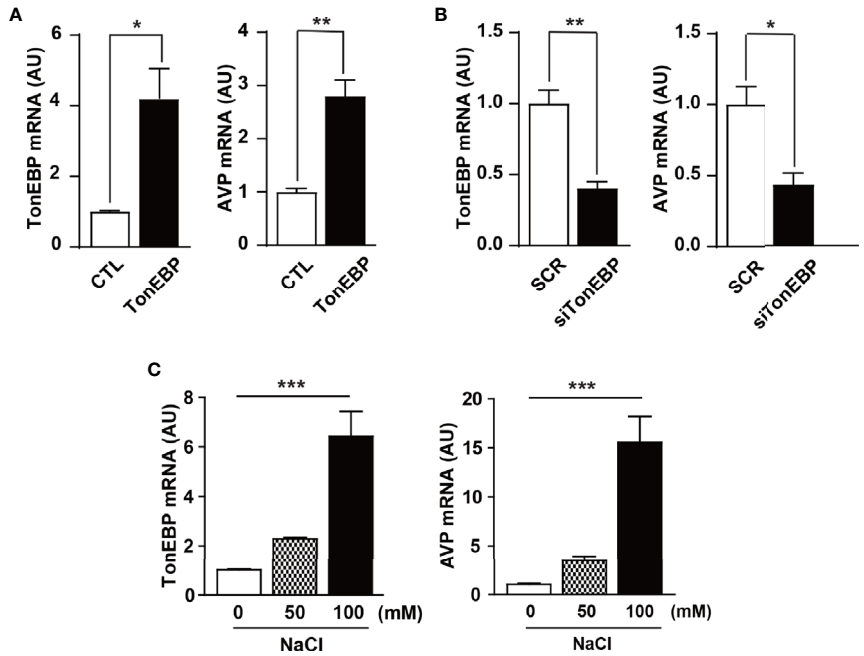

FIGURE 4 | Role of TonEBP in the activation of AVP gene transcription. In *in vitro* experiments, mouse hypothalamic (mHypoA) cells were subjected to real-time PCR to determine interactions between TonEBP and AVP gene transcription. **(A)** The mHypoA cells were transfected with either an expression vector carrying the TonEBP-coding region (500 ng per well) or a control vector for 24 h, and the mRNA expression of TonEBP and AVP was quantified. **(B)** Independently, TonEBP siRNA (siTonEBP, 50 nM per well) or a scrambled control sequence of siRNA (SCR) was transfected into mHypoA cells for 24 h, and the mRNA expression of TonEBP and AVP was quantified. **(C)** Gene transcription of TonEBP and AVP in an environment of osmotic stress was determined in mHypoA cells exposed to different doses of NaCl for 24 h. GAPDH was used as an internal control for all experiments. All data are presented as means ± SEM (n = 6). AU, arbitrary units. *p < 0.05; **p < 0.01; ***p < 0.001.

lethal to animals during development (39). In concert with other results (31), dehydration for 2 days produced a significant increase in mRNA levels of TonEBP in the hypothalamic target regions of the TonEBP (+/+) mice (TonEBP mRNA, 149% of control level in PVN and 210% in SON), but not of the TonEBP (+/-) mice (**Figures 6A, B**), indicating that the entire TonEBP genetic components are necessary in these brain regions for the dehydration-dependent full expression of TonEBP. Importantly, our results further demonstrated a dehydration-induced increase in AVP mRNA levels in the target regions of both animal groups (AVP mRNA from TonEBP (+/+) mice, 382% of control level in PVN and 263% in SON; AVP mRNA from TonEBP (+/-), 332% of control level in PVN and 208% in SON), although a degree of elevation was significantly reduced in TonEBP (+/-) animals (AVP mRNA, 27% reduction to the dehydrated TonEBP (+/+) mice in PVN and 50% reduction in SON). These results suggest an involvement of other mechanisms, together with TonEBP, in the dehydration-dependent AVP gene expression in the PVN and SON. In addition, we investigated a dehydration-induced anorectic effect in TonEBP (+/-) mice (**Figures 6C, D**). Previous investigations, including by our group, have demonstrated that metabolic parameters between TonEBP (+/+) and TonEBP (+/-) mice, such as food intake, body weight gain, glucose and insulin metabolism, and physical activity, are comparable to each other under normal diet conditions (41, 44). However, in this study we found that acute dehydration reduced the daily body-weight gain in the TonEBP (+/+) mice, but not in the TonEBP (+/-) mice [on day 2 of dehydration, -3.4 vs. 0.1 g/day in TonEBP (+/+) mice; -1.6 vs. -1.0 g/day in TonEBP (+/-) mice, dehydrated vs. control, respectively]. Comparing with the daily body-weight changes, the dehydration-dependent daily change in food intake was comparable between the two groups [on day 2 of dehydration, 3.1 vs. 4.0 g/day in TonEBP (+/+) mice; 2.7 vs. 3.8 g/day in TonEBP (+/-) mice, dehydrated vs. control, respectively], although dehydration for 2 days in both animal models showed a considerably reduced food intake when compared to the euhydrated state. These results indicate that TonEBP-dependent hypothalamic AVP synthesis could affect dehydration-induced changes in metabolic parameter.

DISCUSSION

In the brain, AVP-producing cells are densely clustered within the hypothalamic PVN and SON, although scattered AVP cells are also observed in other hypothalamic regions (18). The concentration of AVP in both the brain and plasma depends on the production and release of AVP from those hypothalamic AVP cells. Hypothalamic AVP is strongly implicated in a wide range of physiological processes, including fluid and cardiometabolic homeostasis. For example, deficiency or

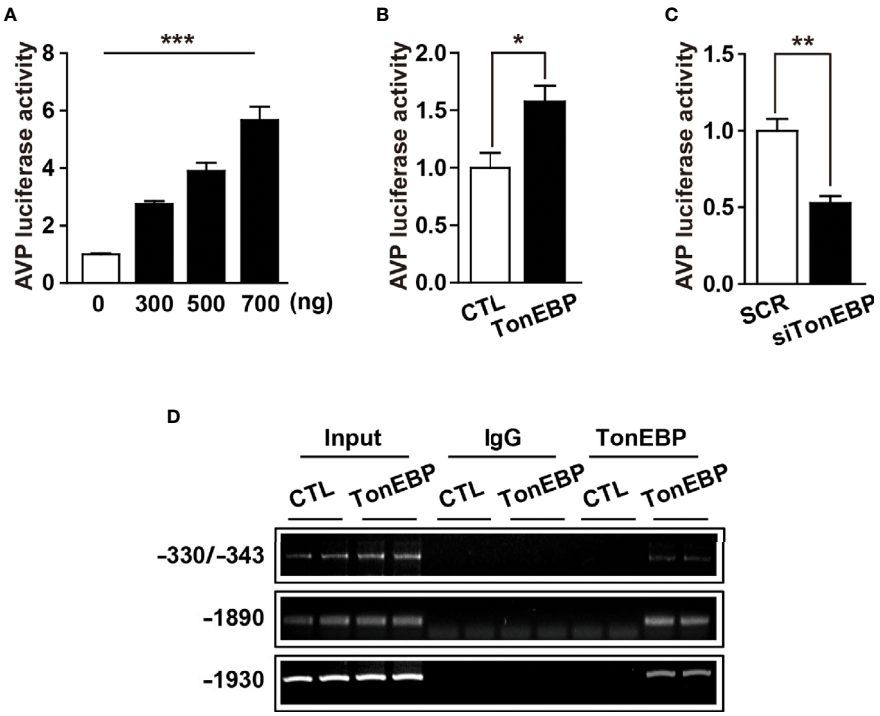

FIGURE 5 | TonEBP binds directly to AVP promoter region and activates dehydration-induced AVP gene transcription. **(A)** Luciferase assays show an increased promoter activity in parallel with an increasing number of AVP-promoter-luciferase constructs. **(B, C)** Luciferase-reporter vectors containing the 5'-flanking region of the AVP gene were co-transfected into mHypoA cells with 500 ng of TonEBP expression vector **(B)**, or 50 nM of TonEBP siRNA/control scrambled sequence **(C)** for 24 h. Then, beta-galactosidase assays were performed to quantify TonEBP-dependent AVP promoter activity. **(D)** ChIP assays were performed to verify whether TonEBP can directly bind to the AVP promoter. Mouse hypothalamic (mHypoA) cells were transiently transfected with pCMV-myc expression vector containing the TonEBP coding region (TonEBP) or control pCMV-myc (CTL), and nuclear DNA samples were immunoprecipitated with TonEBP antibody. Then, PCR amplification was performed using primer sets targeting the indicated TonEBP binding motifs on the AVP gene. Normal rabbit IgG was used as a negative control. All data are presented as means ± SEM (n = 6). $^{**}p < 0.01$; $^{***}p < 0.001$.

overproduction of hypothalamic AVP leads to the development of diabetes insipidus or metabolic problems, including obesity, hypertension, and multiple forms of diabetes, respectively (4, 26, 51–53). Therefore, it is critical to tightly regulate the synthesis, release, and degradation of AVP. Although diverse physiological factors have been found to influence the release of AVP (19–21, 27, 29, 30), it remains unclear what intracellular molecular mechanisms within hypothalamic AVP cells regulate AVP synthesis. Hyperosmolality-sensitive AVP gene activation is of particularly great interest because plasma hyperosmolality is a powerful stimulator of AVP production (54).

In this work, we used *in vitro*, *in vivo*, and *ex vivo* experiments to demonstrate the role of TonEBP in dehydration-dependent hypothalamic AVP gene transcription in rodents. Our results demonstrate synchronized patterns of TonEBP and AVP gene expression in response to osmotic stress. We further found that TonEBP can bind directly to the promoter region of AVP and that TonEBP is responsible for, at least in some degree, dehydration-induced AVP gene expression in the hypothalamic PVN and SON in rodents. This TonEBP-mediated hypothalamic AVP gene expression is necessary for dehydration-dependent body weight loss to occur.

In the rodent brain, TonEBP is widely distributed in neuronal and non-neuronal populations, however, tonicity-dependent induction of TonEBP is observed exclusively in neuronal cells (37). Extracellular hypertonic status induces gene transcription of TonEBP in the hypothalamic PVN and SON (36). Once produced, TonEBP can be rapidly translocated to the nucleus, similar to other transcription factors, to activate the transcription of genes for osmoprotective molecules and protect the cells from osmotic stress (32, 55). In line with other observations (36), our immunohistochemistry results clearly demonstrate an overall dehydration-induced elevation in TonEBP protein in the PVN and SON, especially in the AVP cells in those regions (**Figure 2**). In addition, our results clearly demonstrate an increased TonEBP nuclear translocation in SON AVP cells during dehydration by the localization of TonEBP immunoreactivity (**Figure 2**), western blotting analysis (**Figure 3**), and the results of our ChIP assays (**Figure 5D** and **Supplementary Figure 3**). However, the results of dehydration-induced nuclear translocation of TonEBP in the PVN AVP cells differed from the SON; while abundant TonEBP immunoreactivity following dehydration is observed from our immunohistochemistry, it seemed mostly to be localized in the cytoplasm of AVP cells in this brain region (**Figure 2**). However,

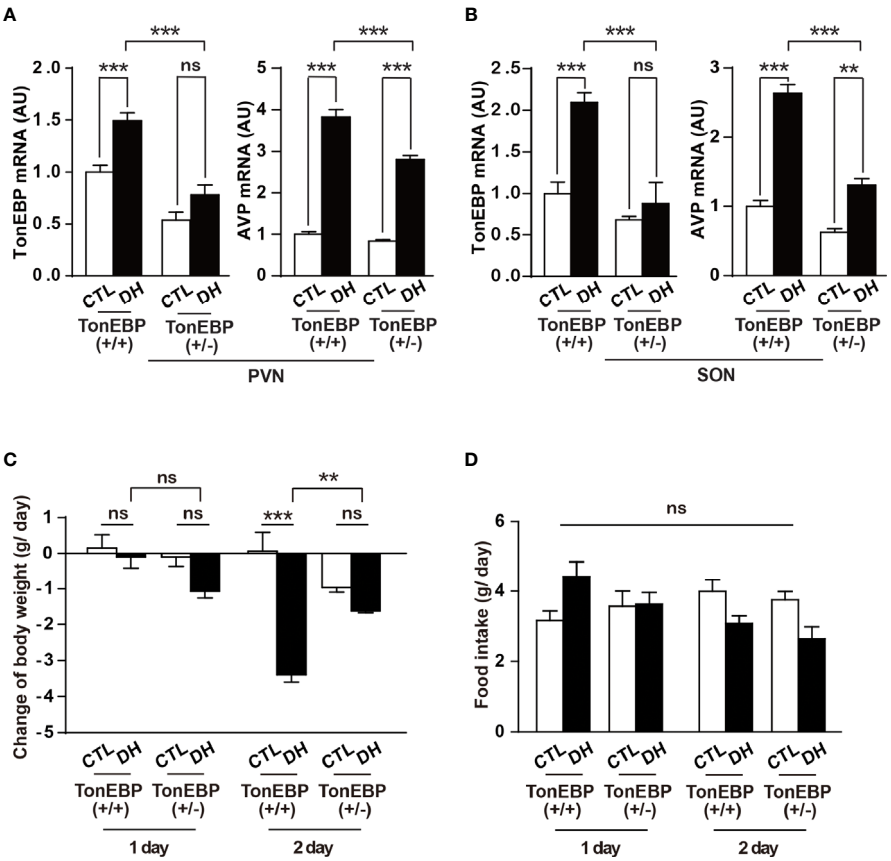

FIGURE 6 | *In vivo* verification of the effects of TonEBP on dehydration-dependent AVP gene transcription and metabolic adaptation. **(A, B)** TonEBP haploinsufficiency [TonEBP (+/-)] and control [TonEBP (+/+)] mice underwent either 2 days of dehydration (DH) or euhydration (CTL), and gene transcription of TonEBP/AVP in the PVN **(A)** and SON **(B)** was quantified by real-time PCR. AU=arbitrary units. **(C, D)** Daily body weight gain **(C)** and daily food intake **(D)** from the same experimental animals were also measured. All data are presented as means ± SEM (n = 4). **p < 0.01; ***p < 0.001; ns, not significant.

our western blotting analysis indicate dehydration-induced increase in TonEBP nuclear translocation in the PVN as well (**Figure 3**). Therefore, detailed investigation that points to PVN AVP-specific and dehydration-dependent TonEBP mechanism is further necessary.

It is worth noting that TonEBP responds to changes in the extracellular osmotic environment and regulates tissue- and cellular-phenotype-specific gene expression for intracellular and matrix homeostasis (32, 55, 56). Therefore, TonEBP has appeared to be a local regulator of fluid balance, rather than a global player. However, our results suggest that hypothalamic TonEBP could act as a global regulator of fluid homeostasis *via* AVP cells in the PVN and SON. Within the hypothalamus, dramatic inter- and intra-cellular modifications occur at the genetic and molecular levels in response to changes in local extracellular osmolality, in concert with changes in plasma volume and osmolality (57, 58). Therefore, the local hypothalamic extracellular osmotic profile is, to a certain degree, a mirror image of the global plasma fluid parameters. This phenomenon could be largely mediated by the forebrain sensory CVOs, including the SFO and OVLT, because those nuclei include osmosensitive cells that directly connect with the circulation and establish massive synaptic networks to the PVN and SON (9, 11, 13, 15, 59). Altogether, these results suggest that the level of TonEBP in the PVN and SON represents not only the local extracellular osmotic status, but also the plasma osmotic environment, and that TonEBP in these regions may be a global regulator of water physiology through the AVP system.

Clearly, TonEBP is the upstream transcription factor for hypothalamic AVP gene transcription, and it contributes to hyperosmolality-dependent AVP synthesis. As a next step, we used a TonEBP haploinsufficiency mouse model to investigate the physiological function of the hypothalamic TonEBP–AVP system in dehydration-dependent metabolic adaptation. TonEBP knockout animals die during development, so TonEBP haploinsufficiency mice have been used extensively to study the physiological and behavioral functions of TonEBP *in vivo* (39, 41, 44). While mRNA levels of TonEBP in the PVN/SON of control mice are increased in response to dehydration, this phenomenon is attenuated in TonEBP haploinsufficiency animals, indicating that TonEBP gene expression in response to dehydration is impaired in the animals with TonEBP

haploinsufficiency. However, AVP gene expression in the PVN/SON is elevated in both animal groups, although a degree of increased AVP gene expression is significantly reduced in TonEBP haploinsufficiency animals. These results suggest that TonEBP may be necessary, but not sufficient by itself, for dehydration-dependent AVP gene expression in the PVN/SON. This also suggests an involvement of other signaling(s), in addition to TonEBP, in such a case. In support of this view, recent investigations have demonstrated that cAMP responsive element-binding protein-3 like-1 (CREB3L1) and caprin-2 are distributed in the PVN/SON, possess an ability to bind directly to promoter and mRNA regions of AVP, respectively, and play a role in AVP-mediated and osmotic stress-dependent physiological adaptations (60, 61). Therefore, it is reasonable to note that a cellular and molecular signaling complex, including TonEBP, is contributing to osmotic stress-dependent hypothalamic AVP synthesis.

Generally, dehydration leads to an increase in hypothalamic AVP cellular activity and plasma AVP concentrations (19–21, 62) and to a decrease in food intake and subsequent body-weight gain in rodents to preserve the body's water and metabolic homeostasis (63–65). However, we found that the dehydration-dependent reduction in body weight in TonEBP (+/+) animals was attenuated in TonEBP haploinsufficiency mice, with a reduced AVP expression in the PVN/SON. It is noteworthy that although our results for food intake did not meet a statistical significance, they showed a considerable reduction in food intake following dehydration in both animal groups. These results suggest a possible involvement of the TonEBP-AVP system in the PVN/SON in osmotic stress-mediated metabolic adaptation, although detailed investigation to uncover a physiological role of the hypothalamic TonEBP-AVP system in stress-dependent metabolic adaptation is further necessary. The anatomical and molecular characteristics of hypothalamic AVP cells are highly complex. For example, multiple investigations have suggested that PVN AVP cells establish multiple synaptic networks, not only to the neurohypophysis but also to several extra-neurohypophyseal targets in the brain (52, 66, 67). These extra-neurohypophyseal projections of PVN AVP cells have been suggested to be implicated in anxiety and stress responses (66, 67). In addition, polysynaptic networks between PVN AVP cells and adipose tissue have also been characterized and suggested to play a role in regulating adipose metabolism (68). Unlike the PVN, most AVP cells within the SON project their fibers to the neurohypophysis to regulate plasma AVP levels (69). Independent investigations have also demonstrated a complex profile of metabolic receptors within hypothalamic AVP cells (27, 70–73). Therefore, hypothalamic AVP–driven metabolic outcomes, such as food intake, body weight gain, energy expenditure, and adipose metabolism, could be mediated by different combinations of anatomical and molecular profiles in individual AVP cells. Therefore, alterations in body weight gain independent offeeding behavior, if this is the case, could possibly be driven by modifications in energy expenditure. In any case, TonEBP contributes to, at least in part, hyperosmolality-dependent AVP synthesis in the hypothalamic neuroendocrine nuclei, such as the PVN and SON.

DATA AVAILABILITY STATEMENT

The raw data supporting the conclusions of this article will be made available by the authors, without undue reservation.

ETHICS STATEMENT

The animal study was reviewed and approved by University of Ulsan for the Care and Use of Laboratory Animals (permission number, BJL-20-050).

AUTHOR CONTRIBUTIONS

DK, JJ, and BL designed the experiments, interpreted results, and wrote the manuscript. DK and KK performed and analyzed most of the experiments. TL and JK performed the histological analyses. HE performed the real-time PCR analysis. JP provided intellectual input. All authors contributed to the article and approved the submitted version.

FUNDING

This research was supported by the Priority Research Centers Program (2014R1A6A1030318) and research funds through the National Research Foundation of Korea (NRF-2020R1I1A1A01068381).

SUPPLEMENTARY MATERIAL

The Supplementary Material for this article can be found online at: https://www.frontiersin.org/articles/10.3389/fendo.2021.627343/full#supplementary-material

Supplementary Figure 1 | Putative AVP 5'-franking promoter sequences in rats. The sequences are obtained from the NCBI GenBank™ database; accession number AF112362.1, and nucleotides are numbered by assigning position +1 to the ATG translation start site. Sequences with underline represent putative TonEBP binding domains as indicated in the Method.

Supplementary Figure 2 | Putative AVP 5'-franking promoter sequences from mouse, rat and human are obtained from the NCBI GenBank™ database; accession gene ID 11998 for mouse, 24221 for rat, and 551 for human, and sequences are aligned, analyzed for the conserved TonEBP binding motifs among species, and deposited at online http://www.ebi.ac.uk/Tools/services/web/toolresult.ebi?tool=clustalo&jobId=clustalo-E20210119-084011-0197-37166704-p1m. As indicated with red boxes, putative TonEBP binding motifs are highly conserved between mouse and rat, and with a less degree with human.

Supplementary Figure 3 | ChIP assays were performed to verify whether TonEBP can directly bind to the AVP promoter under dehydration. Hypothalamic nuclear DNA samples from animals dehydrated for 2 days (DH) and euhydrated control animals (CTL) were immunoprecipitated with TonEBP antibody. Then, PCR amplification was performed using primer sets targeting the indicated TonEBP binding motifs on the AVP gene.

REFERENCES

1. Boschmann M, Steiniger J, Franke G, Birkenfeld AL, Luft FC, Jordan J. Water drinking induces thermogenesis through osmosensitive mechanisms. *J Clin Endocrinol Metab* (2007) 92(8):3334–7. doi: 10.1210/jc.2006-1438
2. Stookey JJ. Negative, Null and Beneficial Effects of Drinking Water on Energy Intake, Energy Expenditure, Fat Oxidation and Weight Change in Randomized Trials: A Qualitative Review. *Nutrients* (2016) 8(1):19. doi: 10.3390/nu8010019
3. Bankir L, Bichet DG, Morgenthaler NG. Vasopressin: physiology, assessment and osmosensation. *J Intern Med* (2017) 282(4):284–97. doi: 10.1111/joim.12645
4. Enhorning S, Melander O. The Vasopressin System in the Risk of Diabetes and Cardiorenal Disease, and Hydration as a Potential Lifestyle Intervention. *Ann Nutr Metab* (2018) 72 Suppl 2:21–7. doi: 10.1159/000488304
5. Chang DC, Basolo A, Piaggi P, Votruba SB, Krakoff J. Hydration biomarkers and copeptin: relationship with ad libitum energy intake, energy expenditure, and metabolic fuel selection. *Eur J Clin Nutr* (2020) 74(1):158–66. doi: 10.1038/s41430-019-0445-6
6. Watts AG, Sanchez-Watts G, Kelly AB. Distinct patterns of neuropeptide gene expression in the lateral hypothalamic area and arcuate nucleus are associated with dehydration-induced anorexia. *J Neurosci* (1999) 19(14):6111–21. doi: 10.1523/JNEUROSCI.19-14-06111.1999
7. Yoshimura M, Nishimura K, Nishimura H, Sonoda S, Ueno H, Motojima Y, et al. Activation of endogenous arginine vasopressin neurons inhibit food intake: by using a novel transgenic rat line with DREADDs system. *Sci Rep* (2017) 7(1):15728. doi: 10.1038/s41598-017-16049-2
8. Zimmerman CA, Lin YC, Leib DE, Guo L, Huey EL, Daly GE, et al. Thirst neurons anticipate the homeostatic consequences of eating and drinking. *Nature* (2016) 537(7622):680–4. doi: 10.1038/nature18950
9. Kinsman BJ, Browning KN, Stocker SD. NaCl and osmolarity produce different responses in organum vasculosum of the lamina terminalis neurons, sympathetic nerve activity and blood pressure. *J Physiol* (2017) 595(18):6187–201. doi: 10.1113/JP274537
10. Mandelblat-Cerf Y, Kim A, Burgess CR, Subramanian S, Tannous BA, Lowell BB, et al. Bidirectional Anticipation of Future Osmotic Challenges by Vasopressin Neurons. *Neuron* (2017) 93(1):57–65. doi: 10.1016/j.neuron.2016.11.021
11. Benz F, Wichitnaowarat V, Lehmann M, Germano RF, Mihova D, Macas J, et al. Low wnt/beta-catenin signaling determines leaky vessels in the subfornical organ and affects water homeostasis in mice. *Elife* (2019) 8:8:e43818. doi: 10.7554/eLife.43818
12. Nomura K, Hiyama TY, Sakuta H, Matsuda T, Lin CH, Kobayashi K, et al. [Na(+)] Increases in Body Fluids Sensed by Central Nax Induce Sympathetically Mediated Blood Pressure Elevations *via* H(+)-Dependent Activation of ASIC1a. *Neuron* (2019) 10160-75(1):e66. doi: 10.1016/j.neuron.2018.11.017
13. Bealer SL, Carithers J, Johnson AK. Fluid regulation, body weight and drinking responses following hypothalamic knife cuts. *Brain Res* (1984) 305 (2):239–45. doi: 10.1016/0006-8993(84)90430-x
14. Oka Y, Ye M, Zuker CS. Thirst driving and suppressing signals encoded by distinct neural populations in the brain. *Nature* (2015) 520(7547):349–52. doi: 10.1038/nature14108
15. Prager-Khoutorsky M, Bourque CW. Anatomical organization of the rat organum vasculosum laminae terminalis. *Am J Physiol Regul Integr Comp Physiol* (2015) 309(4):R324–337. doi: 10.1152/ajpregu.00134.2015
16. Matsuda T, Hiyama TY, Niimura F, Matsusaka T, Fukamizu A, Kobayashi K, et al. Distinct neural mechanisms for the control of thirst and salt appetite in the subfornical organ. *Nat Neurosci* (2017) 20(2):230–41. doi: 10.1038/nn.4463
17. Vandesande F, Dierickx K, De Mey J. The origin of the vasopressinergic and oxytocinergic fibres of the external region of the median eminence of the rat hypophysis. *Cell Tissue Res* (1977) 180(4):443–52. doi: 10.1007/BF00220167
18. Godefroy D, Dominici C, Hardin-Pouzet H, Anouar Y, Melik-Parsadaniantz S, Rostene W, et al. Three-dimensional distribution of tyrosine hydroxylase, vasopressin and oxytocin neurones in the transparent postnatal mouse brain. *J Neuroendocrinol* (2017) 29(12):e12551. doi: 10.1111/jne.12551
19. Yadawa AK, Chaturvedi CM. Expression of stress hormones AVP and CRH in the hypothalamus of Mus musculus following water and food deprivation. *Gen Comp Endocrinol* (2016) 239:13–20. doi: 10.1016/j.ygcen.2016.03.005
20. Armstrong LE, Johnson EC. Water Intake, Water Balance, and the Elusive Daily Water Requirement. *Nutrients* (2018) 10(12):1928. doi: 10.3390/nu10121928
21. Bichet DG. Vasopressin and the Regulation of Thirst. *Ann Nutr Metab* (2018) 72 Suppl 2:3–7. doi: 10.1159/000488233
22. McKenna K, Morris AD, Ryan M, Newton RW, Frier BM, Baylis PH, et al. Renal resistance to vasopressin in poorly controlled type 1 diabetes mellitus. *Am J Physiol Endocrinol Metab* (2000) 279(1):E155–160. doi: 10.1152/ajpendo.2000.279.1.E155
23. Agha A, Smith D, Finucane F, Sherlock M, Morris A, Baylis P, et al. Attenuation of vasopressin-induced antidiuresis in poorly controlled type 2 diabetes. *Am J Physiol Endocrinol Metab* (2004) 287(6):E1100–1106. doi: 10.1152/ajpendo.00214.2004
24. Aoyagi T, Birumachi J, Hiroyama M, Fujiwara Y, Sanbe A, Yamauchi J, et al. Alteration of glucose homeostasis in V1a vasopressin receptor-deficient mice. *Endocrinology* (2007) 148(5):2075–84. doi: 10.1210/en.2006-1315
25. Yi SS, Hwang IK, Kim YN, Kim IY, Pak SI, Lee IS, et al. Enhanced expressions of arginine vasopressin (Avp) in the hypothalamic paraventricular and supraoptic nuclei of type 2 diabetic rats. *Neurochem Res* (2008) 33(5):833–41. doi: 10.1007/s11064-007-9519-2
26. Enhorning S, Struck J, Wirfalt E, Hedblad B, Morgenthaler NG, Melander O. Plasma copeptin, a unifying factor behind the metabolic syndrome. *J Clin Endocrinol Metab* (2011) 96(7):E1065–1072. doi: 10.1210/jc.2010-2981
27. Song Z, Levin BE, Stevens W, Sladek CD. Supraoptic oxytocin and vasopressin neurons function as glucose and metabolic sensors. *Am J Physiol Regul Integr Comp Physiol* (2014) 306(7):R447–456. doi: 10.1152/ajpregu.00520.2013
28. Taveau C, Chollet C, Bichet DG, Velho G, Guillon G, Corbani M, et al. Acute and chronic hyperglycemic effects of vasopressin in normal rats: involvement of V1A receptors. *Am J Physiol Endocrinol Metab* (2017) 312(3):E127–35. doi: 10.1152/ajpendo.00269.2016
29. Robertson GL. The regulation of vasopressin function in health and disease. *Recent Prog Horm Res* (1976) 33:333–85. doi: 10.1016/b978-0-12-571133-3.50015-5
30. Hernandez-Perez OR, Hernandez VS, Nava-Kopp AT, Barrio RA, Seifi M, Swinny JD, et al. A Synaptically Connected Hypothalamic Magnocellular Vasopressin-Locus Coeruleus Neuronal Circuit and Its Plasticity in Response to Emotional and Physiological Stress. *Front Neurosci* (2019) 13:196. doi: 10.3389/fnins.2019.00196
31. Saito N, Fujii M, Sugiura K, Aste N, Shimada K. TonEBP regulates hyperosmolality-induced arginine vasotocin gene expression in the chick (Gallus domesticus). *Neurosci Lett* (2010) 468(3):334–8. doi: 10.1016/j.neulet.2009.11.027
32. Miyakawa H, Woo SK, Dahl SC, Handler JS, Kwon HM. Tonicity-responsive enhancer binding protein, a rel-like protein that stimulates transcription in response to hypertonicity. *Proc Natl Acad Sci U S A* (1999) 96(5):2538–42. doi: 10.1073/pnas.96.5.2538
33. Ko BC, Ruepp B, Bohren KM, Gabbay KH, Chung SS. Identification and characterization of multiple osmotic response sequences in the human aldose reductase gene. *J Biol Chem* (1997) 272(26):16431–7. doi: 10.1074/jbc.272.26.16431
34. Miyakawa H, Woo SK, Chen CP, Dahl SC, Handler JS, Kwon HM. Cis- and trans-acting factors regulating transcription of the BGT1 gene in response to hypertonicity. *Am J Physiol* (1998) 274(4):F753–761. doi: 10.1152/ajprenal.1998.274.4.F753
35. Rim JS, Atta MG, Dahl SC, Berry GT, Handler JS, Kwon HM. Transcription of the sodium/myo-inositol cotransporter gene is regulated by multiple tonicity-responsive enhancers spread over 50 kilobase pairs in the 5'-flanking region. *J Biol Chem* (1998) 273(32):20615–21. doi: 10.1074/jbc.273.32.20615
36. Maallem S, Berod A, Mutin M, Kwon HM, Tappaz ML. Large discrepancies in cellular distribution of the tonicity-induced expression of osmoprotective genes and their regulatory transcription factor TonEBP in rat brain. *Neuroscience* (2006a) 142(2):355–68. doi: 10.1016/j.neuroscience.2006.06.028
37. Maallem S, Mutin M, Kwon HM, Tappaz ML. Differential cellular distribution of tonicity-induced expression of transcription factor TonEBP in the rat brain following prolonged systemic hypertonicity. *Neuroscience* (2006b) 137(1):51–71. doi: 10.1016/j.neuroscience.2005.07.037
38. Go WY, Liu X, Roti MA, Liu F, Ho SN. NFAT5/TonEBP mutant mice define osmotic stress as a critical feature of the lymphoid microenvironment. *Proc Natl Acad Sci U S A* (2004) 101(29):10673–8. doi: 10.1073/pnas.0403139101

39. Lopez-Rodriguez C, Antos CL, Shelton JM, Richardson JA, Lin F, Novobrantseva TI, et al. Loss of NFAT5 results in renal atrophy and lack of tonicity-responsive gene expression. *Proc Natl Acad Sci U S A* (2004) 101 (8):2392–7. doi: 10.1073/pnas.0308703100
40. Shin HJ, Kim H, Heo RW, Kim HJ, Choi WS, Kwon HM, et al. Tonicity-responsive enhancer binding protein haplodeficiency attenuates seizure severity and NF-kappaB-mediated neuroinflammation in kainic acid-induced seizures. *Cell Death Differ* (2014) 21(7):1095–106. doi: 10.1038/cdd.2014.29
41. Lee JY, Jeong EA, Kim KE, Yi CO, Jin Z, Lee JE, et al. TonEBP/NFAT5 haploinsufficiency attenuates hippocampal inflammation in high-fat diet/streptozotocin-induced diabetic mice. *Sci Rep* (2017) 7(1):7837. doi: 10.1038/s41598-017-08319-w
42. Liu C, Choi H, Johnson ZI, Tian J, Shapiro IM, Risbud MV. Lack of evidence for involvement of TonEBP and hyperosmotic stimulus in induction of autophagy in the nucleus pulposus. *Sci Rep* (2017) 7(1):4543. doi: 10.1038/s41598-017-04876-2
43. Choi SY, Lim SW, Salimi S, Yoo EJ, Lee-Kwon W, Lee HH, et al. Tonicity-Responsive Enhancer-Binding Protein Mediates Hyperglycemia-Induced Inflammation and Vascular and Renal Injury. *J Am Soc Nephrol* (2018) 29 (2):492–504. doi: 10.1681/ASN.2017070718
44. Kim HR, Kim DH, Kim KK, Jeong B, Kang D, Lee TH, et al. Tonicity-responsive enhancer binding protein (TonEBP) regulates TNF-alpha-induced hypothalamic inflammation. *FEBS Lett* (2019) 593(19):2762–70. doi: 10.1002/1873-3468.13533
45. Belsham DD, Fick LJ, Dalvi PS, Centeno ML, Chalmers JA, Lee PK, et al. Ciliary neurotrophic factor recruitment of glucagon-like peptide-1 mediates neurogenesis, allowing immortalization of adult murine hypothalamic neurons. *FASEB J* (2009) 23(12):4256–65. doi: 10.1096/fj.09-133454
46. Livak KJ, Schmittgen TD. Analysis of relative gene expression data using real-time quantitative PCR and the 2(-Delta Delta C(T)) Method. *Methods* (2001) 25(4):402–8. doi: 10.1006/meth.2001.1262
47. Choi EJ, Kim DH, Kim JG, Kim DY, Kim JD, Seol OJ, et al. Estrogen-dependent transcription of the NEL-like 2 (NELL2) gene and its role in protection from cell death. *J Biol Chem* (2010) 285(32):25074–84. doi: 10.1074/jbc.M110.100545
48. Ueta Y, Dayanithi G, Fujihara H. Hypothalamic vasopressin response to stress and various physiological stimuli: visualization in transgenic animal models. *Horm Behav* (2011) 59(2):221–6. doi: 10.1016/j.yhbeh.2010.12.007
49. Mucio-Ramirez S, Sanchez-Islas E, Sanchez-Jaramillo E, Curras-Collazo M, Juarez-Gonzalez VR, Alvarez-Gonzalez MY, et al. Perinatal exposure to organohalogen pollutants decreases vasopressin content and its mRNA expression in magnocellular neuroendocrine cells activated by osmotic stress in adult rats. *Toxicol Appl Pharmacol* (2017) 329:173–89. doi: 10.1016/j.taap.2017.05.039
50. Stroud JC, Lopez-Rodriguez C, Rao A, Chen L. Structure of a TonEBP-DNA complex reveals DNA encircled by a transcription factor. *Nat Struct Biol* (2002) 9(2):90–4. doi: 10.1038/nsb749
51. Saleem U, Khaleghi M, Morgenthaler NG, Bergmann A, Struck J, Mosley THJr., et al. Plasma carboxy-terminal provasopressin (copeptin): a novel marker of insulin resistance and metabolic syndrome. *J Clin Endocrinol Metab* (2009) 94(7):2558–64. doi: 10.1210/jc.2008-2278
52. Ribeiro N, Panizza Hdo N, Santos KM, Ferreira-Neto HC, Antunes VR. Salt-induced sympathoexcitation involves vasopressin V1a receptor activation in the paraventricular nucleus of the hypothalamus. *Am J Physiol Regul Integr Comp Physiol* (2015) 309(11):R1369–1379. doi: 10.1152/ajpregu.00312.2015
53. Christ-Crain M, Bichet DG, Fenske WK, Goldman MB, Rittig S, Verbalis JG, et al. Diabetes insipidus. *Nat Rev Dis Primers* (2019) 5(1):54. doi: 10.1038/s41572-019-0103-2
54. Zingg HH, Lefebvre D, Almazan G. Regulation of vasopressin gene expression in rat hypothalamic neurons. Response to osmotic stimulation. *J Biol Chem* (1986) 261(28):12956–9. doi: 10.1016/S0021-9258(18) 69255-5
55. Johnson ZI, Shapiro IM, Risbud MV. Extracellular osmolarity regulates matrix homeostasis in the intervertebral disc and articular cartilage: evolving role of TonEBP. *Matrix Biol* (2014) 40:10–6. doi: 10.1016/j.matbio.2014.08.014
56. Ho SN. The role of NFAT5/TonEBP in establishing an optimal intracellular environment. *Arch Biochem Biophys* (2003) 413(2):151–7. doi: 10.1016/s0003-9861(03)00130-9
57. Mason PA, Durr JA, Bhaskaran D, Freed CR. Plasma osmolality predicts extracellular fluid catechol concentrations in the lateral hypothalamus. *J Neurochem* (1988) 51(2):552–60. doi: 10.1111/j.1471-4159.1988.tb01074.x
58. Greenwood MP, Mecawi AS, Hoe SZ, Mustafa MR, Johnson KR, Al-Mahmoud GA, et al. A comparison of physiological and transcriptome responses to water deprivation and salt loading in the rat supraoptic nucleus. *Am J Physiol Regul Integr Comp Physiol* (2015) 308(7):R559–568. doi: 10.1152/ajpregu.00444.2014
59. Augustine V, Gokce SK, Lee S, Wang B, Davidson TJ, Reimann F, et al. Hierarchical neural architecture underlying thirst regulation. *Nature* (2018) 555(7695):204–9. doi: 10.1038/nature25488
60. Greenwood M, Bordieri L, Greenwood MP, Rosso Melo M, Colombari DS, Colombari E, et al. Transcription factor CREB3L1 regulates vasopressin gene expression in the rat hypothalamus. *J Neurosci* (2014) 34(11):3810–20. doi: 10.1523/JNEUROSCI.4343-13.2014
61. Konopacka A, Greenwood M, Loh SY, Paton J, Murphy D. RNA binding protein Caprin-2 is a pivotal regulator of the central osmotic defense response. *Elife* (2015) 4:e09656. doi: 10.7554/eLife.09656
62. Ji LL, Fleming T, Penny ML, Toney GM, Cunningham JT. Effects of water deprivation and rehydration on c-Fos and FosB staining in the rat supraoptic nucleus and lamina terminalis region. *Am J Physiol Regul Integr Comp Physiol* (2005) 288(1):R311–321. doi: 10.1152/ajpregu.00399.2004
63. Watts AG. Dehydration-associated anorexia: development and rapid reversal. *Physiol Behav* (1999) 65(4-5):871–8. doi: 10.1016/s0031-9384(98)00244-3
64. Schoorlemmer GH, Evered MD. Reduced feeding during water deprivation depends on hydration of the gut. *Am J Physiol Regul Integr Comp Physiol* (2002) 283(5):R1061–1069. doi: 10.1152/ajpregu.00236.2002
65. Bekkevold CM, Robertson KL, Reinhard MK, Battles AH, Rowland NE. Dehydration parameters and standards for laboratory mice. *J Am Assoc Lab Anim Sci* (2013) 52(3):233–9.
66. Hernandez VS, Vazquez-Juarez E, Marquez MM, Jauregui-Huerta F, Barrio RA, Zhang L. Extra-neurohypophyseal axonal projections from individual vasopressin-containing magnocellular neurons in rat hypothalamus. *Front Neuroanat* (2015) 9:130. doi: 10.3389/fnana.2015.00130
67. Hernandez VS, Hernandez OR, Perez de la Mora M, Gomora MJ, Fuxe K, Eiden LE, et al. Hypothalamic Vasopressinergic Projections Innervate Central Amygdala GABAergic Neurons: Implications for Anxiety and Stress Coping. *Front Neural Circuits* (2016) 10:92. doi: 10.3389/fncir.2016.00092
68. Stanley S, Pinto S, Segal J, Perez CA, Viale A, DeFalco J, et al. Identification of neuronal subpopulations that project from hypothalamus to both liver and adipose tissue polysynaptically. *Proc Natl Acad Sci U S A* (2010) 107 (15):7024–9. doi: 10.1073/pnas.1002790107
69. Ishunina TA, Swaab DF. Neurohypophyseal peptides in aging and Alzheimer's disease. *Ageing Res Rev* (2002) 1(3):537–58. doi: 10.1016/s1568-1637(02)00013-2
70. Mozid AM, Tringali G, Forsling ML, Hendricks MS, Ajodha S, Edwards R, et al. Ghrelin is released from rat hypothalamic explants and stimulates corticotrophin-releasing hormone and arginine-vasopressin. *Horm Metab Res* (2003) 35(8):455–9. doi: 10.1055/s-2003-41801
71. Kageyama K, Kumata Y, Akimoto K, Takayasu S, Tamasawa N, Suda T. Ghrelin stimulates corticotropin-releasing factor and vasopressin gene expression in rat hypothalamic 4B cells. *Stress* (2011) 14(5):520–9. doi: 10.3109/10253890.2011.558605
72. Siljee JE, Unmehopa UA, Kalsbeek A, Swaab DF, Fliers E, Alkemade A. Melanocortin 4 receptor distribution in the human hypothalamus. *Eur J Endocrinol* (2013) 168(3):361–9. doi: 10.1530/EJE-12-0750
73. Sandgren JA, Linggonegoro DW, Zhang SY, Sapouckey SA, Claflin KE, Pearson NA, et al. Angiotensin AT1A receptors expressed in vasopressin-producing cells of the supraoptic nucleus contribute to osmotic control of vasopressin. *Am J Physiol Regul Integr Comp Physiol* (2018) 314(6):R770–80. doi: 10.1152/ajpregu.00435.2017

Conflict of Interest: The authors declare that the research was conducted in the absence of any commercial or financial relationships that could be construed as a potential conflict of interest.

frontiers in Neuroscience

PERSPECTIVE
published: 04 May 2021
doi: 10.3389/fnins.2021.665762

QPLOT Neurons—Converging on a Thermoregulatory Preoptic Neuronal Population

Brian A. Upton[1,2,3,4]*, *Shane P. D'Souza*[1,2,3] and *Richard A. Lang*[1,2,5,6]*

[1] The Visual Systems Group, Abrahamson Pediatric Eye Institute, Cincinnati Children's Hospital Medical Center, Cincinnati, OH, United States, [2] Division of Pediatric Ophthalmology, Center for Chronobiology, Cincinnati Children's Hospital Medical Center, Cincinnati, OH, United States, [3] Molecular and Developmental Biology Graduate Program, College of Medicine, University of Cincinnati, Cincinnati, OH, United States, [4] Medical Scientist Training Program, College of Medicine, University of Cincinnati, Cincinnati, OH, United States, [5] Division of Developmental Biology, Cincinnati Children's Hospital Medical Center, Cincinnati, OH, United States, [6] Department of Ophthalmology, College of Medicine, University of Cincinnati, Cincinnati, OH, United States

The preoptic area of the hypothalamus is a homeostatic control center. The heterogeneous neurons in this nucleus function to regulate the sleep/wake cycle, reproduction, thirst and hydration, as well as thermogenesis and other metabolic responses. Several recent studies have analyzed preoptic neuronal populations and demonstrated neuronal subtype-specific roles in suppression of thermogenesis. These studies showed similar thermogenesis responses to chemogenetic modulation, and similar synaptic tracing patterns for neurons that were responsive to cold, to inflammatory stimuli, and to violet light. A reanalysis of single-cell/nucleus RNA-sequencing datasets of the preoptic nucleus indicate that these studies have converged on a common neuronal population that when activated, are sufficient to suppress thermogenesis. Expanding on a previous name for these neurons (Q neurons, which reflect their ability to promote quiescence and expression of *Qrfp*), we propose a new name: QPLOT neurons, to reflect numerous molecular markers of this population and to capture its broader roles in metabolic regulation. Here, we summarize previous findings on this population and present a unified description of QPLOT neurons, the excitatory preoptic neuronal population that integrate a variety of thermal, metabolic, hormonal and environmental stimuli in order to regulate metabolism and thermogenesis.

Keywords: QRFP, PTGER3, Leptin receptor, Opn5, Tacr3, thermoregulation, torpor, neuropsin

OPEN ACCESS

Edited by:
Srinivas Sriramula, The Brody School of Medicine at East Carolina University, United States

Reviewed by:
Stephen B. G. Abbott, University of Virginia, United States
Edward C. Harding, University of Cambridge, United Kingdom

***Correspondence:**
Brian A. Upton
uptonba@mail.uc.edu
Richard A. Lang
richard.lang@cchmc.org

Specialty section:
This article was submitted to Neuroendocrine Science, a section of the journal Frontiers in Neuroscience

Received: *08 February 2021*
Accepted: *06 April 2021*
Published: *04 May 2021*

Citation:
Upton BA, D'Souza SP and Lang RA (2021) QPLOT Neurons—Converging on a Thermoregulatory Preoptic Neuronal Population. Front. Neurosci. 15:665762. doi: 10.3389/fnins.2021.665762

INTRODUCTION

Body temperature regulation is key to survival and reproductive fitness with many mechanisms of regulation evolving throughout speciation. Obligate endotherms, such as mammals, use a variety of processes to regulate temperature, including the generation of heat via both shivering and non-shivering thermogenesis. Shivering thermogenesis results from rapid muscle contractions, whereas non-shivering thermogenesis takes place in specialized fat depots (brown adipose tissue; BAT) via uncoupling of mitochondrial gradients from the electron transport chain mediated by uncoupling protein 1 (Ucp1) (Nedergaard et al., 2001). This utilization of stored energy across the gradient is released as free energy that would have otherwise been incorporated into ATP.

In addition to thermogenesis, organisms can conserve heat by seeking a warmer environment, and increasing blood flow to deep organs while decreasing cutaneous blood flow. Conversely, an organism can dissipate heat by reducing thermogenesis, seeking a cooler environment, increasing cutaneous blood flow, and increasing evaporative heat loss through panting and sweating (Tan and Knight, 2018). While many of these processes occur peripherally, they are regulated by the central nervous system.

Regulation of body temperature and metabolism are energetically demanding processes that are controlled by a region of the anterior hypothalamus known as the preoptic area (POA) (Tan and Knight, 2018). The POA has long been associated with thermoregulation, as c-Fos immunoreactivity increases following warm-exposure and activation of neurons within this nucleus induces a behavioral and physiological response commensurate with heat exposure (e.g., panting and decrease in core body temperature) (Scammell et al., 1993; Bachtell et al., 2003; Tan et al., 2016). Most mammalian biological processes must occur within a narrow thermal range. Given the energetic cost of thermogenesis, the POA must keep this process tightly regulated: Inappropriate thermogenesis wastes stored energy, and, in times of decreased food availability, thermogenesis must be limited to conserve energy.

Recent advances have increased our understanding of the central processes that occur within the hypothalamus for endothermic mammals to regulate temperature, metabolism, and torpor/hibernation, many of which converge upon a single neuronal cell type that when activated, is sufficient to drive these behavioral and physiologic responses.

NUMEROUS GENETIC MARKERS OF THERMOREGULATORY NEURONS ARE EXPRESSED IN A SINGLE PREOPTIC CELLULAR CLUSTER

Warm-responsive neurons (WRNs) are neurons that are activated by exposure to warm stimuli, often indicated by increased expression of c-Fos or phosphorylated riboprotein S6 (pS6) (Sheng and Greenberg, 1990; Knight et al., 2012). This activation, in turn, produces a response that decreases body temperature through inhibition of thermogenesis, redistribution of blood flow to superficial tissues, cold-seeking behavior, and decreased activity (Tan and Knight, 2018). Reactivation of neurons that induce c-Fos following warm exposure results in a decrease in body temperature, even when reactivation occurs at room temperature (Harding et al., 2018). A population of WRNs in the POA are known to be excitatory as chemogenetic activation of POA Vglut2$^+$ neurons, but not Vgat$^+$ neurons, results in a decrease in energy expenditure and core body temperature (Song et al., 2016; Zhao et al., 2017). The identity of WRNs has been further elucidated based on expression of *Adcyap1* and *Bdnf* as optogenetic activation of either neuronal subset decreases core body temperature and facilitates cold-seeking behavior. Furthermore, both *Bdnf* and *Adcyap1* colocalize with pS6 following warm stimulation (Tan et al., 2016). While these markers help to define the molecular identity of WRNs, numerous excitatory POA populations co-express these genes (**Figure 1A**; Moffitt et al., 2018). Another approach that has been used to identify preoptic cellular populations that regulate energy expenditure is to use a tamoxifen-inducible CreER at the *Fos* locus for targeted recombination in active populations (TRAP). When tamoxifen is administered during fasting-induced torpor (torpor-TRAP), neurons that are active during this state of reduced metabolism and thermogenesis can be used to increase expression of cre-dependent genes, such as a fluorescent reporter or designer receptor exclusively activated by designer drugs (DREADDs). Chemogenetic reactivation of torpor-TRAPed neurons in the POA is sufficient to decrease core body temperature, suggesting that at least one of the torpor-TRAPed cell types is able to regulate thermogenesis (Hrvatin et al., 2020). Sequencing of these torpor-TRAPed neurons identifies numerous populations, several of which are excitatory and express both *Bdnf* and *Adcyap1* (**Figure 1A**).

Several additional studies, using different genetic and molecular markers, have been able to precisely identify which of the torpor-TRAPed Bdnf$^+$/Adcyap1$^+$ neuronal populations are responsible for suppressing energy expenditure and decreasing body temperature. Chemogenetic activation of POA neurons using either *Lepr-cre*, *Qrfp-cre*, *Opn5-cre*, or *Esr1-cre* were each individually sufficient to decrease core body temperature and energy expenditure (Yu et al., 2016; Takahashi et al., 2020; Zhang K.X. et al., 2020; Zhang Z. et al., 2020). Additionally, neurokinin B (NKB) signaling within the POA via neurokinin 3 receptor (NK3R; gene: *Tacr3*) results in a rapid drop in body temperature. Furthermore, both *Lepr* and *Sncg* have been colocalized to c-Fos immunoreactivity following warm exposure (Yu et al., 2016; Moffitt et al., 2018). Two independent single-cell/nucleus RNA-sequencing datasets of the POA indicate that these genetic markers of thermoregulatory neurons comprise a single neuronal cluster, identified as e13:*Ghrh/C1ql1* by Moffitt et al. (2018) and e10:*Adcyap1/Opn5* by Hrvatin et al. (2020) (**Figure 1A**). Between these datasets, markers for these clusters overlap and when neurons from the datasets are integrated, a joint cluster is formed as a superimposition of the e10:*Adcyap1/Opn5* and e13:*Ghrh/C1ql1* clusters (**Figures 1A,B**), suggesting that both datasets have identified the same neuronal cell type. From this integrated cluster, *Ptger3*, which encodes the fever-mediating prostaglandin EP_3 receptor (EP_3) and is expressed in *Qrfp-cre* neurons, and *Opn5* are among the most conserved markers for this population (Lazarus et al., 2007; Takahashi et al., 2020; **Figure 1A**).

Taken together, these studies demonstrate that *Lepr*-, *Opn5*-, and *Qrfp*-expressing POA neurons comprise the same cellular population and that activation of this excitatory population is sufficient to decrease metabolism and body temperature. Using progressively more specific cell markers, the molecular identity of these WRNs begins to emerge (**Figure 1C**). A name for this warm-responsive POA population has recently been proposed: quiescence-inducing neurons or Q neurons, based on their ability to induce a hibernation-like

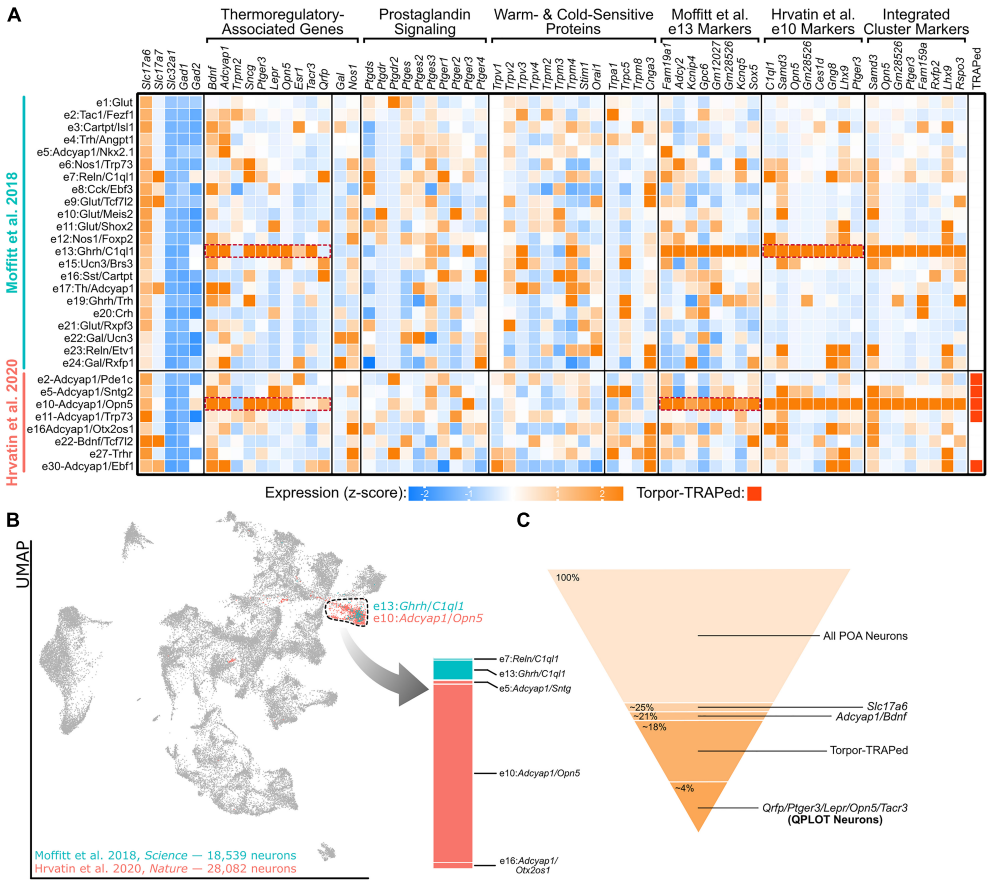

FIGURE 1 | A single molecular identity for QPLOT neurons. **(A)** Heatmap of excitatory POA neurons from Moffitt et al. (2018) and Hrvatin et al. (2020) Known marker genes for thermoregulatory POA neurons, prostaglandin-associated genes, and temperature-sensitive proteins are indicated in columns. Additionally, the top 8 marker genes for excitatory cluster 13 (e13) from Moffitt et al. (2018) and excitatory cluster 10 (e10) from Hrvatin et al. (2020) are provided as well as marker genes for the indicated cluster representing QPLOT neurons when the datasets are merged. Clusters identified in Torpor-TRAP experiments (Hrvatin et al., 2020 clusters only) are indicated. Data is represented as relative expression of each gene within the cluster, averaged over all neuronal clusters, including inhibitory neurons (shown in **Supplementary Figure 1**). **(B)** Uniform manifold projection of 46,621 POA neurons integrated with Seurat v3 (Stuart et al., 2019). Cluster 16, the cluster containing QPLOT neurons, is indicated by the dashed black line. The QPLOT neuron cluster is composed predominantly of e13 from Moffitt et al. (2018) and e10 from Hrvatin et al. (2020) **(C)** Summary of neuronal populations within the POA that are sufficient to reduce body temperature and thermogenesis (**Supplementary Figure 2**).

state when activated, as well as a play on their expression of the neuropeptide pyroglutamylated RFamide peptide or Qrfp (Takahashi et al., 2020).

It is important to mention several limitations of referring to these neurons as "quiescence-inducing". First, these neurons function in more than promoting quiescence, including in temperature and metabolic regulation. Second, not all species undergo similar quiescent states, whether ranging from hibernation to torpor or deep sleep. While these cells may be sufficient to induce quiescence in species that are capable of entering such a state, it is likely that this cellular population exists in all endotherms to regulate energy expenditure. Lastly, *Qrfp* is just one marker among many that is useful in molecularly defining this population. Thus, we propose an expanded definition of the previously defined Q neuron and suggest the name QPLOT neurons, for the markers *Qrfp*, *Ptger3*, *Lepr*, *Opn5*, and *Tacr3* that identify this population. The use of two or more of these markers will allow for precise identification of the population of neurons.

QPLOT NEURONS AS CENTRAL INTEGRATORS OF TEMPERATURE AND METABOLIC INFORMATION

Given the data suggesting that these previous studies have been investigating a singular neuronal population, their published data can be reanalyzed to better understand some of the characteristics of QPLOT neurons. As a unified cellular population, QPLOT neurons can integrate a variety of stimuli to regulate thermogenesis and metabolism. These stimuli include ascending signals from warm and cold sensors in the skin, local changes in hypothalamic temperature, inflammatory-mediated prostaglandin signaling, the hormone leptin, violet light, and estrogen (**Figure 2**).

Ascending Temperature Information

Ambient temperature is detected by cutaneous warm-sensitive and cold-sensitive sensory neurons, which predominantly utilize

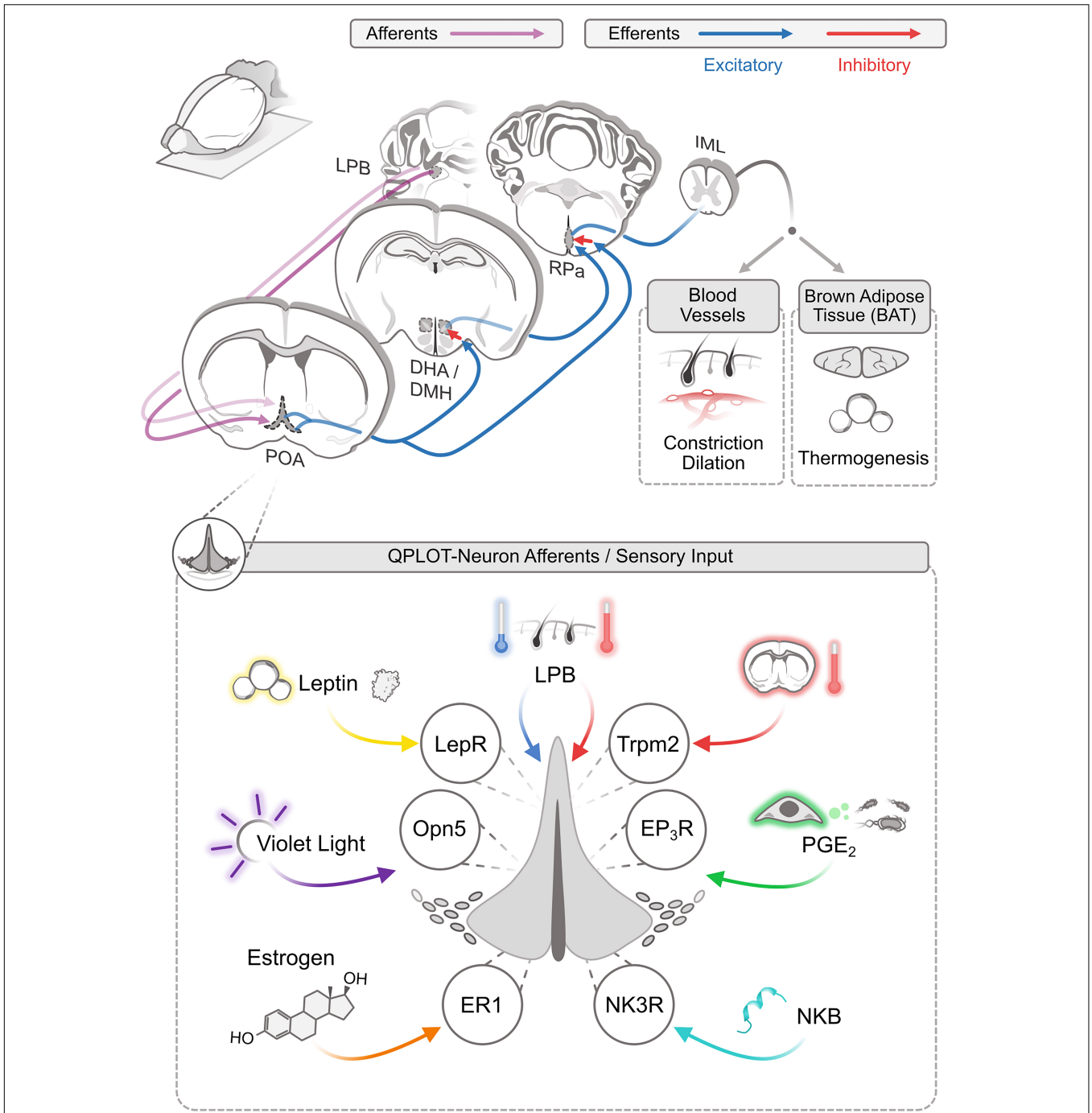

FIGURE 2 | Afferent and efferent thermoregulatory signaling for QPLOT neurons. Schematic of connectivity of QPLOT neurons that mediate body temperature regulation. QPLOT neurons are responsive to numerous stimuli that are integrated to produce the appropriate response.

TRP channels to detect the external temperatures. Trpm8 is necessary for cold-sensitive sensory neurons to detect diminished temperature, whereas Trpv1 is the predominant warm-sensitive protein expressed in sensory neurons (Knowlton et al., 2010, 2013; Pogorzala et al., 2013; Yarmolinsky et al., 2016). This temperature information is conveyed to the brain through multiple pathways, including projections to the lateral parabrachial nucleus (LPB), which in turn projects to the POA. Prior to the POA, warm and cold information is transmitted independently (Geerling et al., 2016). Within the POA, these temperature cues converge, such that activity can be modulated by external increases or decreases in temperature (Morrison and Nakamura, 2011; Yang et al., 2020). Consistent with this model, the LPB has been monosynaptically traced from POA neurons

expressing *Opn5*-cre (Zhang K.X. et al., 2020). These results would indicate that QPLOT neurons themselves receive at least one of these temperature streams directly, rather than through a local circuit within the POA. Thus, in response to ascending external cold or warm stimuli, QPLOT neuron activity can be modulated to adjust to external temperatures or alternatively, interpret external temperature as a cue, along with other stimuli, that the organism should enter torpor.

Intrinsic Temperature Sensitivity

In addition to receiving peripheral thermal information, neurons of the POA have long been known to be intrinsically temperature-sensitive with increased firing rate in response to local increases in temperature and decreased firing in response to local temperature decreases (Magoun et al., 1938; Nakayama et al., 1961, 1963). There is an additional POA neuronal population that functions conversely to these intrinsically warm-sensitive neurons (iWSNs), in which increasing the temperature decreases firing rate while decreasing the hypothalamic temperature increases firing. However, this "cold response" is dependent on synaptic neurotransmission, suggesting that these cells lack an intrinsic ability to respond to local changes in temperature, but are rather responding to extrinsic activity, possibly in direct response to the iWSNs (Kelso and Boulant, 1982; Boulant, 2006; Wang et al., 2019). These iWSNs and cold-responsive POA neurons (CRNs) represent two distinct neuronal populations that likely function together to regulate energy expenditure and the response to external and internal thermal stimuli (Wang et al., 2019).

The molecular identity of iWSNs has not been clearly identified, however, the temperature-sensitive cation channel, Trpm2, is necessary for warm-sensitivity within the POA and functions to limit the fever response induced by either PGE2 or both IL1β and IL6 (Song et al., 2016). *Trpm2* is found in *Opn5*-expressing neurons and chemogenetic activation of *Trpm2*-cre mice results in a decrease in body temperature, demonstrating that Trpm2 is expressed in a neuronal population sufficient to decrease body temperature and metabolism, likely conferring the cell intrinsic temperature sensitivity (Song et al., 2016; Zhang K.X. et al., 2020). Unfortunately, Trpm2 is expressed in a variety of excitatory and inhibitory POA neurons cell types and, therefore, does not serve as a useful marker of any individual population (Song et al., 2016). Thus, Trpm2 is necessary for intrinsic temperature sensitivity of the POA, particularly at high temperatures, but many neuron types within the POA beyond QPLOT neurons utilize this cation channel. There may still be additional temperature-sensitive proteins within the POA that function closer to homeostatic temperatures, rather than at pyretic temperatures. An assumption that has likely limited the molecular identification of iWSNs is that multiple neuronal cell types may be intrinsically temperature sensitive within the POA and that QPLOT neurons only represent one of these. For example, WRNs may use temperature-sensitive proteins, but so could POA neurons involved in the regulation of thirst or sleep. Available sequencing datasets are consistent with this hypothesis, in which no temperature-sensitive proteins are specific to a single neuronal cluster (**Figure 1A**).

Prostaglandin Signaling

Ptger3 is one of the most selective marker genes for QPLOT neurons (**Figure 1A**) and is likely integral to their physiology. Prostaglandins are produced by endothelial cells and microglia within the brain following exposure to endotoxins or inflammatory cytokines (Eskilsson et al., 2017). Prostaglandin EP3 receptor (EP3), encoded by *Ptger3*, is activated by PGE2 to mediate the fever response (Lazarus et al., 2007). This pathway can be suppressed by COX inhibitors to block the synthesis of PGE2, thus reducing fevers. Additionally, targeted ablation of excitatory neurons in the POA or deletion of *Ptger3* from the hypothalamus are sufficient to abolish the inflammatory-induced fever response (Lazarus et al., 2007; Machado et al., 2020). It is clear that both approaches would disrupt the QPLOT neuron population. Accordingly, EP3 activation (G_i-coupled receptor) should reduce QPLOT neuron activity and thus, increase body temperature. In hypothalamic slices, PGE2 has been shown to decrease the firing rate of warm-sensitive neurons, while increasing the activity of temperature-insensitive neurons (Ranels and Griffin, 2003). These results are consistent with a model in which QPLOT neurons are intrinsically temperature-sensitive, express EP3, and upon PGE2 stimulation, decrease their activity, resulting in an increase in body temperature. However, this PGE2-EP3 mechanism may be limited to the inflammatory response, as local changes in hypothalamic temperature do not appear to change PGE2 concentration (Wang et al., 2019).

Leptin Signaling

Leptin is a white adipocyte-derived hormone that conveys information on nutritional status (proportional to adipocyte mass) to other regions of the body, primarily to several hypothalamic brain regions, including the arcuate nucleus (ARC), dorsomedial hypothalamus (DMH), and POA (Schwartz et al., 1996). Systemic leptin regulates food intake and body temperature to correct energy balance during fed and fasting states (Ahima et al., 2000), however these functions are predominantly mediated via leptin receptor (Lepr) activity in the ARC and DMH, respectively (Cowley et al., 2001; Balthasar et al., 2004; Gropp et al., 2005; Luquet et al., 2005; Enriori et al., 2011; Fischer et al., 2016). Activation of *Lepr*-expressing POA neurons decreases food intake, thermogenesis, and energy expenditure, even at thermoneutrality, but local application of leptin into the POA does not alter energy expenditure and only modestly reduces acute food intake (Yu et al., 2016, 2018). Counterintuitively, local deletion of the leptin receptor does not change food intake or energy expenditure when fed; however, a difference in energy expenditure emerges when mice are fasted or given a high fat diet (Yu et al., 2018). Thus, most of the central functions ascribed to leptin can be sufficiently explained via *Lepr*-expressing neurons in the DMH and ARC, though roles for leptin signaling within the POA are emerging.

Interestingly, in the proposed QPLOT neuron, Lepr is functionally positioned to explain several observations. First, following food restriction at subthermoneutral temperatures (a state that would normally induce torpor), leptin treatment

prevents decreases in body temperature (Fischer et al., 2016). Second, mice deficient in leptin spontaneously enter torpor in the absence of fasting or cold exposure (Swoap, 2008). Third, the PGE2-induced fever response is attenuated in fasted mice (Inoue et al., 2008). Since fasting is a state that results in a marked decline in leptin, QPLOT neurons may respond to this drop in hormone level by modulating the thermogenic response to other stimuli. In this manner, the internal metabolic state could directly influence energy utilization when thermoregulation must otherwise be upregulated via integration through a single cellular population. In these examples, the response to the lack of leptin during times of fasting may be the interpreted signal, rather than to increases in leptin.

Violet Light and Opn5

Opn5 encodes the violet light-sensitive atypical opsin, neuropsin, and serves as one of the most specific markers for QPLOT neurons (**Figure 1A**). In birds, neuropsin is known to be expressed in hypothalamic tanycytes, where it regulates seasonal physiology and behavior, although it is not detected in mammalian tanycytes (Tarttelin et al., 2003; Nakane et al., 2010; Yoo et al., 2019). Stimulation of the POA with violet light activates *Opn5-cre* labeled neurons and results in a suppression of metabolism and thermogenesis. This response is absent from *Opn5*-deficient mice. In the absence of *Opn5*, mice have an elevated metabolic rate and body temperature, similar to effects seen following inhibition of putative QPLOT neurons (Song et al., 2016; Zhang K.X. et al., 2020). Despite expression in different cell types between birds and mammals, the functions of hypothalamic *Opn5* in migration, reproduction, metabolism, and torpor suggest a conserved role for Opn5 in regulating seasonal physiology.

Estrogen Receptor

Through a variety of peripheral and central mechanisms, estrogen promotes heat loss and reduced thermogenesis. Estrogen receptor alpha (ERα, *Esr1* gene) is expressed in several POA neuronal populations, including in the QPLOT cluster (**Figure 1A**). Sensitivity to both temperature and estrogen has been noted in a proportion of POA neurons, consistent with *Esr1*-expression in temperature-sensitive QPLOT neurons (Silva and Boulant, 1986; Zhang Z. et al., 2020). Additionally, chemogenetic activation of *Esr1*-cre neurons of the POA leads to a suppression of body temperature and metabolism (Zhang Z. et al., 2020). γ-synuclein, encoded by the warm-induced gene *Sncg*, is known to modulate estrogen signaling, indicating that signaling through ERα may be differentially modulated according to body temperature (Jiang et al., 2004; Moffitt et al., 2018). Taken together, QPLOT neurons appear to be sensitive to estrogen, although how this highly dynamic signaling integrates with other stimuli at the level of the POA remains unclear.

Neurokinin B and NK3R

Kisspeptin-Neurokinin B-Dynorphin-expressing (KNDy) neurons of the arcuate nucleus are another population of estrogen-sensitive neurons that function, in part, in thermoregulation (Rance et al., 2013). These neurons are believed to function in hot flashes. Activation of KNDy projections to the preoptic are sufficient to evoke superficial vasodilation, a decrease in core body temperature, and induction of c-Fos in the POA (Padilla et al., 2018). The thermoregulatory response to KNDy neuron activation is blocked via preoptic inhibition of neurokinin signaling. Since *Tacr3* encode NK3R, the receptor for NKB, and *Tacr3* is enriched in the QPLOT neuronal cluster, it is likely that activation of QPLOT neurons is necessary for KNDy neuron-mediated vasodilation and suppression of body temperature.

ACTIVATION OF QPLOT NEURONS AND THEIR EFFERENT TARGETS

The main thermoregulatory efferents of POA neurons project to the DMH and raphe pallidus (RPa). These projections are excitatory although the targets of these neurons are believed to be inhibitory, a view that has changed in recent years (Saper and Machado, 2020). Activation of QPLOT neurons through various cre lines, either optogenetic or chemogenetic, results in a decrease in body temperature and energy expenditure (Song et al., 2016; Tan et al., 2016; Yu et al., 2016; Hrvatin et al., 2020; Takahashi et al., 2020; Zhang K.X. et al., 2020; Zhang Z. et al., 2020). This effect is likely due to a combination of cutaneous vasodilation, reduced food intake, and a suppression of non-shivering thermogenesis (Abbott and Saper, 2017). Projections from the POA to the DMH convey thermogenic information, as optogenetic activation of *Qrfp-cre* projections to the DMH is sufficient to drive a sustained suppression of BAT thermogenesis. By contrast, activation of *Qrfp-cre* projections directly to the RPa has only a transient suppression of BAT thermogenesis (Takahashi et al., 2020). Similarly, inhibition of the DMH attenuates PGE2 evoked thermogenesis but has no effect on cutaneous vasoconstriction (Rathner et al., 2008). Inhibition of the RPa also inhibits PGE2 evoked thermogenesis, although this could be due to inhibition of direct POA-RPa projections or the POA-DMH-RPa pathway (Yoshida et al., 2009; Zhang et al., 2011). While these two parallel pathways result in similar effects on body temperature, individual neurons in the POA largely project to only one of these efferents, as simultaneous retrograde tracing from the DMH and RPa identifies very few co-labeled neurons (Nakamura et al., 2009). Thus, a subset of QPLOT neurons likely project to the DMH, to regulate thermogenesis, while another subset of QPLOT neurons may project directly to the RPa to regulate vasodilation and potentially additional regulation of thermogenesis. Despite evidence of at least two anatomically distinct populations, there is currently only evidence for one molecularly-defined cellular population. Whether these differences in projection arise from cellular identity/fate decisions or are a result of developmental cues regulating axon guidance remains to be determined. Both the direct and indirect projections reconvene at the RPa, where descending neurons of the RPa project to the preganglionic sympathetic neurons of the IML (intermediolateral cell column) (Nakamura et al., 2004). From the IML, sympathetic neurons innervate BAT and cutaneous blood vessels (**Figure 2**). In addition to these targets of QPLOT neurons, they also project

to the PVN, VMH, and ARC where they likely exert additional influence. These informative studies will need to be revisited with specific markers of the QPLOT neuron population to validate and functionally expand this metabolic circuitry.

A separate thermoregulatory population in the ventrolateral preoptic area (VLPO) is an inhibitory galanin (Gal)-expressing neuron that when activated, promotes NREM sleep and a decrease in core body temperature and when ablated, results in a higher baseline body temperature (Kroeger et al., 2018; Ma et al., 2019). *Gal* is noticeably absent from the QPLOT cluster, although it is expressed in several other clusters (**Figure 1A**; **Supplementary Figure 1**; Guo et al., 2020). Interestingly, VLPO neurons inhibit shivering induced by PGE2 infused into the POA and additionally can inhibit RPa-induced thermogenesis (Conceição et al., 2018). It is conceivable that this VLPO^{Gal} population converges with QPLOT neuron efferents to modulate body temperature and energy expenditure (Zhao et al., 2017; Conceição et al., 2018). Alternatively, or additionally, there may be a local circuit within the anterior hypothalamus between these two thermoregulatory populations. Consistent with this hypothesis, viral tracing from *Qrfp-cre* neurons indicates connectivity within the VLPO and axons from the POA form excitatory synapses with Gal-expressing neurons in the VLPO (Walter et al., 2019; Takahashi et al., 2020). More work with precise genetic markers will be needed to further understand how these separate neuronal populations may function together to regulate body temperature and arousal.

CONCLUSION

Currently available single cell/nucleus sequencing datasets of the POA suggest that there is a unified cellular population known as QPLOT neurons that express *Qrfp*, *Ptger3*, *Lepr*, *Opn5*, *Tacr3*, *Trpm2*, *Esr1*, *Sncg*, *Adcyap1*, and *Bdnf*, that when activated, results in a decrease in core body temperature and energy expenditure. QPLOT neurons are a key cellular population that regulate energy expenditure and thermogenesis by integrating ascending temperature stimuli, local hypothalamic temperature, the internal metabolic state via adipocyte-derived leptin, inflammatory-mediated prostaglandin signaling, ambient violet light, estrogen, and neurokinin signaling. Together, these stimuli modify the activity of QPLOT neurons which function with other neurons in a thermoregulatory circuit to appropriately balance energy utilization and body temperature, keeping an organism within a tightly regulated physiologic range.

DATA AVAILABILITY STATEMENT

The datasets analyzed for this study can be found in the Gene Expression Omnibus (GSE113576 and GSE149344); https://www.ncbi.nlm.nih.gov/geo/query/acc.cgi?acc=GSE113576; https://www.ncbi.nlm.nih.gov/geo/query/acc.cgi?acc=GSE149344.

AUTHOR CONTRIBUTIONS

RL and BU conceived the manuscript. BU drafted and revised the manuscript in discussion with RL and SD'S. BU composed **Figure 1**. SD'S composed **Figure 2**. All authors approved of the submitted version.

FUNDING

This work was supported by the National Institutes of Health (R01EY027077, R01EY027711, R01EY032029 to RL) and (T32GM063483 to UC MSTP), and by funds from the Emma and Irving Goldman Scholar endowment at CCHMC.

SUPPLEMENTARY MATERIAL

The Supplementary Material for this article can be found online at: https://www.frontiersin.org/articles/10.3389/fnins.2021.665762/full#supplementary-material

Supplementary Figure 1 | Heatmaps of excitatory, inhibitory, and hybrid POA neurons from **(A)** Moffitt et al. (2018) and **(B)** Hrvatin et al. (2020) Known marker genes for thermoregulatory POA neurons, prostaglandin-associated genes, and temperature-sensitive proteins are indicated in columns. Additionally, the top 8 marker genes for excitatory cluster 13 (e13) from Moffitt et al. (2018) and excitatory cluster 10 (e10) from Hrvatin et al. (2020) are provided as well as marker genes for the indicated cluster representing QPLOT neurons when the datasets are merged. Clusters identified in Torpor-TRAP experiments (Hrvatin et al., 2020 clusters only) are indicated. Data is represented as relative expression of each gene within the cluster, averaged over all neuronal clusters.

Supplementary Figure 2 | Uniform manifold approximation and projection of integrated single cell/single nucleus RNA-sequencing datasets. Moffitt et al. (2018) and Hrvatin et al. (2020) datasets were integrated in Seurat v3 using 3,000 integration features. UMAP with cells colored based on **(A)** dataset of origin, **(B)** original classification as excitatory, inhibitory, or cholinergic, and **(C)** integrated cluster ID using a resolution of 2.0.

Supplementary Table 1 | QPLOT Neuron Conserved Markers. Marker genes for the QPLOT neuron cluster from integrated POA single cell/nucleus sequencing datasets.

REFERENCES

Abbott, S. B. G., and Saper, C. B. (2017). Median preoptic glutamatergic neurons promote thermoregulatory heat loss and water consumption in mice. *J. Physiol.* 595, 6569–6583. doi: 10.1113/JP274667

Ahima, R. S., Saper, C. B., Flier, J. S., and Elmquist, J. K. (2000). Leptin regulation of neuroendocrine systems. *Front. Neuroendocrinol.* 21, 263–307. doi: 10.1006/frne.2000.0197

Bachtell, R. K., Tsivkovskaia, N. O., and Ryabinin, A. E. (2003). Identification of temperature-sensitive neural circuits in mice using c-Fos expression mapping. *Brain Res.* 960, 157–164. doi: 10.1016/S0006-8993(02)03807-6

Balthasar, N., Coppari, R., McMinn, J., Liu, S. M., Lee, C. E., Tang, V., et al. (2004). Leptin receptor signaling in POMC neurons is required for normal body weight homeostasis. *Neuron* 42, 983–991. doi: 10.1016/j.neuron.2004.06.004

Boulant, J. A. (2006). Neuronal basis of Hammel's model for set-point thermoregulation. *J. Appl. Physiol.* 100, 1347–1354. doi: 10.1152/japplphysiol.01064.2005

Conceição, E. P. S., Madden, C. J., and Morrison, S. F. (2018). Neurons in the rat ventral lateral preoptic area are essential for the warm-evoked inhibition of brown adipose tissue and shivering thermogenesis. *Acta Physiol.* 225:e13213. doi: 10.1111/apha.13213

Cowley, M. A., Smart, J. L., Rubinstein, M., Cerdán, M. G., Diano, S., Horvath, T. L., et al. (2001). Leptin activates anorexigenic POMC neurons through a neural network in the arcuate nucleus. *Nature* 411, 480–484. doi: 10.1038/35078085

Enriori, P. J., Sinnayah, P., Simonds, S. E., Rudaz, C. G., and Cowley, M. A. (2011). Leptin action in the dorsomedial hypothalamus increases sympathetic tone to brown adipose tissue in spite of systemic leptin resistance. *J. Neurosci.* 31, 12189–12197. doi: 10.1523/JNEUROSCI.2336-11.2011

Eskilsson, A., Matsuwaki, T., Shionoya, K., Mirrasekhian, E., Zajdel, J., Schwaninger, M., et al. (2017). Immune-induced fever is dependent on local but not generalized prostaglandin E2 synthesis in the brain. *J. Neurosci.* 37, 5035–5044. doi: 10.1523/JNEUROSCI.3846-16.2017

Fischer, A. W., Hoefig, C. S., Abreu-Vieira, G., de Jong, J. M. A., Petrovic, N., Mittag, J., et al. (2016). Leptin raises defended body temperature without activating thermogenesis. *Cell Rep.* 14, 1621–1631. doi: 10.1016/j.celrep.2016.01.041

Geerling, J. C., Kim, M., Mahoney, C. E., Abbott, S. B. G., Agostinelli, L. J., Garfield, A. S., et al. (2016). Genetic identity of thermosensory relay neurons in the lateral parabrachial nucleus. *Am. J. Physiol. Regul. Integr. Comp. Physiol.* 310, R41–R54. doi: 10.1152/ajpregu.00094.2015

Gropp, E., Shanabrough, M., Borok, E., Xu, A. W., Janoschek, R., Buch, T., et al. (2005). Agouti-related peptide-expressing neurons are mandatory for feeding. *Nat. Neurosci.* 8, 1289–1291. doi: 10.1038/nn1548

Guo, X., Gao, X., Keenan, B. T., Zhu, J., Sarantopoulou, D., Lian, J., et al. (2020). RNA-seq analysis of galaninergic neurons from ventrolateral preoptic nucleus identifies expression changes between sleep and wake. *BMC Genom.* 21:633. doi: 10.1186/s12864-020-07050-7

Harding, E. C., Yu, X., Miao, A., Andrews, N., Ma, Y., Ye, Z., et al. (2018). A neuronal hub binding sleep initiation and body cooling in response to a warm external stimulus. *Curr. Biol.* 28, 2263–2273. doi: 10.1016/j.cub.2018.05.054

Hrvatin, S., Sun, S., Wilcox, O. F., Yao, H., Lavin-Peter, A. J., Cicconet, M., et al. (2020). Neurons that regulate mouse torpor. *Nature* 583, 115–121. doi: 10.1038/s41586-020-2387-5

Inoue, W., Somay, G., Poole, S., and Luheshi, G. N. (2008). Immune-to-brain signaling and central prostaglandin E2 synthesis in fasted rats with altered lipopolysaccharide-induced fever. *Am. J. Physiol. Regul. Integr. Comp. Physiol.* 295, R133–R143. doi: 10.1152/ajpregu.90335.2008

Jiang, Y., Liu, Y. E., Goldberg, I. D., and Shi, Y. E. (2004). γ synuclein, a novel heat-shock protein-associated chaperone, stimulates ligand-dependent estrogen receptor α signaling and mammary tumorigenesis. *Cancer Res.* 64, 4539–4546. doi: 10.1158/0008-5472.CAN-03-3650

Kelso, S. R., and Boulant, J. A. (1982). Effect of synaptic blockade on thermosensitive neurons in hypothalamic tissue slices. *Am. J. Physiol. Regul. Integr. Comp. Physiol.* 243, R480–R490. doi: 10.1152/ajpregu.1982.243.5.r480

Knight, Z. A., Tan, K., Birsoy, K., Schmidt, S., Garrison, J. L., Wysocki, R. W., et al. (2012). Molecular profiling of activated neurons by phosphorylated ribosome capture. *Cell* 151, 1126–1137. doi: 10.1016/j.cell.2012.10.039

Knowlton, W. M., Bifolck-Fisher, A., Bautista, D. M., and McKemy, D. D. (2010). TRPM8, but not TRPA1, is required for neural and behavioral responses to acute noxious cold temperatures and cold-mimetics in vivo. *Pain* 150, 340–350. doi: 10.1016/j.pain.2010.05.021

Knowlton, W. M., Palkar, R., Lippoldt, E. K., McCoy, D. D., Baluch, F., Chen, J., et al. (2013). A sensory-labeled line for cold: TRPM8-expressing sensory neurons define the cellular basis for cold, cold pain, and cooling-mediated analgesia. *J. Neurosci.* 33, 2837–2848. doi: 10.1523/JNEUROSCI.1943-12.2013

Kroeger, D., Absi, G., Gagliardi, C., Bandaru, S. S., Madara, J. C., Ferrari, L. L., et al. (2018). Galanin neurons in the ventrolateral preoptic area promote sleep and heat loss in mice. *Nat. Commun.* 9:4129. doi: 10.1038/s41467-018-06590-7

Lazarus, M., Yoshida, K., Coppari, R., Bass, C. E., Mochizuki, T., Lowell, B. B., et al. (2007). EP3 prostaglandin receptors in the median preoptic nucleus are critical for fever responses. *Nat. Neurosci.* 10, 1131–1133. doi: 10.1038/nn1949

Luquet, S., Perez, F. A., Hnasko, T. S., and Palmiter, R. D. (2005). NPY/AgRP neurons are essentials for feeding in adult mice but can be ablated in neonates. *Science* 310, 683–685. doi: 10.1126/science.1115524

Ma, Y., Miracca, G., Harding, E. C., Miao, A., Yustos, R., Vyssotski, A. L., et al. (2019). Galanin neurons unite sleep homeostasis and a2-Adrenergic sedation. *Curr. Biol.* 29, 3315–3322. doi: 10.1016/j.cub.2019.07.087

Machado, N. L. S., Bandaru, S. S., Abbott, S. B. G., and Saper, C. B. (2020). Ep3R-expressing glutamatergic preoptic neurons mediate inflammatory fever. *J. Neurosci.* 40, 2573–2588. doi: 10.1523/JNEUROSCI.2887-19.2020

Magoun, H. W., Harrison, F., Brobeck, J. R., and Ranson, S. W. (1938). Activation of heat loss mechanisms by local heating of the brain. *J. Neurophysiol.* 1, 101–114. doi: 10.1152/jn.1938.1.2.101

Moffitt, J. R., Bambah-Mukku, D., Eichhorn, S. W., Vaughn, E., Shekhar, K., Perez, J. D., et al. (2018). Molecular, spatial, and functional single-cell profiling of the hypothalamic preoptic region. *Science* 362:eaau5324. doi: 10.1126/science.aau5324

Morrison, S. F., and Nakamura, K. (2011). Central neural pathways for thermoregulation. *Front. Biosci.* 16, 74–104. doi: 10.2741/3677

Nakamura, K., Matsumura, K., Hübschle, T., Nakamura, Y., Hioki, H., Fujiyama, F., et al. (2004). Identification of sympathetic premotor neurons in medullary raphe regions mediating fever and other thermoregulatory functions. *J. Neurosci.* 24, 5370–5380. doi: 10.1523/JNEUROSCI.1219-04.2004

Nakamura, Y., Nakamura, K., and Morrison, S. F. (2009). Different populations of prostaglandin EP3 receptor-expressing preoptic neurons project to two fever-mediating sympathoexcitatory brain regions. *Neuroscience* 161, 614–620. doi: 10.1016/j.neuroscience.2009.03.041

Nakane, Y., Ikegami, K., Ono, H., Yamamoto, N., Yoshida, S., Hirunagi, K., et al. (2010). A mammalian neural tissue opsin (Opsin 5) is a deep brain photoreceptor in birds. *Proc. Natl. Acad. Sci. U.S.A.* 107, 15264–15268. doi: 10.1073/pnas.1006393107

Nakayama, T., Eisenman, J. S., and Hardy, J. D. (1961). Single unit activity of anterior hypothalamus during local heating. *Science* 134, 560–561. doi: 10.1126/science.134.3478.560

Nakayama, T., Hammel, H. T., Hardy, J. D., and Eisenman, J. S. (1963). Thermal stimulation of electrical activity of single units of the preoptic region. *Am. J. Physiol. Content* 215, 389–403. doi: 10.1152/ajplegacy.1963.204.6.1122

Nedergaard, J., Golozoubova, V., Matthias, A., Asadi, A., Jacobsson, A., and Cannon, B. (2001). UCP1: the only protein able to mediate adaptive non-shivering thermogenesis and metabolic inefficiency. *Biochim. Biophys. Acta Bioenerg.* 1504, 82–106. doi: 10.1016/S0005-2728(00)00247-4

Padilla, S. L., Johnson, C. W., Barker, F. D., Patterson, M. A., and Palmiter, R. D. (2018). A neural circuit underlying the generation of hot flushes. *Cell Rep.* 24:37. doi: 10.1016/j.celrep.2018.06.037

Pogorzala, L. A., Mishra, S. K., and Hoon, M. A. (2013). The cellular code for mammalian thermosensation. *J. Neurosci.* 33, 5533–5541. doi: 10.1523/JNEUROSCI.5788-12.2013

Rance, N. E., Dacks, P. A., Mittelman-Smith, M. A., Romanovsky, A. A., and Krajewski-Hall, S. J. (2013). Modulation of body temperature and LH secretion by hypothalamic KNDy (kisspeptin, neurokinin B and dynorphin) neurons: a novel hypothesis on the mechanism of hot flushes. *Front. Neuroendocrinol.* 34, 211–227. doi: 10.1016/j.yfrne.2013.07.003

Ranels, H. J., and Griffin, J. D. (2003). The effects of prostaglandin E2 on the firing rate activity of thermosensitive and temperature insensitive neurons in the ventromedial preoptic area of the rat hypothalamus. *Brain Res.* 964, 42–50. doi: 10.1016/S0006-8993(02)04063-5

Rathner, J. A., Madden, C. J., and Morrison, S. F. (2008). Central pathway for spontaneous and prostaglandin E2-evoked cutaneous vasoconstriction. *Am. J. Physiol. Regul. Integr. Comp. Physiol.* 295, R343–R354. doi: 10.1152/ajpregu.00115.2008

Saper, C. B., and Machado, N. L. S. (2020). Flipping the switch on the body's thermoregulatory system. *Nature* 583, 34–35. doi: 10.1038/d41586-020-01600-5

Scammell, T. E., Price, K. J., and Sagar, S. M. (1993). Hyperthermia induces c-fos expression in the preoptic area. *Brain Res.* 632, 57–67. doi: 10.1016/0006-8993(93)91280-6

Schwartz, M. W., Seeley, R. J., Campfield, L. A., Burn, P., and Baskin, D. G. (1996). Identification of targets of leptin action in rat hypothalamus. *J. Clin. Invest.* 98, 1101–1106. doi: 10.1172/JCI118891

Sheng, M., and Greenberg, M. E. (1990). The regulation and function of c-fos and other immediate early genes in the nervous system. *Neuron* 4, 477–485. doi: 10.1016/0896-6273(90)90106-P

Silva, N. L., and Boulant, J. A. (1986). Effects of testosterone, estradiol, and temperature on neurons in preoptic tissue slices. *Am. J. Physiol. Regul. Integr. Comp. Physiol.* 250:r625. doi: 10.1152/ajpregu.1986.250.4.r625

Song, K., Wang, H., Kamm, G. B., Pohle, J., De Castro Reis, F., Heppenstall, P., et al. (2016). The TRPM2 channel is a hypothalamic heat sensor that limits fever and can drive hypothermia. *Science* 353, 1393–1398. doi: 10.1126/science.aaf7537

Stuart, T., Butler, A., Hoffman, P., Hafemeister, C., Papalexi, E., Mauck, W. M., et al. (2019). Comprehensive integration of single-cell data. *Cell* 177, 1888–1902. doi: 10.1016/j.cell.2019.05.031

Swoap, S. J. (2008). The pharmacology and molecular mechanisms underlying temperature regulation and torpor. *Biochem. Pharmacol.* 76, 817–824. doi: 10.1016/j.bcp.2008.06.017

Takahashi, T. M., Sunagawa, G. A., Soya, S., Abe, M., Sakurai, K., Ishikawa, K., et al. (2020). A discrete neuronal circuit induces a hibernation-like state in rodents. *Nature* 583, 109–114. doi: 10.1038/s41586-020-2163-6

Tan, C. L., Cooke, E. K., Leib, D. E., Lin, Y. C., Daly, G. E., Zimmerman, C. A., et al. (2016). Warm-sensitive neurons that control body temperature. *Cell* 167, 47–59. doi: 10.1016/j.cell.2016.08.028

Tan, C. L., and Knight, Z. A. (2018). Regulation of body temperature by the nervous system. *Neuron* 98, 31–48. doi: 10.1016/j.neuron.2018.02.022

Tarttelin, E. E., Bellingham, J., Hankins, M. W., Foster, R. G., and Lucas, R. J. (2003). Neuropsin (Opn5): a novel opsin identified in mammalian neural tissue. *FEBS Lett.* 554, 410–416. doi: 10.1016/S0014-5793(03)01212-2

Walter, A., van der Spek, L., Hardy, E., Bemelmans, A. P., Rouach, N., and Rancillac, A. (2019). Structural and functional connections between the median and the ventrolateral preoptic nucleus. *Brain Struct. Funct.* 224, 3045–3057. doi: 10.1007/s00429-019-01935-4

Wang, T. A., Teo, C. F., Åkerblom, M., Chen, C., Tynan-La Fontaine, M., Greiner, V. J., et al. (2019). Thermoregulation via temperature-dependent PGD2 production in mouse preoptic area. *Neuron* 103, 309–322.e7. doi: 10.1016/j.neuron.2019.04.035

Yang, W. Z., Du, X., Zhang, W., Gao, C., Xie, H., Xiao, Y., et al. (2020). Parabrachial neuron types categorically encode thermoregulation variables during heat defense. *Sci. Adv.* 6:eabb9414. doi: 10.1126/sciadv.abb9414

Yarmolinsky, D. A., Peng, Y., Pogorzala, L. A., Rutlin, M., Hoon, M. A., and Zuker, C. S. (2016). Coding and plasticity in the mammalian thermosensory system. *Neuron* 167, 897–914. doi: 10.1016/j.neuron.2016.10.021

Yoo, S., Cha, D., Kim, D. W., Hoang, T. V., and Blackshaw, S. (2019). Tanycyte-independent control of hypothalamic leptin signaling. *Front. Neurosci.* 13:240. doi: 10.3389/fnins.2019.00240

Yoshida, K., Li, X., Cano, G., Lazarus, M., and Saper, C. B. (2009). Parallel preoptic pathways for thermoregulation. *J. Neurosci.* 29, 11954–11964. doi: 10.1523/JNEUROSCI.2643-09.2009

Yu, S., Cheng, H., François, M., Qualls-Creekmore, E., Huesing, C., He, Y., et al. (2018). Preoptic leptin signaling modulates energy balance independent of body temperature regulation. *eLife* 7:e33505. doi: 10.7554/elife.33505

Yu, S., Qualls-Creekmore, E., Rezai-Zadeh, K., Jiang, Y., Berthoud, H. R., Morrison, C. D., et al. (2016). Glutamatergic preoptic area neurons that express leptin receptors drive temperature-dependent body weight homeostasis. *J. Neurosci.* 36, 5034–5046. doi: 10.1523/JNEUROSCI.0213-16.2016

Zhang, K. X., D'Souza, S., Upton, B. A., Kernodle, S., Vemaraju, S., Nayak, G., et al. (2020). Violet-light suppression of thermogenesis by opsin 5 hypothalamic neurons. *Nature* 585, 420–425. doi: 10.1038/s41586-020-2683-0

Zhang, Y., Kerman, I. A., Laque, A., Nguyen, P., Faouzi, M., Louis, G. W., et al. (2011). Leptin-receptor-expressing neurons in the dorsomedial hypothalamus and median preoptic area regulate sympathetic brown adipose tissue circuits. *J. Neurosci.* 31, 1873–1884. doi: 10.1523/JNEUROSCI.3223-10.2011

Zhang, Z., Reis, F. M. C. V., He, Y., Park, J. W., DiVittorio, J. R., Sivakumar, N., et al. (2020). Estrogen-sensitive medial preoptic area neurons coordinate torpor in mice. *Nat. Commun.* 11:6378. doi: 10.1038/s41467-020-20050-1

Zhao, Z. D., Yang, W. Z., Gao, C., Fu, X., Zhang, W., Zhou, Q., et al. (2017). A hypothalamic circuit that controls body temperature. *Proc. Natl. Acad. Sci. U.S.A.* 114:201616255. doi: 10.1073/pnas.1616255114

Conflict of Interest: The Lang lab has a sponsored research agreement with BIOS Lighting Inc.

The authors declare that the research was conducted in the absence of any commercial or financial relationships that could be construed as a potential conflict of interest.

frontiers in Endocrinology

ORIGINAL RESEARCH
published: 13 May 2021
doi: 10.3389/fendo.2021.667773

Hippocampal Glycerol-3-Phosphate Acyltransferases 4 and BDNF in the Progress of Obesity-Induced Depression

Yin-qiong Huang[1], *Yaofeng Wang*[1], *Keyue Hu*[1], *Shu Lin*[2,3*] *and Xia-hong Lin*[4*]

[1] *Department of Endocrinology, The Second Affiliated Hospital of Fujian Medical University, Quanzhou, China,* [2] *Centre of Neurological and Metabolic Research, The Second Affiliated Hospital of Fujian Medical University, Quanzhou, China,* [3] *Diabetes and Metabolism Division, Garvan Institute of Medical Research, 384 Victoria Street, Darlinghurst, Sydney, NSW, Australia,* [4] *Department of Endocrinology, The Seventh Affiliated Hospital of Sun Yat-sen University, Shenzhen, China*

Background: Obesity has been reported to lead to increased incidence of depression. Glycerol-3-phosphate acyltransferases 4 (GPAT4) is involved in triacylglycerol synthesis and plays an important role in the occurrence of obesity. GPAT4 is the only one of GPAT family expressed in the brain. The aim of this study is to investigate if central GPAT4 is associated with obesity-related depression and its underlying mechanism.

Results: A high-fat diet resulted in increased body weight and blood lipid. HFD induced depression like behavior in the force swimming test, tail suspension test and sucrose preference test. HFD significantly up-regulated the expression of GPAT4 in hippocampus, IL-1β, IL-6, TNF-α and NF-κB, accompanied with down-regulation of BDNF expression in hippocampus and ventromedical hypothalamus, which was attributed to AMP-activated protein kinase (AMPK) and cAMP-response element binding protein (CREB).

Conclusion: Our findings suggest that hippocampal GPAT4 may participate in HFD induced depression through AMPK/CREB/BDNF pathway, which provides insights into a clinical target for obesity-associated depression intervention.

Keywords: glycerol-3-phosphate acyltransferases 4, depression, high fat diet, hippocampus, ventromedical hypothalamus, inflammation

OPEN ACCESS

Edited by:
Tiemin Liu,
Fudan University, China

Reviewed by:
Qingchun Tong,
University of Texas Health Science Center at Houston, United States
Romana Stark,
Monash University, Australia

****Correspondence:***
Xia-hong Lin
linxiahongdr@fjmu.edu.cn
Shu Lin
shulin1956@126.com

Specialty section:
This article was submitted to Neuroendocrine Science, a section of the journal Frontiers in Endocrinology

Received: *14 February 2021*
Accepted: *19 April 2021*
Published: *13 May 2021*

Citation:
Huang Y-q, Wang Y, Hu K, Lin S and Lin X-h (2021) Hippocampal Glycerol-3-Phosphate Acyltransferases 4 and BDNF in the Progress of Obesity-Induced Depression. Front. Endocrinol. 12:667773. doi: 10.3389/fendo.2021.667773

INTRODUCTION

Obesity is a metabolic disorder caused by excessive accumulation of fat due to increased energy intake. Both environmental factors and genetic factors are responsible for the development of obesity (1, 2). With the development of social economy and lifestyle changes, the incidence of obesity is increasing over years, and it has become a serious public health problem. The main clinical consequences of obesity include diabetes, cardiovascular disease, respiratory distress syndrome, sleep disorders, asthma, and tumors, as well as various mental and psychological diseases (3, 4).

Both epidemiological and clinical studies have shown that there is a positive correlation between obesity and depression. Obese people have a significantly increased risk of depression (5, 6). Body mass index (BMI) is positively correlated with the degree of clinical depressive symptoms (7).

However, although high-energy food can alleviate negative emotions and bad moods in a short period of time, the weight gain caused by long-term consumption will aggravate the depressive symptoms in patients (8, 9). Some scholars have also discovered that depression and obesity have the same candidate genes from the perspective of genetics. Depression and obesity have a high incidence of comorbidities, which seriously endanger the health of patients, but the mechanism is still unclear.

Obesity is related to a high-risk of depression. Both clinical studies and animal experiments have showed that there is a positive relationship between the two. However, the neuropathophysiological mechanism of depression caused by obesity remains unclear. Based on previous studies, neuroinflammation have been implicated in the development of depression. Inflammation, especially neuroinflammation, is an important link between obesity and depression. A high-fat diet activates the inflammatory response in the animal's brain. Animal experiments have shown that IL-1β in the brain can mediate chronic stress-induced depression-like behaviors, while IL-1β receptor knockout mice will not show depression-like behaviors after stress (10).

Glycerol-3-Phosphate Acyltransferases 4 (GPAT4) is the key rate-limiting enzyme in the synthesis of triacylglycerols in the glycerophosphate pathway. Gene overexpression and gene knockout experiments (11, 12) confirmed that GPAT4 plays an important role in the development of obesity, liver steatosis and insulin resistance. Compared with wild-type mice, GPAT4-/- (gene knockout) mice lose weight, have subcutaneous lipodystrophy, reduce triacylglycerol (TAG) content in adipose tissue and liver, and improve insulin resistance (13). And a recent study (14) found that overexpression of GPAT4 in the liver of mice resulted in liver insulin resistance and thus impairs liver glucose metabolism, leading to increased liver gluconeogenesis and reduced glycogen synthesis, and ultimately destroys glucose homeostasis, indicating that GPAT4 may be a new drug target for potential prevention and treatment of obesity, insulin resistance and type 2 diabetes (15). GPAT4 is important in the development of obesity. Besides, GPAT4 is the only one in the GPAT family that is expressed in the brain (16, 17). However, whether central GPAT4 is involved in the development of depression remains unclear.

Brain-derived neurotrophic factor (BDNF) is mainly expressed in the central nervous system, especially in hippocampus and cortex. BDNF has been found to regulate food intake and energy metabolism in the central nervous system, promote body movement, suppress appetite, and improve the leptin resistance and insulin resistance (18). Besides, BDNF is also the main regulator of synaptic plasticity and memory formation (19). It is the major regulator of maintaining neuronal function, regeneration and repair, and preventing neuronal degeneration (20). Obese mice experienced a decline in cognitive function after a long-term high-fat diet, accompanied by corresponding pathological changes in hippocampal neurons, which are closely related to the decline of BDNF levels in hippocampus. Recent studies have found that obesity can induce hippocampal inflammation and impairs emotion related to the hippocampus (21).

High-fat-induced obese mice can lead to the inflammatory state in hippocampus of the mouse and the decrease of BDNF. Studies showed that GPAT4 is also highly expressed in the hippocampus, and GPAT4 is the key rate-limiting enzyme for the synthesis of triacylglycerols in the glycerophosphate pathway. Therefore, this study aims to investigate whether central GPAT4 is associated with obesity-related depression and its underlying mechanism.

MATERIALS AND METHODS

Laboratory Animals and Reagents

Twenty-four 5-week-old male C57BL/6 mice were purchased from the Animal Experimental Center of Fujian Medical University. All mice were housed under standard conditions (constant temperature, constant humidity conditions, and a 12-h light/dark cycle), with free access to food and water. The study followed the National Guidelines for Laboratory Animal Welfare and was approved by the Experimental Animal Ethics Committee of the Second Affiliated Hospital of Fujian Medical University (2020-388).

Establishment of Mice Model

The twenty-four mice were acclimatized for 1 week before conducting the experiments. Then, they were randomized to two groups: normal diet group (ND group, n = 12) and high fat diet group (HFD group, n = 12). The ND group was fed a normal diet (Research Diets, D12450h), and the HFD group were fed a high-fat diet (Research Diets, D12451) for 8 weeks. Six mice in each group were subjected to brain tissue isolation for subsequent qPCR, and the remaining six mice were subjected to perfusion to make frozen sections of brain tissue for *in situ* hybridization.

Behavior Tests

Forced Swimming Test (FST)

The mice were forced to swim for 6 min in a transparent cylindrical container (40cm in height and 20cm in diameter) containing clean water (24°C, 20cm in depth). The duration of immobility state was measured (22).

Tail Suspension Test (TST)

In brief, the mice were suspended approximately 28 ± 2 cm off the floor by fixing its tail (2 cm from the tip of the tail) on the hook. During the experiment immobility time of the mice were automatically recorded for 6 mins (22, 23).

Sucrose Preference

Before starting the experiment, the mice were singly housed and trained to freely drink water and sucrose water in two bottles (the positions of the two water bottles were switched every day) and the daily intake of sucrose water and regular water was recorded for 1 week. The experiment was started after a stable sucrose

water consumption was evident. After 21 days, the sucrose preference test was performed. The detailed test protocol was as follows: after a 12 h period of water fasting, the animals were allowed free access to two bottles respectively containing water and 1% sucrose solution. This test lasted for two hours. Sucrose preference was calculated as the ratio of sucrose water intake to the total volume of liquid intake (24, 25).

Lipid Measurement

Fasting lipid levels including total cholesterol, low density lipoprotein and triglyceride were measured with an automatic biochemistry analyzer.

In Situ Hybridization (ISH) by RNAscope Technology to Determine the mRNA Expression of BDNF in the Hippocampus and Ventromedical Hypothalamus

The animals were perfused with phosphate buffered solution (PBS) at a pH of 7.4 by a cannula inserted in the left ventricle after anesthesia, followed by 4% paraformaldehyde. After perfusion, the brains were immediately removed and were fixed in 4% paraformaldehyde in PBS at 4°C for 12 h and passed through 20 and 30% sucrose gradients prior to embedding in optimum cutting temperature compound (OCT). 20μm tissue sections were air-dried at −20°C and moved to −80°C for long-term storage. Commercially available RNAscope brown reagent kit and RNAscope probes (Advanced Cell Diagnostics, Hayward, CA, Cat No. 322300) were used for transcript detection. ISH was performed according to the manufacturer's instructions for fixed-frozen tissue. The detection was operated in a hybridization oven (HybEZ^{TM}, ACD) with RNAscope Probe- Mm-BDNF (ACD 518751). Each set of probes contained a tag that enabled target transcription to be visualized in a brown color. To compare the expression differences between the two groups, we quantified the integral optical density (IOD) of positive BDNF staining using ImageJ and normalized it by stained area. The mean intensities from three random areas of the same size in target areas were measured for each probe.

TABLE 1 | Primers of qRT-PCR.

Gene		Primers sequence
β-actin	Forward	5' CTACCTCATGAAGATCCTGACC 3'
	Reverse	5' CACAGCTTCTCTTTGATGTCAC 3'
GPAT4	Forward	5' AACCTCCTGGGTATCTCCCTG3'
	Reverse	5' CCGTTGGTGTAGGGCTTGT3'
IL-1β	Forward	5' GAAATGCCACCTTTTGACAGTG3'
	Reverse	5' TGGATGCTCTCATCAGGACAG3'
IL-6	Forward	5' CTCCCAACAGACCTGTCTATAC 3'
	Reverse	5' CCATTGCACAACTCTTTTCTCA 3'
TNF-α	Forward	5' ATGTCTCAGCCTCTTCTCATTC 3'
	Reverse	5' GCTTGTCACTCGAATTTTGAGA 3'
NF-κB	Forward	5' CAAAGACAAAGAGGAAGTGCAA 3'
	Reverse	5' ACTTGATGATCCTCGAGATGTC 3'
AMPK	Forward	5' GTCAAAGCCGACCCAATGATA3'
	Reverse	5' CGTACACGCAAATAATAGGGGTT3'
CREB	Forward	5' AGCAGCTCATGCAACATCATC3'
	Reverse	5' AGTCCTTACAGGAAGACTGAACT3'

β-actin was used as mRNA reference gene, with the 2−ΔΔCt method used for quantitation. Triplicate experiments were performed and repeated at least 3 times.

Quantitative RT-PCR (qRT-PCR)

At the end of each experiment, a microdissection procedure was used to isolate hippocampus. Total RNA was extracted with TRIzol (RNAiso Plus) method (Takara, Japan). RNA was reversed transcribed into cDNA using the two-step method with PrimeScript^{TM} RT reagent Kit with gDNA Eraser (Takara, Japan), according to the manufacturer's instructions. mRNA qRT-PCR was performed with the TB Green^{TM} Premix Ex Taq^{TM} (TliRNaseH Plus) (Takara, Japan) according to the manufacturer's instruction. The procedure was 95°C for 1 min; 95°C for 15 s and 60°C for 34 s, for 40 cycles; 95°C for 15 s, 60°C for 1 min and 95°C for 15 s. The primers were shown in (**Table 1**).

Statistical Analyses

All statistical analyses were performed using the SPSS Statistics 20 software. Data have been expressed in terms of mean ± standard deviation. Statistical significances between two groups of data were determined using unpaired, two-tailed Student's *t*-test. A P value >0.05 was not considered significant, P value <0.05 was labeled as (*), P value <0.01 was labeled as (**), P value <0.001 was labeled as (***).

RESULTS

Metabolic Phenotype in Dietary-Induced Obesity Mice

To determine the metabolic phenotype of mice after a fat-dense diet, we measure the body weight of mice every week. Besides, at the end the of experiment, blood lipid level was measured. We found that 8 weeks of high-fat diet caused increased body weight (**Figures 1A, B**), and blood lipid level including total cholesterol (**Figure 1C**), low density lipoprotein (**Figure 1D**), and triglyceride (**Figure 1E**), compared with ND group.

Depression-Like Phenotype in Dietary-Induced Obesity Mice

To determine whether the consumption of a fat-dense diet plays a causative role in the development of depression, we examined depression-related behaviors among mice fed a ND or HFD. After 8 weeks of high-fat diet (HFD), we examined depression-related behaviors including forced swimming test, tail suspension test and sucrose preference test. Increased immobilization time was observed during forced swim tests (**Figure 2A**) and tail suspension tests (**Figure 2B**) in HFD mice. Also, consumption of sucrose solution (**Figure 2C**) was less in HFD mice compared with control mice on a normal diet.

GPAT4 Expression in Hippocampus Was Decreased After High Fat Diet

GPAT4 is the key rate-limiting enzyme in the synthesis of triacylglycerols in the glycerophosphate pathway and plays an important role in the development of obesity. Besides, GPAT4 is the only one in the GPAT family that is expressed in the brain.

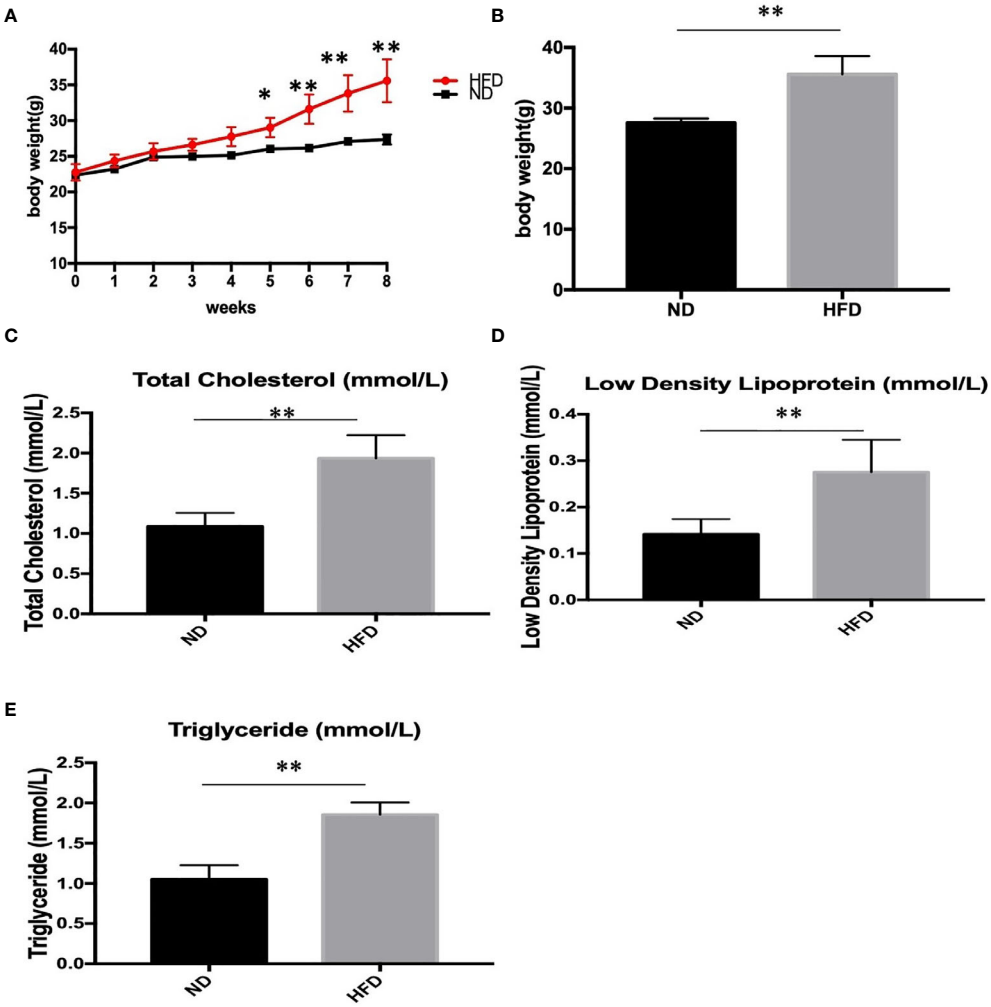

FIGURE 1 | Body weight and blood lipid level after 8 weeks of HFD and ND. **(A)** body weight changes during the 8 weeks; **(B)** Body weight after 8 weeks; **(C)** total cholesterol; **(D)** low density lipoprotein; **(E)** triglyceride. Results are mean ± standard deviation, *P value < 0.05, **P value < 0.01, comparison between the mice fed HFD and ND. (n=6).

To investigate whether central GPAT4 is involved in the development of obesity-related depression, GPAT4 mRNA expression in hippocampus was measured after 8 weeks of high-fat diet (HFD). We found that compared with ND group, GPAT4 mRNA expression in hippocampus was significantly up-regulated in HFD group (**Figure 3A**). We further investigated the correlation between GPAT4 and body weight, we found that the GPAT4 was positive correlated with body weight ($p<0.05$) (**Figure 3B**)

High Fat Diet Induced Inflammation in Hippocampus

Inflammation, especially neuroinflammation, is an important link between obesity and depression. To measure the inflammation in the central nervous system, we examined inflammation markers between HFD mice and normal diet (ND) mice after 8 weeks of high-fat diet (HFD). We found that HFD significantly up-regulated the expression of IL-1β (**Figure 4A**), IL-6 (**Figure 4B**), TNF- α (**Figure 4C**) and NF-κB (**Figure 4D**) in hippocampus.

BDNF Expression in Hippocampus and Ventromedical Hypothalamus Were Decreased After High Fat Diet

BDNF plays a role in emotion regulation, memory function and energy homeostasis as well. To evaluate the role of central BDNF in obesity-related depression, after 8 weeks of high-fat diet (HFD), we examined BDNF expression in hippocampus and ventromedical hypothalamus (VMH). Compared with ND group, BDNF mRNA expression in hippocampus (**Figure 5**), and VMH (**Figure 6**) were significantly down-regulated in HFD group.

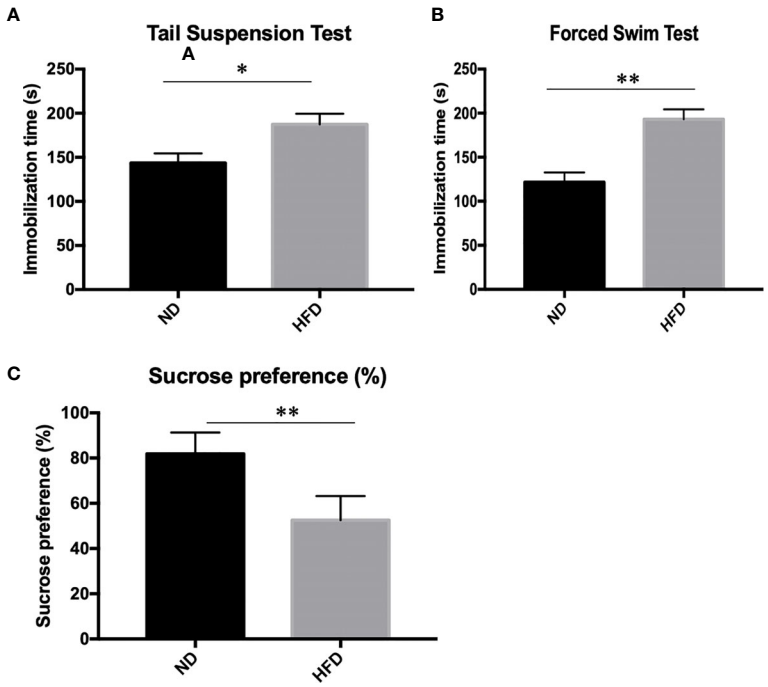

FIGURE 2 | Depression-like phenotype in dietary-induced obesity mice. **(A)** forced swim tests; **(B)** tail suspension tests; **(C)** Sucrose preference test. *P value < 0.05, **P value < 0.01, comparison between the mice fed HFD and ND. (n=6).

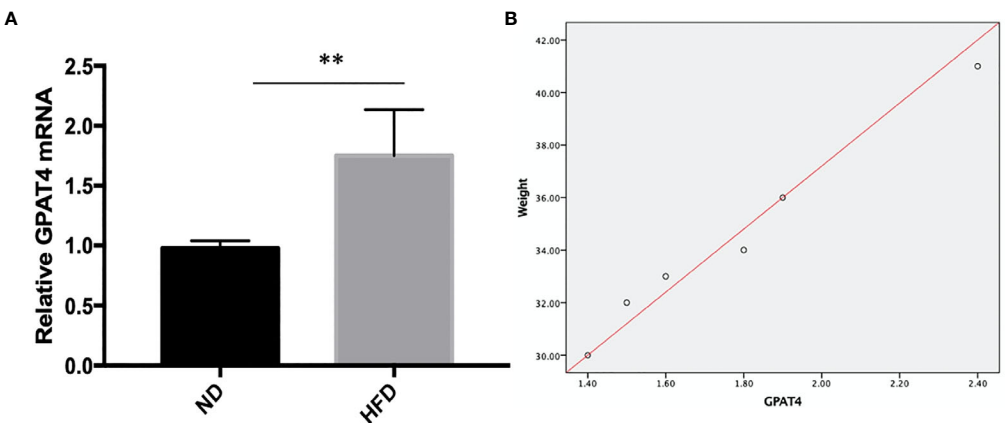

FIGURE 3 | **(A)** GPAT4 expression in hippocampus was decreased after high fat diet. **P value < 0.01, comparison between the mice fed HFD and ND. **(B)** Correlation between GPAT4 expression and body weight. (n=6).

AMPK/CREB Pathway Might Participate in High Fat Diet Induced Depression

To further understand the molecular events underlying the high-fat diet induced depression-like behavior, q-RT PCR was carried out to measure the expression of AMPK and CREB mRNA expression. Our study showed that AMPK and CREB mRNA expression were decreased in HFD group compared with ND group (**Figure 7**).

DISCUSSION

The main findings in our present study include (1) high-fat diet can lead to the development of depression through the use of behavioral paradigms; (2) its mechanism is related to the up-regulation of hippocampal GPAT4 expression and hippocampal inflammation; (3) *in situ* hybridization shows BDNF mRNA expression level, down-regulated in hippocampus and VMH; (4)

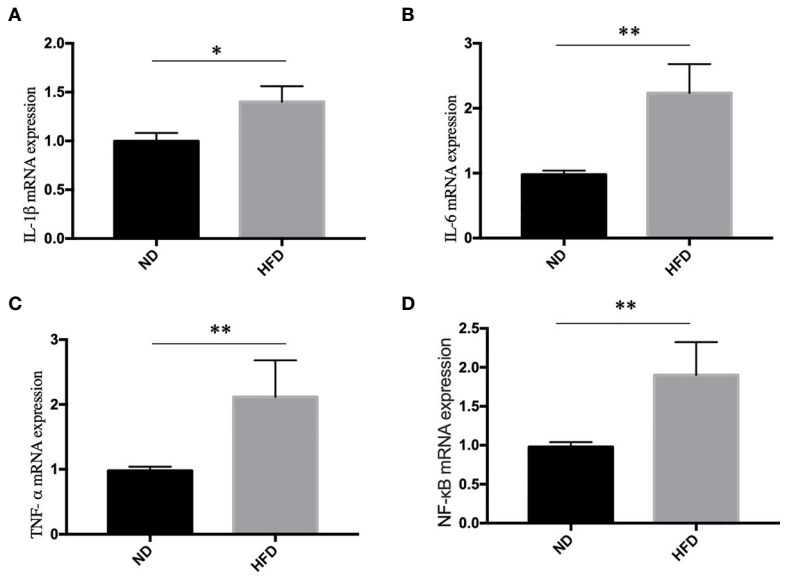

FIGURE 4 | High fat diet induced inflammation in hippocampus. **(A)** IL-1β; **(B)** IL-6; **(C)** TNF- α; **(D)** NF-κB. *P value < 0.05, **P value < 0.01, comparison between the mice fed HFD and ND. (n=6).

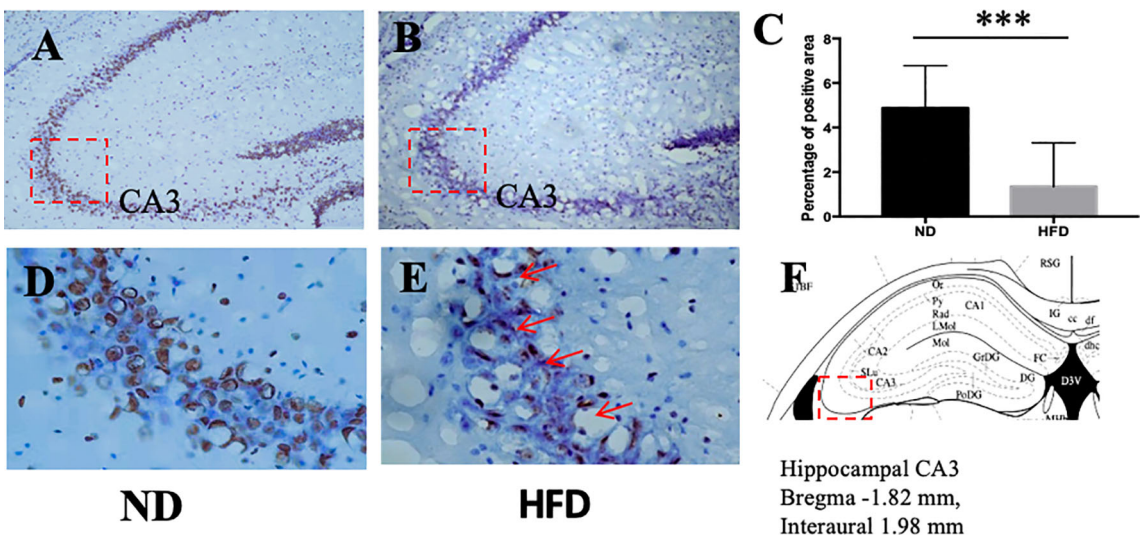

FIGURE 5 | **(A)** BDNF expression in hippocampus in ND group; **(B)** BDNF expression in hippocampus in HFD group; **(C)** percentage of positive area between ND and HFD group; **(D)** higher magnification of **(A)**; **(E)** higher magnification of **(B)**; **(F)** hippocampus area in the brain. ***P value < 0.001, comparison between the mice fed HFD and ND. (n=6).

Real-time quantitative PCR detects the down-regulation of hippocampal AMPK and CREB expression levels in the HFD fed mice.

Depression and obesity are closely related, interact, and are supported by a large amount of epidemiological evidence (26). A systematic review and meta-analysis of the longitudinal relationship between depression, overweight, and obesity discovered that obesity increases the risk of depression (27). Vagena et al. (28) discovered that a high-fat diet can promote the development of depression-like behavior in both groups of mice fed with a high-fat diet for 3 weeks and 8 weeks. In this study, we found that a high-fat diet for 8 weeks induces depression-like behavior, which is consistent with previous studies.

However, the specific mechanism of depression caused by obesity needs to be further explored. The hippocampus is a key area that controls emotions and cognitive behavior in the brain.

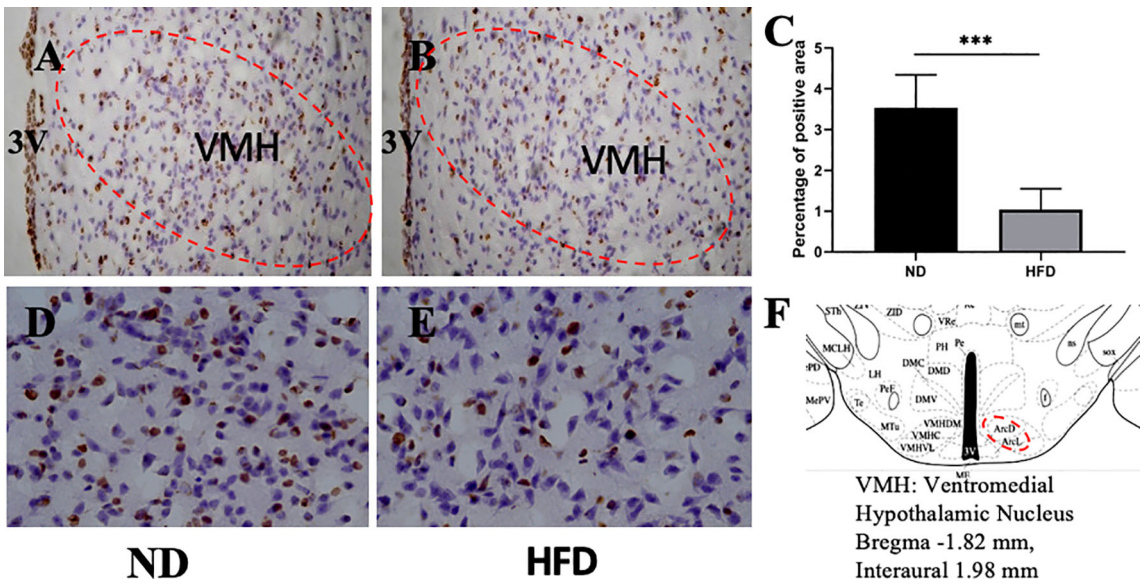

FIGURE 6 | **(A)** BDNF expression in VMH in ND group; **(B)** BDNF expression in VMH in HFD group; **(C)** percentage of positive area between ND group and HFD group; **(D)** higher magnification of **(A)**; **(E)** higher magnification of **(B)**; **(F)** VMH area in the brain. ****P* value < 0.001, comparison between the mice fed HFD and ND. (n=6).

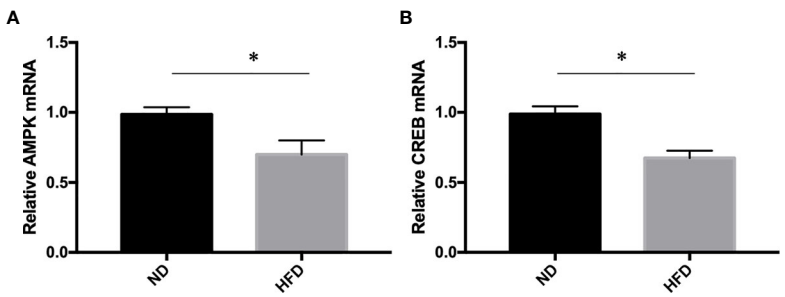

FIGURE 7 | **(A)** AMPK expression; **(B)** CREB expression. **P* value < 0.05, comparison between the mice fed HFD and ND. (n=6).

In obese animal models, high levels of hippocampal and cortical cytokines are expressed in this area (29–31).

GPAT catalyze the first step of synthesis of TAG, which also acts as the rate-limiting enzyme in the *de novo* pathway of glycerophospholipid synthesis. Besides, GPAT4 is the only one in the GPAT family that is expressed in the brain including the hippocampus and the cerebellum. The present study reveals that high fat diet induced GPAT4 overexpression in hippocampus, suggesting that GPAT4 in the hippocampus might play a role in diet-induced depression.

Studies have shown that neurotrophins including BDNF have been documented to play a crucial role in depression. BDNF plays a role in emotion regulation and memory function, especially in the hippocampus area (32). The down-regulation of hippocampal BDNF levels is associated with impaired emotion-related behaviors (33). Many kinds of antidepressants and electroconvulsive therapies significantly increase the expression of BDNF in the hippocampus and prefrontal cortex (34). In addition, direct injection of BDNF into the hippocampus can also show antidepressant effects (35). BDNF plays an important regulatory role in the plasticity of hippocampal structure, and mediate protective effects by enhancing neuron survival (36). What's more, the expression and signal transduction of hippocampal BDNF mRNA negatively regulated by proinflammatory cytokines (37–39). Dexamethasone can reduce the level of pro-inflammatory cytokines, increase the level of anti-inflammatory cytokines, and prevent the decline of BDNF level caused by inflammation (40). The expression of low levels of BDNF in the nervous system may trigger energy homeostasis, thereby developing obesity and

glucose intolerance, and metabolic disorders. BDNF is an important part of the central nervous circuit and participates in regulating energy homeostasis (41). Integrate hippocampus BDNF signal affect the efficacy of antidepressants and the anxiety-like behavior (33).

Obviously, BDNF is related to depression. Previous studies found that the expression of BDNF in hippocampus decreased in depressed mice. However, it is not clear how high-fat diet affect BDNF expression in the central nervous system. In this study, we found that HFD simultaneously induced the down-regulation of BDNF mRNA in hippocampus and VMH, suggesting that BDNF may play a role in depression induced by high-fat diet.

VMH is the satiety center in the brain that regulates food intake, glucose and energy metabolism *via* different downstream targets. A recent research discovers the inhibition of peripheral 5-HT synthesis lead to resistance to HFD-induced obesity and can attenuate HFD-induced depression-like behavior (42).VMH is an important center that integrate peripheral metabolic signal (43). Our previous study found that high fat diet-fed mice with impaired glucose tolerance expressed lower level of BDNF mRNA in VMH. HFD leads to changes of BDNF in VMH by affecting the central insulin signaling pathway (44).

Obesity is linked with chronic low-grade inflammation, which actives the peripheral immunity, transform the inflammation in the central nervous system by the humoral, neural and cellular pathways (45). Central inflammation affects the pathophysiological process of depression, including monoaminergic neurotransmission. There were plenty of evidence justify the role of immune inflammatory disorders. A meta-analysis reported that the level of inflammation markers in depressed patients were higher than those in the control group (46–48). For patients with major depression with elevated plasma inflammatory markers, they respond poorly to antidepressant drugs (49). Higher IL-6 and CRP can predict the development of depression (50). Prospective researches also show that depression can predict the later level changes of IL-6 and CRP (51). A meta-analysis including14 randomized placebo controlled trials showed that anti-inflammatory treatments effectively reduce symptoms in patients with depression (52). Higher levels of peripheral IL-6 were related to brain inflammation (53, 54). IL-6 was negatively

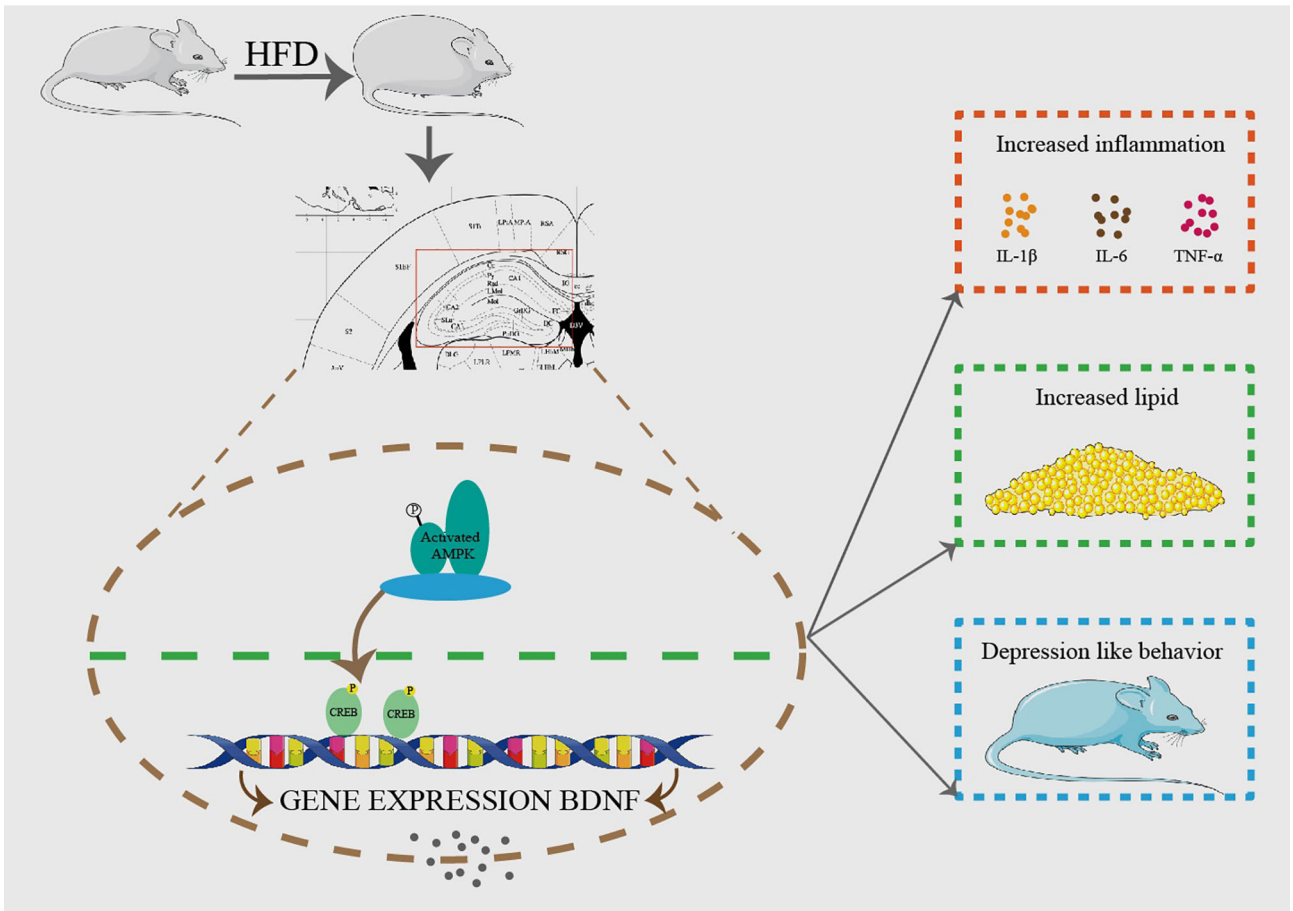

FIGURE 8 | HFD resulted in obesity and depression like behavior. After 8 weeks of HFD, hippocampus GPAT4 and inflammation increased, which was attributed to down-regulation of BDNF, AMP-activated protein kinase (AMPK) and cAMP-response element binding protein (CREB) expression in hippocampus. (n=6).

correlated with hippocampal gray matter volume in healthy adults (53), suggesting that inflammation was a contributing factor to the reduction of hippocampal gray matter. Peripheral inflammation affected hippocampal plasticity, which was due to the activation of microglia and the effects of IL-6 and TNF-α (55, 56). Brain inflammation may negatively affect emotion, study and memory through processes related to neurodegeneration and structural remodeling (57, 58), and mainly affected the hippocampus (59, 60).

5-AMP activated protein kinase (AMPK) is an enzyme involved in energy balance and glucose, and adipose metabolism to help maintain body homeostasis (61, 62). The activation of AMPK can increase the expression of BDNF and active CREB pathway (63). Depression model rats showed overexpression of miR-124 and down-regulation of CREB1 and BDNF in the hippocampus. While knocking down miR-124 improved depression-like behavior in depression rats, which might be related to the increased expression of CREB1 and BDNF in the hippocampus (64). Our study found out downregulation of AMPK and CREB in high-fat fed mice. Depression might be triggered by HFD through AMPK/CREB/BDNF pathway.

There are some limitations in our study. The connection between GPAT4 and BDNF still need to be further confirmed. In our future studies, we will use specific hippocampal GPAT4 knockout mice to further confirm the role of GPAT4 in the hippocampus in the development of depression.

In conclusion, we demonstrate that hippocampal GPAT4 might participate in HFD induced depression by activating AMPK, CREB and BDNF pathways, which provides insights into a clinical target for obesity-associated depression intervention (**Figure 8**).

DATA AVAILABILITY STATEMENT

All relevant data is contained within the article. Further inquiries can be directed to Y-qH by yinqiongh@fumu.edu.cn.

ETHICS STATEMENT

The animal study was reviewed and approved by the Experimental Animal Ethics Committee of the Second Affiliated Hospital of Fujian Medical University (2020-388).

AUTHOR CONTRIBUTIONS

Y-qH, X-hL and SL conceptualized and designed these studies, performed them, and wrote the manuscript. KH and YW contributed through data analyses, data interpretation, and manuscript preparation. All authors contributed to the article and approved the submitted version.

FUNDING

Funding for this work was supported by the Natural science Foundation of Fujian Province (2020J01221); the Key Young Talents Health Training Project of Fujian Province (2020GGA057); Startup Fund for scientific research, Fujian Medical University (2016QH072); Miaopu Fund of the Second Affiliated Hospital of Fujian Medical University (2012MP45).

REFERENCES

1. Herring MP, Sailors MH, Bray MS. Genetic Factors in Exercise Adoption, Adherence and Obesity. *Obes Rev* (2014) 15:29–39. doi: 10.1111/obr.12089
2. Jaaskelainen T, Paananen J, Lindstrom J, Eriksson JG, Tuomilehto J, Uusitupa M, et al. Genetic Predisposition to Obesity and Lifestyle Factors–the Combined Analyses of Twenty-Six Known BMI- and Fourteen Known Waist:Hip Ratio (WHR)-Associated Variants in the Finnish Diabetes Prevention Study. *Br J Nutr* (2013) 110:1856–65. doi: 10.1017/S0007114513001116
3. Gondoni LA, Titon AM, Silvestri G, Nibbio F, Taronna O, Ferrari P, et al. Short Term Effects of Physical Exercise and Low Calorie Diet on Left Ventricular Function in Obese Subjects: A Tissue Doppler Study. *Nutr Metab Cardiovasc Dis* (2007) 17:358–64. doi: 10.1016/j.numecd.2006.01.013
4. Masheb RM, Grilo CM, Rolls BJ. A Randomized Controlled Trial for Obesity and Binge Eating Disorder: Low-Energy-Density Dietary Counseling and Cognitive-Behavioral Therapy. *Behav Res Ther* (2011) 49:821–9. doi: 10.1016/j.brat.2011.09.006
5. Dong C, Sanchez LE, Price RA. Relationship of Obesity to Depression: A Family-Based Study. *Int J Obes Relat Metab Disord* (2004) 28:790–5. doi: 10.1038/sj.ijo.0802626
6. Hamer M, Batty GD, Kivimaki M. Risk of Future Depression in People Who are Obese But Metabolically Healthy: The English Longitudinal Study of Ageing. *Mol Psychiatry* (2012) 17:940–5. doi: 10.1038/mp.2012.30
7. Simon GE, Von Korff M, Saunders K, Miglioretti DL, Crane PK, van Belle G, et al. Association Between Obesity and Psychiatric Disorders in the US Adult Population. *Arch Gen Psychiatry* (2006) 63:824–30. doi: 10.1001/archpsyc.63.7.824
8. Novick JS, Stewart JW, Wisniewski SR, Cook IA, Manev R, Nierenberg AA, et al. Clinical and Demographic Features of Atypical Depression in Outpatients With Major Depressive Disorder: Preliminary Findings From STAR*D. *J Clin Psychiatry* (2005) 66:1002–11. doi: 10.4088/JCP.v66n0807
9. Pagoto S, Schneider KL, Whited MC, Oleski JL, Merriam P, Appelhans B, et al. Randomized Controlled Trial of Behavioral Treatment for Comorbid Obesity and Depression in Women: The Be Active Trial. *Int J Obes (Lond)* (2013) 37:1427–34. doi: 10.1038/ijo.2013.25
10. Goshen I, Kreisel T, Ben-Menachem-Zidon O, Licht T, Weidenfeld J, Ben-Hur T, et al. Brain Interleukin-1 Mediates Chronic Stress-Induced Depression in Mice Via Adrenocortical Activation and Hippocampal Neurogenesis Suppression. *Mol Psychiatry* (2008) 13:717–28. doi: 10.1038/sj.mp.4002055
11. Lewis GF, Carpentier A, Adeli K, Giacca A. Disordered Fat Storage and Mobilization in the Pathogenesis of Insulin Resistance and Type 2 Diabetes. *Endocrine Rev* (2002) 23:201–29. doi: 10.1210/edrv.23.2.0461
12. Takeuchi K, Reue K. Biochemistry, Physiology, and Genetics of GPAT, AGPAT, and Lipin Enzymes in Triglyceride Synthesis. *Am J Physiol Endocrinol Metab* (2009) 296:E1195–209. doi: 10.1152/ajpendo.90958.2008
13. Vergnes L, Beigneux AP, Davis R, Watkins SM, Young SG, Reue K. Agpat6 Deficiency Causes Subdermal Lipodystrophy and Resistance to Obesity. *J Lipid Res* (2006) 47:745–54. doi: 10.1194/jlr.M500553-JLR200
14. Shan D, Li JL, Wu L, Li D, Hurov J, Tobin JF, et al. GPAT3 and GPAT4 are Regulated by Insulin-Stimulated Phosphorylation and Play Distinct Roles in Adipogenesis. *J Lipid Res* (2010) 51:1971–81. doi: 10.1194/jlr.M006304
15. Zhang C, Cooper DE, Grevengoed TJ, Li LO, Klett EL, Eaton JM, et al. Glycerol-3-Phosphate Acyltransferase-4-Deficient Mice are Protected From Diet-Induced Insulin Resistance by the Enhanced Association of Mtor and

Rictor. *Am J Physiol Endocrinol Metab* (2014) 307:E305–15. doi: 10.1152/ajpendo.00034.2014
16. Yu J, Loh K, Song ZY, Yang HQ, Zhang Y, Lin S. Update on Glycerol-3-Phosphate Acyltransferases: The Roles in the Development of Insulin Resistance. *Nutr Diabetes* (2018) 8:34. doi: 10.1038/s41387-018-0045-x
17. Chen YQ, Kuo MS, Li S, Bui HH, Peake DA, Sanders PE, et al. AGPAT6 is a Novel Microsomal Glycerol-3-Phosphate Acyltransferase. *J Biol Chem* (2008) 283:10048–57. doi: 10.1074/jbc.M708151200
18. Vanevski F, Xu B. Molecular and Neural Bases Underlying Roles of BDNF in the Control of Body Weight. *Front Neurosci* (2013) 7:37. doi: 10.3389/fnins.2013.00037
19. Stein S, Winnik S, Matter CM. Brain-Derived Neurotrophic Factor Val66Met Polymorphism in Depression and Thrombosis: SIRT1 as a Possible Mediator. *Eur Heart J* (2017) 38:1436–8. doi: 10.1093/eurheartj/ehv692
20. Molendijk ML, Spinhoven P, Polak M, Bus BA, Penninx BW, Elzinga BM. Serum BDNF Concentrations as Peripheral Manifestations of Depression: Evidence From a Systematic Review and Meta-Analyses on 179 Associations (N=9484). *Mol Psychiatry* (2014) 19:791–800. doi: 10.1038/mp.2013.105
21. Berry A, Mazzelli M, Musillo C, Riva MA, Cattaneo A, Cirulli F. High-Fat Diet During Adulthood Interacts With Prenatal Stress, Affecting Both Brain Inflammatory and Neuroendocrine Markers in Male Rats. *Eur J Neurosci* (2021). doi: 10.1111/ejn.15181
22. Shang C, Liu Z, Chen Z, Shi Y, Wang Q, Liu S, et al. BRAIN CIRCUITS. a Parvalbumin-Positive Excitatory Visual Pathway to Trigger Fear Responses in Mice. *Science* (2015) 348:1472–7. doi: 10.1126/science.aaa8694
23. Crowley JJ, Jones MD, O'Leary OF, Lucki I. Automated Tests for Measuring the Effects of Antidepressants in Mice. *Pharmacol Biochem Behav* (2004) 78:269–74. doi: 10.1016/j.pbb.2004.03.014
24. Forbes NF, Stewart CA, Matthews K, Reid IC. Chronic Mild Stress and Sucrose Consumption: Validity as a Model of Depression. *Physiol Behav* (1996) 60:1481–4. doi: 10.1016/S0031-9384(96)00305-8
25. Lin LY, Zhang J, Dai XM, Xiao NA, Wu XL, Wei Z, et al. Early-Life Stress Leads to Impaired Spatial Learning and Memory in Middle-Aged Apoe4-TR Mice. *Mol Neurodegener* (2016) 11:51. doi: 10.1186/s13024-016-0107-2
26. Milaneschi Y, Simmons WK, van Rossum EFC, Penninx BW. Depression and Obesity: Evidence of Shared Biological Mechanisms. *Mol Psychiatry* (2019) 24:18–33. doi: 10.1038/s41380-018-0017-5
27. Luppino FS, de Wit LM, Bouvy PF, Stijnen T, Cuijpers P, Penninx BW, et al. Overweight, Obesity, and Depression: A Systematic Review and Meta-Analysis of Longitudinal Studies. *Arch Gen Psychiatry* (2010) 67:220–9. doi: 10.1001/archgenpsychiatry.2010.2
28. Vagena E, Ryu JK, Baeza-Raja B, Walsh NM, Syme C, Day JP, et al. A High-Fat Diet Promotes Depression-Like Behavior in Mice by Suppressing Hypothalamic PKA Signaling. *Transl Psychiatry* (2019) 9:141. doi: 10.1038/s41398-019-0470-1
29. Dinel AL, Andre C, Aubert A, Ferreira G, Laye S, Castanon N. Cognitive and Emotional Alterations are Related to Hippocampal Inflammation in a Mouse Model of Metabolic Syndrome. *PloS One* (2011) 6:e24325. doi: 10.1371/journal.pone.0024325
30. Pistell PJ, Morrison CD, Gupta S, Knight AG, Keller JN, Ingram DK, et al. Cognitive Impairment Following High Fat Diet Consumption is Associated With Brain Inflammation. *J Neuroimmunol* (2010) 219:25–32. doi: 10.1016/j.jneuroim.2009.11.010
31. Erion JR, Wosiski-Kuhn M, Dey A, Hao S, Davis CL, Pollock NK, et al. Obesity Elicits Interleukin 1-Mediated Deficits in Hippocampal Synaptic Plasticity. *J Neurosci* (2014) 34:2618–31. doi: 10.1523/JNEUROSCI.4200-13.2014
32. Yamada K, Nabeshima T. Brain-Derived Neurotrophic Factor/Trkb Signaling in Memory Processes. *J Pharmacol Sci* (2003) 91:267–70. doi: 10.1254/jphs.91.267
33. Martinowich K, Manji H, Lu B. New Insights Into BDNF Function in Depression and Anxiety. *Nat Neurosci* (2007) 10:1089–93. doi: 10.1038/nn1971
34. Nibuya M, Morinobu S, Duman RS. Regulation of BDNF and Trkb Mrna in Rat Brain by Chronic Electroconvulsive Seizure and Antidepressant Drug Treatments. *J Neurosci* (1995) 15:7539–47. doi: 10.1523/JNEUROSCI.15-11-07539.1995
35. Shirayama Y, Chen AC, Nakagawa S, Russell DS, Duman RS. Brain-Derived Neurotrophic Factor Produces Antidepressant Effects in Behavioral Models of Depression. *J Neurosci* (2002) 22:3251–61. doi: 10.1523/JNEUROSCI.22-08-03251.2002
36. Suri D, Vaidya VA. Glucocorticoid Regulation of Brain-Derived Neurotrophic Factor: Relevance to Hippocampal Structural and Functional Plasticity. *Neuroscience* (2013) 239:196–213. doi: 10.1016/j.neuroscience.2012.08.065
37. Barrientos RM, Sprunger DB, Campeau S, Watkins LR, Rudy JW, Maier SF. BDNF Mrna Expression in Rat Hippocampus Following Contextual Learning is Blocked by Intrahippocampal IL-1beta Administration. *J Neuroimmunol* (2004) 155:119–26. doi: 10.1016/j.jneuroim.2004.06.009
38. Tanaka S, Ide M, Shibutani T, Ohtaki H, Numazawa S, Shioda S, et al. Lipopolysaccharide-Induced Microglial Activation Induces Learning and Memory Deficits Without Neuronal Cell Death in Rats. *J Neurosci Res* (2006) 83:557–66. doi: 10.1002/jnr.20752
39. Tong L, Balazs R, Soiampornkul R, Thangnipon W, Cotman CW. Interleukin-1 Beta Impairs Brain Derived Neurotrophic Factor-Induced Signal Transduction. *Neurobiol Aging* (2008) 29:1380–93. doi: 10.1016/j.neurobiolaging.2007.02.027
40. Horita J, da Silva MCM, Ferrari CZ, Vieira ELM, Moreira FA, de Oliveira ACP, et al. Evaluation of Brain Cytokines and the Level of Brain-Derived Neurotrophic Factor in an Inflammatory Model of Depression. *Neuroimmunomodulation* (2020) 27:86–96. doi: 10.1159/000511181
41. Benarroch EE. Neural Control of Feeding Behavior: Overview and Clinical Correlations. *Neurology* (2010) 74:1643–50. doi: 10.1212/WNL.0b013e3181df0a3f
42. Karth MM, Baugher BJ, Daly N, Karth MD, Gironda SC, Sachs BD. Brain 5-HT Deficiency Prevents Antidepressant-Like Effects of High-Fat-Diet and Blocks High-Fat-Diet-Induced GSK3beta Phosphorylation in the Hippocampus. *Front Mol Neurosci* (2019) 12:298. doi: 10.3389/fnmol.2019.00298
43. Zhang J, Chen D, Sweeney P, Yang Y. An Excitatory Ventromedial Hypothalamus to Paraventricular Thalamus Circuit That Suppresses Food Intake. *Nat Commun* (2020) 11:6326. doi: 10.1038/s41467-020-20093-4
44. Zhang Y, Zhang SW, Khandekar N, Tong SF, Yang HQ, Wang WR, et al. Reduced Serum Levels of Oestradiol and Brain Derived Neurotrophic Factor in Both Diabetic Women and HFD-Feeding Female Mice. *Endocrine* (2017) 56:65–72. doi: 10.1007/s12020-016-1197-x
45. Capuron L, Miller AH. Immune System to Brain Signaling: Neuropsychopharmacological Implications. *Pharmacol Ther* (2011) 130:226–38. doi: 10.1016/j.pharmthera.2011.01.014
46. Hiles SA, Baker AL, de Malmanche T, Attia J. Interleukin-6, C-Reactive Protein and Interleukin-10 After Antidepressant Treatment in People With Depression: A Meta-Analysis. *Psychol Med* (2012) 42:2015–26. doi: 10.1017/S0033291712000128
47. Dowlati Y, Herrmann N, Swardfager W, Liu H, Sham L, Reim EK, et al. A Meta-Analysis of Cytokines in Major Depression. *Biol Psychiatry* (2010) 67:446–57. doi: 10.1016/j.biopsych.2009.09.033
48. Howren MB, Lamkin DM, Suls J. Associations of Depression With C-Reactive Protein, IL-1, and IL-6: A Meta-Analysis. *Psychosom Med* (2009) 71:171–86. doi: 10.1097/PSY.0b013e3181907c1b
49. Raison CL, Rutherford RE, Woolwine BJ, Shuo C, Schettler P, Drake DF, et al. A Randomized Controlled Trial of the Tumor Necrosis Factor Antagonist Infliximab for Treatment-Resistant Depression: The Role of Baseline Inflammatory Biomarkers. *JAMA Psychiatry* (2013) 70:31–41. doi: 10.1001/2013.jamapsychiatry.4
50. Valkanova V, Ebmeier KP, Allan CL. CRP, IL-6 and Depression: A Systematic Review and Meta-Analysis of Longitudinal Studies. *J Affect Disord* (2013) 150:736–44. doi: 10.1016/j.jad.2013.06.004
51. Copeland WE, Shanahan L, Worthman C, Angold A, Costello EJ. Cumulative Depression Episodes Predict Later C-Reactive Protein Levels: A Prospective Analysis. *Biol Psychiatry* (2012) 71:15–21. doi: 10.1016/j.biopsych.2011.09.023
52. Kohler O, Benros ME, Nordentoft M, Farkouh ME, Iyengar RL, Mors O, et al. Effect of Anti-Inflammatory Treatment on Depression, Depressive Symptoms, and Adverse Effects: A Systematic Review and Meta-Analysis of Randomized Clinical Trials. *JAMA Psychiatry* (2014) 71:1381–91. doi: 10.1001/jamapsychiatry.2014.1611

53. Marsland AL, Gianaros PJ, Abramowitch SM, Manuck SB, Hariri AR. Interleukin-6 Covaries Inversely With Hippocampal Grey Matter Volume in Middle-Aged Adults. *Biol Psychiatry* (2008) 64:484–90. doi: 10.1016/j.biopsych.2008.04.016
54. Andre C, O'Connor JC, Kelley KW, Lestage J, Dantzer R, Castanon N. Spatio-Temporal Differences in the Profile of Murine Brain Expression of Proinflammatory Cytokines and Indoleamine 2,3-Dioxygenase in Response to Peripheral Lipopolysaccharide Administration. *J Neuroimmunol* (2008) 200:90–9. doi: 10.1016/j.jneuroim.2008.06.011
55. Savage JC, St-Pierre MK, Hui CW, Tremblay ME. Microglial Ultrastructure in the Hippocampus of a Lipopolysaccharide-Induced Sickness Mouse Model. *Front Neurosci* (2019) 13:1340. doi: 10.3389/fnins.2019.01340
56. Kohler CA, Freitas TH, Stubbs B, Maes M, Solmi M, Veronese N, et al. Peripheral Alterations in Cytokine and Chemokine Levels After Antidepressant Drug Treatment for Major Depressive Disorder: Systematic Review and Meta-Analysis. *Mol Neurobiol* (2018) 55:4195–206. doi: 10.1007/s12035-017-0632-1
57. Hein AM, Stasko MR, Matousek SB, Scott-McKean JJ, Maier SF, Olschowka JA, et al. Sustained Hippocampal IL-1beta Overexpression Impairs Contextual and Spatial Memory in Transgenic Mice. *Brain Behav Immun* (2010) 24:243–53. doi: 10.1016/j.bbi.2009.10.002
58. Noble F, Rubira E, Boulanouar M, Palmier B, Plotkine M, Warnet JM, et al. Acute Systemic Inflammation Induces Central Mitochondrial Damage and Mnesic Deficit in Adult Swiss Mice. *Neurosci Lett* (2007) 424:106–10. doi: 10.1016/j.neulet.2007.07.005
59. Monje ML, Toda H, Palmer TD. Inflammatory Blockade Restores Adult Hippocampal Neurogenesis. *Science* (2003) 302:1760–5. doi: 10.1126/science.1088417
60. Heyser CJ, Masliah E, Samimi A, Campbell IL, Gold LH. Progressive Decline in Avoidance Learning Paralleled by Inflammatory Neurodegeneration in Transgenic Mice Expressing Interleukin 6 in the Brain. *Proc Natl Acad Sci United States America* (1997) 94:1500–5. doi: 10.1073/pnas.94.4.1500
61. Lopez M, Nogueiras R, Tena-Sempere M, Dieguez C. Hypothalamic AMPK: A Canonical Regulator of Whole-Body Energy Balance. *Nat Rev Endocrinol* (2016) 12:421–32. doi: 10.1038/nrendo.2016.67
62. Hardie DG, Ross FA, Hawley SA. AMPK: A Nutrient and Energy Sensor That Maintains Energy Homeostasis. *Nat Rev Mol Cell Biol* (2012) 13:251–62. doi: 10.1038/nrm3311
63. West AE, Chen WG, Dalva MB, Dolmetsch RE, Kornhauser JM, Shaywitz AJ, et al. Calcium Regulation of Neuronal Gene Expression. *Proc Natl Acad Sci United States America* (2001) 98:11024–31. doi: 10.1073/pnas.191352298
64. Yang W, Liu M, Zhang Q, Zhang J, Chen J, Chen Q, et al. Knockdown of Mir-124 Reduces Depression-Like Behavior by Targeting CREB1 and BDNF. *Curr Neurovasc Res* (2020) 17:196–203. doi: 10.2174/1567202617666200319141755

Conflict of Interest: The authors declare that the research was conducted in the absence of any commercial or financial relationships that could be construed as a potential conflict of interest.

frontiers in Endocrinology

REVIEW
published: 28 May 2021
doi: 10.3389/fendo.2021.667422

Central Regulation of PCOS: Abnormal Neuronal-Reproductive-Metabolic Circuits in PCOS Pathophysiology

Baoying Liao[1,2,3,4], *Jie Qiao*[1,2,3,4] *and Yanli Pang*[1,2,3,4]*

[1] Center for Reproductive Medicine, Department of Obstetrics and Gynecology, Peking University Third Hospital, Beijing, China, [2] National Clinical Research Center for Obstetrics and Gynecology, Peking University Third Hospital, Beijing, China, [3] Key Laboratory of Assisted Reproduction (Peking University), Ministry of Education, Beijing, China, [4] Beijing Key Laboratory of Reproductive Endocrinology and Assisted Reproductive Technology, Peking University Third Hospital, Beijing, China

OPEN ACCESS

Edited by:
Tiemin Liu,
Fudan University, China

Reviewed by:
Stephanie Constantin,
National Institutes of Health (NIH), United States
Jiachao Zhang,
Hainan University, China

***Correspondence:**
Yanli Pang
yanlipang@bjmu.edu.cn

Specialty section:
This article was submitted to Neuroendocrine Science, a section of the journal Frontiers in Endocrinology

Received: *13 February 2021*
Accepted: *07 May 2021*
Published: *28 May 2021*

Citation:
Liao B, Qiao J and Pang Y (2021) Central Regulation of PCOS: Abnormal Neuronal-Reproductive-Metabolic Circuits in PCOS Pathophysiology. Front. Endocrinol. 12:667422. doi: 10.3389/fendo.2021.667422

Polycystic ovary syndrome (PCOS) is a common reproductive endocrine disease. PCOS patients are characterized by hyperandrogenemia, anovulation, and metabolic dysfunction. Hypothalamus–pituitary–ovary axis imbalance is considered as an important pathophysiology underlying PCOS, indicating that central modulation, especially the abnormal activation of hypothalamic GnRH neurons plays a vital role in PCOS development. Increased GnRH pulse frequency can promote LH secretion, leading to ovarian dysfunction and abnormal sex steroids synthesis. By contrast, peripheral sex steroids can modulate the action of GnRH neurons through a feedback effect, which is impaired in PCOS, thus forming a vicious cycle. Additionally, hypothalamic GnRH neurons not only serve as the final output pathway of central control of reproductive axis, but also as the central connection point where reproductive function and metabolic state inter-regulate with each other. Metabolic factors, such as insulin resistance and obesity in PCOS patients can regulate GnRH neurons activity, and ultimately regulate reproductive function. Besides, gut hormones act on both brain and peripheral organs to modify metabolic state. Gut microbiota disturbance is also related to many metabolic diseases and has been reported to play an essential part in PCOS development. This review concludes with the mechanism of central modulation and the interaction between neuroendocrine factors and reproductive or metabolic disorders in PCOS development. Furthermore, the role of the gut microenvironment as an important part involved in the abnormal neuronal–reproductive–metabolic circuits that contribute to PCOS is discussed, thus offering possible central and peripheral therapeutic targets for PCOS patients.

Keywords: polycystic ovary syndrome, hypothalamus–pituitary–ovary axis, ovarian dysfunction, metabolic disorders, gut microbiota

INTRODUCTION

Polycystic ovary syndrome (PCOS) is a common reproductive and endocrine disorder, affecting 6–10% women of reproductive age worldwide (1). It is often characterized by menstrual disorder and infertility, abnormal elevated androgen levels, as well as polycystic ovary morphology (2). Metabolic disorders including IR, obesity, and abnormal lipid metabolism are represented in a considerably large part of PCOS patients. Besides, the long-term risk of type 2 diabetes, cardiovascular diseases, obstetrical complications, and endometrial cancer is significantly increased in women with PCOS than in control (2). The present therapy of PCOS mainly focuses on management of symptoms and prevention of long-term complications, including lifestyle modification, ovulation induction, anti-androgen therapy, and treatment of metabolic disorders (3); etiological treatment is still lacking.

Although it has been a long time since PCOS was discovered, the pathophysiology of PCOS remains unclear. Familial clustering and twin studies indicate the pivotal role genetic factor played in the etiology of PCOS; GWAS also identified PCOS' candidate loci, which provide the studying bases for mechanism research (4, 5). Follicle growth is a complicated process which needs the coordination of LH and FSH, androgen, estrogen, AMH, and other possible factors; follicle growth is impaired in PCOS, leading to follicular arrest, ovulatory dysfunction, and PCOM (6). Induced by inhibition of aromatase activity, hyperandrogenemia and hyperinsulinemia usually impact and facilitate each other and then promote PCOS development (7). Rising pieces of evidence suggest the correlation between gut microbiota and PCOS (8, 9); our studies demonstrated that the gut microbiota–bile acid–IL-22 axis is involved in PCOS development *via* the crosstalk of gut innate immune system and ovary function (9, 10), providing strong evidence for the contribution of the gut microbiota in PCOS pathogenesis, while other possible pathways involved in gut microbiota need to be further explored.

In addition, HPO axis imbalance is considered as an important pathophysiology underlying PCOS. Hypothalamic GnRH neurons act as a central regulator of LH synthesis because of abnormally increased GnRH pulse, LH pulse frequency, and amplitude in women with PCOS, which further enhance androgen synthesis in ovarian theca cell and promote hyperandrogenemia, ovarian dysfunction, and metabolic disorders in women with PCOS (3, 11). GnRH neurons also mediate the effect of peripheral signals on CNS in PCOS development. Here we summarize the mechanism that abnormal neuronal–reproductive–metabolic circuits contributes to PCOS pathogenesis and shed light on central regulation of GnRH neurons mediated by gut microenvironment *via* the gut–brain axis, thus providing new insights into PCOS pathogenesis and treatment.

Abbreviations: PCOS, Polycystic ovary syndrome; GnRH, Gonadotropin-releasing hormone; LH, Luteinizing hormone; PCOM, Polycystic ovary morphology; IR, Insulin resistance; GWAS, Genome-wide association studies; FSH, Follicle stimulating hormone; AMH, AntiMüllerian hormone; IL-22, Interleukin-22; HPO axis, Hypothalamus–pituitary–ovary axis; CNS, Central nervous system; IGF-1, Insulin-like growth factor 1; ARC, Arcuate nucleus; AVPV/PeN, Anteroventral periventricular nucleus/periventricular nucleus continuum; NKB, Neurokinin B; KNDy, Kisspeptin/NKB/dynorphin A; POMC, Pro-opiomelanocortin; GABA, γ-aminobutyric acid; E2, Estradiol; T, Testosterone; AR, Androgen receptor; PNA, Prenatal androgen treated; ARKO, AR knockout; PAMH, Prenatal AMH treated; SHBG, Sex hormone-binding globulin; PVN, Paraventricular nucleus of hypothalamus; GLP-1, Glucagon-like peptide-1; GLP-1R, GLP-1 receptor; SCFAs, Short-chain fatty Acids; PYY, Peptide YY; GF, Germ-free; GDCA, Glycodeoxycholic acid; TUDCA, Tauroursodeoxycholic acid; ILC3s, Group 3 innate lymphoid cells.

THE EFFECT OF GnRH IN PCOS PATHOPHYSIOLOGY

A mounting body of evidence supports that increased GnRH pulse frequency and amplitude can promote LH synthesis over FSH synthesis, leading to a high LH/FSH ratio in women with PCOS (12). Elevating LH levels plays a vital role in the development of reproductive and metabolic disorders, based on the evidence listed below. First, LH promotes the synthesis of androgen in ovarian theca cells, which leads to hyperandrogenemia and arrested follicle development (11). Second, increased LH pulse frequency impairs estrogen and FSH synthesis, thus inhibiting follicle growth and ovulation. Third, LH promotes ovarian secretion of IGF-1 which can further promote LH binding and androgen synthesis in theca cell, and finally contributes to the formation of polycystic ovaries in PCOS patients (13). However, it's still unclear whether the abnormal GnRH function is primary dysfunction of hypothalamus and pituitary or secondary to the complicated effect of reproductive and metabolic disorder, as well as unbalanced immune system and intestinal microenvironment in PCOS patients.

Neuropeptide

Kisspeptin

Located in the hypothalamus, GnRH neurons serve as the final output pathway of central control of the reproductive axis and play a vital role in the control of puberty onset and gonadal function (14). Kisspeptin is the key upstream regulator in GnRH pulse formation: kisspeptin acts through G-protein-coupled receptors GRP54, also known as Kiss1R, to activate hypothalamic GnRH secretion (15); besides, they also transmit peripheral steroid hormone information to the hypothalamus and mediate the steroid feedback control of GnRH secretion (16, 17). Kisspeptin neurons are primarily located in the ARC and the AVPV/PeN of the hypothalamus, while these two clusters of kisspeptin neurons have different effects on the activation of GnRH neurons. Co-expressed with NKB and dynorphin, kisspeptin neurons in the ARC are usually described as one member of the KNDy system that regulates GnRH pulse and LH secretion, as kisspeptin can excite GnRH neurons and NKB work as stimulatory factor and dynorphin as inhibitory factor of kisspeptin production, then modulate downstream GnRH secretion (18). Furthermore, KNDy neurons are involved in the negative feedback regulation of estrogen to the HPO axis

through estrogen receptor (19). On the contrary, kisspeptin neurons in AVPV/PeN are implicated in the formation of estradiol-induced LH surge before ovulation (20). In summary, kisspeptin is an important regulator in the circular regulation from brain to gonads.

It has long been reported that hypothalamic kisspeptin levels are increased in PCOS patients and PCOS animal models, which is the master contributor to increased LH pulse secretion (19, 21). While Panidis et al. found that serum kisspeptin level in PCOS patients was not significantly increased, and even decreased when compared to control (22). As kisspeptin mainly takes effect in the hypothalamus, so serum kisspeptin may be less related to the activation of GnRH neurons and LH pulse synthesis. Apart from NKB and dynorphin, a number of metabolic regulators also contribute to the modulation of kisspeptin neurons. Mice lacking both insulin and leptin receptors in POMC neurons displayed PCOS phenotype, including insulin resistance, elevated testosterone levels and reduced fertility (23); besides, hypothalamic POMC neurons send projections to kisspeptin neurons, indicating the possible role of POMC–kisspeptin pathway in PCOS pathogenesis.

Kisspeptin may also take effect in the ovaries. Gaytán et al. identified the expression of kisspeptin–GPR54 system genes in the human and rat ovary for the first time (24), and ovarian kisspeptin expression was positively regulated by gonadotropins for the fact that KISS1 gene expression increased after puberty onset. Furthermore, it seems that local kisspeptin system may directly modulate ovarian function (25). Recently, Blasco et al. compared the gene expression levels of KISS1/KISS1R, as well as TAC3 and TACR3 (encoding NKB and its G-protein coupled receptor NK3R respectively) in infertile patients and healthy control and found that defected fertility may be associated with the alteration of local KISS1/KISS1R expression in the ovaries (26). Besides, the kisspeptin/KISS1R and NKB/NK3R systems are decreased in PCOS mural granulosa cells and cumulus cells, indicating that abnormal ovarian kisspeptin and NKB may contribute to aberrant follicle development in PCOS patients (27). However, the specific molecular mechanism underlying the local effect of kisspeptin on PCOS ovarian function still needs to be discovered.

Galanin

Found in 1983, neuropeptide galanin is widely distributed in the brain and peripheral organs. Galanin signals through G-protein coupled receptor GAL1-3 which is expressed by ARC GnRH neurons, indicating that galanin is implicated in the modulation of GnRH. Besides, galanin is also implicated in the regulation of glucose metabolism and thermogenesis (28, 29), which makes it a molecular motif integrating metabolism and neuroendocrine-reproduction axis. However, the role galanin played in PCOS development remains unclear. Recently, Azin et al. explored the effect of galanin on estradiol valerate-induced PCOS rat. Intraperitoneal injection of galanin induced increased FSH levels and decreased LH and insulin levels, thus alleviating the metabolic disorders in PCOS rat. Furthermore, serum TNF-α and IL-6 levels were significantly increased in PCOS group, which was reversed with galanin treatment (29). Altinkaya compared serum galanin levels in 44 women with PCOS and 44 age-matched controls and found that women with PCOS were characterized by lower galanin levels than controls (30), indicating that supplementation of galanin may be a new therapeutic approach for PCOS, which still needs more evidence to support.

Neurotransmitters

Neurotransmitters, especially GnRH-regulatory neurotransmitters can be important in the pathogenesis of PCOS (31). Although GABA is usually considered as an inhibitory neurotransmitter in the brain, compelling evidence suggests its stimulatory effect on GnRH neurons (32). It is reported that the number of GABAergic synapses onto KNDy neurons increased significantly in prenatal testosterone exposed ewes, which means that GABA can activate KNDy neurons as well as GnRH neurons, thus elevating the pulse frequency of GnRH and LH in PCOS (33). Furthermore, higher cerebrospinal fluid GABA levels are observed in women with PCOS, along with increased circulating levels of E2 and T (34). Silva et al. investigated the effect of acute stimulation and chronic activation of GABA neurons on LH synthesis and found that both ways can increase LH levels. Besides, chronic activation of GABA neurons induces PCOS-like phenotypes in mice, including high circulating testosterone levels, irregular estrous cycle, and decreased corpora lutea number (32). In addition, the hypothalamic GABA neurons showed less expression of progesterone receptor in PCOS mice, which impairs GABA-mediated feedback effect of progesterone on GnRH neurons (35).

OVARIAN HORMONES MODULATE THE ACTION OF GnRH NEURONS

PCOS patients are characterized by aberrant sex hormone levels; hyperandrogenemia is the most consistent characterization observed in women with PCOS. Besides, aromatase is inhibited in PCOS granulosa cell, leading to aberrant estrogen levels. Abnormally increased AMH levels are also observed in PCOS patients (36); all these sex hormones substantially affect neuronal activity in the brain, which forms a vicious circle, thus promoting ovarian dysfunction and reproductive disorders in women with PCOS.

Androgen

Acting *via* AR, androgen is involved in both intra- and extra-ovarian mechanisms of PCOS pathogenesis. It is reported that AR is hyperactivated in the hypothalamus, ovary, skeletal muscle, and adipose cells in women with PCOS (37), which means the action of androgen in those tissues may mediate PCOS development. Mounting evidence identifies that androgen is implicated in manipulating hypothalamic GnRH neuron activity, as increased LH pulse frequency and amplitude are observed in both PCOS patients and PCOS animal models. In addition, DHT treatment in ovariectomized and estradiol-treated mice increased the connectivity of GABAergic neurons and GnRH neurons, which was inhibited by progesterone treatment (38), indicating the possible role of androgen in

modulating the negative feedback regulation of progesterone on GnRH neurons, and then increasing GnRH pulse frequency and amplitude.

In addition, Kiss1 gene expression and LH pulse frequency are increased in PNA mice, which means that KNDy neurons can be another central target of androgen. ARKO mice exhibit impaired GnRH synthesis pattern and decreased Kiss1 gene expression in anteroventral periventricular nucleus, leading to deficient preovulatory estrogen and LH surge, which is consistent with the reduction of ovarian corpora lutea numbers in ARKO mice (39). To investigate the precise mechanism of AR-mediated androgen action on GnRH synthesis, Cheng et al. generated neuron-specific AR knockout mice (NeurARKO) and found similar neuroendocrine feature to ARKO mice. In terms of ovarian follicle dynamics, increased follicle atresia and reduced ovulation were found in NeurARKO mice (40). Although the effect of androgen on peripheral tissue and organs is implicated in PCOS pathogenesis, the effect of androgen on central nervous system plays a pivotal role in PCOS development, because there is little difference in GnRH synthesis pattern and ovarian follicle dynamics between ARKO mice and NeurARKO mice.

On the other hand, prenatal androgen treated animal models are more often used for research investigating neuroendocrinal pathogenesis in PCOS, considering the high intrauterine androgen environment during pregnancy in women with PCOS, indicating that androgen and androgen activated GnRH synthesis may drive PCOS development since embryo, and this effect consistently exists till adulthood, leading to PCOS in offspring. So, the modulation of androgen on GnRH neurons during pregnancy can be quite important in PCOS development.

Anti-Müllerian Hormone

It is well known that AMH facilitates the modulation of ovarian follicle growth and now is widely used as a predictor of ovarian reserve in clinical work. In women with PCOS, AMH levels are increased due to accumulation of small antral follicles in the ovary (41). On the other hand, AMH can decrease FSH receptor and aromatase expression in granulosa cells (42), which impairs follicle growth and leads to follicular arrest, thus forming a vicious cycle. Apart from the effect on ovary, AMH also takes effect on HPO axis. AMH has high affinity to AMH receptor AMHR2, both AMH and AMHR2 are expressed in GnRH neurons (43, 44). Cimino et al. found that AMH can induce LH secretion *via* stimulating hypothalamic GnRH neurons directly, which needs further research to confirm in PCOS. Recently, Tata et al. found that serum AMH levels are significantly elevated in pregnant women with PCOS than in control women, and they use PAMH mice to investigate the effect of elevated intrauterine AMH levels on neuroendocrine and reproductive function in offspring. It turns out that PAMH mice have significantly higher LH pulse frequency and circulating testosterone levels, as well as longer ano-genital distance which reflects androgenic impregnation, while prenatal GnRH antagonist treatment can reverse the neuroendocrine and reproductive abnormalities in PAMH mice. Besides, GnRH antagonist treatment can normalize the neuroendocrine and reproductive disorders in adult PAMH mice (45), which further confirmed the stimulatory effect of AMH on GnRH neurons.

In conclusion, acting as a stimulator of hypothalamic GnRH neurons, AMH treatment, both pre- and postnatal treatments, can increase LH pulse frequency and induce reproductive disorder like PCOS, and this provides new evidence for the therapeutic effect of GnRH antagonist in women with PCOS.

METABOLIC REGULATION OF GnRH SYNTHESIS IN PCOS

Insulin Resistance

Insulin resistance plays a pivotal role in the pathogenesis of PCOS, the direct consequence of which is abnormally elevated insulin levels. According to human and animal studies concerning the effect of insulin in PCOS development, insulin is considered as a co-effector of gonadotropins. Insulin can promote testosterone biosynthesis in human ovarian theca cell and reduce SHBG production (46), thus contributing to hyperandrogenism in women with PCOS. In addition, insulin can stimulate LH secretion directly (47), leading to aberrant reproductive function in PCOS. As mentioned before, hypothalamic POMC neurons express both insulin receptor and leptin receptor, and knock-out of insulin receptor and leptin receptor in POMC neurons induced PCOS phenotype, indicating the insulin and leptin can be powerful regulators of both kisspeptin and POMC neurons, which further promote PCOS development (23).

Leptin plays a vital role in the central regulation of food intake and energy expenditure, as well as glucose metabolism, which makes leptin an important adipose-derived hormone in promoting insulin resistance. Besides, leptin may contribute to the effect of central and peripheral insulin resistance on obesity; these two pathophysiological changes often work together to promote metabolic disorders in metabolic diseases (48, 49). PCOS patients can be described as leptin resistance, as circulating leptin levels are higher in PCOS patients than in control, which is related to IR in PCOS patients (50, 51), suggesting that leptin may be implicated in the pathogenesis of PCOS. However, down-regulated hypothalamic leptin receptor expression is observed in PNA mice; additionally, leptin receptor is co-localized with kisspeptin and NKB in the ARC of PNA mice, indicating the possible interaction between leptin and kisspeptin/NKB. Further studies show that central administration of leptin can significantly stimulate hypothalamic *Kiss1* gene expression, as well as LH secretion, which can be suppressed by pretreatment with kisspeptin antagonist Kp-234 (52). This study provides a new insight into PCOS pathogenesis by shedding lights on the stimulatory effect of increased leptin levels on KNDy neurons and LH secretion.

Obesity

Obesity is another manifestation of metabolic syndrome in PCOS, while the relationship between obesity and PCOS is much more complex. Firstly, the vicious circle of mutual

reinforcing relationship between obesity and insulin and leptin resistance plays an important role in PCOS pathogenesis (49, 53). Hypothalamic leptin resistance has been identified to increase weight gain; at the same time, enhanced leptin secretion by adipocytes further contributes to induce leptin resistance, thus promoting PCOS development (54). In addition, growing piece of evidence show that kisspeptin also mediate obesity-related effect on reproductive function. To figure out the effect of bariatric surgery (a kind of treatment for PCOS patients to lose weight) on hypothalamic kisspeptin expression, Wen et al. performed sleeve gastrectomy (SG) for PCOS rat. After SG, metabolic disorders in PCOS rat including impaired glucose tolerance, decreased insulin sensitivity, and adiponectin levels are reversed, which is accompanied by decreased KISS1 gene expression in ARC, indicating that over-activated kisspeptin neurons can mediate metabolic regulation of central nervous system, then contribute to metabolic induced reproductive dysfunction in PCOS (55). Interestingly, Wen et al. also found that after SG, there is no significant loss of body weight in PCOS rat, which means that body weight may not implicate in the regulation of KISS1 gene expression. A recent study further confirmed this hypothesis, for the difference of kisspeptin levels between normal-weight PCOS patients and over-weight PCOS patients is insignificant (56). Thus, alternative obesity-related pathway mediating central control of reproductive function needs to be explored.

Growing pieces of evidence suggest that activated sympathetic nervous system takes part in PCOS and obesity pathogenesis (57, 58). Interaction between sympathetic nervous activation and obesity also implicates in PCOS pathogenesis, while the underlying mechanism remains unclear. Adiponectin is an adipocytokine known to play a pivotal role in the regulation of insulin sensitivity, as well as the control of ovarian follicle growth and early embryo development (34, 59). A systemic review identified the lower circulating adiponectin levels in women with PCOS, which are related to IR but not to BMI (60), indicating that there is little correlation between obesity and adiponectin levels in PCOS patients. Instead of the relationship with IR, Shorakae et al. mainly focus on adiponectin's regulation of sympathetic function (61). Muscle sympathetic nerve activity is increased in women with PCOS, along with decreased high molecular weight adiponectin levels. That is to say, similar to other diseases, sympathetic stimulation can reduce adiponectin levels in PCOS. Adiponectin may contribute to PCOS development *via* regulation of insulin resistance and sympathetic nerve activity. Recently, Heras et al. found that increased hypothalamic ceramide levels were involved in an alternative PVN-ovarian sympathetic innervation pathway, rather than the classical GnRH dependent pathway, thus promoting obesity-induced precious puberty (62), which provided new insights for the effect of obesity and sympathetic nervous system activation in PCOS pathogenesis.

Overall, obesity is common in PCOS patient, and lifestyle modifications including weight reduction are the primary treatment to improve metabolic dysfunction and infertility in women with PCOS. While the exact role of obesity or obesity related sympathetic activation in PCOS development still needs to be explored.

IMPACT OF INTESTINAL MICROBIOME ON PCOS PATHOPHYSIOLOGY

The imbalance of gut microenvironment is closely related to the pathogenesis of different kinds of diseases (63). In addition, the crosstalk between gut and brain has long been appreciated (64). This part mainly focuses on the possible mechanism of gut hormones and gut microbiota disturbance affecting the pathogenesis of PCOS through the gut–brain axis.

Gut Hormone

Gut hormones are vital mediators in bidirectional communication of the gut–brain axis and are implicated in different kinds of metabolic diseases. GLP-1 is mainly synthesized by intestinal L cells and acts through G protein-coupled GLP-1R which is found in many tissues in the human body, including brain and reproductive system. A growing body of evidence shows that GLP-1 is now widely used in women suffering PCOS, and the clinical effects of GLP-1 include improvement of ovulation, elevation of menstrual frequency, and promotion of pregnancy rate in women with PCOS (65–67). In terms of sex hormone, liraglutide decreased free testosterone and androstenedione levels and increased SHBG levels in women with PCOS (66). Besides, GLP-1 is recommended as a therapeutic option for obese women with PCOS for its significant weight loss effect. Although GLP-1 has been widely recognized in PCOS treatment, the underlying mechanism remains vague now.

The interaction between GLP-1 and hypothalamic GnRH neurons has long been discovered. Outeiriño-Iglesias et al. investigated the effect of GLP-1 on LH synthesis and found that acute administration of GLP-1significantly increases the amplitude of LH surge before ovulation in adult rats, while GLP-1R agonist Exendin-4 can block the stimulatory effect of GLP-1 on LH synthesis (68). Interestingly, liraglutide, a GLP-1R agonist, is able to depolarize ARC kisspeptin neurons directly but cannot reverse the inhibition of ARC kisspeptin neurons after 48 h fast (69), which means that GLP-1 cannot maintain LH synthesis alone. In addition, GLP-1 can activate GnRH neurons directly *via* GLP-1R, as well as modulation of stimulatory presynaptic GABAergic inputs to GnRH neurons (70). Overall, GLP-1 is identified as a stimulator of GnRH neurons *via* modulation of kisspeptin neurons and GABAergic neurons, indicating that GLP-1 may take part in the modulation of GnRH and LH synthesis, thus contributing to PCOS development.

Except for the regulation of metabolism and LH synthesis, GLP-1 is also a vital mediator of the influence of gut microbiota on host. Gut microbiota fragmentation of non-digestible carbohydrates is known to promote glucose metabolism, increase satiety, and reduce food intake, thus maintaining energy balance (71, 72). Additionally, GLP-1 secretion was augmented by supplementation of dietary fibers, and this process was mediated by SCFAs: as the metabolites of dietary fibers, SCFAs promoted GLP-1 secretion *via* receptors (GPR-41/43) expressed by intestinal enteroendocrine L cells (73–75). So GLP-1 may play an important role in gut microbiota dysbiosis related diseases. Hwang et al. found that antibiotics-induced

reduction of Firmicutes and Bacteroidetes significantly augmented serum GLP-1 levels and GLP-1 expression, thus improving insulin resistance in diet-induced-obesity mice (76). Overall, GLP-1 participated in PCOS pathogenesis through multiple ways; therapeutics targeting GLP-1 secretion can be promising for PCOS treatment.

Gut Microbiota Dysbiosis

Considering the close relationship between gut microbiota and host diseases, the relationship between gut microbiota and PCOS is now attracting more and more attention. It is reported that alpha diversity in PCOS patient is decreased, which may be related to reproductive dysfunction and metabolic dysregulation (8). On the contrary, aberrant sex hormone in PCOS patients may have an impact on gut microbiota as well, which makes it complex to find out the true role of microbiota in PCOS development.

It has been widely reported that the gut microbiota is capable of producing neurotransmitters including dopamine, noradrenaline, serotonin, and GABA (77). As described before, GABA is a powerful neurotransmitter that activates GnRH neurons and increases GnRH pulse frequency and amplitude, thus promoting PCOS development. Furthermore, it's reported that high-fat diet leads to reduced levels of Bacteroides, which reduce GABA levels in rat prefrontal cortex and alleviate depressive-like behavior (78). This indicates that the gut microbiota may modulate neurotransmitter levels in the central nervous system and then change the function of downstream neurons and the emotional state of host. While evidence indicating that microbial-derived neurotransmitter act directly on central neurons is still lacking, the effect of microbial-derived GABA on PCOS neuroendocrine disorder remains unclear. Qi et al. found that the abundance of *B. vulgatus* is increased in PCOS patients (9), which is associated with aberrant hormone levels like high androgen, LH levels, and increased LH/FSH ratio, and this is usually considered as the result of activating GnRH neurons. The relationship between *B. vulgatus* and GABA levels has not been researched; however, GABA may be a dot that connects *B. vulgatus* and neuroendocrine disorders in PCOS. Besides, there are some kinds of GABA-producing bacteria found to be increased and positively correlated with serum LH levels and LH/FSH ratio, which provide a perspective to understand the underlying mechanism of gut–brain axis in PCOS development (79).

Gut microbial metabolites and microbiota-regulated metabolic process also play a vital role in the gut–brain axis. As the most examined gut microbial metabolites, SCFAs have been implicated in maintaining intestinal barrier integrity and host immune homeostasis (64, 80). In addition, SCFAs are involved in gut–brain crosstalk; supplementation of SCFAs can alleviate increased blood–brain barrier permeability in GF mouse and modulate histone acetylation in the cortex of GF mouse. Although it seems like SCFAs play a negative role in the development of Parkinson's disease (81), SCFAs are more thought to be beneficial to host homeostasis. Zhang et al. found that there is a significant decrease in PCOS patients' intestinal SCFA levels, while supplying probiotic *Bifidobacterium lactis* V9 can rescue the decreased SCFA levels in PCOS patients (82). Besides, the colonization of *Bifidobacterium lactis* V9 is related to decreased LH and LH/FSH levels. Furthermore, they explored the correlation among the identified MGS, metabolic parameters, SCFAs, and sex hormones and found that the colonization of *Bifidobacterium lactis* V9 promotes the growth of SCFA-producing microbiotas, thus promoting PYY and ghrelin secretion, which may act on hypothalamus GnRH neurons and mediate the beneficial effect of microbial derived SCFAs in alleviating neuroendocrine disorders of PCOS patients.

As a class of microbial metabolites, bile acids are attracting more and more attention for their serious impact on regulating host immune cell function and modulating host metabolic status, as well as brain function. PCOS is known as a metabolic syndrome with reproductive disorder, aberrant bile acid metabolism may also participate in PCOS development, as Zhang et al. have reported that increased circulating conjugated primary bile acid levels are positively correlated with hyperandrogenemia in women with PCOS (83). On the other hand, Qi et al. found that serum and intestinal secondary bile acid GDCA and TUDCA levels are significantly decreased in PCOS patients (9). Furthermore, GDCA and TUDCA levels were negatively correlated with *B. vulgatus* and bile salt hydrolase (*bsh*) gene abundance, both of which are increased in women with PCOS. So abnormal bile acid metabolism induced by gut microbiota disturbance can be a key segment in PCOS development. In terms of the underlying mechanism, microbial-derived bile acids can activate ILC3s and their secretion of IL-22, thus improving insulin resistance in PCOS patients. Moreover, supplementation of GDCA can decrease serum testosterone levels in DHEA-induced PCOS-like mouse, indicating that bile acid may act through multiple ways to improve PCOS, so bile acids may act through the hypothalamus to regulate sex hormone levels directly.

CONCLUSION

PCOS is the most common endocrine disorder in women of reproductive age, aberrant HPO axis is at the center of PCOS pathogenesis (**Figure 1**). Kisspeptin and GABA are involved in the upstream regulation of GnRH neurons activity, which forms the final common pathway of central regulation of PCOS development. The direct stimulatory effect of androgen and AMH on GnRH neurons is considered as potential key mechanism involved in the origins of the neuroendocrine dysfunctions of PCOS. Besides, metabolic disorders including insulin resistance and leptin resistance also contribute to abnormalities of GnRH neurons in PCOS. However, obesity is more likely to be involved in the sympathetic activation in PCOS development. Gut hormone GLP-1 has long been recommended as treatment for obese women with PCOS; it is also identified as a stimulator of GnRH neurons *via* modulation of kisspeptin neurons and GABAergic neurons. Moreover, gut microbial derived neurotransmitter GABA may take effect in hypothalamic GnRH neurons and thus promoting PCOS

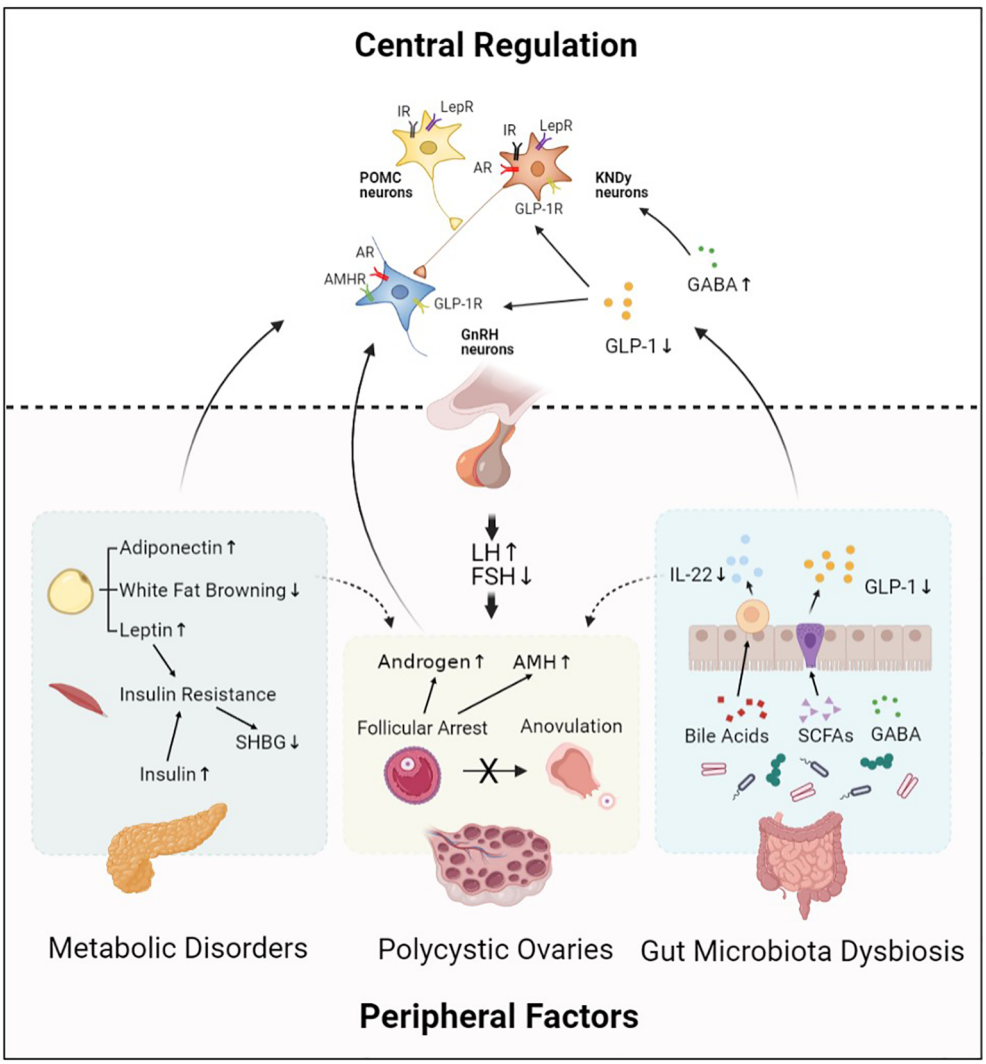

FIGURE 1 | Central regulation of PCOS. Hypothalamic GnRH pulse mediates regulation of LH and FSH synthesis, which plays an important role in PCOS pathophysiology. This process is modulated by central regulators including KNDy neurons, POMC neurons, and neurotransmitters. In addition, peripheral factors including abnormal ovarian hormone levels, metabolic disorders, and gut microbiota dysbiosis also contribute to PCOS development by acting on their receptors expressed in hypothalamic neurons. Moreover, central regulators and peripheral factors interact with each other and form an abnormal neuronal–reproductive–metabolic circuit, thus promoting PCOS development. GnRH, Gonadotropin-releasing hormone; KNDy neurons, kisspeptin/NKB/dynorphin A neurons; POMC neurons, Pro-opiomelanocortin neurons; GABA, γ-aminobutyric acid; GLP-1, Glucagon-like peptide-1; IR, Insulin receptor; LepR, Leptin receptor; AR, Androgen receptor; GLP-1R, Glucagon-like peptide-1 receptor; AMHR, Anti-Müllerian hormone receptor; LH, Luteinizing hormone; FSH, Follicle stimulating hormone; AMH, Anti-Müllerian hormone; SHBG, Sex hormone-binding globulin; IL-22, Interleukin 22; SCFAs, Short-chain fatty acids.

development. Metabolites of the gut microbiota, including SCFAs and bile acids, are effective regulators of GnRH neurons function.

Considering the vital role HPO axis played in PCOS pathogenesis, therapeutics targeting the HPO axis can be effective. Kisspeptin peptides kisspeptin-10 and kisspeptin-54 can increase LH levels in healthy women to promote ovulation (84, 85). With longer terminal half-life time, MVT-602, a novel KISS1R agonist, has longer duration of kisspeptin targeted action of stimulating GnRH synthesis and sustaining peak GnRH levels, consequently promoting LH synthesis in women with PCOS. Besides, estradiol pretreatment before administration of MVT-602 can increase both LH and FSH peak levels to that observed in preovulatory follicular phase, which means that supplementation of estradiol and MVT-602 is a promising treatment for *in vitro* fertilization of PCOS women. It seems that this still belongs to symptomatic treatment; while considering the central role of GnRH in PCOS pathogenesis, therapeutics targeting GnRH neurons can improve endocrine disorders, which further improves metabolic disorders and gut microbiota dysbiosis in PCOS.

Therapeutics improving metabolic disorders including sensitization of tissues to insulin and bariatric surgery to lose

weight can in turn influence GnRH and sex hormone secretion, thus alleviating PCOS. Although the way that peripheral nervous system is implicated in PCOS pathogenesis remains unclear, reduced sympathetic activity is observed in heat-treated obese PCOS women, as well as decreased cardiovascular risk profiles (86). In addition, acupuncture with electrical stimulation also reduces endocrine and reproductive dysfunction in women with PCOS by modulating sympathetic activity (87). However, further research is needed to clarify the underlying mechanism.

Treatment targeting the gut microbiota is an emerging therapeutic for metabolic diseases. It is reported that the gut microbiota *A. muciniphila* increased thermogenesis of brown adipocytes and GLP-1 secretion in HFD mice, thus improving glucose homeostasis (88). High-fiber diet elevated GLP-1 levels in patients with type 2 diabetes *via* promoting the growth of SCFA-producing gut microbiota, and finally improved glucose regulation (89). Fecal bacteria transplantation shows great potential for metabolic disease treatment. A double-blind study was performed to figure out the effect of FMT obese patients. Patients who received FMT capsules presented bile acid profiles comparable to those of lean people (90). The gut microbiota-mediated effect is not just in the gut. Probiotics supplementation increased colonic GLP-1 levels and cerebral GLP-1 receptor expression in mice model of Parkinson disease, indicating that probiotics supplementation could improve cerebral function through the gut microbiota–gut–brain axis (91). Gut microbiota related GABA was implicated in the development of seizure and schizophrenia (92, 93). So, the therapeutic effect of gut microbial-derived metabolites and probiotics in various diseases has been confirmed. Although the effect of gut microbiota-related treatment in women with PCOS still needs further study, fecal bacteria transplantation and supplementation of probiotics all show great potential for PCOS treatment.

In conclusion, the mechanism underlying PCOS pathogenesis is complicated, so is the relationship between neuroendocrine defects, metabolic disorders, and intestinal microbiota dysbiosis in PCOS pathophysiology. In terms of the causal relationship between the central defects and peripheral factors implicated in PCOS pathogenesis, one supposes that reproductive and metabolic disorders lead to defects in the brain of PCOS women, since the effect of exposure to excessive androgen and insulin during pregnancy cannot be ignored for the fact that PCOS mouse model can be established only by androgen injection to pregnant mouse. The other favors the idea that abnormal activation of GnRH neurons is the causality of reproductive and metabolic disorders, as increased GABAergic wiring to hypothalamic GnRH neurons occurred before PCOS mice exhibited disease phenotypes (87). It seems to make sense because of the significant therapeutic effect of inhibiting GnRH neurons in PCOS. But it is still unclear when and how the over-activation of GnRH neurons is formed in the brain, which needs further research studies. Actually, it's more accurate to say that it is the abnormal neuroendocrine–reproductive–metabolic circuit that plays an important role in the pathogenesis of PCOS.

As a rising research field, the gut microbiota is implicated in the development of various diseases through the gut–brain axis, gut-liver axis, *etc.* While direction of the regulation of these pathways remains unclear, one takes the view that the change of the gut microbiota is the cause of metabolic disorders and neuroendocrine defects, for gut microbiota transplantation can transfer donor phenotypes to recipients (94). The other takes the different view that it's just association rather than causality because the composition of gut microbiota is closely related to dietary history, and the gut microbiota transplantation experiments are mainly applied in germ-free mouse which exhibit different intestinal function. However, microbial fingerprinting model was established based on long-term investigation of the compositional and genomic stability of gut microbes, indicating that the gut microbiota composition and metabolites may influence host phenotype in a stable and chronic way. The debate may continue, and more experiments are needed (95).

PCOS is a heterogeneous and complex disorder in women of reproductive age, the pathophysiology of which is not clearly understood yet. Classic theory presumed that the abnormal activation of hypothalamus GnRH neurons and excessive ovarian androgen synthesis are the core of pathogenic mechanism in PCOS. With research studies are getting deeper, the important role of metabolic disorders and gut microbiota dysbiosis in PCOS pathogenesis has been identified. To some extent, reproductive and metabolic disorders and gut microbiota dysbiosis contribute to the impairment of local ovarian function, and their effect on activating GnRH synthesis drives the development of PCOS. However, it's hard to define the accurate onset time and location of this complex syndrome. Abnormal exposure to AMH, androgen, or insulin during pregnancy can promote PCOS development, and the underlying mechanism of which lies in the hyper-secretion of GnRH. Therefore, primary defects in the brain may be the direct cause of PCOS; at the same time, metabolic disorders, local ovarian hormone and gut microbiota dysbiosis can act on GnRH neurons, thus cooperatively promoting PCOS development. Overall, these important insights provide us with a new perspective that the brain plays a key role in the origin of PCOS and opens new avenues for investigating therapeutic interventions for women with PCOS.

AUTHOR CONTRIBUTIONS

All authors listed have made a substantial, direct and intellectual contribution to the work, and approved it for publication.

FUNDING

This work was supported by the National Key Research and Development Program of China (2018YFC1003200, 2018YFC1003900), National Natural Science Foundation of China (82022028, 81730038), Key Clinical Projects of Peking University Third Hospital (BYSYZD2019020), and CAMS Innovation Fund for Medical Sciences (2019-I2M-5-001).

REFERENCES

1. Norman RJ, Dewailly D, Legro RS, Hickey TE. Polycystic Ovary Syndrome. *Lancet* (2007) 370(9588):685–97. doi: 10.1016/S0140-6736(07)61345-2
2. Azziz R, Carmina E, Chen Z, Dunaif A, Laven JS, Legro RS, et al. Polycystic Ovary Syndrome. *Nat Rev Dis Primers* (2016) 2:16057. doi: 10.1038/nrdp.2016.57
3. Jayasena CN, Franks S. The Management of Patients With Polycystic Ovary Syndrome. *Nat Rev Endocrinol* (2014) 10(10):624–36. doi: 10.1038/nrendo.2014.102
4. McAllister JM, Legro RS, Modi BP, Strauss JF, 3rd. Functional Genomics of PCOS: From GWAS to Molecular Mechanisms. *Trends Endocrinol Metab* (2015) 26(3):118–24. doi: 10.1016/j.tem.2014.12.004
5. Shi Y, Zhao H, Shi Y, Cao Y, Yang D, Li Z, et al. Genome-Wide Association Study Identifies Eight New Risk Loci for Polycystic Ovary Syndrome. *Nat Genet* (2012) 44(9):1020–5. doi: 10.1038/ng.2384
6. Dumesic DA, Oberfield SE, Stener-Victorin E, Marshall JC, Laven JS, Legro RS. Scientific Statement on the Diagnostic Criteria, Epidemiology, Pathophysiology, and Molecular Genetics of Polycystic Ovary Syndrome. *Endocr Rev* (2015) 36(5):487–525. doi: 10.1210/er.2015-1018
7. Abbott DH, Nicol LE, Levine JE, Xu N, Goodarzi MO, Dumesic DA. Nonhuman Primate Models of Polycystic Ovary Syndrome. *Mol Cell Endocrinol* (2013) 373(1-2):21–8. doi: 10.1016/j.mce.2013.01.013
8. Thackray VG. Sex, Microbes, and Polycystic Ovary Syndrome. *Trends Endocrinol Metab* (2019) 30(1):54–65. doi: 10.1016/j.tem.2018.11.001
9. Qi X, Yun C, Sun L, Xia J, Wu Q, Wang Y, et al. Gut Microbiota-Bile Acid-Interleukin-22 Axis Orchestrates Polycystic Ovary Syndrome. *Nat Med* (2019) 25(8):1225–33. doi: 10.1038/s41591-019-0509-0
10. Qi X, Yun C, Liao B, Qiao J, Pang Y. The Therapeutic Effect of interleukin-22 in High Androgen-Induced Polycystic Ovary Syndrome. *J Endocrinol* (2020) 245(2):281–9. doi: 10.1530/JOE-19-0589
11. Gilling-Smith C, Willis DS, Beard RW, Franks S. Hypersecretion of Androstenedione by Isolated Thecal Cells From Polycystic Ovaries. *J Clin Endocrinol Metab* (1994) 79(4):1158–65. doi: 10.1210/jc.79.4.1158
12. Taylor AE, McCourt B, Martin KA, Anderson EJ, Adams JM, Schoenfeld D, et al. Determinants of Abnormal Gonadotropin Secretion in Clinically Defined Women With Polycystic Ovary Syndrome. *J Clin Endocrinol Metab* (1997) 82(7):2248–56. doi: 10.1210/jcem.82.7.4105
13. Cara JF, Fan J, Azzarello J, Rosenfield RL. Insulin-Like Growth Factor-I Enhances Luteinizing Hormone Binding to Rat Ovarian Theca-Interstitial Cells. *J Clin Invest* (1990) 86(2):560–5. doi: 10.1172/JCI114745
14. Herbison AE. Control of Puberty Onset and Fertility by Gonadotropin-Releasing Hormone Neurons. *Nat Rev Endocrinol* (2016) 12(8):452–66. doi: 10.1038/nrendo.2016.70
15. Aparicio SA. Kisspeptins and GPR54–the New Biology of the Mammalian GnRH Axis. *Cell Metab* (2005) 1(5):293–6. doi: 10.1016/j.cmet.2005.04.001
16. Zhang C, Bosch MA, Qiu J, Ronnekleiv OK, Kelly MJ. 17beta-Estradiol Increases Persistent Na(+) Current and Excitability of AVPV/PeN Kiss1 Neurons in Female Mice. *Mol Endocrinol* (2015) 29(4):518–27. doi: 10.1210/me.2014-1392
17. Kauffman AS, Clifton DK, Steiner RA. Emerging Ideas About Kisspeptin-Gpr54 Signaling in the Neuroendocrine Regulation of Reproduction. *Trends Neurosci* (2007) 30(10):504–11. doi: 10.1016/j.tins.2007.08.001
18. Cheng G, Coolen LM, Padmanabhan V, Goodman RL, Lehman MN. The Kisspeptin/Neurokinin B/Dynorphin (Kndy) Cell Population of the Arcuate Nucleus: Sex Differences and Effects of Prenatal Testosterone in Sheep. *Endocrinology* (2010) 151(1):301–11. doi: 10.1210/en.2009-0541
19. Tang R, Ding X, Zhu J. Kisspeptin and Polycystic Ovary Syndrome. *Front Endocrinol (Lausanne)* (2019) 10:298. doi: 10.3389/fendo.2019.00298
20. Navarro VM. Metabolic Regulation of Kisspeptin - the Link Between Energy Balance and Reproduction. *Nat Rev Endocrinol* (2020) 16(8):407–20. doi: 10.1038/s41574-020-0363-7
21. Esparza LA, Schafer D, Ho BS, Thackray VG, Kauffman AS. Hyperactive LH Pulses and Elevated Kisspeptin and NKB Gene Expression in the Arcuate Nucleus of a PCOS Mouse Model. *Endocrinology* (2020) 161(4):1–15. doi: 10.1210/endocr/bqaa018
22. Panidis D, Rousso D, Koliakos G, Kourtis A, Katsikis I, Farmakiotis D, et al. Plasma Metastin Levels are Negatively Correlated With Insulin Resistance and Free Androgens in Women With Polycystic Ovary Syndrome. *Fertil Steril* (2006) 85(6):1778–83. doi: 10.1016/j.fertnstert.2005.11.044
23. Hill JW, Elias CF, Fukuda M, Williams KW, Berglund ED, Holland WL, et al. Direct Insulin and Leptin Action on Pro-Opiomelanocortin Neurons is Required for Normal Glucose Homeostasis and Fertility. *Cell Metab* (2010) 11(4):286–97. doi: 10.1016/j.cmet.2010.03.002
24. Gaytan F, Gaytan M, Castellano JM, Romero M, Roa J, Aparicio B, et al. KiSS-1 in the Mammalian Ovary: Distribution of Kisspeptin in Human and Marmoset and Alterations in KiSS-1 Mrna Levels in a Rat Model of Ovulatory Dysfunction. *Am J Physiol Endocrinol Metab* (2009) 296(3):E520–31. doi: 10.1152/ajpendo.90895.2008
25. Qi X, Salem M, Zhou W, Sato-Shimizu M, Ye G, Smitz J, et al. Neurokinin B Exerts Direct Effects on the Ovary to Stimulate Estradiol Production. *Endocrinology* (2016) 157(9):3355–65. doi: 10.1210/en.2016-1354
26. Blasco V, Pinto FM, Fernandez-Atucha A, Gonzalez-Ravina C, Fernandez-Sanchez M, Candenas L. Female Infertility is Associated With an Altered Expression of the Neurokinin B/Neurokinin B Receptor and Kisspeptin/Kisspeptin Receptor Systems in Ovarian Granulosa and Cumulus Cells. *Fertility Sterility* (2020) 114(4):869–78. doi: 10.1016/j.fertnstert.2020.05.006
27. Blasco V, Pinto FM, Fernandez-Atucha A, Prados N, Tena-Sempere M, Fernandez-Sanchez M, et al. Altered Expression of the Kisspeptin/KISS1R and Neurokinin B/Nk3r Systems in Mural Granulosa and Cumulus Cells of Patients With Polycystic Ovarian Syndrome. *J Assist Reprod Genet* (2019) 36(1):113–20. doi: 10.1007/s10815-018-1338-7
28. Fang P, Yu M, Shi M, Bo P, Zhang Z. Galanin Peptide Family Regulation of Glucose Metabolism. *Front Neuroendocrinol* (2020) 56:100801. doi: 10.1016/j.yfrne.2019.100801
29. Azin F, Khazali H. Neuropeptide Galanin and its Effects on Metabolic and Reproductive Disturbances in Female Rats With Estradiol Valerate (Ev) - Induced Polycystic Ovary Syndrome (Pcos). *Neuropeptides* (2020) 80:102026. doi: 10.1016/j.npep.2020.102026
30. Altinkaya SO. Galanin and Glypican-4 Levels Depending on Metabolic and Cardiovascular Risk Factors in Patients With Polycystic Ovary Syndrome. *Arch Endocrinol Metab* (2021). doi: 10.20945/2359-3997000000340
31. Ilie IR. Neurotransmitter, Neuropeptide and Gut Peptide Profile in PCOS-pathways Contributing to the Pathophysiology, Food Intake and Psychiatric Manifestations of PCOS. *Adv Clin Chem* (2020) 96:85–135. doi: 10.1016/bs.acc.2019.11.004
32. Silva MSB, Desroziers E, Hessler S, Prescott M, Coyle C, Herbison AE, et al. Activation of Arcuate Nucleus GABA Neurons Promotes Luteinizing Hormone Secretion and Reproductive Dysfunction: Implications for Polycystic Ovary Syndrome. *Ebiomedicine* (2019) 44:582–96. doi: 10.1016/j.ebiom.2019.05.065
33. Porter DT, Moore AM, Cobern JA, Padmanabhan V, Goodman RL, Coolen LM, et al. Prenatal Testosterone Exposure Alters Gabaergic Synaptic Inputs to GnRH and KNDy Neurons in a Sheep Model of Polycystic Ovarian Syndrome. *Endocrinology* (2019) 160(11):2529–42. doi: 10.1210/en.2019-00137
34. Richards JS, Liu Z, Kawai T, Tabata K, Watanabe H, Suresh D, et al. Adiponectin and its Receptors Modulate Granulosa Cell and Cumulus Cell Functions, Fertility, and Early Embryo Development in the Mouse and Human. *Fertil Steril* (2012) 98(2):471–9 e1. doi: 10.1016/j.fertnstert.2012.04.050
35. Moore AM, Prescott M, Marshall CJ, Yip SH, Campbell RE. Enhancement of a Robust Arcuate GABAergic Input to Gonadotropin-Releasing Hormone Neurons in a Model of Polycystic Ovarian Syndrome. *Proc Natl Acad Sci U S A* (2015) 112(2):596–601. doi: 10.1073/pnas.1415038112
36. Pellatt L, Hanna L, Brincat M, Galea R, Brain H, Whitehead S, et al. Granulosa Cell Production of Anti-Mullerian Hormone is Increased in Polycystic Ovaries. *J Clin Endocrinol Metab* (2007) 92(1):240–5. doi: 10.1210/jc.2006-1582
37. Walters KA. Role of Androgens in Normal and Pathological Ovarian Function. *Reproduction* (2015) 149(4):R193–218. doi: 10.1530/REP-14-0517
38. Sullivan SD, Moenter SM. Gabaergic Integration of Progesterone and Androgen Feedback to Gonadotropin-Releasing Hormone Neurons. *Biol Reprod* (2005) 72(1):33–41. doi: 10.1095/biolreprod.104.033126
39. Cheng XB, Jimenez M, Desai R, Middleton LJ, Joseph SR, Ning G, et al. Characterizing the Neuroendocrine and Ovarian Defects of Androgen Receptor-Knockout Female Mice. *Am J Physiol Endocrinol Metab* (2013) 305(6):E717–26. doi: 10.1152/ajpendo.00263.2013

40. Walters KA, Edwards MC, Tesic D, Caldwell ASL, Jimenez M, Smith JT, et al. The Role of Central Androgen Receptor Actions in Regulating the Hypothalamic-Pituitary-Ovarian Axis. *Neuroendocrinology* (2018) 106 (4):389–400. doi: 10.1159/000487762
41. Desforges-Bullet V, Gallo C, Lefebvre C, Pigny P, Dewailly D, Catteau-Jonard S. Increased Anti-Mullerian Hormone and Decreased Fsh Levels in Follicular Fluid Obtained in Women With Polycystic Ovaries at the Time of Follicle Puncture for *In Vitro* Fertilization. *Fertil Steril* (2010) 94(1):198–204. doi: 10.1016/j.fertnstert.2009.03.004
42. Pellatt L, Rice S, Dilaver N, Heshri A, Galea R, Brincat M, et al. Anti-Mullerian Hormone Reduces Follicle Sensitivity to Follicle-Stimulating Hormone in Human Granulosa Cells. *Fertil Steril* (2011) 96(5):1246–51.e1. doi: 10.1016/j.fertnstert.2011.08.015
43. Cimino I, Casoni F, Liu X, Messina A, Parkash J, Jamin SP, et al. Novel Role for Anti-Mullerian Hormone in the Regulation of GnRH Neuron Excitability and Hormone Secretion. *Nat Commun* (2016) 7:10055. doi: 10.1038/ncomms10055
44. Baarends WM, van Helmond MJ, Post M, van der Schoot PJ, Hoogerbrugge JW, de Winter JP, et al. A Novel Member of the Transmembrane Serine/Threonine Kinase Receptor Family is Specifically Expressed in the Gonads and in Mesenchymal Cells Adjacent to the Mullerian Duct. *Development* (1994) 120(1):189–97. doi: 10.1242/dev.120.1.189
45. Tata B, Mimouni NEH, Barbotin AL, Malone SA, Loyens A, Pigny P, et al. Elevated Prenatal Anti-Mullerian Hormone Reprograms the Fetus and Induces Polycystic Ovary Syndrome in Adulthood. *Nat Med* (2018) 24 (6):834–46. doi: 10.1038/s41591-018-0035-5
46. Nestler JE, Jakubowicz DJ, de Vargas AF, Brik C, Quintero N, Medina F. Insulin Stimulates Testosterone Biosynthesis by Human Thecal Cells From Women With Polycystic Ovary Syndrome by Activating its Own Receptor and Using Inositolglycan Mediators as the Signal Transduction System. *J Clin Endocrinol Metab* (1998) 83(6):2001–5. doi: 10.1210/jcem.83.6.4886
47. Adashi EY, Hsueh AJ, Yen SS. Insulin Enhancement of Luteinizing Hormone and Follicle-Stimulating Hormone Release by Cultured Pituitary Cells. *Endocrinology* (1981) 108(4):1441–9. doi: 10.1210/endo-108-4-1441
48. Yadav A, Kataria MA, Saini V, Yadav A. Role of Leptin and Adiponectin in Insulin Resistance. *Clin Chim Acta* (2013) 417:80–4. doi: 10.1016/j.cca.2012.12.007
49. Konner AC, Bruning JC. Selective Insulin and Leptin Resistance in Metabolic Disorders. *Cell Metab* (2012) 16(2):144–52. doi: 10.1016/j.cmet.2012.07.004
50. Zheng SH, Du DF, Li XL. Leptin Levels in Women With Polycystic Ovary Syndrome: A Systematic Review and a Meta-Analysis. *Reprod Sci* (2017) 24 (5):656–70. doi: 10.1177/1933719116670265
51. Pehlivanov B, Mitkov M. Serum Leptin Levels Correlate With Clinical and Biochemical Indices of Insulin Resistance in Women With Polycystic Ovary Syndrome. *Eur J Contracept Reprod Health Care* (2009) 14(2):153–9. doi: 10.1080/13625180802549962
52. Yan X, Yuan C, Zhao N, Cui Y, Liu J. Prenatal Androgen Excess Enhances Stimulation of the GNRH Pulse in Pubertal Female Rats. *J Endocrinol* (2014) 222(1):73–85. doi: 10.1530/JOE-14-0021
53. Escobar-Morreale HF, San Millan JL. Abdominal Adiposity and the Polycystic Ovary Syndrome. *Trends Endocrinol Metab* (2007) 18(7):266–72. doi: 10.1016/j.tem.2007.07.003
54. Zhao S, Zhu Y, Schultz RD, Li N, He Z, Zhang Z, et al. Partial Leptin Reduction as an Insulin Sensitization and Weight Loss Strategy. *Cell Metab* (2019) 30(4):706–19 e6. doi: 10.1016/j.cmet.2019.08.005
55. Wen L, Lin W, Li Q, Chen G, Wen J. Effect of Sleeve Gastrectomy on Kisspeptin Expression in the Hypothalamus of Rats With Polycystic Ovary Syndrome. *Obes (Silver Spring)* (2020) 28(6):1117–28. doi: 10.1002/oby.22795
56. Araujo BS, Baracat MCP, Dos Santos Simoes R, de Oliveira Nunes C, Maciel GAR, Lobo RA, et al. Kisspeptin Influence on Polycystic Ovary Syndrome-a Mini Review. *Reprod Sci* (2020) 27(2):455–60. doi: 10.1007/s43032-019-00085-6
57. Shorakae S, Lambert EA, Jona E, Ika Sari C, de Courten B, Dixon JB, et al. Effect of Central Sympathoinhibition With Moxonidine on Sympathetic Nervous Activity in Polycystic Ovary Syndrome-A Randomized Controlled Trial. *Front Physiol* (2018) 9:1486. doi: 10.3389/fphys.2018.01486
58. Larabee CM, Neely OC, Domingos AI. Obesity: A Neuroimmunometabolic Perspective. *Nat Rev Endocrinol* (2020) 16(1):30–43. doi: 10.1038/s41574-019-0283-6
59. Bohler H, Mokshagundam S, Winters SJ. Adipose Tissue and Reproduction in Women. *Fertility Sterility* (2010) 94(3):795–825. doi: 10.1016/j.fertnstert.2009.03.079
60. Toulis KA, Goulis DG, Farmakiotis D, Georgopoulos NA, Katsikis I, Tarlatzis BC, et al. Adiponectin Levels in Women With Polycystic Ovary Syndrome: A Systematic Review and a Meta-Analysis. *Hum Reprod Update* (2009) 15 (3):297–307. doi: 10.1093/humupd/dmp006
61. Shorakae S, Abell SK, Hiam DS, Lambert EA, Eikelis N, Jona E, et al. High-Molecular-Weight Adiponectin is Inversely Associated With Sympathetic Activity in Polycystic Ovary Syndrome. *Fertility Sterility* (2018) 109(3):532–9. doi: 10.1016/j.fertnstert.2017.11.020
62. Heras V, Castellano JM, Fernandois D, Velasco I, Rodriguez-Vazquez E, Roa J, et al. Central Ceramide Signaling Mediates Obesity-Induced Precocious Puberty. *Cell Metab* (2020) 32(6):6–8. doi: 10.1016/j.cmet.2020.10.001
63. Schroeder B, Backhed F. Signals From the Gut Microbiota to Distant Organs in Physiology and Disease. *Nat Med* (2016) 22(10):1079–89. doi: 10.1038/nm.4185
64. Cryan JF, O'Riordan KJ, Cowan CSM, Sandhu KV, Bastiaanssen TFS, Boehme M, et al. The Microbiota-Gut-Brain Axis. *Physiol Rev* (2019) 99(4):1877–2013. doi: 10.1152/physrev.00018.2018
65. Elkind-Hirsch K, Marrioneaux O, Bhushan M, Vernor D, Bhushan R. Comparison of Single and Combined Treatment With Exenatide and Metformin on Menstrual Cyclicity in Overweight Women With Polycystic Ovary Syndrome. *J Clin Endocr Metab* (2008) 93(7):2670–8. doi: 10.1210/jc.2008-0115
66. Nylander M, Frossing S, Clausen HV, Kistorp C, Faber J, Skouby SO. Effects of Liraglutide on Ovarian Dysfunction in Polycystic Ovary Syndrome: A Randomized Clinical Trial. *Reprod BioMed Online* (2017) 35(1):121–7. doi: 10.1016/j.rbmo.2017.03.023
67. Salamun V, Jensterle M, Janez A, Bokal EV. Liraglutide Increases Ivf Pregnancy Rates in Obese Pcos Women With Poor Response to First-Line Reproductive Treatments: A Pilot Randomized Study. *Eur J Endocrinol* (2018) 179(1):1–11. doi: 10.1530/EJE-18-0175
68. Outeirino-Iglesias V, Romani-Perez M, Gonzalez-Matias LC, Vigo E, Mallo F. Glp-1 Increases Preovulatory LH Source and the Number of Mature Follicles, As Well As Synchronizing the Onset of Puberty in Female Rats. *Endocrinology* (2015) 156(11):4226–37. doi: 10.1210/en.2014-1978
69. Heppner KM, Baquero AF, Bennett CM, Lindsley SR, Kirigiti MA, Bennett B, et al. Glp-1r Signaling Directly Activates Arcuate Nucleus Kisspeptin Action in Brain Slices But Does Not Rescue Luteinizing Hormone Inhibition in Ovariectomized Mice During Negative Energy Balance. *eNeuro* (2017) 4(1): ENEURO.0198-16.2016. doi: 10.1523/ENEURO.0198-16.2016
70. Farkas I, Vastagh C, Farkas E, Balint F, Skrapits K, Hrabovszky E, et al. Glucagon-Like Peptide-1 Excites Firing and Increases Gabaergic Miniature Postsynaptic Currents (mPSCs) in Gonadotropin-Releasing Hormone (Gnrh) Neurons of the Male Mice *Via* Activation of Nitric Oxide (NO) and Suppression of Endocannabinoid Signaling Pathways. *Front Cell Neurosci* (2016) 10:214. doi: 10.3389/fncel.2016.00214
71. Whelan K, Efthymiou L, Judd PA, Preedy VR, Taylor MA. Appetite During Consumption of Enteral Formula as a Sole Source of Nutrition: The Effect of Supplementing Pea-Fibre and Fructo-Oligosaccharides. *Br J Nutr* (2006) 96 (2):350–6. doi: 10.1079/BJN20061791
72. Archer BJ, Johnson SK, Devereux HM, Baxter AL. Effect of Fat Replacement by Inulin or Lupin-Kernel Fibre on Sausage Patty Acceptability, Post-Meal Perceptions of Satiety and Food Intake in Men. *Br J Nutr* (2004) 91(4):591–9. doi: 10.1079/BJN20031088
73. Samuel BS, Shaito A, Motoike T, Rey FE, Backhed F, Manchester JK, et al. Effects of the Gut Microbiota on Host Adiposity are Modulated by the Short-Chain Fatty-Acid Binding G Protein-Coupled Receptor, Gpr41. *Proc Natl Acad Sci U S A* (2008) 105(43):16767–72. doi: 10.1073/pnas.0808567105
74. Tolhurst G, Heffron H, Lam YS, Parker HE, Habib AM, Diakogiannaki E, et al. Short-Chain Fatty Acids Stimulate Glucagon-Like Peptide-1 Secretion *Via* the G-protein-coupled Receptor Ffar2. *Diabetes* (2012) 61(2):364–71. doi: 10.2337/db11-1019
75. Nohr MK, Pedersen MH, Gille A, Egerod KL, Engelstoft MS, Husted AS, et al. GPR41/FFAR3 and GPR43/FFAR2 as Cosensors for Short-Chain Fatty Acids in Enteroendocrine Cells vs FFAR3 in Enteric Neurons and FFAR2 in Enteric Leukocytes. *Endocrinology* (2013) 154(10):3552–64. doi: 10.1210/en.2013-1142
76. Hwang I, Park YJ, Kim YR, Kim YN, Ka S, Lee HY, et al. Alteration of Gut Microbiota by Vancomycin and Bacitracin Improves Insulin Resistance *Via* Glucagon-Like Peptide 1 in Diet-Induced Obesity. *FASEB J* (2015) 29 (6):2397–411. doi: 10.1096/fj.14-265983

77. Strandwitz P. Neurotransmitter Modulation by the Gut Microbiota. *Brain Res* (2018) 1693(Pt B):128–33. doi: 10.1016/j.brainres.2018.03.015
78. Hassan AM, Mancano G, Kashofer K, Frohlich EE, Matak A, Mayerhofer R, et al. High-Fat Diet Induces Depression-Like Behaviour in Mice Associated With Changes in Microbiome, Neuropeptide Y, and Brain Metabolome. *Nutr Neurosci* (2019) 22(12):877–93. doi: 10.1080/1028415X.2018.1465713
79. Liang Z, Di N, Li L, Yang D. Gut Microbiota Alterations Reveal Potential Gut-Brain Axis Changes in Polycystic Ovary Syndrome. *J Endocrinol Invest* (2021). doi: 10.1007/s40618-020-01481-5
80. Dalile B, Van Oudenhove L, Vervliet B, Verbeke K. The Role of Short-Chain Fatty Acids in Microbiota-Gut-Brain Communication. *Nat Rev Gastroenterol Hepatol* (2019) 16(8):461–78. doi: 10.1038/s41575-019-0157-3
81. Sampson TR, Debelius JW, Thron T, Janssen S, Shastri GG, Ilhan ZE, et al. Gut Microbiota Regulate Motor Deficits and Neuroinflammation in a Model of Parkinson's Disease. *Cell* (2016) 167(6):1469–80 e12. doi: 10.1016/j.cell.2016.11.018
82. Zhang JC, Sun ZH, Jiang SM, Bai XY, Ma CC, Peng QN, et al. Probiotic Bifidobacterium Lactis V9 Regulates the Secretion of Sex Hormones in Polycystic Ovary Syndrome Patients Through the Gut-Brain Axis. *Msystems* (2019) 4(2):e00017–19. doi: 10.1128/mSystems.00017-19
83. Zhang BJ, Shen SM, Gu TW, Hong T, Liu JY, Sun J, et al. Increased Circulating Conjugated Primary Bile Acids are Associated With Hyperandrogenism in Women With Polycystic Ovary Syndrome. *J Steroid Biochem* (2019) 189:171–5. doi: 10.1016/j.jsbmb.2019.03.005
84. Jayasena CN, Nijher GM, Comninos AN, Abbara A, Januszewki A, Vaal ML, et al. The Effects of kisspeptin-10 on Reproductive Hormone Release Show Sexual Dimorphism in Humans. *J Clin Endocrinol Metab* (2011) 96(12): E1963–72. doi: 10.1210/jc.2011-1408
85. Narayanaswamy S, Jayasena CN, Ng N, Ratnasabapathy R, Prague JK, Papadopoulou D, et al. Subcutaneous Infusion of Kisspeptin-54 Stimulates Gonadotrophin Release in Women and the Response Correlates With Basal Oestradiol Levels. *Clin Endocrinol (Oxf)* (2016) 84(6):939–45. doi: 10.1111/cen.12977
86. Ely BR, Francisco MA, Halliwill JR, Bryan SD, Comrada LN, Larson EA, et al. Heat Therapy Reduces Sympathetic Activity and Improves Cardiovascular Risk Profile in Women Who are Obese With Polycystic Ovary Syndrome. *Am J Physiol Regul Integr Comp Physiol* (2019) 317(5):R630–40. doi: 10.1152/ajpregu.00078.2019
87. Maliqueo M, Benrick A, Alvi A, Johansson J, Sun M, Labrie F, et al. Circulating Gonadotropins and Ovarian Adiponectin System are Modulated by Acupuncture Independently of Sex Steroid or Beta-Adrenergic Action in a Female Hyperandrogenic Rat Model of Polycystic Ovary Syndrome. *Mol Cell Endocrinol* (2015) 412:159–69. doi: 10.1016/j.mce.2015.04.026
88. Yoon HS, Cho CH, Yun MS, Jang SJ, You HJ, Kim JH, et al. Akkermansia Muciniphila Secretes a Glucagon-Like Peptide-1-Inducing Protein That Improves Glucose Homeostasis and Ameliorates Metabolic Disease in Mice. *Nat Microbiol* (2021) 6(5):563–73. doi: 10.1038/s41564-021-00880-5
89. Zhao L, Zhang F, Ding X, Wu G, Lam YY, Wang X, et al. Gut Bacteria Selectively Promoted by Dietary Fibers Alleviate Type 2 Diabetes. *Science* (2018) 359(6380):1151–6. doi: 10.1126/science.aao5774
90. Allegretti JR, Kassam Z, Mullish BH, Chiang A, Carrellas M, Hurtado J, et al. Effects of Fecal Microbiota Transplantation With Oral Capsules in Obese Patients. *Clin Gastroenterol Hepatol* (2020) 18(4):855–63.e2. doi: 10.1016/j.cgh.2019.07.006
91. Sun J, Li H, Jin Y, Yu J, Mao S, Su KP, et al. Probiotic Clostridium Butyricum Ameliorated Motor Deficits in a Mouse Model of Parkinson's Disease *Via* Gut microbiota-GLP-1 Pathway. *Brain Behav Immun* (2021) 91:703–15. doi: 10.1016/j.bbi.2020.10.014
92. Olson CA, Vuong HE, Yano JM, Liang QY, Nusbaum DJ, Hsiao EY. The Gut Microbiota Mediates the Anti-Seizure Effects of the Ketogenic Diet. *Cell* (2018) 173(7):1728–41.e13. doi: 10.1016/j.cell.2018.04.027
93. Zheng P, Zeng B, Liu M, Chen J, Pan J, Han Y, et al. The Gut Microbiome From Patients With Schizophrenia Modulates the Glutamate-Glutamine-GABA Cycle and Schizophrenia-Relevant Behaviors in Mice. *Sci Adv* (2019) 5(2):eaau8317. doi: 10.1126/sciadv.aau8317
94. Kootte RS, Levin E, Salojarvi J, Smits LP, Hartstra AV, Udayappan SD, et al. Improvement of Insulin Sensitivity After Lean Donor Feces in Metabolic Syndrome Is Driven by Baseline Intestinal Microbiota Composition. *Cell Metab* (2017) 26(4):611–9.e6. doi: 10.1016/j.cmet.2017.09.008
95. Chen L, Wang D, Garmaeva S, Kurilshikov A, Vich Vila A, Gacesa R, et al. The Long-Term Genetic Stability and Individual Specificity of the Human Gut Microbiome. *Cell* (2021) 184(9):2302–15.e12. doi: 10.2139/ssrn.3653563

Conflict of Interest: The authors declare that the research was conducted in the absence of any commercial or financial relationships that could be construed as a potential conflict of interest.

frontiers in Endocrinology

ORIGINAL RESEARCH
published: 18 June 2021
doi: 10.3389/fendo.2021.705267

Energy Status Differentially Modifies Feeding Behavior and POMC^{ARC} Neuron Activity After Acute Treadmill Exercise in Untrained Mice

Taylor Landry[1,2,3], *Daniel Shookster*[1,2,3], *Alec Chaves*[1,2,3], *Katrina Free*[1,2,3], *Tony Nguyen*[1,2,3] *and Hu Huang*[1,2,3,4*]

[1] East Carolina Diabetes and Obesity Institute, East Carolina University, Greenville, NC, United States, [2] Department of Kinesiology, East Carolina University, Greenville, NC, United States, [3] Human Performance Laboratory, College of Human Performance and Health, East Carolina University, Greenville, NC, United States, [4] Department of Physiology, East Carolina University, Greenville, NC, United States

OPEN ACCESS

Edited by:
Hiroyuki Kaiya, National Cerebral and Cardiovascular Center, Japan

Reviewed by:
María Florencia Andreoli, Consejo Nacional de Investigaciones Científicas y Técnicas (CONICET), Argentina
João Cavalcanti De Albuquerque, Federal University of Rio de Janeiro, Brazil

***Correspondence:**
Hu Huang
huangh@ecu.edu

Specialty section:
This article was submitted to Neuroendocrine Science, a section of the journal Frontiers in Endocrinology

Received: *05 May 2021*
Accepted: *31 May 2021*
Published: *18 June 2021*

Citation:
Landry T, Shookster D, Chaves A, Free K, Nguyen T and Huang H (2021) Energy Status Differentially Modifies Feeding Behavior and POMC^{ARC} Neuron Activity After Acute Treadmill Exercise in Untrained Mice. Front. Endocrinol. 12:705267. doi: 10.3389/fendo.2021.705267

Emerging evidence identifies a potent role for aerobic exercise to modulate activity of neurons involved in regulating appetite; however, these studies produce conflicting results. These discrepancies may be, in part, due to methodological differences, including differences in exercise intensity and pre-exercise energy status. Consequently, the current study utilized a translational, well-controlled, within-subject, treadmill exercise protocol to investigate the differential effects of energy status and exercise intensity on post-exercise feeding behavior and appetite-controlling neurons in the hypothalamus. Mature, untrained male mice were exposed to acute sedentary, low (10m/min), moderate (14m/min), and high (18m/min) intensity treadmill exercise in a randomized crossover design. Fed and 10-hour-fasted mice were used, and food intake was monitored 48h. post-exercise. Immunohistochemical detection of cFOS was performed 1-hour post-exercise to determine changes in hypothalamic NPY/AgRP, POMC, tyrosine hydroxylase, and SIM1-expressing neuron activity concurrent with changes in food intake. Additionally, stains for pSTAT3^{tyr705} and pERK$^{thr202/tyr204}$ were performed to detect exercise-mediated changes in intracellular signaling. Results demonstrated that fasted high intensity exercise suppressed food intake compared to sedentary trials, which was concurrent with increased anorexigenic POMC neuron activity. Conversely, fed mice experienced augmented post-exercise food intake, with no effects on POMC neuron activity. Regardless of pre-exercise energy status, tyrosine hydroxylase and SIM1 neuron activity in the paraventricular nucleus was elevated, as well as NPY/AgRP neuron activity in the arcuate nucleus. Notably, these neuronal changes were independent from changes in pSTAT3^{tyr705} and pERK$^{thr202/tyr204}$ signaling. Overall, these results suggest fasted high intensity exercise may be beneficial for suppressing food intake, possibly due to hypothalamic POMC neuron excitation. Furthermore, this study identifies a novel role for pre-exercise energy status to differentially modify post-exercise feeding behavior and

hypothalamic neuron activity, which may explain the inconsistent results from studies investigating exercise as a weight loss intervention.

Keywords: exercise, food intake, hypothalamus, POMC neuron, NPY/AgRP neuron, tyrosine hydroxylase (th), SIM1 neurons, energy balance

INTRODUCTION

The hypothalamus is a critical nexus of neuron populations that interpret peripheral signals of energy status and deliver diverse efferent outputs to metabolically active tissues (1, 2). These neurons are critical to maintaining metabolic homeostasis, and disruption of their complex neurocircuitry is associated with disordered substrate metabolism and feeding behavior (1, 2). Additionally, emerging evidence identifies a potent role for aerobic exercise to modulate activity and synaptic organization of hypothalamic neurons, especially in the arcuate nucleus (ARC) (3–5). This hypothalamic region contains diverse neuron populations involved in regulating appetite; thus, the ARC presents an attractive target to investigate the regulation of post-exercise feeding behavior.

Identified ARC neurons modulated by acute treadmill exercise include the neuropeptide Y/agouti-related peptide ($NPY/AgRP^{ARC}$) and pro-opiomelanocortin ($POMC^{ARC}$) -expressing neuron populations (3–7). $POMC^{ARC}$ neurons suppress food intake by releasing α-melanocyte-stimulating hormone (αMSH), which binds to melanocortin 4 receptors (MC4R's) to excite satiety-inducing neurons in the paraventricular nucleus of the hypothalamus (PVN) (1, 8). $NPY/AgRP^{ARC}$ neurons have opposite effects on MC4R-expressing neuron activity and feeding *via* co-release of gamma aminobutyric acid (GABA), NPY, and AgRP (1, 2, 9). NPY/AgRP neurons may also directly antagonize POMC neurons *via* GABAergic connections, but the relevance of this phenomenon in physiological conditions is unclear (10).

Both $NPY/AGRP^{ARC}$ and $POMC^{ARC}$ neurons are subject to intricate regulation by appetite-stimulating tyrosine hydroxylase neurons in the ARC (TH^{ARC}) (11). TH is the rate-limiting enzyme in dopamine synthesis (12), and the effects of exercise on TH^{ARC} neurons have yet to be investigated. TH^{ARC} neurons exhibit direct excitatory dopaminergic innervation on $NPY/AgRP^{ARC}$ neurons, as well as direct inhibitory dopaminergic and GABAergic innervation on $POMC^{ARC}$ neurons (11). Moreover, another subpopulation of TH-expressing neurons resides in the PVN (TH^{PVN}) and receives presynaptic inputs from $NPY/AgRP^{ARC}$ neurons to stimulate thermogenesis in brown adipose tissue (13). To date, the potential role of TH^{PVN} neurons in appetite regulation is unknown.

ARC neurons are located adjacent to the third ventricle and the median eminence, which provides convenient access to the cerebrospinal fluid (CSF) and a less selective blood-brain barrier, respectively, and allows for fine responsiveness to changes in energy status. For example, to promote feeding in response to fasting, ghrelin concentrations increase (14), while leptin and insulin levels decrease (15, 16), directly resulting in receptor-mediated increases in NPY/AgRP neuron activity and decreases in POMC neuron activity (17–20). Reduced glucose levels have similar effects on NPY/AgRP and POMC neurons; during which, glucose uptake by glucose transporters is reduced and activity of ATP-sensitive potassium channels is altered (21, 22). Glucose, insulin, leptin, and ghrelin concentrations also differentially fluctuate in response to exercise, depending on intensity and duration (4, 23–25); thus, insight into exercise-mediated changes in hypothalamic neuron activity could be beneficial to understanding of the complex physiological mechanisms regulating post-exercising feeding behavior.

Studies investigating exercise-mediated remodeling of hypothalamic neurocircuits produce conflicting results. For example, Bunner et al. (4) observed acute moderate intensity treadmill exercise (MIE) to increase $NPY/AgRP^{ARC}$ neuron activity and subsequent food intake in fed mice, while He et al. (5) demonstrated opposite effects after fed high intensity interval training (HIIT). Results in $POMC^{ARC}$ neurons are equally equivocal, with one report observing no changes in response to fasted MIE (4) and others observing increased activity after fasted high intensity exercise (HIE) (3) and fed HIIT (5). Notably, all these studies analyzed neuronal activity at a single timepoint immediately after exercise, and exercise-mediated changes in neuronal activity in the hypothalamus can be rapid and transient (5–7). The reported effects may reflect neuroendocrine responses during exercise, rather than changes after exercise, and may also miss critical changes in neuronal activity in the hours after exercise. Moreover, the studies observing appetite-suppressing, NPY/AgRP neuron inhibiting, and/or POMC activating effects after treadmill exercise used electric shock to motivate mice to run, which was not controlled for in sedentary trials (3, 5). This may be a confounding factor, since studies have demonstrated electric shock activates satiety-inducing neurons in the PVN and acute stress stimulates $POMC^{ARC}$-mediated hypophagia (26–28). Alternatively, He et al. (5) may have identified a unique appetite-suppressing effect specific to HIIT. Supporting this hypothesis, other studies have also observed decreased food intake in response to voluntary wheel running in rodents (29, 30), which typically is a more intermittent exercise model (31).

Another potential explanation for variability in investigations into exercise-mediated changes in hypothalamic neuron activity is that these studies contain methodological differences in exercise intensity and pre-exercise feeding (3–5). Considering glucose and metabolic hormone concentrations fluctuate with energy status and exercise intensity (19, 20, 22, 32), it is plausible that post-exercise changes in hypothalamic neuron activity vary depending on energy status and exercise intensity as well. For example, a recent report demonstrates that NPY/AgRP neurons are activated during fed HIIT, but exhibit opposite effects during

fasted HIIT (6). Furthermore, the magnitude of these changes in neuronal activity is directly correlated with exercise intensity (6). Notably, these observations were made during exercise and it remains to be determined if post-exercise changes in hypothalamic neuron activity are similarly dynamic depending on energy status or exercise intensity. This potential phenomenon may explain why the effects of exercise on feeding behavior are inconsistent in the literature and why the success rates of exercise as a weight loss intervention are equally unpredictable (33–44). Overall, the potential confounding factors and methodological differences in studies investigating exercise-mediated modulation of hypothalamic neurons make drawing conclusions challenging; thus, the current study aimed to utilize a translational, well-controlled, within-subject, treadmill exercise protocol to determine the differential effects of fed *vs.* fasted exercise and exercise intensity on subsequent feeding behavior and hypothalamic neuron activity.

MATERIALS AND METHODS

Animals

Male B6.Tg(NPY-hrGFP)1Lowl/J (NPY-GFP reporter) mice were cared for in accordance with the National Institutes of Health *Guide for the Care and Use of Laboratory Animals*, and experimental protocols were approved by Institutional Animal Care and Use Committee of East Carolina University. Mice were fed standard chow ad libitum (3.2kcal/g) and housed at 20–22°C with a 12-h light-dark cycle.

High-Fat Diet-Induced Obesity

5-6-week-old NPY-GFP reporter mice were given ad libitum access to a high-fat diet (5.56kcal/g) with a kilocalorie composition of 58%, 25%, and 17% of fat, carbohydrate, and protein, respectively, for 10 weeks (D12331; Research Diets, New Brunswick, NJ) before undergoing exercise trials.

Acute Treadmill Exercise

Exercise protocols were adapted from a previous study in our lab (4) and all mice were able to successfully complete all exercise trials. Briefly, using a randomized crossover design and commonly used treadmill speeds, untrained mice performed 1-hour sedentary, low (10m/min) (45), moderate (14m/min) (46), and high intensity (18m/min) (3) exercise with one week between bouts. On the day before experiments, mice were familiarized by running for 5 min at 5m/min followed by 5 min at 10m/min. On the day of exercise trials, mice ran at 5m/min for two minutes, 10m/min for two minutes, and then, when applicable, sped up 4m/min every 2 min until the target speed was reached. To minimize stress, a soft bristle brush or gentle puff of air was used to motivate mice, when needed. During sedentary trials, mice were placed in empty cages on top of the running treadmill for 1-hour to simulate stress during exercise bouts. For fasting exercise experiments, food was removed from cages 10-hours before exercise. All sedentary and exercise bouts were performed between 6:30 and 7:30pm., immediately before the dark-phase.

Food Intake and Body Weight Measurements

Food was weighed and added to individually-housed cages immediately after sedentary and exercise bouts (14-15g). Measurements were made 1, 2, 3, 6, 12, 24, and 48-hours post-exercise by subtracting from the total food. Bedding was inspected thoroughly for residual bits of food, which were included in measurements. All food intakes were normalized to body weight, which was measured immediately before sedentary and exercise bouts.

Immunohistochemistry

1-hour post-exercise, when differences in food intake were first observed, mice were intracardially perfused with PBS followed by 10% formalin before immunohistochemistry was performed as described previously (47). Briefly, brains were sliced into 20-µm coronal sections using a freezing microtome (VT1000 S; Leica, Wetzlar, Germany) and incubated overnight in antibody to cFOS (1:250; Santa Cruz Biotechnology, Santa Cruz, CA), POMC (1:6000; Phoenix Pharmaceuticals), tyrosine hydroxylase (TH) (1:100000; Millipore), and SIM1 (1:250; Millipore) followed by incubation with Alexa-fluorophore secondary antibody for 1 h (Abcam). To probe for two proteins with same-source antibodies DAB (3,3′-Diaminobenzidine) staining was performed prior to the immunohistochemistry protocols described above (4). Briefly, brain sections were incubated overnight in antibody to phosphorylated $STAT3^{tyr705}$ (1:500; Cell Signaling Technology) or phosphorylated $ERK^{thr202/tyr204}$ (1:500; Cell Signaling Technology) followed by biotinylated donkey anti-rabbit IgG (Vector; 1:1000) for 2 hours. Sections were then incubated in the avidin–biotin complex (ABC; Vector Elite Kit; 1:500) and incubated in 0.04% DAB, 0.02% cobalt chloride (Fisher Scientific), and 0.01% hydrogen peroxide. Note, $pSTAT3^{tyr705}$ images were inverted (to white) for colocalization. All stains were photographed using an optical microscope (DM6000; Leica), followed by blind analysis using ImageJ. At least three anatomically matched images per mouse were quantified.

Statistical Analysis

For time course food intake experiments, differences among sedentary or exercise bouts were determined using 2-Way-ANOVA with Repeated Measures for time and treatment (n=11/group). Bonferroni corrections were used for multiple comparisons. For comparisons in neuronal activity between sedentary and high intensity exercise, Student's T-tests were used (n=5-7/group for $POMC^{ARC}$ neurons, 4-6/group for $SIM1^{PVN}$ neurons, 5-6/group for TH^{ARC} neurons, 3-5/group for TH^{PVN} neurons, and 4-6/group for $NPY/AgRP^{ARC}$ neurons). All analyses were performed using GraphPad Prism statistics software, and $p<0.05$ was considered statistically significant.

DATA AVAILABILITY STATEMENT

The data sets generated during the current study are available from the corresponding author on reasonable request.

RESULTS

Acute High Intensity Treadmill Exercise Suppresses Food Intake in Fasted Mice

To investigate the effects of varying aerobic exercise intensities on post-exercise food intake, 11 fasted male mice underwent acute sedentary, low intensity (LIE), MIE, and HIE bouts for 1-hour on the treadmill. Cumulative 24-hour food intake was unchanged after LIE and MIE; however, mice ate significantly less after HIE compared to sedentary bouts (5.3%), which persisted for at least 48 hours (6.7%) (**Figures 1A, B**). Further examination of food intake at specific time intervals revealed HIE-mediated appetite suppression occurred 1-2 hours post-exercise, followed by a compensatory increase in food intake at 6-12 hours, and another period of significantly reduced food intake at 12-24 hours (**Figure 1C**). MIE also elicited trends toward reduced food intake 1-2 hours post-exercise, but these effects were not statistically significant (p=0.16), and all exercise intensities elicited increases in food intake at 6-12 hours. Taken together, these data suggest HIE uniquely results in a suppression in appetite 1-2 and 12-24-hours post-exercise, resulting in reduced cumulative food intake for at least 48 hours.

Surprisingly LIE and HIE had no effects on food intake in DIO mice, but MIE significantly reduced 24-hour food intake 8.5% (**Supplemental Figure 1A**) and trended to decrease cumulative food intake at 48 hours (p=0.10; **Supplemental Figure 1B**). Specifically, the reductions in food intake in response to MIE were predominantly observed 2-3 hours post-exercise (**Supplemental Figure 1C**). In summary, these findings suggest, even in overweight mice, fasted aerobic exercise can have an appetite-suppressing effect.

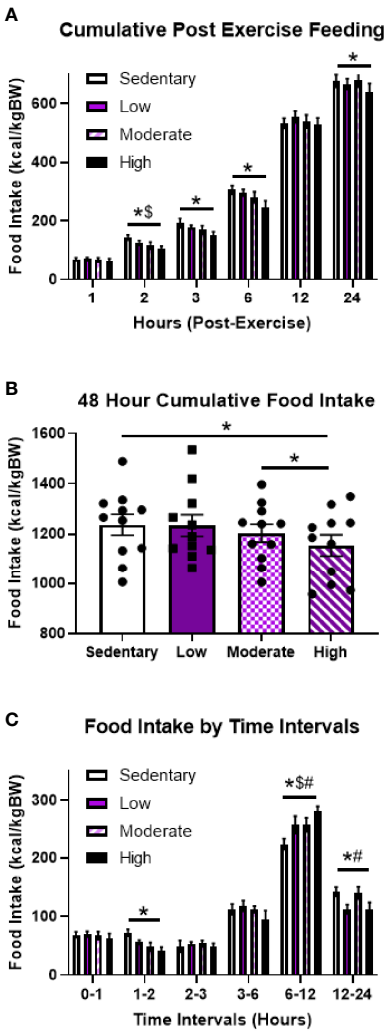

FIGURE 1 | Acute high intensity treadmill exercise suppresses food intake in fasted male mice. **(A)** Timeline of cumulative food intake, **(B)** 48-hour cumulative food intake, and **(C)** food intake by time intervals in fasted male mice in response to different acute treadmill exercise intensities (n = 11). Data represented as mean ± SEM. *indicates $p < 0.05$ high intensity *vs.* sedentary; $^{\$}$indicates $p < 0.05$ moderate intensity *vs.* sedentary; $^{\#}$indicates $p < 0.05$ low intensity *vs.* sedentary.

High Intensity Exercise Increases Activity of POMC^{ARC} and SIM1^{PVN} Neurons in Fasted Mice

Since HIE was the only bout that elicited effects on food intake, brains were removed 1-hour after HIE and immunohistochemical detection for cFOS (a marker of neuronal activity) was performed in the hypothalamus to investigate the associated changes in neuronal activity. Compared to sedentary controls, HIE significantly increased cFOS expression in the dorsomedial hypothalamus (1.8-fold) and ARC (4.4-fold), while trending to increase cFOS in the ventromedial hypothalamus (1.4-fold; p=0.08) (**Figures 2A, B**). Double-staining for cFOS and POMC-expressing neurons revealed that the robust increase in ARC cFOS post-exercise is, in part, due to POMC^{ARC} neuron excitation (2-fold) (**Figures 2C–E**), which are well-documented appetite-suppressing neurons (8). Additionally, HIE increased cFOS colocalization with SIM1^{PVN}-expressing neurons 2.1-fold, which are also satiety-inducing neurons with presynaptic input from POMC neurons (**Figures 2F–H**) (2, 48). These data suggest that the POMC^{ARC}→ SIM1^{PVN} neurocircuit may be activated by HIE.

High Intensity Exercise Also Increases Activity of NPY/AgRP^{ARC} and TH^{PVN} Neurons in Fasted Mice

We also investigated the effects of HIE on activity of appetite-inducing NPY/AgRP^{ARC} and TH^{ARC} neurons. Surprisingly, cFOS colocalization with NPY/AgRP^{ARC} neurons was elevated 1.7-fold 1-hour post-HIE (**Figures 3A–C**). While these data are conflicting with the appetite-suppressing effects of HIE, previous reports suggest exercise-mediated increases in NPY/AgRP neuron activity may be critical to ensuring adequate post-exercise refueling and recovery (4). Moreover, HIE had no effects on cFOS colocalization with TH^{ARC} neurons (**Figures 3D–F**); however, cFOS expression in TH^{PVN} neurons was increased 8.6-fold (**Figures 3G–I**).

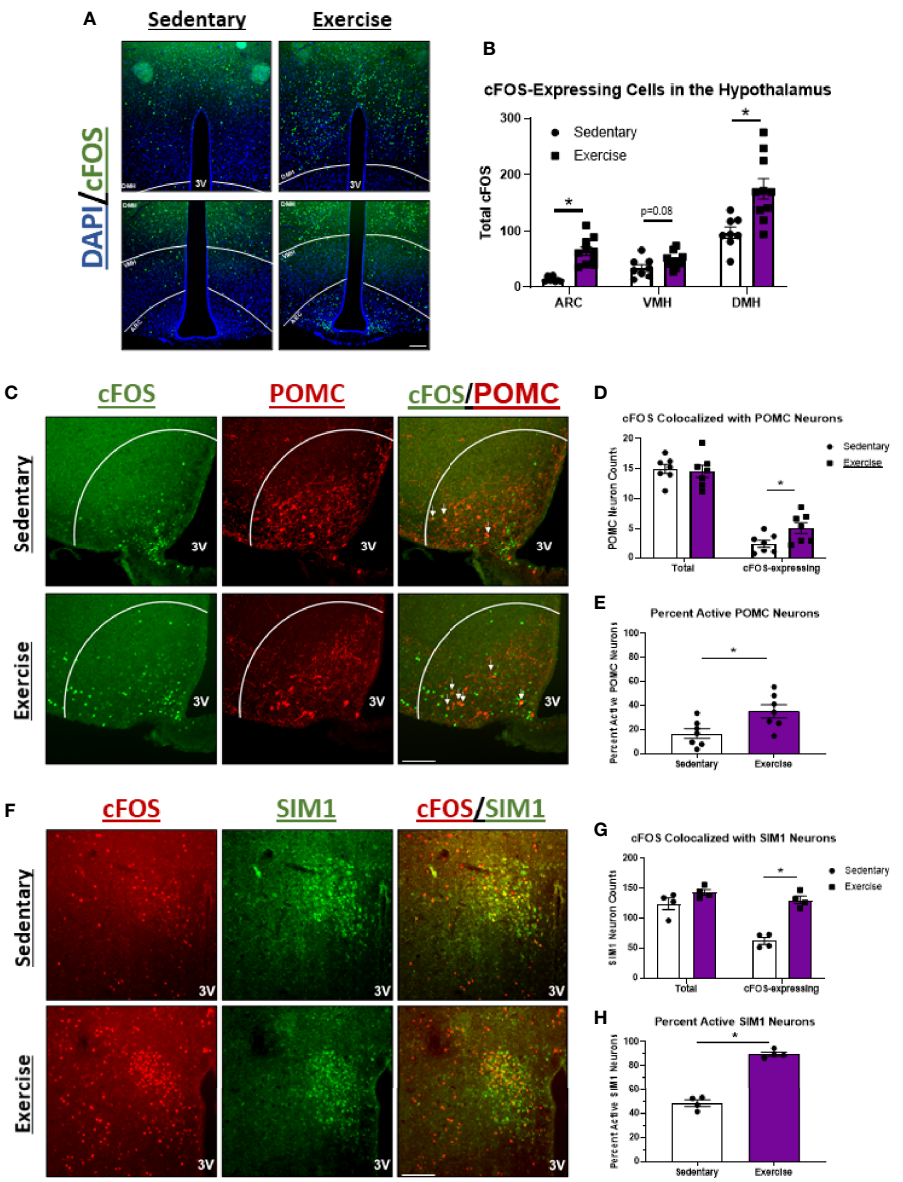

FIGURE 2 | POMC^{ARC} and SIM1^{PVN} neuron activity is elevated 1 hour after acute high intensity treadmill exercise in fasted male mice. **(A)** Representative images of cFOS (green) in the hypothalamus of fasted male mice 1 hour after sedentary trials or high intensity treadmill exercise (DAPI in blue). **(B)** Total cFOS-expressing cells in each region of the hypothalamus (n=10/group) DMH=dorsomedial hypothalamus; VMH=ventromedial hypothalamus; ARC=arcuate nucleus. **(C)** Representative images of cFOS (green) colocalized with POMC^{ARC} neurons (red) in fasted male mice 1 hour after sedentary trials or high intensity treadmill exercise. **(D)** Total and cFOS-expressing POMC^{ARC} neurons and **(E)** Percent active POMC^{ARC} neurons (n = 7/group). **(F)** Representative images of cFOS (red) colocalized with SIM1^{PVN} neurons (green) in fasted male mice 1 hour after sedentary trials or high intensity treadmill exercise. **(G)** Total and cFOS-expressing SIM1^{PVN} neurons and **(H)** Percent active SIM1^{PVN} neurons (n = 4/group). 3V = Third ventricle; Scale bar = 50um. Data represented as mean ± SEM. *indicates $p < 0.05$ *vs.* sedentary trials.

The diverse changes in neuronal activity in response to HIE occurred independent from changes in ARC pSTAT3^{tyr705} and pERK$^{thr202/tyr204}$ intracellular signaling 1-hour post-exercise (**Supplemental Figure 2**). pSTAT3^{tyr705} and pERK$^{thr202/tyr204}$ are downstream mediators of the anorexigenic hormone leptin to activate POMC neurons and inhibit NPY/AgRP neurons (17, 49); therefore, the appetite suppressing effects of HIE may be independent from leptin activity.

Aerobic Exercise in the Fed State Increases Post-Exercise Food Intake

While our data in fasted mice suggests HIE would be beneficial to creating a caloric deficit by increasing energy expenditure and decreasing food intake, recent studies investigating the effects of aerobic exercise on feeding behavior and appetite-controlling neurons produce conflicting results (3–5). Since the hypothalamic neurons affected by aerobic exercise are sensitive to changes in

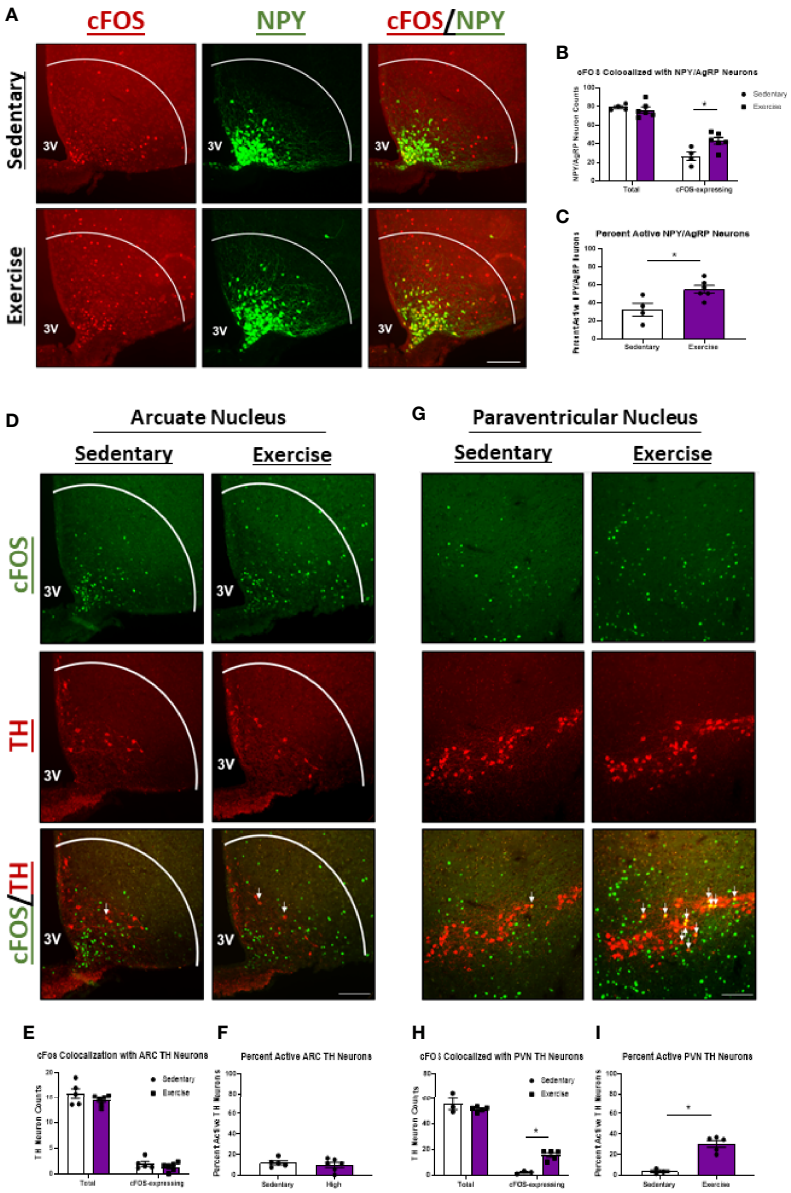

FIGURE 3 | NPY/AgRP^{ARC} and TH^{PVN} neuron activity is elevated 1 hour after acute high intensity treadmill exercise in fasted male mice. **(A)** Representative images of cFOS (red) colocalized with NPY/AgRP^{ARC} neurons (green) in fasted male mice 1 hour after sedentary trials or high intensity treadmill exercise. **(B)** Total and cFOS-expressing NPY/AgRP^{ARC} neurons and **(C)** Percent active NPY/AgRP^{ARC} neurons (n = 4-6/group). **(D)** Representative images of cFOS (green) colocalized with TH^{ARC} neurons (red) in fasted male mice 1 hour after sedentary trials or high intensity treadmill exercise. **(E)** Total and cFOS-expressing TH^{ARC} neurons and **(F)** Percent active TH^{ARC} neurons (n = 5-6/group). **(G)** Representative images of cFOS (green) colocalized with TH^{PVN} neurons (red) in fasted male mice 1 hour after sedentary trials or high intensity treadmill exercise. **(H)** Total and cFOS-expressing TH^{PVN} neurons and **(I)** Percent active TH^{PVN} neurons (n = 3-5/group). 3V = Third ventricle; Scale bar = 50um. Data represented as mean ± SEM. *indicates $p < 0.05$ *vs.* sedentary trials.

glucose and metabolic hormones (19, 20, 22, 32), we hypothesized that changes in pre-exercise energy status may differentially modulate the post-exercise feeding response. Compared to 10-hour-fasted sedentary mice, a separate cohort of ad libitum fed sedentary mice exhibited significantly elevated cFOS colocalization with POMC^{ARC} neurons (3.3-fold) (**Supplemental Figure 3A**) and trends toward decreased cFOS colocalization with NPY/AgRP^{ARC} neurons (p=0.08; 0.6-fold) (**Supplemental Figure 3B**). Moreover, both 1-hour and 24-hour cumulative food intake was decreased in fed mice, overall validating significant differences in pre-exercise energy status between fasted and fed mice (**Supplemental Figure 3C**).

Supporting the hypothesis that pre-exercise energy status dictates post-exercise feeding behavior, all exercise intensities resulted in 8-10% increases in 24-hour food intake compared to the sedentary bout (**Figure 4A**). Notably, these differences were no longer evident

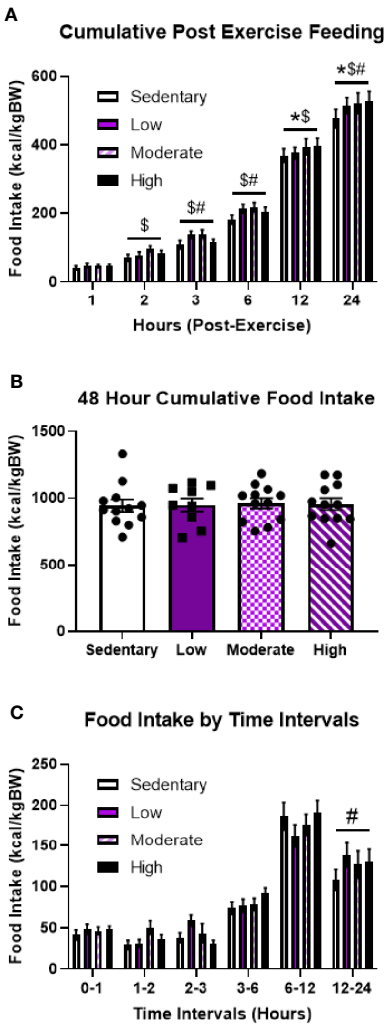

FIGURE 4 | Regardless of intensity, acute treadmill exercise increases food intake in fed male mice. **(A)** Timeline of cumulative food intake, **(B)** 48-hour cumulative food intake, and **(C)** food intake by time intervals in fed male mice in response to different acute treadmill exercise intensities (n = 11). Data represented as mean ± SEM. *indicates $p < 0.05$ high intensity *vs.* sedentary; $^{\$}$indicates $p < 0.05$ moderate intensity *vs.* sedentary; $^{\#}$indicates $p < 0.05$ low intensity *vs.* sedentary.

after 48 hours (**Figure 4B**). Analysis of specific time intervals revealed that LIE specifically elicited increased food intake between 12 and 24 hours post-exercise; however, there were no significant differences at any specific time intervals in response to MIE and HIE (**Figure 4C**). Overall, while time interval data suggests heterogeneity in the specific post-exercise feeding timelines among fed mice, these findings highlight drastic differences in post-exercise feeding behavior depending on energy status.

POMC^{ARC} Neuron Excitation Is Specific to High Intensity Exercise in the Fasted Status

We next aimed to compare changes in hypothalamic neuron activity between exercise in the fasted and fed statuses to better understand the neuron populations responsible for energy status-dependent feeding behavior. Similar to HIE in the fasted status, HIE in fed mice resulted in increased cFOS expression in NPY/AgRP^{ARC} (1.8-fold; **Figures 5A–C**), TH^{PVN} (11.4-fold; **Figures 5D–F**), and SIM1^{PVN} (2.2-fold; **Figures 5G–I**) neurons, with no effects in TH^{ARC} neurons (**Supplemental Figure 4**). The similarities in hypothalamic NPY/AgRP, TH, and SIM1 neuron responses between fed and fasted exercise indicate these neuron populations may not be responsible for energy status-dependent effects of exercise on feeding behavior. Interestingly, unlike in fasted mice, fed HIE had no effects on cFOS colocalization with POMC^{ARC} neurons (**Figure 6**), suggesting POMC excitation may be, in part, responsible for energy status-dependent variations in post-exercise feeding.

DISCUSSION

Recent studies identifying a potent ability for aerobic exercise to modulate hypothalamic neurons involved in appetite regulation produce conflicting results (3–5). These discrepancies may be explained by differences in methods utilized, including exercise intensity, pre-exercise energy status, and stimulus to promote the exercise. Considering this, the current study used a translational, within-subject, acute treadmill exercise protocol to determine that pre-exercise energy status and exercise intensity drastically modify post-exercise feeding behavior and concurrent hypothalamic neuron activity.

The current study identified a beneficial role of fasted aerobic exercise to suppress food intake in mice, which is consistent with some previous reports in rodents and humans (3, 35, 40, 50, 51). Interestingly, reduced food intake occurred only after HIE in lean mice, whereas in DIO mice, this effect was limited to the MIE bout. At first glance, this suggests DIO mice have a lower intensity threshold to elicit exercise-mediated reductions in food intake; however, intensities used in the current study are based on absolute treadmill speeds and do not account for intrinsic aerobic capacities or differences in body weight. Considering DIO mice have lower aerobic capacities compared to lean mice (52), and greater body mass requires more work to perform the same treadmill exercise, the relative intensity at which DIO mice are exercising is higher at any given absolute treadmill speed. Therefore, it is plausible that the HIE and MIE are eliciting similar relative intensities for the lean and DIO mice, respectively. Consequently, these findings suggest fasted aerobic exercise at higher intensities can reduce food intake regardless of obesity, and, coupled with the associated energy expenditure, may be optimal for creating a caloric deficit and inducing weight loss.

Despite our encouraging evidence suggesting higher intensity exercise can suppress appetite, the literature regarding post-exercise feeding produces inconsistent results (35, 36, 39–44, 50, 51, 53–55). The current study demonstrated a novel phenomenon in which post-exercise feeding behavior is dependent on pre-exercise energy status, which may explain these discrepancies. For example, fasted HIE suppressed food

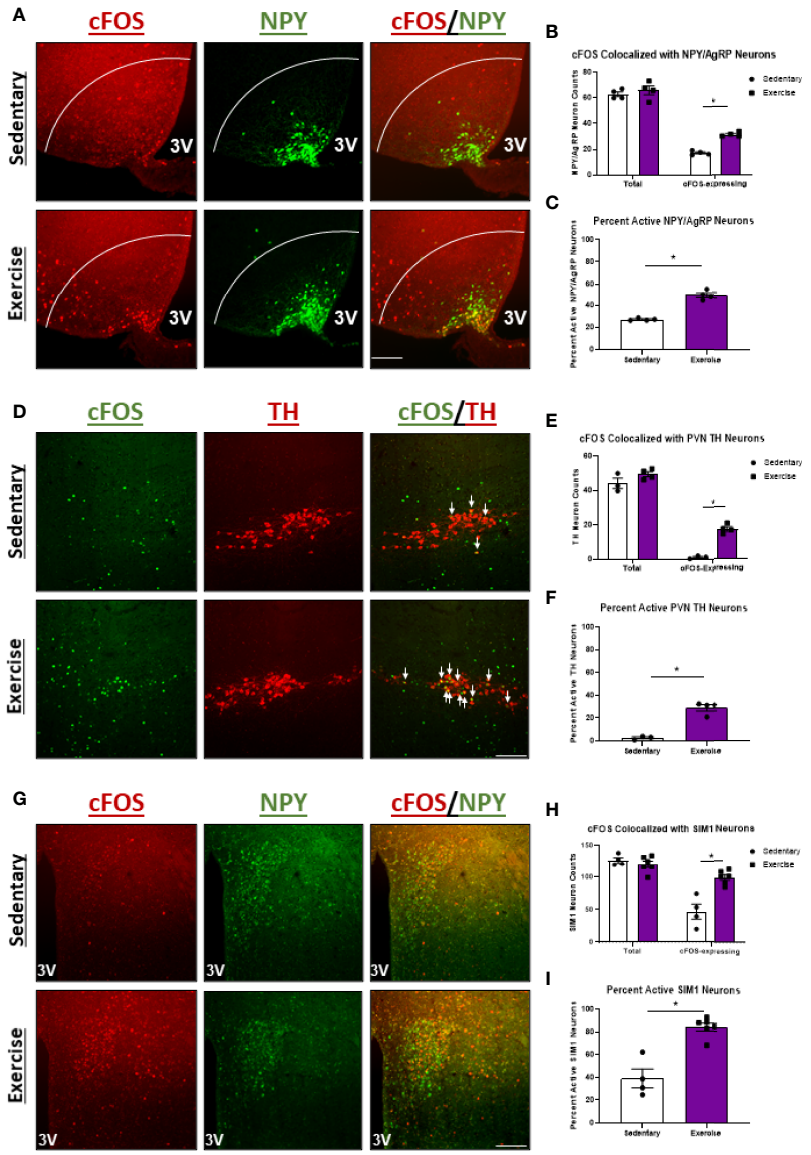

FIGURE 5 | Regardless of energy status, high intensity treadmill exercise increases NPY/AgRP^{ARC}, TH^{PVN}, and SIM1^{PVN} neuron activity. **(A)** Representative images of cFOS (red) colocalized with NPY/AgRP^{ARC} neurons (green) in male mice 1 hour after sedentary trials or high intensity treadmill exercise. **(B)** Total and cFOS-expressing NPY/AgRP^{ARC} neurons and **(C)** Percent active NPY/AgRP^{ARC} neurons (n=4/group). **(D)** Representative images of cFOS (green) colocalized with TH^{PVN} neurons (red) in fed male mice 1 hour after sedentary trials or high intensity treadmill exercise. **(E)** Total and cFOS-expressing TH^{PVN} neurons and **(F)** Percent active TH^{PVN} neurons (n = 3-4/group). **(G)** Representative images of cFOS (red) colocalized with SIM1^{PVN} neurons (green) in fed male mice 1 hour after sedentary trials or high intensity treadmill exercise. **(H)** Total and cFOS-expressing SIM1^{PVN} neurons and **(I)** Percent active SIM1^{PVN} neurons (n = 4-6/group). 3V, Third ventricle; Scale bar = 50um. Data represented as mean ± SEM. *indicates $p < 0.05$ *vs.* sedentary trials.

intake in lean mice, but fed exercise increased food intake regardless of intensity. While the reasons for these energy status-dependent differences in feeding behavior are unclear, glucose and metabolic hormone concentrations also fluctuate with energy status, modulating activity of neuron populations involved in regulating feeding behavior (19, 20, 22, 32). Consequently, recent studies have investigated the potential role for exercise to modulate activity of hypothalamic neurons involved in regulating appetite (3–7).

To elucidate the neuronal mechanisms underlying energy status-dependent post-exercise feeding, we compared the changes in hypothalamic neuron activity after fasted *vs.* fed HIE. The primary difference observed was an increase in anorexigenic POMC^{ARC} neuron activity 1-hour after fasted, but not fed, HIE. Since POMC^{ARC} neurons suppress food intake through excitatory synaptic connections with MC4R^{PVN}-expressing neurons (1, 8), these results may suggest POMC^{ARC} neurons are a mediating factor in fasted HIE-mediated appetite

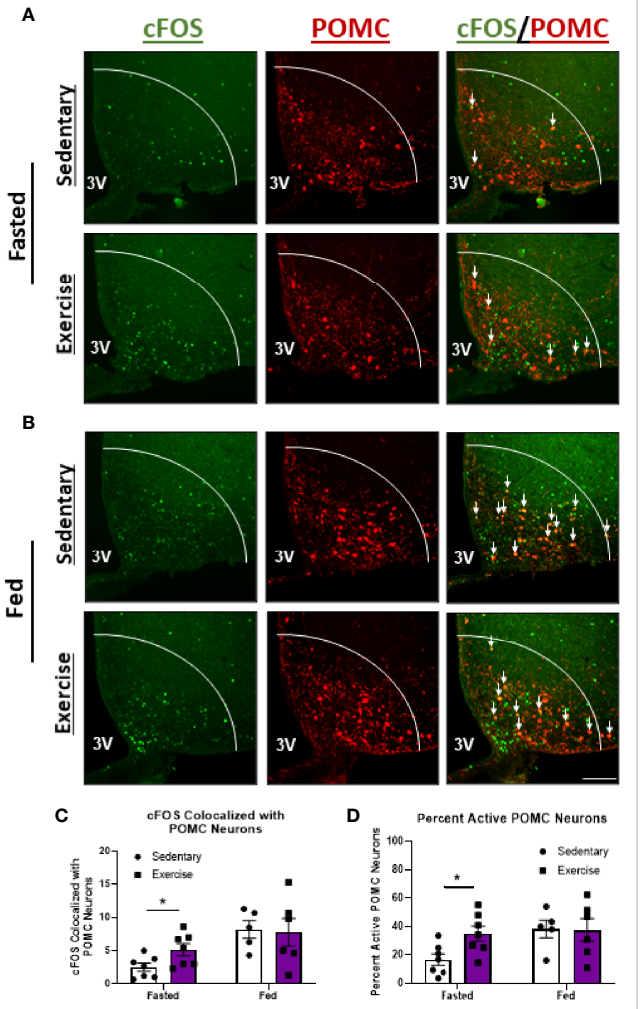

FIGURE 6 | Exercise-mediated POMC^{ARC} activation is specific to the fasted status. Representative images of cFOS (green) colocalized with POMC^{ARC} neurons (red) in **(A)** fasted or **(B)** fed male mice 1 hour after sedentary trials or high intensity treadmill exercise. **(C)** cFOS-expressing POMC^{ARC} neurons and **(D)** Percent active POMC^{ARC} neurons (n = 5-7/group). 3V = Third ventricle; Scale bar = 50um. Data represented as mean ± SEM. *indicates $p < 0.05$ *vs.* sedentary trials.

suppression; although at this time it is unclear what is driving these energy status dependent changes. Feeding increases POMC^{ARC} neuron activity (1, 56); therefore it's possible POMC^{ARC} neuron activity has plateaued before fed exercise, resulting in no additive effects of exercise on these neurons. Mechanistically, exercise has been shown to increase sensitivity to the POMC^{ARC}-stimulating hormone leptin (24, 57); however our data revealed no changes in the ARC in pSTAT3^{tyr705} or pERK$^{thr202/tyr204}$, which are key mediators of leptin activity. Ropelle et al. (57) also observed no effects of exercise on hypothalamic pSTAT3^{tyr705} in lean mice, despite observing augmented appetite suppression in response to intracerebroventricular (ICV) leptin infusion. Since higher intensity exercise can decrease leptin levels (24), the absence of changes in downstream leptin signaling in the hypothalamus post-exercise may suggest compensatory increases in leptin sensitivity. Alternatively, exercise elevates IL-6 concentrations (58), improves insulin sensitivity (57), increases core temperature (3), and decreases ghrelin levels (59), which all can increase POMC^{ARC} neuron activity. Future studies investigating differential modulation of hormones and core temperature by fasted *vs.* fed exercise may provide further explanation into energy-status dependent POMC^{ARC} activation.

While our POMC^{ARC} results are consistent with past reports observing fasting HIE increases POMC^{ARC} neuron activity (3) and no effects of MIE in fed mice (4), one study discovered HIIT has excitatory effects on POMC^{ARC} neurons, even in the fed state (5). It is possible HIIT elicits additional appetite-suppressing benefits compared to steady-state HIE, independent from energy status. This hypothesis is supported by studies observing voluntary wheel running, which is a more intermittent model of exercise (31), to also suppress food intake (29, 30). Alternatively, He et al. (5) utilized electric shock as a stimulus to motivate mice during exercise, which may have been a confounding factor. Electric shock has been shown to activate satiety-inducing neurons in the hypothalamus (28), and acute stress in mice promotes POMC^{ARC}-mediated hypophagia (26, 27). These confounding factors highlight the importance of minimizing and controlling for stress in these studies.

Increased activity of many other neuron populations in the hypothalamus was observed in the present study in response to HIE. For example, NPY/AgRP^{ARC} and SIM1^{PVN} neuron activity was elevated regardless of pre-exercise energy status, suggesting these neuron populations are not driving energy status-dependent feeding behavior after exercise. Activation of the orexigenic NPY/AgRP^{ARC} neuron population was surprising, although a previous study demonstrated NPY/AgRP^{ARC} activation post-exercise was essential to refeeding (4). Therefore, exercise-mediated NPY/AgRP^{ARC} neuron activation may be an evolutionarily preserved mechanism to ensure adequate refueling and recovery. Conversely, He et al., 2018 (5) observed inhibitory effects of HIIT on NPY/AgRP^{ARC} neurons, however, as previously mentioned, these effects may be unique to HIIT or a biproduct of electric shock-induced stress. While the importance of exercise-mediated increases in SIM1^{PVN} neuron activity to feeding behavior is unclear, these findings were consistent with a previous study (4). Past reports using chemogenetic approaches determined exercise-induced SIM1^{PVN} activity is independent from presynaptic NPY/AgRP^{ARC} neurons (4); however, recently a subpopulation of SIM1^{PVN} neurons that exhibit excitatory synapses on NPY/AgRP^{ARC} neurons was identified (60). It is possible that aerobic exercise stimulates a SIM1^{PVN}→NPY/AgRP^{ARC} neurocircuit to promote adequate refeeding, and future studies using chemogenetic inhibition of SIM1^{PVN} neurons before aerobic exercise could help verify this hypothesis.

To our knowledge, the present study was the first to investigate the effects of HIE on hypothalamic TH-expressing neurons. TH^{ARC} neurons stimulate food intake by releasing GABA and dopamine (11); however, no effects of exercise on

TH^{ARC} neuron activity were observed. Interestingly, a striking increase in TH^{PVN} neuron activity was observed in response to both fed and fasted exercise. TH^{PVN} neurons have been implicated in the regulation of brown adipose tissue thermogenesis (13), and they exhibit downstream synaptic connections in various areas of the hypothalamus (61), but their role in appetite regulation is unknown. Regardless, elevated TH^{PVN} neuron activity in response to both fed and fasted exercise suggests these neurons are also not driving factors in energy status-dependent feeding behavior post-exercise.

To summarize the neuronal phenotype in response to acute HIE, $NPY/AgRP^{ARC}$, TH^{PVN}, and $SIM1^{PVN}$ neuron activity are elevated 1-hour post-exercise, regardless of energy status, with no effects on TH^{ARC} neurons. Surprisingly, $POMC^{ARC}$ activity is only increased after fasted exercise, suggesting these neurons may possibly mediate suppression of food intake in response to fasted HIE (**Figure 7**). Notably, the current study only examined neuronal changes 1-hour post-exercise, the time point immediately before changes in food intake were first observed, and changes in neuronal activity after exercise are rapid and transient (5–7). For example, it is unclear what is driving compensatory increases in food intake 6-12-hours after fasted exercise. To better understand the driving factors in post-exercise feeding, future studies into the time course of neuronal activity changes would be valuable.

Overall, our results identify a novel role for pre-exercise energy status to differentially modify post-exercise feeding behavior and hypothalamic neuron activity, which may explain the significant variability in results from studies investigating exercise as a weight loss intervention. Many other factors are also likely involved in mediating differences in post-exercise feeding, such as sex, training status, exercise volume, time of day, and type of exercise. For example, while our study utilized only male mice, female mice exhibit different regulatory mechanisms governing energy balance, including higher POMC expression (62), lower NPY expression (63), and a critical role for estrogen receptors in CNS control of feeding (64). Furthermore, since we investigated acute aerobic exercise, it is unclear if repeated

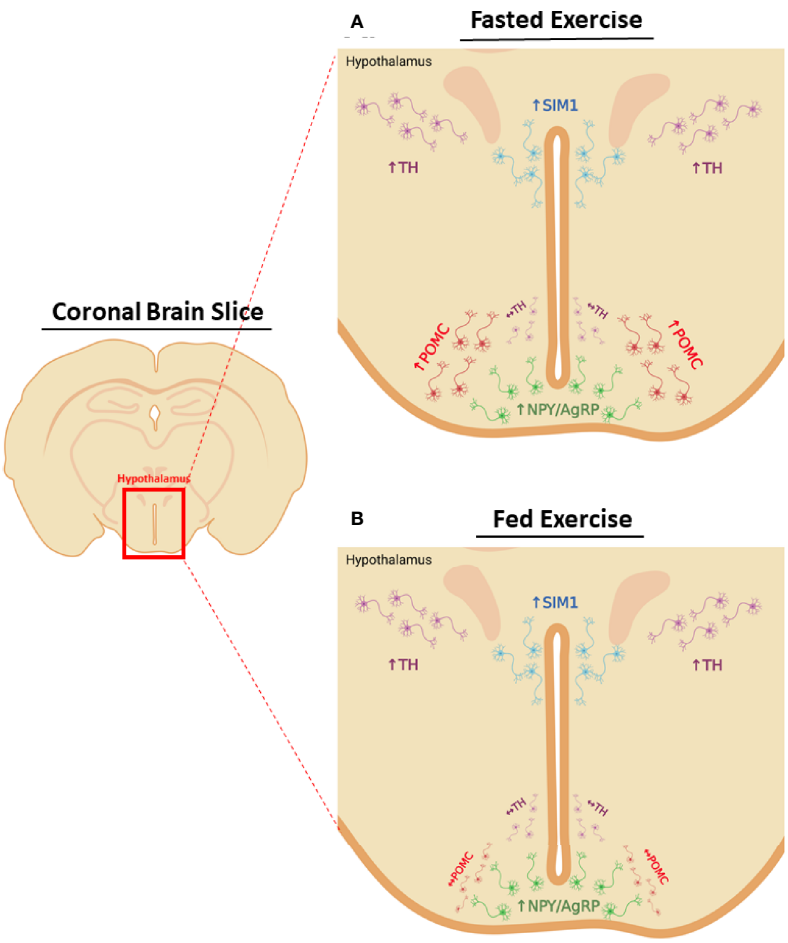

FIGURE 7 | Energy status differentially modifies post-exercise neuronal activity in the hypothalamus. Changes in hypothalamic neuron activity 1-hour after HIE in the **(A)** fasted or **(B)** fed status. Regardless of energy status HIE increases $NPY/AgRP^{ARC}$, $SIM1^{PVN}$, and TH^{PVN} neuron activity, with no effects on TH^{ARC} neurons. $POMC^{ARC}$ neuron activity is only elevated 1-hour after fasted HIE.

aerobic exercise training or resistance training also have differential effects on CNS control of food intake. Lastly, to investigate the effects of exercise intensities on food intake, the current study did not control for total exercise volume or energy expenditure. It is possible that the observed effects of fasted HIE to decrease food intake and increase $POMC^{ARC}$ neuron activity are due to increased exercise volume rather than intensity.

The effect of exercise on hypothalamic neuron activity is a relatively new focus of research and CNS control of feeding behavior is dynamic and complex. While many factors are likely involved, the current study identifies pre-exercise energy status as a novel variable that drastically modifies post-exercise food intake and appetite-controlling neurons. These findings could have implications when tailoring exercise programs to individual goals; for example, in clinical populations, fasted HIE may be beneficial to decreasing food intake and maximizing caloric deficit.

GUARANTOR STATEMENT

HH is the guarantor of this work and, as such, has full access to all the data in the study and takes responsibility for its integrity and the accuracy of the analysis.

DATA AVAILABILITY STATEMENT

The raw data supporting the conclusions of this article will be made available by the authors, without undue reservation.

ETHICS STATEMENT

The animal study was reviewed and approved by Institutional Animal Care and Use Committee of East Carolina University.

AUTHOR CONTRIBUTIONS

TL conceptualization, methodology, validation, formal analysis, investigation, writing – original draft, writing – review and editing, and visualization. DS investigation, writing – review and editing. AC conceptualization, writing – review and editing. KF investigation. TN investigation. HH writing – review and editing, supervision, project administration, funding acquisition. All authors contributed to the article and approved the submitted version.

FUNDING

The funding for this project was provided by East Carolina University start up, the National Institute of Diabetes and Digestive and Kidney Disease (DK121215) to HH.

SUPPLEMENTARY MATERIAL

The Supplementary Material for this article can be found online at: https://www.frontiersin.org/articles/10.3389/fendo.2021.705267/full#supplementary-material

Supplementary Figure 1 | Acute moderate intensity treadmill exercise suppresses food intake in fasted DIO male mice. **(A)** Timeline of cumulative food intake, **(B)** 48 hour cumulative food intake, and **(C)** food intake by time intervals in fasted male mice in response to different acute treadmill exercise intensities (n=11). Data represented as mean ± SEM. $ indicates $p<0.05$ moderate intensity vs. sedentary.

Supplementary Figure 2 | ARC $pSTAT3^{tyr705}$ and $pERK^{thr202/tyr204}$ are unchanged 1 hour after high intensity treadmill exercise in fasted male mice. **(A)** Representative inverted DAB images of $pSTAT3^{tyr705}$ (white) colocalized with $NPY/AgRP^{ARC}$ (green) and $POMC^{ARC}$ neurons (red) in fasted male mice 1 hour after sedentary trials or high intensity treadmill exercise. **(B)** Colocalization with $NPY/AgRP^{ARC}$ neurons and **(C)** Colocalization with POMC neurons. **(D)** Representative DAB images of $pERK^{thr202/tyr204}$ (black) in the ARC. **(E)** Total ARC $pERK^{thr202/tyr204}$ (n=4-5/group). 3V = Third ventricle; Scale bar = 50um. Data represented as mean ± SEM.

Supplementary Figure 3 | Fed mice exhibit elevated $POMC^{ARC}$ neuron activity and reduced food intake. **(A)** Comparison of cFOS colocalized with $POMC^{ARC}$ neurons in sedentary fasted mice vs. sedentary fed mice (original data presented in **Figure 6**). **(B)** Comparison of cFOS colocalized with $NPY/AgRP^{ARC}$ neurons in sedentary fasted mice vs. sedentary fed mice (original data presented in **Figures 3** and **6**). **(C)** Comparison of cumulative food intake in sedentary fasted mice vs. sedentary fed mice (original data presented in **Figures 1** and **4**).

Supplementary Figure 4 | High intensity treadmill exercise has no effects on TH^{ARC} neuron activity. **(A)** Representative images of cFOS (green) colocalized with TH^{ARC} neurons (red) in fed male mice 1 hour after sedentary trials or high intensity treadmill exercise. **(B)** Total and cFOS-expressing TH^{ARC} neurons and **(C)** Percent active TH^{ARC} neurons (n=5-6/group).

REFERENCES

1. Andermann ML, Lowell BB. Toward a Wiring Diagram Understanding of Appetite Control. *Neuron* (2017) 95:757–78. doi: 10.1016/j.neuron.2017.06.014
2. Atasoy D, Nicholas Betley J, Su HH, Sternson SM. Deconstruction of a Neural Circuit for Hunger. *Nature* (2012) 488:172–7. doi: 10.1038/nature11270
3. Jeong JH, Lee DK, Liu SM, Chua SC, Schwartz GJ, Jo YH. Activation of Temperature-Sensitive TRPV1-Like Receptors in ARC POMC Neurons Reduces Food Intake. *PloS Biol* (2018) 16:e2004399. doi: 10.1371/journal.pbio.2004399
4. Bunner W, Landry T, Laing BT, Li P, Rao Z, Yuan Y, et al. Arcagrp/NPY Neuron Activity Is Required for Acute Exercise-Induced Food Intake in Un-Trained Mice. *Front Physiol* (2020) 11:411. doi: 10.3389/fphys.2020.00411
5. He Z, Gao Y, Alhadeff AL, Castorena CM, Huang Y, Lieu L, et al. Cellular and Synaptic Reorganization of Arcuate NPY/AgRP and POMC Neurons After Exercise. *Mol Metab* (2018) 18:107–19. doi: 10.1016/j.molmet.2018.08.011
6. Lieu L, Chau D, Afrin S, Dong Y, Alhadeff AL, Betley JN, et al. Effects of Metabolic State on the Regulation of Melanocortin Circuits. *Physiol Behav* (2020) 224:113039. doi: 10.1016/j.physbeh.2020.113039
7. Miletta MC, Iyilikci O, Shanabrough M, Šestan-Peša M, Cammisa A, Zeiss CJ, et al. AgRP Neurons Control Compulsive Exercise and Survival in an Activity-Based Anorexia Model. *Nat Metab* (2020) 2:1204–11. doi: 10.1038/s42255-020-00300-8
8. Zhan C, Zhou J, Feng Q, Zhang J-E, Lin S, Bao J, et al. Acute and Long-Term Suppression of Feeding Behavior by POMC Neurons in the Brainstem and

Hypothalamus, Respectively. *J Neurosci* (2013) 33:3624–32. doi: 10.1523/JNEUROSCI.2742-12.2013
9. Krashes MJ, Koda S, Ye C, Rogan SC, Adams AC, Cusher DS, et al. Rapid, Reversible Activation of AgRP Neurons Drives Feeding Behavior in Mice. *J Clin Invest* (2011) 121:1424–8. doi: 10.1172/JCI46229
10. Rau AR, Hentges ST. The Relevance of AgRP Neuron-Derived GABA Inputs to POMC Neurons Differs for Spontaneous and Evoked Release. *J Neurosci* (2017) 37:7362–72. doi: 10.1523/JNEUROSCI.0647-17.2017
11. Zhang X, Van Den Pol AN. Hypothalamic Arcuate Nucleus Tyrosine Hydroxylase Neurons Play Orexigenic Role in Energy Homeostasis. *Nat Neurosci* (2016) 19:1341–7. doi: 10.1038/nn.4372
12. Daubner SC, Le T, Wang S. Tyrosine Hydroxylase and Regulation of Dopamine Synthesis. *Arch Biochem Biophys* (2011) 508:1–12. doi: 10.1016/j.abb.2010.12.017
13. Shi YC, Lau J, Lin Z, Zhang H, Zhai L, Sperk G, et al. Arcuate NPY Controls Sympathetic Output and BAT Function Via a Relay of Tyrosine Hydroxylase Neurons in the PVN. *Cell Metab* (2013) 17:236–48. doi: 10.1016/j.cmet.2013.01.006
14. Toshinai K, Mondal MS, Nakazato M, Date Y, Murakami N, Kojima M, et al. Upregulation of Ghrelin Expression in the Stomach Upon Fasting, Insulin-Induced Hypoglycemia, and Leptin Administration. *Biochem Biophys Res Commun* (2001) 281:1220–5. doi: 10.1006/bbrc.2001.4518
15. Frederich RC, Lollmann B, Hamann A, Napolitano-Rosen A, Kahn BB, Lowell BB, et al. Expression of Ob mRNA and its Encoded Protein in Rodents. Impact of Nutrition and Obesity. *J Clin Invest* (1995) 96:1658–63. doi: 10.1172/JCI118206
16. Holmstrup ME, Owens CM, Fairchild TJ, Kanaley JA. Effect of Meal Frequency on Glucose and Insulin Excursions Over the Course of a Day. *E-SPEN* (2010) 5:e277–80. doi: 10.1016/j.eclnm.2010.10.001
17. Varela L, Horvath TL. Leptin and Insulin Pathways in POMC and AgRP Neurons That Modulate Energy Balance and Glucose Homeostasis. *EMBO Rep* (2012) 13:1079–86. doi: 10.1038/embor.2012.174
18. Chen S-R, Chen H, Zhou J-J, Pradhan G, Sun Y, Pan H-L, et al. Ghrelin Receptors Mediate Ghrelin-Induced Excitation of Agouti-Related Protein/Neuropeptide Y But Not Pro-Opiomelanocortin Neurons. *J Neurochem* (2017) 142:512–20. doi: 10.1111/jnc.14080
19. Mayer CM, Belsham DD. Insulin Directly Regulates NPY and AgRP Gene Expression Via the MAPK MEK/ERK Signal Transduction Pathway in mHypoE-46 Hypothalamic Neurons. *Mol Cell Endocrinol* (2009) 307:99–108. doi: 10.1016/j.mce.2009.02.031
20. Qiu J, Zhang C, Borgquist A, Nestor CC, Smith AW, Bosch MA, et al. Insulin Excites Anorexigenic Proopiomelanocortin Neurons Via Activation of Canonical Transient Receptor Potential Channels. *Cell Metab* (2014) 19:682–93. doi: 10.1016/j.cmet.2014.03.004
21. Belgardt BF, Okamura T, Brüning JC. Hormone and Glucose Signalling in POMC and AgRP Neurons. *J Physiol* (2009) 587:5305–14. doi: 10.1113/jphysiol.2009.179192
22. Claret M, Smith MA, Batterham RL, Selman C, Choudhury AI, Fryer LGD, et al. AMPK Is Essential for Energy Homeostasis Regulation and Glucose Sensing by POMC and AgRP Neurons. *J Clin Invest* (2007) 117:2325–36. doi: 10.1172/JCI31516
23. Mani BK, Castorena CM, Osborne-Lawrence S, Vijayaraghavan P, Metzger NP, Elmquist JK, et al. Ghrelin Mediates Exercise Endurance and the Feeding Response Post-Exercise. *Mol Metab* (2018) 9:114–30. doi: 10.1016/j.molmet.2018.01.006
24. Bouassida A, Zalleg D, Bouassida S, Zaouali M, Feki Y, Zbidi A, et al. Leptin, Its Implication in Physical Exercise and Training: A Short Review. *J Sports Sci Med* (2006) 5:172–81.
25. Borghouts LB, Keizer HA. Exercise and Insulin Sensitivity: A Review. *Int J Sports Med* (2000) 21:1–12. doi: 10.1055/s-2000-8847
26. Calvez J, Fromentin G, Nadkarni N, Darcel N, Even P, Tomé D, et al. Inhibition of Food Intake Induced by Acute Stress in Rats Is Due to Satiation Effects. *Physiol Behav* (2011) 104:675–83. doi: 10.1016/j.physbeh.2011.07.012
27. Qu N, He Y, Wang C, Xu P, Yang Y, Cai X, et al. A POMC-originated Circuit Regulates Stress-Induced Hypophagia, Depression, and Anhedonia. *Mol Psychiatry* (2020) 25:1006–21. doi: 10.1038/s41380-019-0506-1
28. Lin X, Itoga CA, Taha S, Li MH, Chen R, Sami K, et al. c-Fos Mapping of Brain Regions Activated by Multi-Modal and Electric Foot Shock Stress. *Neurobiol Stress* (2018) 8:92–102. doi: 10.1016/j.ynstr.2018.02.001
29. Obici S, Magrisso IJ, Ghazarian AS, Shirazian A, Miller JR, Loyd CM, et al. Moderate Voluntary Exercise Attenuates the Metabolic Syndrome in Melanocortin-4 Receptor-Deficient Rats Showing Central Dopaminergic Dysregulation. *Mol Metab* (2015) 4:692–705. doi: 10.1016/j.molmet.2015.07.003
30. O'Neal TJ, Friend DM, Guo J, Hall KD, Kravitz AV. Increases in Physical Activity Result in Diminishing Increments in Daily Energy Expenditure in Mice. *Curr Biol* (2017) 27:423–30. doi: 10.1016/j.cub.2016.12.009
31. Meijer JH, Robbers Y. Wheel Running in the Wild. *Proc R Soc B Biol Sci* (2014) 281:20140210. doi: 10.1098/rspb.2014.0210
32. Pocai A, Morgan K, Buettner C, Gutierrez-Juarez R, Obici S, Rossetti L. Central Leptin Acutely Reverses Diet-Induced Hepatic Insulin Resistance. *Diabetes* (2005) 54:3182–9. doi: 10.2337/diabetes.54.11.3182
33. Johnson NA, Sachinwalla T, Walton DW, Smith K, Armstrong A, Thompson MW, et al. Aerobic Exercise Training Reduces Hepatic and Visceral Lipids in Obese Individuals Without Weight Loss. *Hepatology* (2009) 50:1105–12. doi: 10.1002/hep.23129
34. Swift DL, Johannsen NM, Lavie CJ, Earnest CP, Church TS. The Role of Exercise and Physical Activity in Weight Loss and Maintenance. *Prog Cardiovasc Dis* (2014) 56:441–7. doi: 10.1016/j.pcad.2013.09.012
35. Katch VL, Martin R, Martin J. Effects of Exercise Intensity on Food Consumption in the Male Rat. *Am J Clin Nutr* (1979) 32:1401–7. doi: 10.1093/ajcn/32.7.1401
36. King N, Burley V, Blundell J. Exercise-Induced Suppression of Appetite: Effects on Food Intake and Implications for Energy Balance. *Eur J Clin Nutr* (1994) 48(10):715–24.
37. Thorogood A, Mottillo S, Shimony A, Filion KB, Joseph L, Genest J, et al. Isolated Aerobic Exercise and Weight Loss: A Systematic Review and Meta-Analysis of Randomized Controlled Trials. *Am J Med* (2011) 124:747–55. doi: 10.1016/j.amjmed.2011.02.037
38. Thomas DM, Bouchard C, Church T, Slentz C, Kraus WE, Redman LM, et al. Why do Individuals Not Lose More Weight From an Exercise Intervention at a Defined Dose? An Energy Balance Analysis. *Obes Rev* (2012) 13:835–47. doi: 10.1111/j.1467-789X.2012.01012.x
39. Donnelly JE, Smith BK. Is Exercise Effective for Weight Loss With Ad Libitum Diet? Energy Balance, Compensation, and Gender Differences. *Exerc Sport Sci Rev* (2005) 33:169–74. doi: 10.1097/00003677-200510000-00004
40. King NA, Hopkins M, Caudwell P, Stubbs RJ, Blundell JE. Individual Variability Following 12 Weeks of Supervised Exercise: Identification and Characterization of Compensation for Exercise-Induced Weight Loss. *Int J Obes* (2008) 32:177–84. doi: 10.1038/sj.ijo.0803712
41. Dorling J, Broom DR, Burns SF, Clayton DJ, Deighton K, James LJ, et al. Acute and Chronic Effects of Exercise on Appetite, Energy Intake, and Appetite-Related Hormones: The Modulating Effect of Adiposity, Sex, and Habitual Physical Activity. *Nutrients* (2018) 10:1140. doi: 10.3390/nu10091140
42. Douglas JA, King JA, McFarlane E, Baker L, Bradley C, Crouch N, et al. Appetite, Appetite Hormone and Energy Intake Responses to Two Consecutive Days of Aerobic Exercise in Healthy Young Men. *Appetite* (2015) 92:57–65. doi: 10.1016/j.appet.2015.05.006
43. Ebrahimi M, Rahmani-Nia F, Damirchi A, Mirzaie B, Pur SA. Effect of Short-Term Exercise on Appetite, Energy Intake and Energy-Regulating Hormones. *Iran J Basic Med Sci* (2013) 16:829–34. doi: 10.22038/ijbms.2013.1117
44. Flack KD, Hays HM, Moreland J, Long DE. Exercise for Weight Loss: Further Evaluating Energy Compensation With Exercise. *Med Sci Sports Exerc* (2020) 52:2466–75. doi: 10.1249/MSS.0000000000002376
45. Bobinski F, Teixeira JM, Sluka KA, Santos ARS. Interleukin-4 Mediates the Analgesia Produced by Low-Intensity Exercise in Mice With Neuropathic Pain. *Pain* (2018) 159:437–50. doi: 10.1097/j.pain.0000000000001109
46. Kim Y-A, Pitriani P, Park H-G, Lee W-L. Moderate Intensity Exercise Has More Positive Effects on The Gene Expression of Inflammasome, M1, M2 Macrophage Infiltration and Brown Adipocyte Markers Compared to High Intensity Exercise in Subcutaneous Adipose of Obese Mice Induced by High Fat Diet. *J Life Sci* (2019) 29:303–10. doi: 10.5352/JLS.2019.29.3.303
47. Landry T, Li P, Shookster D, Jiang Z, Li H, Laing BT, et al. Centrally Circulating α-Klotho Inversely Correlates With Human Obesity and

Modulates Arcuate Cell Populations in Mice. *Mol Metab* (2021) 44:101136. doi: 10.1016/j.molmet.2020.101136
48. Millington GWM. The Role of Proopiomelanocortin (POMC) Neurones in Feeding Behaviour. *Nutr Metab* (2007) 4:1–16. doi: 10.1186/1743-7075-4-18
49. Rahmouni K, Sigmund CD, Haynes WG, Mark AL. Hypothalamic ERK Mediates the Anorectic and Thermogenic Sympathetic Effects of Leptin. *Diabetes* (2009) 58:536–42. doi: 10.2337/db08-0822
50. Nadermann N, Volkoff H. Effects of Short-Term Exercise on Food Intake and the Expression of Appetite-Regulating Factors in Goldfish. *Peptides* (2020) 123:170182. doi: 10.1016/j.peptides.2019.170182
51. Thompson DA, Wolfe LA, Eikelboom R. Acute Effects of Exercise Intensity on Appetite in Young Men. *Med Sci Sport Exerc* (1988) 20:222–7. doi: 10.1249/00005768-198806000-00002
52. Setty P, Padmanabha BV, Doddamani BR. Obesity and Cardio Respiratory Fitness. *Int J Med Sci Public Heal* (2013) 2:30–44. doi: 10.5455/ijmsph.2013.2.298-302
53. Staten MA. The Effect of Exercise on Food Intake in Men and Women. *Am J Clin Nutr* (1991) 53:27–31. doi: 10.1093/ajcn/53.1.27
54. Stensel D. Exercise, Appetite and Appetite-Regulating Hormones: Implications for Food Intake and Weight Control. *Ann Nutr Metab* (2010) 57:36–42. doi: 10.1159/000322702
55. Vatansever-Ozen S, Tiryaki-Sonmez G, Bugdayci G, Ozen G. The Effects of Exercise on Food Intake and Hunger: Relationship With Acylated Ghrelin and Leptin. *J Sport Sci Med* (2011) 10:283–91.
56. Mizuno TM, Kleopoulos SP, Bergen HT, Roberts JL, Priest CA, Mobbs CV. Hypothalamic Pro-Opiomelanocortin mRNA Is Reduced by Fasting in Ob/Ob and Db/Db Mice, But is Stimulated by Leptin. *Diabetes* (1998) 47:294–7. doi: 10.2337/diab.47.2.294
57. Ropelle ER, Flores MB, Cintra DE, Rocha GZ, Pauli JR, Morari J, et al. IL-6 and IL-10 Anti-Inflammatory Activity Links Exercise to Hypothalamic Insulin and Leptin Sensitivity Through Ikkβ and ER Stress Inhibition. *PloS Biol* (2010) 8:31–2. doi: 10.1371/journal.pbio.1000465
58. Fischer CP. Interleukin-6 in Acute Exercise and Training: What Is the Biological Relevance? *Exerc Immunol Rev* (2006) 12:6–33.
59. Broom DR, Stensel DJ, Bishop NC, Burns SF, Miyashita M. Exercise-Induced Suppression of Acylated Ghrelin in Humans. *J Appl Physiol* (2007) 102:2165–71. doi: 10.1152/japplphysiol.00759.2006
60. Krashes MJ, Shah BP, Madara JC, Olson DP, Strochlic DE, Garfield AS, et al. An Excitatory Paraventricular Nucleus to AgRP Neuron Circuit That Drives Hunger. *Nature* (2014) 507:238–42. doi: 10.1038/nature12956
61. Ogundele OM, Lee CC, Francis J. Thalamic Dopaminergic Neurons Projects to the Paraventricular Nucleus-Rostral Ventrolateral Medulla/C1 Neural Circuit. *Anat Rec* (2017) 300:1307–14. doi: 10.1002/ar.23528
62. Nohara K, Zhang Y, Waraich RS, Laque A, Tiano JP, Tong J, et al. Early-Life Exposure to Testosterone Programs the Hypothalamic Melanocortin System. *Endocrinology* (2011) 152:1661–9. doi: 10.1210/en.2010-1288
63. Urban JH, Bauer-Dantoin AC, Levine JE. Neuropeptide Y Gene Expression in the Arcuate Nucleus: Sexual Dimorphism and Modulation by Testosterone. *Endocrinology* (1993) 132:139–45. doi: 10.1210/en.132.1.139
64. Qiu J, Rivera HM, Bosch MA, Padilla SL, Stincic TL, Palmiter RD, et al. Estrogenic-Dependent Glutamatergic Neurotransmission From Kisspeptin Neurons Governs Feeding Circuits in Females. *Elife* (2018) 7:e35656. doi: 10.7554/eLife.35656.001

Conflict of Interest: The authors declare that the research was conducted in the absence of any commercial or financial relationships that could be construed as a potential conflict of interest.

frontiers in Neuroscience

SYSTEMATIC REVIEW
published: 24 June 2021
doi: 10.3389/fnins.2021.685031

Proximal Disruption of Brain Energy Supply Raises Systemic Blood Glucose: A Systematic Review

Marie Sprengell†, *Britta Kubera*† *and Achim Peters**

Medical Clinic 1, Center of Brain, Behavior and Metabolism (CBBM), University of Lübeck, Lübeck, Germany

OPEN ACCESS

Edited by:
Srinivas Sriramula, The Brody School of Medicine at East Carolina University, United States

Reviewed by:
Arturo Ortega, Centro de Investigación y de Estudios Avanzados del Instituto Politécnico Nacional, Mexico
Brenton T. Laing, National Institute on Drug Abuse, United States

***Correspondence:**
Achim Peters
achim.peters@uksh.de

†*These authors have contributed equally to this work and share first authorship*

Specialty section:
This article was submitted to Neuroendocrine Science, a section of the journal Frontiers in Neuroscience

Received: *24 March 2021*
Accepted: *28 May 2021*
Published: *24 June 2021*

Citation:
Sprengell M, Kubera B and Peters A (2021) Proximal Disruption of Brain Energy Supply Raises Systemic Blood Glucose: A Systematic Review. Front. Neurosci. 15:685031. doi: 10.3389/fnins.2021.685031

This work joins a series that methodically tests the predictions of the Selfish-Brain theory. The theory postulates a vital ability of the mammalian brain, namely to give priority to its own energy metabolism. The brain behaves "selfishly" in this respect. For the cerebral artery occlusion studied here, the theory predicts an increase in blood glucose concentration, what becomes the hypothesis to be tested. We conducted a systematic review of cerebral-artery-occlusion papers to test whether or not the included studies could confirm this hypothesis. We identified 239 records, screened 231 works by title or abstract, and analyzed 89 by full text. According to strict selection criteria (set out in our PROSPERO preregistration, complying with PRISMA guidelines), 7 papers provided enough information to decide on the hypothesis. Our hypothesis could be fully confirmed for the 3 to 24 h after the onset of a transient 2 h or permanent occlusion. As for the mechanism, the theory predicts that the energy-deprived brain suppresses insulin secretion via the sympathoadrenal system, thereby preventing insulin-mediated glucose uptake into muscle and fat and, as a result, enhancing insulin-independent glucose uptake via the blood-brain barrier. Evidence from our included studies actually demonstrated cerebral insulin suppression. In all, the current work confirms the second major prediction of the Selfish-Brain theory that relates to a proximal bottleneck of the cerebral supply chain, cerebral artery occlusion. Its first major prediction relates to a distal supply bottleneck, caloric restriction, and is fulfilled as shown by our previous work, whereas the prediction of the long held gluco-lipostatic theory, which sees the brain as only passively supplied, is violated (Sprengell et al., 2021). The crucial point was that caloric restriction elicits smaller changes in mass (energy) in the brain than in the body. Taken together, the evidence from the current and previous work clearly shows that the most accurate predictions are possible with a theory that views the brain as an independently self-regulating energy compartment occupying a primary position in energy metabolism.

Keywords: brain energy metabolism, cerebral artery occlusion, blood glucose, cerebral insulin suppression, selfish-brain theory, systematic review

INTRODUCTION

This work is based on the concept of the "cerebral supply chain" where the brain is the end consumer (Peters and Langemann, 2009) (**Figure 1**). The key principle of supply chains is on-demand procurement, which makes the delivery process more economical and less susceptible to disturbances (Slack et al., 2004). We performed a systematic review on the most critical disturbance of the cerebral supply chain: a proximal supply bottleneck caused by cerebral arterial occlusion. It is known that disruption of cerebral fuel supply results in an intraneuronal adenosine triphosphate (ATP) depletion that ultimately leads to ischemic stroke (Wagner et al., 1992). It is also known that patients with acute ischemic stroke often present with hyperglycemia (Bravata et al., 2003), but it remains unclear to what extent this is due to the stroke or undiagnosed diabetes mellitus. What exactly a proximal bottleneck does to the more distal parts of the cerebral supply chain has not yet been studied systematically.

This is our second systematic review on the cerebral supply chain; our first examined the effect of a more distal bottleneck in the supply chain, i.e. caloric restriction (**Figure 2A**). We found that with caloric restriction, the mass (energy) changes in the brain were particularly small (Sprengell et al., 2021). Thus, peripheral energetic intervention has little effect on the central nervous system. In the current systematic review, we examine the reverse case, namely, what effect central energetic interventions have on peripheral energy metabolism. More precisely, we examined what effect the interruption of the brain's energy supply has on the systemic blood glucose concentration. We hypothesize that disruption of brain arterial supply causes a marked rise in blood glucose concentration.

Our hypothesis is a prediction of the Selfish-Brain theory (Peters et al., 2004). This theory deals with the energy allocation within the mammalian organism. It postulates that in case of energy shortage there is a vital ability of the brain, namely to give priority to its own energy metabolism. Rival positions include the long-held gluco-lipostatic theory (Kennedy, 1953; Mayer, 1953) and its modern variants (Chaput and Tremblay, 2009; Schwartz et al., 2017), which all view the brain as only passively supplied.

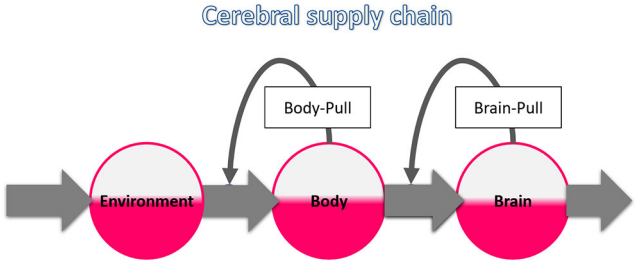

FIGURE 1 | The cerebral supply chain. Energy is transferred from the environment through the body to the brain, the end consumer of the supply chain. The characteristic of supply chains is the procurement on demand, also called pull principle. When the brain needs energy, the brain-pull demands it from the body. When the body needs energy, the body-pull demands it from the environment.

Our first systematic review showed that caloric restriction causes only minor mass (energy) changes in the brain [of the order of −4%] as opposed to major changes in the body [of about −30%] (Sprengell et al., 2021). This finding completely fulfilled the predictions of the Selfish-Brain theory, while those of the gluco-lipostatic theory and its variants were violated. The most accurate predictions are therefore possible with a theory that views the

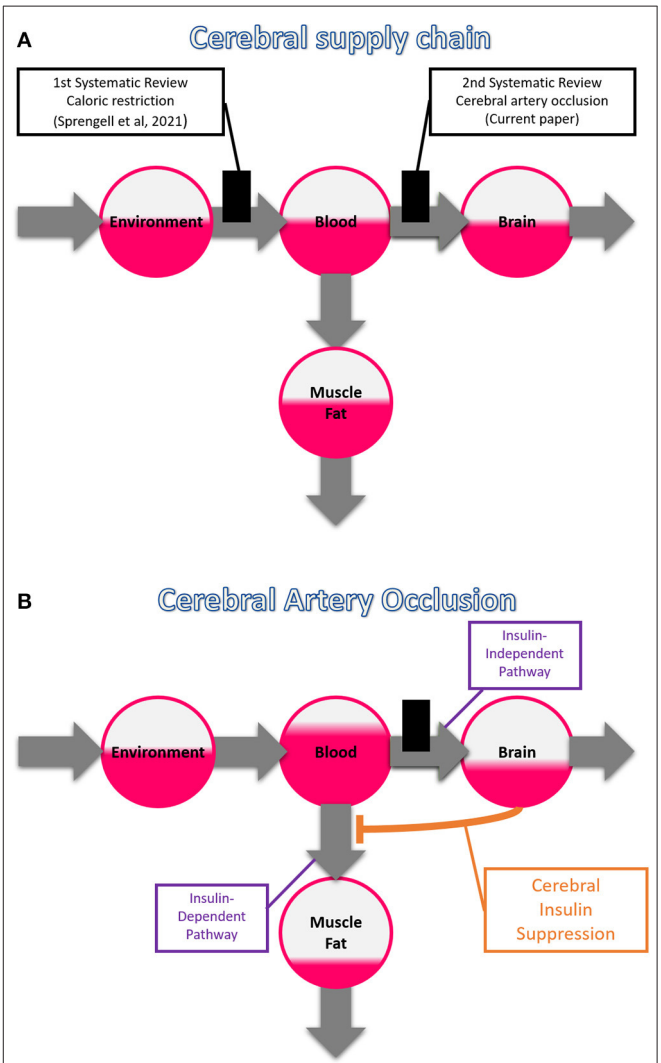

FIGURE 2 | The branched cerebral supply chain. The branching originates from the blood, transmitting energy either to the brain or to muscle or fat tissue. **(A)** Systematic reviews on two different bottlenecks in the cerebral supply chain. The first one deals with a distal bottleneck, i.e. caloric restriction, and is already published (Sprengell et al., 2021); the second one, the current work, deals with a proximal bottleneck, i.e. cerebral artery occlusion. **(B)** Cerebral insulin suppression induced by cerebral artery occlusion. Intraneuronal ATP depletion activates the sympathetic nervous system and the hypothalamic-pituitary-adrenal axis, which both rigorously suppress pancreatic ß-cell secretion, and in so doing block insulin-dependent glucose uptake in muscle and fat tissue. The portion of glucose that is prevented from entering muscle and fat tissue accumulates in the blood, facilitating transfer across the blood-brain barrier via the insulin-independent pathway, allowing partial compensation when brain supply is compromised.

brain as an independently self-regulating energy compartment that occupies a primary position in a hierarchically organized metabolism. Our second systematic review, the current one, aims to examine evidence of this vital ability of the brain. That is, if the hypothesis formulated here can be confirmed by our systematic literature search, an important prediction of the Selfish-Brain theory is fulfilled.

To illustrate how our hypothesis can be deduced from theory, we refer to the cerebral supply chain. It is a mathematical representation of the Selfish-Brain theory (Peters and Langemann, 2009). Logistic supply chains have played an important role in the economy for 80 years, e.g. in automobile production. The mathematical principles of these supply chains could be directly applied to energy metabolism. A general rule for all supply chains is that the flow of goods or energy is composed of two components, one determined by the supplier (push component) and the other by the subsequent recipient (pull component) (Slack et al., 2004). In the cerebral supply chain, energy is transferred from the environment, through the blood, to the end consumer – the brain. As this supply chain is branched, a portion of the energy is transferred from the blood to the muscle and fat tissue. In addition to the antegrade flow of energy toward the brain as the end consumer, there is also a retrograde flow of information consisting of the pull commands.

Brain-pull refers to the brain's ability to procure itself with energy on demand (**Figure 1**). The energy content of the brain (intraneuronal ATP) determines how much energy is demanded from the body. In contrast, the body-pull demands energy from the environment for the body. Both the energy content of the blood (glucose) and that of the body stores (triglycerides) determine how much energy is pulled from the environment. To date, several redundant brain-pull mechanisms have been identified (Peters and McEwen, 2015). These are neuroendocrine in nature and provide the brain with additional energy sources as needed.

Among brain-pull mechanisms, "cerebral insulin suppression" (CIS) is one of the most important (Woods and Porte, 1974; Hitze et al., 2010). Energy sensors in brain regions such as the amygdala (Zhou et al., 2010) and VMH (Spanswick et al., 1997; Routh et al., 2014; Toda et al., 2016) detect even the slightest drop in neuronal ATP and set brain-pull mechanisms in action. VMH activation lowers insulin concentrations and increases blood glucose concentrations (Meek et al., 2016; Stanley et al., 2016). In detail, the VMH activates the sympathoadrenal system, which strongly suppresses insulin secretion from pancreatic ß-cells (Ahren, 2000). Insulin-dependent glucose uptake (GLUT4) in muscle and fat tissue is suppressed, while the remaining circulating glucose is almost completely available to insulin-independent glucose transport (GLUT1) across the blood-brain barrier. For the brain needs virtually no insulin to take up glucose (Hom et al., 1984; Hasselbalch et al., 1999; Seaquist et al., 2001). In summary, GLUT1 glucose uptake safeguards basal energy supply of vital organs, like brain and immune cells (Deng et al., 2014), while GLUT4 allows the storage of surplus energy in muscle and fat cells (Shepherd and Kahn, 1999). Thus, CIS allocates more energy to the brain when needed.

In the case of cerebral artery occlusion, our theory-based prediction is as follows (**Figure 2B**). Occlusion of a cerebral artery restricts the energy flow to the brain, which in the supply chain model corresponds to a reduced blood-push component. Reduced supply (i.e. decreased blood-push) leads to cerebral ATP depletion, resulting in enhanced CIS (i.e. increased brain-pull), which prevents glucose uptake in muscle and fat tissue, and eventually causes glucose accumulation in the blood. While a portion of the circulating glucose cannot enter muscle or fat tissue, this is instead made available to the energy-depleted brain. In this way, the cerebral supply chain model generates a prediction that becomes the hypothesis to be tested here: *Cerebral artery occlusion increases glucose concentration in the blood.*

To this end, we performed a systematic review to examine whether or not the experimental studies found on cerebral artery occlusion can actually confirm this hypothesis.

MATERIALS AND METHODS

The protocol for this systematic review was pre-registered on PROSPERO on 30th of January 2020, and updated versions were published on 28th of September 2020 and 14th of December 2020 (International prospective register of systematic reviews; CRD42020156816). We complied with the PRISMA (Preferred Reporting Items for Systematic Reviews and Meta-analyses) guidelines for systematic reviews of interventions (Moher et al., 2009). Furthermore, the Cochrane Handbook for systematic reviews of interventions was used (Higgins and Thomas, 2019).

Search Strategies

We conducted a systematic search of the literature to identify studies in mammals that focused on how the experimental cerebral artery occlusion affects blood glucose concentration. One reviewer developed the search strategies, which were then discussed with two other reviewers. The databases of MEDLINE and BIOSIS Previews were searched from their inception to 20th December 2020, using a combination of key words and in case of the first database MeSH terms. The full MEDLINE and BIOSIS search strategies are provided in the **Supplementary Material**. Briefly, the search strategies included terms relating to the intervention (cerebral ischemia), to the outcome (blood glucose concentration) and to the methodical approach (experimental study), combined by the Boolean operator AND. Synonyms for terms were combined with the operator OR.

Study Selection

We used the following criteria to include or exclude articles for our systematic review. Only original full research papers published in English or German were included. We included studies that examined mammals of any species or sex. We included only interventional studies that were standardized laboratory experiments or clinical trials and that examined two groups, an interventional group undergoing cerebral artery occlusion and a non-exposed, sham-operated control group. Since we had included clinical trials in our first systematic review (Sprengell et al., 2021), we did the same here for the sake of consistency, but of course did not expect to identify clinical

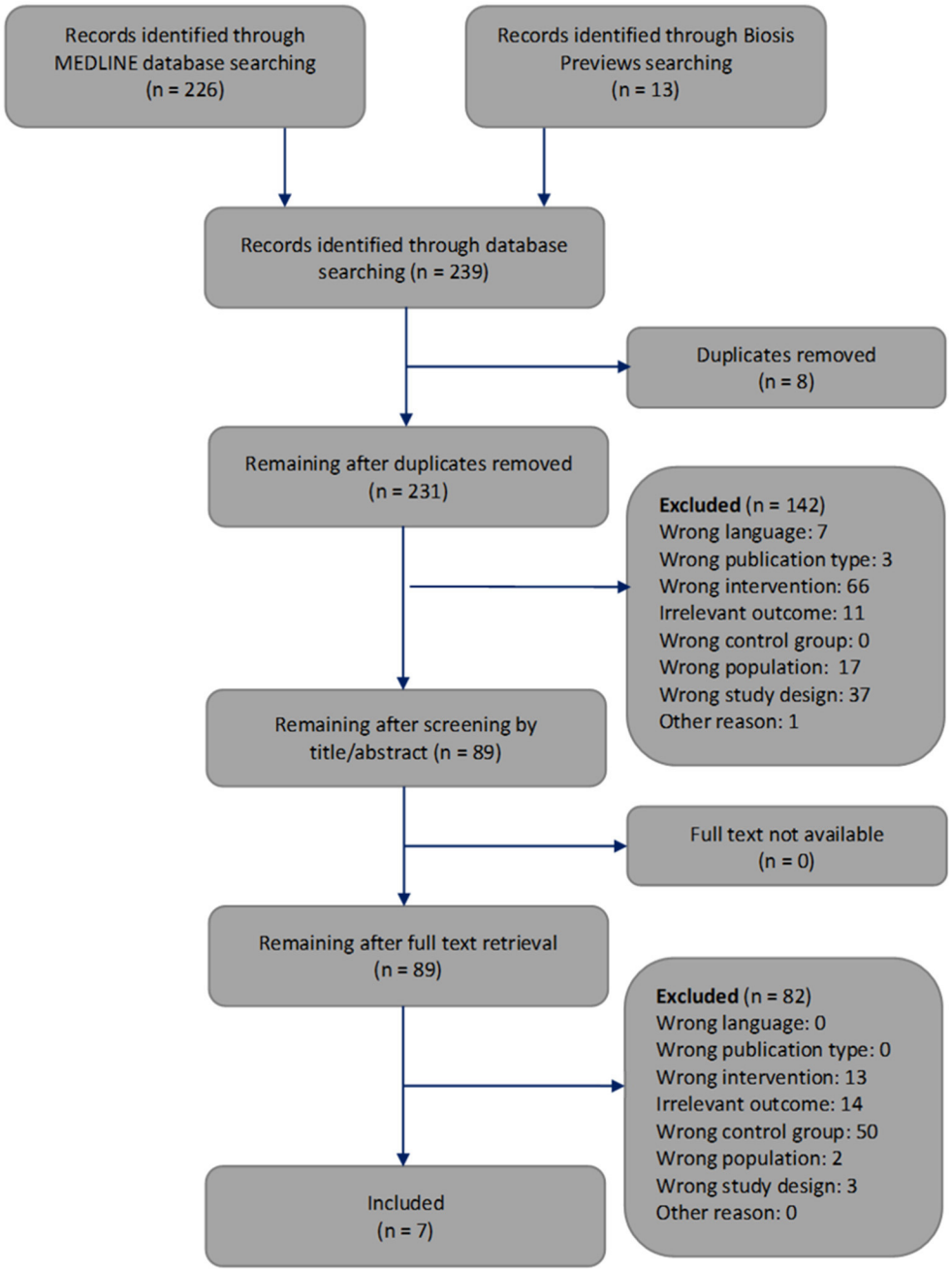

FIGURE 3 | Flowchart through different phases of the systematic review modified according to Moher's publication (Moher et al., 2009).

trials, since cerebral artery occlusion in humans is not ethically defensible. We only included studies that measured blood glucose concentration. We did not include studies that measured outcomes in the intervention and control groups at different time points. We did not include studies, that occluded the vertebral arteries, as cerebral control centers of energy metabolism could have been affected. We did not include studies, in which clots were injected in the aorta, because of unpredictable consequences for other parts of the body. We did not include studies with combined interventions such as cerebral artery occlusion and systemic hypotension. We did not include studies in which the individuals had diseases or were on medication that had been shown to affect energy metabolism; for more details see Sprengell et al. (2021). We did not include trials in pregnant individuals or fetuses, nor in ovariectomized or genetically modified mammals with altered energy metabolism.

The selection of the articles was performed in two steps. We have indicated the reasons for exclusion at each step (**Figure 3**).

First, one reviewer screened the article titles or abstracts against the inclusion and exclusion criteria. This first step of article selection was checked by another reviewer. When a discrepancy occurred regarding the inclusion or exclusion of an article, the two reviewers discussed it until agreement was reached. Otherwise, disagreements were resolved by consulting the third reviewer. Second, two reviewers independently selected the remaining articles by analyzing the full text. Again, disagreements regarding the inclusion or exclusion of an article were resolved by discussion among each other or, if necessary, by consultation with the third reviewer.

Data Extraction

Data from all of the 7 included studies were extracted by one reviewer, independently checked by two other reviewers, and tabulated alphabetically. We recorded the population, sample size, kind of intervention and duration, study design, statistical test applied, baseline blood glucose concentrations as well as blood glucose concentrations after onset of cerebral artery occlusion and secondary outcomes.

Risk of Bias Assessment

To assess the risk of bias of non-human studies the SYRCLE's tool was used (Hooijmans et al., 2014). One reviewer assessed the risk of bias of the 7 included studies. The results were independently checked by two other reviewers. All differences were clarified by discussion.

Hypothesis Decision

Based on the respective statistical test, we decided whether the hypothesis could be confirmed ($p < 0.05$) or not ($p \geq 0.05$).

RESULTS

The systematic search of the literature generated 239 articles, which were processed as summarized in **Figure 3**. Two hundred and thirty one works were screened by title or abstract, and 89 articles were analyzed by full text. We identified seven studies that met all inclusion criteria and focused on how cerebral artery occlusion affects blood glucose concentrations (Harada et al., 2009; Yamazaki et al., 2012, 2014; Wang et al., 2013, 2014; Li et al., 2016; Boujon et al., 2019).

Data Extraction

Table 1 provides details of the 7 included studies. Four studies investigated mice (Harada et al., 2009; Yamazaki et al., 2012, 2014; Boujon et al., 2019) and 3 studies investigated rats (Wang et al., 2013, 2014; Li et al., 2016). The sample sizes varied between 9 and 53.

All included studies provided details on how cerebral artery occlusion was implemented. In 2 studies, the left middle cerebral artery was occluded by insertion of a nylon monofilament (Yamazaki et al., 2012, 2014). Harada and colleagues also occluded the left middle cerebral artery and additionally ligated the left common carotid artery and external carotid artery (Harada et al., 2009). Two other studies performed occlusion by clamping the two common carotid arteries and right middle cerebral artery (Wang et al., 2013, 2014). In one study, the left middle cerebral artery and anterior choroidal arteries were occluded by insertion of a nylon monofilament (Boujon et al., 2019). In a further study, the middle cerebral artery was occluded with nylon suture (Li et al., 2016). The duration of cerebral artery occlusion ranged from 30 min (Boujon et al., 2019) and 2 h (Harada et al., 2009; Yamazaki et al., 2012, 2014; Li et al., 2016) to permanent (Wang et al., 2013, 2014).

Blood glucose concentrations were measured during three phases, where we distinguished the early phase lasting less than 3 h after occlusion onset, the intermediate phase 3 to 24 h after occlusion onset, and the late phase lasting more than 7 days after reperfusion. Work examining the intermediate phase included, firstly, a paper by Wang and coworkers, which reported hourly measurements over 24 h of permanent ischemia, finding that as early as 1 h after the onset of occlusion, the blood glucose profile was elevated and remained elevated above that of controls (all $p < 0.05$) (Wang et al., 2013); secondly, another paper by Wang and coworkers, which reported measurements of blood glucose concentrations at baseline and after 24 h of permanent ischemia, finding that 24 h after the onset of occlusion, blood glucose was higher than in controls ($p < 0.05$) (Wang et al., 2014); thirdly, 2 papers by Yamazaki and coworkers, each reporting in 2 experiments the change in blood glucose concentration 24 h after the onset of a transient 2 h cerebral artery occlusion, finding that blood glucose increased more than in controls (all $p < 0.05$) (Yamazaki et al., 2012, 2014); and finally the work by Harada and coworkers that examined not only the intermediate phase, but also early and late phase, reporting changes in blood glucose concentration at baseline and 1, 3, 6, 12, and 24 h, 3 and 5 days after the onset of transient 2 h cerebral artery occlusion, finding that the blood glucose increase was more pronounced than in controls at 12 and 24 h ($p < 0.01$), while no increase could be detected within the first 6 h or on day 3 or 5 (Harada et al., 2009).

Work examining only the late phase was that of Boujon and co-workers, which reported measurements of blood glucose concentration at baseline and on days 3 and 7 after the onset of transient 30 min cerebral artery occlusion, and found that no increase could be detected on either day 3 or 7 (Boujon et al., 2019). Work examining only the early phase was that of Li and coworkers, who could not demonstrate a difference in blood glucose levels between the intervention and sham-operated groups either during the 2 h occlusion or right afterward (Li et al., 2016).

Secondary outcomes relevant to our research question were provided by (Harada et al., 2009) (insulin concentrations and insulin after glucose load), (Wang et al., 2013) (cortisol, glucagon, fasting insulin concentrations) and (Wang et al., 2014) (fasting insulin, blood norepinephrine, blood epinephrine concentrations, and body weight).

Risk of Bias Assessment

Table 2 provides the risk of bias assessments for all 7 included studies.

TABLE 1 | Characteristics and results of included studies.

References	Population	Sample size	Intervention	Design	Statistical test	Blood glucose [mg/dL]				Secondary outcomes of energy metabolism
						Baseline	**Early Phase < 3h after occlusion onset**	**Intermediate Ph. ≥ 3 and ≤ 24h after occl. onset**	**Late Phase > 24h after occl. onset**	
Boujon et al. (2019)	129S6/ SvEv mice, ~ 10 weeks old, male	Exp: 5[a] Con: 4	**30-min transient** occlusion of left middle cerebral artery and ant. choroidal arteries by inserting nylon monofilament	BG was measured at baseline, on day 3, and on day 7	Two-way ANOVA followed by Turkey's multiple comp. test. Mean ±S.E.M.	Exp: 110±3[b] Con: 120 ±4[ns,b]			**Day 3** Exp: 76±4[b] Con: 84±6[ns,b] **Day 7** Exp: 117±14[b] Con: 128±9[ns,b]	
Harada et al. (2009)	ddY mice, 5 weeks old, male	Exp: 8-17[c] Con: 9-16	**2-h transient** occlusion of the left middle cerebral artery through insertion of nylon monofilament; ligation of the left common carotid artery and external carotid artery	BG was measured at baseline and afterwards at 1h, 3h, 6h, 12h, on day 1, 3 and 5. Increment of BG was calculated.[d]	One-way ANOVA followed by paired student's *t*-test. Data are shown as mean ± S.E.M.[e]	Exp: 0±s[ns,b,d,e] Con: 0±s[b,d,e]	**1h** Exp: 28±s[b,d,e] Con: 38±5 [ns,b,d] (increment)	**3h** Exp: 20±s[b,d,e] Con: 25±s [ns,b,d,e] **6h** Exp: 9±s[b,d,e] Con: 16±s [ns,b,d,e] **12h** Exp: 63±5[b,d] Con: 14±s[**b,d,e] **D1** Exp: 74±16[b,d] Con: 22±s[**b,d,e] (increment)	**Day 3** Exp: 22[b,d,f] Con: 22[ns,b,d,f] **Day 5** Exp: −13±14[b,d] Con: 16±s[ns,b,d,e] (increment)	Insulin, insulin after glucose load
Li et al. (2016)	Sprague-Dawley rats, male	Exp: 23[g] Con: 17	**2-h transient** occlusion of the left middle cerebral artery with nylon suture	BG was measured before, during, and after 2h occlusion	One-way ANOVA	Data not shown	Data not shown. Q: "no significant changes of …. glucose levels… between different groups"; test statistics not shown.			Body weight (data not shown)
Wang et al. (2013)	Sprague-Dawley rats, adult, male	Exp: 6 Con: 6	**Permanent** occlusion through clamping of the 2 common carotid arteries and right middle cerebral artery	BG was measured hourly over 24h	Student's *t*-test. Data are shown in the original paper as mean ± S.D. They were converted by the present reviewers to S.E.M.[h]	Exp: 83[b,f] Con: 83[b,f]	**1h** Exp: 100±2[b,h] Con: 82±2[**b,h] **2h** Exp: 103±2 [b,h] Con: 77±1[**b,h]	**3h** Exp: 93±3 [b,h] Con: 86±2[*b,h] **4h** Exp: 97±4 [b,h] Con: 83±2[**b,h] **5h** Exp: 97±3 [b,h] Con: 86±2[*b,h] **6h** Exp: 98±3[b,h] Con: 78±2[**b,h] **7h** Exp: 102±3[b,h] Con: 79±2[**b,h] **8h** Exp: 104±4[b,h] Con: 77±1[**b,h] **9h** Exp:106±5[b,h] Con: 79±4[**b,h] **10h** Exp: 108±4[b,h] Con: 78±2[**b,h] **11h** Exp: 104±5[b,h] Con: 81±2[**b,h] **12h** Exp: 116±5[b,h] Con: 82±2[**b,h] **24h** Exp:98±4[b,h] Con: 73±2[**b,h]		Cortisol, glucagon, fasting insulin

(Continued)

TABLE 1 | Continued

References	Population	Sample size	Intervention	Design	Statistical test	Blood glucose [mg/dL]				Secondary outcomes of energy metabolism
						Baseline	**Early Phase < 3h after occlusion onset**	**Intermediate Ph. ≥ 3 and ≤ 24h after occl. onset**	**Late Phase > 24h after occl. onset**	
Wang et al. (2014)	Sprague-Dawley rats, adult, male	Exp: 8 Con: 8	**Permanent** occlusion by clamping the 2 common carotid arteries and right middle cerebral artery	BG was measured at baseline and on day 1	Student's unpaired *t*-test. Data are shown as mean ± S.E.M.	Exp: 81.1±5.4[ns,i] Con: 79.3±7.2[i]		**Day 1** Exp: 106.3±5.4[i] Con: 81.1±7.2*[i]		Body weight, fasting insulin, epinephrine, norepi-nephrine
Yamazaki et al. (2012)	ddY mice, 5 weeks old, male	Exp_1: 17 Con_1: 12 Exp_2: 16 Con_2: 8	**2-h transient** occlusion of the left middle cerebral artery through insertion of nylon mono-filament	BG was measured at baseline and on day 1. Increment of BG was calculated[d]	One-way ANOVA followed by Scheffe's test. Mean ±S.E.M.	Not shown		**Day 1** Exp_1: 65±5[b,d] Con_1: 14±7**[b,d] (increment) **Day 1** Exp_2: 60±3[b,d] Con_2: 28±5**[b,d] (increment)		
Yamazaki et al. (2014)	ddY mice, 5 weeks old, male	Exp_1: 7 Con_1: 9 Exp_2: 6 Con_2: 7	**2-h transient** occlusion of the left middle cerebral artery through insertion of nylon mono-filament	BG was measured at baseline and on day 1. Increment of BG was calculated[d]	One-way ANOVA followed by the Scheffe's *post-hoc* test. Mean ±S.E.M.	Not shown		**Day 1** Exp_1: 44±6[b,d] Con_1: 13±5*[b,d] (increment) **Day 1** Exp_2.: 43±3[b,d] Con_2: 13±5**[b,d] (increment)		

*Only information from study arms meeting our inclusion criteria is presented. The sample sizes refer to the number of animals that survived the intervention and the observation period and whose outcomes were measured. Secondary outcomes relevant to our research question are shown in the last column. For time data, onset of ischemia is considered timepoint 0. Data are presented as means ± S.E.M. Abbreviations: Exp: experimental group; Con, Control group; BG, blood glucose; ns, not significant; Q.:Quote; S.D.: Standard deviation; S.E.M.: Standard error of the mean *$p < 0.05$, **$p < 0.01$. [a]One mouse out of six of the interventional group died. [b]Value taken from graph. Some of the values could only be estimated. [c]For the time course experiments, the authors used independent 8–17 mice in every indicated period; that is, they euthanized different numbers of animals at 6 h after the occlusion onset, 12 h, 1 day, 3 day, or 5 day and obtained the respective measurements. [d]Increment of blood glucose was determined by authors using the following formula: increment of BG = BG after occlusion – BG before occlusion. [e]Certain data points within the graphic were displayed so large that they concealed the S.E.M. markers. We estimate the radius of these graphically displayed points to be 5. The variable s stands accordingly for a S.E.M. of ≤ 5mg/dL. [f]Estimation of variances from the figures is not possible if the graphically represented data points of the intervention and control groups overlap. [g]Four out of 27 rats of the interventional group died. [h]The standard deviation was presented in the original paper. It was converted by the present reviewers to the standard error of the mean using the following formula: S.E.M. $= \frac{Standard\ Deviation}{\sqrt{Sample\ Size}}$. The S.E.M. values have been rounded to whole numbers and are presented in the above table. [i]Glucose concentration is expressed in the unit mM in the original paper. The present reviewers have multiplied the concentration value by the conversion factor 18.02.*

TABLE 2 | Risk of bias assessment.

References	Random sequence generation	Baseline characteristics	Addressing of Incomplete outcome data	Selective outcome reporting	Other sources of bias
Boujon et al. (2019)	+	+[a]	–[b]	+	?[c]
Harada et al. (2009)	?	+[d]	+	–[e]	+[f]
Li et al. (2016)	+	-[g]	–[h]	–[h]	+[f]
Wang et al. (2013)	+[i]	+[a]	+[j]	+	+[f]
Wang et al. (2014)	+[i]	+[a]	?[k]	+	+[f]
Yamazaki et al. (2012)	?	+[d]	+[j]	+	+[f]
Yamazaki et al. (2014)	?	+[d]	+[j]	+	+[f]

The SYRCLE's tool (Hooijmans et al., 2014) was used and slightly modified to assess the risk of bias of non-human studies. "+" indicates a low risk of bias, "–" indicates a high risk of bias and "?" indicates that not enough information has been provided on this point. For five items of the SRYCLE tool, i.e. allocation concealment, random housing, blinding of personnel, random outcome assessment and blinding of the outcome assessors, not enough information was available for any of the studies examined here, so that all of them were rated "?". Boujon and coworkers reported, that "experiments were carried out in a blinded fashion", but it remains unclear which procedures this refers to. The item "Selective outcome reporting" refers to data that is related to our research question. [a]Similar baseline characteristics in blood glucose concentration. [b]Attrition bias: 1 out of 6 mice (17%) in the MCAO group died; 1 out of 4 mice (25%) in the sham-operated group was excluded because of poor baseline rotarod performance. [c]First, the study was supported by Roche; Quote: "Roche did not play a role in the conduct of the experiments reported here, nor in the collection, analysis, or interpretation of the data, nor in the preparation of this manuscript." Second, the anesthetics chloral hydrate and isoflurane used in all included studies may increase blood glucose. All included papers described that they used the same anesthesia in the sham control group, Boujon and coworkers probably did the same, but did not mention it explicitly. [d]The increment of blood glucose was presented and analyzed. [e]Quote "We eliminated mice with brain hemorrhage"; effect on results unclear. [f]No evidence for unequal housing conditions, conflict of interests or problems of the study design. [g]Neither baseline blood glucose concentrations nor any other blood glucose concentrations shown. [h]Attrition bias: 4 out of 27 (15%) mice of the intervention group died and were excluded from the analysis, whereas no rat died in the sham-operated control group. Without specifying any test statistics, Li and coworkers reported that they were unable to detect a statistical difference in blood glucose concentration between rats subjected to cerebral ischemia and sham-operated rats. Thus, it cannot be ruled out that the deceased and surviving rats differed in infarct size and blood glucose profile. In this uncertain situation, one would have liked to see the original blood glucose data. [i]Random allocation into study groups; randomization of subgroup allocation not explicitly mentioned. [j]No evidence for dropouts. [k]Initially there were 8 rats per subgroup, the result table mentions 6–8 rats per subgroup; reason remains unclear.

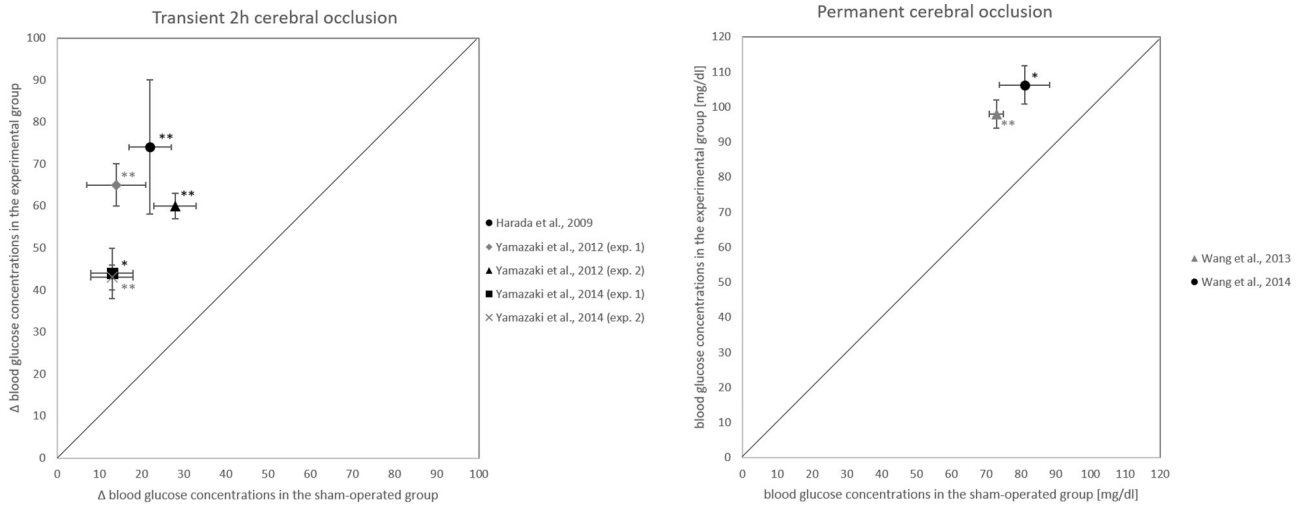

FIGURE 4 | Blood glucose changes 24 h after occlusion onset. **(Left)** Comparison of how experimental and sham-operated groups differ in their blood glucose changes from before to 24 h after the onset of transient 2 h cerebral artery occlusion. **(Right)** Comparison of how experimental and sham-operated groups differ in blood glucose concentrations at 24 h after onset of permanent occlusion. *$P < 0.05$, **$P < 0.01$, significant difference in blood glucose concentrations or their changes between experimental and sham-operated groups.

Hypothesis Decision

All papers which examined the intermediate phase 3 to 24 h after occlusion onset could confirm our hypothesis (Harada et al., 2009; Yamazaki et al., 2012, 2014; Wang et al., 2013, 2014) (**Figure 4**). All of these intermediate phase studies showed that blood glucose concentrations were significantly higher or had changed more in the intervention group than in the sham-operated group (**Table 3**). One work could confirm the hypothesis already for the early phase 1 h after occlusion onset (Wang et al., 2013).

However, the papers that examined the late phase 3 to 7 days after reperfusion onset failed to confirm the hypothesis for the phase (Harada et al., 2009; Boujon et al., 2019). Two papers that examined the early phase could not confirm the hypothesis for

TABLE 3 | Hypothesis decision in the different ischemia phases.

References	Early Phase < 3 h after onset of occlusion	Intermediate Phase ≥ 3 and ≤ 24 h after onset of occlusion	Late Phase > 24 h after onset of occlusion
Boujon et al. (2019)			−
Harada et al. (2009)	−	+	−
Li et al. (2016)	−		
Wang et al. (2013)	+	+	
Wang et al. (2014)		+	
Yamazaki et al. (2012)		++[a]	
Yamazaki et al. (2014)		++[a]	

"+" indicates "hypothesis could be confirmed", "−" indicates "hypothesis could not be confirmed", blank table field indicates that no test has been performed on the hypothesis. Clear evidence for the hypothesis is found for the intermediate phase. Reasons why the hypothesis could not be confirmed may include the measurements not being taken at the optimal time. The pattern of "+" and "−" suggests that it was too early in the early phase to detect an effect on blood glucose, and already too late in the late phase. [a]Hypothesis could be confirmed by two independent experiments in one single paper.

this phase (Harada et al., 2009; Li et al., 2016), in contrast to Wang and coworkers who, as noted, could confirm it (Wang et al., 2013).

DISCUSSION

A total of 231 works was screened by title and abstract, and 89 were analyzed in full text. According to strict selection criteria defined in our PROSPERO pre-announcement and complying with PRISMA guidelines, 7 studies met all inclusion criteria. Of the 7 papers, all 5 that examined the intermediate phase 3 to 24 h after occlusion onset could confirm the hypothesis (Harada et al., 2009; Yamazaki et al., 2012, 2014; Wang et al., 2013, 2014) (**Figure 4**). For the late phase 3 to 7 days after reperfusion onset, the hypothesis could not be confirmed (Harada et al., 2009; Boujon et al., 2019). This evidence suggests that blood glucose elevation during and after cerebral artery occlusion is a temporary phenomenon. In all, our hypothesis could be fully confirmed for the period 3 to 24 h after the onset of a transient 2 h or permanent occlusion, so it holds that cerebral artery occlusion increases blood glucose concentration.

The 7 included studies represent a spectrum of diverse experiments which can be summarized as follows. All studies were published between 2009 and 2019, were performed on mice or rats, and the cerebral artery occlusion was either transient (ranging from 30 min to 2 h) or permanent (Harada et al., 2009; Yamazaki et al., 2012, 2014; Wang et al., 2013, 2014; Li et al., 2016; Boujon et al., 2019). Blood glucose was monitored with varying frequency over a period of about 2 h to 7 days. The papers that examined the intermediate phase reported that blood glucose concentrations 24 h after occlusion onset were 25 to 52 mg/dl higher than those of the control group (all $p < 0.05$). The papers that examined the late phase could no longer demonstrate the blood glucose increase seen in the intermediate phase (Harada et al., 2009; Boujon et al., 2019).

The mechanisms underlying stroke hyperglycemia are unknown, as some authors point out (Arnberg et al., 2015), while others hold overly complex beliefs (Dungan et al., 2009). Given that the Selfish-Brain theory makes accurate predictions in cases where the predictions of conventional theories failed (Sprengell et al., 2021), there is reason to believe that the neuroendocrine mechanisms as assigned by the Selfish-Brain theory provide a reliable explanation for the development of hyperglycemia in stroke. Typically, the Selfish-Brain theory covers topics such as psychosocial stress, depression, anorexia nervosa, obesity, and the development of atherosclerosis, myocardial infarction and stroke (Peters and McEwen, 2015). What is new here is that the theory addresses the consequences of stroke.

In terms of mechanisms, the Selfish-Brain theory refers to the principle of supply chains stating that when "push" fails, "pull" takes over. For the cerebral supply chain, this means that a reduction in the blood-push component (e.g. cerebral artery occlusion) is at least partially compensated by an enhanced brain-pull component. Brain-pull function is exerted by the sympathetic nervous system (SNS) and the hypothalamic-pituitary-adrenal (HPA) axis, which provide additional energy substrates for brain supply when needed. Among the studies found in our current systematic review, 2 studies measured blood concentrations of epinephrine, norepinephrine, and cortisol and showed that the concentrations of these stress hormones 24 h after occlusion onset were two times higher than those of the control group (Wang et al., 2013, 2014).

As mentioned above, several redundant brain-pull mechanisms are at work when the brain needs energy. Here we name three of them: The first brain-pull mechanism is that the SNS and HPA axis cause insulin suppression, which results in more glucose being delivered to the brain (Woods and Porte, 1974; Ahren, 2000). In fact, among the included studies was one that focused on insulin changes, showing that on day 1 after cerebral artery occlusion, an oral glucose load failed to increase plasma insulin concentrations, whereas in the sham-operated control group, the same load caused a 6-fold increase in plasma insulin concentrations (Harada et al., 2009). Thus, Harada and coworkers were able to confirm cerebral artery occlusion to induce CIS. CIS can be diagnosed on the basis of an inappropriately low insulin concentration at a given blood glucose concentration (Hitze et al., 2010). Importantly, CIS also occurs in many other critical situations, where brain energy homeostasis is challenged, including myocardial infarction (Taylor et al., 1969), psychosocial stress (Hitze et al., 2010), mental stress during anticipation of electric shock (Mason et al., 1968), acute hypoxia (Baum and Porte, 1969), deep hypothermia (Baum and Porte, 1971), caloric restriction (Peters et al., 2011) and sleep debt (Spiegel et al., 1999).

The second brain-pull mechanism is that SNS and HPA increase muscular proteolysis and hepatic gluconeogenesis, procuring the brain with even more glucose (Zhang et al., 2018). The third brain-pull mechanism is that SNS and HPA axis increase visceral lipolysis and hepatic ketogenesis, providing ketones as alternative brain substrate (Kubera et al., 2014).

Indeed, it has been shown that brain ischemia via SNS activation induces the formation of ß-hydroxybutyrate (ketogenesis) in the liver and the consumption of ß-hydroxybutyrate in the brain (Koch et al., 2017). Ketones were also shown to exert beneficial effects on pathological and functional outcomes after experimental stroke (Gibson et al., 2012). Overall, brain-pull mechanisms cause the body stores to take in less energy and deliver more.

Replenishing the brain at the expense of body stores is what the supply chain model predicts will lead to weight loss (**Figure 2B**). One of the studies we included showed that compared to sham-operated controls, rats that underwent cerebral ischemia lost 9% of their body weight within 24 h (Wang et al., 2014). This is only a single experiment, and moreover, body weight was only a secondary endpoint. Nevertheless, these results match the prediction that weight loss in cerebral ischemia is caused by energy transfer from the periphery to the brain. Taken together, occlusion of the central cerebral arteries profoundly affects peripheral energy metabolism, with the strongest evidence for an increase in blood glucose concentration.

Hyperglycemia persists even after reperfusion, for which we here provide evidence of both cause and mechanism. In 3 of our included studies, hyperglycemia is still detectable 22 h after reperfusion (Harada et al., 2009; Yamazaki et al., 2012, 2014). While it is clear that impaired cerebral supply during occlusion leads to cerebral ATP deficiency (Wagner et al., 1992), the persistence of this deficiency state after reperfusion seems surprising at first glance. Regarding the cause of such a prolonged hyperglycemia there is evidence demonstrating that cerebral energy consumption increases from the onset of ischemia, particularly in the penumbra, but also in the core ischemic brain regions that undergo infarction (Arnberg et al., 2015). Cerebral energy consumption does not decrease until most ischemic brain regions have succumbed to infarction. As long as the penumbra exhibits increased energy consumption, cerebral ATP concentration as monitored in the VMH can recover only slowly. Thus, even after reperfusion, a prolonged hyperglycemic course seems plausible.

Regarding the mechanism accounting for increased energy consumption in undersupplied brain regions, the Selfish-Brain theory made the following predictions (Peters et al., 2004). ATP binds to low- and high-affinity ATP-sensitive-potassium channels localized on presynaptic GABAergic and postsynaptic glutamatergic neurons, respectively. This type of multi-site neuronal ensemble leads to biphasic responses when neuronal ATP concentrations fall. Mild ATP deficiency hyperpolarizes GABAergic neurons, disinhibits postsynaptic glutamatergic neurons, and thus increases glutamatergic activity and energy expenditure, whereas severe ATP deficiency hyperpolarizes glutamatergic neurons and thus suspends glutamatergic activity. Such a theory-predicted biphasic response to falling ATP levels could indeed be confirmed experimentally (Steinkamp et al., 2007). The clinical correlate of this biphasic course becomes evident when seizure susceptibility increases in moderate hypoglycemia due to facilitated glutamatergic activity, and coma develops in profound hypoglycemia due to ubiquitous silencing of glutamatergic activity (Arieff et al., 1974; Mobbs et al., 2001).

Post-stroke hyperglycemia has long been controversial, with either its deleterious-toxic, its beneficial neuroenergetic, or its Janus-faced dual aspect being held. The deleterious-toxic aspect was supported by the observation that higher blood glucose concentrations were associated with more severe ischemic strokes (Capes et al., 2001). On this basis, it was hypothesized that using insulin to normalize post-stroke hyperglycemia would improve infarct outcome. Several randomized controlled trials were conducted on this issue. Just as diabetologists and intensivists were disappointed with intensified insulin therapy because it caused more deaths in their type 2 diabetic and critically ill patients (Gerstein et al., 2008; The-NICE-SUGAR-Study-Investigators, 2009), so too were neurologists disappointed with intensified insulin treatment of post-stroke hyperglycemia. Specifically, a Cochrane review and the more recent SHINE trial showed that in ischemic stroke, intensified insulin therapy did not improve the outcomes of death, neurological deficit or dependency, but increased risk of symptomatic hypoglycemia (Bellolio et al., 2014; Johnston et al., 2019). While these findings from human studies challenged the deleterious-toxic aspect of post-stroke hyperglycemia, animal studies could indeed demonstrate glucotoxic mechanisms (Kruyt et al., 2010; Khan et al., 2016). This contradiction can be resolved with the Janus-faced dual aspect of post-stroke hyperglycemia, which allows for both deleterious-toxic and beneficial effects (Endres et al., 2008).

The beneficial neuroenergetic aspect of post-stoke hyperglycemia is also advocated (Arnberg et al., 2015). This position was supported by one of the larger randomized controlled trials on intensified insulin therapy, which showed that normalization of post-stroke hyperglycemia led to a 2.5-fold increase in infarct growth (Rosso et al., 2012). In line with this finding, Ginsberg and coworkers could show that rats rendered hyperglycemic by dextrose injection prior to infarct induction developed higher brain glucose concentrations and also smaller infarct volumes than normoglycemic controls (Ginsberg et al., 1987). At this point, a look at the evidence from diabetology and intensive medicine may provide further insight. Hypoglycemia and hypovolemia are among the situations critical for brain supply, in which CIS is essential for increasing blood glucose concentrations (Jarhult and Holst, 1978; Corrall and Frier, 1981). Presumably, neuroenergetic mechanisms such as CIS evolved under evolutionary pressure to survive periods of starvation or injury with blood loss, rather than to survive stroke. Nevertheless, hypoglycemia, hypovolemia, and ischemic stroke display the same neuroenergetic pattern: CIS with increase in blood glucose. This commonality supports the notion that infarct-related systemic hyperglycemia, despite its toxic aspect, is manifestation of an adaptive process that replenishes the energy-depleted brain.

Our systematic review has weaknesses and strengths. The weakness is that our search does not completely represent all relevant studies. However, no systematic review can claim to be complete unless the authors have viewed every paper in full text from all databases – which is not feasible. Authors of systematic reviews must therefore accept a certain degree of incompleteness due to the constraints imposed by their search algorithm. They need to find an optimal trade-off between

sensitivity and specificity for their search. It became clear that our systematic review was not complete either when we had finished the data extraction of all papers. To our surprise, the work of Chen et al. (2016) surfaced. This work would have met all of our inclusion criteria, yet our search algorithm did not detect it. The reason for this was that the search term "ligation" did not appear in this paper, as Chen et al. referred to their previous work regarding their methods, nor was the term indexed for this paper in PubMed. We did not expect such a case when designing our search algorithm. We nevertheless adhered to the protocol and refrained from revising our search algorithm and performing a second search run, as such an approach risks biasing and undermining hypothesis testing.

One of the strengths of our systematic review is the neutrality of its search. We designed our search algorithm to the best of our knowledge and after that was set, had no influence on which studies were found. Even in the case of an incomplete search, this approach would provide us with an unbiased, well-defined set of experimental data against which we could perform hypothesis tests. Basically, compared to hand searching, systematic database searching is much less susceptible to researcher bias in paper selection. Now that we knew the results of Chen's study (Chen et al., 2016), a freedom of choice to either rerun a modified search or to stick with the existing search results would have provided us with an opportunity to influence hypothesis testing. To avoid such bias, we strictly followed our pre-registered PROSPERO protocol and stuck to our original search results. Nevertheless, and for the sake of completeness, we believe it is important to show whether Chen's results, had they been taken into account, would have affected the statement of our work. This was not the case (see **Supplementary Material C**). These considerations point out that when testing a scientific hypothesis in a systematic review it is the degree of completeness that matters, but even more so the neutrality of the search.

In conclusion, our systematic review confirms a major prediction of the Selfish-Brain theory, namely that cerebral artery occlusion elevates blood glucose concentrations. For the causes and effects involved in this blood glucose elevation, the theory makes further predictions such as increase in stress hormones epinephrine, norepinephrine and cortisol, suppression of insulin secretion, and acute body weight loss (Peters and McEwen, 2015), all of which could be fulfilled by findings from our included papers. This is the second major prediction of the Selfish-Brain theory that has been confirmed and that relates to a proximal bottleneck of the cerebral supply chain, the occlusion of the cerebral arteries. The first major prediction, which had also been confirmed, related to a distal supply bottleneck of the cerebral supply chain, caloric restriction (Sprengell et al., 2021). We did not only systematically search the literature databases, but also followed a systematic plan to capture the potential bottlenecks of the cerebral supply chain and predict their impact on cerebral and peripheral energy states. By passing this second test, centered on cerebral ischemia, the Selfish-Brain theory continues to demonstrate the accuracy of its predictions.

DATA AVAILABILITY STATEMENT

The raw data supporting the conclusions of this article will be made available by the authors, without undue reservation.

AUTHOR CONTRIBUTIONS

MS developed the search strategies that BK and AP approved. MS screened the article titles or abstracts against the inclusion and exclusion criteria. BK checked this step, and disagreements were resolved where necessary by consulting the third reviewer AP. MS and BK independently analyzed the full text, and disagreements were resolved where necessary by consultation with the third reviewer AP. MS extracted the data, which BK and AP independently checked. MS assessed the risk of bias, which BK and AP independently checked and approved. BK and AP wrote the manuscript. All authors have read and approved the submitted version.

ACKNOWLEDGMENTS

Our special thanks go to Professor Markus Schwaninger, Chair of the Institute of Experimental and Clinical Pharmacology and Toxicology, University of Luebeck, for his criticism and invaluable comments on this work. We also thank Sabine Wittnebel for expert assistance in the retrieval and acquisition of full text articles.

SUPPLEMENTARY MATERIAL

The Supplementary Material for this article can be found online at: https://www.frontiersin.org/articles/10.3389/fnins.2021.685031/full#supplementary-material

REFERENCES

Ahren, B. (2000). Autonomic regulation of islet hormone secretion-implications for health and disease. *Diabetologia* 43, 393–410. doi: 10.1007/s001250051322

Arieff, A. I., Doerner, T., Zelig, H., and Massry, S. G. (1974). Mechanisms of seizures and coma in hypoglycemia. Evidence for a direct effect of insulin on electrolyte transport in brain. *J. Clin. Invest.* 54, 654–663. doi: 10.1172/JCI107803

Arnberg, F., Grafstrom, J., Lundberg, J., Nikkhou-Aski, S., Little, P., Damberg, P., et al. (2015). Imaging of a clinically relevant stroke model: glucose hypermetabolism revisited. *Stroke* 46, 835–842. doi: 10.1161/STROKEAHA.114.008407

Baum, D., and Porte, D. (1969). Adrenergic regulation of hyperglycemia in acute hypoxia. *Diabetes* 18:346.

Baum, D., and Porte, D. Jr. (1971). Alpha-adrenergic inhibition of immunoreactive insulin release during deep hypothermia. *Am. J. Physiol.* 221, 303–311. doi: 10.1152/ajplegacy.1971.221.1.303

Bellolio, M. F., Gilmore, R. M., and Ganti, L. (2014). Insulin for glycaemic control in acute ischaemic stroke. *Cochrane Database Syst. Rev.* 23:CD005346. doi: 10.1002/14651858.CD005346.pub4

Boujon, V., Uhlemann, R., Wegner, S., Wright, M. B., Laufs, U., Endres, M., et al. (2019). Dual PPARalpha/gamma agonist aleglitazar confers stroke protection in a model of mild focal brain ischemia in mice. *J. Mol. Med.* 97, 1127–1138. doi: 10.1007/s00109-019-01801-0

Bravata, D. M., Kim, N., Concato, J., and Brass, L. M. (2003). Hyperglycaemia in patients with acute ischaemic stroke: how often do we screen for undiagnosed diabetes? *QJM* 96, 491–497. doi: 10.1093/qjmed/hcg087

Capes, S. E., Hunt, D., Malmberg, K., Pathak, P., and Gerstein, H. C. (2001). Stress hyperglycemia and prognosis of stroke in non-diabetic and diabetic patients: a systematic overview. *Stroke* 32, 2426–2432. doi: 10.1161/hs1001.096194

Chaput, J. P., and Tremblay, A. (2009). The glucostatic theory of appetite control and the risk of obesity and diabetes. *Int. J. Obes.* 33, 46–53. doi: 10.1038/ijo.2008.221

Chen, W. Y., Mao, F. C., Liu, C. H., Kuan, Y. H., Lai, N. W., Wu, C. C., et al. (2016). Chromium supplementation improved post-stroke brain infarction and hyperglycemia. *Metab. Brain Dis.* 31, 289–297. doi: 10.1007/s11011-015-9749-y

Corrall, R. J., and Frier, B. M. (1981). Acute hypoglycemia in man: neural control of pancreatic islet cell function. *Metabolism* 30, 160–164. doi: 10.1016/0026-0495(81)90166-9

Deng, D., Xu, C., Sun, P., Wu, J., Yan, C., Hu, M., et al. (2014). Crystal structure of the human glucose transporter GLUT1. *Nature* 510, 121–125. doi: 10.1038/nature13306

Dungan, K. M., Braithwaite, S. S., and Preiser, J. C. (2009). Stress hyperglycaemia. *Lancet* 373, 1798–1807. doi: 10.1016/S0140-6736(09)60553-5

Endres, M., Engelhardt, B., Koistinaho, J., Lindvall, O., Meairs, S., Mohr, J. P., et al. (2008). Improving outcome after stroke: overcoming the translational roadblock. *Cerebrovasc. Dis.* 25, 268–278. doi: 10.1159/000118039

Gerstein, H. C., Miller, M. E., Byington, R. P., Goff, D. C. Jr., Bigger, J. T., Buse, J. B., et al. (2008). Effects of intensive glucose lowering in type 2 diabetes. *N. Engl. J. Med.* 358, 2545–2559. doi: 10.1056/NEJMoa0802743

Gibson, C. L., Murphy, A. N., and Murphy, S. P. (2012). Stroke outcome in the ketogenic state–a systematic review of the animal data. *J. Neurochem.* 123, 52–57. doi: 10.1111/j.1471-4159.2012.07943.x

Ginsberg, M. D., Prado, R., Dietrich, W. D., Busto, R., and Watson, B. D. (1987). Hyperglycemia reduces the extent of cerebral infarction in rats. *Stroke* 18, 570–574. doi: 10.1161/01.STR.18.3.570

Harada, S., Fujita, W. H., Shichi, K., and Tokuyama, S. (2009). The development of glucose intolerance after focal cerebral ischemia participates in subsequent neuronal damage. *Brain Res.* 1279, 174–181. doi: 10.1016/j.brainres.2009.05.014

Hasselbalch, S. G., Knudsen, G. M., Videbaek, C., Pinborg, L. H., Schmidt, J. F., Holm, S., et al. (1999). No effect of insulin on glucose blood-brain barrier transport and cerebral metabolism in humans. *Diabetes* 48, 1915–1921. doi: 10.2337/diabetes.48.10.1915

Higgins, J. P. T., and Thomas, J. M. (2019). *Cochrane Handbook for Systematic Reviews of Interventions, 2nd Edn*. Chichester, UK: John Wiley & Sons Ltd. doi: 10.1002/9781119536604

Hitze, B., Hubold, C., van Dyken, R., Schlichting, K., Lehnert, H., Entringer, S., et al. (2010). How the selfish brain organizes its supply and demand. *Front. Neuroenergetics* 2. doi: 10.3389/fnene.2010.00007

Hom, F. G., Goodner, C. J., and Berrie, M. A. (1984). A [3H]2-deoxyglucose method for comparing rates of glucose metabolism and insulin responses among rat tissues *in viv*o. Validation of the model and the absence of an insulin effect on brain. *Diabetes* 33, 141–152. doi: 10.2337/diab.33.2.141

Hooijmans, C. R., Rovers, M. M., de Vries, R. B., Leenaars, M., Ritskes-Hoitinga, M., and Langendam, M. W. (2014). SYRCLE's risk of bias tool for animal studies. *BMC Med. Res. Methodol.* 14, 43. doi: 10.1186/1471-2288-14-43

Jarhult, J., and Holst, J. J. (1978). Reflex adrenergic control of endocrine pancreas evoked by unloading of carotid baroreceptors in cats. *Acta Physiol. Scand.* 104, 188–202. doi: 10.1111/j.1748-1716.1978.tb06266.x

Johnston, K. C., Bruno, A., Pauls, Q., Hall, C. E., Barrett, K. M., Barsan, W., Fansler, A., Van de Bruinhorst, K., Janis, S., Durkalski-Mauldin, V. L., and Neurological Emergencies Treatment Trials N, the STI (2019). Intensive vs standard treatment of hyperglycemia and functional outcome in patients with acute ischemic stroke: the SHINE randomized clinical trial. *JAMA* 322, 326–335. doi: 10.1001/jama.2019.9346

Kennedy, G. C. (1953). The role of depot fat in the hypothalamic control of food intake in the rat. *Proc. R. Soc. London Ser.* 140, 578–592. doi: 10.1098/rspb.1953.0009

Khan, M. A., Schultz, S., Othman, A., Fleming, T., Lebron-Galan, R., Rades, D., et al. (2016). hyperglycemia in stroke impairs polarization of monocytes/macrophages to a protective non-inflammatory cell type. *J. Neurosci.* 36, 9313–9325. doi: 10.1523/JNEUROSCI.0473-16.2016

Koch, K., Berressem, D., Konietzka, J., Thinnes, A., Eckert, G. P., and Klein, J. (2017). Hepatic ketogenesis induced by middle cerebral artery occlusion in mice. *J. Am. Heart Assoc.* 6. doi: 10.1161/JAHA.117.005556

Kruyt, N. D., Biessels, G. J., Devries, J. H., and Roos, Y. B. (2010). Hyperglycemia in acute ischemic stroke: pathophysiology and clinical management. *Nat. Rev. Neurol.* 6, 145–155. doi: 10.1038/nrneurol.2009.231

Kubera, B., Hubold, C., Wischnath, H., Zug, S., and Peters, A. (2014). Rise of ketone bodies with psychosocial stress in normal weight men. *Psychoneuroendocrinology* 45, 43–48. doi: 10.1016/j.psyneuen.2014.03.008

Li, L., Tian, J., Long, M. K., Chen, Y., Lu, J., Zhou, C., et al. (2016). Protection against experimental stroke by ganglioside GM1 is associated with the inhibition of autophagy. *PLoS One* 11:e0144219. doi: 10.1371/journal.pone.0144219

Mason, J. W., Wherry, F. E., Brady, J. V., Beer, B., Pennington, L. L., and Goodman, A. C. (1968). Plasma insulin response to 72-hr. Avoidance sessions in the monkey. *Psychosom. Med.* 30, 746–759. doi: 10.1097/00006842-196809000-00030

Mayer, J. (1953). Glucostatic mechanism of regulation of food intake. *N. Engl. J. Med.* 249, 13–16. doi: 10.1056/NEJM195307022490104

Meek, T. H., Nelson, J. T., Matsen, M. E., Dorfman, M. D., Guyenet, S. J., Damian, V., et al. (2016). Functional identification of a neurocircuit regulating blood glucose. *Proc. Natl. Acad. Sci. U. S. A.* 113, E2073–E2082. doi: 10.1073/pnas.1521160113

Mobbs, C. V., Kow, L. M., and Yang, X. J. (2001). Brain glucose-sensing mechanisms: ubiquitous silencing by aglycemia vs. hypothalamic neuroendocrine responses. *Am. J. Physiol. Endocrinol. Metab.* 281, E649–E654. doi: 10.1152/ajpendo.2001.281.4.E649

Moher, D., Liberati, A., Tetzlaff, J., Altman, D. G., and PRISMA-P Group (2009). Preferred reporting items for systematic reviews and meta-analyses: the PRISMA statement. *PLoS Med* 6:e1000097. doi: 10.1371/journal.pmed.1000097

Peters, A., Bosy-Westphal, A., Kubera, B., Langemann, D., Goele, K., Later, W., et al. (2011). Why doesn't the brain lose weight, when obese people diet? *Obesity Facts*. 4:151-7.

Peters, A., and Langemann, D. (2009). Build-ups in the supply chain of the brain: on the neuroenergetic cause of obesity and type 2 diabetes mellitus. *Front. Neuroenergetics* 1:2. doi: 10.3389/neuro.14.002.2009

Peters, A., and McEwen, B. S. (2015). Stress habituation, body shape and cardiovascular mortality. *Neurosci. Biobehav. Rev.* 56, 139–150. doi: 10.1016/j.neubiorev.2015.07.001

Peters, A., Schweiger, U., Pellerin, L., Hubold, C., Oltmanns, K. M., Conrad, M., et al. (2004). The selfish brain: competition for energy resources. *Neurosci. Biobehav. Rev.* 28, 143–180. doi: 10.1016/j.neubiorev.2004.03.002

Rosso, C., Corvol, J. C., Pires, C., Crozier, S., Attal, Y., Jacqueminet, S., et al. (2012). Intensive versus subcutaneous insulin in patients with hyperacute stroke: results from the randomized INSULINFARCT trial. *Stroke* 43, 2343–2349. doi: 10.1161/STROKEAHA.112.657122

Routh, V. H., Hao, L., Santiago, A. M., Sheng, Z., and Zhou, C. (2014). Hypothalamic glucose sensing: making ends meet. *Front. Syst. Neurosci.* 8, 236. doi: 10.3389/fnsys.2014.00236

Schwartz, M. W., Seeley, R. J., Zeltser, L. M., Drewnowski, A., Ravussin, E., Redman, L. M., et al. (2017). Obesity pathogenesis: an endocrine society scientific statement. *Endocr. Rev.* 38, 267–296. doi: 10.1210/er.2017-00111

Seaquist, E. R., Damberg, G. S., Tkac, I., and Gruetter, R. (2001). The effect of insulin on *in vivo* cerebral glucose concentrations and rates of glucose transport/metabolism in humans. *Diabetes* 50, 2203–2209. doi: 10.2337/diabetes.50.10.2203

Shepherd, P. R., and Kahn, B. B. (1999). Glucose transporters and insulin action-implications for insulin resistance and diabetes mellitus. *N. Engl. J. Med.* 341, 248–257. doi: 10.1056/NEJM199907223410406

Slack, N., Chambers, S., and Johnston, R. (2004). *Operations Management, 4 Edn*. Harlow: FT Prentice Hall.

Spanswick, D., Smith, M. A., Groppi, V. E., Logan, S. D., and Ashford, M. L. (1997). Leptin inhibits hypothalamic neurons by activation of ATP-sensitive potassium channels. *Nature* 390, 521–525. doi: 10.1038/37379

Spiegel, K., Leproult, R., and Van Cauter, E. (1999). Impact of sleep debt on metabolic and endocrine function. *Lancet* 354, 1435–1439. doi: 10.1016/S0140-6736(99)01376-8

Sprengell, M., Kubera, B., and Peters, A. (2021). Brain more resistant to energy restriction than body: a systematic review. *Front. Neurosci*. 15:639617. doi: 10.3389/fnins.2021.639617

Stanley, S. A., Kelly, L., Latcha, K. N., Schmidt, S. F., Yu, X., Nectow, A. R., et al. (2016). Bidirectional electromagnetic control of the hypothalamus regulates feeding and metabolism. *Nature* 531, 647–650. doi: 10.1038/nature17183

Steinkamp, M., Li, T., Fuellgraf, H., and Moser, A. (2007). K(ATP)-dependent neurotransmitter release in the neuronal network of the rat caudate nucleus. *Neurochem. Int*. 50, 159–163. doi: 10.1016/j.neuint.2006.07.011

Taylor, S. H., Saxton, C., Majid, P. A., Dykes, J. R., Ghosh, P., and Stoker, J. B. (1969). Insulin secretion following myocardial infarction with particular respect to the pathogenesis of cardiogenic shock. *Lancet* 2, 1373–1378. doi: 10.1016/S0140-6736(69)90928-3

The-NICE-SUGAR-Study-Investigators (2009). Intensive versus conventional glucose control in critically ill patients. *N. Engl. J. Med*. 360,1283–1297. doi: 10.1056/NEJMoa0810625

Toda, C., Kim, J. D., Impellizzeri, D., Cuzzocrea, S., Liu, Z. W., and Diano, S. (2016). UCP2 regulates mitochondrial fission and ventromedial nucleus control of glucose responsiveness. *Cell* 164, 872–883. doi: 10.1016/j.cell.2016.02.010

Wagner, K. R., Kleinholz, M., de Courten-Myers, G. M., and Myers, R. E. (1992). Hyperglycemic versus normoglycemic stroke: topography of brain metabolites, intracellular pH, and infarct size. *J. Cereb. Blood Flow Metab*. 12, 213–222. doi: 10.1038/jcbfm.1992.31

Wang, Y. Y., Chen, C. J., Lin, S. Y., Chuang, Y. H., Sheu, W. H., and Tung, K. C. (2013). Hyperglycemia is associated with enhanced gluconeogenesis in a rat model of permanent cerebral ischemia. *Mol. Cell Endocrinol*. 367, 50–56. doi: 10.1016/j.mce.2012.12.016

Wang, Y. Y., Lin, S. Y., Chuang, Y. H., Sheu, W. H., Tung, K. C., and Chen, C. J. (2014). Activation of hepatic inflammatory pathways by catecholamines is associated with hepatic insulin resistance in male ischemic stroke rats. *Endocrinology* 155, 1235–1246. doi: 10.1210/en.2013-1593

Woods, S. C., and Porte, D. Jr. (1974). Neural control of the endocrine pancreas. *Physiol. Rev*. 54, 596–619. doi: 10.1152/physrev.1974.54.3.596

Yamazaki, Y., Harada, S., and Tokuyama, S. (2012). Post-ischemic hyperglycemia exacerbates the development of cerebral ischemic neuronal damage through the cerebral sodium-glucose transporter. *Brain Res*. 1489, 113–120. doi: 10.1016/j.brainres.2012.10.020

Yamazaki, Y., Harada, S., and Tokuyama, S. (2014). Sodium-glucose transporter type 3-mediated neuroprotective effect of acetylcholine suppresses the development of cerebral ischemic neuronal damage. *Neuroscience* 269, 134–142. doi: 10.1016/j.neuroscience.2014.03.046

Zhang, X., Yang, S., Chen, J., and Su, Z. (2018). Unraveling the regulation of hepatic gluconeogenesis. *Front. Endocrinol*. 9:802. doi: 10.3389/fendo.2018.00802

Zhou, L., Podolsky, N., Sang, Z., Ding, Y., Fan, X., Tong, Q., et al. (2010). The medial amygdalar nucleus: a novel glucose-sensing region that modulates the counterregulatory response to hypoglycemia. *Diabetes* 59, 2646–2652. doi: 10.2337/db09-0995

Conflict of Interest: The authors declare that the research was conducted in the absence of any commercial or financial relationships that could be construed as a potential conflict of interest.

frontiers in Endocrinology

ORIGINAL RESEARCH
published: 01 July 2021
doi: 10.3389/fendo.2021.680494

Leptin Receptor Expressing Neurons in the Substantia Nigra Regulate Locomotion, and in The Ventral Tegmental Area Motivation and Feeding

Véronne A. J. de Vrind[1], *Lisanne J. van 't Sant*[1], *Annemieke Rozeboom*[1], *Mieneke C. M. Luijendijk-Berg*[1], *Azar Omrani*[1] *and Roger A. H. Adan*[1,2*]

[1] Brain Center Rudolf Magnus, Department of Translational Neuroscience, University Medical Center Utrecht and University Utrecht, Utrecht, Netherlands, [2] Institute of Neuroscience and Physiology, The Sahlgrenska Academy at the University of Gothenburg, Gothenburg, Sweden

Leptin is an anorexigenic hormone, important in the regulation of body weight. Leptin plays a role in food reward, feeding, locomotion and anxiety. Leptin receptors (LepR) are expressed in many brain areas, including the midbrain. In most studies that target the midbrain, either all LepR neurons of the midbrain or those of the ventral tegmental area (VTA) were targeted, but the role of substantia nigra (SN) LepR neurons has not been investigated. These studies have reported contradicting results regarding motivational behavior for food reward, feeding and locomotion. Since not all midbrain LepR mediated behaviors can be explained by LepR neurons in the VTA alone, we hypothesized that SN LepR neurons may provide further insight. We first characterized SN LepR and VTA LepR expression, which revealed LepR expression mainly on DA neurons. To further understand the role of midbrain LepR neurons in body weight regulation, we chemogenetically activated VTA LepR or SN LepR neurons in LepR-cre mice and tested for motivational behavior, feeding and locomotion. Activation of VTA LepR neurons in food restricted mice decreased motivation for food reward (p=0.032) and food intake (p=0.020), but not locomotion. In contrast, activation of SN LepR neurons in food restricted mice decreased locomotion (p=0.025), but not motivation for food reward or food intake. Our results provide evidence that VTA LepR and SN LepR neurons serve different functions, i.e. activation of VTA LepR neurons modulated motivation for food reward and feeding, while SN LepR neurons modulated locomotor activity.

Keywords: leptin, dopamine, chemogenetics, midbrain, substantia nigra, ventral tegmental area

OPEN ACCESS

Edited by:
Hu Huang, East Carolina University, United States

Reviewed by:
Helene Plamondon, University of Ottawa, Canada
Brenton T. Laing, National Institute on Drug Abuse (NIDA), United States

***Correspondence:**
Roger A. H. Adan
r.a.h.adan@umcutrecht.nl

Specialty section:
This article was submitted to Neuroendocrine Science, a section of the journal Frontiers in Endocrinology

Received: *14 March 2021*
Accepted: *10 June 2021*
Published: *01 July 2021*

Citation:
de Vrind VAJ, van 't Sant LJ, Rozeboom A, Luijendijk-Berg MCM, Omrani A and Adan RAH (2021) Leptin Receptor Expressing Neurons in the Substantia Nigra Regulate Locomotion, and in The Ventral Tegmental Area Motivation and Feeding. Front. Endocrinol. 12:680494. doi: 10.3389/fendo.2021.680494

INTRODUCTION

The current obesity epidemic is a result of overconsumption that exceeds energy requirements. With no truly effective treatments, there is a need for further mechanistic insights into body weight regulation. Hedonic feeding is characterized by the increased consumption of palatable foods and implicates increased motivation for these foods, which ultimately results in obesity (1). Food deprivation or dieting is known to increase motivation for food, which counteracts weight loss (2). In light of the obesity epidemic, it is of interest to gain further knowledge on mechanisms underlying increased motivation for (palatable) food.

Leptin is an anorexic adipose-tissue derived hormone with a central role in body weight regulation. Leptin is secreted in levels proportional to the amount of adipose tissue, i.e. fasting decreases leptin levels, while weight gain increases leptin levels (3–5). Leptin is known to regulate body weight by reducing feeding and increasing energy expenditure (6). Accumulating evidence shows that leptin is also involved in reducing motivation for food in both humans and rodents (7–11). The midbrain, comprising of the ventral tegmental area (VTA) and substantia nigra (SN), is associated with motivational behavior and expresses the leptin receptor (LepR), but it is unclear whether and which of these regions mediate leptin's effect on motivational behavior for food reward (12–14).

Since VTA DA neurons are important for motivational behaviour, VTA DA neurons expressing LepR were proposed to mediate the effect of leptin on food reward (15–18). However, there are data that challenge this idea. An important reward associated pathway are VTA DA neurons projecting to the nucleus accumbens (NAc), but only few VTA-LepR neurons project to the NAc (19). Instead, VTA LepR neurons primarily project to the central amygdala, and these neurons mediate effects of leptin on central amygdala associated behaviors, such as anxiety (18). Indeed, leptin infusion into the VTA of mice decreased anxiety-like behavior (20). Together, these data suggest that VTA (DA) LepR neurons modulate anxiety-like and not motivational behavior. Yet, knockdown of LepR in the whole midbrain increased motivational behavior as assessed by operant responding (21). This suggests that another population of midbrain LepR neurons modulate motivation. In the SN, LepR are almost exclusively expressed on SN DA neurons (18) and SN DA neurons have been implicated in motivational behavior (22). Optogenetic activation of either VTA or SN dopamine neurons demonstrated that dopamine neurons in the VTA and SN exhibited divergent conditioned motivational functions: VTA, but not SN dopamine neurons conferred a signal that made cues attractive and reinforcing; SN dopamine neurons conferred a more general movement invigoration signal: cues paired with their activation evoked vigorous movement not directed at the cue (23). Thus, SN dopamine neurons play a role in motivation and an involvement of SN LepR neurons in mediating the effect of leptin on motivational behavior is possible, but has not yet been determined.

Besides the role of midbrain LepR neurons in motivation for food reward, this region has also been implicated in other aspects of leptin's behavioral effects such as feeding and energy expenditure. Leptin injection into the VTA decreased feeding (15, 24–26) and blocking or decreasing leptin signaling in the VTA increased feeding (15, 25). However, inhibiting leptin signaling in the whole midbrain (21) or specifically in DA neurons of the midbrain (27, 28) did not impact on feeding. These results suggest that perhaps effects on feeding are mediated by non-DA neurons in the VTA. In addition, it remains unknown whether SN LepR neurons contribute to the anorexic effect of leptin.

Effects of midbrain LepR neurons on locomotor activity are contradicting. Whereas leptin infusion into the VTA had no effect on locomotion in ad libitum fed rats (15), RNA interference knockdown of LepR in VTA LepR neurons or ablation of STAT3 in midbrain (SN and VTA) DA neurons increased locomotion (15, 27). One reason for a lack of effect of leptin infusion on locomotion is that endogenous leptin masked effects on locomotion in these experiments since intra-VTA leptin injections were given to ad libitum fed rats that already have high levels of leptin (15). Alternatively, SN LepR neurons could mediate effects of leptin on locomotion. Thus, it remains unclear which midbrain LepR population modulates locomotion.

The aim of the current study was to further insight into the mechanisms underlying the effect of leptin in the midbrain and its involvement in body weight regulation. We started with characterizing the expression of LepR in the midbrain. Next, two questions were of particular interest for behavioral experiments: 1) whether SN LepR neurons modulate motivational, locomotor and feeding behavior and 2) whether VTA LepR neurons mediate anxiety-like, feeding and locomotor behavior. To address these questions, we selectively activated VTA or SN neurons that express leptin receptor, by injecting a viral vector that expresses the CNO receptor hM3Dq (also referred to as chemogenetics) in either the VTA or SN of LepR cre mice. We directly compared behavioral effects of chemogenetically activating VTA LepR or SN LepR neurons on motivational behavior for food reward, feeding, locomotion and anxiety in LepR-cre mice.

MATERIALS AND METHODS

All experiments were approved by the Animal Experimentation Committee of the University Utrecht and were carried out in agreement with Dutch Law (Herziene Wet op Dierproeven, Art 10.a2, 2014) and European regulations (Guideline 2010/63/EU).

Subjects

In house bred, adult male homozygote LepRb-Cre transgenic mice (stock #008320, B6.129-Leprtm2(cre)Rck/J, The Jackson Laboratory, USA) were used for behavioral experiments. Mice were housed individually in plastic cages (Type II L, 365x207x140mm, 530cm^2, Tecniplast, Italy) in a temperature (21 ± 2°C) and humidity (60-70%) controlled room on a reversed day/night (9:00 AM light OFF, 9:00 PM light ON) schedule. We tested all mice first in ad libitum situations (**Figure 1**) and then under food restriction, because leptin levels are correlated with

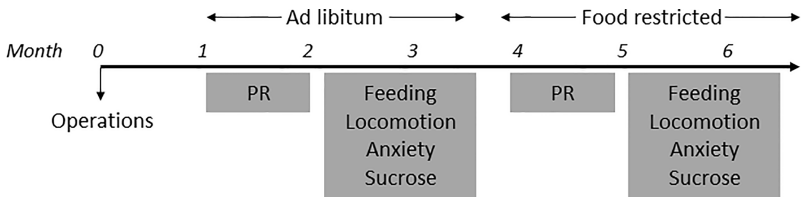

FIGURE 1 | Timeline of experiments.

the amount of fat tissue in mice (3, 5) and leptin influences midbrain DA activity (15, 16, 29). Ad libitum fed mice were given ad libitum access to chow (3,1Kcal/gr, Standard Diet Service, UK) and water. Food-restricted mice were given chow (~3 pieces of standard rodent chow of ±1.3 grams each) after behavioral tasks were performed and maintained on ~90% of the original body weight by adapting the amount of chow given per day. For analysis of DA (determined by staining for TH immunoreactivity) and LepR co-localization, LepRb-Cre mice were crossed with a mouse line that expresses robust tdTomato fluorescence following Cre-mediated recombination (stock # 007914, B6.Cg-Gt(ROSA)26Sortm14(CAG-tdTomato)Hze/J, The Jackson Laboratory, USA). Male mice homozygote for the LepRb-Cre allele and heterozygote for the TdTom allele ("LepR/tdTomato" mice, n=3) were socially housed on a normal day/night cycle (7:00AM lights ON) with ad libitum access to chow and water.

Surgical Procedures

At least 30min prior to anesthetization, mice were given carprofen (5mg/kg, subcutaneous (s.c.), Carporal, AST Farma BV). Mice were anesthetized with an intraperitoneal (i.p.) injection of ketamine (75mg/kg, Narketan, Vetoquinol BV) and medetomidine (1mg/kg, SedaStart, AST Farma BV). Mice were given eye cream (CAF, CEVA Sante Animale BW) and placed in a stereotactic frame (Kopf Instruments, USA). An incision was made in the skin along the midline of the skull and additional analgesia was applied by spraying Xylocaine (lidocaine 100mg/ml, AstraZeneca BV) on the skull. Microinjections of AAV5-hSyn-DIO-hM3DGq-mCherry (0.3ul/side, $3.0*10^9$vp/ul, UNC Vector Core, USA) or AAV-Ef1a-DIO-hChR2-eYFP ("control" mice, 0.3ul/side, 3.0*10^9vp/ul, UNC Vector Core, USA, n=6) were performed bilaterally in the substantia nigra (-3.3 AP, +1.5 ML, -4.4 DV, 0° angle, n=6) or the ventral tegmental area (-3.2 AP, +1.5 ML, -4.8 DV, 10° angle, n=6) at a rate of 0.1ul/min per side followed by a 10min period before retracting the needles. For assessment of SN LepR projection sites mice were injected with AAV-Ef1a-DIO-ChR2-eYFP (0.3ul/side, $3.0*10^9$vp/ul, UNC Vector Core, USA) in the SN (n=4). After the operation, mice were given atipamezole (2.5mg/kg, i.p., SedaStop, AST Farma BV) and saline for rehydration. The following 2 days, mice were given carprofen (5mg/kg, s.c.) and were allowed to recover for at least 1 week after operations. To ensure viral expression, testing commenced 3 weeks after operations were performed. Thus, the mice were exposed to behavioral testing at least four weeks after surgery.

Drugs

Clozapine N-oxide (CNO 99%, AK Scientific, Inc., USA) was dissolved in 0.9% saline and injected i.p. with a commonly used dose of 1.0mg/kg (and 3.0mg/kg for operant testing). For all experiments, each mouse received saline and CNO injections in a latin-square design. Mice were injected with saline or CNO 30 minutes prior to the start of a behavioral task.

Behavioral Procedures

All mice were tested in every behavioral experiment. On test days only one single behavioral experiment was performed (**Figure 1**). Furthermore, between two test days on which mice were injected, there was at least one day on which mice were not injected.

Progressive Ratio Operant Behavior

Mouse operant boxes (ENV-307W, Med Associates Inc., USA) fitted with 2 levers, a cue light above the active lever (AL), a house light, a speaker and a liquid receptacle were used. Throughout all sessions, when the number of AL presses to complete a ratio was reached, the house light and a tone were presented for 5sec, after which a sucrose reward was delivered for 2sec (38ul, 20% w/v sugar solution in tap water). During the training phase, mice were food restricted to ~90% of their original body weight. The first day, mice were habituated for 15min to an operant box, in which we placed a droplet of sugar solution (20% w/v) in the receptacle. The next day, operant training started with a fixed ratio (FR) 1 paradigm for 30min/session. Once mice learned to press on the active lever >20x and <10% on the inactive lever, mice were switched to FR3 (30min/session) and then FR5 (60min/session). Then, once >60 rewards were earned and <10% of the presses were made on the inactive lever, training was switched to the progressive ratio (PR, 60min/session) and mice were returned to ad libitum feeding. PR schedule was based on the formula: $5*e^{(x*0.2)}-5$, rounded to the nearest integer, where x is the position in the ratio sequence (30). Testing with saline/CNO started when PR performance appeared stable, i.e. over 3 days of training no more than ±1 reward from average and no incremental increase or decrease. Operant training and testing were performed during the first 3 hours of the dark phase. Injections were given 30min prior to the start of the PR task. With this test we measured the amount of active lever presses made during 60min of the PR task.

Free Access 20% Sucrose Consumption

Mice were trained to lick for 20% (w/v) granulated sugar solution in an operant box fitted with a spout connected to a pump which delivered 8ul 20% sugar solution upon every detected lick. Mice were trained 4 times prior to testing. Training and testing was performed 3-5h into the dark phase and lasted 30min. On test days, mice were injected with CNO/saline 30min before the start of the test. With this test we measured the number of detected licks during 30 min testing.

Feeding

To simplify finding pieces of chow at measurements, all mice were habituated twice to a second mouse cage, in which no bedding, but only 3 tissues and a water bottle were present, hereafter referred to as 'feeding cage'. During habituation we also habituated the mice to the experimenter taking chow out of the cage with the mice remaining in the cage. Mice were injected with saline/CNO 30min prior to the onset of the dark phase and were directly placed in the feeding cage with a pre-weighed amount of chow on the cage floor. Food intake was measured at 1, 2, 3, 5 and 7h post injection. At these timepoints, we weighed the pieces of chow with mice still in the feeding cage as they were used to from habituation to keep stress levels to a minimum. With this test we measured the amount of chow eaten in grams at the different timepoints.

Locomotion

All mice were habituated 2x1h to an individual plastic cage (Type III H, 425x266x185mm, 800cm^2, Tecniplast, Italy) prior to testing on separate days. The cages were surrounded by white carton to prevent interaction between mice. On the test day, mice were injected with either saline/CNO and placed in the behavioral testing room. 30min later, mice were placed in their own locomotion cage and horizontal movement was tracked using a camera placed above the cages that was coupled to a computer running Ethovision 7 (Noldus Information Technology, the Netherlands). Locomotion tests commenced 4-5h into the dark phase and lasted 1h. With this test we measured the distance mice had travelled in meters in 1h.

Anxiety

Mice were injected with either saline/CNO 30min prior to testing and placed in the front room of the behavioral room where tests would be performed. Mice were lifted by their tails and placed in the center of the elevated plus maze in a brightly lit room and tracked using Ethovision (Noldus, Wageningen) for 5min. Anxiety tests were performed 6-7h into the dark phase. A previous study reported that longer intervals between anxiety tests led to reliable retesting of anxiety (31), so we separated 2 test days by at least 3 weeks. With this test we measured the amount of time mice spent in the open and dark arms and the amount of crossings made.

Tissue Preparation and Immunohistochemical Analysis

Mice were anesthetized with Euthanimal (200mg/ml, Euthanimal, Alfasan BV, the Netherlands) and transcardially perfused with 1x phosphate-buffered saline (PBS) followed by 4% paraformaldehyde in 1xPBS (PFA). Brains were dissected and kept in 4%PFA for 24h at 4°C, after which they were transferred to 30% sucrose in 1xPBS for at least 48h at 4°C. Using a cryostat, the brains were then sectioned to 40um slices and stored in 1xPBS with 0.01% sodium azide. Slices were washed 3x10min in 1xPBS and then blocked for 1h in 1xPBS containing 10% normal goat serum and 0,25% Triton-X100. Slices were then placed in 1xPBS containing the primary antibodies (Rabbit anti-dsRed 1:500, #632496, Clontech, Takara Bio USA Inc, USA; Mouse anti-Th 1:500, MAB318, Milipore) and 2% normal goat serum overnight at 4°C. At room temperature, slices were washed 3x10min in 1xPBS and placed in 1xPBS containing the secondary antibodies (Goat anti-Rabbit 568, 1:500, #ab175471, Abcam plc, UK; Goat anti-Mouse 488 1:500, ab150113, Abcam plc, UK) and 2% normal goat serum for 2h. Finally, slices were washed in 1xPBS and mounted onto slides, dried and covered using Fluorsave (EMD Millipore Corporation, USA) and a coverslip. Images were collected on an epifluorescent microscope (Axio Scope A1, Zeiss, Germany). For behavioral mice, at least 3 representative images were analyzed per mouse from sections ranging from -2.54mm to -3.88mm (bregma).

Data Analysis

Behavioral data was analyzed using Microsoft Excel and GraphPad Prism (version 7.05, GraphPad Software, Inc., USA). Paired t-tests and one- or two-way repeated measures ANOVA and Bonferroni's multiple comparisons tests were used where applicable. A significance criterion of $p<0.05$, two-tailed, was adopted in all the statistical analyses.

RESULTS

The Majority of Midbrain LepR Neurons Are Dopaminergic

To verify previous reports of co-localization of LepR on DA neurons, we assessed LepR expression in the midbrain. To identify LepR neurons in the midbrain, we crossed LepR-cre mice onto the ROSA26-tdTomato reporter mouse line, which allowed robust tdTomato fluorescence following Cre-mediated recombination. Tyrosine hydroxylase (TH) is the rate limiting enzyme in catecholamine production and considering that the VTA and SN are known to be DA producing structures, TH is used as marker for DA neurons. TH- and LepR-tdTomato immunoreactivity revealed that in the VTA 67 ± 1.0% and in the SN 89 ± 3.5% of LepR/tdTomato neurons co-localized with TH (**Figures 2A, B**). Of all TH neurons, only few co-localized with LepR/tdTomato in either region: 16 ± 1.3% in the VTA and 15% in the SN (n=3, **Figure 2C**). Thus, DA neurons that express LepR represented a minority of all DA neurons in VTA and SN, which is consistent with previous reports (15, 17, 18, 32). The majority of SN and VTA neurons expressing leptin receptor (LepR-tdTomato) are DA neurons.

We next aimed to assess the projection areas of midbrain LepR neurons. It has been established that VTA LepR neurons

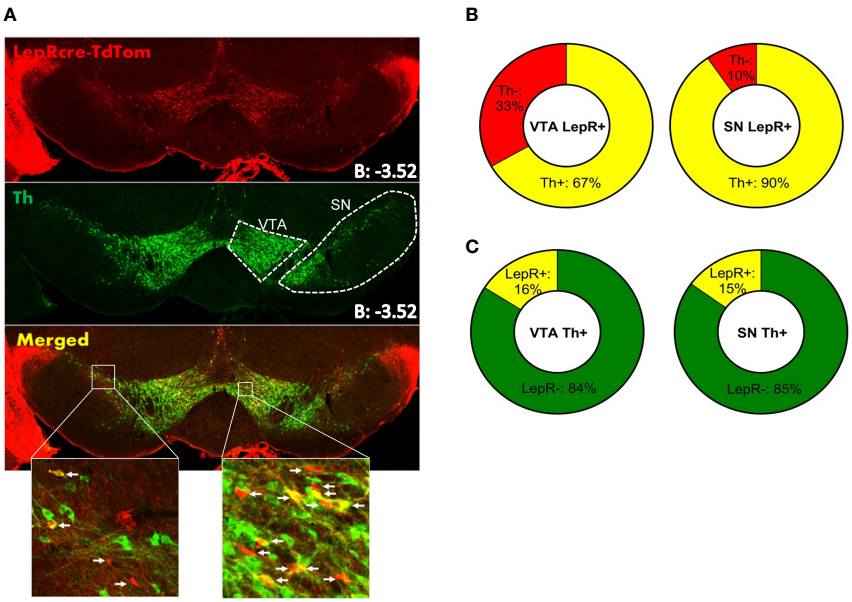

FIGURE 2 | Immunohistochemistry on LepR-cre x TdTomato mice (n=3). **(A)** Both SN and VTA expressed LepR neurons (arrows in insets indicate LepR). **(B)** The majority of LepR neurons co-localized with TH (VTA: 67%, SN: 90%) **(C)** Of all TH neurons, only 16% in the VTA and 15% in the SN expressed the LepR.

primarily project to the central amygdala, while very few project to the NAc (18, 19). SN LepR neurons have been shown to project to the caudate putamen (18) and we sought to further extend on this knowledge. We identified projections of SN LepR neurons by injecting LepR-cre mice with AAV-DIO-ChR2-eYFP into the SN, which also labels axonal projections. We found that SN LepR neurons projected heavily to the caudate putamen and further observed projections to the interstitial nucleus of the posterior limb of the anterior commissure (IPAC) (**Figures 3A–C**). Some eYFP expression was found in the thalamus and in the VTA (**Figures 3D, F**). Finally, labeling of axons with eYFP was also observed within SN pars compacta, SN pars reticula and lateral SN (**Figures 3E–G**). We cannot exclude that the observed staining was due to fibers passing the areas. However the density of fibers in these areas was remarkable compared to surrounding areas.

For behavioral experiments we injected AAV-DIO-hM3DGq-mCherry in the VTA (n=6) or SN (n=6) of LepR-cre mice to generate VTA LepR-Gq and SN LepR-Gq mice. In earlier studies we already demonstrated that in slices of animals with expression of this DREADD receptor in midbrain DA neurons, CNO depolarized DA neurons (33). We examined whether expression of hM3DGq-mCherry was representative for SN LepR or VTA LepR neurons. hM3DGq-mCherry was found mainly in the targeted region, but due to viral spread, some expression was seen in surrounding regions which express LepR-cre: of all hM3DGq-mCherry expressing neurons 68 ± 1.1% were localized in the VTA of VTA LepR-Gq mice and 96 ± 1.1% were localized in the SN of SN LepR-Gq mice (**Figure 4**). The percentage of TH neurons expressing hM3DGq-mCherry or the percentage of hM3DGq-mCherry neurons expressing TH were similar to the numbers presented above of TH/LepR co-localization in LepR-tdTomato mice. Thus, hM3DGq-mCherry targeted neurons were representative for LepR neurons of the VTA or SN.

Control Mice Do Not Show Behavioral Effects After CNO Injections Compared to Saline

Studies show that non-specific effects of CNO may occur in rats and mice due to reverse-metabolism to its parent compound clozapine (34). To ensure this is not the case in our study, we injected AAV-Ef1a-DIO-hChR2-eYFP into the VTA or SN of LepR-cre mice (n=6). This results in expression of channelrhodopsin, which does not respond to CNO or clozapine. As we expected, CNO injections in control mice had no effect on any behavioral parameter tested (**Supplemental Figure**, n=6). Therefore, we conclude that behavioral effects observed in Gq-injected mice are the result of enhanced neuronal activation in VTA LepR-Gq or SN LepR-Gq mice and not due to effects of reverse-metabolism of CNO to clozapine.

Motivation for Sugar Reward Decreased Upon Activation of VTA LepR-Gq Neurons in Food Restricted Mice

To test for motivation, we trained mice to press for a 20% sugar solution reward in the PR task. Once stable, mice were injected with saline and 2 doses of CNO (1.0 and 3.0mg/kg). Ad libitum fed VTA LepR-Gq mice did not alter operant responding after CNO injections compared to saline (**Figure 5A**), but when food restricted, VTA LepR-Gq mice decreased the amount of active

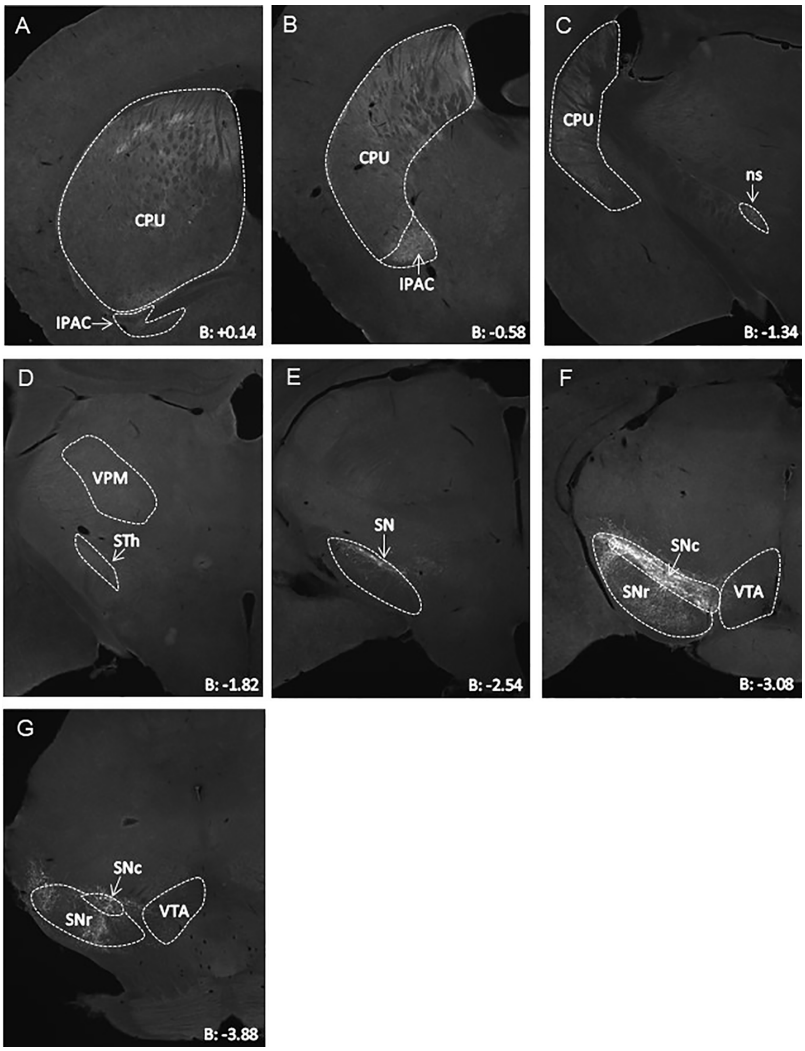

FIGURE 3 | Representative AAV-DIO-ChR2-eYFP tracing of projections from SN LepR neurons in LepR-cre mice (n=4). **(A–G)** eYFP expression in CPU ++, IPAC ++, STh +, VPM + and VTA +/- to which SN LepR neurons sent detectable projections (++ strong eYFP, + eYFP present, +/- scarce eYFP). In **(E–G)**, eYFP soma and tracks within the SN. B = bregma; CPU, caudate putamen; IPAC, interstitial nucleus of the posterior limb of the anterior commissure; ns, nigrostriatal bundle; SN, substantia nigra; SNc, SN pars compacta; SNr, SN pars reticulate; STh, subthalamic nucleus; VPM, Ventral posteromedial thalamus; VTA, ventral tegmental area.

lever presses made during the PR task ($F(1.110,5.549)=7.920$, p=0.032, n=6, **Figure 5C**). Further analyses revealed that both CNO doses significantly decreased performance compared to saline (CNO 1.0mg/kg, p=0.0007; CNO 3.0mg/kg, p=0.019). Operant behavior was not affected upon chemogenetic activation of SN LepR-Gq neurons (n=6, **Figures 5B, D**).

Free Consumption of Sucrose Solution Was Not Affected by VTA LepR or SN LepR Activation

To dissociate motivational behavior from consumption, we assessed free consumption of a 20% sucrose solution. Free consumption was not affected by activation of either VTA LepR or SN LepR, indicating that decreased motivation was driven by motivational behavior without affecting consummatory behavior (**Figure 6**). The apparent difference in baseline sucrose consumption between mice injected in the VTA compared to the SN is most likely due to the fact that these were different batches of mice that were tested at different time points.

Chow Consumption Decreased Upon Activation of VTA LepR-Gq Neurons in Food Restricted Mice

We next tested whether midbrain LepR neurons modulated feeding by measuring chow intake over 7h. Ad libitum fed mice did not alter consumption of chow after chemogenetically

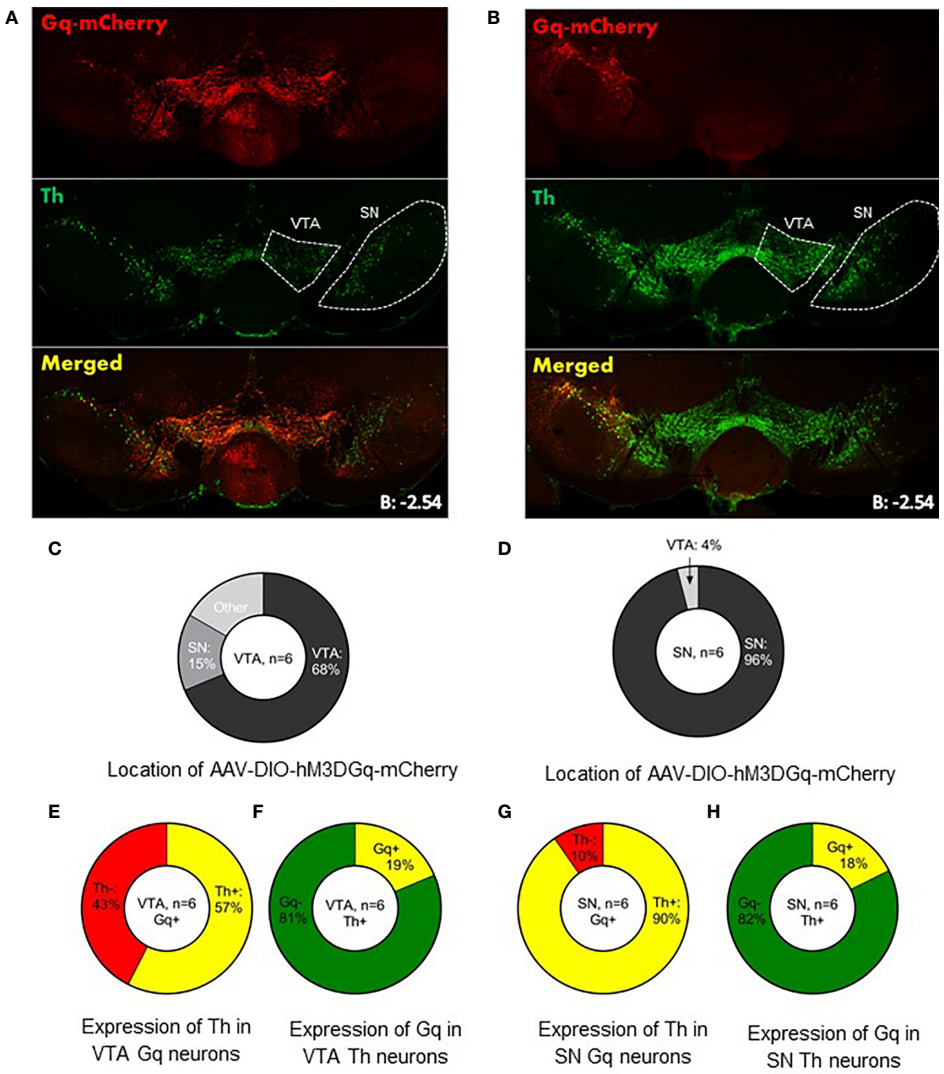

FIGURE 4 | Expression of AAV-DIO-hM3DGq-mCherry in behavioral animals. Representative example of AAV-DIO-hM3DGq-mCherry expression in **(A)** VTA LepR-Gq mice (n=6) and **(B)** SN LepR-Gq mice (n=6). **(C, D)** Analysis of the location of Gq-mCherry expression showed that the majority of Gq-neurons were found in the targeted region. **(E)** Analysis of Gq and TH in VTA LepR-Gq mice showed that 57% of VTA Gq neurons co-localized with TH-immunoreactivity. **(F)** 19% of all VTA TH neurons co-localized with Gq. **(G)** 96% of SN Gq neurons co-localized with TH-immunoreactivity. **(H)** Of all SN Th neurons, 18% co-localized with Gq-mCherry.

activating VTA LepR-Gq (**Figure 7A**) or SN LepR-Gq (**Figure 7B**) neurons. In food restricted VTA LepR-Gq mice, CNO decreased cumulative chow intake compared to saline (main effect of Injection F (1,5)=9.138, p=0.029, **Figure 7C**), but food intake was unaffected in food restricted SN LepR-Gq mice (**Figure 7D**).

Locomotion Decreased Upon Activation of SN LepR-Gq Neurons in Food Restricted Mice

Locomotor activity was assessed by automatically tracking horizontal movement of mice for 1h. CNO injections did not affect locomotor activity in ad libitum fed VTA LepR-Gq mice (**Figure 8A**) or SN LepR-Gq mice (**Figure 8B**). Activating VTA LepR-Gq neurons in food restricted mice did not modulate locomotion (**Figure 8C**), but activation of SN LepR-Gq neurons decreased locomotor activity (interaction effect of Time x Injection F(1.184,5.920)=9.380, p=0.020, **Figure 8D**). Further analyses revealed that CNO decreased locomotion after 40 and 60min in SN LepR-Gq mice (40min, p=0.031; 60min, p=0.025).

Chemogenetically Activating VTA LepR or SN LepR Did Not Affect Anxiety-Like Behavior

Finally, because previous studies showed that VTA LepR modulated anxiety (20, 28), we aimed to verify this in our experiments and determined effects of activating VTA LepR or

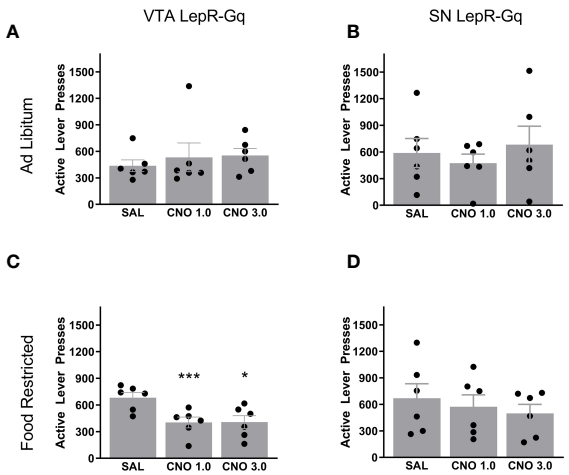

FIGURE 5 | Active lever presses upon chemogenetic activation of VTA LepR or SN LepR neurons. In ad libitum fed mice, CNO (1.0 and 3.0mg/kg) did not affect active lever presses made in **(A)** VTA LepR-Gq (n=6) or **(B)** SN LepR-Gq mice (n=6). **(C)** Food restricted VTA LepR-Gq mice (n=6) decreased active lever presses after CNO compared to saline injections. **(D)** CNO did not affect active lever presses in food restricted SN LepR-Gq mice (n=6). Mean ± SEM. *p<0.05, ***p<0.001.

SN LepR on anxiety-like behavior. To test for anxiety-like behavior, we examined behavior in the elevated plus maze (EPM) for 5min. This test is based on the natural aversion of mice to brightly lit, open and elevated spaces and we therefore report time spent in the avoided part of the EPM, i.e. the brightly lit and elevated open arms. Chemogenetic activation of VTA LepR or SN LepR in food restricted mice did not affect the amount of time spent in the open arm of the EPM (**Figure 9**). Although we increased the time between 2 test days to 3 weeks, anxiety-like behavior may be reduced with repeated exposure to the tasks, so we also analyzed individual test days. However, we did not observe reduced anxiety-like behavior on the second test day. When analyzing the data from the first test day only (comparing between subjects effects), we found no effect of CNO either (data not shown).

DISCUSSION

Leptin suppresses feeding, locomotion, anxiety and motivation to obtain food (15, 20, 28, 35). As the midbrain dopamine system has been implicated in these behaviors as well, we here addressed whether selective chemogenetic activation of leptin receptor expressing midbrain neurons modulated feeding, locomotion, anxiety and motivation. As we confirmed in this study, leptin

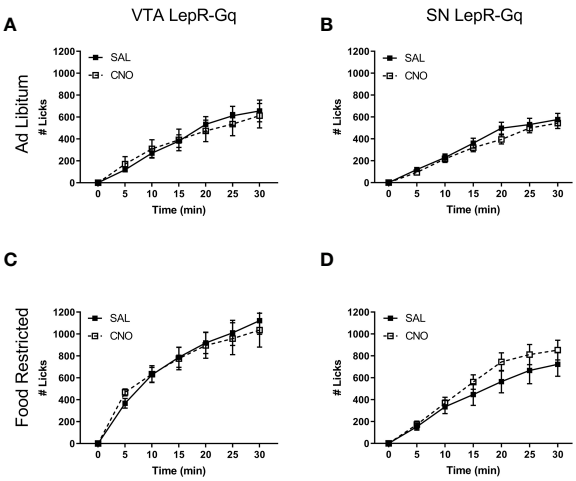

FIGURE 6 | Free 20% sucrose solution consumption upon chemogenetic activation of VTA LepR or SN LepR neurons. CNO (1.0mg/kg) did not affect sucrose solution consumption in ad libitum fed **(A)** VTA LepR-Gq (n=6) and **(B)** SN LepR- Gq (n=6) or food restricted **(C)** VTA LepR-Gq (n=6) and **(D)** SN LepR-Gq (n=6). Mean ± SEM.

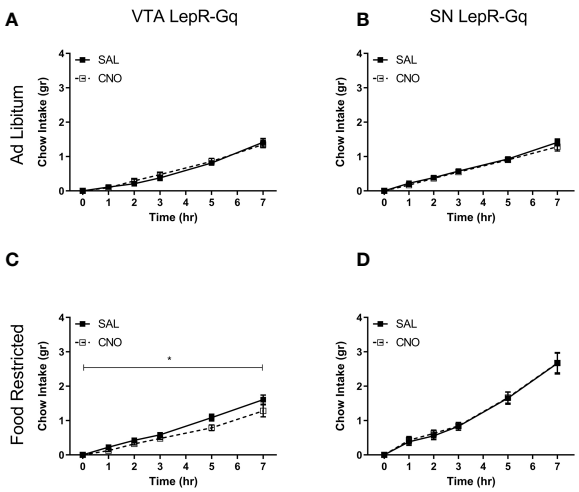

FIGURE 7 | Consumption of chow upon chemogenetic activation of VTA LepR or SN LepR neurons. Chow intake was not affected by CNO (1.0mg/kg) injections in ad libitum fed **(A)** VTA LepR-Gq (n=6) or **(B)** SN LepR-Gq mice (n=6). **(C)** CNO decreased cumulative chow intake in food restricted VTA LepR-Gq mice (n=6). **(D)** CNO did not affect feeding in food restricted SN LepR-Gq mice (n=6). Mean ± SEM. *p<0.05.

receptors are expressed on a subset of VTA and SN neurons. Chemogenetic activation of VTA LepR neurons modulated motivation and feeding, whereas activation of SN LepR neurons modulated locomotion. Activation of neither population altered anxiety-like behavior.

Chemogenetic activation of VTA LepR neurons decreased motivational behavior for food reward. The decrease in motivation was a surprising result as most VTA LepR and SN LepR neurons are DAergic. Increased midbrain DA activity is associated with enhanced motivation (12–14) and chemogenetic activation of VTA DA neurons increases motivation (33). Contrary to our hypotheses, our findings support VTA LepR. A previous study found no effect of leptin infusion into the VTA on motivation in a operant responding task of ad libitum fed rats (21). However the lack of an effect in the study by Davis et al. may be due to the facts that these animals were ad libitum fed. Ad libitum animals have more fat than food restricted animals. Since leptin levels correlate with body fat (3, 5), endogenous leptin levels have been found elevated in ad libitum fed compared to food-restricted animals (5). Thus in ad libitum fed rats endogenous leptin levels are high and may have masked the effect of intra-VTA leptin on motivation. As we found a decrease in motivation by chemogenetically activating LepR-VTA neurons, VTA DA-LepR neurons, most of which project to the amygdala (18), not likely play a role in motivation for food reward. VTA GABA neurons are known to provide local

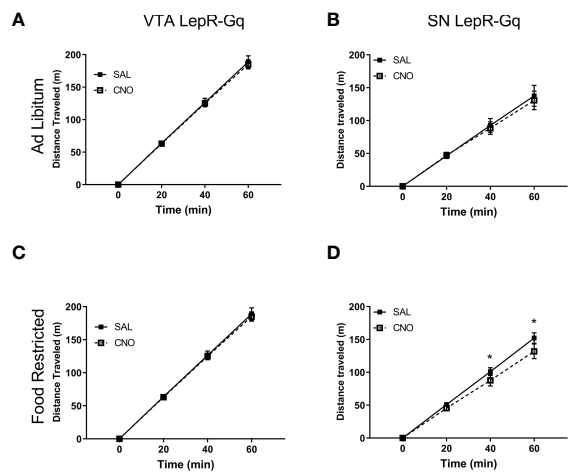

FIGURE 8 | Locomotor activity upon chemogenetic activation of VTA LepR or SN LepR neurons. Locomotion was not affected by CNO (1.0mg/kg) injections in ad libitum fed **(A)** VTA LepR-Gq (n=6) and **(B)** SN LepR-Gq (n=6) or **(C)** food restricted VTA LepR-Gq mice (n=6). **(D)** CNO decreased locomotion in food restricted SN LepR-Gq mice (n=6). Mean ± SEM. *p<0.05.

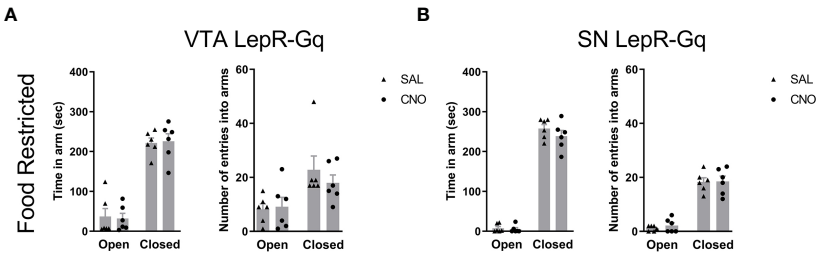

FIGURE 9 | Anxiety-like behavior upon chemogenetic activation of VTA LepR or SN LepR neurons. Anxiety-like behavior in the EPM was not affected by CNO (1.0mg/kg) VTA LepR-Gq (n=6) **(A)** and SN LepR-Gq (n=6) **(B)** injected mice.

inhibition of DA neurons and modulate reward behavior (36). One interpretation of our results is, therefore, that decreased motivation is the result of chemogenetic activation of VTA GABA-LepR neurons that reduce VTA DA activity. Indeed, it was recently found using optogenetic-assisted circuit mapping that VTA GABA neurons expressing the leptin receptor are activated by leptin and directly inhibit VTA DA neurons (37). Similarly, inhibitory input from the lateral hypothalamus to the VTA was shown to inhibit GABA neurons and increase dopamine release in the nucleus accumbens (38, 39). Thus by activating VTA GABA neurons as we have done, one would expect a decrease in motivational behavior in line with our results.

Our data further show that activating LepR neurons in the VTA decreased feeding in food restricted mice. Although the decrease in our study is minimal, this finding is in line with previous studies that reported decreased feeding upon intra-VTA leptin injections (15, 24, 40–42). Interestingly, previous studies reports suggest that non-DA neurons of the VTA mediate leptin effects on feeding: strategies targeting only DA LepR neurons, i.e. LepR deletion in DAT neurons (28) or STAT3 deletion in DAT neurons (27), did not affect feeding and mice with STAT3 deletion in DAT neurons remained responsive to leptin's anorexic effect upon intra-VTA leptin infusions (27). Evenmore, a recent study showed that inhibition of VTA-GABA neurons decreased regular chow intake (43). Our data therefore support the idea that VTA GABA-LepR neurons, like VTA-GABA neurons, modulate feeding, as the decrease in feeding in our experiments is most likely mediated by the activation of these inhibitory neurons.

Given that most SN LepR neurons are DA neurons and chemogenetic activation of SN DA neurons increased locomotion (33), it was unexpected to find that activating SN LepR neurons decreased locomotion. An explanation for this could lie in the fact that only 15% of SN dopaminergic contain LepR and that 10% of SN-LepR neurons are also non-dopaminergic. This suggests that activation of this relatively low amount of DA neurons in the SN is not sufficient to increase locomotion, and also that the few inhibitory SN LepR neurons reduce locomotion. Furthermore, we found no effect of VTA LepR activation on locomotion. However, increased locomotion observed after LepR knockdown in VTA neurons (15) or loss of STAT3 in VTA DA neurons (27) suggest that VTA DA neurons that express LepR modulate locomotion. Similar to the explanation for SN neurons, perhaps activating a low amount of VTA DA neurons was similarly not sufficient to modulate locomotion.

We did not observe changes in anxiety-like behavior upon chemogenetic activation of VTA LepR. However, previous studies report that leptin reduces anxiety by inhibition of VTA DA-LepR neurons that project to the extended central amygdala (18, 20, 28). Furthermore, increased anxiety was seen after deletion of LepR in DA neurons and this was accompanied by increased burst firing of VTA DA neurons (28). Other studies have also suggested that burst firing in VTA DA neurons results in anxiogenic behaviour (44, 45). Together, these results suggest that chemogenetic activation of VTA LepR neurons did not activate VTA DA neurons to the extent of burst firing that is capable of increasing anxiety.

Interestingly, behavioral effects of chemogenetic activation of VTA LepR or SN LepR were only observed in food restricted mice, which have lowered leptin levels (35). As such, we assume that the neurons responsible for changing behavior show decreased activity when leptin levels are low. Since neuronal stimulation resulted in the reduction of the behavior tested, the observed effects were likely driven by the activation of inhibitory non-DA neurons in the VTA or SN, such as GABA neurons. Together, this suggests that GABA neurons mediated the observed reductions in behavior and that GABA neurons are less active with lower leptin levels. Therefore, we propose that leptin stimulates activity of these LepR neurons to contribute to the suppression of motivation, feeding and locomotion. Future studies will be needed to verify this.

There are limitations to the interpretation of the results. The number of mice used in the studies was limited with groups sizes of 6 mice and we performed most experiments with a single dose of CNO. As control for off-target effects of CNO we used mice that expressed a fluorescent protein (channelrhodopsin) not activated by CNO. We cannot exclude that larger group sizes, more doses of CNO or the use of other DREADD receptor ligands for which no off-target effects have been reported would result in unmasking roles of midbrain leptin receptor neurons in the assays we used. Therefore we hope that this study inspires others to replicate and extend our findings.

To conclude, our results show that activating SN LepR neurons decreased locomotion and activating VTA LepR neurons decreased feeding and motivation for food reward. Although both SN LepR and VTA LepR neurons are predominantly DA neurons, which are inhibited by leptin, the effects described here support involvement of inhibitory non-DA neurons in feeding, locomotion and food reward. This is an open question that needs to be addressed to more fully understand the mechanism underlying leptin's effect on motivation for food reward.

DATA AVAILABILITY STATEMENT

The original contributions presented in the study are included in the article/**Supplementary Material**. Further inquiries can be directed to the corresponding author.

ETHICS STATEMENT

The animal study was reviewed and approved by Animal Welfare Body Utrecht Nieuw Gildestein, room 1.81 Bolognalaan 50 3584 CJ Utrecht Phone: (030) 253 15 69 E-mail: info@ivd-utrecht.nl Website: www.ivd-utrecht.nl.

AUTHOR CONTRIBUTIONS

AO performed histology and confocal imaging. VV performed behavioral experiments, histology, and data analysis. ML-B performed stereotaxic virus/implant surgeries. LS and AR contributed to behavioral experiments. RA designed the experiments and wrote the manuscript with inputs from all authors. All authors contributed to the article and approved the submitted version.

FUNDING

This research was supported by the European Union Seventh Framework Programme (grant agreement number 607310; Nudge-it), by the Netherlands Organisation for Scientific Research (grant number ALWOP.137) and by the Swedish Research Council (2018-02588).

SUPPLEMENTARY MATERIAL

The Supplementary Material for this article can be found online at: https://www.frontiersin.org/articles/10.3389/fendo.2021.680494/full#supplementary-material

REFERENCES

1. la Fleur SE, Vanderschuren LJMJ, Luijendijk MC, Kloeze BM, Tiesjema B, Adan RAH. A Reciprocal Interaction Between Food-Motivated Behavior and Diet-Induced Obesity. *Int J Obes* (2007) 31(8):1286–94. doi: 10.1038/sj.ijo.0803570
2. Pickering C, Alsiö J, Hulting A-L, Schiöth HB. Withdrawal From Free-Choice High-Fat High-Sugar Diet Induces Craving Only in Obesity-Prone Animals. *Psychopharmacol (Berl)* (2009) 204(3):431–43. doi: 10.1007/s00213-009-1474-y
3. Frederich RC, Hamann A, Anderson S, Löllmann B, Lowell BB, Flier JS. Leptin Levels Reflect Body Lipid Content in Mice: Evidence for Diet-Induced Resistance to Leptin Action. *Nat Med* (1995) 1(12):1311–4. doi: 10.1038/nm1295-1311
4. Masuzaki H, Ogawa Y, Isse N, Satoh N, Okazaki T, Shigemoto M, et al. Human Obese Gene Expression. Adipocyte-Specific Expression and Regional Differences in the Adipose Tissue. *Diabetes* (1995) 44(7):855–8. doi: 10.2337/diabetes.44.7.855
5. Maffei M, Halaas J, Ravussin E, Pratley RE, Lee GH, Zhang Y, et al. Leptin Levels in Human and Rodent: Measurement of Plasma Leptin and Ob RNA in Obese and Weight-Reduced Subjects. *Nat Med* (1995) 1(11):1155–61. doi: 10.1038/nm1195-1155
6. Halaas JL, Gajiwala KS, Maffei M, Cohen SL, Chait BT, Rabinowitz D, et al. Weight-Reducing Effects of the Plasma Protein Encoded by the Obese Gene. *Science* (1995) 269(5223):543–6. doi: 10.1126/science.7624777
7. Brown JA, Bugescu R, Mayer TA, Gata-Garcia A, Kurt G, Woodworth HL, et al. Loss of Action *Via* Neurotensin-Leptin Receptor Neurons Disrupts Leptin and Ghrelin-Mediated Control of Energy Balance. *Endocrinology* (2017) 158(5):1271–88. doi: 10.1210/en.2017-00122
8. Sharma S, Hryhorczuk C, Fulton S. Progressive-Ratio Responding for Palatable High-Fat and High-Sugar Food in Mice. *J Vis Exp* (2012) (63):e3754. doi: 10.3791/3754
9. Woodworth HL, Batchelor HM, Beekly BG, Bugescu R, Brown JA, Kurt G, et al. Neurotensin Receptor-1 Identifies a Subset of Ventral Tegmental Dopamine Neurons That Coordinates Energy Balance. *Cell Rep* (2017) 20(8):1881–92. doi: 10.1016/j.celrep.2017.08.001
10. Hinkle W, Cordell M, Leibel R, Rosenbaum M, Hirsch J. Effects of Reduced Weight Maintenance and Leptin Repletion on Functional Connectivity of the Hypothalamus in Obese Humans. *PloS One* (2013) 8(3):e59114. doi: 10.1371/journal.pone.0059114
11. Rosenbaum M, Sy M, Pavlovich K, Leibel RL, Hirsch J. Leptin Reverses Weight Loss–Induced Changes in Regional Neural Activity Responses to Visual Food Stimuli. *J Clin Invest* (2008) 118(7):2583–91. doi: 10.1172/JCI35055
12. Ilango A, Kesner AJ, Keller KL, Stuber GD, Bonci A, Ikemoto S. Similar Roles of Substantia Nigra and Ventral Tegmental Dopamine Neurons in Reward and Aversion. *J Neurosci* (2014) 34(3):817–22. doi: 10.1523/JNEUROSCI.1703-13.2014
13. Rossi MA, Sukharnikova T, Hayrapetyan VY, Yang L, Yin HH. Operant Self-Stimulation of Dopamine Neurons in the Substantia Nigra. *PloS One* (2013) 8(6):e65799. doi: 10.1371/journal.pone.0065799
14. Wise RA. Roles for Nigrostriatal–Not Just Mesocorticolimbic–Dopamine in Reward and Addiction. *Trends Neurosci* (2009) 32(10):517–24. doi: 10.1016/j.tins.2009.06.004
15. Hommel JD, Trinko R, Sears RM, Georgescu D, Liu ZW, Gao XB, et al. Leptin Receptor Signaling in Midbrain Dopamine Neurons Regulates Feeding. *Neuron* (2006) 51(6):801–10. doi: 10.1016/j.neuron.2006.08.023
16. van der Plasse G, van Zessen R, Luijendijk MCM, Erkan H, Stuber GD, Ramakers GMJ, et al. Modulation of Cue-Induced Firing of Ventral Tegmental Area Dopamine Neurons by Leptin and Ghrelin. *Int J Obes* (2015) 39(12):1742–9. doi: 10.1038/ijo.2015.131
17. Figlewicz DP, Evans SB, Murphy J, Hoen M, Baskin DG. Expression of Receptors for Insulin and Leptin in the Ventral Tegmental Area/Substantia Nigra (VTA/SN) of the Rat. *Brain Res* (2003) 964(1):107–15. doi: 10.1016/S0006-8993(02)04087-8
18. Leshan RL, Opland DM, Louis GW, Leinninger GM, Patterson CM, Rhodes CJ, et al. Ventral Tegmental Area Leptin Receptor Neurons Specifically Project to and Regulate Cocaine- and Amphetamine-Regulated Transcript Neurons

of the Extended Central Amygdala. *J Neurosci* (2010) 30(16):5713–23. doi: 10.1523/JNEUROSCI.1001-10.2010
19. Fulton S, Pissios P, Manchon RP, Stiles L, Frank L, Pothos EN, et al. Leptin Regulation of the Mesoaccumbens Dopamine Pathway. *Neuron* (2006) 51 (6):811–22. doi: 10.1016/j.neuron.2006.09.006
20. Liu J, Guo M, Lu X-Y. Leptin/LepRb in the Ventral Tegmental Area Mediates Anxiety-Related Behaviors. *Int J Neuropsychopharmacol* (2016) 19(2):pyv115. doi: 10.1093/ijnp/pyv115
21. Davis JF, Choi DL, Schurdak JD, Fitzgerald MF, Clegg DJ, Lipton JW, et al. Leptin Regulates Energy Balance and Motivation Through Action at Distinct Neural Circuits. *Biol Psychiatry* (2011) 69(7):668–74. doi: 10.1016/j.biopsych.2010.08.028
22. Drui G, Carnicella S, Carcenac C, Favier M, Bertrand A, Boulet S, et al. Loss of Dopaminergic Nigrostriatal Neurons Accounts for the Motivational and Affective Deficits in Parkinson's Disease. *Mol Psychiatry* (2014) 19(3):358–67. doi: 10.1038/mp.2013.3
23. Saunders BT, Richard JM, Margolis EB, Janak PH. Dopamine Neurons Create Pavlovian Conditioned Stimuli With Circuit-Defined Motivational Properties. *Nat Neurosci* (2018) 21(8):1072–83. doi: 10.1038/s41593-018-0191-4
24. Trinko R, Gan G, Gao X-B, Sears RM, Guarnieri DJ, DiLeone RJ. Erk1/2 Mediates Leptin Receptor Signaling in the Ventral Tegmental Area. *PloS One* (2011) 6(11):e27180. doi: 10.1371/journal.pone.0027180
25. Scarpace PJ, Matheny M, Kirichenko N, Gao YX, Tümer N, Zhang Y. Leptin Overexpression in VTA Trans-Activates the Hypothalamus Whereas Prolonged Leptin Action in Either Region Cross-Desensitizes. *Neuropharmacology* (2013) 65:90–100. doi: 10.1016/j.neuropharm.2012.09.005
26. Matheny M, Strehler KYE, King M, Tumer N, Scarpace PJ. Targeted Leptin Receptor Blockade: Role of Ventral Tegmental Area and Nucleus of the Solitary Tract Leptin Receptors in Body Weight Homeostasis. *J Endocrinol* (2014) 222(1):27–41. doi: 10.1530/JOE-13-0455
27. Fernandes MFA, Matthys D, Hryhorczuk C, Sharma S, Mogra S, Alquier T, et al. Leptin Suppresses the Rewarding Effects of Running *Via* STAT3 Signaling in Dopamine Neurons. *Cell Metab* (2015) 22(4):741–9. doi: 10.1016/j.cmet.2015.08.003
28. Liu J, Perez SM, Zhang W, Lodge DJ, Lu XY. Selective Deletion of the Leptin Receptor in Dopamine Neurons Produces Anxiogenic-Like Behavior and Increases Dopaminergic Activity in Amygdala. *Mol Psychiatry* (2011) 16 (10):1024–38. doi: 10.1038/mp.2011.36
29. Murakami T, Enjoji M, Koyama S. Leptin Attenuates D_2 Receptor-Mediated Inhibition of Putative Ventral Tegmental Area Dopaminergic Neurons. *Physiol Rep* (2018) 6(7):e13631. doi: 10.14814/phy2.13631
30. Richardson NR, Roberts DC. Progressive Ratio Schedules in Drug Self-Administration Studies in Rats: A Method to Evaluate Reinforcing Efficacy. *J Neurosci Methods* (1996) 66(1):1–11. doi: 10.1016/0165-0270(95)00153-0
31. Schneider P, Ho Y-J, Spanagel R, Pawlak CR. A Novel Elevated Plus-Maze Procedure to Avoid the One-Trial Tolerance Problem. *Front Behav Neurosci* (2011) 5:43. doi: 10.3389/fnbeh.2011.00043
32. Scott MM, Lachey JL, Sternson SM, Lee CE, Elias CF, Friedman JM, et al. Leptin Targets in the Mouse Brain. *J Comp Neurol* (2009) 514(5):518–32. doi: 10.1002/cne.22025
33. Boekhoudt L, Omrani A, Luijendijk MCM, Wolterink-Donselaar IG, Wijbrans EC, van der Plasse G, et al. Chemogenetic Activation of Dopamine Neurons in the Ventral Tegmental Area, But Not Substantia Nigra, Induces Hyperactivity in Rats. *Eur Neuropsychopharmacol* (2016) 26(11):1784–93. doi: 10.1016/j.euroneuro.2016.09.003
34. Manvich DF, Webster KA, Foster SL, Farrell MS, Ritchie JC, Porter JH, et al. The DREADD Agonist Clozapine N-Oxide (CNO) Is Reverse-Metabolized to Clozapine and Produces Clozapine-Like Interoceptive Stimulus Effects in Rats and Mice. *Sci Rep* (2018) 8(1):3840. doi: 10.1038/s41598-018-22116-z
35. Ahima RS, Prabakaran D, Flier JS. Postnatal Leptin Surge and Regulation of Circadian Rhythm of Leptin by Feeding. Implications for Energy Homeostasis and Neuroendocrine Function. *J Clin Invest* (2018) 101(5):1020–7. doi: 10.1172/JCI1176
36. Creed MC, Ntamati NR, Tan KR. Vta GABA Neurons Modulate Specific Learning Behaviors Through the Control of Dopamine and Cholinergic Systems. *Front Behav Neurosci* (2014) 8:8. doi: 10.3389/fnbeh.2014.00008
37. Omrani A, de Vrind VAJ, Lodder B, Stoltenborg I, Kooij K, Wolterink-Donselaar IG, et al. Identification of Novel Neurocircuitry Through Which Leptin Targets Multiple Inputs to the Dopamine System to Reduce Food Reward Seeking. *Biol Psychiatry* (2021) [in press]. doi: 10.1016/j.biopsych.2021.02.017
38. Nieh EH, Vander Weele CM, Matthews GA, Presbrey KN, Wichmann R, Leppla CA, et al. Inhibitory Input From the Lateral Hypothalamus to the Ventral Tegmental Area Disinhibits Dopamine Neurons and Promotes Behavioral Activation. *Neuron* (2016) 90(6):1286–98. doi: 10.1016/j.neuron.2016.04.035
39. Schiffino FL, Siemian JN, Petrella M, Laing BT, Sarsfield S, Borja CB, et al. Activation of a Lateral Hypothalamic-Ventral Tegmental Circuit Gates Motivation. *PloS One* (2019) 14(7):e0219522. doi: 10.1371/journal.pone.0219522
40. Bruijnzeel AW, Qi X, Corrie LW. Anorexic Effects of intra-VTA Leptin are Similar in Low-Fat and High-Fat-Fed Rats But Attenuated in a Subgroup of High-Fat-Fed Obese Rats. *Pharmacol Biochem Behav* (2013) 103(3):573–81. doi: 10.1016/j.pbb.2012.10.012
41. Bruijnzeel AW, Corrie LW, Rogers JA, Yamada H. Effects of Insulin and Leptin in the Ventral Tegmental Area and Arcuate Hypothalamic Nucleus on Food Intake and Brain Reward Function in Female Rats. *Behav Brain Res* (2011) 219(2):254–64. doi: 10.1016/j.bbr.2011.01.020
42. Morton GJ, Blevins JE, Kim F, Matsen M, Figlewicz DP. The Action of Leptin in the Ventral Tegmental Area to Decrease Food Intake Is Dependent on Jak-2 Signaling. *Am J Physiol Endocrinol Metab* (2009) 297(1):E202–10. doi: 10.1152/ajpendo.90865.2008
43. Chen L, Lu YP, Chen HY, Huang SN, Guo YR, Zhang JY, et al. Ventral Tegmental Area GABAergic Neurons Induce Anxiety-Like Behaviors and Promote Palatable Food Intake. *Neuropharmacology* (2020) 173. doi: 10.1016/j.neuropharm.2020.108114
44. Coque L, Mukherjee S, Cao J-L, Spencer S, Marvin M, Falcon E, et al. Specific Role of VTA Dopamine Neuronal Firing Rates and Morphology in the Reversal of Anxiety-Related, But Not Depression-Related Behavior in the ClockΔ19 Mouse Model of Mania. *Neuropsychopharmacology* (2011) 36 (7):1478–88. doi: 10.1038/npp.2011.33
45. Sagheddu C, Aroni S, De Felice M, Lecca S, Luchicchi A, Melis M, et al. Enhanced Serotonin and Mesolimbic Dopamine Transmissions in a Rat Model of Neuropathic Pain. *Neuropharmacology* (2015) 97:383–93. doi: 10.1016/j.neuropharm.2015.06.003

Conflict of Interest: The authors declare that the research was conducted in the absence of any commercial or financial relationships that could be construed as a potential conflict of interest.

frontiers in Endocrinology

ORIGINAL RESEARCH
published: 09 July 2021
doi: 10.3389/fendo.2021.694162

Neuropeptide Y Plays an Important Role in the Relationship Between Brain Glucose Metabolism and Brown Adipose Tissue Activity in Healthy Adults: A PET/CT Study

Qiongyue Zhang[1,2†‡], Qing Miao[1†], Yehong Yang[1†], Jiaying Lu[3], Huiwei Zhang[3], Yonghao Feng[1], Wei Wu[1], Xiaoming Zhu[1], Boni Xiang[1], Quanya Sun[1], Yihui Guan[3], Yiming Li[1*], Chuantao Zuo[3*‡] and Hongying Ye[1*‡]*

[1] Division of Endocrinology and Metabolism, Department of Internal Medicine, Huashan Hospital, Shanghai Medical College, Fudan University, Shanghai, China, [2] Shanghai Key Laboratory of Metabolic Remodeling and Health, Institute of Metabolism & Integrative Biology, Fudan University, Shanghai, China, [3] Positron Emission Tomography (PET) Center, Huashan Hospital, Shanghai Medical College, Fudan University, Shanghai, China

Introduction: Brown adipose tissue (BAT) becomes the favorite target for preventing and treating metabolic diseases because the activated BAT can produce heat and consume energy. The brain, especially the hypothalamus, which secretes Neuropeptide Y (NPY), is speculated to regulate BAT activity. However, whether NPY is involved in BAT activity's central regulation in humans remains unclear. Thus, it's essential to explore the relationship between brain glucose metabolism and human BAT activity.

Methods: A controlled study with a large sample of healthy adults used Positron emission tomography/computed tomography (PET/CT) to noninvasively investigate BAT's activity and brain glucose metabolism *in vivo*. Eighty healthy adults with activated BAT according to the PET/CT scan volunteered to be the BAT positive group, while 80 healthy adults without activated BAT but with the same gender, similar age, and BMI, scanning on the same day, were recruited as the control (BAT negative). We use Statistical parametric mapping (SPM) to analyze the brain image data, Picture Archiving & Communication System (PACS), and PET/CT Viewer software to calculate the semi-quantitative values of brain glucose metabolism and BAT activity. ELISA tested the levels of fasting plasma NPY. The multiple linear regression models were used to analyze the correlation between brain glucose metabolism, the level of NPY, and the BAT activity in the BAT positive group.

Results: (1) Compared with controls, BAT positive group showed significant metabolic decreases mainly in the right Insula (BA13a, BA13b) and the right claustrum (uncorrected $P < 0.01$, adjusted BMI). (2) The three brain regions' semi-quantitative values in the BAT positive group were significantly lower than the negative group (all P values < 0.05). (3) After adjusting for age, gender, BMI, and outside temperature, there was a negative correlation between brain metabolic values and BAT activity (all P values < 0.05). However, after further adjusting for NPY level, there were no significant differences between the

OPEN ACCESS

Edited by:
Riccarda Granata,
University of Turin, Italy

Reviewed by:
Paolo Magni,
University of Milan, Italy
Xiaodan Lu,
The People's Hospital of Jilin Province, China

***Correspondence:**
Hongying Ye
yehongying@huashan.org.cn
Chuantao Zuo
zuochuantao@fudan.edu.cn
Yiming Li
yimingli.fudan@gmail.com
Qiongyue Zhang
qiongyue_zhang@fudan.edu.cn

†These authors have contributed equally to this work and share first authorship

‡These authors have contributed equally to this work and share last authorship

Specialty section:
This article was submitted to Neuroendocrine Science, a section of the journal Frontiers in Endocrinology

Received: 12 April 2021
Accepted: 11 June 2021
Published: 09 July 2021

Citation:
Zhang Q, Miao Q, Yang Y, Lu J, Zhang H, Feng Y, Wu W, Zhu X, Xiang B, Sun Q, Guan Y, Li Y, Zuo C and Ye H (2021) Neuropeptide Y Plays an Important Role in the Relationship Between Brain Glucose Metabolism and Brown Adipose Tissue Activity in Healthy Adults: A PET/CT Study. Front. Endocrinol. 12:694162. doi: 10.3389/fendo.2021.694162

BA13b metabolic values and BAT activity (P>0.05), while the correlation between the BA13a metabolic values and BAT activity still was significant (P< 0.05).

Conclusions: Regional brain glucose metabolism is closely related to healthy adults' BAT activity, which may be mediated by NPY.

Keywords: brown adipose tissue, positron-emission tomography and computed tomography, brain glucose metabolism, neuropeptide Y, statistical parametric mapping

INTRODUCTION

Brown adipose tissue (BAT) has been well recognized as a significant thermogenic tissue to maintain the body temperature in rodents and newborn humans because of its high expression of uncoupling protein 1 (UCP1) (1). Besides, recent studies have proved that BAT can be activated and also present in adults, which are detected by ^{18}F-fluorodeoxyglucose (^{18}F-FDG) positron emission tomography/computed tomography (PET/CT) (2, 3). Stimulating BAT activity is expected to be a new approach to treat obesity and other metabolic diseases (4, 5), but the precise regulatory mechanism of BAT activity is still unclear.

The central nervous system (CNS) is the core of regulating energy metabolism, which may be related to heat generation and energy consumption of BAT (6), especially the hypothalamus, which is involved in the regulation of BAT activity (7). The hypothalamus is the center of feeding behavior, body temperature regulation, and metabolism control (8). As the region of information integration in the brain, the insular cortex (Insula) regulates temperature, pain, appetite, and energy metabolism, which has a fibrous connection with the hypothalamus (9). The claustrum is a small region subcortical structure and contiguous the insula. Mammal species studies have shown that there are networks between the insula and claustrum, which may influence many aspects of the brain's function together (10, 11).

Previous invasive methods of studying the structure and function of CNS do not apply to the human body. Emerging molecular functional imaging technology PET/CT is mainly used to diagnose and evaluate tumors, infectious diseases (12), and central nervous system diseases (13), such as lung cancer (14), lymphoma (15), etc. al. Since detection of ^{18}F-FDG uptake is the gold standard for reflecting BAT activity, PET/CT imaging has become the most common platform for investigating the human BAT (16). Studies have shown that PET/CT can not only detect the activity of adult BAT (17), but also evaluate the glucose metabolism in specific brain regions (18) and can noninvasively semi-quantitative analyze the brain structure and function. So far, most PET/CT studies focused on oncology patients (19) or with a small sample (20). In several retrospective studies, the prevalence of activated BAT ranged from 1.3% to 6.7%, while our previous retrospective study found that there were 410 of the 31088 subjects (1.32%) identified by PET/CT scanning as activated BAT (21). In our cross-sectional study, the BAT positive rate was 1.77%(105/5945). Moreover, adults with activated BAT were younger, had lower BMI, higher insulin sensitivity, and better lipid profiles than those without activated BAT positive (22).

In view of many factors, such as disease status, age, gender, temperature, and environment, may affect brain metabolism and BAT activity. Therefore, we adopted the ^{18}F-FDG PET/CT imaging technology and the Statistical Parametric Mapping (SPM) software, enlarged the sample size, and recruited healthy adults who came to the PET center for the purpose of physical examination in order to precisely explore the relationship between the brain glucose metabolism and healthy adult BAT activity. In addition, this controlled study not only analyzed the relationship between brain glucose metabolism and BAT activity but also verified whether the Neuropeptide Y (NPY), which was secreted by the hypothalamus, was involved in brain glucose metabolism to regulate BAT's activity. To provide clues and basis for revealing the mechanism of central regulation of BAT activity.

MATERIALS AND METHODS

Subjects and Workflow

About six thousands of individuals underwent a whole-body imaging scan using ^{18}F-FDG PET/CT in the PET Center of Huashan Hospital Affiliated with Fudan University from September 2009 to March 2011. Eighty healthy adults with activated BAT detected by PET/CT scan were recruited as the BAT positive group after reviewing the medical history, physical examination, and tested fasting blood sample. Each BAT positive subject was matched to a healthy adult without activated BAT detected by PET/CT scan on the same day, with the same gender and similar age (± 5 years). Furthermore, in the BAT positive group, there were 15 subjects who volunteered to stay at thermoneutrality (28°C, two hours, in the climate chamber) and then re-examined PET/CT scan to confirm that BAT was undetected within two weeks, and took a fasting blood test for the level of NPY. All subjects were healthy Chinese adults (aged between 20-50 with BMI < 30), and had no history of diabetes, hypertension, heart disease, severe infection, chronic liver or kidney disease, or cancers, and did not take any regular medications (especially adrenergic receptor blockers, antidepressants, or psychiatric drugs, et al.). Pregnant women and subjects with implantable medical electronic devices should be excluded. The workflow of the study is shown in **Figure 1**. The Ethics Committee approved the study design of Huashan Hospital at Fudan University. All of the subjects volunteered for scientific research and signed informed consent. The trial was already registered at Clinical Trials.gov (NCT01387438).

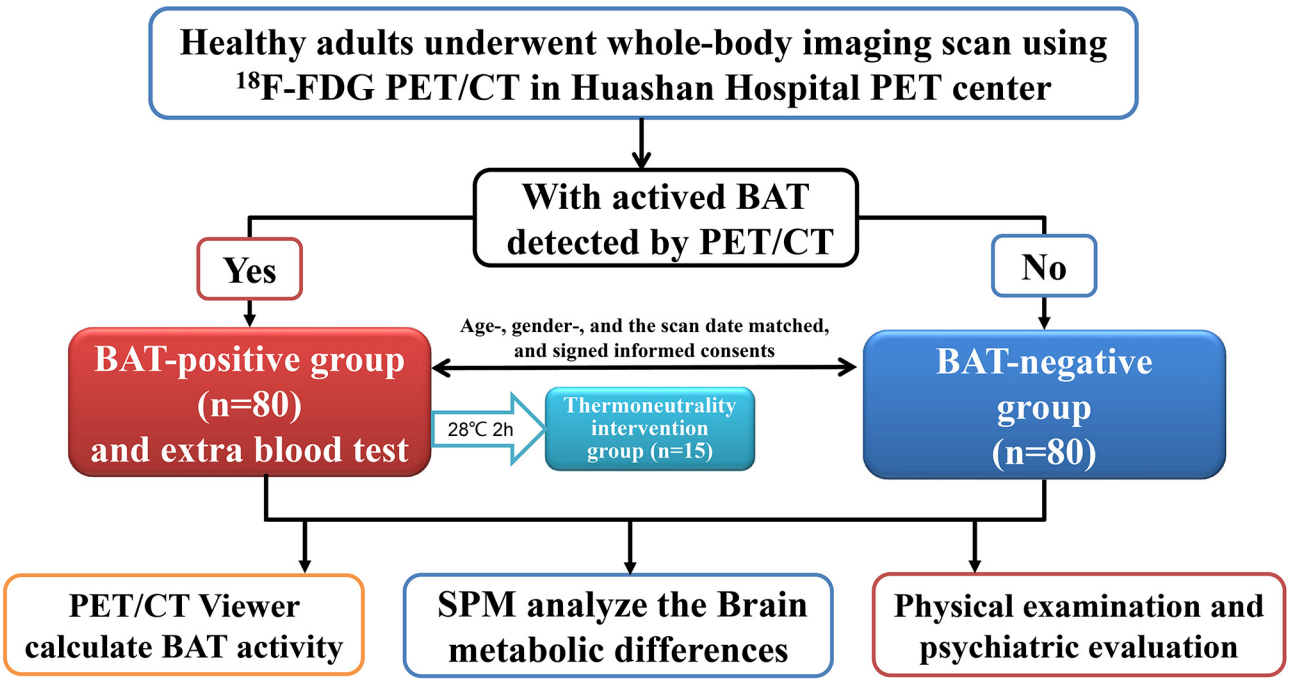

FIGURE 1 | Subjects and Workflow. Flowchart of the PET/CT study: This research is a cross-sectional control study with a large sample. Subjects were divided into two groups according to ^{18}F-FDG uptake of BAT detected by PET-CT. Eighty healthy adults with activated BAT detected by PET/CT scan were recruited as the BAT positive group, while each BAT positive subject was matched to a healthy adult without activated BAT detected by PET/CT scan on the same day, with the same gender, and similar age (± 5 years), who became the BAT negative control group. There were 15 BAT positive subjects who volunteered to stay in thermoneutrality (28°C, two hours), repeat the PET/CT scan, and take a blood test for the NPY level. Every subject performed the whole-body PET/CT scan, the physical examination, and the blood test.

Medical Assessment and Blood Sample Collection

Demographics and clinical data, including age, gender, body mass index (BMI), medical history, medication utilization, diagnosis, and daily average outdoor temperature, were obtained from all subjects (shown in **Table 1**). The blood samples were drawn in the fasting and resting state, and the fast blood glucose (FBG) levels were measured using an automatic biochemical analyzer (Hitachi 7600, Japan) before the PET/CT scan. The concentrations of NPY in the BAT positive group were determined by enzyme-linked immunosorbent assay (Raybiotech, American) after the PET/CT scan. The other medical assessment, such as the heart rate, systolic blood pressure (SBP), diastolic blood pressure (DBP), was performed on the two groups.

TABLE 1 | Characteristics of the subjects with activated BAT (BAT Positive) and without ^{18}F-FDG BAT uptake (BAT Negative)*.

	BAT-Positive group (n = 80)	BAT-Negative group (n = 80)	*P* value†
Demographic features			
Gender (men: women)	20: 60	20: 60	1.000
Age (year)	36.84 ± 6.71	36.90 ± 6.24	0.951
Handedness (R:L:N/A)	78: 1: 1	77: 2: 1	—
Outdoor temperature (°C)	8 (6 – 11)	8 (6 – 11)	1.000
Clinical Characteristics			
BMI (Kg/m^2)	21.06 ± 2.38	21.71 ± 1.83	0.053
SBP (mmHg)	123.13 ± 12.46	122.55 ± 10.38	0.752
DBP (mmHg)	79.79 ± 9.54	81.05 ± 8.62	0.381
Heart rate (beats/min)	72.60 ± 7.34	71.00 ± 6.34	0.142
Fasting glucose (mmol/l)	4.86 ± 0.52	4.82 ± 0.57	0.663

**BAT denotes brown adipose tissue, SBP denotes systolic blood pressure, and DBP denotes diastolic blood pressure. BMI (Body-mass index) is the weight in kilograms divided by the square of the height in meters. The continuous variables of the normal distribution are expressed by mean ± standard deviation, and the continuous variables of non-normal distribution are described by median (quaternary interval P25~P75).*

†P values were obtained by a two-sided test using two independent sample tTest.

PET/CT Scan and Imaging Processing

All subjects fasted for at least 8 hours before performing the whole-body PET/CT scan (PET/CT Biograph 64, SIEMENS) at room temperature, which was maintained at 21~23℃. According to the PET/CT scanning protocol, the PET tracer (^{18}F-FDG) was administered intravenously with a dose of 5.55-7.40MBq/kg. Then the subjects rested for 45 minutes until imaging began. After a CT transmission scan for attenuation correction, PET scans were acquired and reconstructed with the three-dimensional (3D) reprojection method. Commonly, transmission and emission modes are used alternately to scan brain images. The peak voltage was 120kV, the electric current was 300mA, the scanning time for each bed is 1.5 minutes, and the collection time is at least 10 minutes. The body's emission scan was 2 minutes per bed position, and five to six bed positions per subject were needed to cover the BAT areas. Brain PET images were reconstructed by - the ordered subset expectation maximization method and Hanning filtering with matrix 168×168×148 and pixel 2.04mm×2.04mm×1.5mm, giving a transaxial and axial cut-off frequency of 0.5. The Leonardo workstation of Siemens fused the images. Both PET and CT images were reconstructed in transaxial, coronal, and sagittal images with a slice thickness of 3 mm. BAT positive was defined, and BAT activity was calculated according to the standard of Cypess et al. (23): 1) the CT value was adipose tissue (-250 to -50 Hounsfield units), 2) the diameter of the area is greater than 4mm, 3) the maximum of ^{18}F-FDG Standardized uptake value (SUV_{max}) of BAT exceeds 2.0g/ml. All studies in patients and healthy subjects were performed in a resting state in a quiet and dimly lit room.

Statistical Analysis

Image Data Preprocess

SPM8 software was used to analyze the locations of brain regions with different metabolic between the BAT positive and negative groups, and also to measure the glucose metabolism of different brain regions and the semi-quantitative value of BAT's activity. Firstly, PET scans were spatially normalized to Montreal Neurological Institute (MNI) space, by using the default PET template in SPM8 software (Wellcome Department of Imaging Neuroscience, Institute of Neurology, London, UK, Version 8) applied in MATLAB 8.4.0 (Mathworks Inc, Sherborn, MA). Then, in order to increase the signal-to-noise ratio for statistical analysis, the normalized PET scans were smoothed by a Gaussian filter of 10 mm full width at half maximum over a 3D space. Voxel-wise analysis was performed to detect regional differences in mean glucose metabolism between two groups by SPM8 software. A two-sample t-test according to the general linear model at each voxel and the mean signal differences over the whole brain were removed by analysis of covariance in each individual subject. And BMI was included as the covariate. The threshold was set as P<0.01 (uncorrected) over whole brain regions with an extent threshold was empirically chosen to be more than two times of the expected voxels per cluster estimated in the SPM run. Significant regions were localized by Talairach-Daemon software (Research Imaging Center, University of Texas Health Science Center, San Antonio, TX, USA). The SPM map for altered glucose metabolism was overlaid on a standard T1-weighted MRI brain template in stereotaxic space. Next, a spherical volume of interest (VOI), four mm in radius within the image space, centered at the peak voxel of clusters significant in SPM analysis, were constructed to quantify metabolic changes in specific regions (**Figure 2**). We subsequently calculated the individual values of each region as a relative measure of regional cerebral metabolism [VOI value/whole-brain value] using ScAnVP freely available (http://www.feinstein-neuroscience.org at Center for Neuroscience, the Feinstein Institute for Medical Research, Manhasset, NY) in MATLAB.

Clinical Data Analysis

SPSS software (Spss Inc., Chicago, IL, USA, version 20.0) was used to analyze the differences in clinical data and semi-quantitative values of brain regions between the BAT positive and negative groups. The Kolmogorov-Smimov test was performed first. Continuous variables of the normal distribution were described by Means ± standard deviation (SD), and Student's *t*-test was used to compare the differences between the two groups. Data that are not normally distributed are represented as medians (interquartile intervals), and logarithmic conversion is performed before further analysis. Multiple linear regression models were used to analyze the correlation between the semi-quantitative value of brain region and BAT activity and to adjust for possible confounding factors such as age, BMI, gender, outdoor temperature, and the plasma NPY level. All *P* values were two-tailed, and the values less than 0.05 are considered to be statistically significant.

RESULTS

Baseline and Characteristics

A total of 80 healthy subjects with detected BAT by PET-CT scan were enrolled into the BAT-positive group, and 80 subjects with well-matched gender (P=1.000), outdoor temperature (P=1.000), and age (P=0.951) and handedness (P=1.000) without detected BAT by PET-CT scan were served as the BAT negative control group. Clinical characteristics between the two groups, such as BMI (21.06 ± 2.38 *vs.* 21.71 ± 1.83, $P = 0.053$), SBP($P = 0.752$), DBP ($P = 0.381$), heart rate ($P = 0.234$), and FBG ($P = 0.663$) were not statistically different (**Table 1**).

Differences in Brain Glucose Metabolism Between the BAT Positive Group and the BAT Negative Group

The voxel-wise analysis found that there were differences in three brain regions between the BAT positive group and the BAT negative group (**Figure 3**, and **Table 2**). As shown in **Figure 4**, compared with the BAT negative control group, the local glucose metabolic activities of the right Insula (BA13a, Z =3.08), the right Insula (BA13b, Z =3.05), and the right claustrum (Z =3.16) in the BAT positive group were lower (uncorrected P<0.01, threshold K≥321.6 voxels, adjusting for BMI) (**Table 2**). Then, the semi-quantitative values of glucose metabolism in the three different brain regions were further calculated and analyzed as continuous variables, shown in **Table 3**. Compared with BAT negative controls, the BAT positive subjects' semi-quantitative metabolic activities of brain regions in

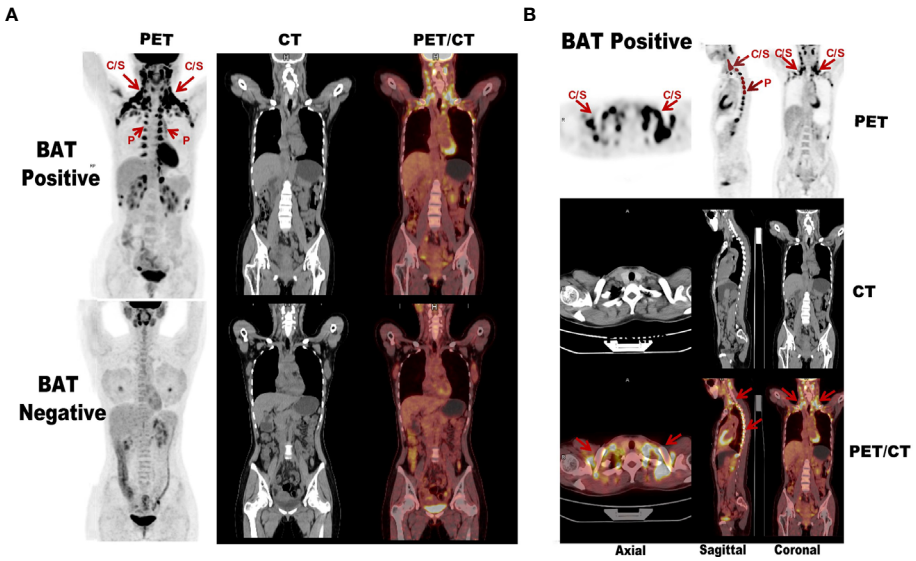

FIGURE 2 | Comparison diagram of subjects with and without activated BAT assessed by ^{18}F-FDG PET/CT. **(A)** The above images shows extended BAT uptake of ^{18}F-FDG in cervical, supraclavicular, axillary, and paravertebral regions in healthy adult. The below images The below image of the other subject with the same gender, similar age and BMI in whom PET/CT was performed in the same day shows no BAT uptake of ^{18}F-FDG in the same regions. **(B)** The subject with activated BAT mainly located in the central axis areas such as the cervical-supraclavicular and paravertebral on the PET maximum intensity projection. "C/S" means cervical/supraclavicular and "P" denotes paravertebral (red arrows).

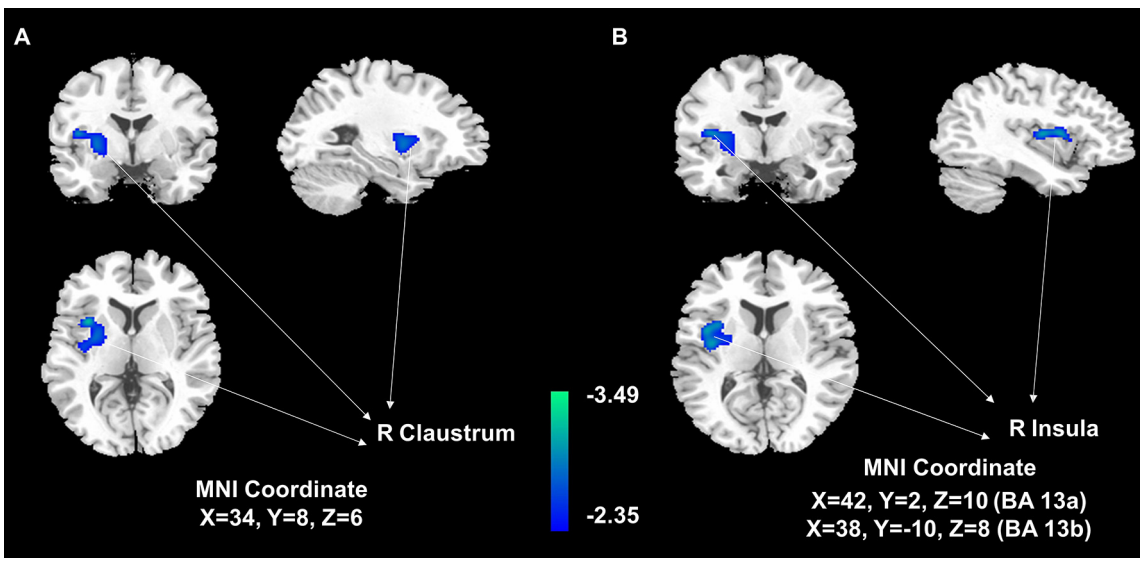

FIGURE 3 | Areas of significant differences of glucose metabolism in subjects with activated BAT, compared with controls. Statistical Parametric Mapping (SPM) results: It is displayed on a T1 template overlaid with magnetic resonance images at the threshold of uncorrected $P<0.01$, threshold K>321.6, and the gray-scale figures are a T1 structural MRI that are representative of MNI space. The blue areas represent relatively hypometabolic regions of decreased ^{18}F-FDG uptake in the right claustrum **(A)** and right Insula **(B)** in BAT-positive subjects than in negative control subjects.

TABLE 2 | Areas of significant differences of glucose metabolism in subjects with activated BAT (BAT-positive group), compared with controls (BAT-negative group)*.

Metabolic change	Cluster Size (mm^3)	T_{max}	Z_{max}	Coordinates			Brain regions
				x	y	z	
Decreased	7864	3.13	3.08	42	2	10	Right Sub-lobar, Insula, Brodmann area 13_a
	7864	3.10	3.05	38	-10	8	Right Sub-lobar, Insula, Brodmann area 13_b
	7864	3.21	3.16	34	8	6	Right Claustrum, Brodmann area/

Coordinates are displayed in MNI standard space. Regions are significant at voxel threshold P < 0.01 (uncorrected, adjusted for BMI), extent threshold =321.6 voxels (2572.8 mm^3).

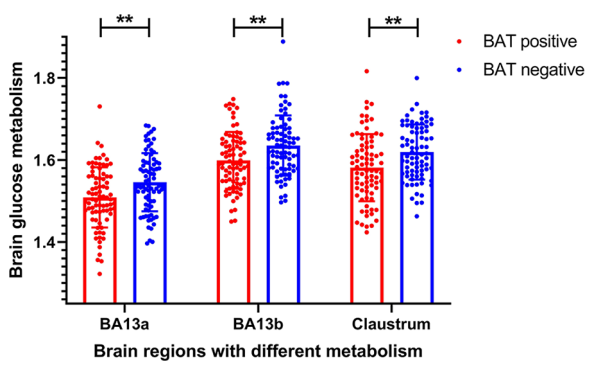

FIGURE 4 | Differences of semi-quantitative metabolic values of brain regions between BAT positive group and BAT negative group. The semi-quantitative metabolic values of three brain region in BAT positive group were significantly lower than these in BAT negative group ($BA13_a$ $P = 0.001$; $BA13_b$ $P = 0.002$; Right claustrum $P = 0.002$). BA denotes the Brodmann area. *P* values are based on Independent-Samples *t*Test. ** denotes *P* value < 0.01.

the right Insula(BA13a, BA13b) and right claustrum were significantly decreased (**Figure 4** and **Table 3**).

Correlation Analysis of Brain Glucose Metabolism and BAT Activity

As shown in **Figure 5**, there was a negative correlation between the BAT activity and the average outdoor temperature on the examination day in the BAT positive group (r = -0.366, P = 0.001). And more importantly, the semi-quantitative values of the three different brain regions were both negatively correlated with BAT Activity in the BAT positive group ($BA13_a$ r = -0.293, P = 0.008; $BA13_b$ r = -0.374, P = 0.001; right claustrum r = -0.279, P = 0.012).

Multiple Linear Regression Analysis of Brain Glucose Metabolism, NPY Level, and BAT Activity

In order to reduce the interference of confounding factors, multiple linear regression models were used to analyze the

TABLE 3 | The semi-quantitative values of brain regions with significant metabolic differences between BAT positive group and BAT negative group*.

Brain region	BAT -positive (n = 80)	BAT-negative (n = 80)	*P* value†
Right Sub-lobar, Insula ($BA13_a$)	1.509 ± 0.008	1.546 ± 0.008	0.001
Right Sub-lobar, Insula ($BA13_b$)	1.599 ± 0.008	1.635 ± 0.008	0.002
Right Claustrum	1.581 ± 0.009	1.619 ± 0.008	0.002

Indicated are mean values ± SE, BA denotes Brodmann area.
†*P values are based on Independent-Samples tTest.*

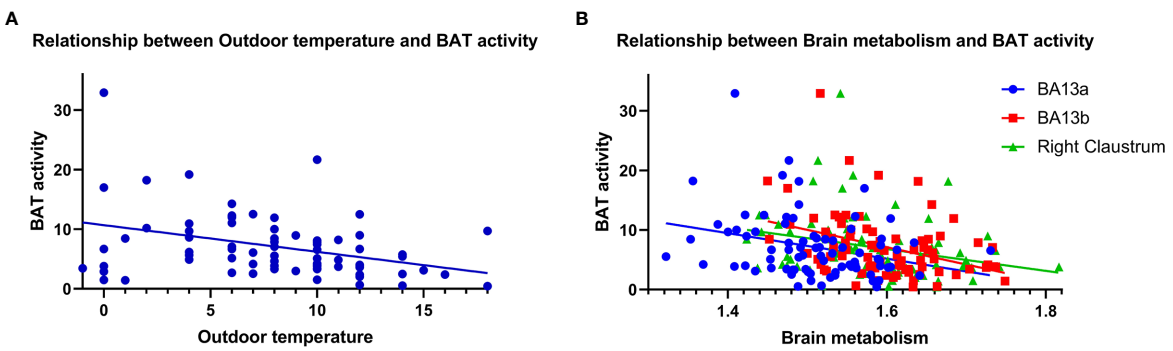

FIGURE 5 | Correlation analysis of brain semi-quantitative metabolism values and average outdoor temperature with BAT activity. BAT activity was negatively correlated with average outdoor temperature [**(A)**, r = -0.366, P = 0.001] and semi-quantitative values of brain metabolism. [**(B)**, BA13a r = -0.293, P = 0.008; BA13b r = -0.374, P = 0.001; right claustrum r = -0.279, P = 0.012].

correlation between variables in the BAT positive group. The BAT activity was taken as the dependent variable, and the semi-quantitative metabolic values of the three brain regions, as well as the plasma NPY level in the BAT positive group, were analyzed as the independent variable.

As shown in **Table 4**, after adjusting for age, gender, BMI, and outside temperature in the regression model 1 and 2, the semi-quantitative metabolic values of right insula and claustrum areas were still significantly negatively correlated with BAT activity. While adjusting for the NPY level in the regression model 3, the correlation between the semi-quantitative values of brain metabolism ($BA13_a$ and right claustrum) and the BAT activity was statistically negative ($P = 0.025$, $P = 0.027$). It was suggested that the correlation between the other brain region's semi-quantitative value and BAT activity was affected by NPY levels. However, NPY level was negatively correlated with BAT activity. This negative correlation was still statistically significant even after adjusting for the three brain regions' semi-quantitative values in the last model ($P < 0.001$), which indicated that the level of NPY was an independent factor affecting BAT activity. The NPY levels of 15 BAT positive subjects were lower than their negative controls', which also increased after thermoneutrality (**Figure 6**).

DISCUSSION

This research carried out a controlled study in healthy people with a large sample size to explore BAT activity's central regulatory mechanism noninvasively and in-vivo and minimizing distractions. Advanced molecular functional imaging PET-CT technology was used to semi-quantitatively analyze the relationship between brain glucose metabolism and BAT activity. Moreover, the plasma NPY level of multiple groups (BAT negative group, BAT positive group, and BAT positive group after thermal neutral intervention) was further detected by Elisa. It provides a new clue to study the central regulatory mechanism of BAT activity.

It is known that the CNS is involved in maintaining energy metabolism and substance metabolism homeostasis, especially the hypothalamus area, which plays an essential role in this process (24). Even though animal studies have shown that knockdown of NPY expression in the dorsomedial hypothalamus could stimulate BAT activity (25), there is no direct evidence that the hypothalamus regulates BAT activity in healthy adults. Our results show apparent metabolic differences in brain regions (such as right insula and claustrum) between BAT positive subjects and their negative controls, but do not show the glucose metabolism values of the hypothalamus region are different between the two groups, which is consistent with the conclusion of the Taiwan study of cancer patients (26). Our research group has also analyzed the changes in brain glucose metabolism in the BAT positive subjects before and after the thermoneutrality intervention, and the metabolic changes in the hypothalamus region were not statistically significant either (18). It may be the hypothalamus region is relatively small, and the PET/CT imaging resolution is limited, so it is difficult to find the area with a difference of less than 2mm. Thus, the possibility of false negatives is likely to exist. The central neuroendocrine regulation is a complex network, and the hypothalamus may play an indirect role through the combination of other fibers or the brain structure.

In this study, SPM8 software and ^{18}F-FDG PET/CT related image analysis software were used to further calculate the three brain regions' semi-quantitative values with metabolic differences and BAT activity. Results show that the semi-quantitative values of the brain regions in the right sub-lobar insula and right claustrum of the BAT positive group were significantly lower than those of the negative group (**Figures 3**, **4** and **Table 3**), which not only analyzed the spatial structure but also semi-quantitatively found that the metabolism of specific brain regions was negatively correlated with BAT activity. These computation results are statistically significant and highly reliable.

TABLE 4 | Multiple linear regression models for associations of brain glucose metabolism and NPY with the activity of BAT*.

Independent Variable	Model	β	Standard error of the coefficient	*t*	*p*
Region1	1	-22.778	8.380	-2.718	0.008
	2	-22.028	7.812	-2.820	0.006
	3†	-15.046	6.585	-2.285	0.025
Region2	1	-30.296	8.353	-3.627	0.001
	2	-29.471	7.754	-3.801	<0.001
	3†	-14.261	7.404	-1.926	0.058
Region3	1	-19.221	7.310	-2.630	0.010
	2	-21.880	6.718	-3.257	0.002
	3†	-13.256	5.872	-2.257	0.027
Lg(NPY)‡	1	-8.331	1.315	-6.334	<0.001
	2	-7.764	1.247	-6.226	<0.001
	3§	-6.815	1.343	-5.074	<0.001

Values of β are regression coefficients; Region 1, 2, 3 denote the semi-quantitative metabolic values of brain regions(BA13a, BA13b, Right Claustrum) respectively; NPY denotes neuropeptide Y; model 1, after adjustment for age, gender, BMI; model 2, after further adjustment for the outside temperature.

†*Model 3, after further adjustment for NPY.*

‡*We used the logarithmic transformation to transform data to the normal distribution and described them as Lg(X) instead of X.*

§*Model 3, after further adjustment for Region1, Region2, Region3.*

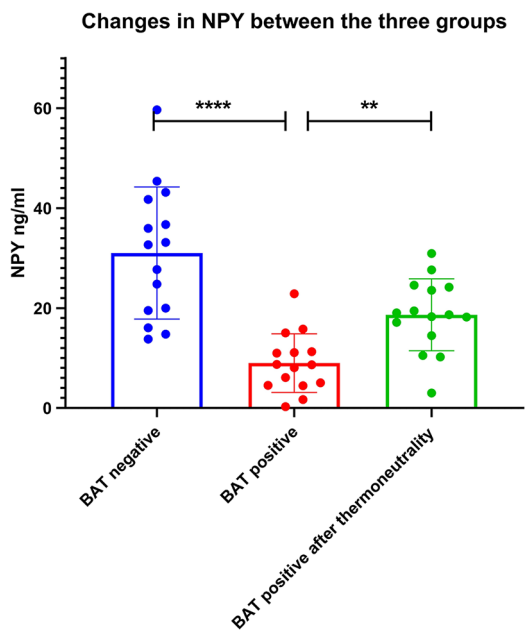

FIGURE 6 | Changes in NPY between the three groups. The NPY levels of 15 BAT positive subjects were lower than their negative controls' ($P < 0.001$), which also increased after thermoneutrality ($P = 0.003$). ** denotes P value < 0.01, **** denotes P value < 0.001.

Confounding factors such as tumor diseases, age, gender, and temperature can directly influence the glucose metabolism of the human brain and the activity of the BAT (23, 27, 28). Therefore, 160 healthy adults were recruited as this research's subjects, whether activated BAT detected by PET/CT scan is divided into BAT positive group and negative control group, in accordance with the 1:1 matching of gender and scan date. Demographic characteristics (such as age, gender, hand dominance, and average outdoor temperature) of the two groups were not significantly different, as well as clinical data (such as blood pressure, heart rate, fasting glucose, and BMI) (**Table 1**).

To further reduce the interference of confounding factors, this study establishes the multivariate linear regression models to adjust for age, gender, BMI, and the average outdoor temperature. Despite adjusting for these factors, the semi-quantitative metabolism values of the right insula and claustrum were still negatively correlated with BAT activity. Nevertheless, after further correction of NPY level, only partial right insula and claustrum metabolism values were significantly negatively correlated with BAT activity. These results indicated that the brain glucose metabolism was closely related to BAT activity, which was not affected by age, gender, BMI, and outdoor temperature, but might be affected by the level of NPY.

Although there was no significant metabolic difference in the hypothalamus region between the two groups, in the multiple linear regression models, the level of NPY was consistently negatively correlated with BAT activity after successively adjusting for age, gender, BMI, outdoor mean temperature, and the semi-quantitative values of the three brain regions. The results of this study highly suggested that the level of hypothalamic neuroendocrine factor NPY was closely related to BAT activity and was not affected by other factors. NPY is made up of 36 amino acids, is one of the most critical neuroendocrine factors, mainly secreted by the hypothalamus, stimulates the appetite. While the permeability of the blood-brain barrier is different between individuals, the hypothalamic arcuate nucleus of NPY content is the most abundant. The circulating NPY level is closely related to the central brain source of NPY and can be integrated into the metabolic response of the central and peripheral nervous systems. Our clinical study revealed that under a fasting state, NPY was negatively correlated with BAT activity, and these brain regions might regulate the activity of BAT through the action of NPY. The NPY levels of 15 BAT positive subjects were lower than their negative controls', which also increased after thermoneutrality intervention. This changing trend of NPY further confirms the negative correlation between NPY and BAT activity.

In this study, the classical Brodmann area (BA) based on the neuroanatomical cellular structure was used to represent the distribution locations of metabolic different brain regions (29). Our study identified the three brain regions of BA13a, BA13b, and right claustrum, which are parts of the right sub-lobar insula and belong to the limbic system. The insula is the only cortex of the human brain hidden deep in the cerebral tissue, in the shape of an inverted triangle, about the size of a "plum". The insular lobe is involved in many physiological processes such as emotional and psychological regulation, visceral and somatosensory, motion control, etc. (30–32). The insular lobe receives physiological signals (such as temperature, visceral sensation, pain, etc.) that the body senses and then integrates information and transmits it to related structures in the brain. The structure and fiber connections around the insula are the material basis for successfully completing the "bridge" work of the insula. The anterior part of the insula is connected to the anterior lobe of the brain and the posterior portion to the temporal and parietal lobes. In addition, the insular lobe can also be closely associated with the surrounding brain tissue through the superior longitudinal tract, hooklike tract, frontal occipital tract, and other white matter fibers (33, 34). Both the insular lobe (which belongs to the cortical structure) and the hypothalamus (which belongs to the subcortical structure) are components of the limbic system and share a common molecular biomarker, limbic system-associate membrane protein (LAMP). It has a unique function in a specific area and also plays a holistic role through a complex network of peripheral structures, fibrous connections, and loops that interact with other tissues in the brain (35).

As the center of body temperature regulation, the hypothalamus can stimulate BAT activity to produce heat through the sympathetic nervous system, and the insula is the signal receiving station and integration center of the body to the external temperature. Therefore, when the human body is stimulated by ambient temperature, the metabolism of the insula region of the cerebral cortex changes, and the integrated signal is transmitted to the hypothalamus through fiber

connections, thereby regulating the thermogenic activity of BAT. However, after the adjustment of outdoor temperature in the multiple linear regression model, it was still found that the metabolism of brain regions was related to BAT activity, suggesting that there were some regulatory mechanisms independent of temperatures, such as mental factors and visceral sensation factors.

There are still some limitations to this study. As a single-center, cross-sectional study, it was observed that glucose metabolism was closely related to BAT activity in some brain regions, but the causal relationship could not be fully explained. Further mechanism studies using transgenic animals are expected. This study focused on the hypothalamic region and NPY, while it is not known that other neuroendocrine factors may be involved in the central regulation of BAT activity. There are still many mysteries in the regulation mechanism of BAT activity, especially in the CNS regulation mechanism. We hope to conduct in-depth research on the mechanism of central regulation of metabolism *in vivo* through micro PET/CT of animals.

CONCLUSION

This study revealed that the glucose metabolism in some brain regions (such as the insula-claustrum region) was closely related to BAT activity, and NPY mostly excreted from the hypothalamus may play an essential role in it. This is a new clue added to the central regulation of energy metabolism, which provides valuable experience for opening up new research methodology.

DATA AVAILABILITY STATEMENT

The data analyzed in this study is subject to the following licenses/restrictions: The data may be related to the privacy of clinical subjects. Requests to access these datasets should be directed to qiongyue_zhang@fudan.edu.cn.

ETHICS STATEMENT

The studies involving human participants were reviewed and approved by the ethics committees of Huashan Hospital, Fudan University in Shanghai. The patients/participants provided their written informed consent to participate in this study.

AUTHOR CONTRIBUTIONS

HY, CZ, QZ, YL, and YY designed this study. QZ, QM, YY, WW, QS, BX, JL, and HZ contributed to the recruitment and conducted experiments. QZ and QM wrote the paper. XZ, YF, JL and HZ analyzed data and revised the article. HY, CZ, YL and YG supervised the study. All authors contributed to the article and approved the submitted version.

FUNDING

This work was supported by grants from the National Key Research and Development Program of China (2019YFA0801900, 2016YFC1305105), the National Natural Science Foundation of China (81800691, 81670751, 81770840, 81971641, and 81671239), China Postdoctoral Science Foundation (2021M690680), the Shanghai Committee of Science and Technology, China (No. 10JC1401002), the Research project of Shanghai Health Commission (2020YJZX0111), Shanghai Municipal Commission of Health and Family Planning (20144Y0070, 20164Y0041), Clinical Research Plan of SHDC (SHDC2020CR1038B).

ACKNOWLEDGMENTS

We sincerely thank the volunteers who participated in this study, the staff from the PET Center at Shanghai Huashan Hospital for facilitating the assessment of subjects, and the Center of Laboratory Medicine Huashan Hospital for their technical assistance.

REFERENCES

1. Cannon B, Nedergaard J. Brown Adipose Tissue: Function and Physiological Significance. *Physiol Rev* (2004) 84(1):277–359. doi: 10.1152/physrev.00015.2003
2. van Marken Lichtenbelt WD, Vanhommerig JW, Smulders NM, Drossaerts JM, Kemerink GJ, Bouvy ND, et al. Cold-Activated Brown Adipose Tissue in Healthy Men. *N Engl J Med* (2009) 360(15):1500–8. doi: 10.1056/NEJMoa0808718
3. Virtanen KA, Lidell ME, Orava J, Heglind M, Westergren R, Niemi T, et al. Functional Brown Adipose Tissue in Healthy Adults. *N Engl J Med* (2009) 360 (15):1518–25. doi: 10.1056/NEJMoa0808949
4. Farmer SR. Obesity: Be Cool, Lose Weight. *Nature* (2009) 458(7240):839–40. doi: 10.1038/458839a
5. Seale P, Lazar MA. Brown Fat in Humans: Turning Up the Heat on Obesity. *Diabetes* (2009) 58(7):1482–4. doi: 10.2337/db09-0622
6. Whittle AJ, López M, Vidal-Puig A. Using Brown Adipose Tissue to Treat Obesity - the Central Issue. *Trends Mol Med* (2011) 17(8):405–11. doi: 10.1016/j.molmed.2011.04.001
7. Waterson MJ, Horvath TL. Neuronal Regulation of Energy Homeostasis: Beyond the Hypothalamus and Feeding. *Cell Metab* (2015) 22(6):962–70. doi: 10.1016/j.cmet.2015.09.026
8. Henningsen JB, Scheele C. Brown Adipose Tissue: A Metabolic Regulator in a Hypothalamic Cross Talk? *Annu Rev Physiol* (2021) 83:279–301. doi: 10.1146/annurev-physiol-032420-042950
9. Livneh Y, Ramesh RN, Burgess CR, Levandowski KM, Madara JC, Fenselau H, et al. Homeostatic Circuits Selectively Gate Food Cue Responses in Insular Cortex. *Nature* (2017) 546(7660):611–6. doi: 10.1038/nature22375
10. Qadir H, Krimmel SR, Mu C, Poulopoulos A, Seminowicz DA, Mathur BN. Structural Connectivity of the Anterior Cingulate Cortex, Claustrum, and the Anterior Insula of the Mouse. *Front Neuroanat* (2018) 12:100. doi: 10.3389/fnana.2018.00100
11. Reser D, Picard F. Editorial: Structure and Function of the Insula-Claustrum Region. *Front Neuroanat* (2020) 14:14. doi: 10.3389/fnana.2020.00014
12. Steinberg J, Thomas A, Iravani A. F-Fluorodeoxyglucose PET/CT Findings in a Systemic Inflammatory Response Syndrome After COVID-19 Vaccine. *Lancet (London England)* (2021) 397(10279):e9. doi: 10.1016/S0140-6736(21)00464-5
13. Rusthoven CG, Doebele RC. Management of Brain Metastases in ALK-Positive Non-Small-Cell Lung Cancer. *J Clin Oncol* (2016) 34(24):2814–9. doi: 10.1200/JCO.2016.67.2410
14. Fischer B, Lassen U, Mortensen J, Larsen S, Loft A, Bertelsen A, et al. Preoperative Staging of Lung Cancer With Combined PET-CT. *New Engl J Med* (2009) 361(1):32–9. doi: 10.1056/NEJMoa0900043

15. Johnson P, Federico M, Kirkwood A, Fosså A, Berkahn L, Carella A, et al. Adapted Treatment Guided by Interim Pet-CT Scan in Advanced Hodgkin's Lymphoma. *New Engl J Med* (2016) 374(25):2419–29. doi: 10.1056/NEJMoa1510093
16. Chen KY, Cypess AM, Laughlin MR, Haft CR, Hu HH, Bredella MA, et al. Brown Adipose Reporting Criteria in Imaging Studies (BARCIST 1.0): Recommendations for Standardized Fdg-Pet/Ct Experiments in Humans. *Cell Metab* (2016) 24(2):210–22. doi: 10.1016/j.cmet.2016.07.014
17. Kim K, Huang S, Fletcher LA, O'Mara AE, Tal I, Brychta RJ, et al. Whole Body and Regional Quantification of Active Human Brown Adipose Tissue Using 18f-FDG Pet/Ct. *J Vis Exp* (2019) 146. doi: 10.3791/58469
18. Miao Q, Zhao XL, Zhang QY, Zhang ZY, Guan YH, Ye HY, et al. Stability in Brain Glucose Metabolism Following Brown Adipose Tissue Inactivation in Chinese Adults. *AJNR Am J Neuroradiol* (2012) 33(8):1464–9. doi: 10.3174/ajnr.A3006
19. Pace L, Nicolai E, Basso L, Garbino N, Soricelli A, Salvatore M. Brown Adipose Tissue in Breast Cancer Evaluated by [(18)F] FDG-PET/CT. *Mol Imaging Biol* (2020) 22(4):1111–5. doi: 10.1007/s11307-020-01482-z
20. Fischer JGW, Maushart CI, Becker AS, Muller J, Madoerin P, Chirindel A, et al. Comparison of [(18)F]FDG PET/CT With Magnetic Resonance Imaging for the Assessment of Human Brown Adipose Tissue Activity. *EJNMMI Res* (2020) 10(1):85. doi: 10.1186/s13550-020-00665-7
21. Zhang Z, Cypess AM, Miao Q, Ye H, Liew CW, Zhang Q, et al. The Prevalence and Predictors of Active Brown Adipose Tissue in Chinese Adults. *Eur J Endocrinol* (2014) 170(3):359–66. doi: 10.1530/EJE-13-0712
22. Zhang Q, Ye H, Miao Q, Zhang Z, Wang Y, Zhu X, et al. Differences in the Metabolic Status of Healthy Adults With and Without Active Brown Adipose Tissue. *Wiener Klin Wochenschrift* (2013) 125(21-22):687–95. doi: 10.1007/s00508-013-0431-2
23. Cypess AM, Lehman S, Williams G, Tal I, Rodman D, Goldfine AB, et al. Identification and Importance of Brown Adipose Tissue in Adult Humans. *New Engl J Med* (2009) 360(15):1509–17. doi: 10.1056/NEJMoa0810780
24. Zhang W, Cline MA, Gilbert ER. Hypothalamus-Adipose Tissue Crosstalk: Neuropeptide Y and the Regulation of Energy Metabolism. *Nutr Metab (Lond)* (2014) 11:27. doi: 10.1186/1743-7075-11-27
25. Chao PT, Yang L, Aja S, Moran TH, Bi S. Knockdown of NPY Expression in the Dorsomedial Hypothalamus Promotes Development of Brown Adipocytes and Prevents Diet-Induced Obesity. *Cell Metab* (2011) 13(5):573–83. doi: 10.1016/j.cmet.2011.02.019
26. Huang YC, Hsu CC, Huang P, Yin TK, Chiu NT, Wang PW, et al. The Changes in Brain Metabolism in People With Activated Brown Adipose Tissue: A PET Study. *Neuroimage* (2011) 54(1):142–7. doi: 10.1016/j.neuroimage.2010.07.058
27. Lee HY, Chung JK, Jeong JM, Lee DS, Kim DG, Jung HW, et al. Comparison of FDG-PET Findings of Brain Metastasis From Non-Small-Cell Lung Cancer and Small-Cell Lung Cancer. *Ann Nucl Med* (2008) 22(4):281–6. doi: 10.1007/s12149-007-0104-1
28. Willis MW, Ketter TA, Kimbrell TA, George MS, Herscovitch P, Danielson AL, et al. Age, Sex and Laterality Effects on Cerebral Glucose Metabolism in Healthy Adults. *Psychiatry Res* (2002) 114(1):23–37. doi: 10.1016/s0925-4927(01)00126-3
29. Zilles K, Amunts K. Centenary of Brodmann's Map–Conception and Fate. *Nat Rev Neurosci* (2010) 11(2):139–45. doi: 10.1038/nrn2776
30. Naqvi NH, Bechara A. The Hidden Island of Addiction: The Insula. *Trends Neurosci* (2009) 32(1):56–67. doi: 10.1016/j.tins.2008.09.009
31. Ruiz S, Lee S, Soekadar SR, Caria A, Veit R, Kircher T, et al. Acquired Self-Control of Insula Cortex Modulates Emotion Recognition and Brain Network Connectivity in Schizophrenia. *Hum Brain Mapp* (2013) 34(1):200–12. doi: 10.1002/hbm.21427
32. Menon V, Uddin LQ. Saliency, Switching, Attention and Control: A Network Model of Insula Function. *Brain Struct Funct* (2010) 214(5-6):655–67. doi: 10.1007/s00429-010-0262-0
33. Cauda F, D'Agata F, Sacco K, Duca S, Geminiani G, Vercelli A. Functional Connectivity of the Insula in the Resting Brain. *Neuroimage* (2011) 55(1):8–23. doi: 10.1016/j.neuroimage.2010.11.049
34. Kang Y, Williams LE, Clark MS, Gray JR, Bargh JA. Physical Temperature Effects on Trust Behavior: The Role of Insula. *Soc Cognit Affect Neurosci* (2011) 6(4):507–15. doi: 10.1093/scan/nsq077
35. Shah A, Jhawar SS, Goel A. Analysis of the Anatomy of the Papez Circuit and Adjoining Limbic System by Fiber Dissection Techniques. *J Clin Neurosci* (2012) 19(2):289–98. doi: 10.1016/j.jocn.2011.04.039

Conflict of Interest: The authors declare that the research was conducted in the absence of any commercial or financial relationships that could be construed as a potential conflict of interest.

frontiers in Endocrinology

REVIEW
published: 21 July 2021
doi: 10.3389/fendo.2021.694204

Central 5-HTR2C in the Control of Metabolic Homeostasis

Ting Yao[1,2†‡], Jiehui He[3†], Zhicheng Cui[3], Ruwen Wang[1], Kaixuan Bao[4], Yiru Huang[3], Ru Wang[1*‡] and Tiemin Liu[3,4,5,6*‡]*

[1] School of Kinesiology, Shanghai University of Sport, Shanghai, China, [2] Department of Physiology and Pathophysiology, School of Basic Medical Sciences, Xi'an Jiaotong University School of Medicine, Xi'an, China, [3] School of Life Sciences, Fudan University, Shanghai, China, [4] Human Phenome Institute, Fudan University, Shanghai, China, [5] State Key Laboratory of Genetic Engineering, Fudan University, Shanghai, China, [6] State Key Laboratory of Pharmaceutical Biotechnology, Nanjing University, Nanjing, China

OPEN ACCESS

Edited by:
Etienne Challet, Université de Strasbourg, France

Reviewed by:
Jin Kwon Jeong, George Washington University, United States
Lourdes Mounien, Aix-Marseille Université, France

***Correspondence:**
Ting Yao
xiaciweixiao@yeah.net
Ru Wang
wangru@sus.edu.cn
Tiemin Liu
tiemin_liu@fudan.edu.cn

†These authors have contributed equally to this work and share first authorship

‡These authors have contributed equally to this work and share last authorship

Specialty section:
This article was submitted to Neuroendocrine Science, a section of the journal Frontiers in Endocrinology

Received: *12 April 2021*
Accepted: *06 July 2021*
Published: *21 July 2021*

Citation:
Yao T, He J, Cui Z, Wang R, Bao K, Huang Y, Wang R and Liu T (2021) Central 5-HTR2C in the Control of Metabolic Homeostasis. Front. Endocrinol. 12:694204. doi: 10.3389/fendo.2021.694204

The 5-hydroxytryptamine 2C receptor (5-HTR2C) is a class G protein-coupled receptor (GPCR) enriched in the hypothalamus and the brain stem, where it has been shown to regulate energy homeostasis, including feeding and glucose metabolism. Accordingly, 5-HTR2C has been the target of several anti-obesity drugs, though the associated side effects greatly curbed their clinical applications. Dissecting the specific neural circuits of 5-HTR2C-expressing neurons and the detailed molecular pathways of 5-HTR2C signaling in metabolic regulation will help to develop better therapeutic strategies towards metabolic disorders. In this review, we introduced the regulatory role of 5-HTR2C in feeding behavior and glucose metabolism, with particular focus on the molecular pathways, neural network, and its interaction with other metabolic hormones, such as leptin, ghrelin, insulin, and estrogens. Moreover, the latest progress in the clinical research on 5-HTR2C agonists was also discussed.

Keywords: 5-HTR2C, feeding behavior, glucose homeostasis, obesity, hypothalamus, neural network, energy metabolism, lorcaserin

INTRODUCTION

Serotonin, or 5-hydroxytryptamine (5-HT), is an essential neurotransmitter that has been shown to be involved in the regulation of multiple physiological and behavioral functions, including emotion, cognition, sleep, exercise, and energy homeostasis (1, 2). There are seven classes of receptors in the 5-HT family, most of which are G-protein coupled receptors (3, 4). Among them, 5-HTR2C has been shown as a key regulator for feeding and glucose homeostasis. Knock-out of 5-HTR2C in mice resulted in increased food intake, insulin resistance, and obesity (5, 6), while pharmacological activation of the 5-HTR2C inhibits food intake (7). Thus, 5-HTR2C has become a hot target for anti-obesity treatment. For example, the non-selective 5-HTR2C agonist D-Fenfluramine (d-Fen) (**Table 2**), and selective 5-HTR2C agonist lorcaserin (**Table 2**) were approved by Food and Drug Administration for body weight management. However, they were withdrawn due to associated side effects. A better understanding of the mechanism of 5-HTR2C on energy homeostasis will facilitate the development of improved drugs targeting 5-HTR2C pathways for metabolic diseases. In this review, we recapped the molecular mechanisms and discussed the neural circuits of 5-HTR2C in regulating energy metabolism. In addition, the functional interactions between 5-HTR2C and other

appetite-regulatory signaling pathways were discussed. Since 5-HTR2C has become one of the most promising targets for treating obesity, we also discussed the clinical application of 5-HTR2C as a potential therapeutic target in treating metabolic diseases.

5-HTR2C SIGNAL TRANSDUCTION

5-HTR2C is one of the first sequenced and cloned 5-HT receptors (8). The gene coding 5-HTR2C is located at chromosome Xq24 in humans. It contains three introns (instead of two, such as 5-HTR2A and 5-HTR2B) and encodes a protein product with seven transmembrane regions. There is more than 80% homology of 5-HTR2C in the transmembrane regions among mice, rats, and humans (9). 5-HTR2C is widely expressed in the central nervous system (CNS) compared to the peripheral nervous system (10). In the CNS, 5-HTR2C is expressed in these known brain areas that are related to energy metabolism, including the ventral tegmental area (VTA), the arcuate nucleus (ARC), the nucleus tractus solitarius (NTS), paraventricular nucleus of the hypothalamus (PVN), and lateral parabrachial nucleus (LPBN) (11). Genetic studies with loss or gain function of 5-HTR2C indicate a key role of 5-HTR2C in these brain regions in maintaining energy homeostasis (12). Pharmacological studies using its agonists or antagonists also revealed that central 5- HTR2C is involved in various metabolic diseases such as diabetes and obesity (13). In line, a higher density of 5-HTR2C was found in the hypothalamus in Prader-Willi syndrome (PWS) patients showing hyper appetite and obesity (14).

The best understood function of 5-HTR2C is food intake regulation through 5-HTR2C action in pro-opiomelanocortin (POMC) neurons in the hypothalamus (**Figure 1**). Serotonin binding to 5-HTR2C leads to the dissociation of a heterotrimeric G protein that binds to the second intracellular loop of 5-HTR2C. Upon dissociation, the subunit $G_{\alpha/q11}$, activates phospholipase C, generating inositol triphosphate (IP3) and diacylglycerol (DAG), which activates Protein Kinase C (PKC). PKC activates the extracellular regulated kinase (ERK) pathway, leading to the phosphorylation of c-*Fos* and POMC synthesis. POMC is processed into α-melanocyte-stimulating hormone (α-MSH) that activates neurons in the PVN *via* melanocortin 4 receptors (MC4Rs) (15). Activation of PVN neurons induces satiety, i.e., cessation of eating, an anorexic response.

Of note, 5-HTR2C is the only known GPCR whose mRNA undergoes post-transcriptional editing to yield different receptor isoforms (16). This RNA editing process further modulates the basal activity of 5-HTR2C and/or the sensitivity of 5-HTR2C (17). The 5-HTR2C mRNA is edited in 5 distinct sites (18) resulting in at least 33 distinct mRNAs and 25 distinct isoforms of the protein in humans (19). The activity of the 5-HTR2C is regulated through the ratio of these truncated to full-length receptors. An increase in the truncated receptor sequesters the full-length receptor intracellularly, decreasing 5-HTR2C signaling (20). Overexpression of fully-edited receptors decreased the expression of POMC in the hypothalamus and caused hyperphagia in mice (21). In addition, mutation of SNORD115, a small RNA that regulates alternative splicing of 5-HTR2C, is observed in most in PWS patients who are characterised by hyperphagia and obesity (14).

Taken together, 5-HTR2C is associated with multiple signal transduction pathways, mobilizing various intracellular signaling molecules. An in-depth understanding of the gene-editing processes of 5-HTR2C in the central regulation of metabolism may help to identify the differentially expressed targets for pharmacological operations and the development of new drugs.

FEEDING BEHAVIOR

5-HTR2C in POMC Neurons in the ARC and NTS

POMC neurons in the ARC are characterized as the first-order neurons that regulate energy balance in the hypothalamus (22). In the ARC, most of POMC neurons co-express 5-HTR2C (23) and receive inputs from serotoninergic nerve fibers terminate (24). 5-HTR2C has also been proved to regulate energy homeostasis. Mice with global mutation or knock-out of the *5-HTR2C* gene (2C-null) developed hyperphagia and obesity (**Table 1**) (5, 25, 26), and 5-HTR2C agonist d-Fen was reported to suppress mice food intake, contributing to the anorexigenic effects (27). Electrophysiological studies showed that selective 5-HTR2C agonists, including m-chlorophenyl piperazine (mCPP), d-Fen (23), could activate ARC POMC neurons and stimulate POMC expression by increasing the mRNA level (28–30). ARC POMC neurons produce α-MSH, an endogenous agonist of MC4Rs (31–33). It was reported that the mutation of the *MC4R* gene led to insensitivity to the anorectic effect of d-Fen (34), suggesting that the function of ARC 5-HTR2C required a central melanocortin pathway. In particular, the involved MC4R population was probably located at the single minded-1 (SIM1) neurons in the PVN, because the restoration of MC4Rs in SIM1 neurons in MC4R KO mice was sufficient to rescue anorexigenic effects caused by the 5-HTR2C agonist (32, 35, 36). Moreover, deleting the 5-*HTR2C* gene only in POMC neurons (POMC-2C-null) increased mice food intake (**Table 1**) (15), while re-expressed 5-HTR2C in POMC neurons (POMC-2C-RE) could rescue this phenotype (**Table 1**) (25). Further, at the cellular level, transient receptor potential cation 5 (TrpC5) was required to activate POMC neurons by 5-HTR2C, as the intraperitoneal injections of 5-HTR2C agonist failed to suppress food intake in *TrpC5* KO mice (37). Thus, the feeding inhibitory effect by activating 5-HTR2C was at least partly mediated by the POMC neurons in the ARC (**Figure 2**) (23, 38).

In addition to the ARC, NTS, a brainstem center for satiety signals, also contains substantial POMC-expressing neurons that co-express 5-HTR2C (39, 40). Studies have shown that 5-HT2CR in the NTS is involved in the anorexic effect of the two 5-HT2CR agonists, lorcaserin and WAY161,503 and chemogenetics activation of 5-HTR2C-expressing neurons in the NTS decrease food intake in mice (38). Interestingly, different from

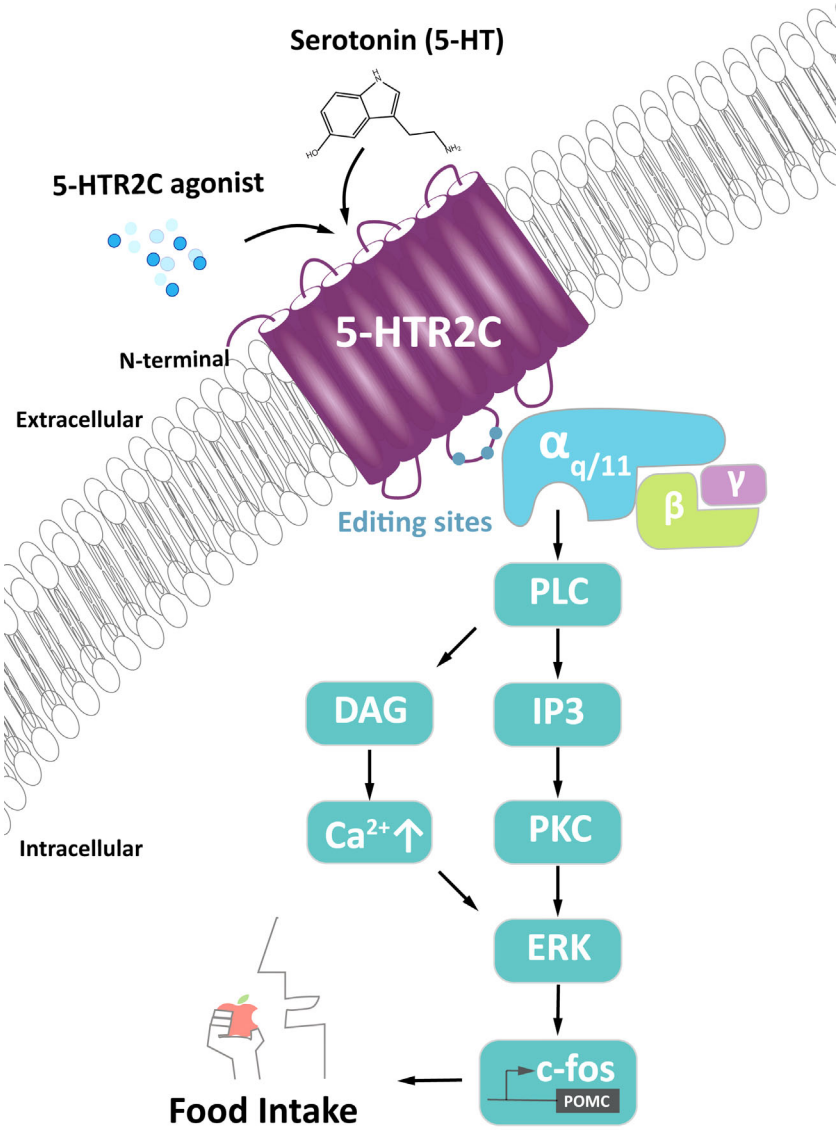

FIGURE 1 | Signaling of 5-HTR2C in POMC neurons generating food intake. Activation of $\alpha_{q/11}$ promotes phospholipase C (PLC) to produce diacylglycerol (DAG) and inositol-1,4,5-triphosphate (IP3). IP3 promotes release of intracellular calcium (Ca^{2+}) while DAG binds to downstream effector protein kinase C (PKC), both of which activates c-*Fos via the* extracellular regulated kinase pathway (ERK). C-*Fos* turns on the pro-opiomelanocortin (POMC) promoter, which signals to neurons regulating the food intake signal. This signal is also regulated by 5-HTR2C agonist and serotonin.

TABLE 1 | Phenotypes of the 5-HTR2C deficient mice.

Mice Model	Body Weight	Fat Mass	Lean Mass	Food Intake	Binge-like Eating	Hepatic Glucose Production	Reference
2C-null	↑	↑	↓	↑	↓	↑	(5, 25)
POMC-2C-null	↑	↑	↓	↑	↓	↑	(15)
POMC-2C-RE	↔	↔	↔	↔	/	↔	(25)
DA-2C-RE	/	/	/	↑	↔	/	(15)
DA-2C-KO	/	/	/	↑	↓	/	(15)

'↑', Increased; '↓', Reduced; '↔', No change; '/', Unknown. 2C-null is a loxed transcription blocker (loxTB) 5-HTR2C mouse line lacking functional 5-HTR2C globally; POMC-2C-null mice with previously characterized animals in which cre is constitutively (developmentally) expressed in POMC neurons to ablate 5-HTR2C specifically; POMC-2C-RE mice with 5-HTR2C re-expressed specifically and only in POMC neurons; DA-2C-RE mice with the expression of endogenous 5-HTR2C only in DA neurons; DA-2C-KO with deletion of endogenous 5-HTR2C only in DA neurons.

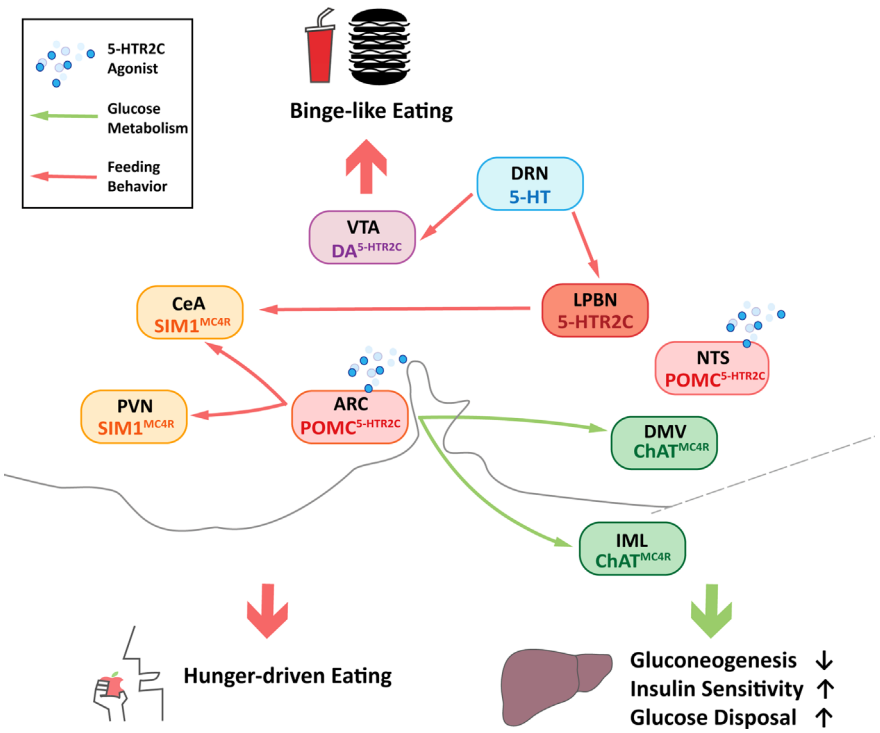

FIGURE 2 | Central neuronal circuits of 5-HTR2C that regulate feeding behavior and glucose homeostasis. Central Nervous System (CNS) 5-hydroxytryptamine receptor 2C (5-HTR2C) may regulate energy metabolism through neuronal circuits. Red arrows designate circuits that regulate three types of feeding behavior which are binge-like eating, sodium intake and hunger-driven eating, while the green arrows show the circuits that regulate glucose homeostasis by reducing gluconeogenesis, increasing insulin sensitivity and glucose disposal. Pink boxes indicate nuclei containing POMC neurons that co-express 5-HTR2C ($POMC^{5\text{-}HTR2C}$); Green boxes indicate nuclei containing cholinergic neurons that co-express melanocortin 4 receptors ($ChAT^{MC4R}$); Yellow boxes indicate nuclei containing single minded-1 (SIM1) neurons that co-express melanocortin 4 receptors ($SIM1^{MC4R}$); Light purple box indicates nuclei containing DA neurons that co-express 5-HTR2C ($DA^{5\text{-}HTR2C}$); Light blue box indicates nuclei containing 5-HT neurons and orange box indicates nuclei containing a subset of neurons expressing 5-HTR2C. ARC, arcuate nucleus; NTS, nucleus tractus solitarius; PVN, paraventricular nucleus of the hypothalamus; CeA, central amygdala; LPBN, lateral parabrachial nucleus; DRN, dorsal raphe nucleus; VTA, ventral tegmental area; DMV, dorsal motor nucleus of the vagus; IML, intermediolateral nucleus.

ARC POMC neurons, NTS POMC neurons decreased food intake more significantly and rapidly, in other words, 5-HTR2C agonist lorcaserin required a longer time to decrease mice food intake in the ARC as effectively as in the NTS (38, 41). Therefore, NTS POMC neurons appear to mediate the inhibitory effects of lorcaserin on feeding, but the downstream pathway remains elusive (**Figure 2**). Studies had shown that PVN and central amygdala (CeA) could be innervated by NTS POMC neurons (42). Both of them are key brain regions involved in the regulation of feeding behavior, but the roles of these brain regions warrant further investigation.

5-HTR2C in Dopamine Neurons in the VTA

Apart from homeostatic feeding, 5-HTR2C is also involved in hedonic feeding behaviors, defined as ingestion of a large amount of food in a short timeframe for pleasure (43, 44). The central dopamine (DA) system has been implicated in the pathophysiology of binge eating (45); 5-HT releasing neurons in the dorsal raphe nucleus (DRN) directly innervate DA neurons in VTA (46). In the VTA, DA neurons were proved to co-express 5-HTR2C (47), suggesting that 5-HTR2C probably interacted with VTA DA neurons to regulate binge eating. Moreover, intraperitoneal injections of 5-HTR2C agonists significantly suppressed binge-like eating in wild-type mice, while the 2C-null mice showed no effect (48). Indeed, specific knock-out of *5-HTR2C* gene in the VTA DA neurons (DA-VTA-KO) blunted the suppression of binge-like eating by 5-HTR2C agonist (**Table 1**) (48). These observations indicate that 5-HTR2C can act downstream the DRN 5-HT neurons to inhibit food intake. However, the feeding control by VTA DA 5-HTR2C-expressing neurons seemed specific to hedonic rather than hunger-driven eating, as re-expression of 5-HTR2C in DA neurons (DA-2C-RE) did not affect normal food intake in mice even when administered with the 5-HTR2C agonist (**Table 1**) (48). But the downstream neural circuits of the DA 5-HTR2C-expressing neurons still remain unclear. Studies have found that administration of cocaine can increase DA releases in the nucleus accumbens (NAc), an effect that can be blocked by local injections of 5-HTR2C agonist in the VTA (49). Given the abundant connectivity between VTA neurons and the NAc, it would be interesting to know that DA 5-HTR2C neurons in the VTA regulate binge eating by projecting to the NAc (**Figure 2**).

5-HTR2C in the LPBN on Sodium Intake

Sodium ions are important minerals for maintaining extracellular fluid and blood volume (50). Studies have found clues for 5-HTR2C in the LPBN to regulate sodium appetite (51). Ingestion of high-concentration sodium-containing food increased c-*Fos* expression in neurons that co-express 5-HTR2C in the LPBN (52–54). Furthermore, specific activation of LPBN 5-HTR2C neurons rapidly suppressed sodium intake in mice. By contrast, inhibition of the 5-HTR2C neurons of LPBN increased the intake of sodium-containing foods (55). Furthermore, electrophysiological studies suggested an abundant connectivity between LPBN 5-HTR2C neurons and CeA (**Figure 2**) (54). In vivo optogenetics stimulation further indicated that LPBN 5-HTR2C neurons could suppress sodium appetite *via* projections to CeA (54). Moreover, raphe nuclei probably modulate the neurons in the LPBN through serotoninergic projections. The injection of retrobeads into the LPBN of wildtype mice showed co-localization of 5-HT and retro bead-labeled cells in the DRN and the median raphe nucleus (MnR) (54). In conclusion, LPBN 5-HTR2C neurons may receive 5-HT signals from median raphe nucleus (MRN)/DRN and project to the CeA to regulate sodium intake (**Figure 2**).

ENERGY EXPENDITURE

The 5-HT signaling pathway is closely related to individual energy storage and expenditure. Inhibiting the 5-HT signaling pathway can increase individual thermogenesis in mice (56). Studies found that the knock-out of 5-HTR2C affected the activity level and energy expenditure in mice. The mutant mice exhibited hyperactivity, and increased total energy expenditure, while reducing energy expenditure during exercise. At nine months old, elevated mRNA levels of uncoupling protein 2 (UCP2) were detected in the liver, skeletal muscle, and white adipose tissue of the mutant mice (57). The mice targeted restoration of POMC only within 5-HTR2C expressing cells showed sex differences in physical activity, energy expenditure, and the development of obesity (58). In addition, mutation of the 5-HTR2C gene can increase the mRNA level of UCP1 in brown adipose tissues and reduce fat accumulation in mice (59–61). In summary, 5-HTR2C can affect the energy expenditure of tissues or individuals in diverse ways.

GLUCOSE HOMEOSTASIS

In addition to regulating food intake, serotonin is essential in regulating glucose homeostasis. 5-HT produced by enterochromaffin cells in the gut can act as an paracrine signal modulating islet β cell activity and proliferation (62, 63). It has been shown that 5-HTR2B agonists could promote insulin secretion (64). Meanwhile, studies have revealed the role of 5-HTR2C in the POMC neurons in mediating blood glucose, suggesting a central role of 5-HTR2C in glucose metabolism. Indeed, 2C-null mice manifested insulin resistance (15, 25), and POMC-2C-RE mice was sufficient to rescue the impairment (**Table 1**) (6). On the other hand, 5-HTR2C agonist lorcaserin could significantly improve glucose and insulin tolerance in wild-type mice, and these effects were abolished in *POMC* gene deficient mice (POMC-NEO) and restored in POMC-2C-RE mice (65). Studies showed that the glycemic effect of 5-HTR2C in POMC neurons was mediated by cholinergic (ChAT) MC4Rs in dorsal motor nucleus of the vagus (DMV) and the intermediolateral nucleus (IML) (32, 65, 66), which was different from the forebrain SIM1 MC4Rs implicated in feeding behavior, indicating the subsets of POMC 5-HTR2C neurons in controlling feeding behavior and glucose homeostasis might be different (**Figure 2**). It was shown that 5-HTR2C agonist m-CPP and lorcaserin can improve glycemic control independently of body weight (6, 15, 65, 67). The improved glucose tolerance in mice by lorcaserin was found to be mediated by reducing the hepatic glucose production and improving glucose disposal, without change of insulin secretion (65) (**Table 1** and **Figure 2**). Interestingly, a recent study showed that a subset of POMC neurons may have the ability to promote hepatic glucose production, which was speculated to be relevant with the heterogeneity of POMC neurons (68). Given the complex functions of POMC neurons in the brain, the relationship between this subset of POMC neurons and POMC 5-HTR2C neurons remains to be further elucidated. In analyzing the heterogeneity of different parts of the same tissue, the spatial transcriptomics studies may be helpful. Studies had preliminarily used the spatial transcriptome to reveal the heterogeneity of tumor tissue (69). Integrating the transcriptome profiles and projection patterns of individual neurons may help to clarify how POMC 5-HTR2C neurons process various stimuli at the single-neuron level.

INTERACTION OF 5-HTR2C WITH BODYWEIGHT REGULATORY SIGNALS

Leptin

Leptin, a key regulator for the metabolism, is secreted from adipocytes (70). It prevents bodyweight gain by suppressing feeding and increasing energy expenditure (71). Mutations of the gene encoding leptin in mice (*ob/ob*) lead to severe obesity and increased appetite (72). The leptin receptor (LepR) mediates the effects of leptin on body weight, and it is involved in the majority of leptin's actions in the brain (73). Double fluorescent *in situ* hybridization experiments showed that in the hypothalamic, the neurons which express LepR also co-express 5-HTR2C, including the ARC and the ventromedial hypothalamus (VMH) (74, 75). However, selective knock-out of LepR in 5-HTR2C-expressed neurons exhibited neither hyperglycemia nor alteration in serum insulin or leptin concentrations (76). Further, single-cell transcriptomic data showed that the LepR-expressing POMC cells formed a molecularly distinct cluster relative to POMC neurons expressing the 5-HTR2C (77, 78), indicating that leptin probably affected systemic energy balance through different POMC neuronal subsets. In particular, Daniel D et al. clarified that brain 5-HT neurons did not express LepR and therefore not directly

responded to leptin (79). In conclusion, whether the leptin signaling pathway interacts with 5-HT remains controversial, which needs further research.

Ghrelin

Ghrelin is a stomach-derived body weight regulatory signal stimulating feeding *via* the growth hormone secretagogue receptors (GHSRs). The ghrelin signaling pathway interacts with 5-HT. The appetite-stimulating activity of ghrelin is shown to be mediated by the inhibition of serotonin release (80). GHSRs in ARC is expressed in 94% of nerve peptide Y (NPY) neurons and 8% of POMC neurons (81), and is co-localized with 5-HTR2C neurons. Studies have shown that the 5-HTR2C is dimerized with the GHSRs to inhibit its orexigenic activity (82). The activation of 5-HTR2B and 5-HTR2C reduced the gastric and hypothalamic secretion of ghrelin (83). 5-HTR2C agonist like lorcaserin inhibits the increase of plasma ghrelin level induced by fasting. Besides, 5-HTR2C antagonism reduces dimerization and increases GHSR-induced food intake, indicating that 5-HTR2C can change the regulation of ghrelin on feeding (84, 85). Overall, 5-HTR2C and its interaction with GHSR are probably a valuable target for designing new compounds to prevent obesity.

Insulin

Insulin efficiently crosses the blood-brain barrier *via* receptor-mediated transport (86). Besides, the insulin receptor is widely expressed in the CNS, including the cerebral cortex, hippocampus, and hypothalamus (87). Mice with targeted mutation in the 5-HTR2C gene resulted in insulin resistance and type 2 diabetes (T2D), with antecedent hyperphagia and obesity (26, 88), suggesting an interaction of insulin with 5-HTR2C on energy metabolism. Infusion of insulin in the hypothalamic could briefly enhance 5-HT release in rostromedial hypothalamus (89), and systemic administration of 5-HTR2C agonist mCPP by osmotic minipumps could reduce fasting plasma insulin level through POMC neurons in diet-induced obesity (DIO) mice without altering blood glucose (90). However, single-cell transcriptomic data showed the subset of POMC neurons that expressing 5-HTR2C and insulin receptor were not the same (77), which should be further investigated.

Estrogens

The gene encoding 5-HTR2C has been mapped to human chromosome X, suggesting a sex-dependent role for 5-HTR2C signaling (91). When 5-HTR2C agonists and antagonists were used in elderly mice exposed to stress, different feeding phenotypes were found in females and males (92). When food is reduced due to stress, the female mice recovered more quickly than the male mice (92). In aged male mice, exposure to novelty stress promoted 5-HTR2C protein synthesis in PVN stress-specific neurons and activated neurons that expressed 5-HTR2C (93). In contrast, there was no change in 5-HTR2C and *c-Fos* co-positive cell counts in the PVN of aged female mice exposed to stress (93). It was unclear if these sex differences were due to gonadal hormones or the organizational effect, but estradiol was reported to enhance 5-HTR2C protein synthesis in the DRN region (94), caudal brainstem, and hypothalamus (93, 95).

Cholecystokinin

As a bodyweight regulatory signal, cholecystokinin(CCK), secreted by the gastrointestinal tract and neurons in brain, stimulates satiety and suppresses feeding behavior (96, 97). Some studies have found that CCK can act synergistically with 5-HT to inhibit food intake by simultaneously activating CCK-1 and 5-HTR3A (98, 99), and 5-HTR1A are also involved in CCK induced anorexic behavior (100, 101). However, there is little research on the association between 5-HTR2C and CCK signaling in CNS (102), which is probably a direction for future research.

NPY/AgRP

Studies have confirmed co-expression of NPY and 5-HTR2C in the lateral hypothalamus, the basolateral nucleus and ARC (103–105). Intraperitoneal injection with 5-HTR2C agonist lorcaserin could significantly reduce the expression of NPY mRNA in the ARC, while 5-HTR2C antagonist risperidone caused the opposite effect (103). In addition, injection of 5-HTR2A/2C agonist 1-(2,5-dimethoxy-4-iodophenyl)-2-aminopropane (DOI) into the PVN, but not the perifornical hypothalamus and VMH, could suppress NPY-induced feeding behavior (106, 107). In summary, the effect of 5-HTR2C on feeding seems to be highly associated with NPY/AgRP signaling, and more research on how 5-HTR2C affects NPY/AgRP neurons is required for further investigation.

CLINICAL APPLICATION

Obesity

Obesity prevalence calls for new methods of appetite suppression and weight loss. Satiety and appetite control pathways have been widely studied in animals and humans, but the exact underlying molecular mechanism is still unclear (108, 109). Nowadays, some drugs used to treat obesity have side effects. At present, 5-HTR2C is one of the most promising targets for new weight-loss drugs. Many modulators targeting 5-HT signaling, including sibutramine (serotonin and adrenaline reuptake inhibitors) (**Table 2**), mCPP, and fenfluramine (also named as fluoxetine, selective serotonin reuptake inhibitors) (**Table 2**) have been used as appetite suppressants (27, 110, 111). Sibutramine and fluoxetine can increase extracellular serotonin levels *in vivo*, non-selectively stimulate all postsynaptic subtypes, and then stimulate 5-HTR2C to suppress food intake (112, 113). Heisler (114) reported that mCPP did not inhibit food intake in 5-HTR2C knock-out mice and weakened the swallowing effect of fenfluramine (serotonin releasing agent and reuptake inhibitor), demonstrating the key role of 5-HTR2C in satiety induction by d-fenfluramine. Fenfluramine, an effective treatment for obesity, sold as Pondimin ®/Redux ®, reduces appetite. Fenfluramine binds weakly to the serotonin 5-HTR2C, d-Fen binds to and activates the serotonin 5-HTR2B and 5-HTR2C with high affinity and the serotonin 5-HTR2A with moderate affinity (115–117). However, fenfluramine is associated with side effects of valvular heart disease and pulmonary hypertension, prompting it to withdraw from clinical use (118, 119).

Lorcaserin is an effective and selective 5-HTR2C agonist that reduces food intake and body weight in rodents in a dose-

TABLE 2 | 5-HTR2C related drugs in this review.

Name	Mechanism of Action	Side Effect	Application
Lorcaserin	selective 5-HTR2C agonist	headache, fatigue, nausea, dry mouth, and constipation	weight-loss drug
D-Fen	serotonin releasing agent and reuptake inhibitor	cardiac complications	weight-loss drug
Sibutramine	serotonin and adrenaline reuptake inhibitor	stroke, myocardial infarction	weight-loss drug
Fluoxetine	selective serotonin reuptake inhibitor	anorexia	an approved drug to treat depression and obsessive-compulsive disorder
m-CPP	agonist of 5-HTR2C and 5-HTR1B	anxiety, negative mood measured	decrease food intake and enhance microstructural measures of satiety

dependent manner (120). Lorcaserin was approved by Food and Drug Administration for weight management in adults with body mass index (BMI) ≥ 30 kg/m^2 or BMI ≥ 27 kg/m^2 with at least one weight-related complication. Since 2013, lorcaserin has been sold in the United States under the name of Belviq ®. The safety and efficacy of lorcaserin have been determined by three phases III clinical trials, one cardiovascular (CV) outcome trial, and four randomized controlled trials (121–123). Animal experiments showed that after 28 days of treatment in diet-induced obesity rats, there was no aortic and mitral regurgitation in any treatment group (124). A 6-month randomized, placebo-controlled, double-blind clinical trial also found that lorcaserin could reduce weight and improve cardiac metabolic risk factors in obese adults, thus modifying circulating body weight regulatory signals associated with energy balance and decreasing the risk of cardiovascular disease (125). Recent follow-up data have shown that the drug probably increases cancer risk, and further research is needed. The role of 5-HTR2C in POMC neurons and the new role in neural circuits suggest that the new anti-obesity drugs act directly on the CNS, thereby reducing the negative effects caused by acting on the periphery, which will be discussed in the future.

Diabetes

As a chronic disease, the prevalence of T2D continues to rise worldwide, highlighting the clinical need for a variety of treatment options. The current first-line drugs for T2D target peripheral tissue to improve blood glucose and insulin function (126, 127). 5-HTR2C has been found to regulate glucose homeostasis during weight loss, which is expected to become a candidate target (128, 129) for the treatment of diabetes. Yuan et al. discovered that the-759C/T polymorphism of the *5-HTR2C* gene was associated with obesity and T2D (130). The lower frequency of-759T allele in the *5-HTR2C* gene was associated with T2D but not associated with obesity in men and women (131), resulting from alleles type from promoter activity and transcriptional level, thus preventing the development of T2D.

A retrospective analysis of the Phase III BLOOM-DM study showed that lorcaserin combined with diet and exercise decreased blood glucose within 2 weeks (132–134). In the study of the effect of lorcaserin on weight loss in patients with T2D, lorcaserin could also decrease the Hemoglobin A1c of diabetic patients, providing direct evidence support for the treatment of diabetes. Besides, reducing fasting plasma glucose and Hemoglobin A1c was greater in people with no significant weight loss, suggesting that it could benefit blood sugar independent of weight loss. Besides, more clinical studies are needed to demonstrate this regulation in the future.

Cardiovascular System

Obesity and metabolic syndrome can increase the risk of cardiovascular disease. Weight-loss drugs can affect cardiovascular health by losing weight and directly acting on the cardiovascular system (135, 136). It was found that subcutaneous injection of 5-HTR2C agonist mCPP (3 mg/kg) had no significant effect on heart rate and meant arterial blood pressure (137). Lorcaserin, a selective 5-HTR2C agonist, did not seem to have a negative effect on the cardiovascular system at very high concentrations (125). Alpana P Shukla et al. (7) summarized the pharmacodynamic and pharmacokinetic characteristics of lorcaserin and discussed efficacy and safety data from major clinical trials. The bodyweight could be reduced by a certain dose of treatment. Therefore, the cardiac metabolic parameters could be significantly improved. In the CAMELLIA-TIMI 61 trial, the incidence of adverse cardiovascular events and conversion to T2D in obese and overweight subjects with cardiovascular disease or multiple cardiovascular risk factors was assessed. It was concluded that the safety of the drug could be guaranteed.

In conclusion, as the first selective 5-HTR2C agonist approved for human weight control, the 5-HTR2C agonist lorcaserin has been widely used in clinical and scientific research after being launched in 2012. Although CAMELLIA-TIMI 61 research found no significant difference in cancer incidence during the first few months of treatment, the imbalance increased with the duration of lorcaserin, suggesting that the drug increased the risk of cancer. The cardiovascular effects of other anti-obesity drugs like liraglutide, bupropion/naltrexone, and phentermine/topiramate remain uncertain (138). Due to the side effects of drugs, there is no better drug to treat obesity. Although 5-HTR2C is the target of several anti-obesity drugs, its side effects limit their clinical application. However, the specific neural circuits of 5-HTR2C expressing neurons and the detailed molecular pathways of 5-HTR2C signaling on metabolic regulation will help to develop better treatment strategies for metabolic disorders. To solve the side

effects caused by other drugs on the peripheral spectrum, future drugs that target the CNS will give us more inspiration.

DISCUSSION

In summary, the action of CNS 5-HTR2C neuron contributes to the regulation of energy homeostasis and have greatly advanced the understanding of the physiology and behavioral functions of 5-HTR2C in the brain. However, there are many questions. As a GPCR, understanding the *5-HTR2C* gene-editing processes is helpful to study the weight-loss drug. However, the detailed molecular mechanisms remain unclear. Furthermore, there is growing interest in brain control of metabolism. Here, we summarized the 5-HTR2C related metabolic circuit of feeding behavior and glucose homeostasis in the brain, and we found that the mechanism of 5-HTR2C in the central cortex still needs to be further clarified. To explore the systemic effects of 5-HTR2C, we also discussed the relationship between metabolic hormones and 5-HTR2C. From the perspective of clinical application, the functions of weight-loss drugs now are mostly concentrated on systemic administration, resulting in negative effects. In the future, 5-HTR2C in the brain may become a potential for the treatment of obesity and type 2 diabetes.

AUTHOR CONTRIBUTION

JH, ZC, and RWW conceived and wrote the manuscript. KB modified the figure drawing. YH revised the overall framework of the article. TY, RW, and TL were responsible for the article structure, scientific logic, and innovative examination of the overall article. All authors contributed to the article and approved the submitted version.

FUNDING

The study was funded by a grant from the National Key Research and Development Program of China (2019YFA0801900, 2018YFA0800300), the National Natural Science Foundation of China (31971074), and the open fund of state key laboratory of Pharmaceutical Biotechnology, Nan-jing University, China (KF-GN-201701).

ACKNOWLEDGMENTS

We wish to thank ZZ, YZ and FMX for critical reading of the manuscript.

REFERENCES

1. Tecott LH. Serotonin and the Orchestration of Energy Balance. *Cell Metab* (2007) 6(5):352–61. doi: 10.1016/j.cmet.2007.09.012
2. Yabut JM, Crane JD, Green AE, Keating DJ, Khan WI, Steinberg GR. Emerging Roles for Serotonin in Regulating Metabolism: New Implications for an Ancient Molecule. *Endocr Rev* (2019) 40(4):1092–107. doi: 10.1210/er.2018-00283
3. Barrera NP, Herbert P, Henderson RM, Martin IL, Edwardson JM. Atomic Force Microscopy Reveals the Stoichiometry and Subunit Arrangement of 5-HT3 Receptors. *Proc Natl Acad Sci USA* (2005) 102(35):12595–600. doi: 10.1073/pnas.0503253102
4. Bennet H, Mollet IG, Balhuizen A, Medina A, Nagorny C, Bagge A, et al. Serotonin (5-HT) Receptor 2b Activation Augments Glucose-Stimulated Insulin Secretion in Human and Mouse Islets of Langerhans. *Diabetologia* (2016) 59(4):744–54. doi: 10.1007/s00125-015-3847-6
5. Tecott LH, Sun LM, Akana SF, Strack AM, Lowenstein DH, Dallman MF, et al. Eating Disorder and Epilepsy in Mice Lacking 5-HT2c Serotonin Receptors. *Nature* (1995) 374(6522):542–6. doi: 10.1038/374542a0
6. Xu Y, Berglund ED, Sohn JW, Holland WL, Chuang JC, Fukuda M, et al. 5-HT2CRs Expressed by Pro-Opiomelanocortin Neurons Regulate Insulin Sensitivity in Liver. *Nat Neurosci* (2010) 13(12):1457–9. doi: 10.1038/nn.2664
7. Shukla AP, Kumar RB, Aronne LJ. Lorcaserin Hcl for the Treatment of Obesity. *Expert Opin Pharmacother* (2015) 16(16):2531–8. doi: 10.1517/14656566.2015.1096345
8. Pazos A, Hoyer D, Palacios JM. Mesulergine, a Selective Serotonin-2 Ligand in the Rat Cortex, Does Not Label These Receptors in Porcine and Human Cortex: Evidence for Species Differences in Brain Serotonin-2 Receptors. *Eur J Pharmacol* (1984) 106(3):531–8. doi: 10.1016/0014-2999(84)90056-6
9. Bonhaus DW, Bach C, DeSouza A, Salazar FH, Matsuoka BD, Zuppan P, et al. The Pharmacology and Distribution of Human 5-Hydroxytryptamine2b (5-HT2B) Receptor Gene Products: Comparison With 5-HT2A and 5-HT2C Receptors. *Br J Pharmacol* (1995) 115(4):622–8. doi: 10.1111/j.1476-5381.1995.tb14977.x
10. Pasqualetti M, Ori M, Castagna M, Marazziti D, Cassano GB, Nardi I. Distribution and Cellular Localization of the Serotonin Type 2C Receptor Messenger RNA in Human Brain. *Neuroscience* (1999) 92(2):601–11. doi: 10.1016/s0306-4522(99)00011-1
11. Clemett DA, Punhani T, Duxon MS, Blackburn TP, Fone KC. Immunohistochemical Localisation of the 5-HT2C Receptor Protein in the Rat CNS. *Neuropharmacology* (2000) 39(1):123–32. doi: 10.1016/s0028-3908(99)00086-6
12. Chou-Green JM, Holscher TD, Dallman MF, Akana SF. Repeated Stress in Young and Old 5-HT(2C) Receptor Knockout Mice. *Physiol Behav* (2003) 79(2):217–26. doi: 10.1016/s0031-9384(03)00096-9
13. Palacios JM, Pazos A, Hoyer D. A Short History of the 5-HT(2C) Receptor: From the Choroid Plexus to Depression, Obesity and Addiction Treatment. *Psychopharmacol (Berl)* (2017) 234(9-10):1395–418. doi: 10.1007/s00213-017-4545-5
14. Garfield AS, Davies JR, Burke LK, Furby HV, Wilkinson LS, Heisler LK, et al. Increased Alternate Splicing of Htr2c in a Mouse Model for Prader-Willi Syndrome Leads Disruption of 5HT(2C) Receptor Mediated Appetite. *Mol Brain* (2016) 9(1):95. doi: 10.1186/s13041-016-0277-4
15. Berglund ED, Liu C, Sohn JW, Liu T, Kim MH, Lee CE, et al. Serotonin 2C Receptors in Pro-Opiomelanocortin Neurons Regulate Energy and Glucose Homeostasis. *J Clin Invest* (2013) 123(12):5061–70. doi: 10.1172/jci70338
16. Gurevich I, Tamir H, Arango V, Dwork AJ, Mann JJ, Schmauss C. Altered Editing of Serotonin 2C Receptor pre-mRNA in the Prefrontal Cortex of Depressed Suicide Victims. *Neuron* (2002) 34(3):349–56. doi: 10.1016/s0896-6273(02)00660-8
17. Berg KA, Cropper JD, Niswender CM, Sanders-Bush E, Emeson RB, Clarke WP. RNA-Editing of the 5-HT(2C) Receptor Alters Agonist-Receptor-Effector Coupling Specificity. *Br J Pharmacol* (2001) 134(2):386–92. doi: 10.1038/sj.bjp.0704255
18. Deffit SN, Hundley HA. To Edit or Not to Edit: Regulation of ADAR Editing Specificity and Efficiency. *Wiley Interdiscip Rev RNA* (2016) 7(1):113–27. doi: 10.1002/wrna.1319
19. Stamm S, Gruber SB, Rabchevsky AG, Emeson RB. The Activity of the Serotonin Receptor 2C is Regulated by Alternative Splicing. *Hum Genet* (2017) 136(9):1079–91. doi: 10.1007/s00439-017-1826-3
20. Zhang Z, Shen M, Gresch PJ, Ghamari-Langroudi M, Rabchevsky AG, Emeson RB, et al. Oligonucleotide-Induced Alternative Splicing of Serotonin

2C Receptor Reduces Food Intake. *EMBO Mol Med* (2016) 8(8):878–94. doi: 10.15252/emmm.201506030
21. Morabito MV, Abbas AI, Hood JL, Kesterson RA, Jacobs MM, Kump DS, et al. Mice With Altered Serotonin 2C Receptor RNA Editing Display Characteristics of Prader-Willi Syndrome. *Neurobiol Dis* (2010) 39(2):169–80. doi: 10.1016/j.nbd.2010.04.004
22. Morton GJ, Cummings DE, Baskin DG, Barsh GS, Schwartz MW. Central Nervous System Control of Food Intake and Body Weight. *Nature* (2006) 443(7109):289–95. doi: 10.1038/nature05026
23. Heisler LK, Cowley MA, Tecott LH, Fan W, Low MJ, Smart JL, et al. Activation of Central Melanocortin Pathways by Fenfluramine. *Science* (2002) 297(5581):609–11. doi: 10.1126/science.1072327
24. Kiss J, Léránth C, Halász B. Serotoninergic Endings on VIP-Neurons in the Suprachiasmatic Nucleus and on ACTH-Neurons in the Arcuate Nucleus of the Rat Hypothalamus. A Combination of High Resolution Autoradiography and Electron Microscopic Immunocytochemistry. *Neurosci Lett* (1984) 44(2):119–24. doi: 10.1016/0304-3940(84)90068-5
25. Xu Y, Jones JE, Kohno D, Williams KW, Lee CE, Choi MJ, et al. 5-HT2CRs Expressed by Pro-Opiomelanocortin Neurons Regulate Energy Homeostasis. *Neuron* (2008) 60(4):582–9. doi: 10.1016/j.neuron.2008.09.033
26. Nonogaki K, Strack AM, Dallman MF, Tecott LH. Leptin-Independent Hyperphagia and Type 2 Diabetes in Mice With a Mutated Serotonin 5-HT2C Receptor Gene. *Nat Med* (1998) 4(10):1152–6. doi: 10.1038/2647
27. Vickers SP, Clifton PG, Dourish CT, Tecott LH. Reduced Satiating Effect of D-Fenfluramine in Serotonin 5-HT(2C) Receptor Mutant Mice. *Psychopharmacology* (1999) 143(3):309–14. doi: 10.1007/s002130050952
28. Sohn JW, Xu Y, Jones JE, Wickman K, Williams KW, Elmquist JK. Serotonin 2C Receptor Activates a Distinct Population of Arcuate Pro-Opiomelanocortin Neurons *via* TRPC Channels. *Neuron* (2011) 71 (3):488–97. doi: 10.1016/j.neuron.2011.06.012
29. Doslikova B, Garfield AS, Shaw J, Evans ML, Burdakov D, Billups B, et al. 5-HT2C Receptor Agonist Anorectic Efficacy Potentiated by 5-HT1B Receptor Agonist Coapplication: An Effect Mediated *via* Increased Proportion of Pro-Opiomelanocortin Neurons Activated. *J Neurosci* (2013) 33(23):9800–4. doi: 10.1523/jneurosci.4326-12.2013
30. Lam DD, Przydzial MJ, Ridley SH, Yeo GS, Rochford JJ, O'Rahilly S, et al. Serotonin 5-HT2C Receptor Agonist Promotes Hypophagia *via* Downstream Activation of Melanocortin 4 Receptors. *Endocrinology* (2008) 149(3):1323–8. doi: 10.1210/en.2007-1321
31. Fenselau H, Campbell JN, Verstegen AM, Madara JC, Xu J, Shah BP, et al. A Rapidly Acting Glutamatergic ARC→PVH Satiety Circuit Postsynaptically Regulated by α-MSH. *Nat Neurosci* (2017) 20(1):42–51. doi: 10.1038/nn.4442
32. Balthasar N, Dalgaard LT, Lee CE, Yu J, Funahashi H, Williams T, et al. Divergence of Melanocortin Pathways in the Control of Food Intake and Energy Expenditure. *Cell* (2005) 123(3):493–505. doi: 10.1016/j.cell.2005.08.035
33. Garfield AS, Li C, Madara JC, Shah BP, Webber E, Steger JS, et al. A Neural Basis for Melanocortin-4 Receptor-Regulated Appetite. *Nat Neurosci* (2015) 18(6):863–71. doi: 10.1038/nn.4011
34. Heisler LK, Jobst EE, Sutton GM, Zhou L, Borok E, Thornton-Jones Z, et al. Serotonin Reciprocally Regulates Melanocortin Neurons to Modulate Food Intake. *Neuron* (2006) 51(2):239–49. doi: 10.1016/j.neuron.2006.06.004
35. Bergman B, Brismar B. Characteristics of Imprisoned Wife-Beaters. *Forensic Sci Int* (1994) 65(3):157–67. doi: 10.1016/0379-0738(94)90271-2
36. Xu Y, Jones JE, Lauzon DA, Anderson JG, Balthasar N, Heisler LK, et al. A Serotonin and Melanocortin Circuit Mediates D-Fenfluramine Anorexia. *J Neurosci* (2010) 30(44):14630–4. doi: 10.1523/JNEUROSCI.5412-09.2010
37. Gao Y, Yao T, Deng Z, Sohn JW, Sun J, Huang Y, et al. TrpC5 Mediates Acute Leptin and Serotonin Effects *via* Pomc Neurons. *Cell Rep* (2017) 18 (3):583–92. doi: 10.1016/j.celrep.2016.12.072
38. D'Agostino G, Lyons D, Cristiano C, Lettieri M, Olarte-Sanchez C, Burke LK, et al. Nucleus of the Solitary Tract Serotonin 5-HT(2C) Receptors Modulate Food Intake. *Cell Metab* (2018) 28(4):619–30.e5. doi: 10.1016/j.cmet.2018.07.017
39. Fan W, Ellacott KL, Halatchev IG, Takahashi K, Yu P, Cone RD. Cholecystokinin-Mediated Suppression of Feeding Involves the Brainstem Melanocortin System. *Nat Neurosci* (2004) 7(4):335–6. doi: 10.1038/nn1214
40. Huo L, Grill HJ, Bjørbaek C. Divergent Regulation of Proopiomelanocortin Neurons by Leptin in the Nucleus of the Solitary Tract and in the Arcuate Hypothalamic Nucleus. *Diabetes* (2006) 55(3):567–73. doi: 10.2337/diabetes.55.03.06.db05-1143
41. Zhan C, Zhou J, Feng Q, Zhang JE, Lin S, Bao J, et al. Acute and Long-Term Suppression of Feeding Behavior by POMC Neurons in the Brainstem and Hypothalamus, Respectively. *J Neurosci: Off J Soc Neurosci* (2013) 33 (8):3624–32. doi: 10.1523/jneurosci.2742-12.2013
42. Wang D, He X, Zhao Z, Feng Q, Lin R, Sun Y, et al. Whole-Brain Mapping of the Direct Inputs and Axonal Projections of POMC and AgRP Neurons. *Front Neuroanat* (2015) 9:40. doi: 10.3389/fnana.2015.00040
43. Patrick L. Eating Disorders: A Review of the Literature With Emphasis on Medical Complications and Clinical Nutrition. *Altern Med Rev* (2002) 7 (3):184–202.
44. Berthoud HR. Metabolic and Hedonic Drives in the Neural Control of Appetite: Who Is the Boss? *Curr Opin Neurobiol* (2011) 21(6):888–96. doi: 10.1016/j.conb.2011.09.004
45. van Gestel MA, Kostrzewa E, Adan RA, Janhunen SK. Pharmacological Manipulations in Animal Models of Anorexia and Binge Eating in Relation to Humans. *Br J Pharmacol* (2014) 171(20):4767–84. doi: 10.1111/bph.12789
46. Beier KT, Steinberg EE, DeLoach KE, Xie S, Miyamichi K, Schwarz L, et al. Circuit Architecture of VTA Dopamine Neurons Revealed by Systematic Input-Output Mapping. *Cell* (2015) 162(3):622–34. doi: 10.1016/j.cell.2015.07.015
47. Bubar MJ, Cunningham KA. Distribution of Serotonin 5-HT2C Receptors in the Ventral Tegmental Area. *Neuroscience* (2007) 146(1):286–97. doi: 10.1016/j.neuroscience.2006.12.071
48. Xu P, He Y, Cao X, Valencia-Torres L, Yan X, Saito K, et al. Activation of Serotonin 2c Receptors in Dopamine Neurons Inhibits Binge-Like Eating in Mice. *Biol Psychiatry* (2017) 81(9):737–47. doi: 10.1016/j.biopsych.2016.06.005
49. Navailles S, Moison D, Cunningham KA, Spampinato U. Differential Regulation of the Mesoaccumbens Dopamine Circuit by Serotonin2c Receptors in the Ventral Tegmental Area and the Nucleus Accumbens: An *In Vivo* Microdialysis Study With Cocaine. *Neuropsychopharmacology* (2008) 33(2):237–46. doi: 10.1038/sj.npp.1301414
50. Johnson AK, Thunhorst RL. The Neuroendocrinology of Thirst and Salt Appetite: Visceral Sensory Signals and Mechanisms of Central Integration. *Front Neuroendocrinol* (1997) 18(3):292–353. doi: 10.1006/frne.1997.0153
51. Castro L, Athanazio R, Barbetta M, Ramos AC, Angelo AL, Campos I, et al. Central 5-HT2B/2C and 5-HT3 Receptor Stimulation Decreases Salt Intake in Sodium-Depleted Rats. *Brain Res* (2003) 981(1-2):151–9. doi: 10.1016/s0006-8993(03)03015-4
52. Yamamoto T, Shimura T, Sako N, Sakai N, Tanimizu T, Wakisaka S. C-Fos Expression in the Parabrachial Nucleus After Ingestion of Sodium Chloride in the Rat. *Neuroreport* (1993) 4(11):1223–6. doi: 10.1097/00001756-199309000-00003
53. Geerling JC, Loewy AD. Sodium Deprivation and Salt Intake Activate Separate Neuronal Subpopulations in the Nucleus of the Solitary Tract and the Parabrachial Complex. *J Comp Neurol* (2007) 504(4):379–403. doi: 10.1002/cne.21452
54. Park S, Williams KW, Liu C, Sohn JW. A Neural Basis for Tonic Suppression of Sodium Appetite. *Nat Neurosci* (2020) 23(3):423–32. doi: 10.1038/s41593-019-0573-2
55. Menani JV, Thunhorst RL, Johnson AK. Lateral Parabrachial Nucleus and Serotonergic Mechanisms in the Control of Salt Appetite in Rats. *Am J Physiol* (1996) 270(1 Pt 2):R162–8. doi: 10.1152/ajpregu.1996.270.1.R162
56. Oh C-M, Namkung J, Go Y, Shong KE, Kim K, Kim H, et al. Regulation of Systemic Energy Homeostasis by Serotonin in Adipose Tissues. *Nat Commun* (2015) 6(1):1–12. doi: 10.1038/ncomms7794
57. Nonogaki K, Abdallah L, Goulding EH, Bonasera SJ, Tecott LHJD. Hyperactivity and Reduced Energy Cost of Physical Activity in Serotonin 5-HT2C Receptor Mutant Mice. *Diabetes* (2003) 52(2):315–20. doi: 10.2337/diabetes.52.2.315
58. Burke LK, Doslikova B, D'Agostino G, Greenwald-Yarnell M, Georgescu T, Chianese R, et al. Sex Difference in Physical Activity, Energy Expenditure and Obesity Driven by a Subpopulation of Hypothalamic POMC Neurons. *Mol Metab* (2016) 5: (3):245–52. doi: 10.1016/j.molmet.2016.01.005

59. Fitzgerald LW, Iyer G, Conklin DS, Krause CM, Marshall A, Patterson JP, et al. Messenger RNA Editing of the Human Serotonin 5-HT 2C Receptor. *Neuropsychopharmacology* (1999) 21(1):82–90. doi: 10.1038/sj.npp.1395328
60. Burns CM, Chu H, Rueter SM, Hutchinson LK, Canton H, Sanders-Bush E, et al. Regulation of Serotonin-2C Receptor G-Protein Coupling by RNA Editing. *Nature* (1997) 387(6630):303–8. doi: 10.1038/387303a0
61. Kawahara Y, Grimberg A, Teegarden S, Mombereau C, Liu S, Bale TL, et al. Dysregulated Editing of Serotonin 2C Receptor mRNAs Results in Energy Dissipation and Loss of Fat Mass. *J Neurosci* (2008) 28(48):12834–44. doi: 10.1523/JNEUROSCI.3896-08.2008
62. Sanger GJ. 5-Hydroxytryptamine and the Gastrointestinal Tract: Where Next? *Trends Pharmacol Sci* (2008) 29(9):465–71. doi: 10.1016/j.tips.2008.06.008
63. Fung TC, Vuong HE, Luna CDG, Pronovost GN, Aleksandrova AA, Riley NG, et al. Intestinal Serotonin and Fluoxetine Exposure Modulate Bacterial Colonization in the Gut. *Nat Microbiol* (2019) 4(12):2064–73. doi: 10.1038/s41564-019-0540-4
64. Georgescu T, Lyons D, Heisler LK. Role of Serotonin in Body Weight, Insulin Secretion and Glycaemic Control. *J Neuroendocrinol* (2021) 33(4):e12960. doi: 10.1111/jne.12960
65. Burke LK, Ogunnowo-Bada E, Georgescu T, Cristiano C, de Morentin PBM, Valencia Torres L, et al. Lorcaserin Improves Glycemic Control *via* a Melanocortin Neurocircuit. *Mol Metab* (2017) 6(10):1092–102. doi: 10.1016/j.molmet.2017.07.004
66. Rossi J, Balthasar N, Olson D, Scott M, Berglund E, Lee CE, et al. Melanocortin-4 Receptors Expressed by Cholinergic Neurons Regulate Energy Balance and Glucose Homeostasis. *Cell Metab* (2011) 13(2):195–204. doi: 10.1016/j.cmet.2011.01.010
67. Wade JM, Juneja P, MacKay AW, Graham J, Havel PJ, Tecott LH, et al. Synergistic Impairment of Glucose Homeostasis in Ob/Ob Mice Lacking Functional Serotonin 2C Receptors. *Endocrinology* (2008) 149(3):955–61. doi: 10.1210/en.2007-0927
68. Kwon E, Joung HY, Liu SM, Chua SCJr., Schwartz GJ, Jo YH. Optogenetic Stimulation of the Liver-Projecting Melanocortinergic Pathway Promotes Hepatic Glucose Production. *Nat Commun* (2020) 11(1):6295. doi: 10.1038/s41467-020-20160-w
69. Berglund E, Maaskola J, Schultz N, Friedrich S, Marklund M, Bergenstråhle J, et al. Spatial Maps of Prostate Cancer Transcriptomes Reveal an Unexplored Landscape of Heterogeneity. *Nat Commun* (2018) 9(1):2419. doi: 10.1038/s41467-018-04724-5
70. Leibel RL, Chung WK, Chua SCJr. The Molecular Genetics of Rodent Single Gene Obesities. *J Biol Chem* (1997) 272(51):31937–40. doi: 10.1074/jbc.272.51.31937
71. Trayhurn P, Thurlby PL, James WP. Thermogenic Defect in Pre-Obese Ob/Ob Mice. *Nature* (1977) 266(5597):60–2. doi: 10.1038/266060a0
72. Frederich RC, Hamann A, Anderson S, Löllmann B, Lowell BB, Flier JS. Leptin Levels Reflect Body Lipid Content in Mice: Evidence for Diet-Induced Resistance to Leptin Action. *Nat Med* (1995) 1(12):1311–4. doi: 10.1038/nm1295-1311
73. Tartaglia LA. The Leptin Receptor. *J Biol Chem* (1997) 272(10):6093–6. doi: 10.1074/jbc.272.10.6093
74. Yadav VK, Oury F, Suda N, Liu ZW, Gao XB, Confavreux C, et al. A Serotonin-Dependent Mechanism Explains the Leptin Regulation of Bone Mass, Appetite, and Energy Expenditure. *Cell* (2009) 138(5):976–89. doi: 10.1016/j.cell.2009.06.051
75. Pasqualetti M, Ori M, Marazziti D, Castagna M, Nardi I. Distribution of 5-HT2c and 5-Ht5a Receptor mRNA in Human Brain. *Ann NY Acad Sci* (1998) 861:245. doi: 10.1111/j.1749-6632.1998.tb10202.x
76. Rupp AC, Allison MB, Jones JC, Patterson CM, Faber CL, Bozadjieva N, et al. Specific Subpopulations of Hypothalamic Leptin Receptor-Expressing Neurons Mediate the Effects of Early Developmental Leptin Receptor Deletion on Energy Balance. *Mol Metab* (2018) 14:130–8. doi: 10.1016/j.molmet.2018.06.001
77. Lam BYH, Cimino I, Polex-Wolf J, Nicole Kohnke S, Rimmington D, Iyemere V, et al. Heterogeneity of Hypothalamic Pro-Opiomelanocortin-Expressing Neurons Revealed by Single-Cell RNA Sequencing. *Mol Metab* (2017) 6(5):383–92. doi: 10.1016/j.molmet.2017.02.007
78. Quarta C, Claret M, Zeltser LM, Williams KW, Yeo GSH, Tschöp MH, et al. POMC Neuronal Heterogeneity in Energy Balance and Beyond: An Integrated View. *Nat Metab* (2021) 3(3):299–308. doi: 10.1038/s42255-021-00345-3
79. Lam DD, Leinninger GM, Louis GW, Garfield AS, Marston OJ, Leshan RL, et al. Leptin Does Not Directly Affect CNS Serotonin Neurons to Influence Appetite. *Cell Metab* (2011) 13(5):584–91. doi: 10.1016/j.cmet.2011.03.016
80. Brunetti L, Recinella L, Orlando G, Michelotto B, Di Nisio C, Vacca M. Effects of Ghrelin and Amylin on Dopamine, Norepinephrine and Serotonin Release in the Hypothalamus. *Eur J Pharmacol* (2002) 454(2-3):189–92. doi: 10.1016/s0014-2999(02)02552-9
81. Benoit S, Schwartz M, Baskin D, Woods SC, Seeley RJ. CNS Melanocortin System Involvement in the Regulation of Food Intake. *Horm Behav* (2000) 37(4):299–305. doi: 10.1006/hbeh.2000.1588
82. Schellekens H, De Francesco PN, Kandil D, Theeuwes WF, McCarthy T, van Oeffelen WE, et al. Ghrelin's Orexigenic Effect Is Modulated *via* a Serotonin 2c Receptor Interaction. *ACS Chem Neurosci* (2015) 6(7):1186–97. doi: 10.1021/cn500318q
83. Hattori T, Yakabi K, Takeda H. Cisplatin-Induced Anorexia and Ghrelin. *Vitam Horm* (2013) 92:301–17. doi: 10.1016/B978-0-12-410473-0.00012-X
84. Lu S, Guan JL, Wang QP, Uehara K, Yamada S, Goto N, et al. Immunocytochemical Observation of Ghrelin-Containing Neurons in the Rat Arcuate Nucleus. *Neurosci Lett* (2002) 321(3):157–60. doi: 10.1016/s0304-3940(01)02544-7
85. Cowley MA, Smith RG, Diano S, Tschöp M, Pronchuk N, Grove KL, et al. The Distribution and Mechanism of Action of Ghrelin in the CNS Demonstrates a Novel Hypothalamic Circuit Regulating Energy Homeostasis. *Neuron* (2003) 37(4):649–61. doi: 10.1016/s0896-6273(03)00063-1
86. King GL, Johnson SM. Receptor-Mediated Transport of Insulin Across Endothelial Cells. *Science* (1985) 227(4694):1583–6. doi: 10.1126/science.3883490
87. Havrankova J, Roth J, Brownstein M. Insulin Receptors are Widely Distributed in the Central Nervous System of the Rat. *Nature* (1978) 272(5656):827–9. doi: 10.1038/272827a0
88. Bonasera SJ, Tecott LH. Mouse Models of Serotonin Receptor Function: Toward a Genetic Dissection of Serotonin Systems. *Pharmacol Ther* (2000) 88(2):133–42. doi: 10.1016/s0163-7258(00)00087-5
89. Orosco M, Rouch C, Gerozissis K. Activation of Hypothalamic Insulin by Serotonin is the Primary Event of the Insulin-Serotonin Interaction Involved in the Control of Feeding. *Brain Res* (2000) 872(1-2):64–70. doi: 10.1016/s0006-8993(00)02449-5
90. Zhou L, Sutton GM, Rochford JJ, Semple RK, Lam DD, Oksanen LJ, et al. Serotonin 2C Receptor Agonists Improve Type 2 Diabetes *via* Melanocortin-4 Receptor Signaling Pathways. *Cell Metab* (2007) 6(5):398–405. doi: 10.1016/j.cmet.2007.10.008
91. Lappalainen J, Zhang L, Dean M, Oz M, Ozaki N, Yu D-h, et al. Identification, Expression, and Pharmacology of a Cys23-Ser23 Substitution in the Human 5-HT2c Receptor Gene (HTR2C). *Genomics* (1995) 27(2):274–9. doi: 10.1006/geno.1995.1042
92. Qiu J, Xue C, Bosch MA, Murphy JG, Fan W, Rønnekleiv OK, et al. Serotonin 5-Hydroxytryptamine2c Receptor Signaling in Hypothalamic Proopiomelanocortin Neurons: Role in Energy Homeostasis in Females. *Mol Pharmacol* (2007) 72(4):885–96. doi: 10.1124/mol.107.038083
93. Yamada C, Sadakane C, Nahata M, Saegusa Y, Nakagawa K, Okubo N, et al. Serotonin 2C Receptor Contributes to Gender Differences in Stress-Induced Hypophagia in Aged Mice. *Psychoneuroendocrinology* (2015) 55:81–93. doi: 10.1016/j.psyneuen.2015.02.006
94. Henderson JA, Bethea CL. Differential Effects of Ovarian Steroids and Raloxifene on Serotonin 1A and 2C Receptor Protein Expression in Macaques. *Endocrine* (2008) 33(3):285–93. doi: 10.1007/s12020-008-9087-5
95. Santollo J, Yao D, Neal-Perry G, Etgen AM. Middle-Aged Female Rats Retain Sensitivity to the Anorexigenic Effect of Exogenous Estradiol. *Behav Brain Res* (2012) 232(1):159–64. doi: 10.1016/j.bbr.2012.04.010
96. Noble F, Roques BJ. Cholecystokinin Peptides in Brain Function. *Handb Neurochem Mol Neurobiol* (2006), 545–71. doi: 10.1007/978-0-387-30381-9_24
97. Ivy A, Oldberg EJA. A Hormone Mechanism for Gall-Bladder Contraction and Evacuation. *JoP-LC* (1928) 86(3):599–613. doi: 10.1152/ajplegacy.1928.86.3.599

98. Hayes MR, Covasa MJP. CCK and 5-HT Act Synergistically to Suppress Food Intake Through Simultaneous Activation of CCK-1 and 5-HT3 Receptors. *Peptides* (2005) 26(11):2322–30. doi: 10.1016/j.peptides.2005.03.045
99. Hayes MR, Covasa M. Dorsal Hindbrain 5-HT3 Receptors Participate in Control of Meal Size and Mediate CCK-Induced Satiation. *JBr* (2006) 1103 (1):99–107. doi: 10.1016/j.brainres.2006.05.058
100. Hayes MR, Moore RL, Shah SM, Covasa MJ. 5-HT3 Receptors Participate in CCK-Induced Suppression of Food Intake by Delaying Gastric Emptying. *AJoP-R Integrative Physiol C* (2004) 287(4):R817–R23. doi: 10.1152/ajpregu.00295.2004
101. Voigt J-P, Fink H, Marsden CJ. Evidence for the Involvement of the 5-HT 1A Receptor in CCK Induced Satiety in Rats. *N-Ssaop* (1995) 351(3):217–20. doi: 10.1007/BF00233239
102. Asarian L, Geary N, Langhans WJA. Serotonin 2C Receptor (5HT2CR) Signaling is Necessary for, and Dissociates the Neural Pathways of, the Satiating Effects of Cholecystokinin (CCK) and Glucagon-Like Peptide-1 (GLP-1). *Appetite* (2008) 2(51):352. doi: 10.1016/j.appet.2008.04.029
103. Wan XQ, Zeng F, Huang XF, Yang HQ, Wang L, Shi YC, et al. Risperidone Stimulates Food Intake and Induces Body Weight Gain via the Hypothalamic Arcuate Nucleus 5-HT2c Receptor—NPY Pathway. *CNS Neurosci Ther* (2020) 26(5):558–66. doi: 10.1111/cns.13281
104. Bonn M, Schmitt A, Lesch K-P, Van Bockstaele E, Asan EJBS. Function. Serotonergic Innervation and Serotonin Receptor Expression of NPY-Producing Neurons in the Rat Lateral and Basolateral Amygdaloid Nuclei. *Brain Struct Funct* (2013) 218(2):421–35. doi: 10.1007/s00429-012-0406-5
105. Bocchio M, McHugh SB, Bannerman DM, Sharp T, Capogna MJ. Serotonin, Amygdala and Fear: Assembling the Puzzle. *Finc* (2016) 10:24. doi: 10.3389/fncir.2016.00024
106. Currie PJ, Saxena N, Tu AYJN. 5-HT2A/2C Receptor Antagonists in the Paraventricular Nucleus Attenuate the Action of DOI on NPY-Stimulated Eating. *Neuroreport* (1999) 10(14):3033–6. doi: 10.1097/00001756-199909290-00029
107. Currie PJ, Coscina DVJN. Stimulation of 5–HT2A/2C Receptors Within Specific Hypothalamic Nuclei Differentially Antagonizes NPY-Induced Feeding. *Neuroreport* (1997) 8(17):3759–62. doi: 10.1097/00001756-199712010-00020
108. Isaac M. Serotonergic 5-HT2C Receptors as a Potential Therapeutic Target for the Design Antiepileptic Drugs. *Curr Topics Medicinal Chem* (2005) 5 (1):59–67. doi: 10.2174/1568026053386980
109. Ahima RS, Antwi DA. Brain Regulation of Appetite and Satiety. *Endocrinol Metab Clin North Am* (2008) 37(4):811–23. doi: 10.1016/j.ecl.2008.08.005
110. Dalton GL, Lee MD, Kennett GA, Dourish CT, Clifton PG. Serotonin 1B and 2C Receptor Interactions in the Modulation of Feeding Behaviour in the Mouse. *Psychopharmacology* (2006) 185(1):45–57. doi: 10.1007/s00213-005-0212-3
111. Dalton GL, Lee MD, Kennett GA, Dourish CT, Clifton PG. mCPP-Induced Hyperactivity in 5-HT2C Receptor Mutant Mice Is Mediated by Activation of Multiple 5-HT Receptor Subtypes. *Neuropharmacology* (2004) 46(5):663–71. doi: 10.1016/j.neuropharm.2003.11.012
112. Higgs S, Cooper AJ, Barnes NM. Reversal of Sibutramine-Induced Anorexia With a Selective 5-HT(2C) Receptor Antagonist. *Psychopharmacology* (2011) 214(4):941–7. doi: 10.1007/s00213-010-2106-2
113. Halford JC, Harrold JA. 5-HT(2C) Receptor Agonists and the Control of Appetite. *Handb Exp Pharmacol* (2012) 209):349–56. doi: 10.1007/978-3-642-24716-3_16
114. Heisler LK, Chu HM, Tecott LH. Epilepsy and Obesity in Serotonin 5-HT2C Receptor Mutant Mice. *Ann NY Acad Sci* (1998) 861:74–8. doi: 10.1111/j.1749-6632.1998.tb10175.x
115. Garattini S, Mennini T, Bendotti C, Invernizzi R, Samanin R. Neurochemical Mechanism of Action of Drugs Which Modify Feeding *via* the Serotoninergic System. *Appetite* (1986) 7 Suppl:15–38. doi: 10.1016/s0195-6663(86)80050-2
116. Oluyomi AO, Gibson EL, Barnfield AM, Curzon G. D-Fenfluramine and D-Norfenfluramine Hypophagias Do Not Require Increased Hypothalamic 5-Hydroxytryptamine Release. *Eur J Pharmacol* (1994) 264(1):111–5. doi: 10.1016/0014-2999(94)90646-7
117. Gibson EL, Kennedy AJ, Curzon G. D-Fenfluramine- and D-Norfenfluramine-Induced Hypophagia: Differential Mechanisms and Involvement of Postsynaptic 5-HT Receptors. *Eur J Pharmacol* (1993) 242(1):83–90. doi: 10.1016/0014-2999(93)90013-8
118. Khan MA, Herzog CA, St Peter JV, Hartley GG, Madlon-Kay R, Dick CD, et al. The Prevalence of Cardiac Valvular Insufficiency Assessed by Transthoracic Echocardiography in Obese Patients Treated With Appetite-Suppressant Drugs. *N Engl J Med* (1998) 339(11):713–8. doi: 10.1056/NEJM199809103391101
119. Gardin JM, Schumacher D, Constantine G, Davis KD, Leung C, Reid CL. Valvular Abnormalities and Cardiovascular Status Following Exposure to Dexfenfluramine or Phentermine/Fenfluramine. *Jama* (2000) 283(13):1703–9. doi: 10.1001/jama.283.13.1703
120. Thomsen WJ, Grottick AJ, Menzaghi F, Reyes-Saldana H, Espitia S, Yuskin D, et al. Lorcaserin, A Novel Selective Human 5-Hydroxytryptamine2c Agonist: *In Vitro* and *In Vivo* Pharmacological Characterization. *J Pharmacol Exp Ther* (2008) 325(2):577–87. doi: 10.1124/jpet.107.133348
121. Smith SR, Weissman NJ, Anderson CM, Sanchez M, Chuang E, Stubbe S, et al. Multicenter, Placebo-Controlled Trial of Lorcaserin for Weight Management. *N Engl J Med* (2010) 363(3):245–56. doi: 10.1056/NEJMoa0909809
122. Fidler MC, Sanchez M, Raether B, Weissman NJ, Smith SR, Shanahan WR, et al. A One-Year Randomized Trial of Lorcaserin for Weight Loss in Obese and Overweight Adults: The BLOSSOM Trial. *J Clin Endocrinol Metab* (2011) 96(10):3067–77. doi: 10.1210/jc.2011-1256
123. Chan EW, He Y, Chui CS, Wong AY, Lau WC, Wong IC. Efficacy and Safety of Lorcaserin in Obese Adults: A Meta-Analysis of 1-Year Randomized Controlled Trials (RCTs) and Narrative Review on Short-Term RCTs. *Obes Reviews: An Off J Int Assoc Study Obes* (2013) 14(5):383–92. doi: 10.1111/obr.12015
124. Higgins GA, Desnoyer J, Van Niekerk A, Silenieks LB, Lau W, Thevarkunnel S, et al. Characterization of the 5-HT2C Receptor Agonist Lorcaserin on Efficacy and Safety Measures in a Rat Model of Diet-Induced Obesity. *Pharmacol Res Perspect* (2015) 3(1):e00084. doi: 10.1002/prp2.84
125. Tuccinardi D, Farr OM, Upadhyay J, Oussaada SM, Mathew H, Paschou SA, et al. Lorcaserin Treatment Decreases Body Weight and Reduces Cardiometabolic Risk Factors in Obese Adults: A Six-Month, Randomized, Placebo-Controlled, Double-Blind Clinical Trial. *Diabetes Obes Metab* (2019) 21(6):1487–92. doi: 10.1111/dom.13655
126. Intensive Blood-Glucose Control With Sulphonylureas or Insulin Compared With Conventional Treatment and Risk of Complications in Patients With Type 2 Diabetes (UKPDS 33). UK Prospective Diabetes Study (UKPDS) Group. *Lancet* (1998) 352(9131):837–53. doi: 10.1016/S0140-6736(98)07019-6
127. Effect of Intensive Blood-Glucose Control With Metformin on Complications in Overweight Patients With Type 2 Diabetes (UKPDS 34). UK Prospective Diabetes Study (UKPDS) Group. *Lancet* (1998) 352(9131):854–65. doi: 10.1016/S0140-6736(98)07037-8
128. Meyer J, Saam W, Mossner R, Cangir O, Ortega GR, Tatschner T, et al. Evolutionary Conserved Microsatellites in the Promoter Region of the 5-Hydroxytryptamine Receptor 2C Gene (HTR2C) are Not Associated With Bipolar Disorder in Females. *J Neural Transm* (2002) 109(5-6):939–46. doi: 10.1007/s007020200077
129. Hill MJ, Reynolds GP. 5-HT2C Receptor Gene Polymorphisms Associated With Antipsychotic Drug Action Alter Promoter Activity. *Brain Res* (2007) 1149:14–7. doi: 10.1016/j.brainres.2007.02.038
130. Yuan X, Yamada K, Ishiyama-Shigemoto S, Koyama W, Nonaka K. Identification of Polymorphic Loci in the Promoter Region of the Serotonin 5-HT2C Receptor Gene and Their Association With Obesity and Type II Diabetes. *Diabetologia* (2000) 43(3):373–6. doi: 10.1007/s001250050056
131. Iordanidou M, Tavridou A, Vasiliadis MV, Arvanitidis KI, Petridis J, Christakidis D, et al. The -759c/T Polymorphism of the 5-HT2C Receptor is Associated With Type 2 Diabetes in Male and Female Caucasians. *Pharmacogenetics Genomics* (2008) 18(2):153–9. doi: 10.1097/FPC.0b013e3282f4ae93
132. Magkos F, Nikonova E, Fain R, Zhou S, Ma T, Shanahan W. Effect of Lorcaserin on Glycemic Parameters in Patients With Type 2 Diabetes Mellitus. *Obesity* (2017) 25(5):842–9. doi: 10.1002/oby.21798

133. O'Neil PM, Smith SR, Weissman NJ, Fidler MC, Sanchez M, Zhang J, et al. Randomized Placebo-Controlled Clinical Trial of Lorcaserin for Weight Loss in Type 2 Diabetes Mellitus: The BLOOM-DM Study. *Obesity* (2012) 20 (7):1426–36. doi: 10.1038/oby.2012.66
134. Handelsman Y, Fain R, Wang Z, Li X, Fujioka K, Shanahan W. Lorcaserin Treatment Allows for Decreased Number Needed to Treat for Weight and Glycemic Parameters in Week 12 Responders With >/=5% Weight Loss. *Postgraduate Med* (2016) 128(8):740–6. doi: 10.1080/00325481.2016.1240591
135. Ma C, Avenell A, Bolland M, Hudson J, Stewart F, Robertson C, et al. Effects of Weight Loss Interventions for Adults Who Are Obese on Mortality, Cardiovascular Disease, and Cancer: Systematic Review and Meta-Analysis. *BMJ* (2017) 359:j4849. doi: 10.1136/bmj.j4849
136. Carbone S, Lavie CJ, Arena R. Obesity and Heart Failure: Focus on the Obesity Paradox. *Mayo Clinic Proc* (2017) 92(2):266–79. doi: 10.1016/j.mayocp.2016.11.001
137. Stiedl O, Misane I, Koch M, Pattij T, Meyer M, Ogren SO. Activation of the Brain 5-HT2C Receptors Causes Hypolocomotion Without Anxiogenic-Like Cardiovascular Adjustments in Mice. *Neuropharmacology* (2007) 52(3):949–57. doi: 10.1016/j.neuropharm.2006.10.012
138. Cataldi M, Cignarelli A, Giallauria F, Muscogiuri G, Barrea L, Savastano S, et al. Cardiovascular Effects of Antiobesity Drugs: Are the New Medicines All the Same? *Int J Obes Suppl* (2020) 10(1):14–26. doi: 10.1038/s41367-020-0015-3

Conflict of Interest: The authors declare that the research was conducted in the absence of any commercial or financial relationships that could be construed as a potential conflict of interest.

frontiers in Endocrinology

ORIGINAL RESEARCH
published: 16 September 2021
doi: 10.3389/fendo.2021.693669

Successful Diagnoses and Remarkable Metabolic Disorders in Patients With Solitary Hypothalamic Mass: A Case Series Report

Boni Xiang[1†], Quanya Sun[1†], Min He[1], Wei Wu[1], Bin Lu[1], Shuo Zhang[1], Zhaoyun Zhang[1], Yehong Yang[1], Yiming Li[1], Yue Wu[2], Zhenwei Yao[2], Haixia Cheng[3], Li Pan[4,5], Qing Miao[1], Yongfei Wang[4*] and Hongying Ye[1*]*

[1] Department of Endocrinology and Metabolism, Huashan Hospital, Fudan University, Shanghai, China, [2] Department of Radiology, Huashan Hospital, Fudan University, Shanghai, China, [3] Department of Pathology, Huashan Hospital, Fudan University, Shanghai, China, [4] Department of Neurosurgery, Huashan Hospital, Fudan University, Shanghai, China, [5] Shanghai Gamma Hospital, Fudan University, Shanghai, China

Background: Solitary intracranial hypothalamic mass occurs rarely. The etiological diagnosis of solitary hypothalamus lesion is challenging and often unachievable. Although previous studies indicated that lesions affecting the hypothalamus often cause significant metabolic disorders, few reports about the metabolic disturbances of patients with solitary hypothalamic mass have been reported.

Method: Twenty-five patients with solitary hypothalamus lesions who had been evaluated and treated in Huashan Hospital from January 2010 to December 2020 were retrospectively enrolled. The clinical manifestations, radiological features, endocrine and metabolic disorders, and pathology were analyzed.

Results: The male to female ratio was 5/20. The median age of onset was 22 (19, 35) years old. The most common initial symptom was polydipsia/polyuria (19/25, 76.0%) and amenorrhea (9/20, 45.0%). A high prevalence of hypopituitarism of different axes was found, with almost all no less than 80%. Central hypogonadism (21/22, 95.5%) and central diabetes insipidus (19/21, 90.5%) were the top two pituitary dysfunctions. Conclusive diagnoses were achieved by intracranial surgical biopsy/resection or stereotactic biopsy in 16 cases and by examining extracranial lesions in 3 cases. The pathological results were various, and the most common diagnoses were Langerhans cell histiocytosis (7/19) and hypothalamitis (5/19). The mean timespan from onset to diagnosis in the 19 cases was 34 ± 26 months. Metabolic evaluations revealed remarkable metabolic disorders, including hyperlipidemia (13/16, 81.3%), hyperglycemia (10/16, 62.5%), hyperuricemia (12/20, 60%), overweight/obesity (13/20, 65.0%), and hepatic adipose infiltration (10/13, 76.6%).

Conclusion: Either surgical or stereotactic biopsy will be a reliable and relatively safe procedure to help to confirm the pathological diagnosis of solitary hypothalamic mass. Metabolic disorders were severe in patients with solitary hypothalamic mass.

OPEN ACCESS

Edited by:
Hu Huang,
East Carolina University, United States

Reviewed by:
Jose Maria Pascual,
Hospital Universitario La Princesa, Spain
Bing Xing,
Peking Union Medical College Hospital (CAMS), China
Zhu Huijuan,
Peking Union Medical College Hospital (CAMS), China

***Correspondence:**
Hongying Ye
yehongying@huashan.org.cn
Yongfei Wang
eamns@hotmail.com
Qing Miao
carmel@139.com

[†]These authors have contributed equally to this work

Specialty section:
This article was submitted to Neuroendocrine Science, a section of the journal Frontiers in Endocrinology

Received: 11 April 2021
Accepted: 25 August 2021
Published: 16 September 2021

Citation:
Xiang B, Sun Q, He M, Wu W, Lu B, Zhang S, Zhang Z, Yang Y, Li Y, Wu Y, Yao Z, Cheng H, Pan L, Miao Q, Wang Y and Ye H (2021) Successful Diagnoses and Remarkable Metabolic Disorders in Patients With Solitary Hypothalamic Mass: A Case Series Report. Front. Endocrinol. 12:693669. doi: 10.3389/fendo.2021.693669

The management of such cases should cover both the treatment of the primary disease, as well as the endocrine and metabolic disorders

Keywords: hypothalamus, hypopituitarism, metabolic disorders, hypothalamic obesity, stereotactic biopsy

INTRODUCTION

Hypothalamus is one of the essential regions of the brain and acts as the regulatory center of the endocrine system. It plays vital roles in regulating endocrine functions, water metabolism, food intake, body weight, body temperature, sleep/wake cycle, and emotions (1). Patients with hypothalamic or peri-hypothalamic lesions may present with similar hormonal or neurologic disorders due to mass effect upon the hypothalamus or direct invasion of this diencephalic region. The etiology of hypothalamic lesions is various, includes congenital developmental malformations, primary tumors, metastatic tumors, hemangioma, inflammatory and granulomatous diseases, trauma, infections, etc. (1). Cases of intracranial solitary hypothalamic mass are rarely reported. Such patients, despite different etiologies, can have similar clinical manifestations and radiological features. The etiological diagnosis of solitary hypothalamus lesion is crucial to determine the treatment. But it is very challenging in practice and often unachievable. Few cases about intracranial solitary hypothalamus mass with a confirmed pathological diagnosis were reported (2, 3). Considering the vital role in regulating metabolism and energy balance, patients with hypothalamic lesions tend to have metabolic disorders. However, few reports have addressed the subject comprehensively. To explore the diagnosis procedures and to reveal the endocrine and metabolic consequences of solitary hypothalamus lesions, we present a case series report of 25 patients with intracranial solitary hypothalamic mass.

METHOD

This is a retrospective study including 25 patients with intracranial solitary hypothalamic lesions admitted to Huashan Hospital from January 2010 to December 2020. The clinical manifestations, endocrine and metabolic disorders, and pathology were reviewed.

Radiological Examinations

Magnetic resonance imaging (MRI) was performed in all patients, using a 3-T scanner (Signa; GE Medical Systems, Shanghai, China). Precontrast T1-weighted spin-echo images and T2-weighted fast spin-echo images were recorded, followed by contrast-enhanced T1-weighted imaging (T1WI). An intracranial solitary hypothalamic lesion is defined as the radiologically proved lesion within the anatomical area of the hypothalamus in MRI. The pre-operation/biopsy/treatment MRI images were reviewed by experienced radiologists, particularly focusing on the neuroradiological variables including size, shape, and consistency of the lesion, enhancement pattern, third ventricle floor status, degree of third ventricle expansion, displacement/atrophy of mammillary bodies, degree of pituitary stalk infiltration, presence of hydrocephalus, and optic chiasm invasion. The size of each lesion was measured at the greatest diameter in each of the three planes. Total-body 18-fluorodeoxyglucose positron emission tomography-CT (18-FDG-PET-CT) was performed in 9 cases, using a combined PET/CT scanner (Siemens Biograph Sensation 16; Siemens, Berlin, Germany).

Surgery and Biopsy

Stereotactic hypothalamic biopsy in 6 patients, surgical biopsy through transcranial approaches or endoscopic endonasal approach in 10 patients, and surgical resection of the hypothalamus lesions in 4 patients were performed. The detailed procedure of stereotactic biopsy can be referred to in our published paper (4).

Endocrine Evaluation

Endocrine functions were routinely evaluated in most patients. Blood and urine samples were obtained at 8:00 AM before any medication. Central adrenal insufficiency (CAI) was defined as a serum cortisol level <3 μg/dL or a peak serum cortisol level <18.1 μg/dL at 30 or 60 minutes in a corticotropin stimulation test (5). Central hypothyroidism (CHT) was defined as a free T4 level below the laboratory reference range in conjunction with a low, normal, or mildly elevated thyroid-stimulating hormone (5, 6). The diagnosis of central hypogonadism (CHG) was made based on low morning serum total testosterone levels with non-raised gonadotropin levels in men or a low serum estradiol level simultaneously low luteinizing hormone and follicle-stimulating hormone in women presenting oligomenorrhea or amenorrhea (7). Hyperprolactinemia (HPL) was defined as a serum PRL level above the laboratory reference range. Central diabetes insipidus (CDI) was confirmed by a water deprivation test followed by a desmopressin test. A urine osmolality of less than 300 mOsm/kg in the presence of fluid deprivation and subsequent rise of urine osmolality by no less than 50% after arginine vasopressin stimulation supported the diagnosis of CDI (7). Besides, for patients with significant polyuria (more than 50 mL/kg of body weight/24 hours), CDI could also be diagnosed by the presence of low urine specific gravity and a good response to a therapeutic trial of desmopressin (5, 7). Evaluation of the growth hormone (GH) axis only included the assessment of IGF-1 levels.

Metabolic Evaluation

Metabolic evaluations, including body mass index (BMI), liver ultrasonography, fasting/postprandial blood glucose

(FBG/PBG), HbA1c, lipid profile, and serum uric acid (SUA), were performed in some cases.

Statistical Analyses

Normal distributed continuous variables were expressed as mean values ± standard deviation (SD). Differences between groups were estimated using the Fisher's exact test or the Mann-Whitney test. Simple linear regression coefficients and multiple regression analysis were used to examine the correlation among parameters. SPSS software (version 21.0, SPSS Inc) was used to perform statistical analyses. A two-tailed P value <0.05 was considered statistically significant.

Ethical Approval

The study was approved by the ethics committee of Huashan Hospital affiliated to Fudan University. Consent was obtained after a full explanation of the study purpose and procedures.

RESULTS

Symptoms

A short description of patients was shown in **Table 1**. The male to female ratio was 5/20. The median age of onset was 22 (ranging from 10 to 70) years old. The most common initial symptoms (**Figure 1A**) were polydipsia and polyuria (19/25, 76.0%) and amenorrhea (9/20, 45%, Patient No.5 had had menopause before onset). Other symptoms at onset included hyperphagia (3/25), cognitive impairment (3/25, mainly memory deterioration together with reduced ability to solve problems), affective disorders (2/25, manifesting as irritability), weight loss (2/25), weight gain (1/25), anorexia (1/25), lactation (1/25), headache (1/25), fever (1/25), dizziness (1/25), visual disorder (1/25), somnolence (1/25), nausea and vomiting (1/25). With the progression of the disease, new manifestations showed up subsequently (**Figure 1B**). Altogether, amenorrhea in females (19/20, 95%) and sexual dysfunction in males (4/4, 100%) were the top two symptoms, followed by polydipsia and polyuria (20/25, 80.0%). Oligodipsia occurred in 3 cases after the onset of diabetes insipidus. Hyperphagia was seen in 12/25 cases, and weight gain in 8/25. Specially, one patient (No.4) had anorexia and weight loss in the beginning but had hyperphagia and weight gain afterward. Besides, affective disorders like irritability or mood swings and cognitive impairment were common, which were seen in 12/25 and 9/25 separately. Fever with no evidence of infection occurred in 7 cases. Some patients showed symptoms related to mass effects, such as headache (4/25), visual disorders (7/25), nausea, and vomiting (1/25). Disturbance of consciousness developed, such as somnolence (6/25) and even coma (1/25, No.23), which may be related to severe hypernatremia (over 160mmol/L). This patient complained of symptoms of auditory and visual hallucination, too. Subcutaneous lumps were seen in two cases (No. 20&21), who were diagnosed with Langerhans cell histiocytosis (LCH). Patient No. 21 had systemic skin lesions manifesting as itches, ulceration, and exudation.

Radiological Features

Table 2 shows a summary of the neuroradiological variables. The pre-operation/biopsy/treatment MR images of patients No. 2, 3, 18, 22, 25 were missing. The T1-weighted postcontrast coronal and sagittal views of MR images of two typical cases (patients No. 7 and 10) were shown in **Figure 2**. The MRI features mainly demonstrated hypointense or isointense T1WI and hyperintense T2WI for the hypothalamic lesions. In contrast-enhanced T1WI, all lesions showed enhancement patterns, either heterogeneous or homogeneous. Hydrocephalus was seen in 7 patients. In 5 (71.4%) of them, the lesions` maximum diameter in any of the three planes was no less than 2cm. The lesions took on an elliptical (6/20), round (7/20), polygonal (4/20), or lobulated (3/20) shape. A consistency of pure solid was seen in most cases (17/20), while mixed solid-cystic lesion was found in cases No. 4 and 9, and solid with small cystic change lesion in patient No. 11. Atrophy of mammillary bodies wasn`t found, but their displacement was observed in 8 cases, either downward (6/20) or upward (2/20). In 9/20 cases, the pituitary stalk was partially infiltrated, and in 3/20 wholly infiltrated. The bright signals in the posterior lobe of the pituitary were absent for all cases. Optic chiasm was partially infiltrated in 15/20 cases and wholly infiltrated in 3/20. Among the 18 patients, 6 had visual disorders. The third ventricle floor (TVF) identification was examined. The TVFs were completely identifiable in 3/20 cases, not visible in 10/20 patients, and in 7/20 cases, only mammillary bodies were visible. Third ventricle involvement was seen in 15/20 cases, with 1 wholly invaded and 14 partially invaded.

The correlations between complex hypothalamic symptoms (including cognitive impairment, affective disorder, hyperphagia, weight gain, fever, and somnolence) and the lesion size (using the maximum diameter in any of the three planes as the variable), TVF identification, and third ventricle involvement were analyzed. The absence of any of such symptoms was only seen in cases with lesion sizes less than 1cm (see the blue bars in **Figure 3A**). Also, a larger size is a marked predictor of developing affective disorders and hyperphagia (P=0.032 and 0.005, respectively). Patients having cognitive impairment tend to have larger lesions than those who didn`t too, but the difference is not statistically significant (P=0.088). Similarly, patients with wholly identifiable TVFs showed no manifestations of such complex hypothalamic symptoms (**Figure 3B**). Those with more notable involvement of the TVFs were more likely to have symptoms of affective disorders and hyperphagia (P=0.042 for both). Generally, patients with these complex symptoms had higher degrees of the third ventricle involvement (**Figure 3C**), despite the statistic insignificance. Patient No. 9, whose third ventricle was completely invaded, developed all the six symptoms described above.

High FDG metabolism of the solitary hypothalamic lesions was found in 18-FDG-PET-CT for the nine evaluated cases, with the maximum standardized uptake values (SUVs) ranging from 5.1 to 33 (**Supplementary Table 1**). In 6/9 of the cases whose diagnoses were confirmed, the SUVs of those who had LCH were

TABLE 1 | Short description of patients.

No	Gender	Age of Onset (y/o)	Initial symptoms	All symptoms	AI	CHT	CHG	HPL	Low IGF-1	CDI	Diagnosis	DfOtD (months)	Treatment	Follow-up period (months)	Outcome
1	F	38	polydipsia, polyuria	polydipsia, polyuria, amenorrhea	N*	N	Y†	Y	Y	Y	Unknown	/	Radiotherapy	4	Stable lesion
2	F	26	amenorrhea	amenorrhea, polyphagia, irritability, memory deterioration	N/A‡	Y	Y	Y	N/A	Y	Unknown	/	/	16	Stable lesion
3	F	25	polydipsia, polyuria, anorexia, weight loss	polydipsia, polyuria, anorexia, weight loss, depressed mood, memory deterioration, polyphagia, weight gain	N/A	N/A	N/A	N/A	N/A	N/A	LCH	66	Surgical resection	44	Stable lesion
4	F	17	irritability, memory deterioration, difficulty with problem-solving, polyphagia, weight gain	irritability, memory deterioration, difficulty with problem-solving, polyphagia, weight gain, amenorrhea	N/A	N/A	Y	N/A	N/A	N/A	Germinoma	15	Radiotherapy	39	Lesion shrinkage after radiotherapy and stable afterwards
5	F	58	polydipsia, polyuria	polydipsia, polyuria, fever	Y	Y	Y	Y	N	Y	LCH	48	Radiotherapy	25	Lesion shrinkage after treatment and stable afterwards
6	F	21	polydipsia, polyuria, somnolence	polydipsia, polyuria, somnolence, amenorrhea, polyphagia, weight gain	Y	Y	Y	Y	Y	Y	Unknown	/	Gamma knife radiosurgery	9	Lesion shrinkage after treatment and stable afterwards
7	M	34	polydipsia, polyuria	polydipsia, polyuria, sexual dysfunction	Y	Y	Y	Y	N	Y	Hypothalamitis	33	Methylprednisolone and azathioprine	47	Lesion shrinkage after treatment and stable afterwards
8	M	22	nausea, vomiting	nausea, vomiting, headache, sexual dysfunction	Y	Y	Y	Y	Y	Y	Germinoma	26	Radiotherapy and chemotherapy	25	Lesion shrinkage after treatment and stable afterwards
9	F	21	polydipsia, polyuria	polydipsia, polyuria, amenorrhea, visual disorder, irritability, memory deterioration, polyphagia, weight gain, fever, somnolence	Y	Y	Y	N/A	N/A	Y	Embryonic germ cell tumors	3	Radiotherapy and chemotherapy	110	Lesion shrinkage after treatment and stable afterwards
10	F	37	polydipsia, polyuria, amenorrhea, weight loss	polydipsia, polyuria, amenorrhea, weight loss, apathy	Y	Y	Y	N/A	Y	Y	LCH	15	Radiotherapy and chemotherapy	40	Lesion shrinkage after treatment, death of systemic disease spread afterwards
11	F	32	polydipsia, polyuria	polydipsia, polyuria, polyphagia, weight gain, fever, somnolence, oligodipsia, disorientation, loss of memory	Y	Y	Y	Y	N	Y	Hypothalamitis	29	Methylprednisolone	/	Lesion shrinkage, lost to follow-up afterwards
12	F	17	polydipsia, polyuria, amenorrhea, fever	polydipsia, polyuria, amenorrhea, fever, irritability, polyphagia, weight gain, somnolence, oligodipsia	Y	Y	Y	Y	Y	Y	Hypothalamitis	30	Methylprednisolone and azathioprine	/	Lost to follow-up
13	F	19	polydipsia, polyuria, amenorrhea	polydipsia, polyuria, amenorrhea	Y	Y	Y	Y	N	Y	Hypothalamitis	24	Diagnostic radiotherapy; Methylprednisolone and azathioprine after biopsy	12	Lesion shrinkage; sudden death of unknown reason afterwards
14	F	35	polydipsia, polyuria	polydipsia, polyuria, amenorrhea, irritability, polyphagia, weight loss	Y	Y	Y	Y	Y	Y	Granulosa cell tumor	77	/	/	Lost to follow-up

(Continued)

TABLE 1 | Continued

No	Gender	Age of Onset (y/o)	Initial symptoms	All symptoms	AI	CHT	CHG	HPL	Low IGF-1	CDI	Diagnosis	DfOtD (months)	Treatment	Follow-up period (months)	Outcome
15	F	35	amenorrhea	polydipsia, polyuria, amenorrhea, lactation, fever, somnolence, apathy	N/A	Y	Y	Y	Y	Y	LCH	35	Gamma knife radiosurgery	25	Death
16	F	22	polydipsia, polyuria, amenorrhea, polyphagia	polydipsia, polyuria, amenorrhea, polyphagia	N/A	N	Y	N	N/A	Y	Rosai-Dorfman disease	53	Gamma knife radiosurgery	8	Lesion shrinkage; death of acute pancreatitis afterwards
17	M	20	polydipsia, polyuria, irritability, memory deterioration, polyphagia	polydipsia, polyuria, irritability, memory deterioration, polyphagia, sexual dysfunction	Y	Y	Y	Y	N/A	Y	Hypothalamitis	3	Dexamethasone, methylprednisolone and azathioprine	132	Lesion shrinkage after treatment and stable afterwards
18	M	70	polydipsia, polyuria	polydipsia, polyuria, sexual dysfunction	Y	Y	Y	Y	N	Y	Metastatic carcinoma from lung	4	/	/	Lost to follow-up
19	F	19	amenorrhea	polydipsia, polyuria, amenorrhea, irritability, memory deterioration, difficulty with problem-solving, polyphagia, weight gain, somnolence, oligodipsia	N/A	Y	Y	Y	N/A	N/A	Unknown	/	Radiotherapy, methylprednisolone and azathioprine	78	Lesion shrinkage in the beginning; death afterwards
20	F	10	polydipsia, polyuria	polydipsia, polyuria, amenorrhea, headache, weight gain, subcutaneous lump on the forehead	N	Y	Y	N	Y	N	LCH	77	Chemotherapy	56	Lesion shrinkage after treatment and stable afterwards
21	F	15	polydipsia, polyuria, amenorrhea	polydipsia, polyuria, amenorrhea, subcutaneous lump on the occiput, skin itches/ulceration/exudation	Y	Y	Y	Y	Y	Y	LCH	17	Chemotherapy	/	Lost to follow-up
22	F	22	polydipsia, polyuria, headache, loss of memory	polydipsia, polyuria, headache, loss of memory, amenorrhea, lactation	N/A	N/A	N/A	N/A	N/A	N/A	LCH	81	Chemotherapy	/	Lesion shrinkage after treatment and stable afterwards
23	F	34	polydipsia, polyuria	polydipsia, polyuria, amenorrhea, mood swings, polyphagia, fever, auditory hallucination, visual hallucination, coma	N/A	Y	N/A	Y	N/A	Y	Unknown	/	Gamma knife radiosurgery	14	No change after treatment
24	F	40	polydipsia, polyuria	polydipsia, polyuria, amenorrhea, mood swings, visual disorder, loss of memory, fever	Y	Y	Y	Y	Y	Y	Unknown	/	/	11	Stable lesion
25	M	14	visual disorder, dizziness	visual disorder, dizziness	N	N	N	Y	N	N	Pilocytic astrocytoma	3	Surgical resection	/	Lost to follow-up

AI, adrenal insufficiency; CHT, central hypothyroidism; CHG, central hypogonadism; HPL, hyperprolactinemia; CDI, central diabetes insipidus; DfOtD, duration from onset to diagnosis; LCH, Langerhans cell histiocytosis. N: no. Y†: yes. N/A‡: not available.*

The follow-up period refers to the time span from the treatment to the timepoint of the last follow-up/death. For those no treatment was given, the follow-up period refers to the time span from the first admission to the timepoint of last follow-up/death.

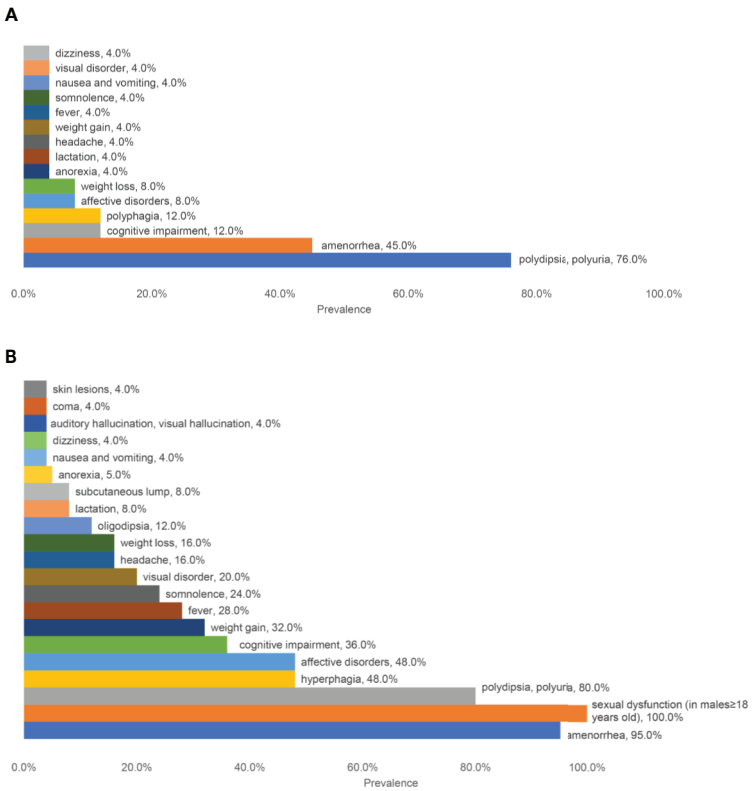

FIGURE 1 | A summary of the prevalence of different symptoms. **(A)** The prevalence of initial symptoms; **(B)** The prevalence of all the symptoms.

significantly higher than those who didn`t (20.87 ± 5.92 *vs.* 6.37 ± 1.17, P=0.047). Besides the primary lesions, elevated uptake of FDG was found in patient No.1 (bone marrow), No.6 (bilateral cervical, axillary, mesenteric, and retroperitoneal lymph nodes), No.18 (left upper lung, mediastinal, and bilateral pulmonary hilar lymph nodes), No.21(hepatic hilar region, skins of bilateral chest wall and axillae, muscles of the left buttock), No.22 (bilateral temporal-mandibular joint, bilateral cervical, left clavicular lymph nodes), and No.24 (bilateral submandibular, bilateral axillary, right inguinal lymph nodes and a pulmonary nodule in the right lung).

Diagnosis

Histopathological diagnoses were confirmed in 19 of the 25 patients. The mean timespan from onset to diagnosis was 34 ± 26 months. The diagnoses were various, and the most common diseases were Langerhans cell histiocytosis (7/19) and hypothalamitis (5/19). **Figures 4**, **5** show the histopathologic findings of patients No. 10 and 17, which were diagnosed with LCH and hypothalamitis separately. Marked histiocyte proliferation was found in case No. 10. Immunohistochemistry examination reflected significant abundance in CD1a cells, scattered CD68 positive results for anti-CD68 antibody (KP1) and leukocyte common antigen (LCA), and few CD138 cells. Abundant lymphocyte, plasma cells, and histiocyte were seen in case No.17. Immunohistochemical analysis revealed scattered CD68, CD138, and CD3 cells, with IgG deposition. CD20 and CD1a cells were absent. Those with hypothalamitis were treated with glucocorticoids and/or azathioprine, and post-therapeutic MRI revealed mass volume reduction. In the 20 patients receiving neurosurgical biopsy/resection or stereotactic biopsy, definite histopathological diagnosis was not achieved in 4 of them (No.1, 6, 20, and 24). Only gliosis and inflammatory cell infiltration were found, with no diagnostic immunohistochemical features. For patient No.20, two years after the surgical biopsy through craniotomy, a subcutaneous lump on the forehead gradually arose. The biopsy of the lump later suggested the diagnosis of LCH. Patient No.21 received a skin biopsy, and it turned out to be LCH. Patient No. 18, the eldest case of all, was found to have mediastinal lymph node enlargement in the chest computed tomography (CT) scan. The lymph node biopsy helped to confirm the histopathological diagnosis of low-differentiated neuroendocrine carcinoma originated from the lung. Thus, the mass of the patient's hypothalamus was thought of as the metastatic lesion of the lung carcinoma.

Pituitary Dysfunctions and Metabolic Disorders

In the evaluation of pituitary functions, central hypogonadism (21/22, 95.5%) and central diabetes insipidus (19/21, 90.5%) were found the two most commonly affected axes (**Figure 6A**). The prevalence of hypopituitarism of almost all different axes

TABLE 2 | Summary of neuroradiological variables.

No	Hydrocephalus	T1WI	T2WI	Size (cm)	Shape	Lesion consistency	Enhancement pattern	Displacement of MBs	Atrophy of MBs	Pituitary stalk	Optic chiasm invasion	Third ventricle involvement	TVF identification
1	N*	hypointensity	hyperintensity	1.2×1.3×0.9	elliptical	pure solid	marked homogeneous enhancement	Y† (downward)	N	partially infiltrated	partially infiltrated	partial invasion	only MBs visible
2							Images N/A‡						
3							Images N/A						
4	N	mild hypointensity	hyperintensity	2.1×2.1×2.5	lobulated	mixed solid-cystic	marked homogeneous enhancement	N	N	not affected	partially infiltrated	partial invasion	not visible
5	N	mild hypointensity	mild hyperintensity	0.8×1.3×1.2	elliptical	pure solid	marked homogeneous enhancement	Y(downward)	N	partially infiltrated	partially infiltrated	not affected	only MBs visible
6	Y	mild hypointensity	mild hyperintensity	1.6×1.3×2.1	polygonal	pure solid	marked homogeneous enhancement	Y(downward)	N	wholly infiltrated	partially infiltrated	partial invasion	only MBs visible
7	N	hypointensity	hyperintensity	0.5×0.9×0.7	round	pure solid	marked homogeneous enhancement	N	N	not affected	partially infiltrated	not affected	wholly identifiable
8	N	hypointensity	hyperintensity	0.6×0.5×0.6	round	pure solid	marked homogeneous enhancement	N	N	not affected	not affected	not affected	wholly identifiable
9	Y	hypointensity	hyperintensity	2.1×2.0×2.2	round	mixed solid-cystic	marked heterogeneous enhancement	Y(downward)	N	wholly infiltrated	wholly infiltrated	whole invasion	only MBs visible
10	N	mild hypointensity	mild hyperintensity	1.3×1.1×1.2	round	pure solid	marked homogeneous enhancement	Y(downward)	N	partially infiltrated	partially infiltrated	not affected	only MBs visible
11	Y	hypointensity	hyperintensity	1.7×1.4×1.9	elliptical	solid with small cystic change	marked homogeneous enhancement	N	N	partially infiltrated	partially infiltrated	partial invasion	not visible
12	N	hypointensity	hyperintensity	1.3×1.8×1.5	lobulated	pure solid	marked homogeneous enhancement	N	N	partially infiltrated	wholly infiltrated	partial invasion	not visible
13	N	hypointensity	hyperintensity	0.6×0.6×0.5	round	pure solid	marked homogeneous enhancement	N	N	not affected	partially infiltrated	not affected	wholly identifiable
14	Y	hypointensity	hyperintensity	2.1×2.0×2.2	round	mixed solid-cystic	marked heterogeneous enhancement	Y(downward)	N	wholly infiltrated	wholly infiltrated	whole invasion	only MBs visible
15	N	mild hypointensity	mild hyperintensity	1.8×1.4×1.6	polygonal	pure solid	marked homogeneous enhancement	N	N	partially infiltrated	partially infiltrated	partial invasion	not visible
16	N	mild hypointensity	mild hyperintensity	2.1×1.9×1.1	elliptical	pure solid	marked homogeneous enhancement	Y(upward)	N	not affected	partially infiltrated	partial invasion	not visible
17	Y	mild hypointensity	mild hyperintensity	1.8×2.0×2.2	round	pure solid	marked heterogeneous enhancement	N	N	partially infiltrated	not affected	partial invasion	not visible
18							Images N/A						
19	Y	mild hypointensity	mild hyperintensity	2.0×1.9×1.3	polygonal	pure solid	marked homogeneous enhancement	Y(upward)	N	not affected	partially infiltrated	partial invasion	not visible
20	N	hypointensity	hyperintensity	1.7×1.2×1.5	round	pure solid	marked homogeneous enhancement	Y(downward)	N	not affected	partially infiltrated	partial invasion	only MBs visible
21	N	hypointensity	hyperintensity	2.1×1.1×2.4	polygonal	pure solid	marked homogeneous enhancement	N	N	not affected	partially infiltrated	partial invasion	not visible
22							Images N/A						
23	Y	hypointensity	hyperintensity	2.4×2.3×1.6	elliptical	pure solid	marked heterogeneous enhancement	N	N	partially infiltrated	partially infiltrated	partial invasion	not visible
24	N	mild hypointensity	mild hyperintensity	1.8×1.1×1.7	elliptical	pure solid	marked homogeneous enhancement	N	N	partially infiltrated	partially infiltrated	partial invasion	not visible
25							Images N/A						

MBs, mammillary bodies; TVF, third ventricle floor; N, no; Y†, yes; N/A‡, not available.*

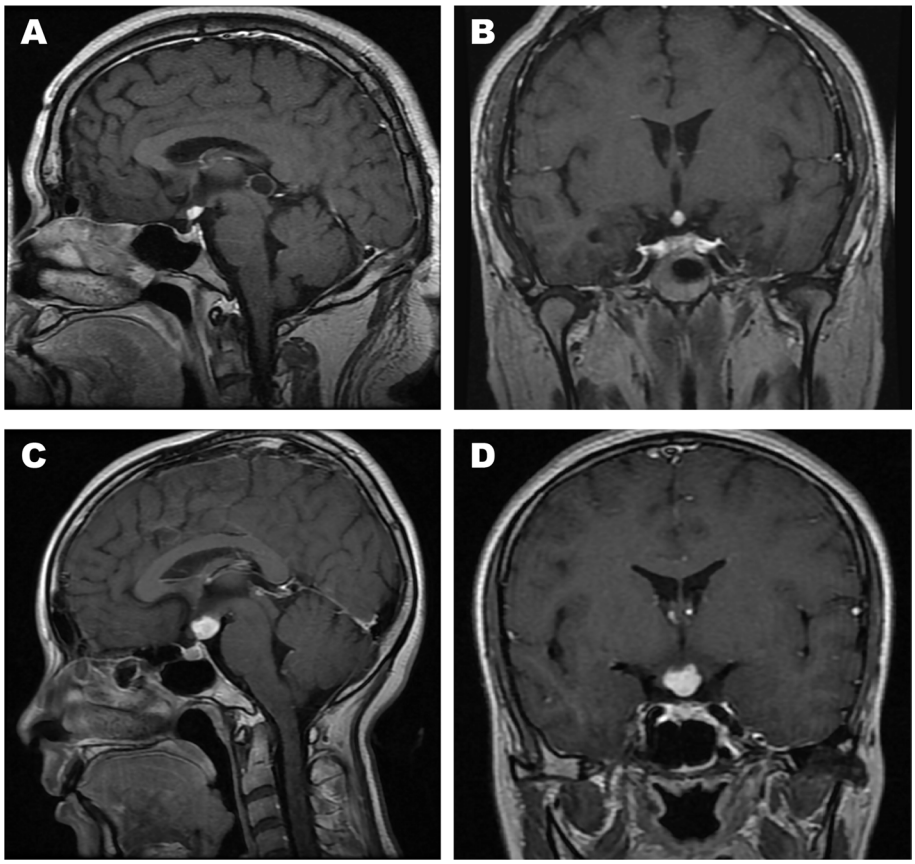

FIGURE 2 | The T1-weighted postcontrast MR images of two typical cases. **(A)** Sagittal view of patient No. 7; **(B)** Coronal view of patient No. 7; **(C)** Sagittal view of patient No. 10; **(D)** Coronal view of patient No. 10.

(including the adrenal gland, thyroid gland, gonadal glands, prolactin, and neurohypophysis) in the evaluated patients exceeded 80%. Insulin-like growth factor-1 (IGF-1) levels below the age- and gender-matched reference range were found in 10 of the 16 patients.

Metabolic evaluation in the cases revealed remarkable metabolic disorders. Pre-operation/treatment data of body mass index (BMI) were available in 20 cases (**Figure 6B**). Overweight (24≤BMI ≤ 27.9) was found in 8 (40.0%), and obesity (BMI≥28) in 5 (25.0%). Hyperlipidemia developed in 13 of the 16 evaluated cases. The levels of triglyceride (TG), total cholesterol (TC), low-density lipoprotein-cholesterol (LDL-c), and high-density lipoprotein-cholesterol (HDL-c) were 4.87 ± 5.78, 5.77 ± 1.90, 3.00 ± 1.14, 0.90 ± 0.36 (mmol/L), respectively. Among them, elevated triglyceride (TG) was found in all 13 cases. Patient No. 5 even had a TG level as high as 25.0mmol/L (**Figure 6C**). In the evaluation of glucose metabolism, 7/16 cases were proved to have diabetes mellitus (DM), 3/16 had impaired glucose tolerance (IGT). Hyperuricemia was found in 10 of the 15 females and 2 of the 5 males, with serum uric acid levels of 0.460 ± 0.156mmol/L and 0.342 ± 0.120mmol/L separately (**Figure 6D**). No onset of gout was reported. In the 12 patients with hyperuricemia, 5 cases had no elevated serum sodium level. Liver ultrasonography demonstrated hepatic adipose infiltration in 11 of the 16 evaluated patients. No history of excessive drinking was reported, nor evidence of viral/autoimmune/congenital hepatic diseases was found. Levels of the serum lipid profile, HbA1c, FBG, PBG, were not significantly related to BMI, while levels of SUA were positively related to BMI (r=0.652, P=0.003). The BMIs of those who had fatty liver infiltration were notably higher than patients who didn`t (P=0.027).

DISCUSSION

Previous reports had given descriptions of the manifestations of patients with hypothalamic lesions, resulting from the mass effects or the dysfunction in the regulation of endocrine disorders (insipidus diabetes, amenorrhea, sexual dysfunction), sleep, food intake, body temperature, water metabolism, emotion, which were called hypothalamic syndrome (1). Early in the 1950s, Bauer reported 60 cases with various lesions in the hypothalamus (8). Neurologic symptoms were the most common clinical manifestations (including neuro-ophthalmologic abnormalities, pyramidal tract or sensory nerve involvement, headaches,

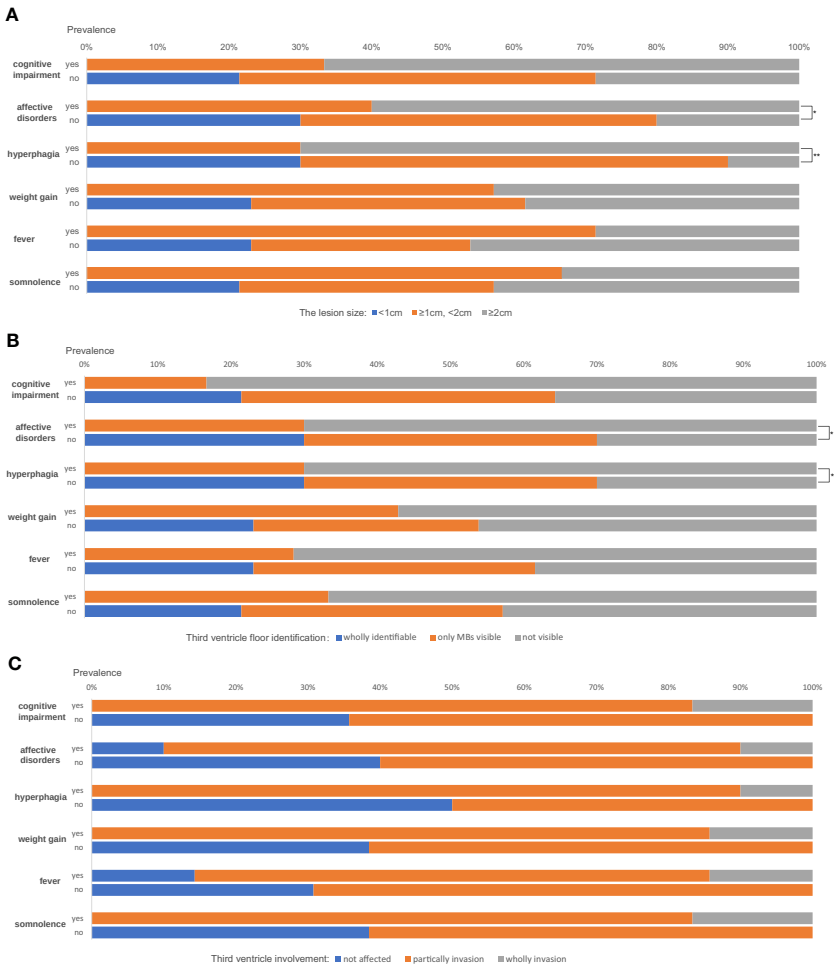

FIGURE 3 | The correlations between complex hypothalamic symptoms and the lesion size **(A)**, the third ventricle floor (TVF) identification **(B)** and third ventricle involvement **(C)**. *P < 0.05, **P < 0.01.

extrapyramidal cerebellar signs, and recurrent vomiting). As for the symptoms related to the hypothalamus itself, sexual abnormalities, diabetes insipidus, and psychic disturbances were the top three manifestations. Specially, precocious puberty was seen in 40% of the cases, which may result from the selection bias. However, few reports had described the symptoms of solitary hypothalamic lesions. In our case series, diabetes insipidus was the most common initial manifestation, affecting 76% of all cases, and the prevalence of polyuria and polydipsia rose to 80% later. Hypogonadism in females was another frequently reported initial symptom (in 9 of the 20 cases). In addition, with the progress of the diseases, manifestations of hypogonadism developed in all the patients over 18 years old. Other symptoms include cognitive impairment, affective disorders, food intake disorders, body weight alternations (either gain or loss), fever, somnolence, oligodipsia, lactation, neurologic symptoms, psychiatric symptoms, and cutaneous/subcutaneous involvement. Our institution mainly deals with adult patients. The youngest age of onset was ten years old in our report. That`s why precocious puberty wasn`t seen. Compared to Bauer`s report, symptoms linked to hypothalamus dysfunction were more common in our case series rather than neurological symptoms. This could be explained by the localized involvement of the hypothalamus, with the adjacent anatomic structures (such as the optic chiasm, the optic nerve, the internal capsule, the pituitary, the pituitary stalk, and the thalamus, etc.) less (or not) affected.

The lesions involving different nuclei and regions of the hypothalamus can result in related symptoms. Central diabetes insipidus mainly results from destructions of the supraoptic and paraventricular nuclei (9). In addition, the dysfunctions of the thirst center osmoreceptors lead to oligodipsia, which may cause severe hypernatremia. As diabetes insipidus was the most common initial symptom in our report, it could be inferred that a primary hypothalamus lesion often firstly affects the supraoptic and paraventricular nuclei. The susceptibility of developing hypogonadism can be another characteristic of solitary hypothalamus lesions. In our study's evaluation of pituitary functions, central hypogonadism had the highest

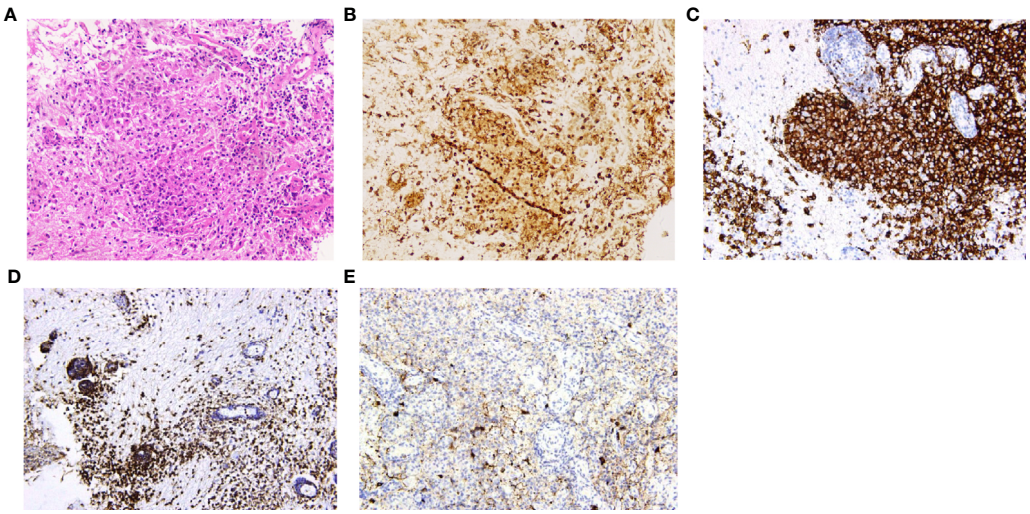

FIGURE 4 | Histopathology and immunohistochemistry manifestations of Langerhans cell histiocytosis (LCH) in patient No. 10. **(A)** H&E staining reflected marked histiocyte proliferation (H&E, ×200 original magnification); Immunohistochemistry indicated clusters of various immunophenotypical markers [**(B)**: CD68+, **(C)**: CD1a+, **(D)**: leukocyte common antigen (LCA)+, **(E)**: CD138+, ×200 original magnification].

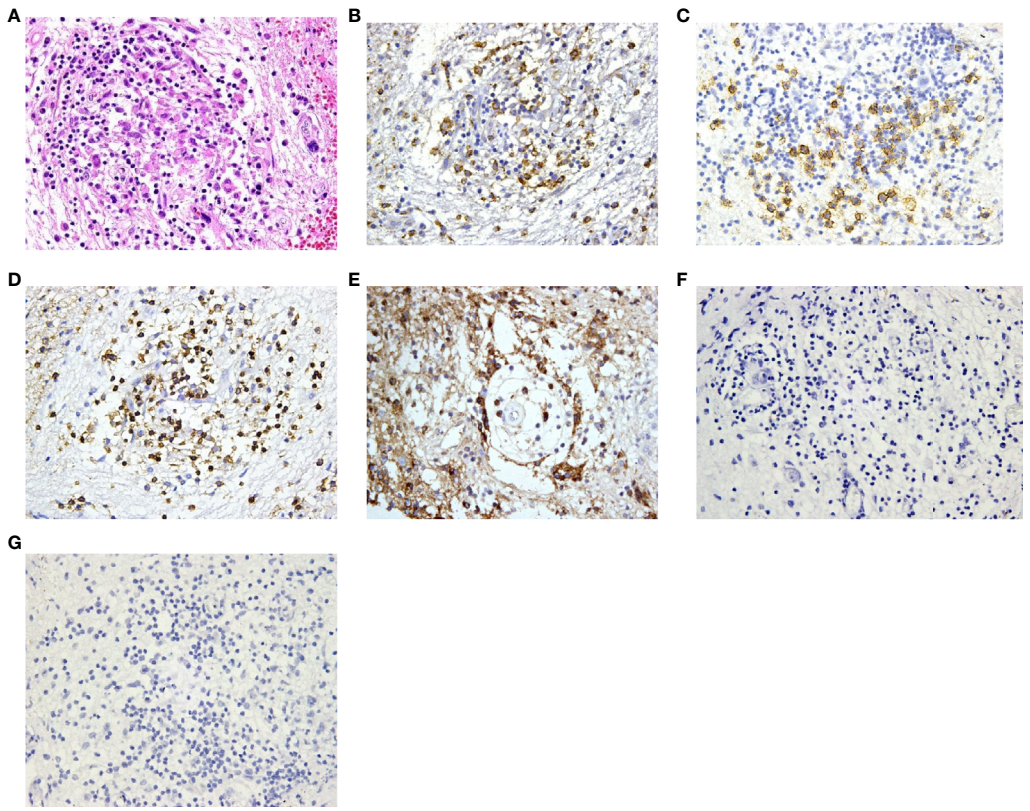

FIGURE 5 | Histopathology and immunohistochemistry manifestations of hypothalamitis in patient No. 17. **(A)** Notable proliferation of lymphocyte, plasma cells and histiocyte was found in H&E staining (H&E, ×200 original magnification); Immunohistochemical analysis revealed scattered CD68 **(B)**, CD138 **(C)** and CD3 **(D)** cells, with IgG deposition **(E)**. CD20 **(F)** and CD1a **(G)** cells were absent.

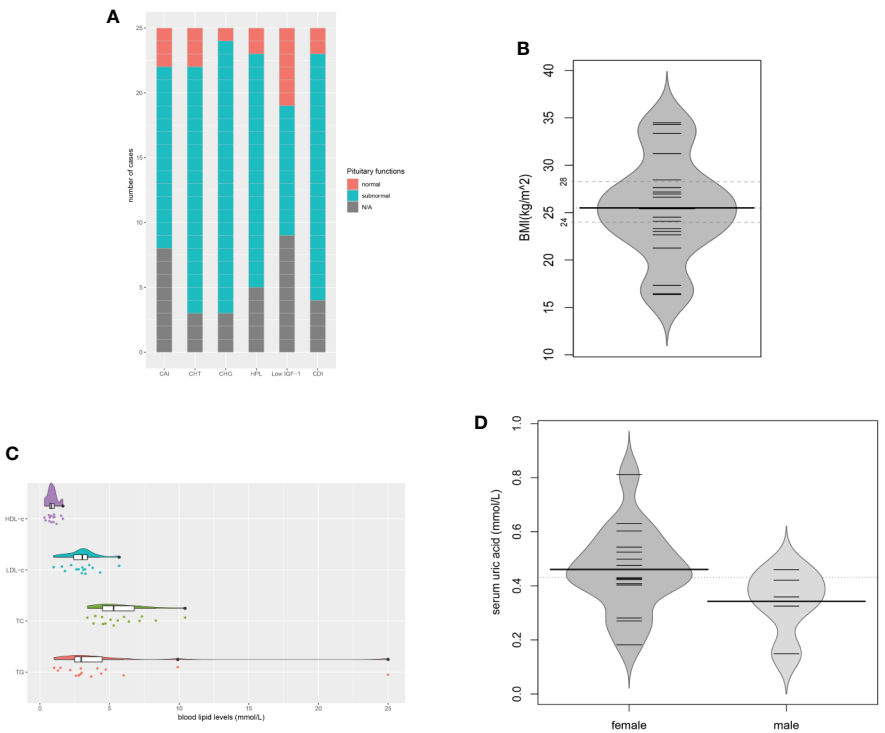

FIGURE 6 | Pituitary dysfunctions and metabolic disorders. **(A)** Description of hypopituitarism of all the cases; **(B)** BMIs of the evaluated cases (n = 20); **(C)** Blood lipid levels of the evaluated cases (n = 16); **(D)** Serum uric acid levels of the evaluated cases (n = 20). CAI, central adrenal insufficiency; CHT, central hypothyroidism; CHG, central hypogonadism; HPL, hyperprolactinemia; CDI, central diabetes insipidus; N/A, not available.

prevalence (95.5%) of all axes. Similarly, as one of the most frequently affected axis in sellar lesions, the previously reported prevalence of central hypogonadism could be as high as 95% in patients with sellar tumors and after surgery or radiotherapy (5). The mechanisms of hypothalamic hypogonadism are complex, including the disorders of gonadotropin-releasing hormone (GnRH) secretion/transportation, pulsatile release of luteinizing hormone (LH) and follicle-stimulating hormone (FSH), and/or hyperprolactinemia, etc. (1) Manifestations of somnolence were common in our and the previous reports (8). The mechanisms of sleep-wake cycle regulation are rather complex. The hypothalamus harbors nuclei and regions controlling sleep-wake cycles, and they communicate with other areas of the brain, especially the reticular activating system of the brain stem, to maintain a normal circadian rhythm (10). Destructions of the hypothalamus could impair normal wakefulness and arousal and lead to prolonged hours of sleep (1). Fever with no evidence of infection occurred in 7 cases. The preoptic area (POA) of the hypothalamus is thought to be the key integratory site for thermoregulation in the brain (11). The symptoms of fevers in such patients could very possibly result from the abnormal central regulation of body temperature. Affective disorders, especially irritability, were found in some of our cases. Lesions in the ventromedial nucleus have been found to be related to aggressive and even violent behaviors in animals (1). Early in 1969, Reeves and Plum described a case whose ventromedial hypothalamus was destroyed by a small neoplasm manifested rage attacks, hyperphagia, and dementia (12). Bilateral involvement of ventromedial nuclei and adjacent pathways contribute to such a triad. Cognition impairment in our reports mainly manifested as memory deterioration, which might be associated with dysfunctions of ventromedial nuclei and the communications between the hypothalamus and brain stem reticular formation and limbic system (1). Also, posteriorly the tuber cinereum lie the mammillary bodies. They include important nuclei of the memory circuit, and hypothalamic lesions affecting the fornices and the afferent input to the mammillary bodies could cause memory defects (13). Such manifestations had been widely described in Korsakoff's syndrome, which is mainly characterized by amnesia (both retrograde and anterograde) (14). The pathology in Korsakoff's syndrome almost always involves the mammillary bodies. Although Korsakoff's syndrome is most frequent in alcoholics, it is also described for craniopharyngiomas affecting the third ventricle (15). It can be inferred that Korsakoff-like amnesia could be a significant determinant of memory deteriorations in our case series. Besides, disorders of the sleep-wake cycle and poor quality of sleep could increase the possibility of cognitive impairment as well (10). In addition to emotional and cognitive alterations, strange behaviors and changes in personality, even accompanied by psychotic symptoms can occur, as was in the case No. 23. Such symptoms reflect lesions affecting more

diffusely the hypothalamic networks and the connectivity of the hypothalamus with the medial-basal frontal cortices and limbic system (16). Our study validates the hypothalamic lesions as a clinical model of psychiatric disturbances, similarly to the case of craniopharyngiomas developing or invading the third ventricle. Accordingly, a wider set of symptoms than the insufficiency of hormones of the endocrine axes controlled by the hypothalamus can be grouped under the term "hypothalamic syndrome" in contrast to the restricted involvement of the infundibulum-tuber cinereum.

In craniopharyngiomas, a clinical-topographical correlation between the patient's syndrome and the anatomical structures involved by the tumor had been proven (17). Structural/functional impairment of the infundibulum-tuber cinereum complex encompassing damage of the median eminence, arcuate nucleus, and tubero-mammillary nuclei, leads to the infundibulo-tuberal syndrome. It was originally described by French authors Claude and Lhermitte in 1917 (18), including symptoms of Fröhlich`s syndrome, obesity, diabetes insipidus, and/or sleep alterations due to lesion of the histaminergic neurons in the tuberomammillary nucleus (19). Infundibulo-tuberal syndrome was found to occur in craniopharyngiomas which replaced or invaded the TVFs (17). Furthermore, injury to structures above the infundibulum and tuber cinereum level (ventromedial and dorsomedial hypothalamus and fornices) induces complex psychiatric, behavioral, or emotional alterations, memory impairment (including Korsakoff's syndrome), abnormal body temperature, and so on. In our study, the clinical-topographical correlation was also confirmed. Hyperphagia and somnolence, as typical manifestations of infundibulo-tuberal syndrome, were only seen in cases with the TVF involvement. Besides, those with complex hypothalamic symptoms associated to cognition, mood and body temperature tended to have larger mass sizes, wider involvement of third ventricle and TVFs.

The solitary hypothalamic lesion occurs rarely, and patients with different etiology could have similar clinical manifestations and MR imaging features. Final diagnoses highly depend on histopathological evidence. The surgical procedures in the hypothalamus region could be risky and challenging. Diagnostic radiation and steroid treatment are alternatives when the etiology is hard to confirm. However, the treatment can be ineffective and induce lots of complications. Only in very few case reports the pathological diagnoses were established (2–4). In our case series, stereotactic hypothalamic biopsy/surgical biopsy/surgical resection was performed in 20 patients by the most experienced surgeons in our institution. 16 of the 20 cases achieved histopathological diagnoses. Either surgical or stereotactic biopsy will be a reliable and relatively safe procedure to help to reach the pathological diagnosis of solitary hypothalamic mass. The stereotactic biopsy can be used for most hypothalamic primary lesions with diameters≥5mm. For lesions located at the bottom area of the hypothalamus or close to the pituitary stalk, a surgical biopsy is more likely to be chosen. In patients No.1, 6, 20, and 24, only gliosis and inflammatory cell infiltration were found, with no diagnostic immunohistochemical features. However, the following subcutaneous lump in patient No. 20 gave rise to the final diagnosis of LCH. Similarly, the skin lesions in patient No. 22 made the diagnosis of LCH. The lymph node biopsy in Patient No.18 helped to confirm the histopathological diagnosis of low-differentiated neuroendocrine carcinoma originated from the lung. So, the mass of the hypothalamus was thought of as a metastatic lesion. Such cases indicated that careful systemic evaluations are critical, including detailed physical examination and history-taking, evaluation of important diagnostic markers, and comprehensive radiological examinations. CT scan and whole body 18-FDG-PET-CT scan can help to find potential extracranial lesions for biopsy or surgery. Also, the multi-disciplinary workup and consultation consisting of specialties of different departments can be vital to reach the final diagnosis. Here we present an algorithm of diagnosis of a solitary hypothalamus lesion (**Figure 7**).

In our cases, the metabolic disorders were remarkable, which appeared before any etiological therapy. Previous reports seldom emphasized the problems of metabolism. The hypothalamus plays a vital role in regulating body weight by balancing the intake of food and energy expenditure and storage. Hypothalamic obesity (HO) is defined as significant hyperphagia and weight gain after any damage to the energy-controlling center of the hypothalamus (20).HO is most commonly described in the context of craniopharyngioma, and most patients with HO have large lesions or extensive involvement of the hypothalamus (21). Previous reports indicate that obesity occurs in approximately 25% of individuals with anatomically proven lesions in the hypothalamus (8, 9). The prevalence of weight gain could be as high as 90% in craniopharyngioma after surgery (21). In our reports, hyperphagia was seen in 48% (12/25) of cases, and overweight/obesity was found in 65% (13/20). The mechanisms of HO could be various, including hyperphagia, impaired energy expenditure and thermoregulation, vagally mediated hyperinsulinemia, and defective hypothalamic leptin signal transduction (1, 22). Lesions affecting the arcuate nucleus, the paraventricular nucleus, the ventromedial nucleus, the dorsomedial nucleus, and the dorsal hypothalamic area could contribute to HO, which play vital roles in the regulation of satiety and energy expenditure (23). Besides, some patients in our study presented with amenorrhea, sexual dysfunction, HO and hyperphagia. Early in 1901, Alfred Fröhlich published his famous work describing a 14-year-old boy with a large pituitary tumor presenting sexual infantilism and obesity (24). These manifestations were defined as Fröhlich's syndrome or adiposogenital dystrophy, which featured excessive eating, obesity, pubertal delay, and hypogonadism (25). The destruction/anatomic distortion of the median eminence, where axonal endings from GnRH neurons establish their synaptic contacts with the complex capillary network of fenestrated vessels and tanycytes, could contribute to the development of Fröhlich's syndrome (26, 27). In addition, the interrupted communication between GnRH neurons and the network of astrocytes processing the feedback metabolic

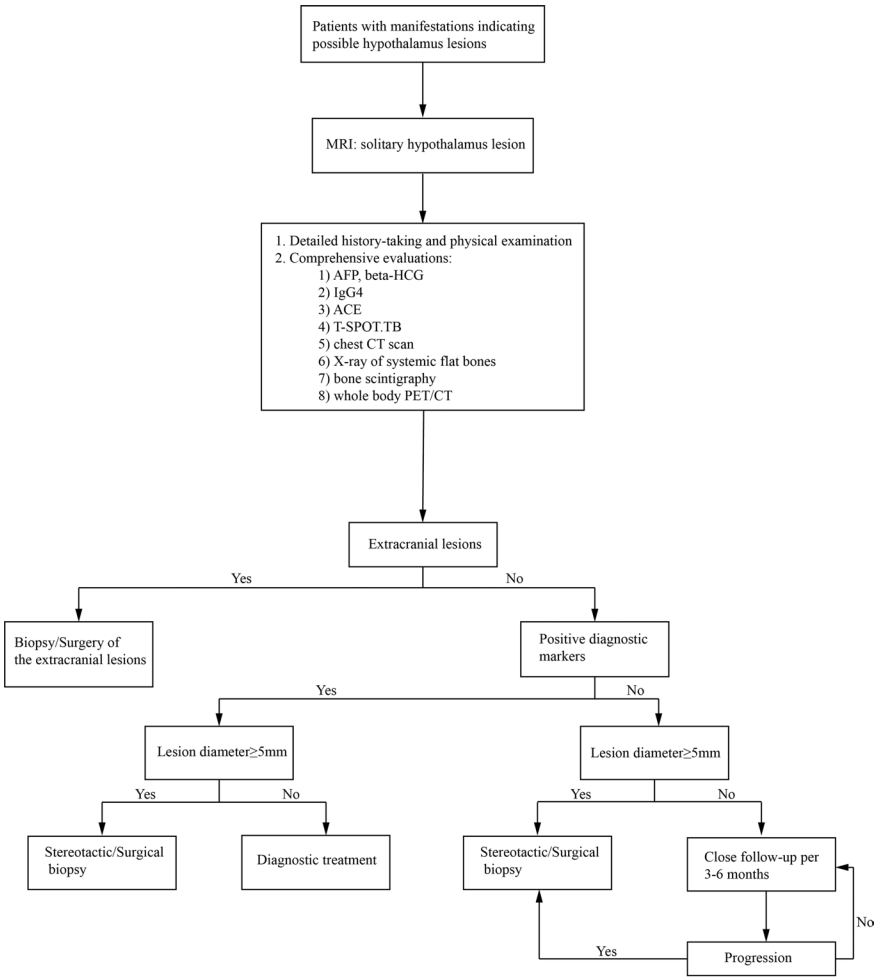

FIGURE 7 | An algorithm of the diagnosis of an intracranial solitary hypothalamus lesion. MRI, magnetic resonance imaging; ACE, angiotensin-converting enzyme; T-SPOT.TB, T-cell spot of tuberculosis test; CT, computed tomography; PET/CT, Positron emission tomography-computed tomography.

information of blood energy molecules and hormones to the arcuate nucleus is also a fundamental anatomical correlate of such a functional impairment (26, 28, 29). HO has a significant adverse impact on quality of life and increases the risk of cardio- and cerebrovascular mortality. In spite of a great deal of theoretical understanding, an effective treatment for hypothalamic obesity has not been developed. The trials with GLP-1 (30, 31) and gastric bypass surgery (32) have proved to be effective. We expect more effective therapy in the future. Hyperlipidemia developed in 81.3% (13/16), and hepatic adipose infiltration in 68.8% (11/16) of the evaluated cases. Fatty liver infiltration might be induced by obesity, considering the significant difference in BMI between those with and without fatty liver. Hyperglycemia and fatty liver infiltration were also reported in the follow-up of craniopharyngioma (33). Abnormal glucose metabolism (either DM or IGT) was found in 62.5% (10/16). The disorders in lipid and glucose metabolism could be caused by HO, hypopituitarism, and disturbed central metabolic regulation. Specially, we had reported a case of hypothalamitis who presented a notable elevation of blood glucose along with the increase of the size of the lesion, and the blood glucose returned to normal after post-therapeutic size decrease of the lesion (4). For this case, it can be inferred that the hyperglycemia was mainly caused by the lesion itself, which induced severely impaired hypothalamic regulation of glucose homeostasis. The diabetes mellitus resulting from reasons like this could be defined as a new type: hypothalamic diabetes mellitus. SUA levels were elevated in 60% (12/20) patients, in which 5 cases had no elevated serum sodium level. All the patients with hyperuricaemia were asymptomatic. Aside from diabetes insipidus and the following dehydration, hyperuricaemia was generally thought to be associated with genes, obesity, gender, diet, insulin resistance, drug use, chronic kidney disease, and so on (34). Levels of SUA were positively related to BMI in our study, indicating the contribution of obesity in the development of hyperuricaemia. Besides, it has been reported that electrical stimulation of the ventromedial hypothalamus in rats can induce a rise of plasma uric acid, which possibly can be due to the

acceleration of epinephrine release from the adrenal medulla (35, 36). More researches are needed to explore how serum uric acid levels are regulated by the hypothalamus.

CONCLUSION

Either surgical or stereotactic biopsy will be a reliable and relatively safe procedure to help to confirm the pathological diagnosis of solitary hypothalamic mass. Metabolic disorders were severe in patients with solitary hypothalamic mass. The management of such cases should cover both the treatment of the primary disease and the endocrine and metabolic disorders. Effective therapy of the metabolism disorders related to hypothalamus destructions, especially hypothalamic obesity, are to be explored in the future.

DATA AVAILABILITY STATEMENT

The raw data supporting the conclusions of this article will be made available by the authors, without undue reservation.

ETHICS STATEMENT

The study was approved by the ethics committee of Huashan Hospital attached to Fudan University. Written informed consent to participate in this study was provided by the participants' legal guardian/next of kin. Written informed consent was obtained from the [individual(s) and/or minor(s)' legal guardian/next of kin] for the publication of any potentially identifiable data included in this article.

AUTHOR CONTRIBUTIONS

HY, YFW, and QM designed the study. BX, QS, MH, WW, QM, BL, SZ, ZZ, YY, YL, YW, ZY, HC, LP, YFW, and HY diagnosed, treated, and followed the patients. YW and ZY analyzed the MRI images. HC reviewed the histopathology results. LP conducted the stereotactic biopsies, and YFW performed the intracranial neurosurgeries. BX, QS, and HY analyzed the data, wrote and edited the manuscript. All authors contributed to the article and approved the submitted version.

FUNDING

This work was supported by the National Key R&D Program of China (2019YFA0801900), the National Project in promoting the diagnosis and treatment of major diseases by MDT, and the National Natural Science Foundation for Young Scientists of China (Grant No. 81800691).

ACKNOWLEDGMENTS

The authors acknowledge the collaboration of the patients and all the doctors involved in the diagnosis, treatment, and follow-up.

SUPPLEMENTARY MATERIAL

The Supplementary Material for this article can be found online at: https://www.frontiersin.org/articles/10.3389/fendo.2021.693669/full#supplementary-material

REFERENCES

1. Giustina A, Frara S, Spina A, Mortini P. "Chapter 9 - The Hypothalamus". In: S Melmed, editor. *The Pituitary, 4th ed*. London, the United Kingdom: Academic Press (2017). p. 291–327.
2. Niri T, Horie I, Kawahara H, Ando T, Fukuhara N, Nishioka H, et al. A Case of Isolated Hypothalamitis With a Literature Review and a Comparison With Autoimmune Hypophysitis. *Endocr J* (2020) 68(1):119–27.
3. Türe U, De Bellis A, Harput MV, Bellastella G, Topcuoglu M, Yaltirik CK, et al. Hypothalamitis: A Novel Autoimmune Endocrine Disease. A Literature Review and Case Report. *J Clin Endocrinol Metab* (2020) 106(2): e415–29.
4. Zhang S, Ye H, Zhang Z, Lu B, Yang Y, He M, et al. Successful Diagnosis of Hypothalamitis Using Stereotactic Biopsy and Treatment. *Medicine* (2015) 94 (5):e447. doi: 10.1097/MD.0000000000000447
5. Fleseriu M, Hashim IA, Karavitaki N, Melmed S, Murad MH, Salvatori R, et al. Hormonal Replacement in Hypopituitarism in Adults: An Endocrine Society Clinical Practice Guideline. *J Clin Endocrinol Metab* (2016) 101 (11):3888–921. doi: 10.1210/jc.2016-2118
6. Ursula K, Ken K, Ho Y. Pituitary Physiology and Diagnostic Evaluation. In: M Shlomo, S Kenneth, P Polonsky, RP Larsen, HM Kronenberg, editors. *Williams Textbook of Endocrinology, 13th*. Philadelphia, PA: Elsevier (2016). p. 176–231. doi: 10.1016/S0140-6736(16)30053-8
7. Higham CE, Johannsson G, Shalet SM. Hypopituitarism. *Lancet* (2016) 388 (10058):2403–15.
8. Bauer HG. Endocrine and Other Clinical Manifestations of Hypothalamic Disease; a Survey of 60 Cases, With Autopsies. *J Clin Endocrinol Metab* (1954) 14(1):13–31.
9. Bauer HG. Endocrine and Metabolic Conditions Related to Pathology in The Hypothalamus: A Review. *J Nervous Ment Dis* (1959) 128(4):323–38. doi: 10.1097/00005053-195904000-00005
10. Saper CB, Scammell TE, Lu J. Hypothalamic Regulation of Sleep and Circadian Rhythms. *Nature* (2005) 437(7063):1257–63. doi: 10.1038/nature04284
11. Tan CL, Knight ZA. Regulation of Body Temperature by the Nervous System. *Neuron* (2018) 98(1):31–48. doi: 10.1016/j.neuron.2018.02.022
12. Reeves AG, Plum F. Hyperphagia, Rage, and Dementia Accompanying a Ventromedial Hypothalamic Neoplasm. *Arch Neurol* (1969) 20(6):616–24. doi: 10.1001/archneur.1969.00480120062005
13. Uwaifo GI. *The Human Hypothalamus: Anatomy, Dysfunction and Disease Management*. BC Carmen, VC Simona, GF Adriana, editors. Cham, Switzerland: Humana Press (2020) p. 7–13.
14. Vann SD, Aggleton JP. The Mammillary Bodies: Two Memory Systems in One? *Nat Rev Neurosci* (2004) 5(1):35–44. doi: 10.1038/nrn1299
15. Savastano LE, Hollon TC, Barkan AL, Sullivan SE. Korsakoff Syndrome From Retrochiasmatic Suprasellar Lesions: Rapid Reversal After Relief of Cerebral Compression in 4 Cases. *J Neurosurg* (2018) 128(6):1731–6. doi: 10.3171/2017.1.JNS162719
16. Pascual JM, Prieto R, Castro-Dufourny I, Mongardi L, Rosdolsky M, Strauss S, et al. Craniopharyngiomas Primarily Involving the Hypothalamus: A Model of Neurosurgical Lesions to Elucidate the Neurobiological Basis of Psychiatric Disorders. *World Neurosurg* (2018) 120:e1245–78. doi: 10.1016/j.wneu.2018.09.053
17. Castro-Dufourny I, Carrasco R, Prieto R, Barrios L, Pascual JM. The Infundibulo-Tuberal Syndrome Caused by Craniopharyngiomas:

Clinicopathological Evidence From an Historical French Cohort (1705-1973). *Pituitary* (2015) 18(5):642–57. doi: 10.1007/s11102-014-0623-4
18. Claude H, Lhermitte J. Le Syndrome Infundibulaire Dans Un Cas De Tumeur Du Troisième Ventricule. *Presse Med* (1917) 41:417–8.
19. Castro-Dufourny I, Carrasco R, Prieto R, Pascual JM. Infundibulo-Tuberal Syndrome: The Origins of Clinical Neuroendocrinology in France. *Pituitary* (2015) 18(6):838–43. doi: 10.1007/s11102-015-0660-7
20. Bereket A, Kiess W, Lustig RH, Muller HL, Goldstone AP, Weiss R, et al. Hypothalamic Obesity in Children. *Obes Rev* (2012) 13(9):780–98. doi: 10.1111/j.1467-789X.2012.01004.x
21. DeVile CJ, Grant DB, Hayward RD, Stanhope R. Growth and Endocrine Sequelae of Craniopharyngioma. *Arch Dis Child* (1996) 75: (2):108–14. doi: 10.1136/adc.75.2.108
22. Pinkney J, Wilding J, Williams G, MacFarlane I. Hypothalamic Obesity in Humans: What do We Know and What Can Be Done? *Obes Rev* (2002) 3 (1):27–34. doi: 10.1046/j.1467-789X.2002.00052.x
23. Abuzzahab MJ, Roth CL, Shoemaker AH. Hypothalamic Obesity: Prologue and Promise. *Horm Res Paediatr* (2019) 91(2):128–36. doi: 10.1159/000496564
24. Fröhlich A. Ein Fall Von Tumor Der Hypophysis Cerebri Ohne Akromegalie. *Wien Klin Rundschau 15* (1901) 15(883–886):906–8.
25. Pascual JM, Prieto R. Harvey Cushing and Pituitary Case Number 3 (Mary D.): The Origin of This Most Baffling Problem in Neurosurgery. *Neurosurg Focus* (2016) 41(1):E6. doi: 10.3171/2016.2.FOCUS1592
26. Clasadonte J, Prevot V. The Special Relationship: Glia-Neuron Interactions in the Neuroendocrine Hypothalamus. *Nat Rev Endocrinol* (2018) 14(1):25–44. doi: 10.1038/nrendo.2017.124
27. Le Tissier P, Campos P, Lafont C, Romanò N, Hodson DJ, Mollard P. An Updated View of Hypothalamic–Vascular–Pituitary Unit Function and Plasticity. *Nat Rev Endocrinol* (2017) 13(5):257–67. doi: 10.1038/nrendo.2016.193
28. Rodriguez EM, Blazquez JL, Guerra M. The Design of Barriers in the Hypothalamus Allows the Median Eminence and the Arcuate Nucleus to Enjoy Private Milieus: The Former Opens to the Portal Blood and the Latter to the Cerebrospinal Fluid. *Peptides* (2010) 31(4):757–76. doi: 10.1016/j.peptides.2010.01.003
29. García-Cáceres C, Balland E, Prevot V, Luquet S, Woods SC, Koch M, et al. Role of Astrocytes, Microglia, and Tanycytes in Brain Control of Systemic Metabolism. *Nat Neurosci* (2019) 22(1):7–14. doi: 10.1038/s41593-018-0286-y
30. Cegla J, Troke RC, Jones B, Tharakan G, Kenkre J, McCullough KA, et al. Coinfusion of Low-Dose GLP-1 and Glucagon in Man Results in a Reduction in Food Intake. *Diabetes* (2014) 63(11):3711–20. doi: 10.2337/db14-0242
31. Montelius C, Erlandsson D, Vitija E, Stenblom EL, Egecioglu E, Erlanson-Albertsson C. Body Weight Loss, Reduced Urge for Palatable Food and Increased Release of GLP-1 Through Daily Supplementation With Green-Plant Membranes for Three Months in Overweight Women. *Appetite* (2014) 81:295–304. doi: 10.1016/j.appet.2014.06.101
32. Zhang X, Cheng Z, Xiao Z, Du X, Du J, Li Y, et al. Comparison of Short- and Mid-Term Efficacy and the Mechanisms of Gastric Bypass Surgeries on Managing Obese and Nonobese Type 2 Diabetes Mellitus: A Prospective Study. *Arch Med Res* (2015) 46(4):303–9. doi: 10.1016/j.arcmed.2015.06.003
33. Amayiri N, Swaidan M, Yousef Y, Halalsheh H, Abu-Hijlih R, Kalaldeh S, et al. Review of Management and Morbidity of Pediatric Craniopharyngioma Patients in a Low-Middle-Income Country: A 12-Year Experience. *Child's Nervous Syst* (2017) 33(6):941–50. doi: 10.1007/s00381-017-3411-4
34. Joosten LAB, Crisan TO, Bjornstad P, Johnson RJ. Asymptomatic Hyperuricaemia: A Silent Activator of the Innate Immune System. *Nat Rev Rheumatol* (2020) 16(2):75–86. doi: 10.1038/s41584-019-0334-3
35. Sumi T, Umeda Y. Adrenal Epinephrine in Hyperuricemia Induced by Hypothalamic Stimulation of the Rat. *Am J Physiol Endocrinol Metab* (1979) 236(3):E212–5. doi: 10.1152/ajpendo.1979.236.3.E212
36. Sumi T, Umeda Y. Epinephrine-Independent Production of Hyperuricemia by Means of Hypothalamic Stimulation in the Conscious Rat. *Life Sci* (1981) 28(10):1183–8. doi: 10.1016/0024-3205(81)90696-2

Conflict of Interest: The authors declare that the research was conducted in the absence of any commercial or financial relationships that could be construed as a potential conflict of interest.

frontiers in Endocrinology

ORIGINAL RESEARCH
published: 18 October 2021
doi: 10.3389/fendo.2021.668193

Metabolic Consequences of Neuronal HIF1α-Deficiency in Mediobasal Hypothalamus in Mice

Azmat Rozjan[1], *Weibi Shan*[2] *and Qiaoling Yao*[1]*

[1] Department of Physiology, School of Basic Medical Sciences, Xinjiang Medical University, Urumqi, China, [2] Department of Dermatology, The First Affiliated Hospital of Xinjiang Medical University, Urumqi, China

Objective: This study aims to investigate whether hypoxia-inducible factor 1α (HIF1α) in the neurons of the mediobasal hypothalamus is involved in the regulation of body weight, glucose, and lipid metabolism in mice and to explore the underlying molecular mechanisms.

Methods: HIF1$\alpha^{flox/flox}$ mice were used. The adeno-associated virus that contained either cre, GFP and syn, or GFP and syn (controls) was injected into the mediobasal hypothalamus to selectively knock out HIF1α in the neurons of the mediobasal hypothalamus. The body weight and food intake were weighed daily. The levels of blood glucose, insulin, total cholesterol (TC), triglyceride (TG), free fatty acid (FFA), high-density lipoprotein (HDL), and low-density lipoprotein (LDL)were tested. Intraperitoneal glucose tolerance test (IPGTT) was performed. The insulin-stimulated Akt phosphorylation in the liver, epididymal fat, and skeletal muscle were examined. Also, the mRNA expression levels of HIF1α, proopiomelanocortin (POMC), neuropeptide Y (NPY), and glucose transporter protein 4 (Glut4) in the hypothalamus were checked.

Results: After selectively knocking out HIF1α in the neurons of the mediobasal hypothalamus (HIF1αKOMBH), the body weights and food intake of mice increased significantly compared with the control mice ($p < 0.001$ at 4 weeks). Compared with that of the control group, the insulin level of HIF1αKOMBH mice was 3.5 times higher ($p < 0.01$). The results of the IPGTT showed that the blood glucose level of the HIF1αKOMBH group at 20–120 min was significantly higher than that of the control group ($p < 0.05$). The serum TC, FFA, HDL, and LDL content of the HIF1αKOMBH group was significantly higher than those of the control group ($p < 0.05$). Western blot results showed that compared with those in the control group, insulin-induced AKT phosphorylation levels in liver, epididymal fat, and skeletal muscle in the HIF1αKOMBH group were not as significantly elevated as in the control group. Reverse transcription-polymerase chain reaction (RT-PCR) results in the whole hypothalamus showed a significant decrease in Glut4 mRNA expression. And the mRNA expression levels of HIF1α, POMC, and NPY of the HIF1αKOMBH group decreased significantly in ventral hypothalamus.

OPEN ACCESS

Edited by:
Tiemin Liu,
Fudan University, China

Reviewed by:
Pingwen Xu,
University of Illinois at Chicago, United States
Qingchun Tong,
University of Texas Health Science Center at Houston, United States

***Correspondence:**
Qiaoling Yao
ql.yao@hotmail.com

Specialty section:
This article was submitted to Neuroendocrine Science, a section of the journal Frontiers in Endocrinology

Received: *15 February 2021*
Accepted: *16 September 2021*
Published: *18 October 2021*

Citation:
Rozjan A, Shan W and Yao Q (2021) Metabolic Consequences of Neuronal HIF1α-Deficiency in Mediobasal Hypothalamus in Mice. Front. Endocrinol. 12:668193. doi: 10.3389/fendo.2021.668193

Conclusions: The hypothalamic neuronal HIF1α plays an important role in the regulation of body weight balance in mice under normoxic condition. In the absence of hypothalamic neuronal HIF1α, the mice gained weight with increased appetite, accompanied with abnormal glucose and lipid metabolism. POMC and Glut4 may be responsible for this effect of HIF1α.

Keywords: HIF1α in the hypothalamus, obesity, glucose, lipid metabolism, insulin resistance

BACKGROUND

Obesity refers to a metabolic disease in which the energy intake exceeds the energy expenditure, leading to increased body weight and body fat content. In 2015, 107.7 million children and 603.7 million adults were obese in the world, and about 1.9 billion were overweight (1, 2). The epidemics of obesity and obesity-related diseases, such as dyslipidemia, hypertension, and type 2 diabetes, are rapidly increasing worldwide (3, 4). Researchers never stopped exploring the treatment of obesity, but to date, no absolute safe and effective weight loss method or drug have been found. Therefore, studying the pathogenesis of obesity from different perspectives and finding possible treatments are still necessary.

The hypoxia-inducible factor (HIF) is a transcription factor that is stably expressed in hypoxic cells and participates in various adaptive responses (5, 6). Three isoforms of HIF, namely, HIF1α, HIF2α, and HIF3α, are identified. Studies showed that HIF1α and HIF2α are stably expressed in the brain, including hypothalamus under normoxic condition (7, 8). Moreover, studies showed that the hypothalamic HIFs play an important role in appetite regulation in mice. Studies demonstrated that increased hypothalamic glucose level activates HIF and inhibits feeding in mice (7). The knockdown of both HIF1α and HIF2α in proopiomelanocortin (POMC) neurons or arcuate nucleus (ARC) results in pronounced weight gain under high-fat diet (HFD) (7, 9). The HIF2α expression decreases with the aging of the mice, and the deletion of HIF2α in hypothalamic POMC neurons can lead to age-dependent weight gain and increased body fat content in mice with mild glucose intolerance and insulin resistance (8). These studies suggested that HIFs, especially HIF2α, in hypothalamic ARC, precisely POMC neurons may be involved in appetite regulation and body weight regulation in mice fed with HFD. However, it is not clear whether hypothalamic neuronal HIF1α itself plays a role in body weight regulation in mice, especially under normal diet and whether it affects the glucose and lipid metabolism.

Therefore, in our study, HIF1α$^{flox/flox}$ mice were selected, and adeno-associated viruses containing *cre* fragments and neuron-specific promoter *syn* were injected into mediobasal hypothalamus to knock out HIF1α selectively in the neurons of the mediobasal hypothalamus. The body weight and food intake of the mice are recorded under chow diet. Also, the glucose metabolism and the lipid metabolism of the mice were examined. As a first step to understand the role of HIF1α in body weight control, we aim to identify the metabolic phenotype of neuronal HIF1α-deficiency in mediobasal hypothalamus in mice.

MATERIALS AND METHODS

Animals

Breeding pairs of HIF1α$^{flox/flox}$ mice were gifts from Polotsky Laboratory (10) of Johns Hopkins University and bred at the Animal Experimentation Center of Xinjiang Medical University. Male HIF1α$^{flox/flox}$ mice aged 6–8 weeks and weighing approximately 23 g were used for the study. Male C57BL/6J mice aged 6–8 weeks were used to test the effect of viruses on body weight. All mice had free access to water and were housed in a standard specific pathogen free (SPF)-grade laboratory environment at 22°C–23°C with a 12-h light/dark cycle (09:00–21:00/21:00–09:00). Mice were anesthetized by intraperitoneal injection of 4% chloral hydrate (0.13 ml/10 g) for all surgeries. After virus injection, up to five mice were kept in one cage on chow diet (9.4% kcal from fat) (11), and cages were changed twice a week. The daily food intake of mice is calculated by cage: the total food intake of the cage/the number of mice. All animal experiments were approved by the Animal Ethics Committee of Xinjiang Medical University and conducted in accordance with the guidelines established by this committee.

Mediobasal Hypothalamic Injection of Virus to Knock Down HIF1α

For both HIF1α$^{flox/flox}$ mice and C57BL/6J mice, AAV-hSyn-cre-GFP (cre) and AAV-hSyn-GFP (GFP) (serotype 9, GENE, AAV9CON323) were injected into the mediobasal hypothalamus by stereotaxic injection at the following coordinates: 1.5 mm form bregma; midline, ± 0.5 (both sides); and dorsoventral, −5.8 (from cranial surface). Each side was given an injection of 0.5 μl virus at a concentration of 1.45 E^{+13} v g/ml.

Experimental Design

The mice with significant weight gain were divided into three batches 28–35 days after the virus injection. In the first batch, the brain of the mice was harvested after whole body perfusion for frozen section. Intraperitoneal glucose tolerance test (IPGTT) and insulin signaling pathway were examined in the mice of the second batch. The blood and the fresh hypothalamus were harvested in the mice of the third batch for future use.

Frozen Sections to Observe the Location of Injections and Expression of Viruses

The HIF1α$^{flox/flox}$ mice were anesthetized and rapidly perfused with sterile normal saline and 4% paraformaldehyde 28–35 days after virus injection. The brains were carefully removed, postfixed in 4% paraformaldehyde at 4°C for overnight. The next morning, the brains were cytoprotected in 20% sucrose solution at 4°C for 24 h. Then, the brains were frozen and stored at −80°C. Whole brains were fixed with the O.C.T. compound and 30 μm of sections were cut and stored in PBS buffer. Then the brain slices were mounted on the slide. After sealing with antifade solution (Solarbio, S2100, Beijing, China), the injection location and virus expression were observed and pictured by confocal microscope (Leica, SP8, Wetzlar, Germany) with full-slice scanning using ×10 magnification.

IPGTT

IPGTT were performed after 6 h fasting. The glucose solution (1 g/kg) (BIOFROXX, 1179GR500, Einhausen, Germany) was intraperitoneally injected into the mice after testing blood glucose at baseline. The blood glucose was measured at the tip of the tail using a handheld glycemic meter (Roche Accu-Chek, Active, Indianapolis, IN, USA) at 10, 20, 30, 60, 90, and 120 min after injection of glucose.

Biochemical Measurements

The triglyceride (TG) assay kit (Elabscience, E-BC-K238, Wuhan, China) was used to detect TG content in serum. The total cholesterol (TC) ELISA kit (Elabscience, E-BC-K179) was used to detect the content of TC in serum. The mouse free fatty acids (FFA) ELISA kit (TW-reagent) was used to detect the content of FFA in serum. The glucose content in serum was detected using the mouse glucose ELISA Kit (Elabscience, E-BC-K268). The serum insulin content was measured using the mouse insulin ELISA Kit (Raybio, ELM-Insulin, Peachtree Corners, GA, USA).

Insulin Signaling Pathway Detection

Insulin signaling pathway activation in mice was performed by administering 5 U/kg insulin intraperitoneally 15 min prior to the sacrifice of the mice. In control mice, saline was injected. Liver, epididymal fat, and skeletal muscle tissue were collected, snap frozen in liquid nitrogen, and stored at −80°C. Tissues were homogenized through the Ripa buffer (ThermoFisher, VH310061, Waltham, MA, USA). The gels for Western blot were made by a gel-making kit (Solarbio, PC0020). Proteins (30 μg) were applied to each lane. For total and phosphorylated Akt measurements, we used antibody phospho-Akt (Ser473) (D9E) XP rabbit mAb (Cell Signaling, #4060, Danvers, MA, USA) and Akt (pan) (11E7) rabbit mAb (Cell Signaling, #4685). The optical densities of bands were measured using the ImageJ software. Insulin signaling was assessed by calculation of the ratio of pAkt to actin or total Akt after insulin injection.

Quantitative RT-PCR of HIF1α, POMC, Neuropeptide Y, and Glut4

The total RNA was extracted from the homogenized hypothalamus by using TRIzol (Takara, 15596026, Ambion, Austin, TX, USA), and the RNA was reverse transcribed into cDNA by using rapid reverse transcription kits (RR047A, Kusatsu, Japan). Real-time fluorescence quantitative PCR was performed (Takara, RR820A). The amplification reaction conditions were as follows: stage 1: one cycle at 95°C for 30 s; stage 2: 40 cycles at 95°C for 5 s and 60°C for 34 s; stage 3: one cycle at 95°C for 15 s, 60°C for 1 min, and 95°C for 15 s. The CT values of the samples were measured using the Applied Biosystems 7500 Real-time PCR System. The relative expression level was calculated using 18S as reference, and the $2^{-\Delta\Delta Ct}$ method was used to analyze the data. The primers of the target mRNAs are as follows: HIF1α: sense, 5′-CAGCAAG ATCTCGGCGAAGC-3′; antisense, 5′-TGATGGTGAGCC TCATAACAGA-3′. POMC: sense, 5′-CAAGGACAAGC GTTACGGTG-3′; antisense, 5′-GGGGCCTTGGAATGAGAA G-3′. Neuropeptide Y (NPY): sense, 5′-AGAAAACGCCCCCA GAACAA-3′; antisense, 5′-TAGTGGTGGCATGCATTGGT-3′. Glucose transporter protein 4 (Glut4): sense, 5′-CCAACAGCT CTCAGGCATCA-3′; antisense, 5′-CCGAGACCAA CGTGAAGA-3′. 18S: sense, 5′-TTGACGGAAGGGCACCA CCAG-3′; antisense, 5′-GCACCACCACCCACGGAATCG-3′.

Statistical Analyses

Mean ± SEM was used to calculate the results, and two-sided unpaired *t*-tests were used for both data sets. Pearson correlation tests for correlation between variables and normal distributions were performed using IBM SPSS Statistics 26 analysis software, as well as repeated measures ANOVA for weight and food intake for HIF1αKOMBH, C57BL/6J, and controls, and Bonferroni was used for multiple comparisons. GraphPad Prism 9 was used to calculate the area under the curve. Data are expressed as mean ± SEM, and $p < 0.05$ was considered statistically significant.

RESULTS

Localization and Expression of Viruses

Frozen sections of the brains were collected 28–35 days after HIF1α$^{flox/flox}$ mice were injected with AAV-hsyn-GFP and AAV-hsyn-cre-GFP to observe the locations and expressions of virus injection. The green fluorescence in **Figures 1A, B** are the expression locations of AAV-hsyn-GFP and AAV-hsyn-cre-GFP, respectively. The green fluorescence in **Figures 1C, D** are the expression locations of AAV-hsyn-GFP and AAV-hsyn-cre-GFP in wild-type (WT) C57BL/6J mice. The injection and expression sites of viruses can be seen around the third ventricle, in the mediobasal hypothalamus. Due to variations of the injections, the small differences of expression positions can be seen in the figure. The leakage of the viruses can also be seen through the injection route.

Increased Body Weight and Food Intake in HIF1αKOMBH Mice

No significant difference in mean body weight was found between the HIF1αKOMBH and control groups before virus injection. On 16 to 28 days after virus injection, the body weights

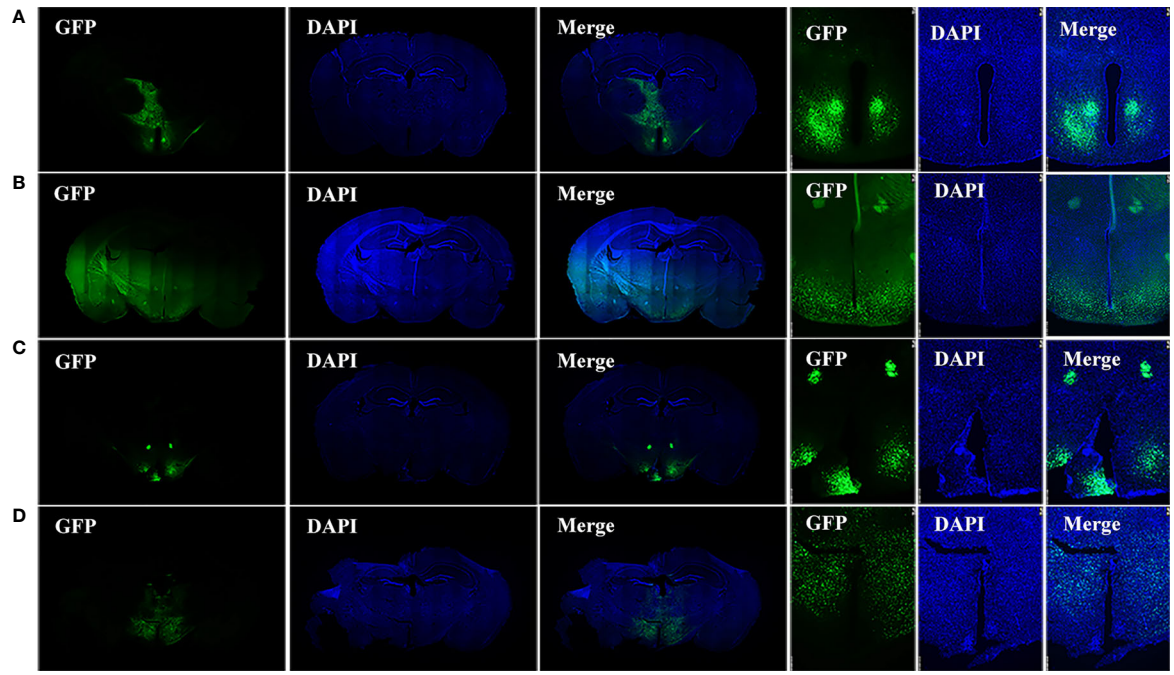

FIGURE 1 | Injection site of viruses. **(A)** Brain sections of HIF1$\alpha^{flox/flox}$ mice injected with AAV-hSyn-GFP virus in the mediobasal hypothalamus. **(B)** Brain sections of HIF1$\alpha^{flox/flox}$ mice injected with AAV-hSyn-cre-GFP virus in the mediobasal hypothalamus. **(C)** Brain sections of wild-type C57BL/6J mice injected with AAV-hSyn-GFP virus at the mediobasal hypothalamus. **(D)** Brain sections of wild-type C57BL/6J mice injected with AAV-hSyn-cre-GFP virus at the medial mediobasal hypothalamus.

of HIF1αKOMBH mice increased significantly compared with the control mice (**Figure 2B**). The repeated measures ANOVA analysis showed that the interaction term was statistically significant, F (23, 897) = 17.880, $p < 0.05$, bias $\eta^2 = 0.314$, suggesting an interaction effect of group and time change on body weight in mice. By comparing the difference in body weight of mice seen in the two groups, the results showed that $F = 7.006$, $p < 0.05$, deviation $\eta^2 = 0.152$, indicating that the difference in body weight of mice in the two groups was significant. Twenty-eight days after virus injection, the mean body weight of mice in the HIF1αKOMBH group reached 33.68 ± 1.43 g ($n = 26$), which was 1.3 times that of the control mice (26.01 ± 0.48 g, $n = 15$; **Figure 2B**). The maximum body weight of mice in the HIF1αKOMBH group reached 46.2 g (**Figure 2A**). For wild-type C57BL/6J mice, significant increases in body weight on days 24 and 27 after virus injection were seen in the cre group compared with the control group ($p < 0.05$) ($n = 9$, **Figure 2D**). However, the maximum body weight of the C57BL/6J mice in the cre group on day 27 after virus injection was only 30.9 g. The two-way ANOVA analysis showed that the interaction term for wild-type C57BL/6J mice in this study was statistically significant, F (8, 128) = 79.076, $p < 0.05$, deviation $\eta^2 = 0.832$, but there was no significant difference in weight between the two groups ($F = 0.825$, $p > 0.05$, deviation $\eta^2 = 0.049$).

The food intake of HIF1$\alpha^{flox/flox}$ mice injected with AAV-hsyn-cre-GFP significantly increased compared with that of the control mice. The two-way ANOVA analysis showed that the interaction term was statistically significant, F (23, 575) = 2.389, $p < 0.05$, bias $\eta^2 = 0.087$, suggesting an interaction effect of group and time change on the change of food intake. Statistical significance was observed between the two groups of mice from days 10 to 13, 15, and 17–29 ($p < 0.05$, $p < 0.01$, and $p < 0.001$, respectively; **Figure 2C**). The results of the comparison of the difference in the amount of food eaten by the mice between the different groups showed a significant difference in the weight of food eaten by the mice between the two groups ($F = 10.914$, $p < 0.05$, deviation $\eta^2 = 0.304$). For WT C57BL/6J mice, the number of days and group interaction had a significant effect on mouse feeding (F (5, 75) = 7.476, $p < 0.05$, deviation $\eta^2 = 0.333$). However, there was no difference in mouse feeding between groups ($F = 0.044$, $p > 0.05$, deviation $\eta^2 = 0.003$) ($n = 9$, **Figure 2E**).

Blood Glucose and Insulin Levels in HIF1αKOMBH Mice

Thirty days after AAV-hsyn-GFP and AAV-hsyn-cre-GFP injection in the mediobasal hypothalamus of HIF1$\alpha^{flox/flox}$ mice, serum insulin and fasting blood glucose were detected. No significant differences were shown in fasting blood glucose level between HIF1αKOMBH mice ($n = 8$) and control mice ($n = 7$) (**Figure 3A**). However, the serum insulin level of HIF1αKOMBH mice reached 49.70 ± 14.18 UIU/ml ($n = 12$), which was 4.9 times higher than that of the control mice ($n = 23$,

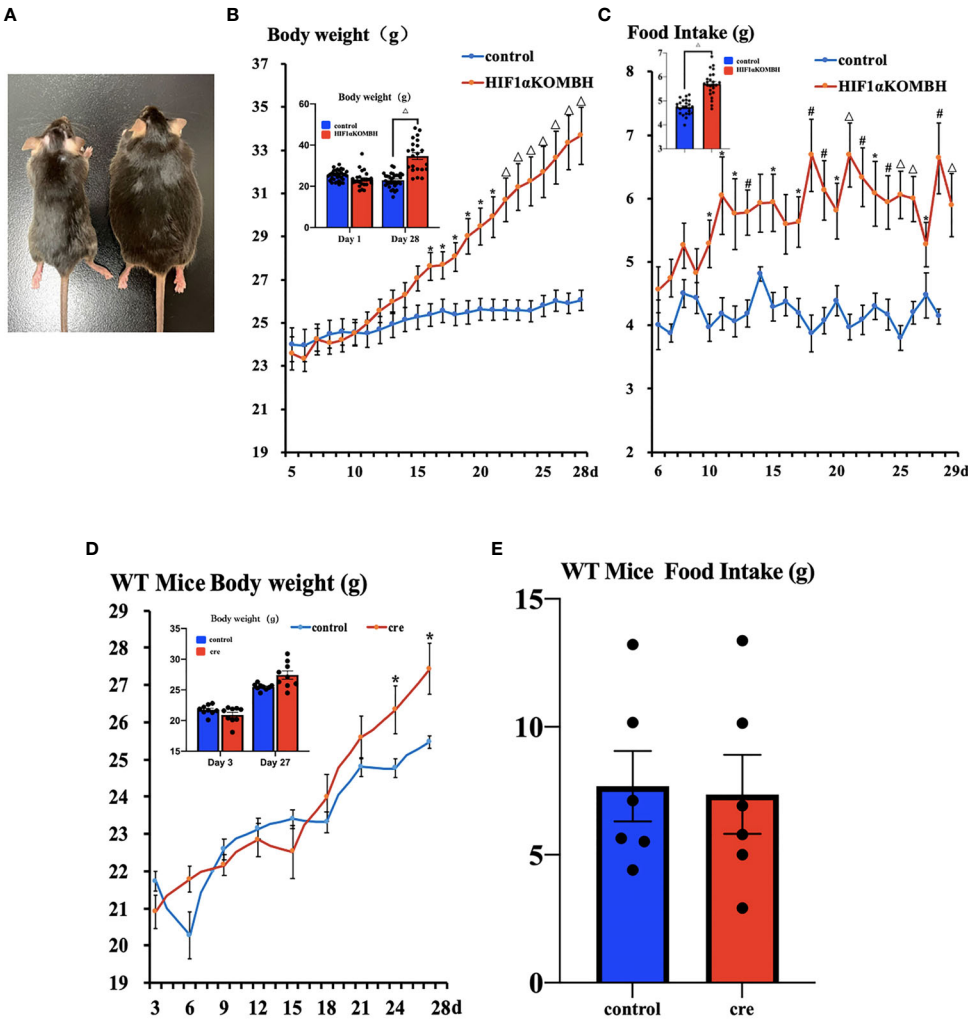

FIGURE 2 | Changes in the body weight and food intake of HIF1α$^{flox/flox}$ mice injected with AAV-hSyn-cre-GFP and AAV-hSyn-GFP at the mediobasal hypothalamus. **(A)** HIF1α$^{flox/flox}$ mice injected with AAV-hSyn-GFP (left) and AAV-hSyn-cre-GFP (right) at the mediobasal hypothalamus for 28 days. **(B)** Changes in body weight of HIF1α$^{flox/flox}$ mice after injections of AAV-hSyn-cre-GFP and AAV-hSyn-GFP at the mediobasal hypothalamus. **(C)** Effects of AAV-hSyn-cre-GFP and AAV-hSyn-GFP injections at the medial mediobasal hypothalamus of HIF1α$^{flox/flox}$ mice on food intake. **(D)** Changes in body weight of wild-type C57BL/6J mice after injections of AAV-hSyn-cre-GFP and AAV-hSyn-GFP at the mediobasal hypothalamus. **(E)** Effects of AAV-hSyn-cre-GFP and AAV-hSyn-GFP injections at the mediobasal hypothalamus of wild-type C57BL/6J mice on food intake. $^{*}p < 0.05$, $^{\#}p < 0.01$, and $^{\triangle}p < 0.001$.

$p < 0.01$, **Figure 3B**). The correlation analysis in HIF1αKOMBH mice showed that the serum insulin level was positively correlated with weight gain ($p < 0.05$, $r = 0.669$, $n = 11$; **Figure 3C**).

Impaired Glucose Tolerance in HIF1αKOMBH Mice

IPGTT was performed 28–35 days after virus injection to investigate the glucose tolerance of mice. The results showed that both groups had peak blood glucose levels 20 min after glucose injection. There were no significant differences for the baseline glucose level of the two groups, similar with the fasting glucose level we tested before. However, HIF1αKOMBH mice had higher blood glucose levels at each time point after glucose injection than control mice, and the statistical significances were seen at 20, 30, 60, 90, and 120 min after glucose injection ($n = 11$; $p < 0.05$, $p < 0.01$, and $p < 0.001$, **Figure 4A**). The area under the curve (AUC) of the HIF1αKOMBH knockout mice (1,880.38 ± 138.69) was 1.2 times higher than that of the control mice (1,350.38 ± 49.51, $p < 0.01$; **Figure 4B**).

Attenuated Insulin Signaling Pathway in HIF1αKOMBH Mice

In control mice, p-Akt protein expression significantly increased in the liver, epididymal fat, and skeletal muscle in insulin injection group ($n = 5$; **Figure 5**), which implied a normal insulin signaling pathway in these mice. However, there was no significant difference in Akt phosphorylation in liver, epididymal fat, and skeletal muscle of HIF1αKOMBH mice between insulin injection group and saline injection group

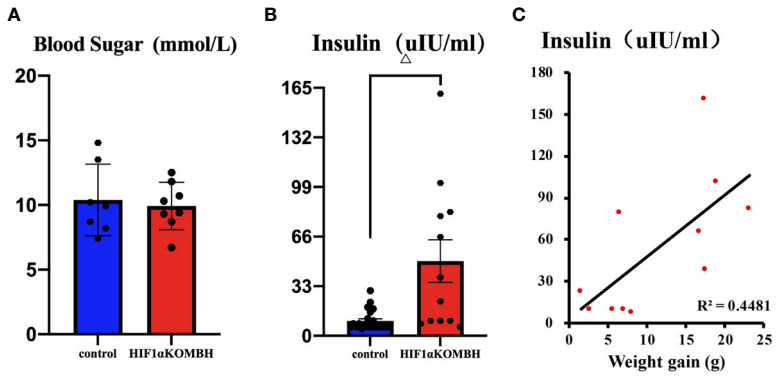

FIGURE 3 | Changes in blood glucose and insulin content and the correlation between serum insulin content and body weight of mice after injections of AAV-hSyn-GFP and AAV-hSyn-cre-GFP in the mediobasal hypothalamus of HIF1α$^{flox/flox}$ mice. **(A)** Serum blood glucose levels of HIF1α$^{flox/flox}$ mice injected with AAV-hSyn-cre-GFP and AAV-hSyn-GFP. **(B)** Serum insulin contents of HIF1α$^{flox/flox}$ mice injected with AAV-hSyn-cre-GFP and AAV-hSyn-GFP. **(C)** Correlation analysis between serum insulin content of HIF1α$^{flox/flox}$ mice and body weight changes after injections of AAV-hSyn-GFP and AAV-hSyn-cre-GFP ($^{\triangle}p < 0.001$).

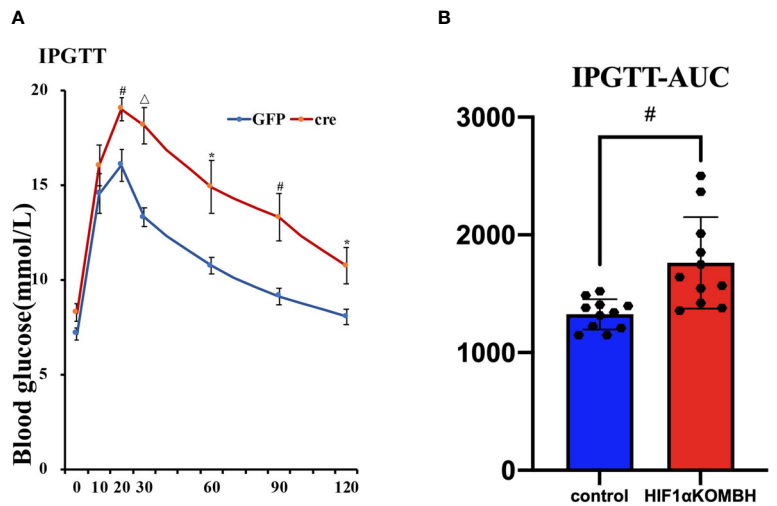

FIGURE 4 | Effects of AAV-hSyn-GFP and AAV-hSyn-cre-GFP injections into the mediobasal hypothalamus HIF1α$^{flox/flox}$ mice on the intraperitoneal glucose tolerance (IPGTT) and subsurface area (AUC). Changes in **(A)** glucose tolerance, **(B)** area under the glucose tolerance test curve. ($^{*}p < 0.05$, $^{\#}p < 0.01$, and $^{\triangle}p < 0.001$).

(**Figure 5**), indicating the impaired insulin sensitivity in HIF1αKOMBH mice.

Abnormal Lipid Metabolism in HIF1αKOMBH Mice

The investigation of TC, TG, FFA, high-density lipoprotein (HDL), and low-density lipoprotein (LDL) levels in the serum of HIF1αKOMBH mice showed that lipid metabolism was also abnormal in HIF1αKOMBH mice. No significant difference was found in the serum TG content between the two groups (**Figure 6A**). The serum total cholesterol and FFA level in HIF1αKOMBH mice was significantly higher than control mice ($p < 0.01$ and $p < 0.05$, respectively, **Figures 6B, C**). For lipoprotein levels, the HDL and LDL content in HIF1αKOMBH mice was also significantly higher than those in control mice ($p < 0.01$ and $p < 0.05$, respectively, **Figures 6D, E**).

Changes in the Expression of Protein and Appetite-Related Neuropeptides Associated With Systemic Energy Homeostasis in HIF1αKOMBH Mice

Fresh hypothalamus were harvested 28–35 days after virus injections to detect the mRNA expression of HIF1α, POMC, NPY, and Glut4 by RT-PCR. Tests on the whole hypothalamus

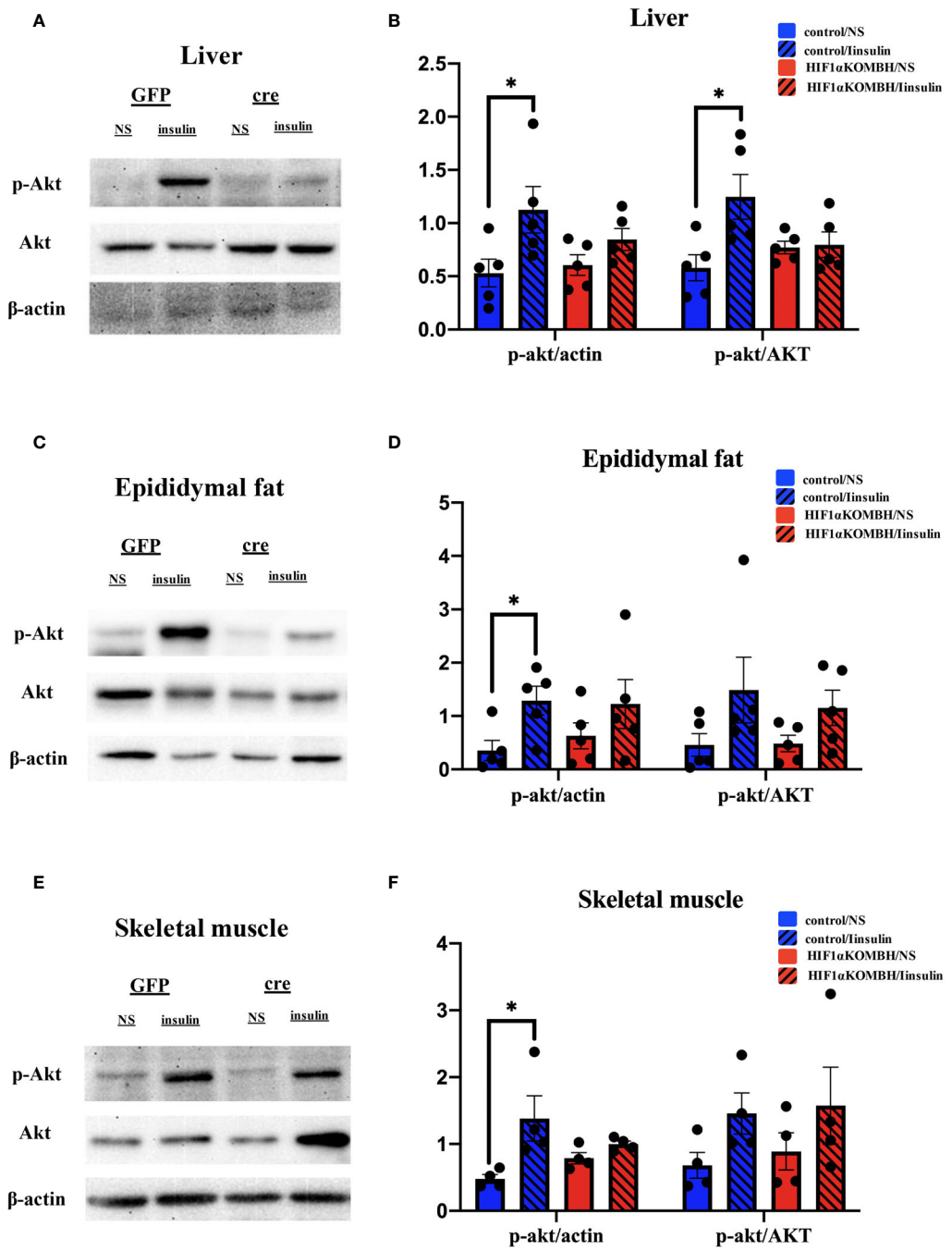

FIGURE 5 | Effects of AAV-hSyn-GFP and AAV-hSyn-cre-GFP injections into the mediobasal hypothalamus of HIF1α$^{flox/flox}$ mice on insulin signaling pathway. **(A)** Detection of the p-Akt and Akt protein expression levels in the mouse liver after AAV-hSyn-GFP and AAV-hSyn-cre-GFP injection into the mediobasal hypothalamus of HIF1α$^{flox/flox}$ mice. **(B)** Quantitative analysis results of p-Akt, Akt, and actin protein expression in the liver of HIF1α$^{flox/flox}$ mice after injections of AAV-hSyn-GFP and AAV-hSyn-cre-GFP into the mediobasal hypothalamus. **(C)** Expression of p-Akt and Akt protein in mouse epididymal fat detected after injections of AAV-hSyn-GFP and AAV-hSyn-cre-GFP into the mediobasal hypothalamus of HIF1α$^{flox/flox}$ mice. **(D)** Quantitative analysis results of p-Akt, Akt, and actin protein expression in the epididymal fat of HIF1α$^{flox/flox}$ mice after injections of AAV-hSyn-GFP and AAV-hSyn-cre-GFP into the mediobasal hypothalamus. **(E)** Expression of p-Akt and Akt protein in mouse skeletal muscle detected after injections of AAV-hSyn-GFP and AAV-hSyn-cre-GFP into the mediobasal hypothalamus of HIF1αflox/flox mice. **(E)** Quantitative analysis results of p-Akt, Akt and actin protein expression in the skeletal muscle of HIF1α$^{flox/flox}$ mice after injections of AAV-hSyn-GFP and AAV-hSyn-cre-GFP into the mediobasal hypothalamus (*$p < 0.05$).

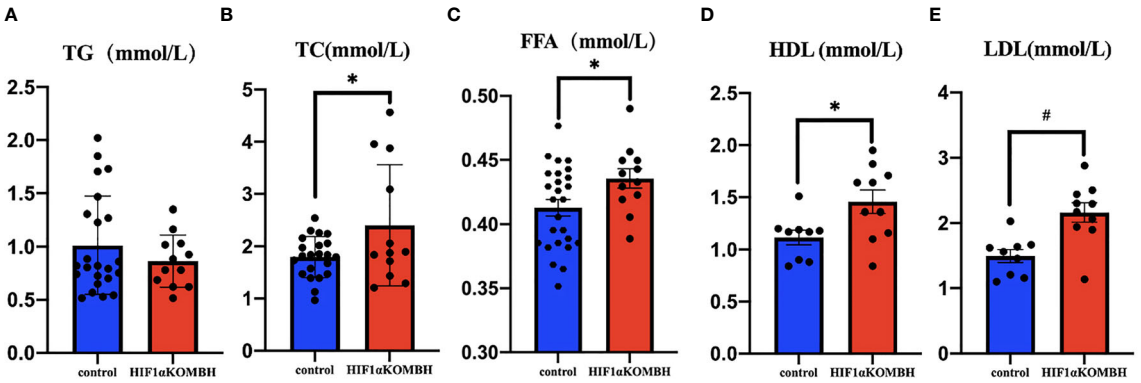

FIGURE 6 | Changes in triglyceride, total cholesterol, free fatty acid, high-density lipoprotein and low-density lipoprotein content in the serum of HIF1αKOMBH mice. **(A)** Serum triglyceride, **(B)** serum total cholesterol, **(C)** free fatty acid contents, **(D)** high-density lipoprotein, and **(E)** low-density lipoprotein (*$p < 0.05$, #$p < 0.01$).

showed no significant changes in HIF1α (n = 16), POMC (n = 17), and NPY (n = 17) between two groups. However, a 2.05 times increase in Glut4 mRNA levels compared with the controls were seen (n = 18) (**Figure 7A**). While tests on the ventral hypothalamus showed that the expression of HIF1α in HIF1αKOMBH mice (n = 4) was 74% less than the control group (n = 3) ($p < 0.05$), indicating that the neuronal HIF1α knockout in mediobasal hypothalamus of mice was successful. In ventral hypothalamus, the expression of POMC mRNA and NPY mRNA in HIF1αKOMBH mice (n = 4) was significantly reduced ($p < 0.05$) compared with the control group (n = 3), but the Glut4 expression in the hypothalamus of HIF1αKOMBH mice (n = 4) was not significantly different from the control group (n = 3) in ventral hypothalamus (**Figure 7B**).

DISCUSSION

In the central nervous system, the hypothalamus is the basic center for the regulation of energy metabolism and has a powerful regulatory role in energy intake, energy expenditure, and weight control (12–15), but the underlying mechanisms are unclear. Our study showed that HIF1α in neurons of mediobasal hypothalamus plays an important role in the regulation of body weight in mice under normoxic conditions. In the absence of HIF1α in neurons of mediobasal hypothalamus, the mice gained weight with increased food intake, accompanied with abnormal glucose and lipid metabolism.

The hypothalamus senses and regulates many signals of biometabolic dynamics (16, 17). In food-induced obesity, the whole-body energy homeostasis is disrupted (18), which may be related to abnormalities in hypothalamic neurons, e.g., NPY/agouti gene-related peptidergic neurons stimulating POMC/cocaine- and amphetamine-induced transcriptergic neurons (19–21). Conditional knockout of HIF in mouse hypothalamic POMC neurons using genetic methods and the knockout of HIF1β in the hypothalamic ARC have not revealed significant changes in feeding and body weight in mice fed with chow diet, but a significant increase in feeding and body weight is observed in those mice fed with HFD (7). In the present study, adeno-

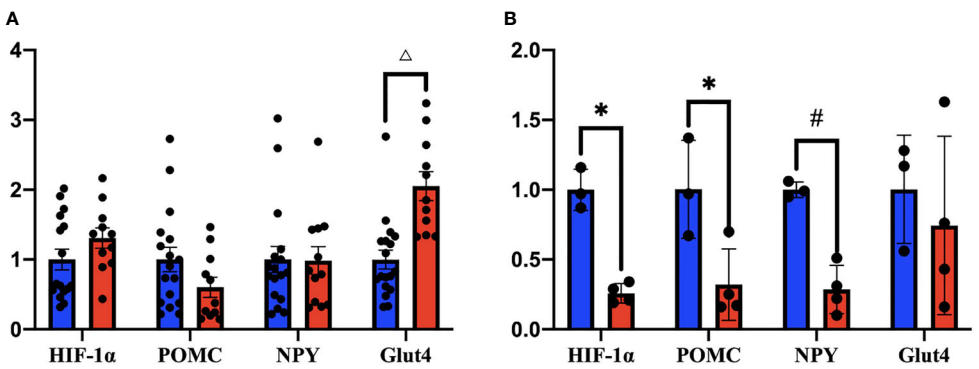

FIGURE 7 | mRNA expression levels of HIF1α, POMC, NPY, and Glut4 in the hypothalamus of HIF1α^{flox} mice after injection of AAV-hSyn-cre and AAV-hSyn-GFP (*$p < 0.05$, #$p < 0.01$, and △$p < 0.001$). **(A)** Changes in the expression levels of HIF1α, POMC, NPY, and Glut4 mRNA in the whole hypothalamus. **(B)** Changes in HIF1α, POMC, NPY, and Glut4 mRNA expression levels in the ventral hypothalamus.

associated viruses containing *syn* (neuron-specific promoter) and *cre* fragments were injected into mediobasal hypothalamus of mice by stereotaxic injection, and HIF1α was conditionally knocked out in this site, confirmed by RT-PCR. Although we knocked out only HIF1α, rather than the HIF precursor, the body weight and food intake of mice with the chow diet increased significantly ($p < 0.05$), suggesting that neuronal HIF1α itself in mediobasal hypothalamus could be important for body weight and appetite control, although part of the reason may be due to broad regional HIF1α knockout neurons in the hypothalamus in our study. In addition to the hypothalamic POMC neurons and ARC region, HIF1α in other parts of the hypothalamic neurons may be involved in the regulation of body weight as well. In our results, the increase in body weight occurred earlier than the increase in food intake, suggesting that HIF1α in neurons of mediobasal hypothalamus might affect both the appetite and metabolic rate in mice. To exclude the effect of AAV-cre on body weight and food intake, we injected the same viruses in WT C57BL/6J mice. We did see the increase of body weight on 24 and 27 days after virus injection, but the increase of body weight was much less than HIF1α$^{flox/flox}$ mice. Moreover, the increase in food intake was not seen in WT mice. These results confirmed that the prominent weight gain and increased food intake in HIF1αKOMBH mice was due to loss of neuronal HIF1α in mediobasal hypothalamus.

Studies found that the loss of HIF1α in the vascular endothelial cells of mice leads to a significant increase in the fasting glucose level, slow insulin response after intravenous glucose injection, delayed glucose clearance in the blood, and significantly impeded glucose absorption by the brain and heart (22). These results indicated that HIF1α plays an important role in glucose metabolism. Other studies showed that HIF induction can enhance hypothalamic glucose sensing (7), and the inhibition of hypothalamic HIF1 lead to glucose intolerance and increased serum insulin level (8). In our study, impaired glucose metabolism was present in HIF1αKOMBH mice. Although there were no significant changes in blood glucose levels in HIF1αKOMBH mice, the serum insulin levels of HIF1αKOMBH mice were significantly increased, suggesting that mice with neuronal HIF1α knockout in the mediobasal hypothalamus developed insulin resistance. In addition, the normal blood glucose levels might be the result of increased insulin secretion. The results of correlation analysis showed that the increase in insulin content was positively correlated with increased body weight in mice, indicating that the increase in insulin secretion might be the consequence of the increased body weight in mice.

IPGTT and insulin signaling results further confirmed abnormal glucose tolerance and insulin resistance in HIF1αKOMBH mice. The higher blood glucose levels in the knockout mice after glucose injection suggested that the mediobasal hypothalamic neuronal HIF1α knockout mice caused abnormal glucose tolerance in mice. The HIF1α KOMBH mice had a significantly delayed decrease in blood glucose after glucose injection, indicating that the absence of HIF1α in the neurons of medial basal hypothalamus might lead to impaired glucose clearance in the blood of mice. The glucose intolerance in HIF1αKOMBH mice may be due to higher insulin secretion baseline in these mice, which leads to insulin deficiency when facing glucose challenge. Akt, also known as PKB or Rac, plays a critical role in the control of survival and apoptosis (23–25). Insulin promotes a variety of important biological responses (26) and can stimulate the disposal of blood glucose primarily in target tissues, such as skeletal muscle and adipocytes, where the sugar is either oxidized or stored as glycogen or fatty acids. In both tissues, insulin promotes a rapid activation of specific PKB isoforms. Our results showed that the insulin-induced activation of AKT signaling pathway in the liver, epididymal fat, and skeletal muscle of HIF1αKOMBH mice was significantly lower than that of the control mice, confirming the reduced insulin sensitivity in these mice.

To investigate the lipid metabolism of HIF1α knockout mice in the mediobasal hypothalamus, we measured the serum TG, TC, FFA, HDL, and LDL levels in HIF1α$^{flox/flox}$ mice after virus injection. Although there are no significant changes in the serum TG content, the serum TC and FFA content in knockout mice significantly increased. The abnormal blood lipid content still appeared in the mice under chow diet, suggesting that HIF1α in the neurons in the mediobasal hypothalamus was also involved in blood lipid metabolism to some extent. The increased HDL and LDL level may be the consequence of increased lipid level.

To confirm that the HIF1α was indeed knocked out in HIF1αKOMBH mice, the RT-PCR of HIF1α was performed. When we checked the HIF1α in the whole hypothalamus, we found that the HIF1α did not decrease. Since the virus injections are mainly in the mediobasal hypothalamus, we took the ventral part of the hypothalamus to perform the RT-PCR again. As a result, the expression of HIF1α mRNA in HIF1αKOMBH mice decreased by 74%, indicating that AAV-hSyn-cre-GFP had a knockdown effect on HIF1α. Considering the knockout is neuronal specific, 74% decrease in HIF1α expression is reasonable.

The ARC in the hypothalamus has two distinct functional types of neurons that are important for appetite regulation. These neurons are related peptide agouti-related protein (AGRP)/NPY neurons, which express food-derived (appetite-stimulating) NPY and AGRP, and POMC neurons, which express POMC and inhibit appetite (27). NPY, as a polypeptide widely distributed in the central and peripheral nervous systems, plays an important role in body weight regulation. The main role of NPY is to increase food intake and reduce the thermogenic effect of satiated animals. The RT-PCR in the whole hypothalamus suggested nonchanged expression of POMC and NPY. Interestingly, however, in ventral hypothalamus, the mRNA expression of POMC and NPY were significantly reduced in HIF1αKOMBH group. The decreased POMC expression may explain the increased food intake in knockout mice, while the decrease in NPY mRNA expression might be the result of negative feedback regulation due to overeating in mice.

Previous study found that Glut4 is also expressed in the hypothalamus (28) and plays an important role in sensing glucose and regulating systemic glucose homeostasis. The

knockdown of Glut4 in the mouse brain leads to impaired glucose tolerance, reduced insulin sensitivity, and impaired glucose-lowering regulation in mice (29). Moreover, the deletion of HIF1α in skeletal muscle cells leads to impaired Glut4 function (30). By contrast, the insulin receptor substrate 1-associated phosphatidylinositol 3-phosphate kinase can activate Glut4 translocation to the plasma membrane, thereby importing glucose into the cell. Therefore, Glut4 is a key factor in skeletal muscle insulin sensitivity. The results of the present study showed a decreased Glut4 mRNA expression in HIF1αKOMBH mice in the whole hypothalamus, suggesting that Glut4 may be involved in the weight gain and abnormal glucose metabolism of these mice. However, the expression of Glut4 did not change in ventral hypothalamus, suggesting that the effect of HIF1α may act on the dorsal part of hypothalamus.

In summary, our study showed that neuronal HIF1α knockout at the mediobasal hypothalamus could lead to weight gain in mice accompanied with impaired glucose metabolism and lipid metabolism. POMC and Glut4 may be related to this effect of HIF1α. Whether the abnormal glucose metabolism and lipid metabolism was directly and causally related to the deletion of HIF1α at the mediobasal hypothalamus in mice remained unclear. In the future study, we will further investigate the effects of hypothalamic neuronal HIF1α on hypothalamic glucose sensing, insulin signaling pathway, and lipid regulatory pathway and mechanisms.

DATA AVAILABILITY STATEMENT

The raw data supporting the conclusions of this article will be made available by the authors, without undue reservation.

ETHICS STATEMENT

The animal study was reviewed and approved by Animal Ethics Committee of Xinjiang Medical University.

AUTHOR CONTRIBUTIONS

AR, WS, and QY performed experiments and analyzed data. AR and QY prepared the figures and drafted the manuscript. QY conceived and designed the research and approved the final version of manuscript. All authors contributed to the article and approved the submitted version.

REFERENCES

1. GBD 2015 Obesity Collaborators, Afshin A, Forouzanfar MH, Reitsma MB, Sur P, Estep K, et al. Health Effects of Overweight and Obesity in 195 Countries Over 25 Years. *N Engl J Med* (2017) 377(1):13–27. doi: 10.1056/NEJMoa1614362
2. Gregg EW, Shaw JE. Global Health Effects of Overweight and Obesity. *N Engl J Med* (2017) 377(1):80–1. doi: 10.1056/NEJMe1706095
3. Saito H, Tanaka T, Sugahara M, Tanaka S, Fukui K, Wakashima T, et al. Inhibition of Prolyl Hydroxylase Domain (PHD) by JTZ-951 Reduces Obesity-Related Diseases in the Liver, White Adipose Tissue, and Kidney in Mice With a High-Fat Diet. *Lab Invest* (2019) 99(8):1217–32. doi: 10.1038/s41374-019-0239-4
4. López-Pastor AR, Infante-Menéndez J, Escribano Ó, Gómez-Hernández A. Mirna Dysregulation in the Development of non-Alcoholic Fatty Liver Disease and the Related Disorders Type 2 Diabetes Mellitus and Cardiovascular Disease. *Front Med (Lausanne)* (2020) 7:527059. doi: 10.3389/fmed.2020.527059
5. Semenza GL. HIF-1 and Mechanisms of Hypoxia Sensing. *Curr Opin Cell Biol* (2001) 13(2):167–71. doi: 10.1016/s0955-0674(00)00194-0
6. Semenza GL. Hypoxia-Inducible Factor 1 (HIF-1) Pathway. *Sci STKE* (2007) 2007(407):cm8. doi: 10.1126/stke.4072007cm8
7. Zhang H, Zhang G, Gonzalez FJ, Park SM, Cai D. Hypoxia-Inducible Factor Directs POMC Gene to Mediate Hypothalamic Glucose Sensing and Energy Balance Regulation. *PloS Biol* (2011) 9(7):e1001112. doi: 10.1371/journal.pbio.1001112
8. Wang Z, Khor S, Cai D. Age-Dependent Decline of Hypothalamic HIF2α in Response to Insulin and its Contribution to Advanced Age-Associated Metabolic Disorders in Mice. *J Biol Chem* (2019) 294(13):4946–55. doi: 10.1074/jbc.RA118.005429
9. Gaspar JM, Mendes NF, Corrêa-da-Silva F, Lima-Junior JC, Gaspar RC, Ropelle ER, et al. Downregulation of HIF Complex in the Hypothalamus Exacerbates Diet-Induced Obesity. *Brain Behav Immun* (2018) 73:550–61. doi: 10.1016/j.bbi.2018.06.020
10. Mesarwi OA, Shin MK, Bevans-Fonti S, Schlesinger C, Shaw J, Polotsky VY. Hepatocyte Hypoxia Inducible Factor-1 Mediates the Development of Liver Fibrosis in a Mouse Model of Nonalcoholic Fatty Liver Disease. *PloS One* (2016) 11(12):e0168572. doi: 10.1371/journal.pone.0168572
11. Zhang Y, Guan Y, Pan S, Yan L, Wang P, Chen Z, et al. Hypothalamic Extended Synaptotagmin-3 Contributes to the Development of Dietary Obesity and Related Metabolic Disorders. *Proc Natl Acad Sci USA* (2020) 117(33):20149–58. doi: 10.1073/pnas.2004392117
12. Schwartz MW, Porte D. Diabetes, Obesity, and the Brain. *Science* (2005) 307(5708):375–9. doi: 10.1126/science.1104344
13. Cakir I, Nillni EA. Endoplasmic Reticulum Stress, the Hypothalamus, and Energy Balance. *Trends Endocrinol Metab* (2019) 30(3):163–76. doi: 10.1016/j.tem.2019.01.002
14. Coll AP, Yeo GS. The Hypothalamus and Metabolism: Integrating Signals to Control Energy and Glucose Homeostasis. *Curr Opin Pharmacol* (2013) 13(6):970–6. doi: 10.1016/j.coph.2013.09.010
15. SC W, S RJ, C D. Regulation of Food Intake Through Hypothalamic Signaling Networks Involving Mtor. *Annu Rev Nutr* (2008) 28:295–311. doi: 10.1146/annurev.nutr.28.061807.155505
16. Timper K, Brüning JC. Hypothalamic Circuits Regulating Appetite and Energy Homeostasis: Pathways to Obesity. *Dis Model Mech* (2017) 10(6):679–89. doi: 10.1242/dmm.026609
17. Sisley S, Sandoval D. Hypothalamic Control of Energy and Glucose Metabolism. *Rev Endocr Metab Disord* (2011) 12(3):219–33. doi: 10.1007/s11154-011-9189-x
18. Velloso LA, Schwartz MW. Altered Hypothalamic Function in Diet-Induced Obesity. *Int J Obes* (2011) 355:1455–65. doi: 10.1038/ijo.2011.56
19. Thaler JP, Yi CX, Schur EA, Guyenet SJ, Hwang BH, Dietrich MO, et al. Obesity is Associated With Hypothalamic Injury in Rodents and Humans. *J Clin Invest* (2012) 122(1):153–62. doi: 10.1172/JCI59660
20. Valdearcos M, Douglass JD, Robblee MM, Dorfman MD, Stifler DR, Bennett ML, et al. Microglial Inflammatory Signaling Orchestrates the Hypothalamic Immune Response to Dietary Excess and Mediates Obesity Susceptibility. *Cell Metab* (2017) 26(1):185–197.e3. doi: 10.1016/j.cmet.2017.05.015
21. Valdearcos M, Robblee MM, Benjamin DI, Nomura DK, Xu AW, Koliwad SK. Microglia Dictate the Impact of Saturated Fat Consumption on Hypothalamic Inflammation and Neuronal Function. *Cell Rep* (2014) 9(6):2124–38. doi: 10.1016/j.celrep.2014.11.018

22. Huang Y, Lei L, Liu D, Jovin I, Russell R, Johnson RS, et al. Normal Glucose Uptake in the Brain and Heart Requires an Endothelial Cell-Specific HIF-1α-Dependent Function. *Proc Natl Acad Sci USA* (2012) 109(43):17478–83. doi: 10.1073/pnas.1209281109
23. Franke TF, Kaplan DR, Cantley LC. PI3K: Downstream Aktion Blocks Apoptosis. *Cell* (1997) 88(4):435–7. doi: 10.1016/s0092-8674(00)81883-8
24. Burgering BM, Coffer PJ. Protein Kinase B (C-Akt) in Phosphatidylinositol-3-OH Kinase Signal Transduction. *Nature* (1995) 376(6541):599–602. doi: 10.1038/376599a0
25. Franke TF, Yang SI, Chan TO, Datta K, Kazlauskas A, Morrison DK, et al. The Protein Kinase Encoded by the Akt Proto-Oncogene is a Target of the PDGF-Activated Phosphatidylinositol 3-Kinase. *Cell* (1995) 81(5):727–36. doi: 10.1016/0092-8674(95)90534-0
26. Hajduch E, Litherland GJ, Hundal HS. Protein Kinase B (PKB/Akt)–a Key Regulator of Glucose Transport? *FEBS Lett* (2001) 492(3):199–203. doi: 10.1016/s0014-5793(01)02242-6
27. Gropp E, Shanabrough M, Borok E, Xu AW, Janoschek R, Buch T, et al. Agouti-Related Peptide-Expressing Neurons are Mandatory for Feeding. *Nat Neurosci* (2005) 28(10):1289–91. doi: 10.1038/nn1548
28. McEwen BS, Reagan LP. Glucose Transporter Expression in the Central Nervous System: Relationship to Synaptic Function. *Eur J Pharmacol* (2004) 490(1-3):13–24. doi: 10.1016/j.ejphar.2004.02.041
29. Reno CM, Puente EC, Sheng Z, Daphna-Iken D, Bree AJ, Routh VH, et al. Brain Glut4 Knockout Mice Have Impaired Glucose Tolerance, Decreased Insulin Sensitivity, and Impaired Hypoglycemic Counterregulation. *Diabetes* (2017) 66(3):587–97. doi: 10.2337/db16-0917
30. Kim JH, Kim H, Hwang KH, Chang JS, Park KS, Cha SK, et al. WNK1 Kinase is Essential for Insulin-Stimulated Glut4 Trafficking in Skeletal Muscle. *FEBS Open Bio* (2018) 8(11):1866–74. doi: 10.1002/2211-5463.12528

Conflict of Interest: The authors declare that the research was conducted in the absence of any commercial or financial relationships that could be construed as a potential conflict of interest.

Publisher's Note: All claims expressed in this article are solely those of the authors and do not necessarily represent those of their affiliated organizations, or those of the publisher, the editors and the reviewers. Any product that may be evaluated in this article, or claim that may be made by its manufacturer, is not guaranteed or endorsed by the publisher.

frontiers in Endocrinology

ORIGINAL RESEARCH
published: 17 December 2021
doi: 10.3389/fendo.2021.697445

Brain Permeable AMP-Activated Protein Kinase Activator R481 Raises Glycaemia by Autonomic Nervous System Activation and Amplifies the Counterregulatory Response to Hypoglycaemia in Rats

*Ana M. Cruz[1], Katie M. Partridge[1], Yasaman Malekizadeh[1], Julia M. Vlachaki Walker[1], Paul G. Weightman Potter[1], Katherine R. Pye[1], Simon J. Shaw[2], Kate L. J. Ellacott[1] and Craig Beall[1]**

[1] Institute of Biomedical and Clinical Sciences, College of Medicine and Health, University of Exeter, Exeter, United Kingdom, [2] Rigel Pharmaceuticals Inc., South San Francisco, CA, United States

OPEN ACCESS

Edited by:
Sebastien G. Bouret,
INSERM U1172 Centre de Recherche Jean Pierre Aubert (INSERM), France

Reviewed by:
Xavier Fioramonti,
INRA UMR1286 Laboratoire NutriNeuro, France
Christelle Le Foll,
University of Zurich, Switzerland

***Correspondence:**
Craig Beall
c.beall@exeter.ac.uk

Specialty section:
This article was submitted to Neuroendocrine Science, a section of the journal Frontiers in Endocrinology

Received: 19 April 2021
Accepted: 15 November 2021
Published: 17 December 2021

Citation:
Cruz AM, Partridge KM, Malekizadeh Y, Vlachaki Walker JM, Weightman Potter PG, Pye KR, Shaw SJ, Ellacott KLJ and Beall C (2021) Brain Permeable AMP-Activated Protein Kinase Activator R481 Raises Glycaemia by Autonomic Nervous System Activation and Amplifies the Counterregulatory Response to Hypoglycaemia in Rats. Front. Endocrinol. 12:697445. doi: 10.3389/fendo.2021.697445

Aim: We evaluated the efficacy of a novel brain permeable "metformin-like" AMP-activated protein kinase activator, R481, in regulating glucose homeostasis.

Materials and Methods: We used glucose sensing hypothalamic GT1-7 neuronal cells and pancreatic αTC1.9 α-cells to examine the effect of R481 on AMPK pathway activation and cellular metabolism. Glucose tolerance tests and hyperinsulinemic-euglycemic and hypoglycemic clamps were used in Sprague-Dawley rats to assess insulin sensitivity and hypoglycemia counterregulation, respectively.

Results: *In vitro*, we demonstrate that R481 increased AMPK phosphorylation in GT1-7 and αTC1.9 cells. In Sprague-Dawley rats, R481 increased peak glucose levels during a glucose tolerance test, without altering insulin levels or glucose clearance. The effect of R481 to raise peak glucose levels was attenuated by allosteric brain permeable AMPK inhibitor SBI-0206965. This effect was also completely abolished by blockade of the autonomic nervous system using hexamethonium. During hypoglycemic clamp studies, R481 treated animals had a significantly lower glucose infusion rate compared to vehicle treated controls. Peak plasma glucagon levels were significantly higher in R481 treated rats with no change to plasma adrenaline levels. *In vitro*, R481 did not alter glucagon release from αTC1.9 cells, but increased glycolysis. Non brain permeable AMPK activator R419 enhanced AMPK activity *in vitro* in neuronal cells but did not alter glucose excursion *in vivo*.

Conclusions: These data demonstrate that peripheral administration of the brain permeable "metformin-like" AMPK activator R481 increases blood glucose by activation of the autonomic nervous system and amplifies the glucagon response to hypoglycemia in rats. Taken together, our data suggest that R481 amplifies the counterregulatory response to hypoglycemia by a central rather than a direct effect on the pancreatic

α-cell. These data provide proof-of-concept that central AMPK could be a target for future drug development for prevention of hypoglycemia in diabetes.

Keywords: AMPK, hypoglycemia, glucagon, hypoglycemic clamp, glucose homeostasis, counterregulation

INTRODUCTION

Achieving more time in the target blood glucose (BG) range is a daily challenge for people with diabetes. This can become increasingly challenging with tightening glycemic control using insulin treatment, which increases the risk of hypoglycaemia. Moreover, disease progression and frequent exposure to hypoglycaemia can lead to impaired awareness of and defective counterregulatory responses (CRR) to hypoglycaemia (1).

AMP-activated protein kinase (AMPK) has emerged as a central component of cellular energy sensing over the past two decades. The enzyme is a heterotrimeric complex composed of α, β and γ-subunits, with the α-subunit containing the catalytic domain (2). There are two isoforms of the α-subunit, AMPKα1 and AMPKα2, with the latter isoform having a more prominent role in glucose sensing (3–5). This enzyme plays an important role in regulating whole body energy homeostasis through its actions in the hypothalamus (6) and pancreas (7, 8). Previous studies have shown that direct pharmacological activation of AMPK in the ventromedial nucleus of the hypothalamus (VMH), an important hypoglycemia-sensing brain region (9), increases the response to hypoglycemia in healthy (10), recurrently hypoglycemic and diabetic BB rats (11) by increasing hepatic glucose production (HGP) with or without concomitant increases in glucagon and adrenaline levels. Moreover, suppression of AMPK activity using shRNA diminishes the glucagon and adrenaline response to hypoglycemia (12). Recurrent glucoprivation in rats leads to attenuated AMPK activation in hypothalamic nuclei during hypoglycemia (13), suggesting, at least in part, that recurrent hypoglycemia (RH) may lead to defective CRR through suppression of hypothalamic AMPK activity. Importantly, previous studies have, thus far, only used direct injection of AMPK activators into the brain. Rigel Pharmaceuticals (CA, USA) has developed novel AMPK activating compounds with a similar mechanism of action to metformin [complex I inhibition (14)] but with greater potency. One novel compound, R481, is brain permeable and has a positive brain:plasma distribution. We assessed the effect of R481 on glucose homeostasis and used this novel compound to test the hypothesis that peripheral delivery of a brain-permeable AMPK activator may improve the CRR to hypoglycemia.

RESEARCH DESIGN AND METHODS

Reagents

R481 and R419 were kindly gifted by Rigel Pharmaceuticals Inc (San Francisco, USA). Chemical structures for compounds are shown in **Figure 1**. SBI-0206965 was purchased from Cayman Chemical, hexamethonium bromide from Sigma Aldrich, 50% glucose solution from Centaur Services, and Novo Nordisk Actrapid insulin was purchased from Covetrus.

Cell Culture

Immortalized GT1-7 mouse hypothalamic cells were a kind gift from Pamela Mellon, Salk Institute, San Diego, California, USA. GT1-7 cells were cultured in growth medium, as previously described (15), and experiments conducted at physiological brain glucose levels (2.5 mmol/L) in experimental medium (**Table 1**). The murine pancreatic α-cell line αTC1 clone 9 (referred to as αTC1.9) was a kind gift from Hannah Welters, University of Exeter, UK. αTC1.9 cells were cultured in growth medium at physiological peripheral glucose levels (5.5 mmol/L) and experiments conducted in experimental medium, KBH buffer or XF medium (**Table 1**). Cell lines were confirmed as mycoplasma free using a commercial kit (MycoAlert, Lonza, Slough, UK).

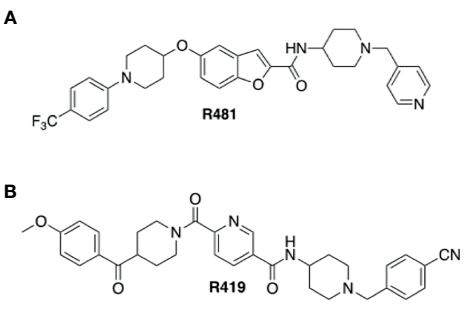

FIGURE 1 | Structures of indirect AMPK activators R481 and R419. Chemical structures of brain permeable R481 **(A)** and non-brain permeable R419 **(B)** indirect AMPK activators.

TABLE 1 | Media composition for *in vitro* experiments.

Cell line	Medium	Components
GT1-7	Growth medium	High glucose (25 mmol/L) DMEM (D5671, Sigma) supplemented with 10% FBS (102070-106 Gibco), 4% L-glutamine (ThermoFisher) and 2% penicillin/streptomycin (pen/strep; 100 U/ml; 100 µg/ml; Gibco)
GT1-7	Plating medium	Glucose-free DMEM (11966, ThermoFisher) with 2% L-glutamine supplemented with 7.5 mmol/L glucose, 10% FBS and 2% pen/strep
GT1-7	Experimental medium	Glucose-free DMEM, serum free, supplemented with 2.5 mmol/L glucose
αTC1.9	Growth/plating medium	Glucose free DMEM supplemented with 5.5 mmol/L glucose, 10% FBS (102070-106), 0.02% wt/vol fatty acid free BSA, 0.34 mmol/L mixed essential amino acids, 1 mmol/L pyruvate, 15 mmol/L HEPES and 2% pen/strep
αTC1.9	Experimental medium	Glucose-free DMEM, serum free, supplemented with 1 mmol/L glucose
αTC1.9	Kreb's-Ringer bicarbonate HEPES (KBH)	In sterile ddH_2O, 130 mmol/L NaCl, 3.6 mmol/L KCl, 1/5 mmol/L $CaCl_2$, 0.5 mmol/L KH_2PO_4, 0.5 mmol/L $MgSO_4$, 2 mmol/L Na_2CO_3, 10 mmol/L HEPES and 0.1% wt/vol fatty acid free BSA, pH 7.4
αTC1.9	Seahorse XF medium	XF DMEM pH 7.4 supplemented with 2.5 mmol/L sodium pyruvate and 2 mmol/L L-glutamine with 0.5 mmol/L glucose or glucose free.

Immunoblotting

Cells were grown to 60-80% confluence in 60 mm round petri dishes. Following drug treatment, cell lysates were collected for protein quantification using the Bradford method (16). For tissues, brains were dissected from healthy Sprague Dawley rats following administration with R481 (20 mg kg^{-1}; i.p), R419 (20 mg kg^{-1}; i.p) or vehicle (0.5% HPMC, 0.1% TWEEN-80; i.p) during glucose tolerance tests (2 g kg^{-1}) 120 minutes following drug administration and snap frozen in liquid nitrogen. 2 mm sections encompassing the medial basal hypothalamus (MBH) were cut using the rat brain matrix (A1TO 1mm World Precision instruments) and MBH dissected with a scalpel. Protein was extracted from the region of interest by mechanical homogenisation, in lysis buffer, and quantified using the Bradford method. Extracted protein was separated using SDS-PAGE and transferred to nitrocellulose membranes. Immunoreactivity for total and phosphorylated protein was detected and semi-quantified using infrared fluorescence on the Licor Odyssey scanner. Primary antibodies used were: pThr172 AMPK (1:1,000; catalogue #2531), AMPKα (total AMPK 1:1000, catalogue #2535), pSer79 acetyl CoA carboxylase (ACC; 1:1000; catalogue #3661) from Cell Signalling Technologies, total ACC (1:1,000; catalogue #05-1098) from Merck Millipore and β-actin (1:10,000; catalogue #NB600-501) from Biotechne.

Determination of ATP Concentrations

GT1-7 cells were cultured in 96-well plates overnight and intracellular ATP concentrations were measured using the ATPlite two-step assay (PerkinElmer, UK) as per manufacturer's instructions and as previously described (17).

Measurement of Glucagon Release

For glucagon assessments, αTC1.9 cells were seeded in 12-well plates overnight, incubated in serum-free medium for 2 hrs and treated for 1 hr with R481 (50 nmol/L) or vehicle in KBH buffer (**Table 1**) supplemented with 0.5 mmol/L glucose. Media was collected for glucagon quantification using glucagon ELISA (Mercodia, Uppsala, Sweden) and cells lysed for protein quantification. Data analyzed by 4-parameter logistic curve analysis.

Assessment of Cellular Metabolism

Measurement of basal oxygen consumption rate (OCR), extracellular acidification rate (ECAR) and glycolytic rate assays were performed using the Agilent Seahorse Bioanalyzer according to manufacturer's instructions with minor modifications (Agilent, United Kingdom). Briefly, αTC1.9 cells were plated on poly-L-lysine (PLL; 4 µg/ml) coated XFe96 microplates (3 x 10^4 cells/well) in growth medium (**Table 1**) and incubated overnight at 37°C, 5% CO_2 before experiments. For glucose concentration response experiment, following overnight incubation, cells were washed and incubated in glucose-free XF DMEM at 37°C in non-CO_2 incubator (de-gas) and treated with R481 (50 nmol/L) or vehicle for 60 minutes. Baseline OCR and ECAR measurements were taken before injection of increasing glucose concentrations (0.1-11.7 mmol/L). For glycolytic rate assays, cells were incubated overnight, as above, and subsequently treated with R481 (50 nmol/L) or vehicle with and without SBI-0206965 (30 µmol/L) for 60 minutes in 0.5 mmol/L glucose containing XF DMEM. Basal ECAR was measured and used to determine glycolytic proton efflux rate (glycoPER), calculated according to manufacturer's instructions using in house buffer capacity assays. After assays, cells were lysed with NaOH (50 mmol/L) for protein quantification using the method of Bradford. Baseline OCR and ECAR represent an average of the first 4 cycles of each assay.

Animals

All animals in these studies were male Sprague-Dawley rats (200-350 g) purchased from Charles River Laboratories (Margate, UK). Rats were group-housed in double decker clear plastic cages with ample bedding material and environmental enrichment (wooden chew blocks and a cardboard tube) and maintained on a 12-hour light cycle (06:30 am lights on), temperature 22-23°C, 55% humidity with *ad libitum* access to food (Lab Diet; catalogue number 5LF2) and water. Animals were randomized to treatment groups (computerized randomization) and for most studies, the lead investigator was blinded to treatments (excluding pilot and/or dose finding studies). Rats were fasted for 16 hrs prior to all experiments. All procedures were approved by the University of Exeter Animal Welfare and Ethical Review body and were

performed in accordance with the UK Animals Scientific Procedures Act (1986).

Glucose Tolerance Tests and Feeding Studies

For glucose assessments using SBI-0206965 (3 mg kg^{-1}) and hexamethonium (50 mg kg^{-1}) or saline vehicle, either drug was delivered 30 minutes before glucose (2 g kg^{-1}) ± R481 (5-20 mg kg^{-1}); R419 (20 mg kg^{-1}) or vehicle (0.5% HPMC + 0.1% TWEEN-80) in a single injection. Substances were administered *via* the intraperitoneal (i.p.) route. Blood glucose was measured at 0, 15, 30, 60 and 120 minutes from a tail vein prick by handheld glucometer (AccuCheck, Roche). Blood samples at 15 minutes were collected from the tail vein using sodium heparin coated capillary tubes. Blood was centrifuged at 5000 rpm for 10 minutes at 4°C and plasma collected and snap frozen in liquid nitrogen for insulin quantification. For feeding studies, food hopper containing chow was weighed after 1-24 hours, depending on the study.

Hyperinsulinemic Clamp Studies

Male Sprague-Dawley rats (200-300 g) with pre-implanted jugular vein and carotid artery catheters were purchased from Charles River (Margate, UK). Catheters were exteriorized using a dual-channel vascular access button (Instech, USA) and covered using a lightweight aluminium cap, enabling social housing following surgery. This improved body weight curves post-surgery. Catheter patency was maintained by flushing the catheters every 3-5 days with heparinized glucose catheter lock solution. R481 (20 mg kg^{-1}; i.p.) or vehicle (0.5% HPMC, 0.1% TWEEN-80; i.p.) were administered following overnight fast, 1 hr prior to the hyperinsulinemic-euglycemic or hypoglycemic clamp. Blood glucose was measured every 5-10 min and larger blood samples for hormone analysis were collected every 30 min from the carotid artery catheter. During euglycemic clamps, animals received a fixed continuous insulin infusion of 20 mU kg^{-1} min^{-1} and a variable dextrose (20% w/v; i.v.) infusion rate to maintain glycaemia at approximately 5.5 mmol/L. To induce hypoglycemia, rats received a bolus insulin infusion of 80 mU kg^{-1} min^{-1} for 10 minutes, followed by a maintenance dose of 20 mU kg^{-1} min^{-1} for the remainder of the clamp. A variable 20% (w/v) dextrose infusion was used to maintain blood glucose levels at approximately 2.8-3 mmol/L at nadir. Six animals were excluded from the study for poor catheter patency issues. Overall patency rates were approximately 85% for animals maintained up to 21 days post-surgery.

Hormone and Metabolite Analysis

Plasma glucagon, C-peptide and insulin were measured using ELISA (Mercodia, Uppsala, Sweden). Plasma adrenaline was measured using the Demeditec Adrenaline ELISA (Kiel, Germany).

Statistical Analysis

A one-sample t-test was used to determine significant changes in phosphorylated or total protein expression relative to control in immunoblotting experiments. Unpaired t-tests were used to compare groups in non-normalized immunoblotting data. Blood glucose levels, glucose infusion rates and plasma analytes were analyzed using a two-way ANOVA with repeated measures or mixed-effects analysis in cases where datasets were missing data points. Peak hormone levels were analyzed using an unpaired t-test. Analyses were performed using the GraphPad Prism (Prism 8, GraphPad, La Jolla, CA, USA). Results are expressed as mean ± SEM, with $p < 0.05$ considered statistically significant.

RESULTS

R481 Activates AMPK in Hypothalamic Neuronal Cells

To confirm that R481 activated AMPK in neuronal cells, we utilized the mouse hypothalamic glucose-sensing GT1-7 line (3). In GT1-7 cells, treatment for 30 minutes with increasing concentrations of R481 (0-50 nmol/L) increased AMPK phosphorylation at threonine 172 (**Figures 2A, B**). Phosphorylation of the downstream AMPK substrate, ACC, was also significantly increased by R481 (**Figures 2A, C**). Despite AMPK activation, total intracellular ATP levels were not compromised by R481, even at concentrations up to 200 nmol/L (**Figure 2D**). Treatment with R419 (50 nmol/L) did not alter AMPK phosphorylation in GT1-7 cells (**Supplementary Figure 2**) but did increase phosphorylation of ACC, suggesting modest AMPK activation by an AMP-dependent mechanism, as expected for a mild mitochondrial complex I inhibitor.

R481 Raises Peak Glycaemia Which Is Attenuated by AMPK Inhibitor SBI-0206965 and Abolished by Autonomic Blockade

Dosing studies in mice demonstrated that R481 rapidly enters the brain (**Supplementary Figure 1A**), displaying a brain:plasma ratio of >3 (**Supplementary Figure 1B**) and increases whole brain AMPK phosphorylation following bolus intravenous infusion in mice (**Supplementary Figure 1C**). In contrast, a related compound R419 did not display significant brain permeability (data courtesy of Rigel Pharmaceuticals. Inc). To determine whether R481 altered glucose tolerance, rats were given a combined intraperitoneal injection of R481 (5-20 mg kg^{-1}) and glucose (2 g kg^{-1}). R481 treated rats showed significantly higher peak glucose excursions yet glucose levels were not significantly different between groups at 2 hrs post-injection, suggesting effective clearance of glucose. This effect was not reproduced following treatment with non-brain permeable R419 (peak glucose 15.7 ± 1.7 mmol/L in Veh, 23.4 ± 1.8 mmol/L in R481 and 18.3 ± 1.6 in R419 groups; **Figure 3A**). The R481-mediated increase in peak glucose levels was attenuated by pre-treatment with AMPK/Uncoordinated (Unc)-51-like kinase (ULK-1) inhibitor SBI-0206965 (3 mg kg^{-1}; peak glucose 20.7 ± 1.2 mmol/L in R481 vs 17.4 ± 1.1 mmol/L in R481+SBI group; **Figure 3B**) (18), which has demonstrated brain penetrance and been shown to inhibit autophagy in the brain (19). To examine whether the autonomic nervous system (ANS) played a role in raising glucose levels, we pre-treated rats with pan autonomic blocker hexamethonium (50 mg kg^{-1}) prior to glucose tolerance testing. Glucose excursion in hexamethonium treated rats was not altered

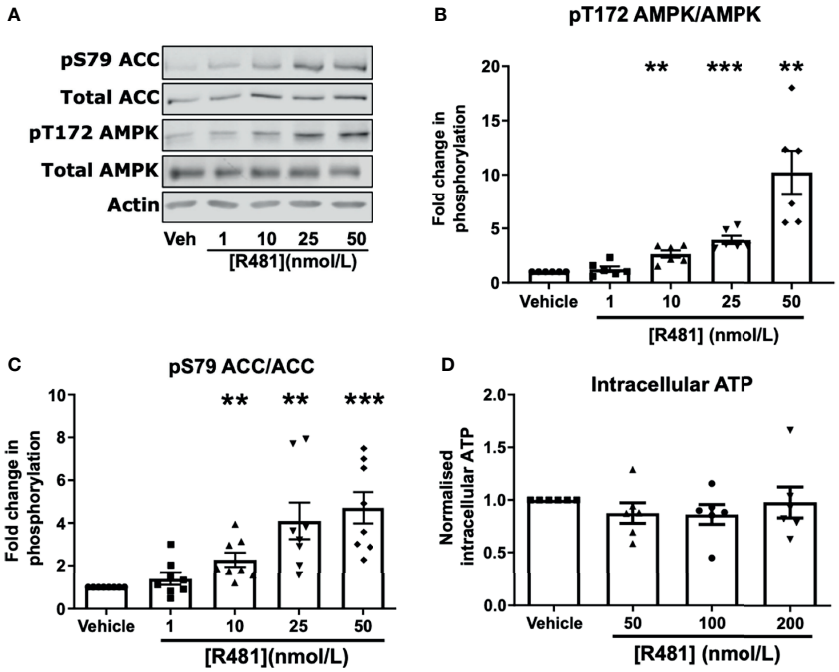

FIGURE 2 | AMPK is activated in GT1-7 hypothalamic neuronal cells by R481. Mouse GT1-7 hypothalamic neurons treated with increasing concentrations of R481 for 30 minutes. **(A)** Representative Western blots for AMPK (pT172), total AMPK, ACC (pS79), total ACC and Actin. Densitometric analysis of the mean pooled data for phospho-AMPK normalized to total AMPK shown in **(B)** (n=6) and phospho-ACC normalized to total ACC in **(C)** (n=8; **P<0.01; ***P<0.001; One-sample t-test in comparison to control). **(D)** Intracellular ATP levels of GT1-7 cells treated with R481, normalized to vehicle (30 minutes; n=6).

by R481 treatment, suggesting that autonomic blockage completely abolished the effect of R481 on glycaemia (peak glucose 22.3 ± 0.7 mmol/L R481 vs 17.6 ± 1.1 mmol/L in R481 + Hex group; **Figure 3C**). At peak glucose levels (15 minutes), insulin concentrations were comparable between vehicle and R481 treated rats (37.2 ± 8.3 pmol/L Veh vs 45.3 ± 22.6 pmol/L R481; **Figure 3D**). Together with R419 data this supports a central action of R481 in regulating glycaemia. On examination of AMPK phosphorylation in the medial basal hypothalamus of R481 and R419 treated rats, there was modestly but not significantly increased levels compared to vehicle controls (>10% increase), with no change seen following R419 treatment (**Supplementary Figure 3**).

As hypothalamic AMPK activation increases feeding (6) and leptin-induced repression of feeding requires inhibition of AMPK (20), we postulated that a brain permeable AMPK activator may increase feeding behavior. However, R481 treatment did not alter *ad libitum*, fasting or hypoglycemia-induced feeding in rats (**Supplementary Figure 4**).

R481 Does Not Alter Glucose Infusion Rates During a Hyperinsulinemic-Euglycemic Clamp

R481 (20 mg kg^{-1}) or vehicle were administered 60 minutes before insulin infusion (see study design, **Figure 4A**; blood glucose target: 5.5 mmol/L). Baseline glucose levels were moderately increased in R481 treated animals (t = -60 minutes; 7.2 ± 0.2 mmol/L vs t = 0; 7.5 ± 0.2 mmol/L), compared to vehicle group, as blood glucose levels decreased in the latter following drug treatment (t= -60 minutes 7.1 ± 0.6 to t= 0 6.3 ± 0.2 mmol/L). This produced a significant relative increase in blood glucose at the start of the clamp in R481 treated animals (n=8; **Figure 4B**). Glucose levels were well-matched during the last 30 minutes of the clamp (**Figure 4B**), with no difference in the glucose infusion rate (GIR; **Figure 4C**). The levels of C-peptide were not different between groups (**Figure 4D**).

R481 Reduces the GIR and Increases Glucagon Levels During A Hyperinsulinemic-Hypoglycemic Clamp

To determine the potential influence of central AMPK activation, using R481, on CRR, we induced hypoglycemia (2.8 mmol/L) during a 90 minute clamp study (Study design **Figure 5A**). Glucose levels during the clamp were well-matched between vehicle and R481-treated rats (**Figure 5B**). Exogenous glucose infusion required to maintain hypoglycemia was significantly lower in R481-treated animals (**Figure 5C**). Peak plasma glucagon levels were significantly higher in the R481 treated group (**Figures 5D, E**). Adrenaline levels were not different between groups (**Figures 5F, G**).

R481 Activates AMPK and Enhances Glucose Utilization in Pancreatic α-Cells During Low Glucose Exposure

Given that R481 significantly augmented peak glucagon levels, murine αTC1.9 cells were used as a model of pancreatic α-cell to

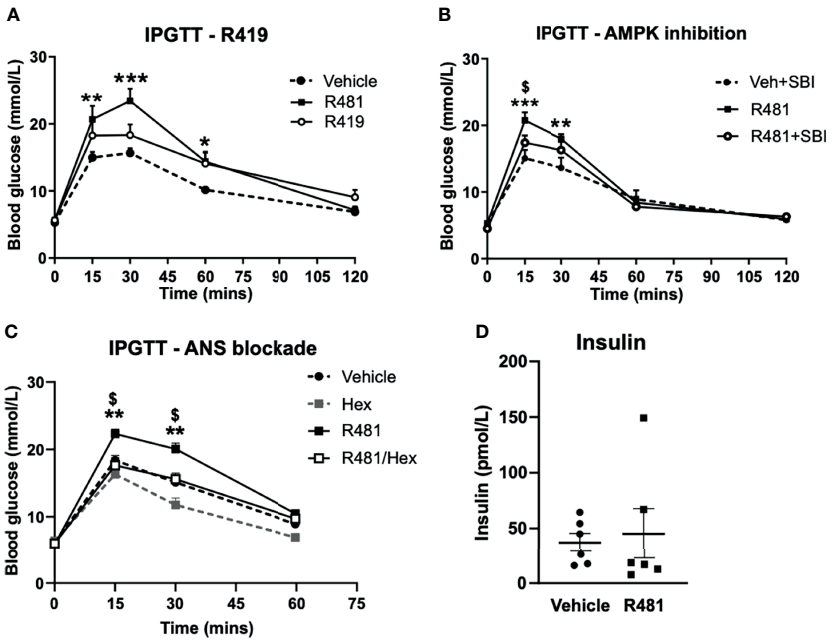

FIGURE 3 | R481 increases peak glucose excursion in a manner that is attenuated by AMPK inhibitor SBI-0206965 and ANS blocker hexamethonium and does not alter insulin levels. Glucose tolerance tests in male Sprague-Dawley rats fasted for 16 hrs. **(A)** Rats were administered glucose (2 g kg-1; i.p.) together with either vehicle (HPMC/Tween-80; n=6), R419 (20 mg kg-1; n=6) or R481 (20 mg kg-1;n=6) Two-way ANOVA with repeated measures, *P(drug)<0.05, ***P(time)<0.001, **P (interaction)<0.01, with Bonferroni's analysis *P<0.05, **P<0.01, ***P<0.001 for R481 against vehicle; no significant difference between R419 and vehicle groups. **(B)** Rats were administered SBI-0206965 (3 mg kg-1; i.p.) or vehicle 30 minutes before R481 (5 mg kg-1; i.p.) or vehicle (HPMC/Tween-80; i.p.) together with glucose (2 g kg-1; i.p.)(SBI-0206965 n=6; R481 n=10; R481+SBI-0206965 n=8); Two-way ANOVA with repeated measures *P(drug)<0.05, ***P(time)<0.001, ***P (interaction)<0.001 and Bonferroni's multiple comparisons analysis, **P<0.01, ***P<0.001 for R481 against vehicle, $P<0.05 for R481 *versus* R481+SBI-0206965. **(C)** Rats were treated with hexamethonium (Hex; 50 mg kg-1) or vehicle (saline) 30 minutes before combined administration of glucose (2 g kg-1; i.p.) and R481 (20 mg kg-1; i.p.) or vehicle (HPMC/Tween-80; i.p.); Two-way ANOVA with repeated measures ***P(drug)<0.001, ***P(time)<0.001, ***P(interaction)<0.001 Veh (n=8); Hex (n=3); R481 (n=7); R481/Hex (n=8) with Bonferroni's analysis **P<0.01 for R481 against vehicle and $^{\$}$P<0.05 for R481 against R481/Hex. **(D)** Plasma insulin levels measured from 15 minute sample of vehicle (n=7) and R481 (n=7) groups in C by ELISA.

examine the effect of R481 on AMPK activation, glucagon secretion and cellular metabolism during low glucose exposure. Treatment of αTC1.9 cells for 60 minutes with R481 (50 nmol/L) at 1 mmol/L glucose significantly enhanced AMPK phosphorylation at threonine 172 (**Figures 6A, B**) and ACC phosphorylation at serine 79 (**Figures 6A, C**). Glucagon release following 60 minute treatment with R481 (50 nmol/L) or vehicle at 0.5 mmol/L glucose was not different between groups (Veh 1044 ± 141.3; R481 832.6 ± 68.0 pg/mg; **Figure 6D**). To assess changes to cellular metabolism in these glucose sensing cells, αTC1.9 cells were treated for 60 minutes with R481 (50 nmol/L) in the absence of glucose; oxygen consumption rate (OCR) was measured, and cells were treated with increasing glucose concentrations to assess changes to extracellular acidification rate (ECAR) as a proxy for glycolysis. Baseline OCR levels were modestly but significantly decreased in R481 treated cells compared to vehicle, as expected (**Figure 6E**). The glucose-dependent increase in ECAR was augmented by R481, which tended to increase at 0.5 mmol/L and was significantly elevated in R481 treated cells from 1 mmol/L to 11.7 mmol/L glucose (**Figure 6F**). Finally, to test the effect of AMPK inhibition on the R481-mediated ECAR response, cells were treated with R481 (50 nmol/L) with or without AMPK inhibitor SBI-0206965 (30 μmol/L) for 60 minutes in 0.5 mmol/L glucose. The R481-mediated increase in basal ECAR was blunted by treatment with SBI-0206965 (**Figure 6G**). To distinguish whether this represents mitochondria derived proton acidification or glycolysis derived acidification, glycoPER, or glycolytic proton efflux rate was measured. Cells treated with R481 showed significantly higher glycolytic rates compared to vehicle and this increase was completely abolished by SBI-0206965 treatment. Moreover, SBI-0206965 treatment alone significantly lowered basal glycoPER, most likely driven by endogenous increases in AMPK activity during low glucose exposure (**Figure 6H**).

DISCUSSION

AMPK activators have been developed for glucose lowering in Type 2 Diabetes (T2D), largely by acting on skeletal muscle to promote glucose disposal (21, 22). The R481 analogue, R419 (non-brain permeable), activates AMPK in skeletal muscle and increases insulin sensitivity in high-fat fed mice (23).

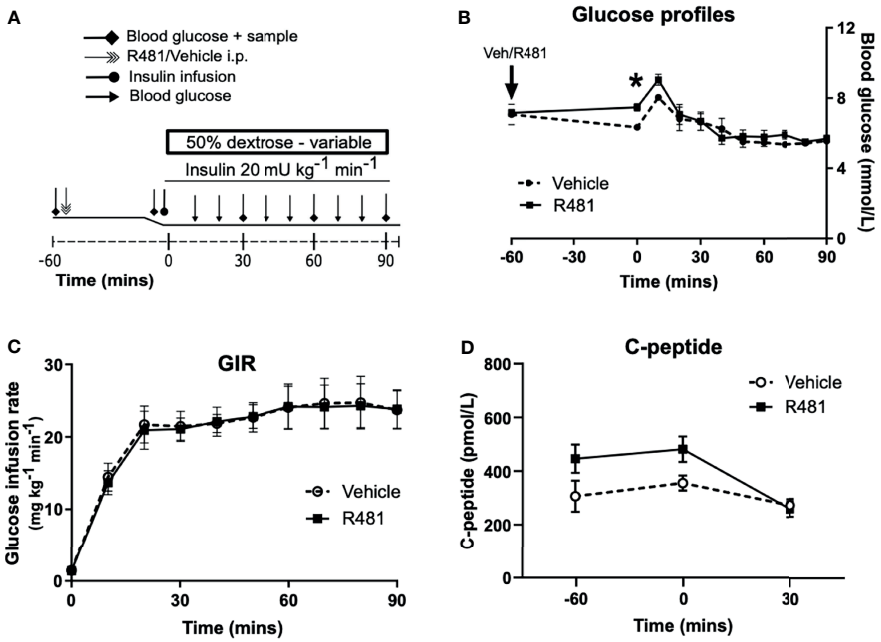

FIGURE 4 | R481 does not alter glucose infusion rate during hyperinsulinemic-euglycemic clamp or alter endogenous insulin secretion. Hyperinsulinemic-euglycemic clamps performed in male Sprague-Dawley rats. **(A)** Study design. **(B)** Blood glucose profiles (Vehicle n=8, R481 n=8; 20 mg kg^{-1}; i.p.). No overall drug effect P(drug) >0.05; mixed-effects analysis of repeated measures, but *P<0.05 for R481 against vehicle at t=0 minutes, using Bonferroni's *post-hoc* test. **(C)** Glucose infusion rate (GIR; mg kg^{-1} min^{-1}) during the clamp using a 50% dextrose solution (Vehicle n=8; R481 n=8). **(D)** Plasma C-peptide measured by ELISA (Vehicle n=8; R481 n=7).

We demonstrate here that R481 (brain permeable) raises glucose levels during GTTs, without negatively impacting glucose clearance, in a manner that was attenuated by AMPK inhibition and completely abolished by autonomic blockade, suggesting R481 acts centrally to mediate these effects. Previous studies have shown that genetic or pharmacological suppression of hypothalamic AMPK activity decreases hepatic glucose production [HGP (24)]. Conversely, direct infusion of non-specific AMPK activator AICAR into the hypothalamus stimulates HGP (24, 25). In addition, fructose ingestion has been shown to increase hypothalamic AMPK activity and increase HGP (26). In combination, these studies indicate that hypothalamic AMPK activity regulates HGP and supports the suggestion that R481 may require hypothalamic AMPK activation to stimulate HGP, possibly *via* the brain stem circuit, as demonstrated previously (25). Our data concur with these earlier observations and extend them by demonstrating that peripheral delivery of a brain permeable AMPK activator can increase glycaemia. Defining the specific brain nuclei and the neural circuitry involved will be important in future studies.

Kume and colleagues (27) demonstrated that activation of hypothalamic AMPK suppressed first phase glucose-stimulated insulin secretion (GSIS) through autonomic innervation of α-adrenergic pancreatic nerves. This was suggested to be a physiological response to promote glucose delivery to the brain during fasting (27), a mechanism that may also occur during hypoglycemia. However, in our study, R481 did not alter glucose-stimulated insulin secretion nor did it alter C-peptide levels during the clamp studies, suggesting that R481 does not suppress basal insulin secretion and likely increases glycaemia by stimulating HGP, as has been previously reported following viral and pharmacological manipulation of hypothalamic AMPK activity (24–26).

We postulated that R481 treatment may increase the GIR during the euglycemic clamp by enhancing skeletal muscle glucose uptake. However, the GIR during the euglycemic clamp was not altered by R481. This suggests that the compound is not having a direct metformin-like effect in the liver to suppress HGP. However, given that R481 has a positive brain:plasma ratio, it is plausible that there is insufficient compound accumulation in the liver to significantly change glucose production directly. Moreover, we examined glucose homeostasis following a single injection of the drug in lean rats and saw no direct evidence of glucose lowering, again suggesting that there is little effect in peripheral tissues such as skeletal muscle or adipose tissue. Whether acute and/or chronic R481 treatment would have a glucose lowering effect in rats fed a high-fat diet (HFD) remains to be determined. However, a previous study demonstrated that the R481 analogue R419, given chronically to HFD fed mice (23), enhanced skeletal muscle glucose uptake and insulin sensitivity. It is important to highlight that our data suggest the transient increase in blood glucose levels by R481 was not mediated by a change to insulin secretion or sensitivity. Moreover, despite the fact that glucose levels peaked higher in the R481 treated animals during the GTT, glucose levels at 2 hours post glucose administration were not

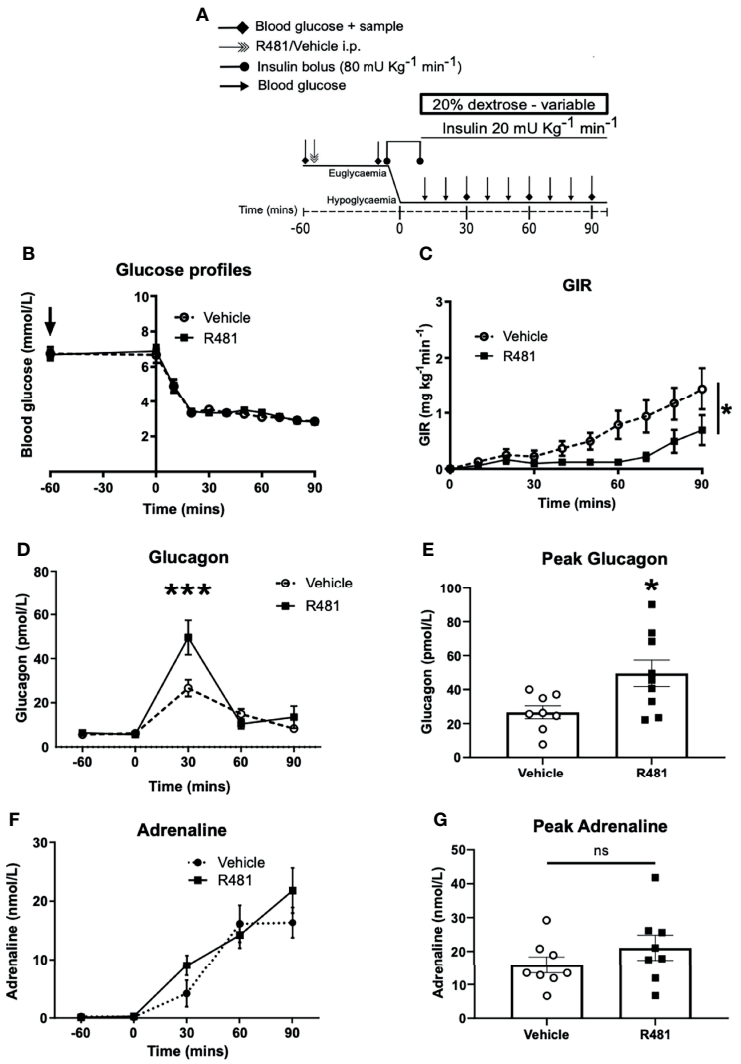

FIGURE 5 | R481 delays exogenous glucose requirements during hyperinsulinaemic-hypoglycaemic clamp by augmenting glucagon levels during hypoglycaemia. Hyperinsulinaemic-hypoglycaemic clamps performed in male Sprague-Dawley rats. **(A)** Study design. Animals were fasted for 16 hrs. R481 (20 mg kg^{-1}; i.p.) or vehicle (HPMC/Tween-80; i.p.) were administered 60 minutes before the start of the clamp. **(B)** Blood glucose profiles before and during clamp (Vehicle n=10; R481 n=8). **(C)** Glucose infusion rates (GIR; mg kg^{-1} min^{-1}) during the clamp using a 20% dextrose solution. *P(drug)<0.05, ***P(time)<0.05, *P(interaction)<0.05; Two-way ANOVA with repeated measures. **(D)** Plasma glucagon profile with peak shown in **(E)**, measured by ELISA (Vehicle n=9; R491 n=9; *P<0.05, unpaired t-test). **(F)** Plasma adrenaline profile with peak shown in **(G)**, measured by ELISA (Vehicle n=8; R481 n=8; ns, not significant).

different from controls, suggesting that glucose clearance was not altered and possibly greater compared to vehicle treated animals. Using glucose tracers to determine the rates of glucose appearance and disappearance will be important going forward to closely examine HGP and skeletal muscle glucose uptake.

In previous studies with non-diabetic rats, direct pharmacological activation of AMPK in the VMH using AICAR amplified HGP during hypoglycemia, without altering glucagon or adrenaline release (10). In line with this, basal glucagon and adrenaline release in our study were not altered by R481. Importantly, previous studies have demonstrated that pharmacological and genetic activation of AMPK in pancreatic α-cells was sufficient to stimulate glucagon release (7, 8). Taken together with our data, it is plausible that R481 may have direct actions in pancreatic α-cells to augment glucagon release. To assess this further we treated pancreatic α-cells *in vitro* with R481 during exposure to low glucose. Our data suggest that treatment with R481 increases AMPK activation at low glucose and, like other indirect AMPK activators, appears to cause mild mitohormesis, evidenced by decreased basal oxygen consumption. However, R481 did not alter glucagon secretion during low glucose treatment, at least in this cell model. In contrast, R481 treatment significantly enhanced glucose utilization by amplifying glucose-dependent glycolytic rate, which would be expected to result in suppression of glucagon release. This R481-mediated increase in glycolysis was completely

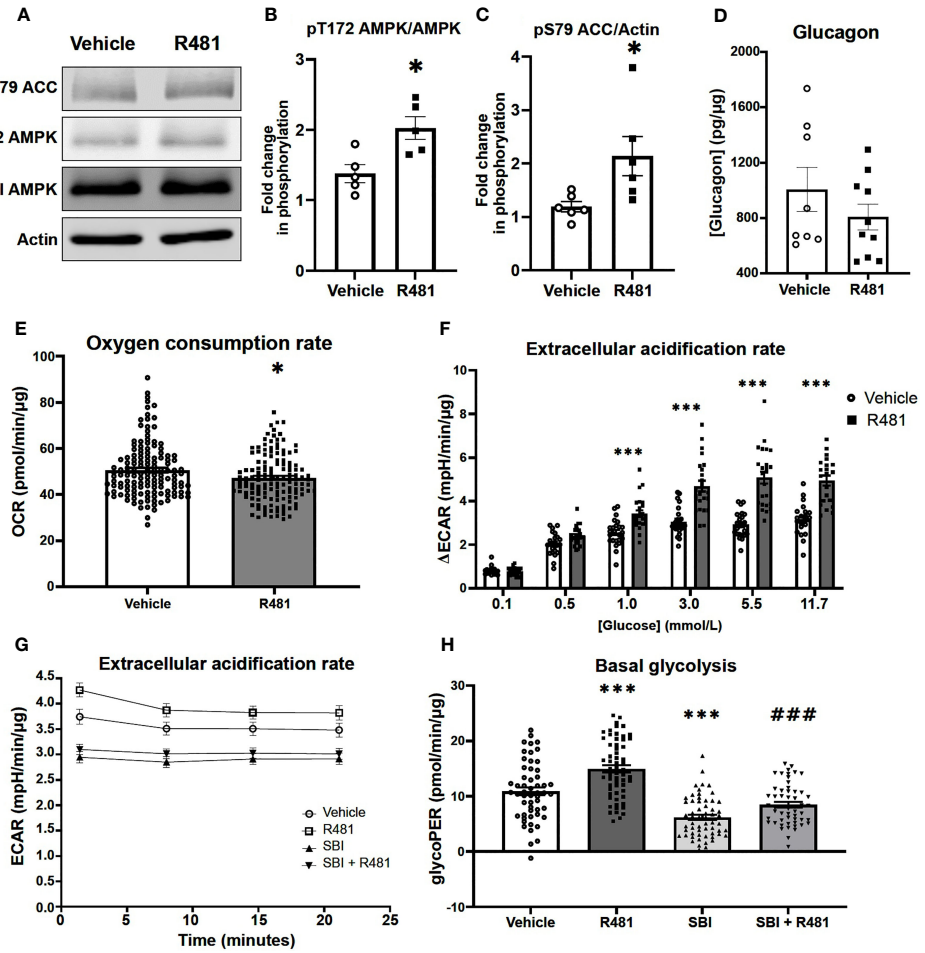

FIGURE 6 | R481 activates AMPK and enhances glycolysis during low glucose in murine pancreatic α-cells. Murine αTC1.9 pancreatic α-cells treated with R481 during hypoglycemia. **(A)** Representative Western blot for AMPK (pT172), total AMPK, ACC (pS79), total ACC and Actin. Densitometric analysis of the mean pooled data for phospho-AMPK normalized to total AMPK in **(B)** (n=5) and phopho-ACC normalized to total ACC in **(C)** (n=6) for cells treated with R481 (50 nmol/L) or vehicle in 1 mmol/L glucose (*P<0.05 unpaired t-test). **(D)** Glucagon measured by ELISA in αTC1.9 cells treated with R481 (50 nmol/L) or vehicle for 1 hr in 0.5 mmol/L glucose (Veh n=8; R481 n=10). Measurement of baseline oxygen consumption rate in **(E)** (n= 138; *P<0.05; unpaired t-test) prior to and change in extracellular acidification rate in **(F)** (n= 24; delta reflects change from baseline glucose-free levels) following acute treatment with glucose (0.1-11.7 mmol/L) in cells treated for 1 hr with R481 (50 nmol/L) or vehicle. **(G)** Representative trace of basal ECAR for cells treated with R481 (50 nmol/L) or vehicle with or without SBI-0206967 (Vehicle n=54; R481 n=60, SBI n=59, R481+SBI n=54) in 0.5 mmol/L glucose with assessment of glycolytic proton efflux rate (glycoPER) in **(H)** (***P<0.001 compared to vehicle; ###P<0.001 compared to R481 group).

abolished by pre-treatment with allosteric AMPK inhibitor SBI-0206965, indicating the R481-induced changes in cellular metabolism are most likely AMPK mediated, although it should be noted that SBI-0206965 can also inhibit ULK1 at these concentrations (18). Taken together, these actions of R481 suggest that the compound does not alter glucagon secretion through a pancreatic α-cell-mediated mechanism and provides evidence that *in vivo*, R481 may raise glucagon levels during hypoglycemia by a centrally-mediated pathway.

In streptozotocin-induced diabetic rats, VMH AICAR injection can augment both glucagon and adrenaline responses during hypoglycemia (11). Given that both hyperglycemia and recurrent hypoglycemia/glucoprivation suppress hypothalamic AMPK activation (6, 13) and that direct genetic suppression of VMH AMPK expression/activity suppresses the glucagon and adrenaline responses to hypoglycemia (12), it is plausible that hypothalamic AMPK activity is blunted in diabetes, leading, at least in part, to defective CRR. In our study, R481 may activate an AMPK-ANS-HGP axis, whilst also increasing plasma glucagon levels to better defend against hypoglycemia. Delineating the central *versus* peripheral actions of pharmacological AMPK activation during hypoglycemia requires further study. It will also be interesting to determine the effect of R481 when given chronically and by a method that provides slower release of R481, such as with an osmotic mini-pump, as the action of R481 was limited to 2-2.5 hours when delivered by the intraperitoneal

route. One of the limitations of our study was that we were unable to conclusively demonstrate increased AMPK phosphorylation or activity in brains from rats treated with R481. We have demonstrated a trend towards increased AMPK phosphorylation following R481 but not R419 treatment in the medial basal hypothalamus. However, we did not observe statistically significant differences, which may be due to increased basal AMPK activation as a consequence of hypoxia during anaesthesia prior to tissue extraction (28).

Importantly, our data highlight that the likely net effect of brain AMPK activation is to increase glucose delivery to the brain (27), indicating that, at the level of the whole organism, central AMPK activation may supersede peripheral activation in a hierarchical manner, akin to that suggested for subcellular pools of AMPK (29). This raises the interesting possibility that centrally biased AMPK activating drugs could be used to raise blood glucose levels and peripheral activators to reduce glycaemia, meaning that a drug or combination of drugs that activate central and peripheral AMPK could be used to attenuate the peaks and troughs in blood glucose seen in diabetes. Our data also raise the interesting possibility that if metformin were to activate AMPK in the brain, this possible glucose-raising action could compete with the effect of metformin in the liver to suppress gluconeogenesis (30). The blood brain barrier is more leaky in T2D/obesity (31–33) and several clinical studies have shown possible central effects of metformin (34, 35), suggesting that metformin may enter the brain at efficacious levels in some circumstances. Taken together, this could raise the possibility that metformin "failure" in T2D could be caused by metformin-induced activation of brain AMPK, stimulating ANS-mediated HGP, competing against the actions of the drug in the liver.

In summary, our data indicate that peripheral delivery of a brain permeable AMPK activator raises glycaemia, likely to protect brain function. We provide proof-of-concept that pharmacological activation of central AMPK may be a suitable therapeutic target for amplifying the defense against hypoglycemia. This requires testing in rodent models of T1D and T2D and in rodents with defective CRR where careful optimization of the dose to amplify CRR without worsening fasting/fed hyperglycemia will be needed. To be clinically useful, any anti-hypoglycemic drug would need to be taken prior to the unpredictable development of hypoglycemia. A drug with an optimized pharmacodynamic/pharmacokinetic profile permitting dosing, for example, before bedtime, could be taken to prevent the development of nocturnal hypoglycemia. It will also be interesting to determine whether central AMPK activating drugs could be used as a treatment for severe hypoglycemia to promote rapid recovery of blood glucose levels. In conclusion, development of brain permeable allosteric activators of AMPK could be useful for the prevention/treatment of hypoglycemia in diabetes.

DATA AVAILABILITY STATEMENT

The raw data supporting the conclusions of this article will be made available by the authors, without undue reservation.

ETHICS STATEMENT

The animal study was reviewed and approved by University of Exeter Animal Welfare and Ethical Review Board.

AUTHOR CONTRIBUTIONS

A.M.C, K.M.P, Y.M., J.M.V.W., P.G.W.P, K.R.P, and C.B. researched data. A.M.C., K.M.P, J.M.V.W., S.J.S., K.L.J.E., and C.B., contributed to study design. All authors contributed to writing the manuscript and approved the final version. C.B. conceived the study, had access to all the data collected at the University of Exeter and takes responsibility for the accuracy and integrity of the data.

FUNDING

This study was funded by: a JDRF Innovative grant (1-INO-2016-214-A-N) to CB and KE; a JDRF postdoctoral fellowship (3-PDF-2020-941-A-N) to PW, a Diabetes UK RD Lawrence Fellowship to CB (13/0004647); a Diabetes UK PhD studentship to CB and KE for KMP. (18/0005914); a Society for Endocrinology early career grant to CB and a British Society for Neuroendocrinology practical skills grant to CB. AC was funded by a University of Exeter Medical School PhD studentship.

ACKNOWLEDGMENTS

We wish to thank Jennifer Gallagher, Dr Alison McNeilly, Prof Rory McCrimmon and Gary Park. We also wish to thank Prof René Remie for surgical refinements. Parts of this work were presented at the ADA 79th Scientific Sessions, Diabetes UK APC 2019, AMPK2018, AMPK2019 and EASD 2020 conferences. This study represents independent research supported by the National Institute of Health Research Exeter Clinical Research Facility.

SUPPLEMENTARY MATERIAL

The Supplementary Material for this article can be found online at: https://www.frontiersin.org/articles/10.3389/fendo.2021.697445/full#supplementary-material

REFERENCES

1. Segel SA, Paramore DS, Cryer PE. Hypoglycemia-Associated Autonomic Failure in Advanced Type 2 Diabetes. *Diabetes* (2002) 51:724–33. doi: 10.2337/diabetes.51.3.724

2. Carling D, Clarke PR, Zammit VA, Hardie DG. Purification and Characterization of the AMP-Activated Protein Kinase. Copurification of Acetyl-Coa Carboxylase Kinase and 3-Hydroxy-3-Methylglutaryl-Coa Reductase Kinase Activities. *Eur J Biochem* (1989) 186:129–36. doi: 10.1111/j.1432-1033.1989.tb15186.x

3. Beall C, Hamilton DL, Gallagher J, Logie L, Wright K, Soutar MP, et al. Mouse Hypothalamic GT1-7 Cells Demonstrate AMPK-Dependent Intrinsic Glucose-Sensing Behaviour. *Diabetologia* (2012) 55:2432–44. doi: 10.1007/s00125-012-2617-y
4. Sun G, Tarasov AI, McGinty J, McDonald A, da Silva Xavier G, Gorman T, et al. Ablation of AMP-Activated Protein Kinase Alpha 1 and Alpha 2 From Mouse Pancreatic Beta Cells and RIP2.Cre Neurons Suppresses Insulin Release *In Vivo*. *Diabetologia* (2010) 53:924–36. doi: 10.1007/s00125-010-1692-1
5. Beall C, Piipari K, Al-Qassab H, Smith MA, Parker N, Carling D, et al. Loss of AMP-Activated Protein Kinase Alpha 2 Subunit in Mouse Beta-Cells Impairs Glucose-Stimulated Insulin Secretion and Inhibits Their Sensitivity to Hypoglycaemia. *Biochem J* (2010) 429:323–33. doi: 10.1042/BJ20100231
6. Minokoshi Y, Alquier T, Furukawa N, Kim YB, Lee A, Xue BZ, et al. AMP-Kinase Regulates Food Intake by Responding to Hormonal and Nutrient Signals in the Hypothalamus. *Nature* (2004) 428:569–74. doi: 10.1038/nature02440
7. Sun G, da Silva Xavier G, Gorman T, Priest C, Solomou A, Hodson DJ, et al. LKB1 and Ampkalpha1 are Required in Pancreatic Alpha Cells for the Normal Regulation of Glucagon Secretion and Responses to Hypoglycemia. *Mol Metab* (2015) 4:277–86. doi: 10.1016/j.molmet.2015.01.006
8. Leclerc I, Sun G, Morris C, Fernandez-Millan E, Nyirenda M, Rutter GA. AMP-Activated Protein Kinase Regulates Glucagon Secretion From Mouse Pancreatic Alpha Cells. *Diabetologia* (2011) 54:125–34. doi: 10.1007/s00125-010-1929-z
9. Borg MA, Sherwin RS, Borg WP, Tamborlane WV, Shulman GI. Local Ventromedial Hypothalamus Glucose Perfusion Blocks Counterregulation During Systemic Hypoglycemia in Awake Rats. *J Clin Invest* (1997) 99:361–5. doi: 10.1172/JCI119165
10. McCrimmon RJ, Fan X, Ding Y, Zhu W, Jacob RJ, Sherwin RS. Potential Role for AMP-Activated Protein Kinase in Hypoglycemia Sensing in the Ventromedial Hypothalamus. *Diabetes* (2004) 53:1953–8. doi: 10.2337/diabetes.53.8.1953
11. Fan X, Ding Y, Brown S, Zhou L, Shaw M, Vella MC, et al. Hypothalamic AMP-Activated Protein Kinase Activation With AICAR Amplifies Counterregulatory Responses to Hypoglycemia in a Rodent Model of Type 1 Diabetes. *Am J Physiol Regul Integr Comp Physiol* (2009) 296:R1702–8. doi: 10.1152/ajpregu.90600.2008
12. McCrimmon RJ, Shaw M, Fan X, Cheng H, Ding Y, Vella MC, et al. Key Role for AMP-Activated Protein Kinase in the Ventromedial Hypothalamus in Regulating Counterregulatory Hormone Responses to Acute Hypoglycemia. *Diabetes* (2008) 57:444–50. doi: 10.2337/db07-0837
13. Alquier T, Kawashima J, Tsuji Y, Kahn BB. Role of Hypothalamic Adenosine 5 '-Monophosphate Activated Protein Kinase in the Impaired Counterregulatory Response Induced by Repetitive Neuroglucopenia. *Endocrinology* (2007) 148:1367–75. doi: 10.1210/en.2006-1039
14. Jenkins Y, Sun T-Q, Markovtsov V, Foretz M, Li W, Nguyen H, et al. AMPK Activation Through Mitochondrial Regulation Results in Increased Substrate Oxidation and Improved Metabolic Parameters in Models of Diabetes. *PloS One* (2013) 8:e81870. doi: 10.1371/journal.pone.0081870
15. Beall C, Haythorne E, Fan X, Du Q, Jovanovic S, Sherwin R, et al. Continuous Hypothalamic KATP Activation Blunts Glucose Counter-Regulation *In Vivo* in Rats and Suppresses KATP Conductance In Vitro. *Diabetologia* (2013) 56:2088–92. doi: 10.1007/s00125-013-2970-5
16. Bradford MM. Rapid and Sensitive Method for Quantitation of Microgram Quantities of Protein Utilizing Principle of Protein-Dye Binding. *Analytical Biochem* (1976) 72:248–54. doi: 10.1016/0003-2697(76)90527-3
17. Vlachaki Walker JM, Robb JL, Cruz AM, Malhi A, Weightman Potter PG, Ashford MLJ, et al. AMP-Activated Protein Kinase (AMPK) Activator a-769662 Increases Intracellular Calcium and ATP Release From Astrocytes in an AMPK-Independent Manner. *Diabetes Obes Metab* (2017) 19:997–1005. doi: 10.1111/dom.12912
18. Dite TA, Langendorf CG, Hoque A, Galic S, Rebello RJ, Ovens AJ, et al. AMP-Activated Protein Kinase Selectively Inhibited by the Type II Inhibitor SBI-0206965. *J Biol Chem* (2018) 293(23):8874–85. doi: 10.1074/jbc.RA118.003547
19. Rocchi A, Yamamoto S, Ting T, Fan Y, Sadleir K, Wang Y, et al. A Becn1 Mutation Mediates Hyperactive Autophagic Sequestration of Amyloid Oligomers and Improved Cognition in Alzheimer's Disease. *PloS Genet* (2017) 13:e1006962.
20. Dagon Y, Hur E, Zheng B, Wellenstein K, Cantley LC, Kahn BB. P70s6 Kinase Phosphorylates AMPK on Serine 491 to Mediate Leptin's Effect on Food Intake. *Cell Metab* (2012) 16:104–12. doi: 10.1016/j.cmet.2012.05.010
21. Merrill GF, Kurth EJ, Hardie DG, Winder WW. AICA Riboside Increases AMP-Activated Protein Kinase, Fatty Acid Oxidation, and Glucose Uptake in Rat Muscle. *Am J Physiol-Endocrinol Metab* (1997) 36:E1107–12. doi: 10.1152/ajpendo.1997.273.6.E1107
22. Kurth-Kraczek EJ, Hirshman MF, Goodyear LJ, Winder WW. 5 ' AMP-Activated Protein Kinase Activation Causes GLUT4 Translocation in Skeletal Muscle. *Diabetes* (1999) 48:1667–71. doi: 10.2337/diabetes.48.8.1667
23. Marcinko K, Bujak AL, Lally JS, Ford RJ, Wong TH, Smith BK, et al. The AMPK Activator R419 Improves Exercise Capacity and Skeletal Muscle Insulin Sensitivity in Obese Mice. *Mol Metab* (2015) 4:643–51. doi: 10.1016/j.molmet.2015.06.002
24. Yang CS, Lam CKL, Chari M, Cheung GWC, Kokorovic A, Gao S, et al. Hypothalamic Amp-Activated Protein Kinase Regulates Glucose Production. *Diabetes* (2010) 59:2435–43. doi: 10.2337/db10-0221
25. Lam CK, Chari M, Rutter GA, Lam TK. Hypothalamic Nutrient Sensing Activates a Forebrain-Hindbrain Neuronal Circuit to Regulate Glucose Production In Vivo. *Diabetes* (2011) 60:107–13. doi: 10.2337/db10-0994
26. Kinote A, Faria JA, Roman EA, Solon C, Razolli DS, Ignacio-Souza LM, et al. Fructose-Induced Hypothalamic AMPK Activation Stimulates Hepatic PEPCK and Gluconeogenesis Due to Increased Corticosterone Levels. *Endocrinology* (2012) 153:3633–45. doi: 10.1210/en.2012-1341
27. Kume S, Kondo M, Maeda S, Nishio Y, Yanagimachi T, Fujita Y, et al. Hypothalamic AMP-Activated Protein Kinase Regulates Biphasic Insulin Secretion From Pancreatic Beta Cells During Fasting and in Type 2 Diabetes. *EBioMedicine* (2016) 13:168–80. doi: 10.1016/j.ebiom.2016.10.038
28. Scharf MT, Mackiewicz M, Naidoo N, O'Callaghan JP, Pack AI. AMP-Activated Protein Kinase Phosphorylation in Brain is Dependent on Method of Killing and Tissue Preparation. *J Neurochem* (2008) 105:833–41. doi: 10.1111/j.1471-4159.2007.05182.x
29. Zong Y, Zhang C-S, Li M, Wang W, Wang Z, Hawley SA, et al. Hierarchical Activation of Compartmentalized Pools of AMPK Depends on Severity of Nutrient or Energy Stress. *Cell Res* (2019) 29:460–73. doi: 10.1038/s41422-019-0163-6
30. Hunter RW, Hughey CC, Lantier L, Sundelin EI, Peggie M, Zeqiraj E, et al. Metformin Reduces Liver Glucose Production by Inhibition of Fructose-1-6-Bisphosphatase. *Nat Med* (2018) 24:1395–406. doi: 10.1038/s41591-018-0159-7
31. Pallebage-Gamarallage M, Lam V, Takechi R, Galloway S, Clark K, Mamo J. Restoration of Dietary-Fat Induced Blood-Brain Barrier Dysfunction by Anti-Inflammatory Lipid-Modulating Agents. *Lipids Health Dis* (2012) 11:117. doi: 10.1186/1476-511X-11-117
32. Davidson TL, Monnot A, Neal AU, Martin AA, Horton JJ, Zheng W. The Effects of a High-Energy Diet on Hippocampal-Dependent Discrimination Performance and Blood-Brain Barrier Integrity Differ for Diet-Induced Obese and Diet-Resistant Rats. *Physiol Behav* (2012) 107:26–33. doi: 10.1016/j.physbeh.2012.05.015
33. Chang HC, Tai YT, Cherng YG, Lin JW, Liu SH, Chen TL, et al. Resveratrol Attenuates High-Fat Diet-Induced Disruption of the Blood-Brain Barrier and Protects Brain Neurons From Apoptotic Insults. *J Agric Food Chem* (2014) 62:3466–75. doi: 10.1021/jf403286w
34. Zhao M, Li XW, Chen Z, Hao F, Tao SX, Yu HY, et al. Neuro-Protective Role of Metformin in Patients With Acute Stroke and Type 2 Diabetes Mellitus *via* AMPK/Mammalian Target of Rapamycin (Mtor) Signaling Pathway and Oxidative Stress. *Med Sci Monitor: Int Med J Exp Clin Res* (2019) 25:2186–94. doi: 10.12659/MSM.911250
35. Lin Y, Wang K, Ma C, Wang X, Gong Z, Zhang R, et al. Evaluation of Metformin on Cognitive Improvement in Patients With non-Dementia Vascular Cognitive Impairment and Abnormal Glucose Metabolism. *Front Aging Neurosci* (2018) 10:227–7. doi: 10.3389/fnagi.2018.00227

Author Disclaimer: The views expressed are those of the author(s) and not necessarily those of the NHS, the NIHR or the Department of Health and Social Care.

Conflict of Interest: SJS is an employee and shareholder of Rigel Pharmaceuticals, Inc.

The remaining authors declare that the research was conducted in the absence of any commercial or financial relationships that could be construed as a potential conflict of interest.

Publisher's Note: All claims expressed in this article are solely those of the authors and do not necessarily represent those of their affiliated organizations, or those of the publisher, the editors and the reviewers. Any product that may be evaluated in this article, or claim that may be made by its manufacturer, is not guaranteed or endorsed by the publisher.

Advantages of publishing in Frontiers

OPEN ACCESS
Articles are free to read for greatest visibility and readership

FAST PUBLICATION
Around 90 days from submission to decision

HIGH QUALITY PEER-REVIEW
Rigorous, collaborative, and constructive peer-review

TRANSPARENT PEER-REVIEW
Editors and reviewers acknowledged by name on published articles

Frontiers
Avenue du Tribunal-Fédéral 34
1005 Lausanne | Switzerland

Visit us: www.frontiersin.org
Contact us: frontiersin.org/about/contact

REPRODUCIBILITY OF RESEARCH
Support open data and methods to enhance research reproducibility

DIGITAL PUBLISHING
Articles designed for optimal readership across devices

FOLLOW US
@frontiersin

IMPACT METRICS
Advanced article metrics track visibility across digital media

EXTENSIVE PROMOTION
Marketing and promotion of impactful research

LOOP RESEARCH NETWORK
Our network increases your article's readership